THE PRODUCTION OF CLINICAL DEXTRAN USING MEMBRANE PROCESSES

ANDREW TILL

Doctor of Philosophy

THE UNIVERSITY OF ASTON IN BIRMINGHAM

October 1988

THE UNIVERSITY OF ASTON IN BIRMINGHAM

THE PRODUCTION OF CLINICAL DEXTRAN USING MEMBRANE PROCESSES

Andrew Till (BSc) PhD October 1988

SUMMARY

Clinical dextran is used as a blood volume expander. The British Pharmacopeia (BP) specification for this product requires the amount of dextran below 12,000 MW and above 98,000 MW to be strictly controlled. Dextran is presently fractionated industrially using ethanol precipitation.

The aim of this work was to develop an ultrafiltration system which could replace the present industrial process. Initially these molecular weight (MW) bands were removed using batch ultrafiltration. A large number of membranes were tested. The correct BP specification could be achieved using these membranes but there was a significant loss of saleable material. To overcome this problem a four stage ultrafiltration cascade (UFC) was used. This work is the first known example of a UFC being used to remove both the high and low MW dextran. To remove the high MW material it was necessary to remove 90% of the MW distribution and retain the remaining 10%.

The UFC signficantly reduced the amount of dialysate required. To achieve the correct specification below 12,000 MW, the UFC required only 2.5 - 3.0 diavolumes while the batch system required 6 - 7. The UFC also improved the efficiency of the fractionation process. The UFC could retain up to 96% of the high MW material while the batch system could only retain 82.5% using the same number of diavolumes. On average the UFC efficiency was approximately 10% better than the equivalent batch system.

The UFC was found to be more predictable than the industrial process and the specification of the final product was easier to control.

The UFC can be used to improve the fractionation of any polymer and also has several other potential uses including enzyme purification.

A dextransucrase bioreactor was also developed. This preliminary investigation highlighted the problems involved with the development of a successful bioreactor for this enzyme system.

Key words:

Dextran, Ultrafiltration, Cascading, Bioreactor, Dextransucrase

DEDICATED

TO MY FATHER

A SKILLED CRAFTSMAN

WHO IS MISSED BY US ALL

ACKNOWLEDGEMENTS

The Author is indebted to the following:

Dr E L Smith and the Department of Chemical Engineering and Applied Chemistry for making available the facilities for research.

Professor P E Barker who supervised this work, for his help and guidance throughout this project.

For the provision of a scholarship by the Science and Engineering Research Council and the Directors of Fisons Plc for their financial support.

Mr N Roberts and all the technical staff, especially Mr D Bleby whose electronic expertise and patience helped to solve many annoying problems.

April, my sister, for her patience during the typing of this thesis.

Finally, my parents for their support and encouragement throughout my PhD.

LIST OF CONTENTS

LIST OF FIGURES

LIST OF TABLES

1.0 INTRODUCTION

1.0 INTRODUCTION

Dextran is a natural polymer of glucose in which the glucosidic bonds are predominantly of the γ-1,6 type. Interest in dextran goes back to 1874 when it was named by Scheibler (1).

Probably the largest dextran usage is in the pharmaceutical industry as a blood volume restorer. The molecular weight distribution within this product is strictly controlled. The British Pharmacopeia (BP) standard for a dextran 40 requires 85% of its molecular weight range to be between 12,000 daltons and 98,000 daltons (2). Another common use for dextran is in the form of iron dextran, which is used in the treatment of anaemia.

Dextran is produced from sucrose using the extra cellular enzyme dextransucrase. The product of this fermentation stage is known as 'native dextran'. The molecular weight of this native dextran ranges from several hundred thousand to at least 50 million daltons. To obtain the final clinical dextran product several steps are involved. Firstly the native dextran is subjected to partial acid hydrolysis to give a product with a molecular weight range of 180 daltons to 3 million daltons. This product is commonly known as the dextran hydrolysate.

The final fractionation of the dextran hydrolysate is accomplished using a process known as ethanol fractionation. This process makes use of the dextrans reducing solubility with increasing molecular weight. The first addition of ethanol to an aqueous solution of dextran results in the precipitation of the largest dextran molecules. A second ethanol addition is then used to increase the ethanol concentration to a point where the smaller molecules are precipitated [3,4].

This process suffers from high energy cost due to the need for ethanol recovery by distillation and is also a potential fire hazard.

Using an ultrafiltration system to perform this fractionation avoids these problems although maintaining sterility would be more difficult in an aqueous solution than in ethanol. Vlachogiannis [5] investigated the potential of the ultrafiltration system using a range of Amicon membranes. Vlachogiannis found that he could achieve the correct BP specification below 12,000 MW using diafiltration but unfortunately substantial amounts of the saleable 12,000 MW to 98,000 MW band was also lost.

To improve the efficiency of the fractionation process Poland [6] developed an ultrafiltration cascade system. Using this four stage ultrafiltration cascade to remove dextran with a molecular weight below 12,000 MW Poland was able to show that the cascade aided the removal of the low molecular weight material and also enhanced the retention of the saleable 12,000 MW to 98,000 MW band. Unfortunately Poland found that the Amicon 5000 MW cut-off membranes were not ideal for this particular fractionation since the cross-over point (the point below which the cascade aids the removal and above which it enhances the retention of material) occurred at a value of 6000 MW not the desired value of 12,000 MW. The aims of this project were as follows:

(a) To complete a detailed investigation into the removal of dextran below 12,000 MW using the ultrafiltration cascade.

(b) To gain a detailed understanding of the factors effecting the performance of the ultrafiltration cascade.

(c) To use the ultrafiltration cascade to remove the dextran above 98,000 MW.

(d) To develop a mathematical model which may be used to predict the performance of the experimental cascade.

(e) To undertake preliminary studies into an ultrafiltration bioreactor system for the production of dextran and fructose from sucrose using the enzyme dextransucrose.

Figure 1.1 Clinical Dextran Fractionation from Hydrolysate

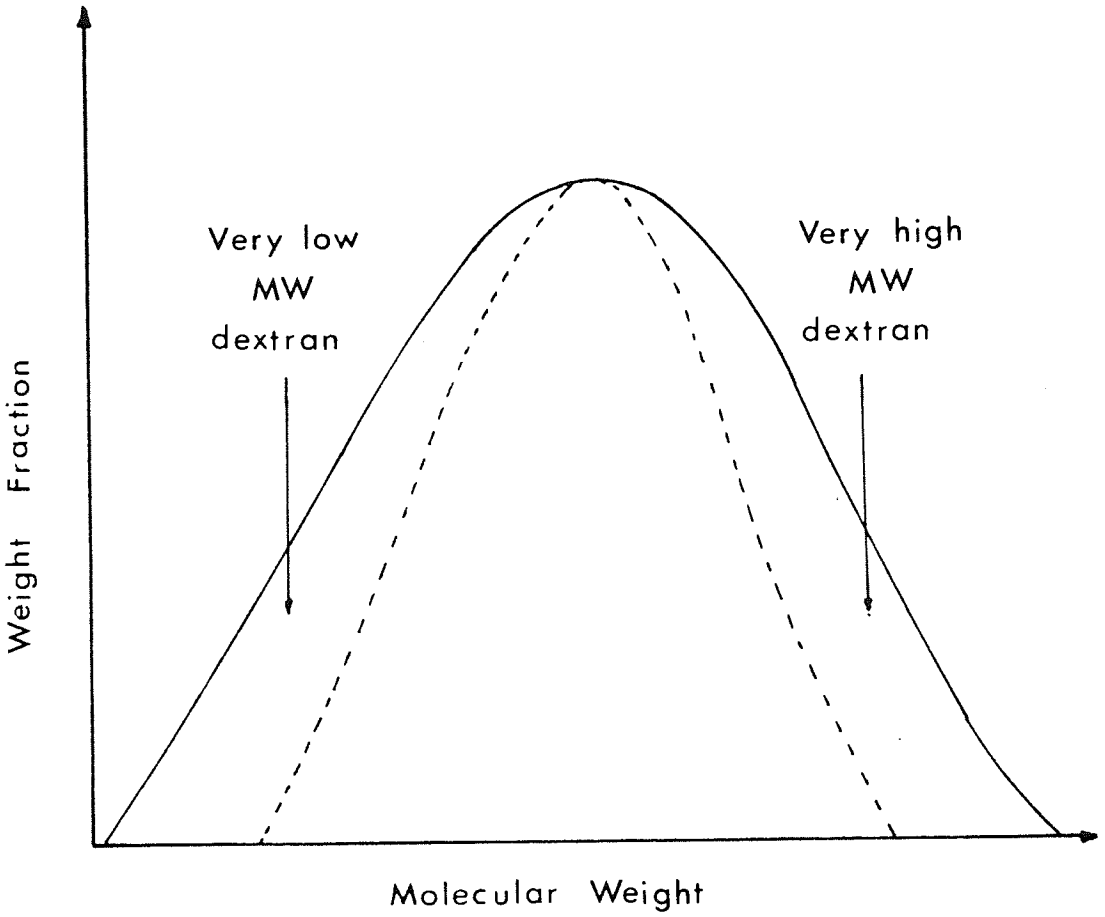

——— Dextran Hydrolysate

– – – – – Clinical Dextran

Specification of clinical dextran 40

British Pharmacopeia

85 % of dextran between 12000 - 98000 MW

Fisons Ltd

90 % of dextran between 12000 - 98000 MW

2.0 ULTRAFILTRATION OF MACROMOLECULES

2.0 ULTRAFILTRATION OF MACROMOLECULES

2.1 INTRODUCTION

Ultrafiltration is only one of a wide spectrum of membrane processes which can be distinguished by the size of the molecules they retain. See figure 2.1. The borderline between each process is diffuse, however broadly speaking ultrafiltration operates in the macromolecular weight range while reverse osmosis is used to separate smaller molecules such as inorganic ions and small organics and microfiltration, larger material such as bacteria, cells and cell fragments.

Although ultrafiltration has been possible on a laboratory scale for many years using materials such as collodion and cellophane the practical application of this process only became possible with the advent of a new range of membranes which exibited a high flux and were able to distinguish among molecular species in the 1nm to 10 μm size range. These membranes manufactured from cellulose acetate were a direct spin off from the rapid development of reverse osmosis technology. In more recent years the range of polymers used has rapidly increased, for example polysulphone, polyamides, polycarbonates and polyvinyl chloride have all been used. The polysulphone membranes in particular are now widely available and have now replaced the earlier cellulose acetate membranes from most applications apart from those requiring very tight membranes. To obtain the best performance from these membranes a wide range of equipment designs have been developed, these include hollow fibre cartridges, plate and frame, spiral wound and tubular systems.

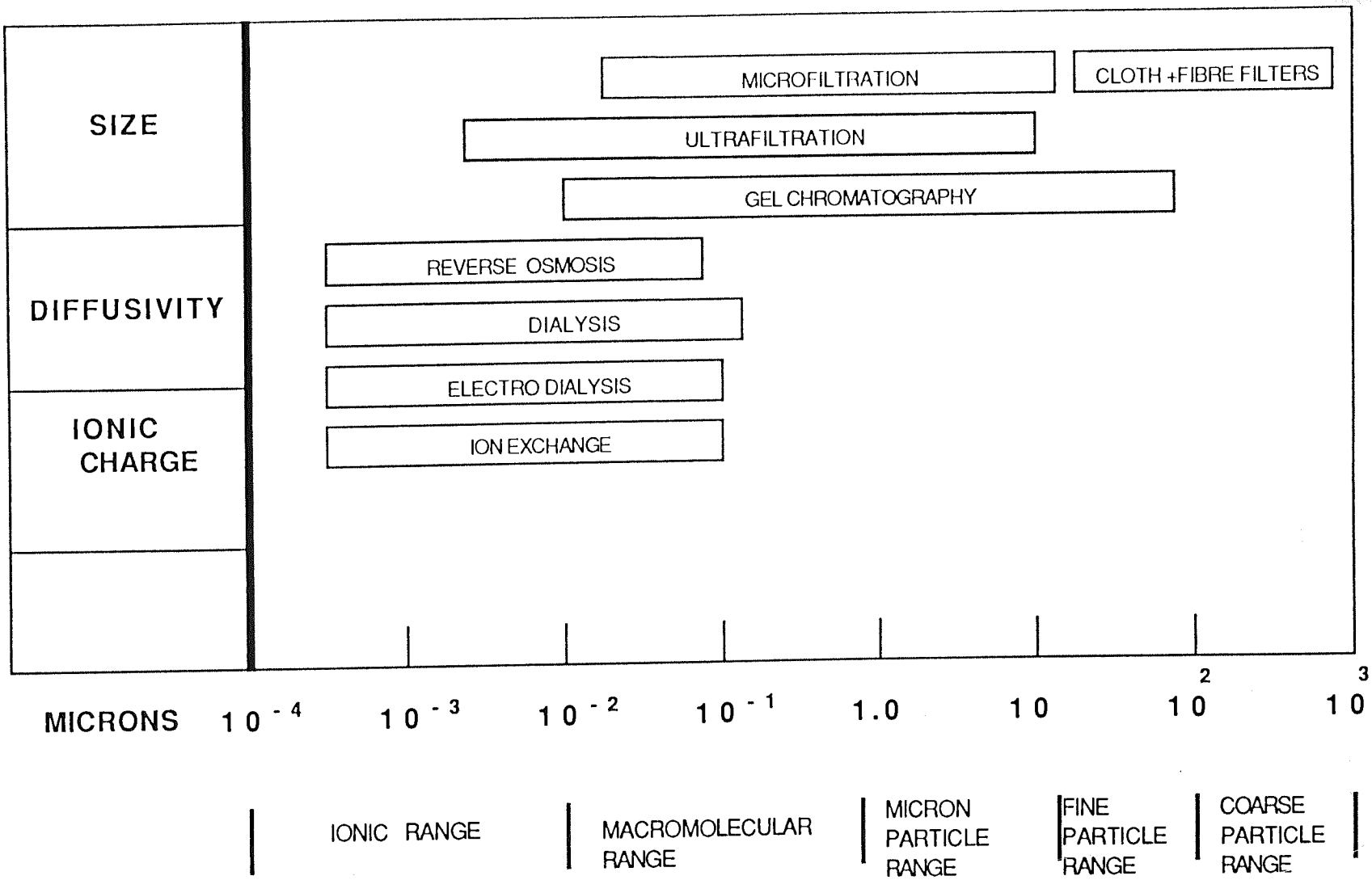

Figure 2.1 Comparison of Membrane Processes

Since the ultrafiltration process is athermal it avoids problems such as thermal and oxadative degradation common with other unit operations such as evaporation and freeze drying. Furthermore since no phase changes are involved the operating costs are typically far lower.

Ultrafiltration can now be found within the food processing, chemical processing, pharmaceutical and medical industries, for the concentration, purification and sterilization of macromolecules and colloidal solutions. Furthermore ultrafiltration can also be found in novel applications such as enzyme bioreactors which show great promise for future commercial exploitation.

2.2 ULTRAFILTRATION

2.2.1 MEMBRANE MANUFACTURE

The technique known as phase inversion is currently the most important method of preparing synthetic membranes. Although the process has now been refined the basic technique is very simple. The polymer is first dissolved in a suitable solvent and a layer of the solution up to 2 mm thick is cast onto a suitable plate. At this stage the film may be left to allow solvent to evaporate or to allow water to be absorbed from the atmosphere, or in some cases both. The film is then quenched in a gelation (or precipitation) medium, usually water, which is a non-solvent. During the quenching stage the polymer solution splits into two phases, a polymer rich solid phase which forms the membrane and a polymer depleted solvent phase which fills the pores in the membranes structure. Since the gelation occurs far more rapidly at the surface where the polymer meets the gelation medium, the pores formed in this layer are far smaller than in the bulk, giving rise to a skin or active layer. These membranes with a dense surface skin and a highly porous

sub-structure are typically categorised as asymmetrical membranes because of their unique structure.

Since these membranes are required to withstand high operating pressures these membranes are often cast onto a porous support medium which can take the form of paper sheet, a braided mat of polyester fibres or a sintered plastic sheet. Hollow fibres on the otherhand are manufactured by extrusion and rely on the fact that if the lumen of the tube is sufficiently small a material with only a modest mechanical strength can be adequate to withstand relatively high operating pressures. Typically these fibres have an internal diameter of only 0.5 mm to 1.0 mm.

The other common types of membranes include thin film composite membranes, track etched and stretched formed membranes. The thin film composite membranes are similar to the asymmetric membranes, however the active membrane and the porous sublayers are manufactured separately and bonded together. Since it is possible to manufacture both layers in different polymers it is possible to optimise both to give the membrane better properties.

Track etched membranes are made from thin polymeric films typically about 10-20 μm thick. This film is irradiated with α-particles and then chemically etched. This process produces a membrane with uniform cylindrical pores though the depth of the membrane, unlike the asymmetric membranes mentioned earlier.

Stretch formed membranes are formed by consecutive steps of cold stretching, hot stretching and heat setting of a polypropylene film. This results in a membrane containing elliptically shaped, but uniform pores. These membranes are available with a molecular weight cut-off of about 100,000 MW which puts them within the ultrafiltration range.

2.2.2 ULTRAFILTRATION EQUIPMENT

For the successful application of ultrafiltration as an efficient separation process, the design of the module used to contain the membrane and the layout of the system in which the module is installed, are as important as the selection of the correct membrane. The four most common systems are the tubular module, the plate and frame module, the spiral-wound module and the hollow fibre module.

The tubular membrane system consists of a membrane which is normally between 1.0 to 2.5 cm in diameter which is supported within a porous stainless steel or fibreglass tube. The pressurized fluid flows down the tube bore and the product solution permeates through the membrane and collects in the outer shell. The tubes may be installed in series or in parallel if there is a high pressure drop. See figure 2.2. The advantages of the tubular system are the control of concentration polarization by the adjustment of the feed flow velocity over a wide range, and the possibility of mechanical cleaning if excessive membrane fouling makes this necessary. While the disadvantages of the tubular system are the relatively high investment and operating costs, and the low ratio of membrane surface area to system volume.

The plate and frame designs were among the first systems introduced in large scale ultrafiltration and reverse osmosis units. The membranes, porous membranes support material and spacers forming the feed flow channel are clamped together and stacked between two endplates. The feed solution is channelled across the surface of the membrane by the feed side spacers, see figure 2.3. There are a variety of plate and frame designs on the market differing primarily in the design of the feed flow channel. All these plate and frame systems provide a large membrane area per unit volume. In general the control of concentration polarization is more difficult in these units than in

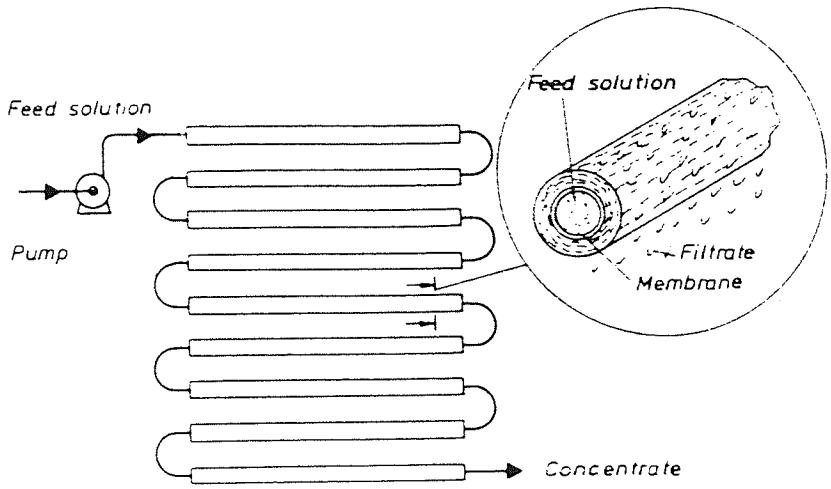

Figure 2.2 A Tubular Membrane Module

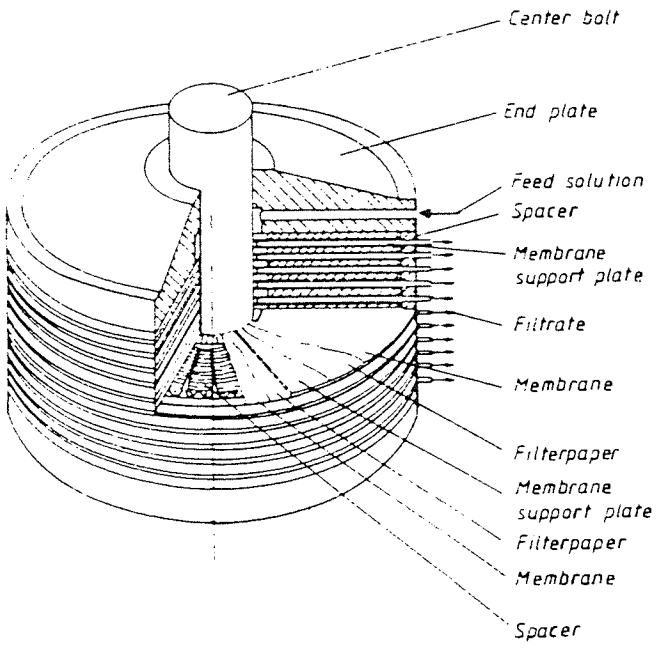

Figure 2.3 A Plate and Frame Module

tubular systems, and plugging of the feed flow channel can be a problem particularly with solutions containing large quantities of suspended solid matter. In general the capital costs are somewhat lower than the tubular system and the operating costs are also lower.

The spirally wound module is basically a plate and frame system which has been rolled up, see figure 2.4. The feed flow channel, the membrane, and the porous membrane support are all rolled up and placed inside an outer tubular casing. The permeate is collected in a tube in the centre of the roll. The spiral wound design allows a high surface area to volume ratio and the operating costs are also low. However it can be difficult to control concentration polarization and membrane fouling with this design.

The capillary or hollow fibre design can come in several forms. The most commonly used modules are those produced by Amicon and Romicon. These units consist of a bundle of fibres typically 0.5 to 1.1 mm in diameter cast into epoxy header blocks within a PVC or polysulphone permeate shroud, see figure 2.5. The feed solution passes down the lumen of the fibre and the filtrate permeates through the wall of the capillary. This design has a low capital cost combined with a relatively high surface area to volume ratio. The system provides good feed flow control, however plugging of the fibre lumen can be a problem when dirty solutions are used and therefore effective prefiltering must be provided.

Since these ultrafiltration modules vary significantly in design and performance a detailed comparison of capital costs and operating costs is difficult, however a more general comparison has been made in table 2.1.

Figure 2.4 A Spiral Wound Module

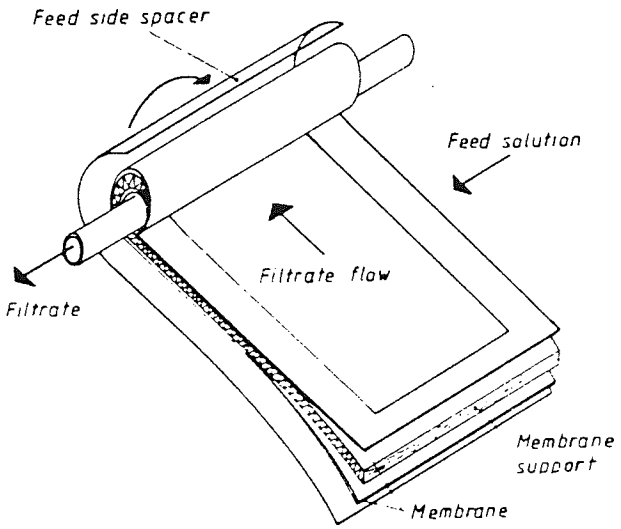

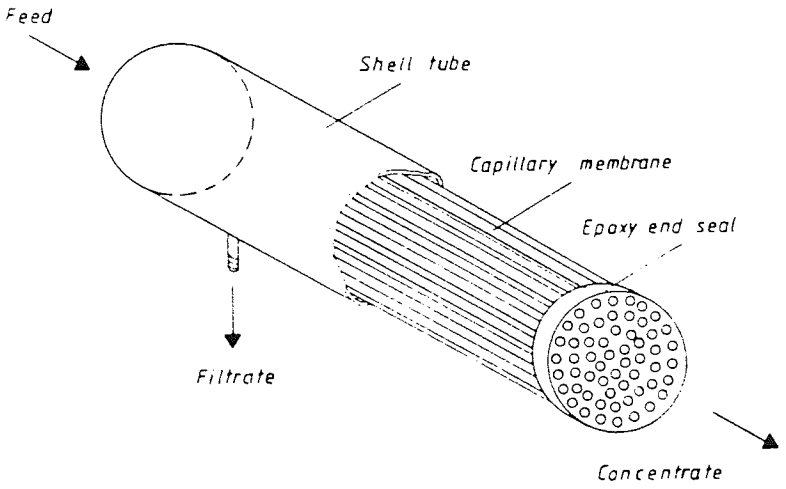

Figure 2.5 A Capillary Membrane Module

Table 2.1 Comparison of Ultrafiltration Systems (22)

Module Type	Membrane Surface area for Module Volume (m^2/m^3)	Investment Cost	Operating Cost	Flow Control	Ease of Cleaning in Place
Tubular	24 to 50	High	High	Good	Good
Plate and Frame	400 to 600	High	Low	Fair	Poor
Spiral Wound	800 - 1000	Very low	Low	Poor	Poor
Capillary	600-1200	Low	Low	Good	Fair

2.2.3 MODES OF OPERATION

An ultrafiltration system can be operated in three modes, concentration, diafiltration and dialysis.

By applying a positive pressure to a macromolecular solution retained by a membrane the solvent can be removed through the walls of the membrane while retaining the macromolecules. Therefore a solution can be concentrated. Removal of low molecular weight impurities can also be partially effected during concentration, however the purification of solutes using diafiltration (or constant concentration) is often more successful. In the diafiltration mode the solute to be purified is neither concentrated or diluted with respect to the solvent. As the permeate containing the low molecular weight material passes through the membrane, dialysate (pure solvent) flows into the retentate reservoir at the same rate. In the final mode, namely the dialysis mode, the feed solution flows across the membrane on the high pressure side while the fresh solvent flows across the other side. This allows a rapid removal of impurities since the molecules are able to diffuse into

the dialysate liquid through the membrane and are also convectively transported through the membrane as permeate.

2.3 ULTRAFILTRATION - THE IDEAL SYSTEM

2.3.1 RETENTIVITY

Unlike reverse osmosis membranes, ultrafiltration membranes have a distinct pore structure and the selectivity of the membrane is defined by the sieving action of the pores in the membranes structure. Normally a membrane will contain a distribution of pore sizes and a certain fraction (R) of these pores will be too small to allow passage of the solute through the membrane. If all the larger pores allow the solute to pass through the membrane unhindered, the solute flux can be defined as

$$J_2 = C_B(1-R)J_1 \qquad \ldots 2.1$$

where J_1 is the solvent flux and C_B the bulk concentration of the solute in the retentate.

Since the mass balance dictates that

$$J_2 = J_1 C_P \qquad \ldots 2.2$$

where C_P is the concentration of the solute in the permeate then

$$R = 1 - \frac{C_P}{C_B} \qquad \ldots 2.3$$

Although this is a commonly used method of defining the selectivity (R) of the membrane. There are several limitations of its use. The expression can only be valid if the concentration of the solute remains constant. This would only be true if the concentration of the permeate (C_P) was equal to the concentration of the retentate (C_B), ie if R equals zero. In any case where R is greater than zero the concentration of the retentate would change, thus changing C_P. To reduce this problem very large volumes of test solution can be employed and only small volumes of permeate removed, so that any changes in C_B would be negligible. Dilute solutions should also be employed to avoid concentration polarization. The effect of non-ideality such as concentration polarization is discussed in section 2.4.

Since the volume of the retentate often changes during ultrafiltration, it is advisable to take this into account when calculating the rejection coefficient [7]. Based on the retentate stream the rejection coefficient can be obtained from

$$R_{ret} = \frac{Ln(Ct/Co)}{Ln(Vo/Vt)} \qquad \ldots 2.4$$

This expression is only valid if the concentration mode of operation is used. For the diafiltration mode of operation another simple expression can be developed based on either the permeate or retentate streams.

$$C_{r(t)} = C_{r(o)} \exp\left[- \frac{V_{(t)}}{V_o} (1-R) \right] \qquad \ldots 2.5$$

$$\text{Ln}C_p(t) = \text{Constant} - (1-R)\frac{V_t}{V_o} \quad \ldots 2.6$$

where V_t is the volume of permeate collected from the beginning of the experiment to time t : V_o is the volume of the UF cell, which is constant; $C_{r(t)}$, $C_{p(t)}$ are the concentrations of the retentate and permeate at time t, $C_{r(o)}$ is the initial concentration of the retentate and R is the rejection coefficient.

R can be simply determined by plotting $\text{Ln}Cp_{(t)}$ versus V_t/V_o which gives a slope of -[1-R]. In both the concentration and diafiltration mode of testing, dilute solutions must be used to avoid concentration polarization.

Normally the molecular weight cut-off quoted by manufacturers are determined by using a range of solutes with differing molecular weights. Typically the values correspond to the solute which gives greater than 90% retention.

The simple rejection models described above indicate that the rejection coefficient is effectively constant and pressure independent, however under normal working conditions this will not be true. To take into account such factors as solute shape, charge, adsorption onto the membrane and membrane fouling more complex models are required; these are discussed later.

2.3.2 MEMBRANE PERMEATION

For the ideal system operating isothermally and at steady state the flux can be determined using the relationship proposed by Kaden and Katchalsky [8].

$$J_1 = Lp\ \{(P_A - P_P) - (\pi_A - \pi_P)\} = L_P(\Delta P - \Delta\pi) \qquad \ldots 2.7$$

where π_A and π_P are osmotic pressures corresponding to the retentate concentration C_A and the permeate concentration C_P. P_A and P_P are the pressures corresponding to the feed and permeate side of the membrane. L_p is the membrane permeability constant which is stable over a wide range of pressures and concentrations.

Where the solute molecules are large and uncharged the osmotic pressure difference across the membrane can be assumed to be negligible compared to the applied pressure.

If the membrane can be assumed to contain straight uniform cylindrical pores, for example within a track etched membrane, the water flux can be determined using the Hagen-Poiseuille equation for viscous flow through a cylindrical pipe [9].

$$J_1 = \frac{\epsilon r^2\ \Delta P}{8\ \mu\ \Delta x} \qquad \ldots 2.8$$

Where J_1 is the solvent flux, ϵ is the fraction of the membrane containing pores, r is the pore radius, ΔP is the pressure drop across the membrane, μ is the viscosity and Δx the membrane thickness.

Where the pore structure is non uniform, for example in a asymmetric membrane this equation can lead to a substantial error. Another model proposed by Rautenback [10] was based on the Carman Kozeny equation and was developed for flow through a porous bed containing irregular pores:

$$J_1 = \frac{\epsilon^2}{2K_c\,(1-\epsilon)^2\,F(V)^2} * \frac{\epsilon\ \Delta P}{\mu\ \Delta x} \qquad \ldots 2.9$$

where F(V) is the surface area per unit volume and K_c is the Carman factor.

The solute flux of the membrane is given by equation 2.1.

$$J_2 = J_1\,(1-R)\,C_B \qquad \ldots 2.1$$

These simple models indicate that the solvent flux is directly proportional to the applied pressure and the solute flux is dependent on the solvent flux. Under normal operating conditions this is not valid.

2.4 THE NON-IDEAL SYSTEM

2.4.1 MEMBRANE PERMEATION

It was discovered in the early studies of ultrafiltration that the simple proportionality between membrane flux and applied pressure difference was only valid for the pure solvent and very dilute solutions of macromolecules. As the concentration was increased an anomalous result was observed. The linear flux/pressure relationship was evident at only very low pressures; as the applied pressure was increased the

rate of flux increase decreased until no further change occurred, normally at a value far below that for the pure solvent. After this point the flux became pressure independant. This effect is commonly known as concentration polarization.

When a macromolecular mixture is brought to the membrane surface by a pressure driving force some molecules will permeate the membrane whilst others will be retained. This leads to an accumulation of the retained components and a depletion of the permeating components in the boundary layer adjacent to the membrane surface. Eventually a sufficiently high concentration can be reached where the solubility limit of the solute is exceeded, this will cause the solute to precipitate on the membrane surface. This is commonly known as gel layer formation. Whether this layer is a true gel is difficult to assess, however it is generally agreed that the solute molecules are approaching a 'close-packed' configuration.

The effect of concentration polarization may be modelled by two fundamentally different approaches. These are the film model originally proposed by Sourirajan [11] for reverse osmosis and the osmotic pressure model. These models will now be considered.

The film model is equally effective at modelling the concentration polarization and gel layer regimes. The model assumes that even in turbulent flow a laminar boundary layer is present next to the membrane surface. During the filtration process, a steady state is achieved where the convective transport of solutes to the membrane surface is counter-balanced by a diffusive flow of the rejection material from the membrane surface back into the bulk solution. Therefore a constant concentration profile of the rejected solute is found in the boundary layer. A schematic diagram can be found in figure 2.6. Where C_W and C_B are the concentration at the membrane surface and the bulk solute

concentration, Y_b is the boundary layer thickness. The back diffusion from the membrane can be assumed to occur accordingly to Ficks law:

$$B = D \frac{dc}{dy} \qquad \ldots 2.10$$

where B is the back diffusion, D the diffusivity of the species and (dc/dy) is the rate of change of the solute concentration.

Since the membrane is assumed to be only partly retentive the mass of material at the membrane surface by convective transport will be:

$$J_1C - J_1C_P \qquad \ldots 2.11$$

Where J_1 is the solvent flux and C_P the concentration of the permeate. At a steady state:

$$J_1 (C-C_P) = -D \frac{dc}{dy} \qquad \ldots 2.12$$

rearranging 2.12 and intergrating over the boundary layer:

$$\frac{J_1 Y_b}{D} = \text{Ln} \left(\frac{C_W - C_P}{C_B - C_P} \right) \qquad \ldots 2.13$$

If the membrane is very highly retentive then it is often possible to assume that $C_P = 0$. If K the mass transfer coefficient is defined as:

$$K = D / Y_b \qquad \ldots 2.14$$

then equation 2.13 can be rearranged to give;

$$J_1 = K \ln \frac{C_W}{C_B} \qquad \ldots 2.15$$

The ratio of C_W/C_B is often known as the concentration polarization modulus.

This model predicts that the degree of concentration polarization is determined by the diffusion coefficient, the filtration rate and the thickness of the boundary layer. The diffusion coefficient is usually determined by the solute and the solvent used and the filtration rate purposely maintained as high as possible, so the effect of concentration polarization is normally controlled by reducing the thickness of the boundary layer. This is normally achieved by using a high recirculation rate to create turbulence near the membrane surface.

It was mentioned earlier that the flux will become independent of the applied pressure; this behaviour was explained by Michaels [12] and Blatt [13] by the so called gel polarization theory that suggested that the macromolecular solution reaches an upper concentration limit (C_g) at high values of the polarization modules and displays properties analogous to that of a gel. Naturally if a gel layer is present equation 2.15 will no longer be valid. However using the same approach as used previously, the effect of the gel layer can be modelled. See figure 2.7;

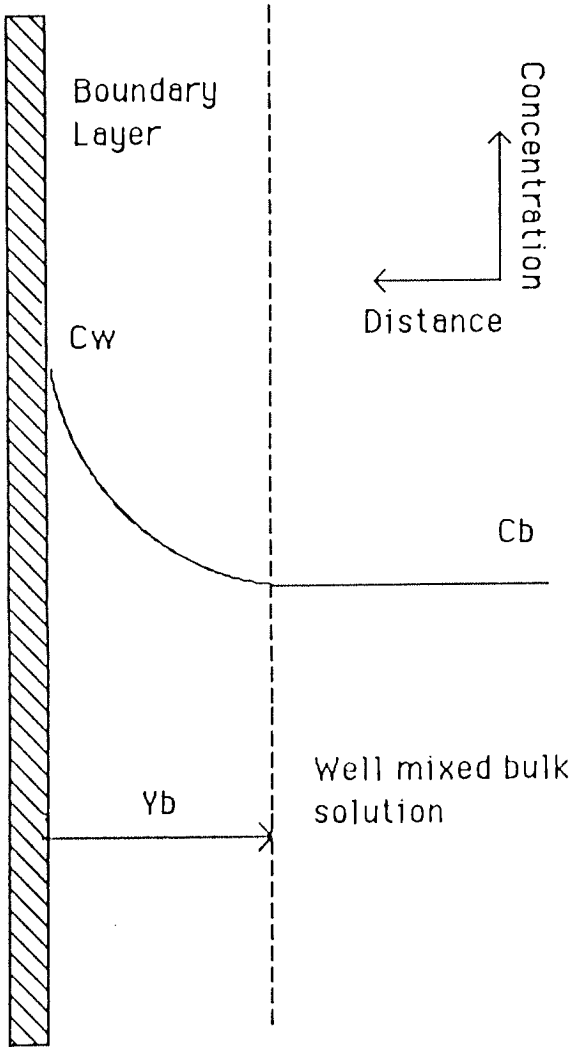

Figure 2.6 Concentration Profile in the Boundary Layer for well Developed Turbulent Flow

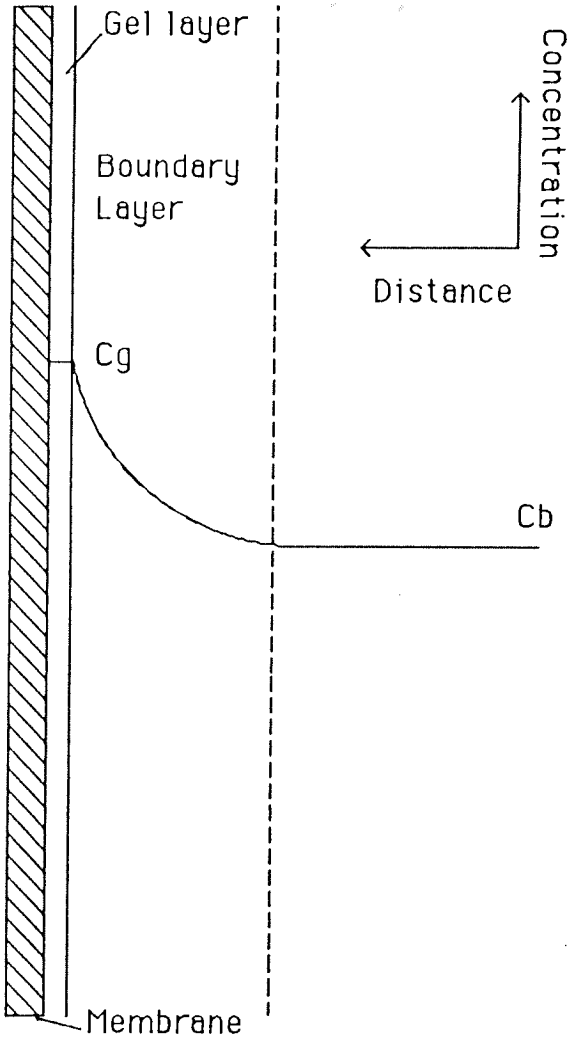

Figure 2.7 Gel Formation in Concentration Polarization

$$J_1 = K \ln \frac{C_g}{C_B} \quad \ldots 2.16$$

The gel layer concentrations can be determined by plotting J_1 versus In C_b, theory dictates that when $J_1 = 0$ the concentration must equal C_g.

It was noticed by several workers that since film theory was being used the mass transfer coefficient could be determined using mass transfer and heat transfer analogies. Porter [14] found that for the laminar flow region the Graetz [15] or Leveque [16] solutions could be used. For all thin channel systems the Leveques solution can be expressed as:

$$Sh = 1.62 \, (Re \, Sc \, d_h/L)^{0.33} \quad \ldots 2.17$$

for $100 < Re \, Sc \, d_h/L < 5000$

where Sh = Sherwood number $= \frac{K \, d_h}{D}$ ... 2.18

Re = Reynolds number $= \frac{U \, d_h}{v}$ ... 2.19

Sc = Schmidt number $= \frac{v}{D}$ ... 2.20

and d_h = equivalent hydraulic diameter, L the channel length, U the average velocity, v the Kinematic viscosity and D the diffusivity.

For fully developed turbulent flow Porter found that the Dittus and Boelter [17] correlation gave satisfactory results:

$$Sh = 0.023\ Re^{0.8}\ Sc^{0.33} \qquad \ldots 2.21$$

for $Re > 2000$.

The major assumption of the model mentioned above is that the osmotic pressure of macromolecules are always negligible. However this has been shown to be only partly true, Vilkers et al [18] measured the osmotic pressure of bovine serum albumin at concentrations up to 475 g/litre. They found that these highly concentrated solutions had osmotic pressures comparable to the normally applied pressure in ultrafiltration. The supporters of the osmotic pressure model suggest that the high macromolecule concentrations found at the membrane surface results in a significant osmotic pressure, which would cause the rate of increase of the membrane flux to decrease as the transmembrane pressure is increased. The pressure independent flux region occurs when an increase in transmembrane pressure causes a corresponding equal increase in osmotic pressure.

A typical example of this model was proposed by Clifton [19]. In the absence of any membrane fouling the only effect which operates to reduce the membrane permeation rate is the osmotic pressure in contact with the membrane. Therefore the basic equation of Kaden and Katchalsky can be applied:

$$J_1 = L_p\ (\Delta P - \Delta\pi) \qquad \ldots 2.7$$

Where $\Delta\pi$ is the osmotic pressure difference caused by the macromolecules at the membrane surface and those in the permeate.

The variation of osmotic pressure with concentration is given by the relationship:

$$\pi_{(c)} = (RT/M_N)\ [C + \Gamma_2 C^2 + \Gamma_3 C^3] \qquad \ldots 2.22$$

where the first term is this expression corresponds to the Van't Hoff Law and Γ_2 and Γ_3 are viral coefficients.

Clifton [19] showed that this type of approach could be used to model the effect of concentration polarisation. Wijmans [20] compared the two approaches and concluded that the two approaches were essentially equivalent.

2.4.2 RETENTIVITY

Since concentration polarization causes a high solute concentration at the membrane wall the rejection coefficient based on the bulk solution concentration will be lower than expected. The observed rejection is given by:

$$R = 1 - \frac{C_P}{C_B} \qquad \ldots 2.3$$

while the true rejection is given by:

$$Ro = 1 - \frac{C_P}{C_W} \qquad \ldots 2.23$$

where C_W is the concentration at the membranes surface. The observed rejection can be related to the true rejection by a mass transfer model

proposed by Colton [21] for a stirred batch ultrafiltration system. This mass transfer model is based on the relative rate of solute transfer to the membrane by convection, compared to the rate of transfer away from the membranes surfaces by diffusion:

$$Ro = R \exp (J_v/K) \; / \; ((1-R) + R \exp (J_v/K)) \qquad \ldots 2.24$$

where J_v = total volume of permeate and K the mass transfer coefficient.

The mass transfer coefficient can be obtained from:

$$K = 0.0443 \; [\; D/r \;] \; [\; v \; /D \;]^{0.333} \; [\; \omega r^2/v \;]^{0.746} \qquad \ldots 2.25$$

D is the solute diffusivity, r is the membrane radius, v is the Kinematic viscosity and ω is the rotational velocity of the stired batch cell.

By combining equations 2.3 and 2.13 the rejection can be related to the boundary layer thickness, the diffusion coefficient and flux:

$$\frac{C_W}{C_B} = \frac{\exp (J \; Y_b/D)}{R + (1-R) \exp (J \; Y_b/D)} \qquad \ldots 2.26$$

C_W/C_B is often known as the concentration polarization modulus.

This equation can only hold true if the diffusion coefficient is independent of the solute concentration, and the boundary layer is constant over the entire membrane. These assumptions will normally only be valid for dilute solutions in the down stream region of turbulent flow [22].

Another commonly used model can also be developed by combining equations 2.13, 2.14 and also introducing the sieving coefficient which is defined as :

$$\phi = \frac{C_p}{C_W} \qquad \ldots 2.27$$

to give

$$\frac{1-R}{R} = \frac{\phi}{1-\phi} \exp(J/K) \qquad \ldots 2.28$$

This model was proposed for dilute solutions. For a fixed sieving factor, (ie. C_p must increase as C_W increases to keep ϕ constant) as concentration polarization increases, C_p must increase and hence R decreases. This then shows that for a dilute solution as the pressure increases the rejection decreases.

When high solute concentrations are used these equations are no longer valid since concentration polarization often results in the formation of a gel layer which can act as a secondary membrane. The secondary sieving effects of the gel layer are well known, for example, the presence of γ - globulin in a protein mixture containing human serum albumin (HSA) can create a dynamic membrane. The rejection of HSA being proportional to the square root of the γ - globulin concentration [13]. This secondary membrane is often more retentive than the primary membrane and therefore the rejection coefficient tend to increase as concentration polarization increases. An extreme example of this effect is the use of the gel layer as a dynamic membrane. Johnson [23] found that he could obtain a satisfactory solute rejection by forming a

dynamic membrane on the surface of a porous support which exhibit no initial selectivity.

To model the effects of the gel layer, Nakao [24] assumed that the gel layer acted as a membrane in series with the ultrafiltration membrane. Therefore the gel is considered to have a specific pore size, solute permeability (P_g) and reflection coefficient (σ_g).

For this analysis, transport equations for water and solute flow through two different membranes in series are necessary. These equations have been developed by Jagur - Grodzinski and Kadem [25]. The real rejection of this system is given by:

$$R = \frac{(1-F_g)\,(1-\sigma_m) + F_g\,(1-\sigma_g)\,(1-F_m\,\sigma_m) - (1-\sigma_g)\,(1-\sigma_m)}{(1-F_g)\,(1-\sigma_m) + F_g\,(1-\sigma_g)\,(1-F_m\,\sigma_m)} \qquad \ldots 2.29$$

where the suffixes g and m correspond to the gel layer and the membrane.

$$F_g = \exp\left[\frac{-Jv\,(1-\sigma_g)}{P_g}\right] \qquad \ldots 2.30$$

$$Fm = \exp\left[\frac{-Jv\,(1-\sigma_m)}{Pm}\right] \qquad \ldots 2.31$$

When Nakao used a steric hindrance pore model to determine the parameters σ and P he found a good agreement between theory and experimental. However the main draw-backs of the model are its complexity and the considerable amount of experimental data required to evaluate some of the parameters used in the model.

2.4.3 MEMBRANE FOULING AND ADSORPTION EFFECTS

Membrane fouling is a commonly found problem which results in the long term decline of the membrane flux. Although fouling is normally used to describe the long term loss of membrane performance which cannot easily be regained even by cleaning, Fane [27] considered fouling more broadly. He considered the fouling of a membrane over its whole lifespan, for example he felt that fouling had three phases. The first phase is the period of membrane usage prior to ultrafiltration during which the membrane is normally washed and the flux measured. Fane showed that even trace amounts of bacteria or colloids rapidly reduced the flux. Other factors that caused flux decline were hydrolysis and membrane compaction. The second phase of fouling is caused principally by the build-up of the concentration polarization boundary layer; normally this effect occurs rapidly over a period of seconds or minutes at the start of ultrafiltration. This stage of fouling is normally considered to be reversible with cleaning. The third phase is the long term flux decline region which is often classed as irreversible. The long term flux decline can be modelled by the simple equation:

$$J = P / (Rm + Rs (1-a)) \qquad \ldots 2.32$$

where Rm is the membrane resistance, Rs the resistance of the polarization layer and a is an aging function obtained from:

$$a = \frac{a_{max} \cdot t}{Kt + t} \qquad \ldots 2.33$$

where t is time and the parameters a_{max} and K_t must be correlated as a function of the cross flow velocity for a particular system.

Reducing of this long term flux decline is important if the useful life of a membrane unit is to be extended. Many attempts have been made to reduce the flux decline, these have included the modification of the membrane to include charged groups [27] and the immobilization of enzymes on the membrane surface [28]. Both methods have been shown to be reasonably successful.

There is little doubt that adsorption of solutes onto the membrane surface and into the pores are major causes of membrane fouling. However the effect is very specific to the membrane and solute under consideration. This makes it very difficult to develop a general theory. Most researchers at present have confined their studies to well defined model systems, in particular bovine serum albumin. For example Mathiason [29] measured the binding capacity of polysulphone, cellulose acetate and polyamide membranes using ^{14}C labelled BSA in an unstirred cell. He found that the loss of membrane performance corresponded to the degree of binding.

Zeman [30] noticed that adsorption changed the rejection characteristics of a membrane. To model these changes he developed a model based on the simple steric rejection of spheres by a capillary:

$$R = [\, \lambda'(\lambda' - 2) \,]^2 \qquad \ldots 2.34$$

where

$$\lambda' = \frac{r_2}{r_3 - \Delta r_3} \qquad \ldots 2.35$$

and r_2 is the radius of the solute, Δr_3 denotes the adsorbed layer thickness and r_3 is the membrane pore radius.

For the case of adsorbing spheres equation 2.35 becomes:

$$\lambda' = \frac{r_2}{r_3 - 2r_2} \qquad \ldots 2.36$$

and for random coils a reasonable approximation can be given by:

$$\lambda' = \frac{r_2}{r_3 - K[\eta]_2} \qquad \ldots 2.37$$

where $[\eta]_2$ is the intrinsic viscosity of the solute and K is a proportionality constant. In this latter case Zeman assumed that a random coil behaved like a sphere with a diameter proportional to $[\eta]_2$.

The relative thickness of the absorbed layer can be determined using the relationship:

$$\frac{\Delta r_3}{r_3} = \left| -\left(\frac{J_{w,2}}{J_{w,1}} \right)^{0.25} \right. \qquad \ldots 2.38$$

where J_{w1} and J_{w2} are the water flux prior to solute adsorption and after solute adsorption.

Using the model mentioned above Zeman was able to obtain reasonable agreement with his experimental results. Furthermore, Zeman found that generally hydrophobic solutes gave higher rejections coefficients than hydrophilic solutes of the same size with the same membrane. Since increasing hydrophobicity of the solute leads to an increased entrophy gain due to hydrophobic dehydration on adsorption this is reflected in stronger solute-membrane interaction and greater pore constriction.

2.5 MODELLING THE PERFORMANCE OF MEMBRANES

To model the passage of the macromolecules through the pores within the membranes surface, two approaches have been considered. These can be classified as the hard sphere model and the flexible molecule model.

The hard sphere model has been developed extensively by Zeman and Wales [31, 32]. The original Ferry formula [33] for the rejection of a sphere by a capillary can be written as:

$$R = 1 - C_P/C_B = (\lambda(\lambda - 2))^2 \qquad \lambda \leqslant 1 \qquad \ldots 2.39$$

where $\lambda = a/r$ where a is the radius of the sphere and r is the capillary radius.

In an enclosed space the terminal velocity of a sphere with respect to a moving liquid is not the same as in free space. This effect is known as hydrodynamic lag. The viscous drag force on a solute sphere that reflects the proximity of the wall can be written as:

$$F = -6\pi r a (K_1 U - K_2 V) \qquad \ldots 2.40$$

where U is the velocity of the sphere with respect to some reference point, V is the velocity of the liquid with respect to the same reference, K_1 and K_2 are drag coefficients.

At steady state

$$U/V = K_2/K_1 \qquad \ldots 2.41$$

and the hindrance to convection becomes:

$$W = 1-R = \frac{Cp}{C_B} = \frac{K2}{K_1} \quad (1 - (\lambda (\lambda - 2))^2) \qquad \ldots 2.42$$

The values of K_1 and K_2 were determined by Paine and Scherr [34]:

$$W = 1 - R = \{1-[\lambda (\lambda -2)]^2 \} \exp (- 0.7146 \lambda ^2) \qquad \ldots 2.43$$

Zeman tested the model experimentally using very dilute solutions of dextran and PEG; the low concentrations being important to avoid concentration polarization.

To approximate the hard sphere radius for the dextran Zeman used the Stokes radius for the dextran, r_S was determined from:

$$r_S = 10^{(0.47 \log Mw - 0.513)} \qquad \ldots 2.44$$

plotting λ versus rejection for three Nuclepore membranes, Zeman found good agreement up to $\lambda = 0.7$, however above this value the model over predicted the rejection, see figure 2.8. Unfortunately Zeman could find no satisfactory explanation for this effect. Long and Jacobs [34] also investigated the use of the hard sphere model. Long considered a wider variety of molecules than Zeman. These included polystyrene latex, the tobacco mosaic virus as well as dextran. Instead of using the Stokes radius to determine (a) Long used the Einstein radius (R_e) determined from:

$$= 2.5 \left(\frac{4}{3} R_e^3 \right) \frac{N_A}{M_W} \qquad \ldots 2.45$$

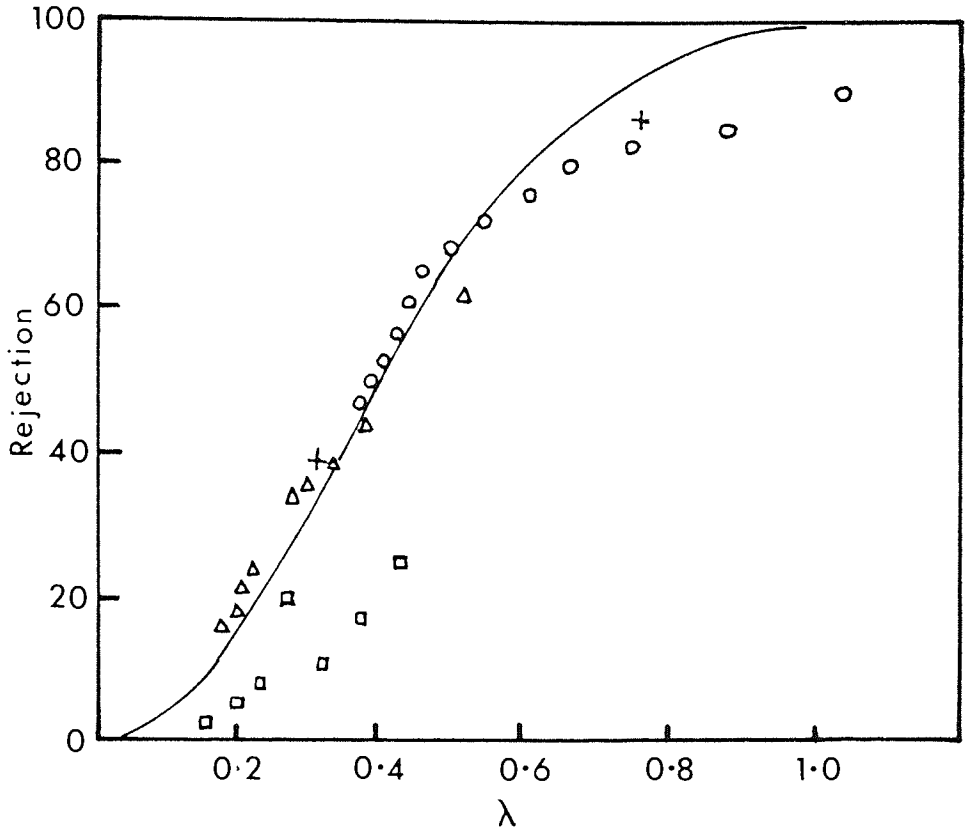

Figure 2.8 Results Obtained by Zeman Using the Hard Sphere Model for Dextran. Solid Line Denotes Model Prediction (31)

where η is the intrinsic viscosity of the dextran sample and N_A is Avogadro's number.

Long found that using the Einstein radius gave equally as good results as the Stokes radius and concluded that dextran molecules could be modelled as hard spheres.

The accuracy of this method for modelling materials such as dextran would appear to be dependent on the operating parameters such as concentration (concentration polarization) and shear rate, therefore under normal operating conditions the model would probably not hold. This was confirmed by Munch [35] using polyacrylamide with a molecular weight of approximately 3×10^6. Munch found that the rejection of this polymer was far lower than the hard sphere model predicted. He felt that this effect was predominantly caused by shear rate effects.

The flexible molecule model has been considered extensively by several workers [36-39]. A soluble macromolecule exposed to a shear flow can be distorted by a difference in velocity between the two sides of the random coil, however the Brownian fluctuations in the chain configuration tend to produce a relaxation of the distortion. If the shear rate is lower than a critical value S_c, the entropic restoring force wins and the distortion decays. If the shear rate is higher than S_c the stretching flow wins and the polymer chain becomes strongly stretched. In the later case the chain follows perfectly the deformation imposed by the solvent flow; this type of deformation is called "affine" deformation [39]. The critical value S_c is of the order of the relaxation frequency of the soluble polymer. In a dilute solution the relaxation frequency of a macromolecule is the Zimm relaxation frequency of the polymer chain:

$$S_c \simeq r_z^{-1} \simeq K_B \; T \epsilon \; / \; \eta_o \; R_F^3 \qquad \ldots 2.46$$

where r_z is the Zimm relaxation time, η_o is the viscosity of the solvent, R_F is the Flory radius of gyration of a dissolved molecule, T is the temperature in degrees Kelvin, and K_B is the Boltzmann constant.

In the semi-dilute solutions where there is some overlap of polymer coils, the characteristic time for the reorganization of the transient network is the reptation time r_R which is linked to the Zimm relaxation time r_z and the concentration C by the relationship [36];

$$S_c \simeq r_R^{-1} \qquad \ldots 2.47$$

where $$r_R \simeq r_z \left(\frac{C}{C^*}\right)^{3/2} \qquad \ldots 2.48$$

and $$C^* \simeq N/R_F^3 \qquad \ldots 2.49$$

where N is the number of monomer units in a macromolecule.

Daoudi [38] showed that to drive a macromolecule into a pore the elongational shear should have to obtain a critical threshold S_c ($S_c \simeq r_z^{-1}$) for a dilute regime; $S_c \simeq r_R^{-1}$ for the semi dilute regime) at a minimal distance from the pore opening of the order of the characteristic dimension of the dissolved macromolecules. The latter condition for the passage of macromolecules is the necessary condition to obtain the transversal dimension of the deformed chains equal to or lower than that of the pore. For a dilute solution the characteristic dimension is the radius of gyration R_F.

$$S(r = R_F) \simeq \frac{J\, Ro^2}{\epsilon R_F^3} \gtrsim K_B \frac{T}{\eta_o R_F^3} \qquad \ldots 2.50$$

or

$$J^* \gtrsim K_B T \epsilon / \eta_o R_o^2 \quad \ldots 2.51$$

where S is the longitudinal gradient of velocity, r is the distance from the pore opening, J is the average flux per unit membrane area, R_o the pore opening radius, ϵ the surface porosity of the membrane skin, K_B is the Boltzmann constant, η_o the viscosity of the solvent and T the temperature in Kelvin.

For a semi dilute solution the characteristic dimensions of the dissolved macromolecule is the correlation length:

$$\xi \simeq R_F (C^*/C)^{3/4} \quad \ldots 2.52$$

thus

$$J^* \gtrsim \frac{k_B T \epsilon}{\eta_o R_o^2} \left(\frac{C^*}{C} \right)^{15/4} \quad \ldots 2.53$$

From this theory it can be seen that the critical flux (J*) depends on both the membrane skin parameters, and the macromolecular solution parameters. Furthermore the critical flux is independent of the concentration of the solution in the dilute regime but it decreases by $C^{-15/4}$ in the semi dilute regime.

This behaviour could be explained by the difference in the physical state of the macromolecules in these two regimes: in dilute solutions the relaxation of the independent macromolecules is rapid and of the same frequency. Once the semi dilute regime is reached the polymer coils becomes more and more entangled with increasing concentration and the thermic motion of their segments is retarded. The shear required for their deformation is consequently lower. Also the deformation would

be easier with a membrane with large pores and low surface porosity because of the higher shear obtained at the same flux of filtrate.

Since the critical flux is dependent on the concentration only in the semi dilute regime, this suggests that there is a critical concentration at the transition point from the dilute to the semi-dilute regime. This was tested experimental by Nguyen [40] using PEG. For low concentrations the rejection of the PEG remained constant but once the critical concentration had been reached, both the flux and rejection fell sharply, the critical flux dropping according to $C^{-15/4}$.

2.6 ULTRAFILTRATION OF DEXTRAN

Dextran has been used extensively to investigate the ultrafiltration of polymers and to characterize membranes [41,42] since it is cheap, water soluble and available in a wide range of molecular weights.

The fractionation of dextran has been shown to be effected by the normal range of operating parameters such as pressure, recirculation rate and temperature, but also by such factors as the molecular weight average M_w of the dextran, the pH and ionic strength.

Using a range of dextran T fractions Baker [43] found that the rejection of dextran was dependent on the applied transmembrane pressure. As the transmembrane pressure increased he found that the rejection decreased. Interestingly this decrease was far more dramatic with the dextran solutions than either proteins or polyelectrolites. See figure 2.9.

Figure 2.9 Plot of Rejection Against Varying Operating Pressures for a Range of Dextran Samples (43)

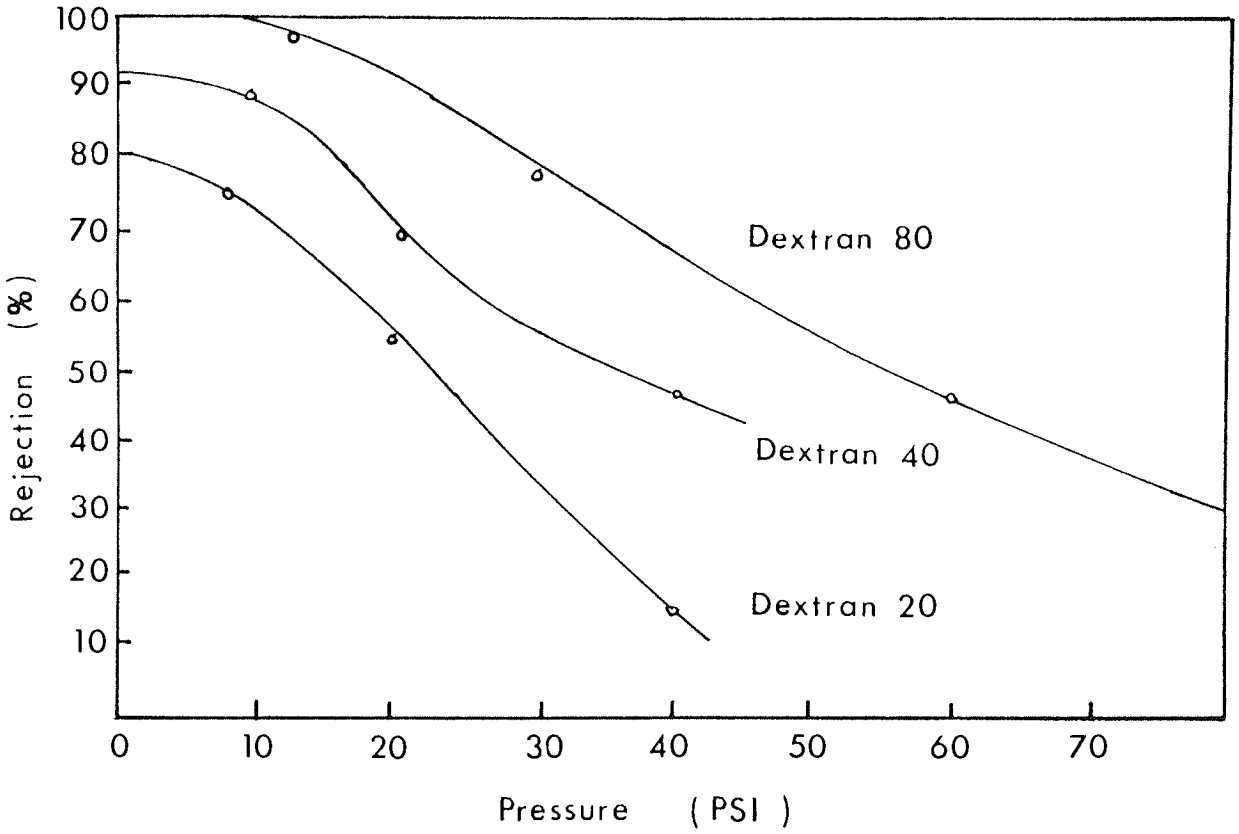

Both Bottino [44] and Baker [43] found that rejection of dextran was increased by increasing the recirculation rate. Baker postulated that this increase was a result of the lower dextran concentrations at the membrane wall. See figure 2.10

The flux was also found by Bottino [44] to be dependent on the recirculation rate; increasing the recirculation rate increased the flux. Bottino also showed that the flux became more sensitive to recirculation rate as the weight average M_W of the dextran sample used increased. He also found that dextrans with low M_W values gave higher fluxes than dextrans with high M_W values at the same concentration. See figure 2.11. He concluded that these effects were caused by the rejection of the high molecular weight material; this accumulated at the membranes surface and caused a higher degree of concentration polarization.

The retention of dextran is generally far lower than other materials such as proteins of the same molecular weight. Both Baker [43] and Bodzek [42] examined this phenomenon and concluded that this effect was probably due to the high stear forces present in ultrafiltration. These forces could deform the large dextran molecules and allow them to pass through small diameter pores.

While investigating the concentration of dextran solution Vlachogiannis [45] found that increasing the temperature increased the flux and allowed a higher concentration to be achieved but this also caused the rejection to decrease. At 20°C he found that only 1.8% of the material was lost but this increased to 13.6% at 40°C. Vlachogannis felt that this was caused by a higher dextran concentration at the membrane wall as a result of the higher flux.

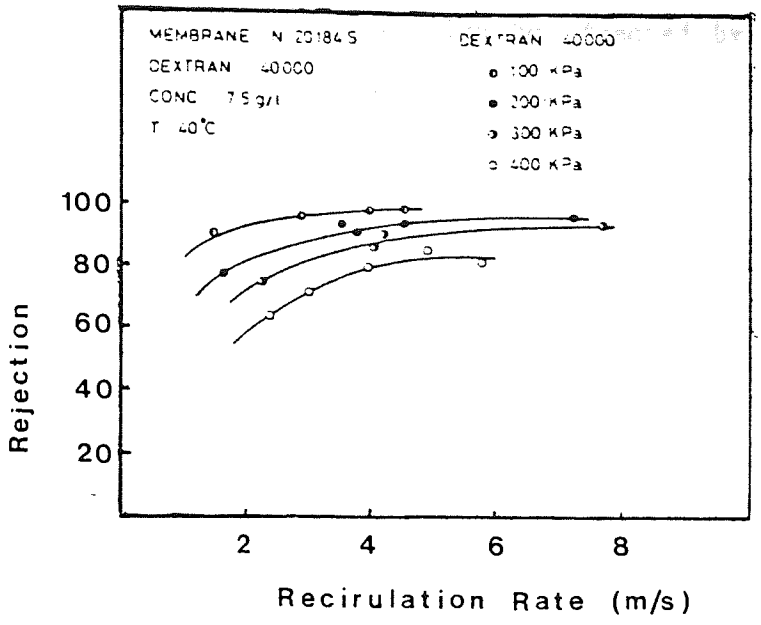

Figure 2.10 Influence of Recirculation Rate on the Membrane at Varying Operating Pressures (44)

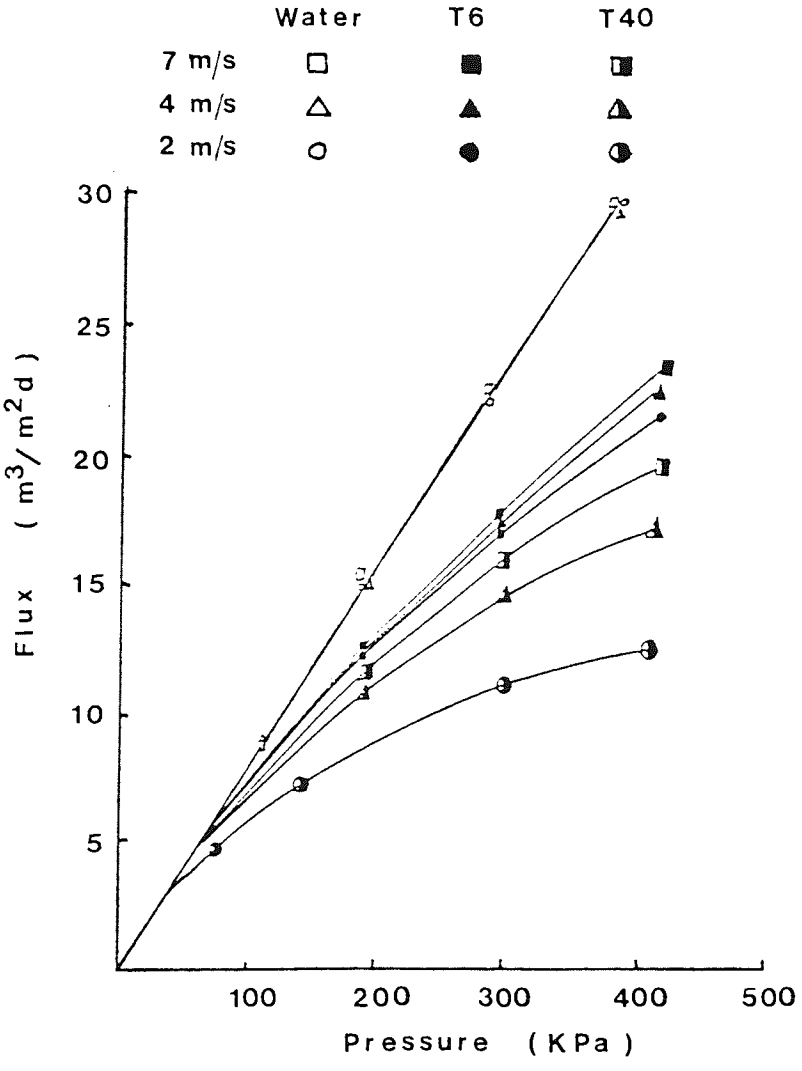

Figure 2.11 Effect of Recirulation Rate on Membrane Flux (44)

The ultrafiltration of dextran can also be affected by the ionic charge on the dextran molecules. Michaels [12] when examining the sieving curves for ionically charged dextran and neutral dextran found that the negatively charged macromolecules were sieved more effectively; while positively charged ones less effectively than neutral macromolecules. He concluded that this result was consistent with the existence of a negative charge on the membranes surface. Long [34] also found that blue dextran was adsorbed onto track eteched Nuclepore membranes while a T70 solution was not. He also found that the rejection of blue dextran was reduced when the ionic strength of the solution was increased. He concluded that this was caused by dextran adopting a more compact configuration at the higher ionic strength.

In his experiments Baker calculated the molecular weights of his samples from the intrinsic viscosity. Hence if he had a product of low viscosity he assumed it contained only low molecular weight material. However, the sample could contain high molecular weight material as well, the intrinsic viscosity would only measure the average molecular weight. Therefore this could not be used to characterize the rejection at a specific molecular weight of dextran. This problem was partly solved by Edberg [46] using the sedimentation equlibrium method of Van Hode and Baldwin. Using this technique Edberg was able to calculate both the weight average (M_W) and the number average (M_N) molecular weight, from the ratio of the two he was able to find the range of the distribution in his samples. Using a simple cascade system Edberg fractionated a dextran feed into several products of different weight average molecular weights and narrow range distribution. A similar system was also employed by Porter [47] to fractionate dextran, in both designs each of the three stages contained a membrane with a different molecular weight cut-off.

The problem of measuring actual molecular weights of dextran instead of averages was solved with the advent of gel permeation chromatography (GPC) as an analytical tool. Using GPC Cooper [48] was able to characterize membranes using dextrans of several molecular weight distributions (T fractions). He found that if the rejection coefficients were plotted against molecular weight on log probability paper, linear relationships were observed. This plot allowed the rejection (R), molecular weight (MW) relationship to be defined by two parameters, (a) the mean value of log MW at P = 0.5, and (b) the standard deviation, which is one half the difference in log MW at R = 0.84 and 0.16. Cooper found that the R-MW relationship was not independent of the polymer samples molecular weight distribution. While investigating the performance of a 10,000 MW cut-off membrane he found it to be less retentive at a given molecular weight for the higher M_W sample (40,000) than the lower M_W sample (10,000). However when the two polymer samples were mixed the R-MW relationship was very similar to that obtained with the lower M_W sample alone, see figure 2.12. This suggested that the presence of the lower molecular weight material was increasing the rejection of the higher molecular weight material. This effect was also found by Bottino [44] when investigating the ultrafiltration of PEG. To determine the effect of the low M_W sample on the rejection characteristics of a high M_W sample Bottino mixed a sample of PEG of 35,000 M_W with a sample of 3000 M_W. He found that even in small quantities the low M_W material increased the rejection coefficient of the mixture above that of the pure 35,000 M_W sample.

All the work mentioned above is concerned with either using dextran to characterize membranes or showing that membranes can be used to separate dextran into products of differing M_W. However work done by Barker and Vlachogiannis [5] and Poland and Barker [6] has shown that ultrafiltration could be used to fractionate dextran on a commercial

Figure 2.12 Effect of Molecular Weight and its Distribution on the Determination of Rejection - Molecular Weight Relationships (48)

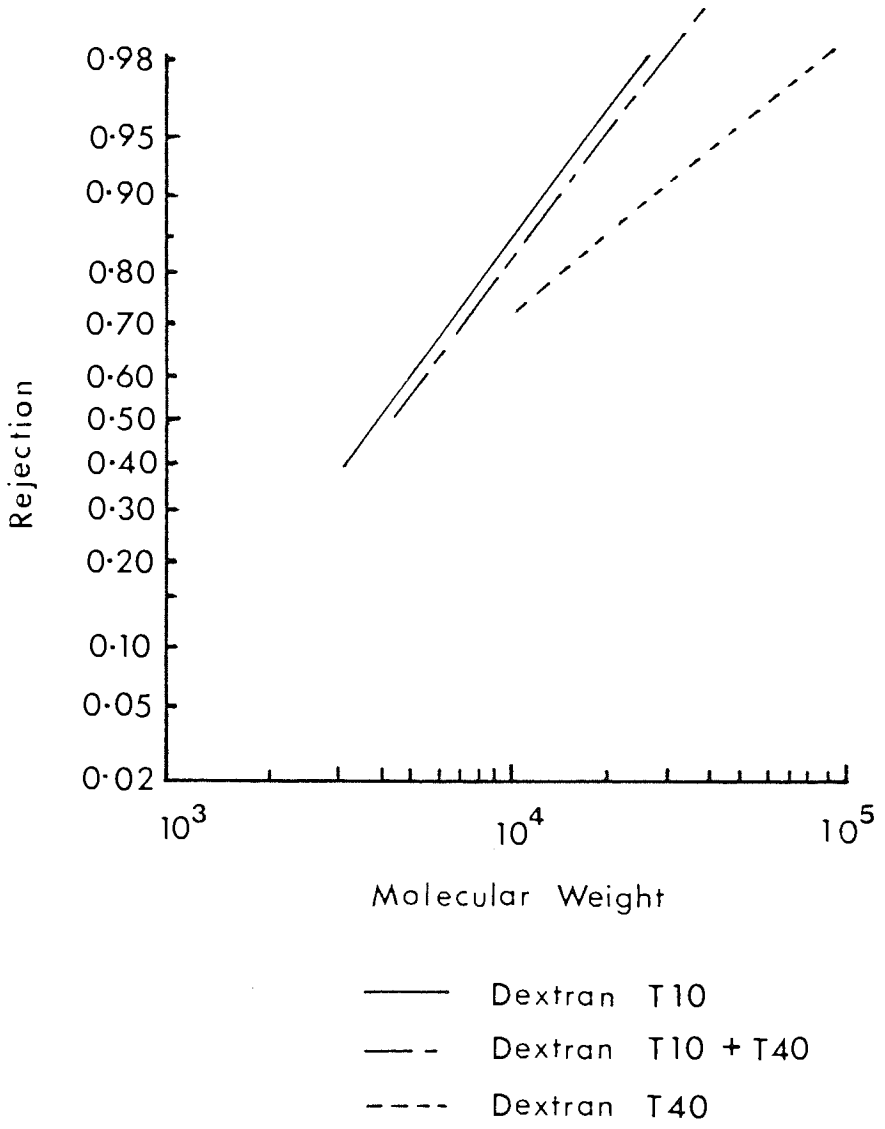

basis. This work was concerned with the removal of dextran of 12000 MW and less, from an industrial hydrolysate with a wide molecular weight range. Both Vlachogiannis and Poland found that a 5000 MW cut-off membrane used in the diafiltration mode of operation could be used to remove the low molecular weight material. Unfortunately they found that when they used the diafiltration mode, molecules as large as 70,000 MW could be readily 'washed' through the membrane, this resulted in a significant loss of the 'saleable' 12,000 MW to 98,000 MW band. Both workers were however able to show that ultrafiltration could be used to fractionate the hydrolysate to a clinical standard. Baker and Vlachogiannis also showed that dextran solutions could be easily concentrated from low concentrations (1%) to high concentrations (20%) using either a 5000 MW or 2000 MW cut-off membrane.

Poland and Barker developed a practical diafiltration cascade, from a design proposed by Cooper [49] to enhance the retention of the 12,000 MW to 98,000 MW band when removing the dextran below 12,000 MW. They found that the cascade improved the retention of this band by 10% and also aided the removal of the low molecular weight material.

2.7 ULTRAFILTRATION CASCADE SYSTEMS

Ultrafiltration is generally regarded as a method of purifying one component by the removal of a second. Normally the material to be purified has a molecular weight far greater than the nominal molecular weight cut-off of the membrane and hence can be assumed to be 100% rejected, while the impurity is able to pass freely through the membrane. Under these ideal conditions a batch process would be satisfactory, however in many processes the molecular weights of the two components are similar, so it may be impossible to remove the impurity

without incurring excessive loss of the material to be purified. To aid the separation of the two components a cascade process can be employed. A cascade process is a system where, by means of permeate and retentate recycling a purity and efficiency greater than the batch system can be obtained. There are several different designs of cascade which can be classified by their mode of operation; the two main groups are those using concentration and diafiltration, however a dialysis cascade has also been proposed.

Both Baker [50] and Porter [47] developed simple concentration cascade systems. Using a three stage system Baker fractionated both PVP and dextran into different M_W products. The system was designed to remove the high and low molecular weight fractions from a polymeric product. The first two stages were responsible for the removal of the high molecular weight material. Any high molecular material not retained by stage one was recaptured in the second stage. The permeate from stage two which contained the middle and low molecular weight material was then used as feed for the third stage. The third stage consisted of four cells each containing identical membranes. These membranes where chosen to allow only the passage of the low molecular weight material hence the final middle molecular weight product was obtained as the retentate product from this stage. By choosing the correct number of stages any medium molecular weight purity could be obtained. See figure 2.13.

The system proposed by Porter consisted of a very similar design, however each stage contained a membrane of differing molecular weight cut-off allowing the removal of different molecular weight fractions from each stage.

The development of the true concentration cascade has close links with the gaseous diffusion cascade used during the second world war for the separation of uranium isotopes. This design of cascade can be split

into two sections, an enriching section and a stripping section with the feed inlet between the two. The required product is removed from the 'top' of the cascade stage N and the unwanted waste product from stage one. See figure 2.14. This type of cascade can be used for the separation of two or more components. It is usual for the membranes used in each stage to be identical unlike the other forms of cascade mentioned earlier.

The fractionation within the cascade occurs in the following manner. The initial separation of the components occurs in the feed stage. The component to be removed and the lost product leaves the stage as permeate and passes into the stripping section. Within the stripping section the lost product is recovered and recycled back into the feed stage. By careful selection of the number of stages within the stripping section it is theoretically possible to obtain any degree of recovery of the product.

The retentate product from the feed stage enters the enriching section where the contamination is removed, naturally with some loss of the desired product. Therefore the permeates in this section are recycled back down the cascade to recover the lost product. As with the stripping section the number of stages can be chosen to give the required purity.

The key operating parameters affecting this type of cascade are the number of stages used, the position of the feed point, the difference between the rejection coefficients of the components and the ratio of permeate and retentate products. Several workers have considered these factors on an theoretical basis. Tutunjian and Reti [51] developed a model of a five stage cascade unit by solving a series of mass balances over the whole cascade and each individual stage. Several assumptions were made to simplify the problem, firstly the flow of material through

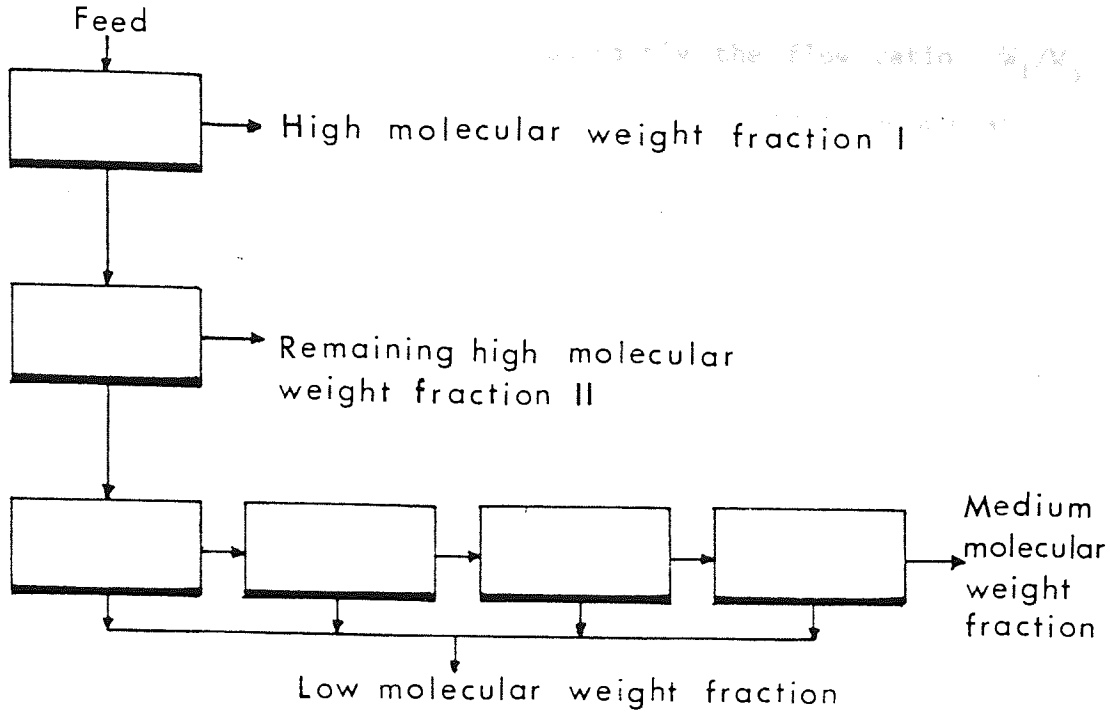

Figure 2.13 Concentration Cascade Used by Baker (50) for the Fractionation of Dextran

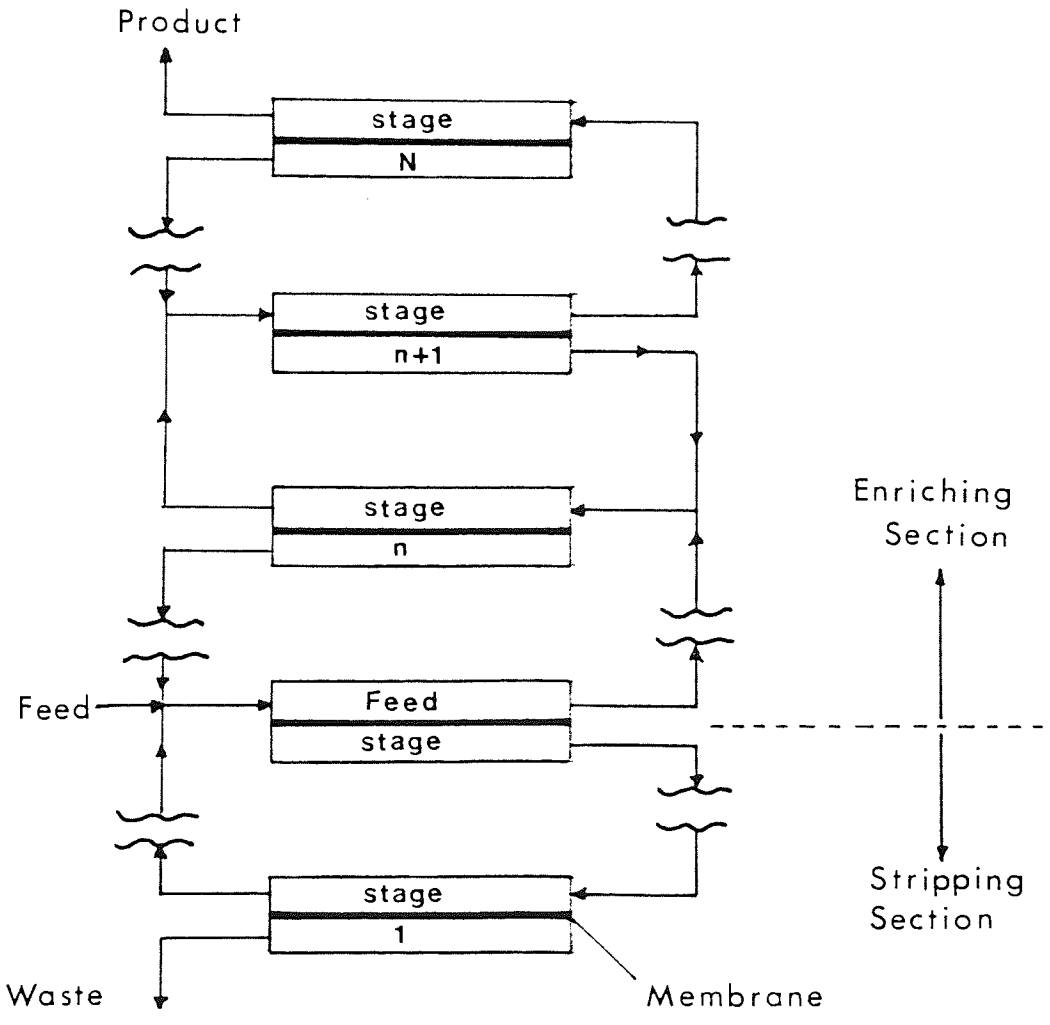

Figure 2.14 Concentration Cascade Used for the Separation of Uranium Isotopes

each stage was plug flow and more importantly the flow ratio W_i/W_o which was defined as the ratio of flow at the inlet to retentate at the outlet, was identical in all the stages.

A summary of their results is given graphically in figures 2.15 to 2.18. In these figures the passage (P) is the fractional passage of the component through the membrane, ie, (1-R). The flow ratio defined earlier is W_i/W_o, N the number of stage and F the feed stage. Using these graphs the relative separation of a two component system can be considered. Starting with a feed containing equal concentrations of A and B which have a passage of 0.7 and 0.3 (rejection of 0.3 and 0.7), a feed point at stage three and a flow ratio of 6 the fraction of each solute in the permeate can be read directly from figure 2.15.

Cascade

Permeate A = 0.94 (78% purity)

B = 0.26

Single Stage

Permeate A = 0.71 (63% purity)

B = 0.42

Cascade

Retentate A = 0.06

B = 0.74 (93% purity)

Single Stage

Retentate A = 0.29

B = 0.58 (67% purity)

changing the flow ratio on the cascade to 3 gave:-

Permeate A = 0.61 (92% purity)

B = 0.05

Retentate A = 0.39

B = 0.95 (71% purity)

Tutunjian concluded that reducing the flow ratio increased the purity of the permeate stream but the recovery of the main component (A) was reduced. This effect can be seen clearly in figure 2.16, as the flow rate decreases the fraction of any component in the permeate decreases. Increases the flow ratio will have the same effect on the retentate stream.

The dependence of the separation on the number of stages is shown in figure 2.17. As the number of stages is increased the relative separation is increased; this is shown graphically by the increase in the slope of the lines. Tutunjian also found that moving the feed point away from the permeate product stage has the same effect as decreasing the flow ratio, ie. decreasing the fraction of any component in the permeate product.

Using a similar approach Ward [52] developed a model for a three stage cascade which he tested by using an experimental cascade. Using glucose and S-ovalbumin he demonstrated that the cascade gave a higher separation and extraction than could be obtained using a single ultrafilter. However the separation obtained was generally less than those predicted by the model. Ward attributed this to the models inability to adequately predict the effect of concentration polarization.

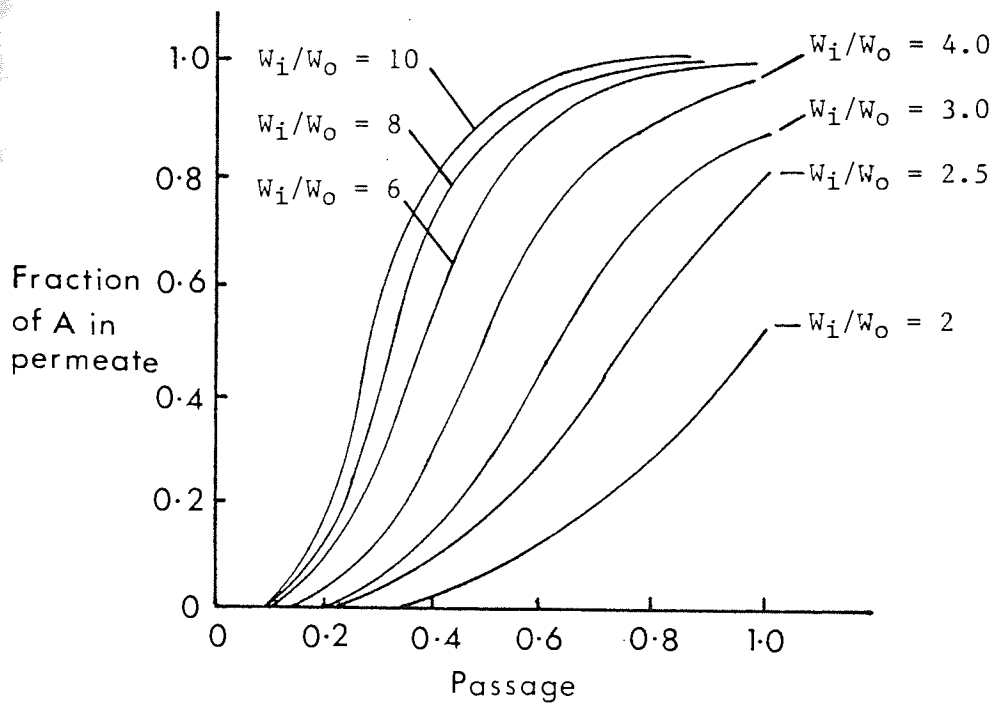

Figure 2.15 Permeate Product as a Function of Passage

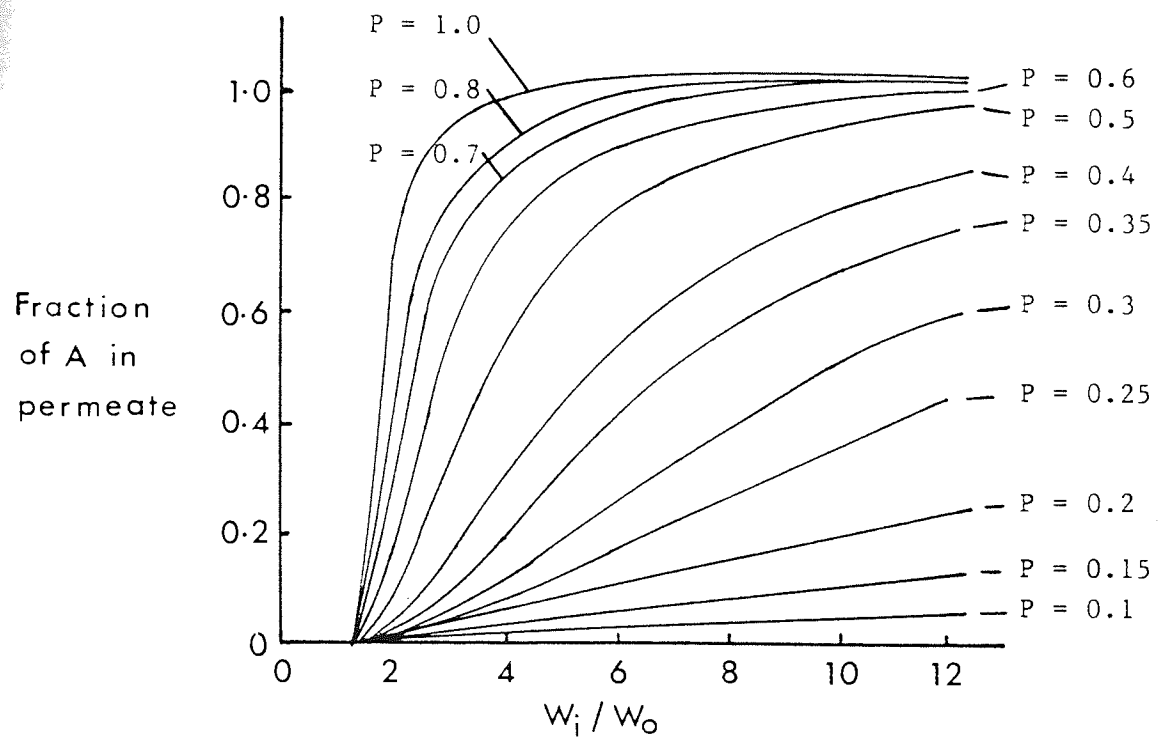

Figure 2.16 Permeate Product as a Function of Flow Ratio

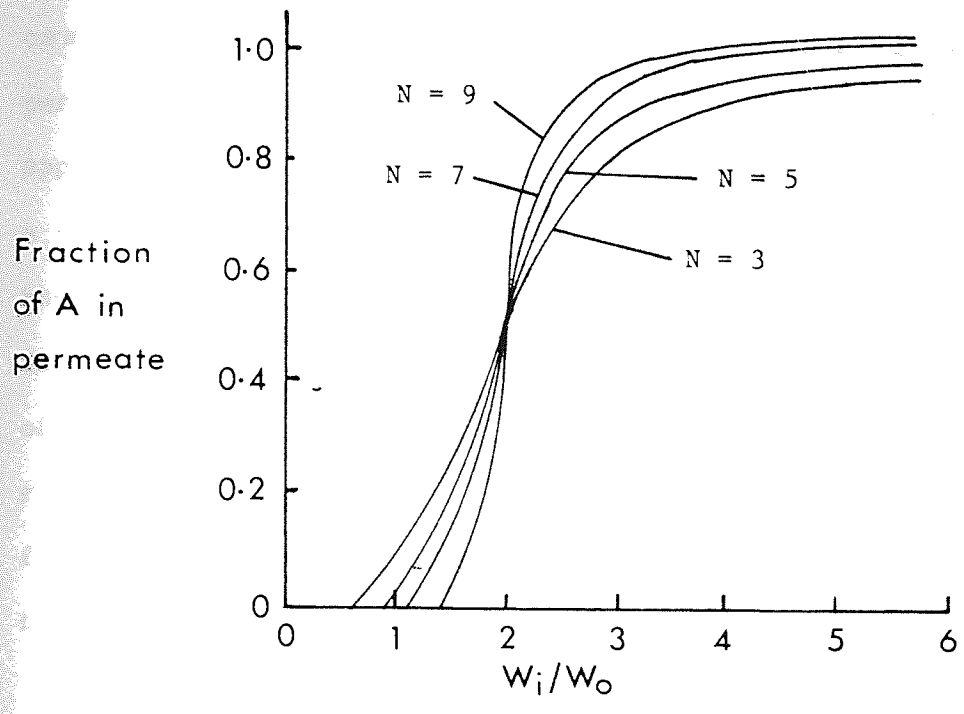

Figure 2.17 Permeate Product for Various Numbers of Stages

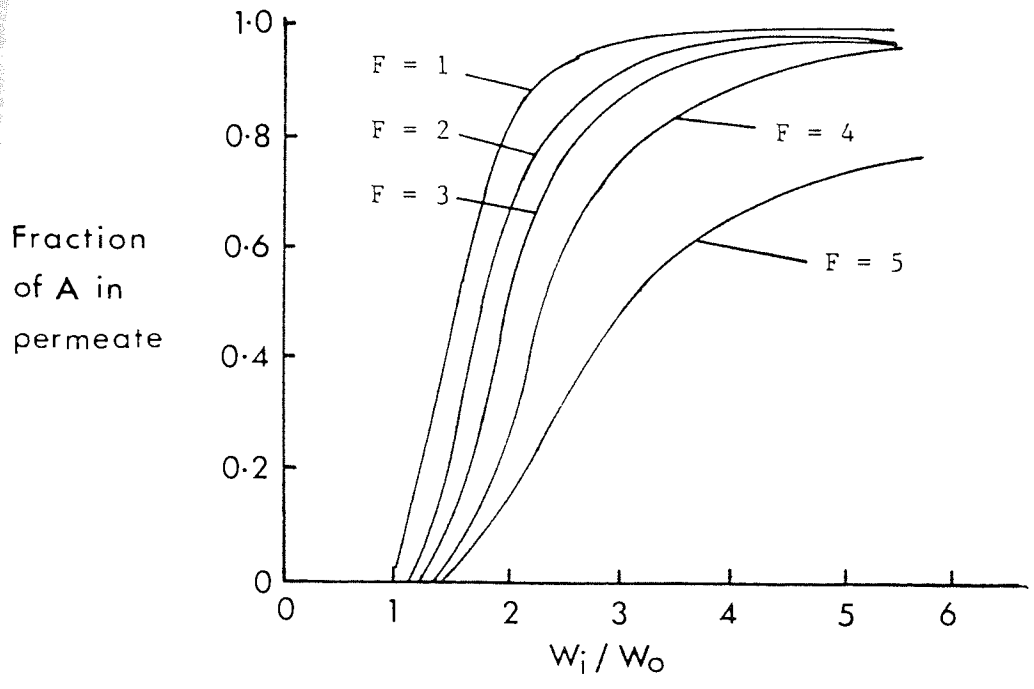

Figure 2.18 Permeate Product for Various Feed Stages

Another novel cascade system was considered by Mitrovic [53]. The cascade which was developed for use with reverse osmosis or pervaporation membranes consists of dual cells with two membranes of opposite perm-selective characteristics which were treated as stages of a separation battery. Mitrovic used McCabe-Thiele techniques to define the optimum number of stages and reflux ratios for both the dual cell cascade and the single cell cascade mentioned above. For the separation of ethyl alcohol and p-xylene Mitrovic found that the dual cell system required fewer stages to obtain the same degree of separation, furthermore the energy consumption of the dual cell system was less then the single cell system.

Both Tutanjian and Ward simplified the mass balances required for their models by using a constant flow ratio for each cascade stage, and by considering a cascade with a maximum of five stages

In these cases numerical iteration methods such as the multi dimensional Newton-Raphson method can be used. The solution of these equations has been investigated by many workers [54-56].

The purification of a solute using diafiltration normally produces large volumes of waste solvent, on an industrial scale and this would result in storage, pumping and effluent problems. To reduce the amount of dialysate (wash solvent) required Porter and Michaels [47] proposed a three stage cascade system. See figure 2.19. The fresh dialysate enters into the third stage and the permeate from this stage is recycled back to stage two and used as dialysate for this stage, similarly the permeate from stage two is used as dialysate in stage one. Using this system one volume of dialysate was used where the batch process would have required three.

Figure 2.19 Continuous Counter-Current Diafiltration Cascade (47)

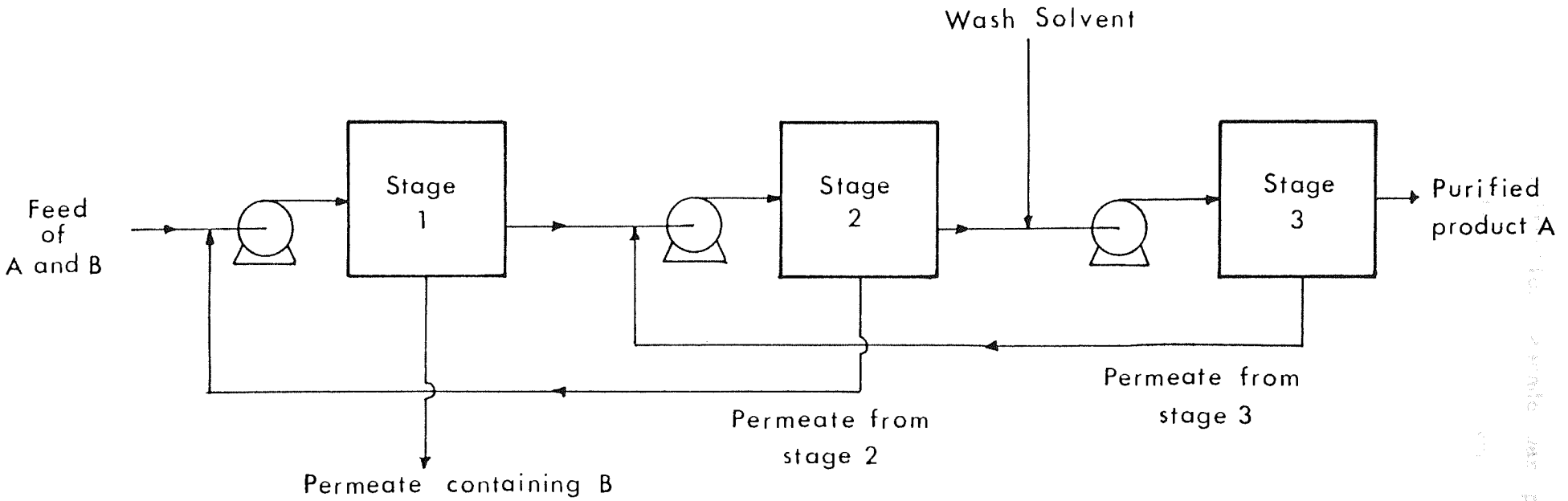

A further example of the diafiltration cascade was proposed by Cooper [49] as a method of reducing the amount of solvent used during the purification of polymeric dyes. See figure 2.20. The system operated in the same manner as the cascade system proposed by Porter but the final permeate product was sent to a solvent recovery stage. Cooper developed a model for the system by solving a series of mass balances over the cascade. Using this model Cooper was able to obtain a relationship which showed how the number of stages (K) and rejection coefficient (σ) of the impurity would effect the purity of the final product. For simplicity Cooper combined the rejection (σ) and the number of diavolumes used (N) as a single expression $Z = (1 - \sigma)N$. The results of this analysis can be found in figure 2.21 and 2.22. Cooper found that for increasing values of K and Z the value of ψ increased non linearly at low values of Z and linearly at higher values of Z.

To confirm the benefits of the cascade Cooper compared the operating costs of the batch and cascade systems. The main processing costs such as solvent price, fractional loss of solvent in the solvent recovery stage and individual membrane life were assumed to be identical in both the cascade and batch systems. Cooper was able to show that the cascade had a significant economic advantage over the batch system especially when the solvent costs were high.

The practical application of the diafiltration cascade system was considered by Poland [6]. Using a computer controlled four stage cascade Poland investigated the fractionation of a dextran polymer. He was able to show that below the nominal cut-off of the membranes he used the amount to dextran removed was significantly improved, while above this value the retention of the dextran was increased. For all his experiments Poland used 5000 MW cut-off hollow fibre membranes obtained from Amicon.

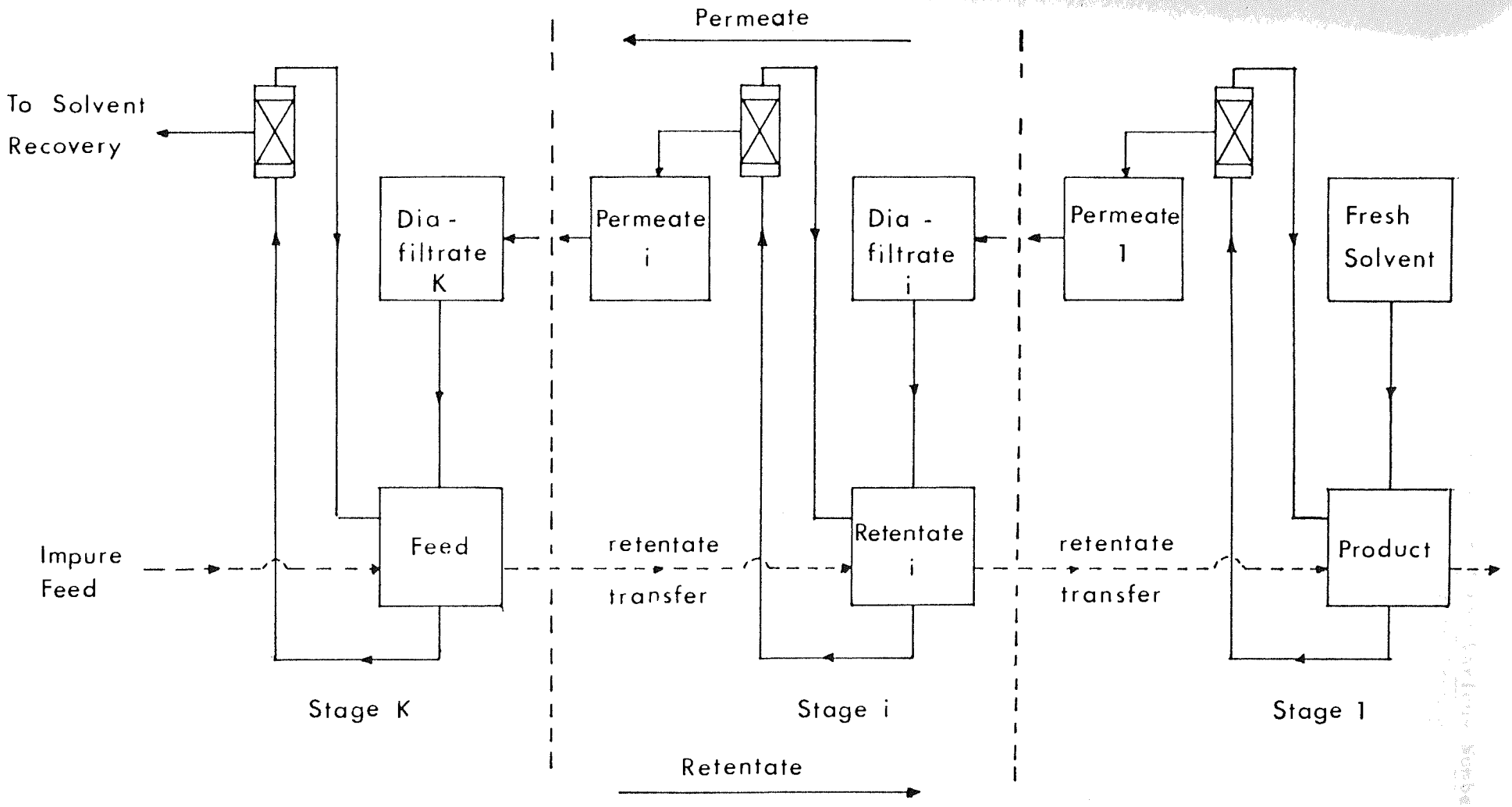

Figure 2.20 Schematic Diagram of Diafiltration Cascade Proposed by Cooper (49)

Figure 2.21 Effect of High Values of Z for Various Numbers of Stages (K) on Product Purity from a Diafiltration Cascade

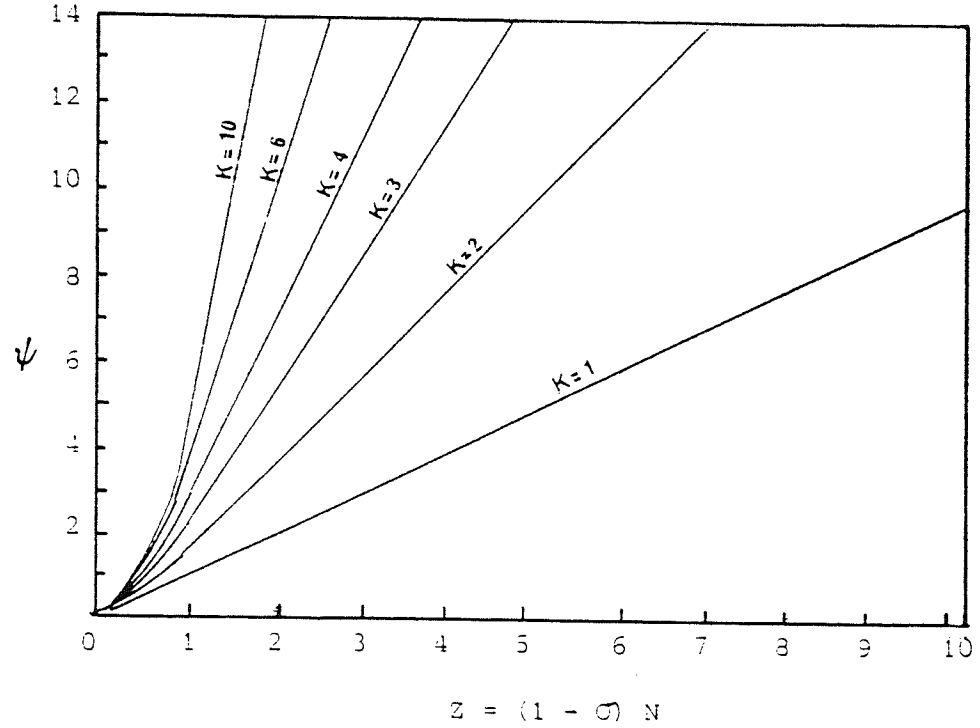

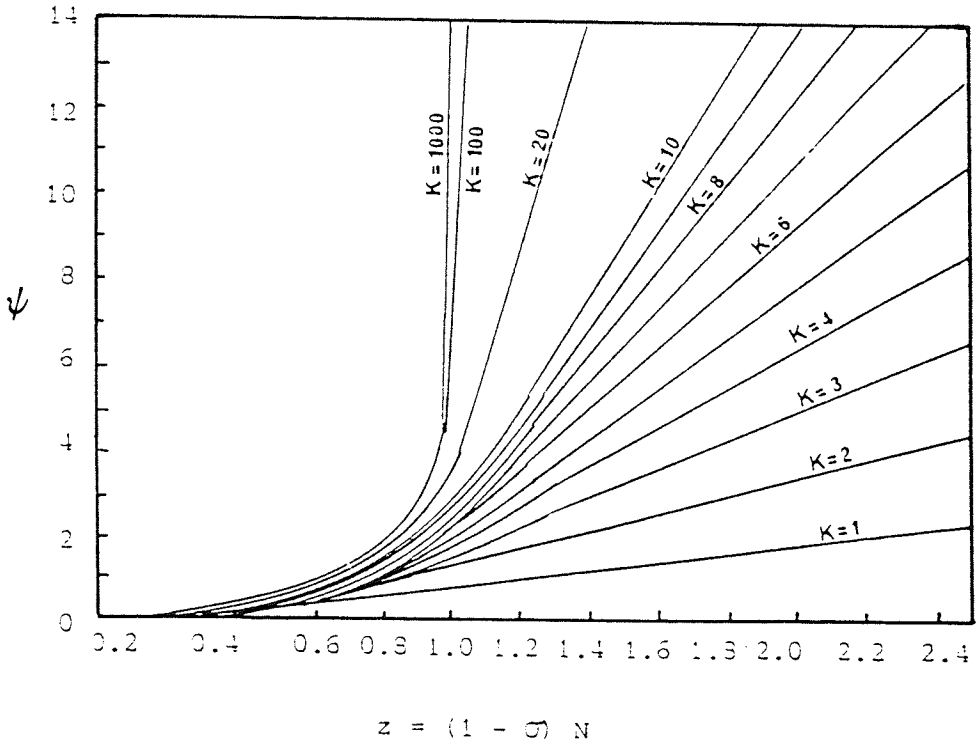

Figure 2.22 Effect of Low Values of Z for Various Numbers of Stages (K) on Product Purity from a Diafiltration Cascade

The development of a dialysis cascade was considered theoretically by Noda and Gryte [57]. They were able to show that a simple countercurrent cascade of dialysers was not able to increase the selectivity of the dialysis unit. However by combining the dialysis units with a series of non-selective concentrators the solute selection could be increased. These concentrators could either be reverse osmosis, distillation or evaporation units.

An schematic diagram of the system is given in figure 2.23. The rectifying section above the feed point has N stages and the section below the feed point has M stages. Each stage corresponds to a concentration-dialyzer pair. The top stream has a molar flow rate of Vm and is divided into the top product stream and the reflux stream. The ratio of the reflux molar flow rate to the overhead product molar flow rate Vd is the rectifying reflux ratio r. The bottom stream Um is also divided into the reflux stream and the bottom product stream. The ratio of the reflux molar flow rate to the bottom product molar flow rate Ub, is the stripping section reflux ratio S. F and G are the molar flow rates of the solute in the feed. This design of counter current cascade can be found in many other separation processes for example gaseous diffusion and in a similar form for reverse osmosis.

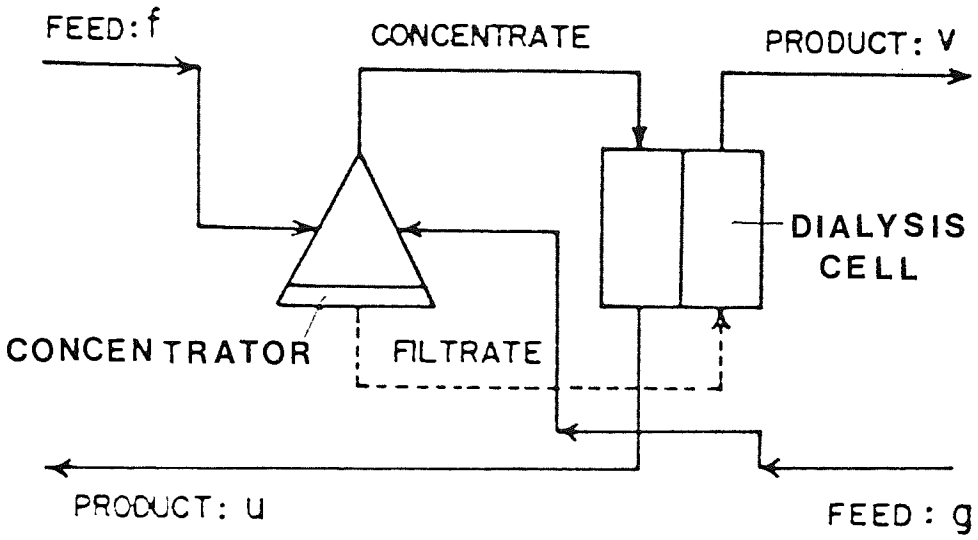

A concentrator dialyzer pair (CDP)

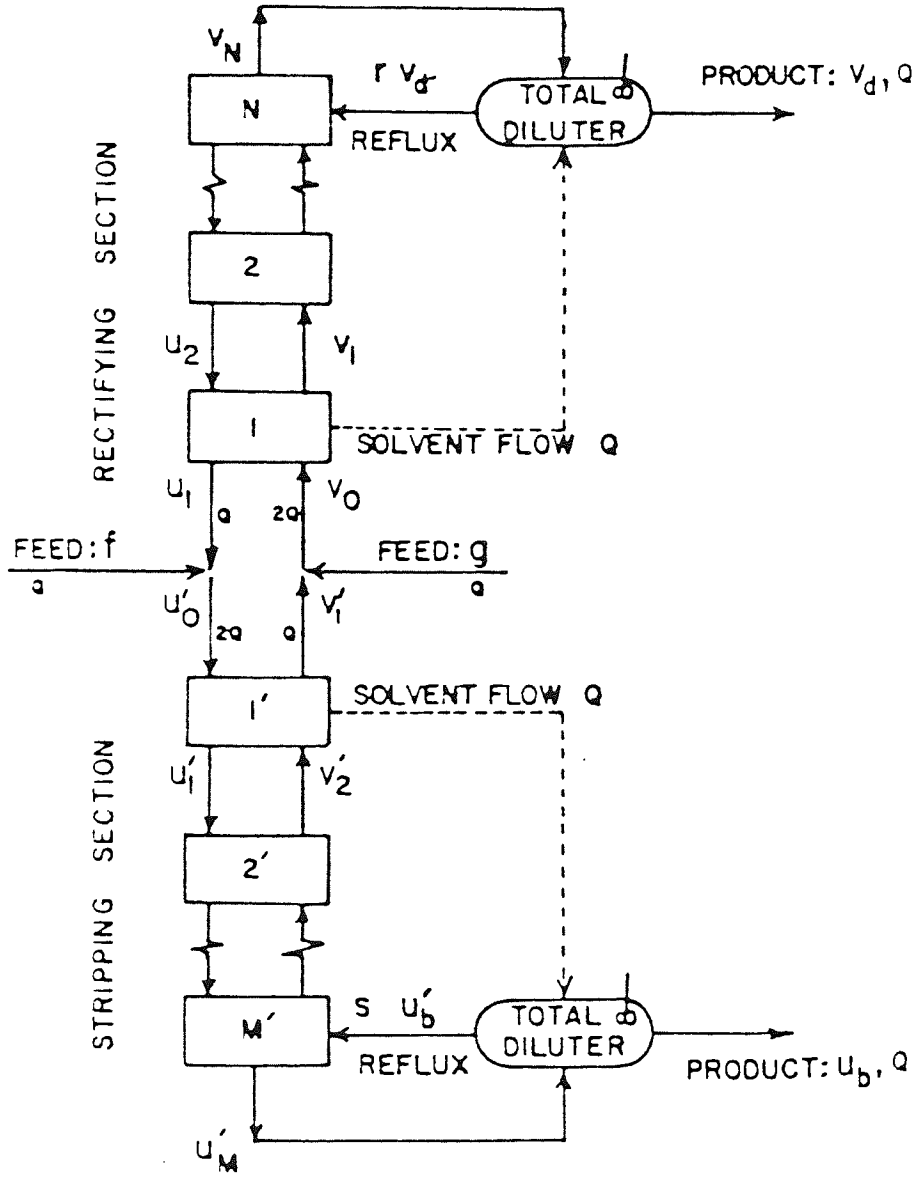

Figure 2.23 A Counter-Current Dialysis Cascade where each Stage Corresponds to a CDP

3.0 THE IMMOBILIZATION OF ENZYMES WITHIN ULTRAFILTRATION SYSTEMS

3.0 IMMOBILIZATION OF ENZYMES WITHIN ULTRAFILTRATION SYSTEMS

3.1 INTRODUCTION

The immobilization of biocatalysts using ultrafiltration membranes was first reported by Blatt [58] in 1968. This was followed by a rapid expansion of research as membranes improved and became more varied.

The underlying principle in any form of ultrafiltration bioreactor system is the use of a membrane which is retentive to biocatalyst but will freely pass the products of the reaction. It is convenient to separate the wide variety of membrane reactors into two basic groups, those which retain the biocatalyst distributed in the retentate stream and those which retain the biocatalyst within the membrane structure. At present the most widely used bioreactor system is the former of the two.

3.2 BIOREACTORS WITH DISPERSED BIOCATALYSTS

One of the simplest forms of enzyme reactor is the enzyme CSTR/UF reactor. See figure 3.1. The system typically consists of a reaction vessel connected to a ultrafiltration module. Solution from the reaction vessel containing the substrate, product and biocatalyst is continuously pumped through the membrane module. Ideally the membrane should be selected to allow only the passage of the product molecules, therefore at steady state a continuous flow of product leaves in the permeate stream and the unreacted substrate and enzyme is returned to the reaction vessel. Fresh substrate is added to the reaction vessel to maintain the level of substrate. Although this is a very simple approach, this system is the only type of enzyme reactor known to be

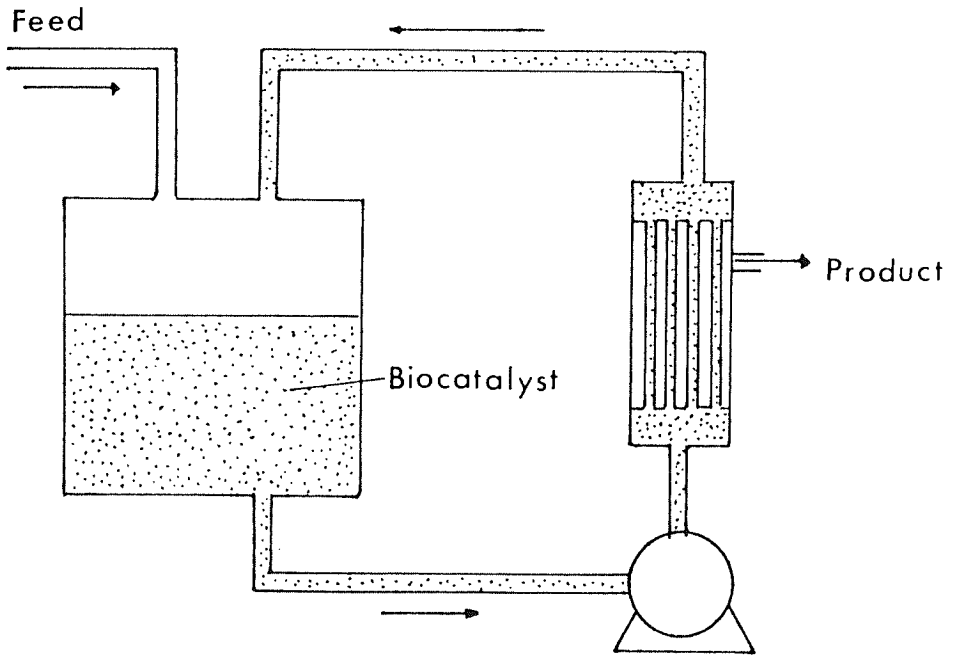

Figure 3.1 A CSTR/Ultrafiltration Reactor

used on a commercial basis. A number of nutritionally important amino acids are now either being synthesized or optically resolved on an industrial scale in both Japan and Germany via CSTR/UF enzymic reactors (59, 60).

The necessity of using a CSTR/UF bioreactor where the biocatalyst is present in a great volume of water would appear to be totally unnecessary since the compartments in the membrane unit, (ie. in a hollow fibre cartridge) can serve to contain the biocatalyst. Hollow fibre cartridges have been found to be particularly suitable for containing biocatalysts since they have a high surface area to volume ratio, the membrane is self-supporting and can be backflushed without the membrane separating from its support.

Two approaches can be used, the biocatalyst can be contained in either the shell side or tube side of the hollow fibre cartridge. See figure 3.2 and 3.3. The entrapment of the biocatalyst in the lumen of the hollow fibres was first suggested by Rony [61, 62]. In the system used by Rony the movement of substrate and product into and out of the fibre was purely by diffusion. The substrate solution being constantly pumped through the shell side of hollow fibre cartridge. Kitano [63] used this type of reactor to entrap urease and uricase. He found that the half life of the entrapped urease was typically only 60-80% of the free enzyme, this was probably due to pH variations within the lumen of the fibres as a result of the chemical reactions involved, for example the production of ammonia by the urease. Furthermore the apparent Michaelis Menton constant obtained for this reactor was always larger than that of the free enzyme because the rate determining step was the diffusion of the substrate across the membrane.

Figure 3.2 Hollow Fibre Enzyme Reactor with Enzyme Located Inside the Fibres (61)

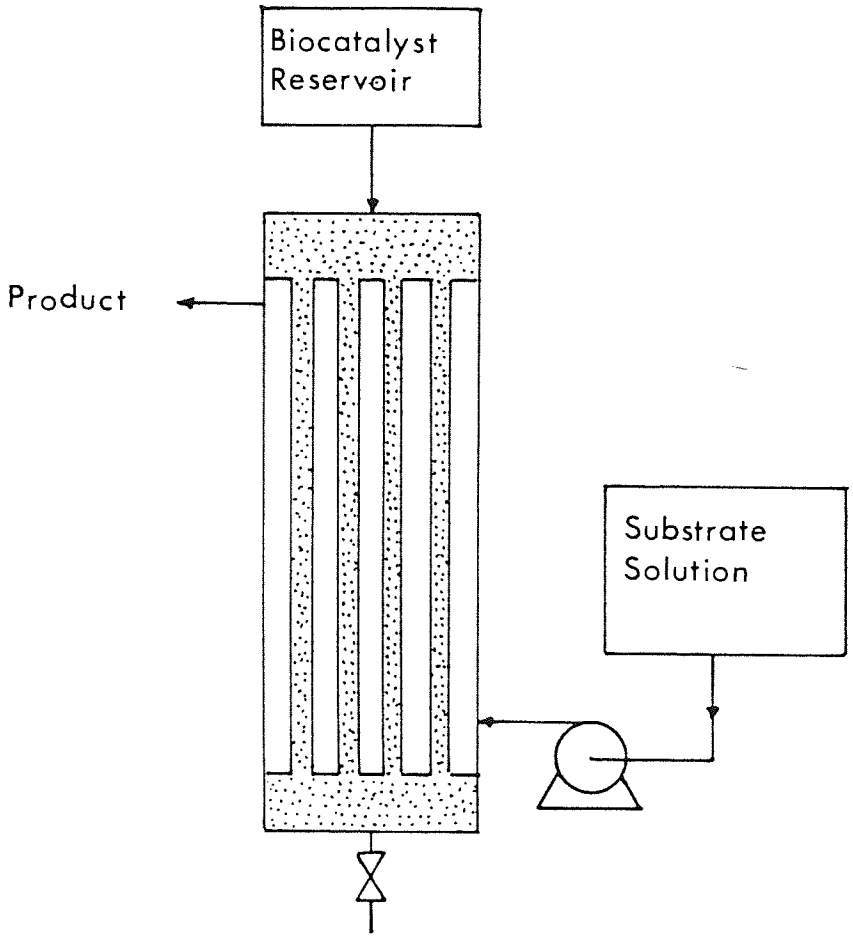

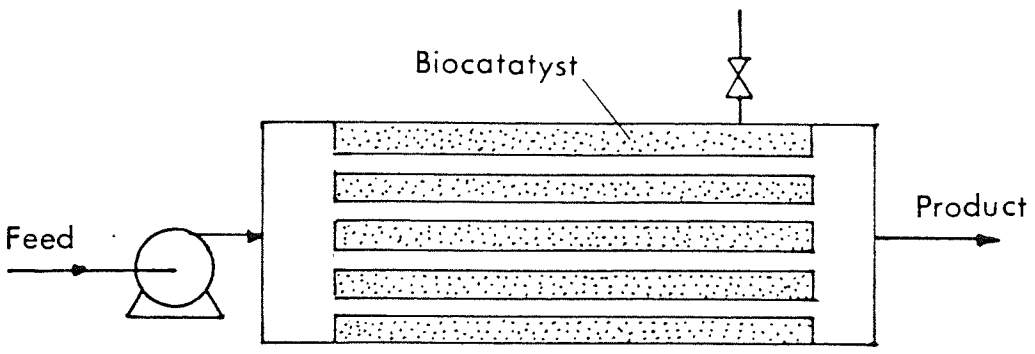

Figure 3.3 Hollow Fibre Enzyme Reactor with the Enzyme Located in the Shell Side

Simple mathematical models and experiments [64] have indicated that it is adventageous for most applications to have the biocatalyst solution sealed in the shell side and the substrate flowing through the fibres. There are many examples of this form of reactor [65, 66, 67] involving enzymes such as B-glucosidase, alkaline phosphatase and whole cells (for the production of urocanic acid). In the simplest form of this reactor the substrate and products move through the membrane by diffusion only [66, 67], however it is also possible to use a pressure driving force to aid the transfer of substrate and product. The operating procedure is simple, the process stream flows through the lumen of the fibres, if for example an inlet pressure of 25 psi and outlet pressure of 10 psi is used the sealed shell will equilibrate at a pressure which is essentially equal to the average of the inlet and outlet pressures, ie. 17.5 psi. Therefore when the reactor is operated the pressure at the beginning of the hollow fibres is greater than that in the shell side and hence permeate flows from the inside of fibre to the cartridge shell. Similarly at the opposite end of the cartridge a zone would exist where the pressure within the fibre would be less than that in the shell side and hence permeate flow would occur back from the shell side into the fibres. See figure 3.4. Klei and Sundstrom [65] used this type of reactor for the production of sugars from cellobiose. In this example the cellobiose solution was pumped from a reservoir through a Romicon PM10 cartridge (10,000 MW cut-off), the unreacted cellobiose and reaction products were then returned to reservoir. The B-glucosidase enzyme was put into the shell side of the cartridge by either backflushing or by immobilizing the enzyme onto alumina powder and then pumping the alumina powder as a slurry into the shell side. The system used by Klei and Sundstrom also contained an enzyme reservoir connected to the membrane cartridge so that fresh enzyme could be introduced into the reactor. Since the B-glucosidase enzyme was .pn89

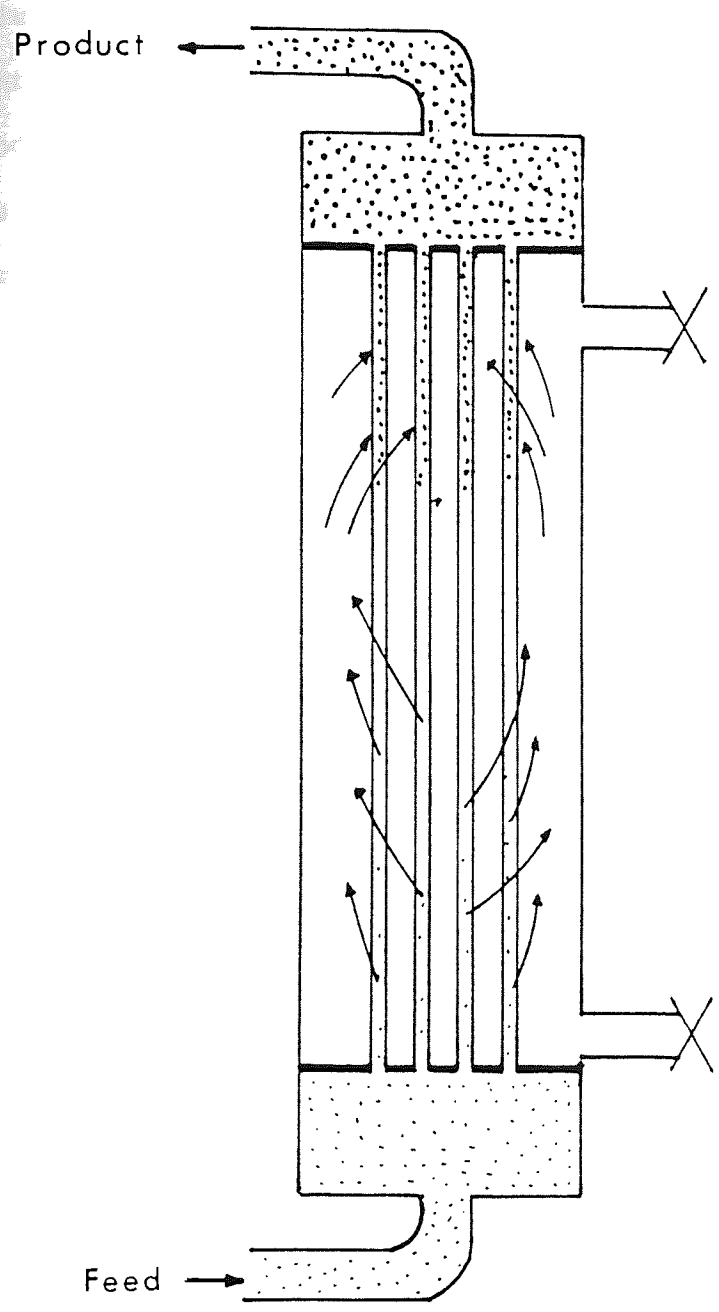

Figure 3.4 Shell Side Enzyme Immobilization with Convective Flow out from and Back into the Fibres

unstable and easily denatured this approach proved to be highly satisfactory. See figure 3.5. In another reactor scheme considered by Klei and Sundstrom a multi-enzyme system was used. See figure 3.6. The process tank contained a slurry of cellulose fibres suspended in a solution of cellulase enzyme. The slurry from the process tank was continually pumped through a hollow fibre cartridge so that the reaction products, the soluble low molecular weight sugars such as cellobiose would be removed in the permeate from this membrane. The permeate then passed to a second membrane which contained the immobilized B-glucosidase. The enzyme was retained in the shell side of this membrane. The glucose produced by this reaction was able to permeate into the fibre lumens and was returned back to the process tank.

This system is particularly interesting since two enzymes could be employed in one reactor without mixing the enzymes. Using this approach the total yield of sugars was increased and the cellulase enzyme requirements were significantly reduced.

In a design proposed by Michaels [68], enzymes or whole cells could be contained by sandwiching them between two membranes which were freely permeable to nutrients, cell products and metabolites. This system could be used in either a diffusion controlled mode or in a convection controlled mode as shown in figure 3.7. This system is really a simpler form of a hollow fibre reactor and can provide a compact and efficient bioreactor.

3.3 BIOREACTORS USING CHEMICAL AND PHYSICAL IMMOBILIZATION

In this group the biocatalyst is immobilized on or within the actual structure of the membrane, and so do not rely exclusively on the retenture nature of the membrane to contain the biocatalyst. This type

Figure 3.5 Shell Side Immobilization System Used by Klei and Sundstrom (65)

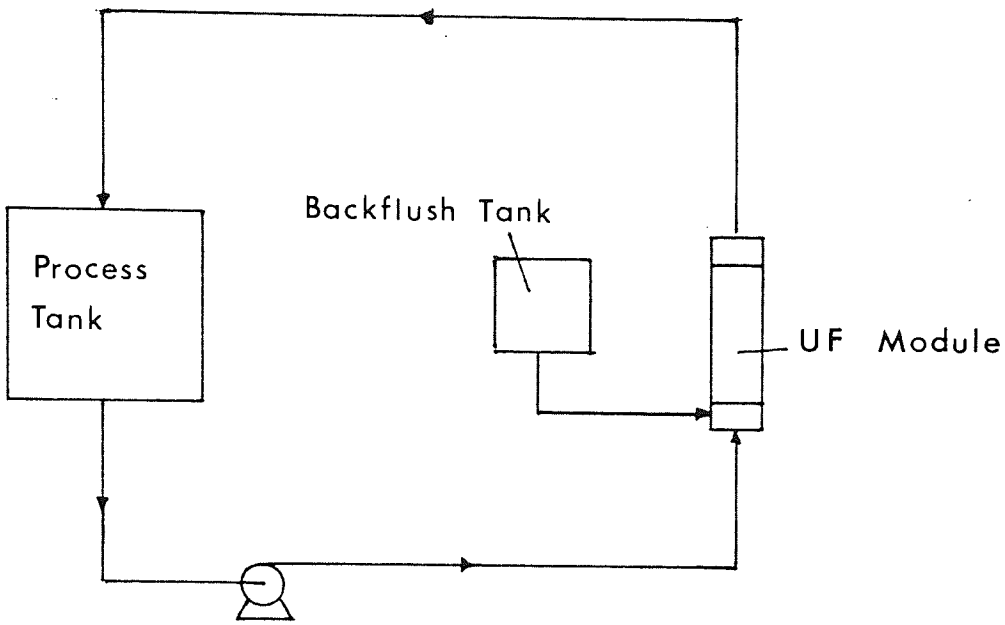

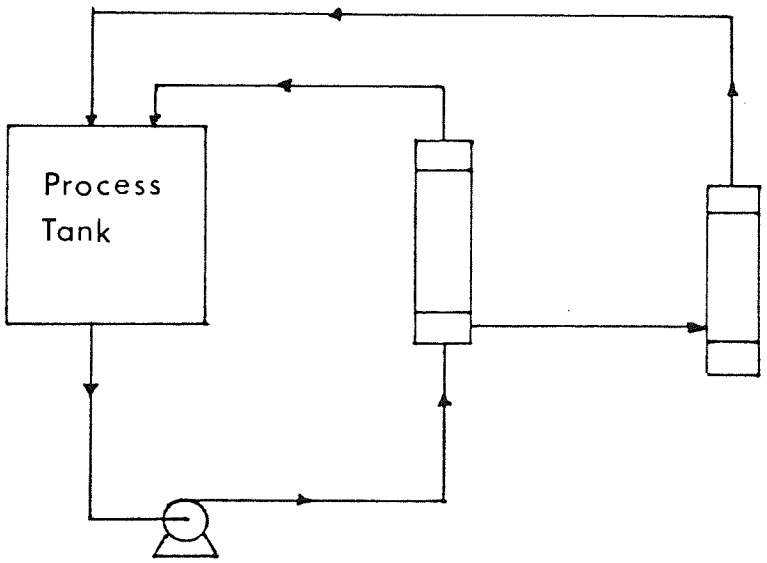

Figure 3.6 Immobilized Multi-Enzyme System Used by Klei and Sundstrom (65)

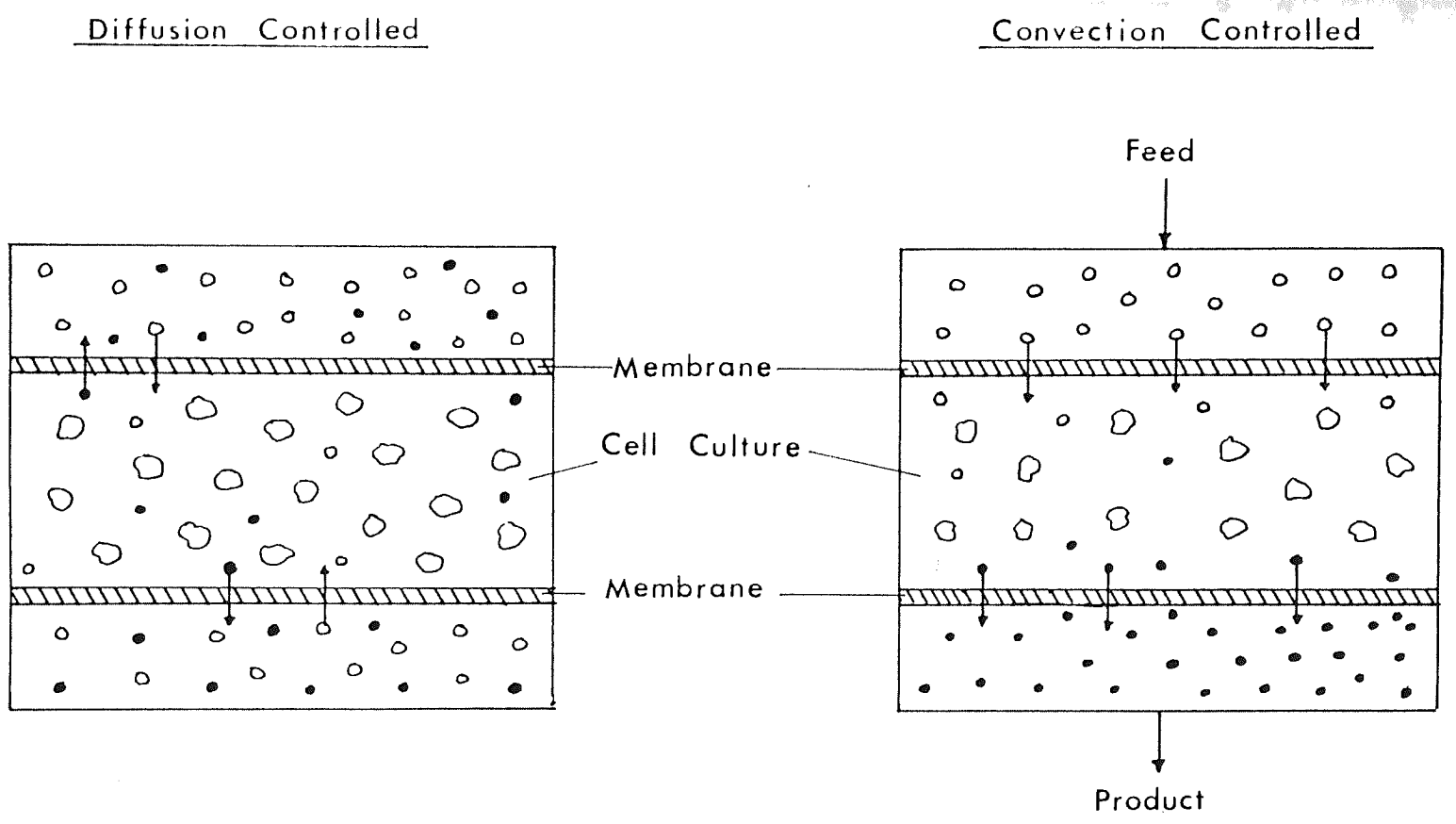

Figure 3.7 Immobilized Cell Bioreactor Proposed by Michaels (68)

of immobilization can be split into two subsections. That which involves physical immobilization such as the formation of gel layers and also for simplicity adsorption, and those which are immobilized by the action of a chemical coupling agent.

In the simplest forms of physical immobilization the biocatalyst can be adsorbed onto the porous substructure of the membrane. The adsorption of proteins onto membranes is normally considered a severe problem and has been linked to membrane fouling. The adsorption of proteins has been studied in some detail by using bovine serum albumin (BSA) labelled with iodine 125 [69]. It was found that when an ultrafiltration membrane was brought into contact with the BSA, even under conditions where there was no liquid permeation and minimal hydrostatic pressure, proteins would spontaneously adsorb onto the membrane. The amount of protein adsorbed was a function of several factors. The amount of BSA absorbed was firstly a function of time, with more BSA being adsorbed with longer contact time. Furthermore they found that the protein adsorption depended quite strongly on both the membrane material and the nominal molecular weight cut-off. In general, hyrophobic membranes and those with higher molecular weight cut-offs adsorbed the greatest quantities of protein. This first effect was probably due to the BSA having greater non-polar than polar characteristics and thus adsorbed more readily onto hydrophobic (non-polar) material. This is an important consideration when attempting to physically immobilize enzymes within the membrane structure. It was also observed that BSA (68,000 MW) was able to diffuse through the separating layers of a membrane with a nominal molecular cut-off as low as 10,000 MW. In addition there was in some cases sufficient transport through the membrane so that 80% of the adsorbed BSA was found in the porous support behind the membrane.

These experiments also demonstrated that the adsorption of protein onto the membrane caused a decrease in flux. This reduction was found to be as much as 50% in some cases. Naturally the smaller the membranes molecular weight cut-off the greater the effect. It was concluded that the reduction in flux was due to a combination of reduced flow area and pore blockage by the protein.

The practical application of this effect was considered by Korus [70]. Korus attempted to immobilize α-glactosidase and invertase within polysuphone hollow fibres. Two methods were used. In the first method the enzyme was added to the cartridge shell and allowed to stand overnight. The shell was then emptied of liquid. In the second method enzyme was pumped into the shell and permeate removed from the lumen to concentrate the enzyme in the porous support. Korus found that both enzymes could be immobilized with no detectable enzyme leakage and they had stabilities approaching the stability of the free enzyme. Naturally immobilization under pressure gave a higher enzyme loading. Korus also commented that immobilization within hollow fibre cartridges compared favourably with other methods of immobilization since this approach allowed easy enzyme loading, operation, cleaning and sterilization and also regeneration was relatively simple.

The main disadvantage of enzyme adsorption is that it is a dynamic process and under the right conditions the enzyme will be lost from the membrane structure. These systems are typically operated at low permeate flow rates to avoid the enzyme being washed out of the porous substructure, this often results in the reaction being diffusion controlled. This problem was found by Korus when using the invertase enzyme.

The backflush reactor system can be used to overcome some of the problems mentioned above. This approach is more applicable to hollow fibre membranes than flat membranes since there is less tendency for the membrane skin to separate from the porous support during operation. Once the biocatalyst has been loaded into the porous substructure of the membrane, by either simple adsorption or by forcing the biocatalyst into the substructure using pressure, the flow of substrate is directed through the shell side of the reactor so that the substrate permeates the porous substructure and the products of the reaction leave via the lumen of the fibre. This method allows a high permeate flow rate and reduces enzyme losses, see figure 3.8. The main disadvantage of this type of reactor is the low flux which can result if the biocatalyst blocks the channels in the porous support [71].

Another non-chemical method of biocatalyst immobilization makes use of the well-known effect of concentration polarization and gel layer formation. This aspect of immobilization has been investigated in great detail by Drioli, Catapano and others [72 - 75].

The effect of concentration polarization is generally considered to be caused by the accumulation of macromolecules at the membrane/solution interface. Owing to the low diffusion coefficients of most macromolecules the back diffusion is small and a concentration profile develops at the membrane surface. If the solubility limit of the solute is exceeded then the solute precipitates out as a gel layer on the membrane surface.

To immobilize the enzyme a solution of biocatalyst is completely ultrafiltered, or if this is not possible, until only a very small volume of liquid remains. Since the membrane is 100% retentive to the biocatalyst, the biocatalyst is left as a gel on the membrane surface. Once the immobilization has been completed the substrate solution can be added to the cell or the membrane can be stored for future use. This

Figure 3.8 An Immobilized Enzyme Backflush Reactor

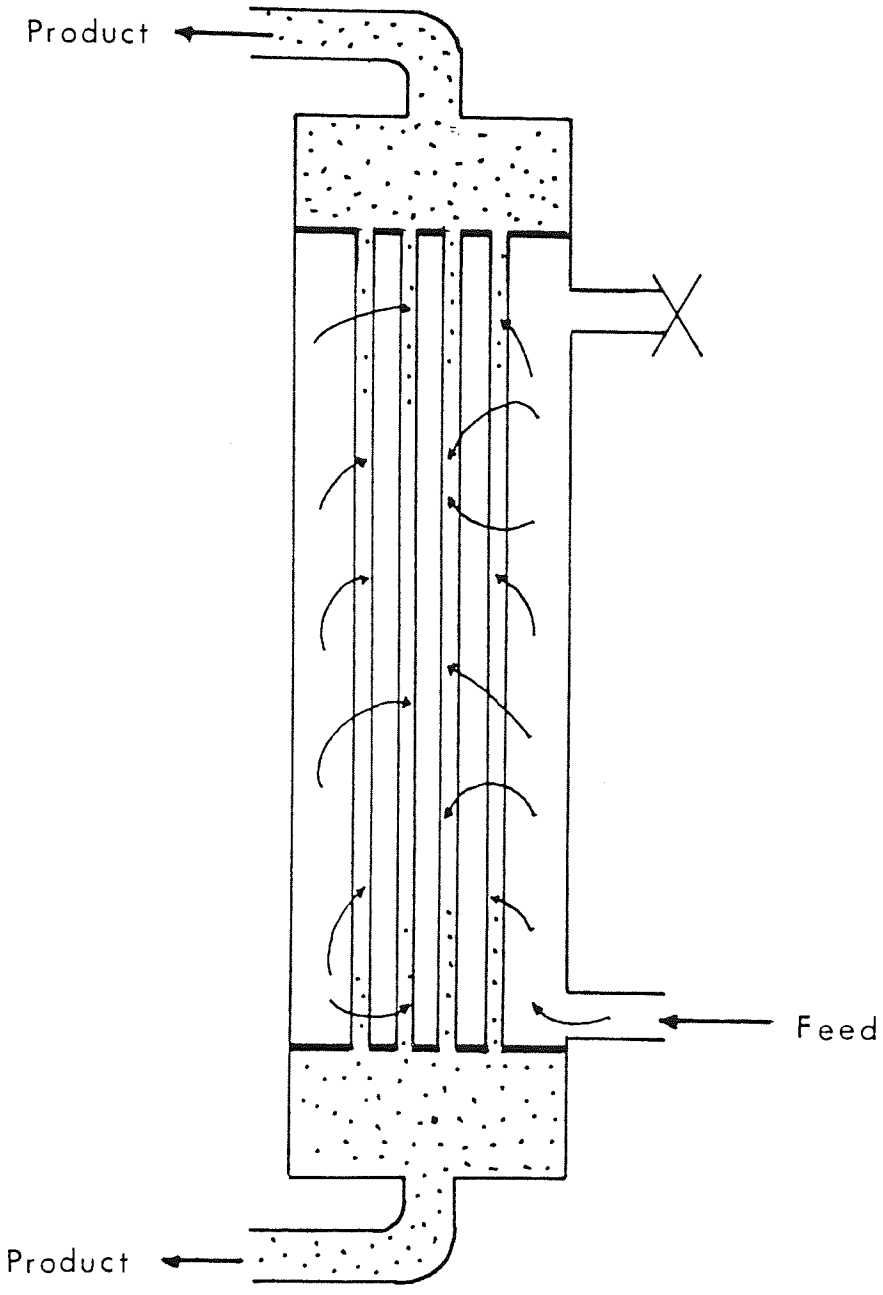

technique has been used for a wide range of enzymes including acid phosphatase [73], urease [72], B-glucosidase [72] and malic enzyme [74]. Generally it was found that the enzyme maintained its activity when immobilized. A further advantage of the immobilization was that reversible reactions could be considered irreversible if the rejection of the products was very low.

In most cases an unstirred system was used [72, 73] since turbulence at the membrane wall tended to cause the gel layer to break down. This was particularly noticable when malic enzyme was immobilized in a hollow fibre cartridge. At low flow rates a better conversion could be obtained but at higher flow rates the resultant shear stresses caused complete removal of the gel layer.

Using this technique multi-layer enzyme immobilization can also be achieved. Greco [76] immobilized acid phosphatase in two distinct layers on the surface of an ultrafiltration membrane. The immobilization was achieved by firstly applying a layer of enzyme using the techniques mentioned earlier, followed by a layer of PHSA (polymerised human serum albumin). This was then repeated for subsequent enzyme layers. Although Greco used only one enzyme, two or more different enzymes could be used.

This method has the advantage that no chemical manipulation was required to produce the multi-layer system, however with the acid phosphatase system the author found that the enzyme activity was impaired by the immobilization.

Bonding the biocatalyst to the membrane using chemical coupling agents has several advantages over the physical types of immobilization. The system can be run with a transmembrane pressure without the enzyme being lost from the membrane and the immobilization process can also improve the stability of the enzyme. The stability of the enzyme is improved since the bonding helps to maintain the protein structure under adverse conditions.

The normal method of bonding is covalent bonding. To obtain a good bond between the enzyme and the membrane it is important to see that both enzyme and membrane have the correct reactive groups. Furthermore, the bonding agent must be selected to avoid damage to the enzyme and so may be specific to a particular enzyme. Glutaraldehyde and cyanogen bromide are two common bonding agents which have been used with many enzymes. [77, 78, 79].

Chemical bonding can be achieved in a similar manner to the adsorption techniques mentioned earlier. The enzyme can be introduced into the structure of the membrane by either using diffusion or by applying a transmembrane pressure. When immobilizing the enzyme using the diffusion method, the membrane (normally polysulphone membranes since they contain the correct reactive groups) is firstly soaked in a solution of the immobilizing agent and then placed in the enzyme solution. The membrane is left to soak for up to 24 hours and then washed to remove any free enzyme. In the second approach the bonding agent is flushed through the membrane followed by the enzyme solution. After bonding the membrane is washed to remove any free enzyme. Typically the immobilization under pressure gives a higher enzyme loading. Both these methods were employed by Staude [77] to immobilize dextranase and urease. As with the adsorption immobilized techniques it is usual for the enzyme to be immobilized in the porous substructure of the membrane.

Further work by Gregor [78] on the immobilization of chymotrypsin using cyanogen bromide showed clearly the advantages of chemical immobilization. Firstly Gregor found that coupling under pressure gave a far higher retention of enzyme activity (70% compared to 40%). However more importantly the thermal and chemical stability of the enzyme was also better, see figure 3.9.

This technique is normally only applicable to stable enzymes, since chemical bonding is difficult to reverse and the membrane cannot be reused, for example chymotrypsin which loses only 1% of its activity per week at room temperature.

The membrane can also suffer from reduced flux, this is caused by the presence of the enzyme in the porous substructure reducing the flow area.

3.4 WHOLE CELL IMMOBILIZATION

The immobilization of whole cells has several advantages over enzyme immobilization. Firstly since the cells are typically far larger, immobilization is far easier, and secondly the useful life of the reactor should be longer since the activity of the reactor is maintained as the cells grow and replicate.

Whole cells can be easily immobilized within an ultrafiltration membrane. The most common method used is immobilization within the spongy support material of the membrane either by chemical or physical bonding [68]. This type of reactor has been shown to have potential for the production of monoclonial antibodies and hormones [80].

Figure 3.9 The Effect of Temperature on the Chymotrypsin Enzyme (78)

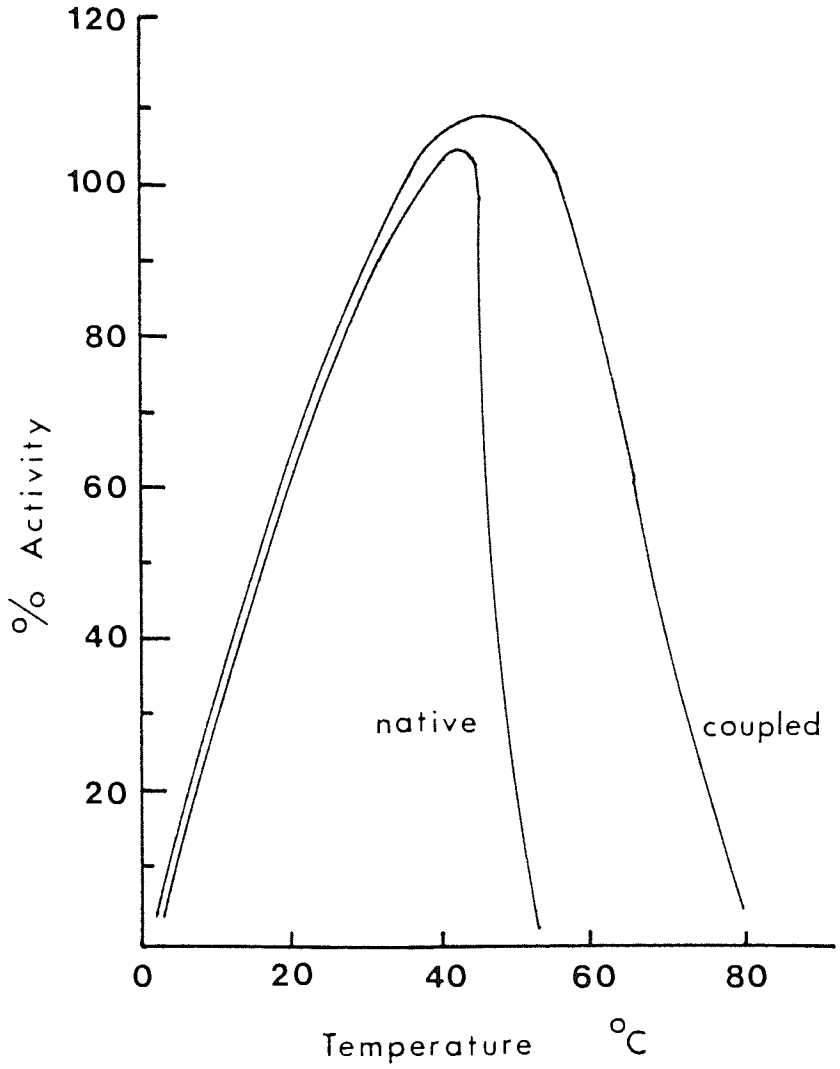

The immobilization of whole cells can also be achieved during the phase inversion stage of the membrane formation process. Naturally this technique gives the most secure bond between the cells and the membrane, but the cells must be thermally and chemically resistant if the procedure is to be successful. Drioli [81] immobilized C.acidophila cells into cellulose acetate and polysulphone membranes during the phase inversion process. The C.acidophila cells were particularly suitable since they could withstand low pH and had an optimal temperature of 90-100°C. The cells were used for their B-galactosidase activity, but as Drioli commented, the cells could be used to investigate other cytoplasmic enzymes by simply changing the substrate used.

Drioli confirmed that the physico-chemical properties of the B-galactosidase immobilized in the membrane were similar to those shown by the enzyme in the free cells, and that the cells showed good stability within the membranes.

3.5 THE USE OF FREE AND IMMOBILIZED DEXTRANSUCRASE

Dextransucrases are mainly extra cellular trans-glycosylases which are responsible for the conversion of sucrose to dextran and fructose. Unlike many other enzymes dextransucrases do not require the presence of cofactors or other high energy related phosphorylated intermediates and therefore have a greater possibility of being used in reactors other than the conventional batch reactor.

The dextransucrase enzyme used for the industrial manufacture of dextran is normally obtained from the bacterium Leuconostoc Mesenteroides, NRRL B512F. This strain has the ability to produce enzyme which gives linear chained molecules with only 5% branching. The enzyme dextransucrase synthesizes dextran from sucrose according to the overall equation:-

$$n \cdot (C_{12}H_{22}O_{11}) \longrightarrow (C_6H_{10}O_5)_n + n \cdot (C_6H_{12}O_6)$$

sucrose — dextran — fructose

Robyt et al (82) investigated the mechanism of chain growth using pulse and chase techniques with [^{14}C] labelled sucrose. Robyt proposed a mechanism for the synthesis in which two nucleophiles at the active sites, X_1 and X_2, (see figure 3.10) attack two bound sucrose molecules displacing the fructose units leaving two glucosyl units covalently linked to the nucleophiles through C_1 of the molecule. In subsequent steps the C_6 - hydroxyl (the primary hydroxyl group) of one of the glucose units effects a nucleophilic attack on C_1 of the other glucose unit forming an α- 1,6 glucosidic linkage. Simultaneously this transformation releases the active site nucleophile which can then attack another sucrose molecule to give a new glucosyl unit attached to the active site. The C_6 - hydroxyl of this new glucosyl unit then attacks the C_1 unit of the isomaltosyl unit forming another α-1,6 linkage. In the presence of sufficient sucrose, this process continues with the two necleophile groups X_1 and X_2 at the active site, alternatively forming covalent complexes with glucose and the growing dextran chain. The process is stopped when an acceptor molecule interacts with the active site resulting in the release of the chain from the enzyme. Robyt found over 30 different acceptor products, these included a wide range of carbohydrate molecules. Examples of these molecules are fructose, maltose, isomoltose, glucose, mannose and glactose.

Figure 3.10 Reaction Mechanism for Dextran Synthesis (82)

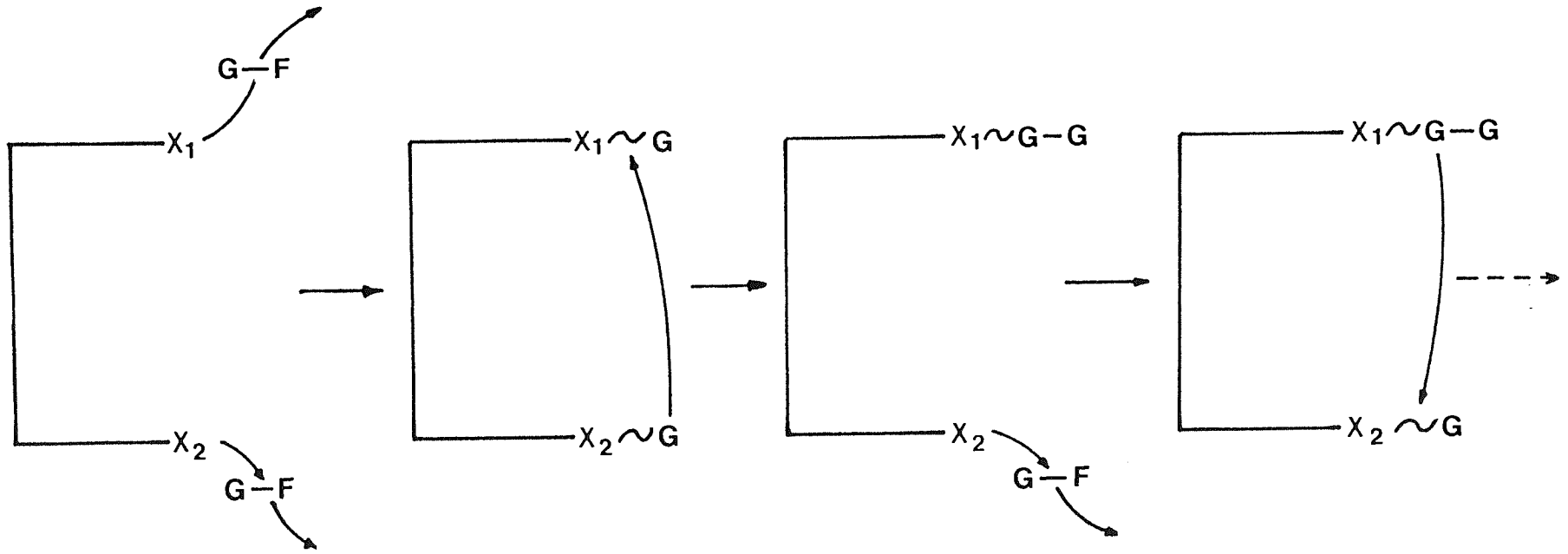

G—F : Sucrose G : Glucose F : Fructose

The second reaction product fructose is a relatively strong acceptor. Theoretically stoichimetry predicts that 100 g of sucrose gives 52.6 g monosaccharides (fructose) and 47.4 g of high molecular weight (HMW) dextran. In practice however disaccharides and lower molecular weight dextrans are formed due to the acceptor reactions. Alsop [83] investigated the effect of fructose on the enzyme reaction in a batch system. See table 3.1.

Table 3.1 Yields of carbohydrate fractions from dextransucrase at various sucrose strengths (g per 100 g sucrose)

Sucrose % W/V	Mono-saccharides	Disaccharides	Total Dextran	HMW Dextran	LMW Dextran
2	52.2	1.9	45.9	45.9	0
4	50.0	4.4	45.6	45.6	0
6	51.3	4.3	44.4	44.4	0
10	51.2	6.8	42.0	39.0	3.0
15	55.5	9. 4	35.3	25.3	10.0
20	56.9	11.2	31.9	17.9	14.0
(Theory)	52.6	0	47.4	47.4	0

When a 2% sucrose concentration was used the reaction was almost stoichimetric resulting in quantitative yields of dextran and monosaccharides, the dextran being exclusively high molecular weight and the monosaccaride was fructose. As the sucrose concentration increased from 2% to 20% the amount of monosaccharide marginally increased and the amount of disaccharide (shown to be mainly leucrose) increased markedly. The amount of low molecular weight dextran including oligosaccharides also increased, particularly when concentrations above 10% were used. As a consequence of these changes the total yield of dextran fell dramatically. It can be seen that if high sucrose concentrations are to be used the fructose must be removed from the reaction mixture before it can interfere with the chain growth.

The dextransucrase activity (DSU) is most commonly defined as the amount of enzyme which would convert 1 mg of sucrose to dextran in 1 hour under actual operating conditions, ie. pH 5.2 and 25^{o}C. This definition was used throughout this work. The dextransucrase activity can be determined using either HPLC, GPC or Hostettlers method [92].

The optimum pH for dextransucrase is 5.2 although between pH 4.8 and 5.6 the enzyme retains 90% of its maximum activity, outside this range the activity drops sharply. Dextransucrase has its maximum activity at 30^{o}C but an operating temperature of 25^{o}C is recommended since at higher temperatures a rapid decay occurs. At 4^{o}C the enzyme was found to be stable for 3 weeks, at 35^{o}C for 1 hour and at 40^{o}C it was completely destroyed in 15 minutes.

The precise molecular weight of the dextransucrase enzyme is unclear since it is often associated with large dextran molecules. Jackson and Stewart [92] reported a molecular weight of 171,000 Daltons, while Ebert and Schenk [93] claimed that when associated with dextran it had a molecular weight of 280,000 Daltons.

Monsan and Lopez [84] investigated the effect of reaction time on chain growth. See figure 3.11. They found that the molecular weight appeared to increase with reaction time and the distribution which was rather disperse at the beginning, became sharper as the reaction time increased. These results confirmed the results obtained by Braswell [85] and Bovey [86].

Over the last few years many attempts have been made to immobilize the purified dextransucrase onto porous suports. Both Reilly and Kaboli (87, 88), and Monsan (84, 89, 90) have made significant progress in this area. Reilly and Kaboli [87] initially immobilized dextransucrase onto Whatman number 1 filter paper (using cyanuric chloride), to DEAE-cellulose, DEAE-sephadex A-25 and A50 and SP-sephadex C-25 and C-50 but the retained activity was very low. With the three DEAE carriers virtually all the dextransucrase was ionically attached to the carrier but at best only 10% remained active. Reilly and Kaboli obtained their best results by immobilizing the enzyme onto a porous silica using a glutaraldehyde solution. Using this method they obtained a retained activity of up to 19.6%. Reilly and Kaboli also investigated the effect of pH and temperature on the immobilized enzyme and compared this to the 'free' enzyme. See figure 3.12 and 3.13. They found that the optimum pH remained the same at pH 5.2, but the enzyme activity decreased less rapidly at pH values well removed from the optimum. The temperature/activity relationship showed the same trends, the enzyme showed maximum activity at 30^{o}C but the rate of activity loss above this temperature was far lower than the free enzyme.

More recently Monsan (84,89,90) obtained immobilized dextransucrase activities as high as 800 DSU/gm for dextransucrase immobilized onto amino porous silica (spherosil) using glutaraldehyde. This higher activity was achieved by the addition of maltose to the enzyme solution during the coupling reaction. Monsan felt that the addition of maltose

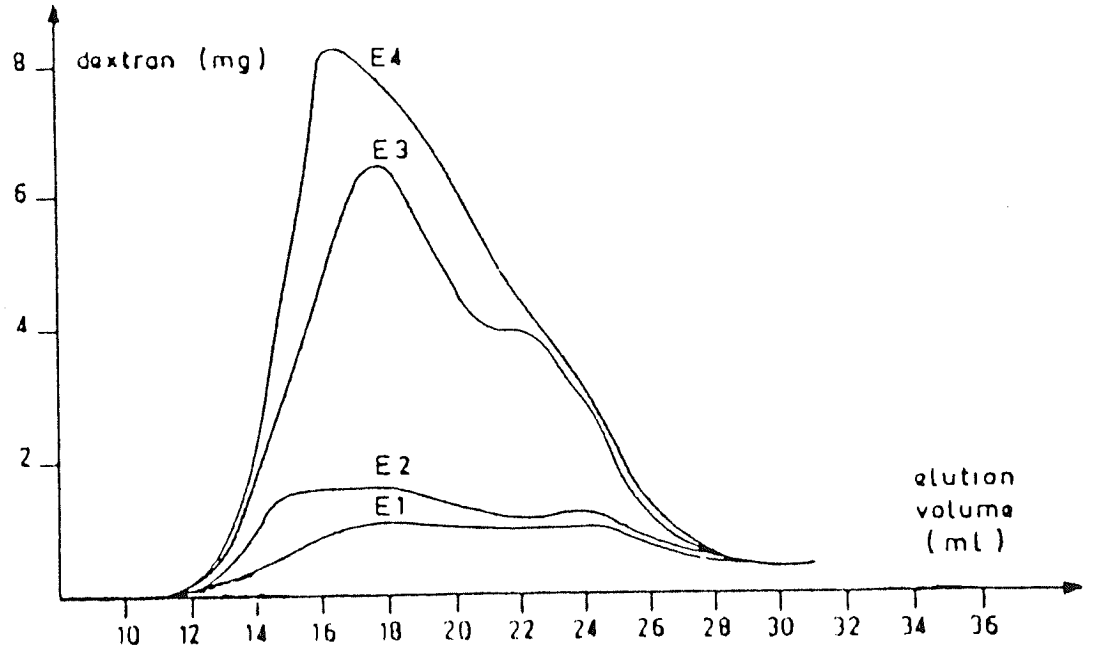

Dextran molecular weight distribution at different times of reaction (E1 = 25 min.; E2 = 50 min.; E3 = 131 min.; E4 = 190 min.)
Dextran was fractionated by GPC on Ultrogel A2.

Figure 3.11 How the Molecular Weight Distribution Changes during the Fermentation Process (84)

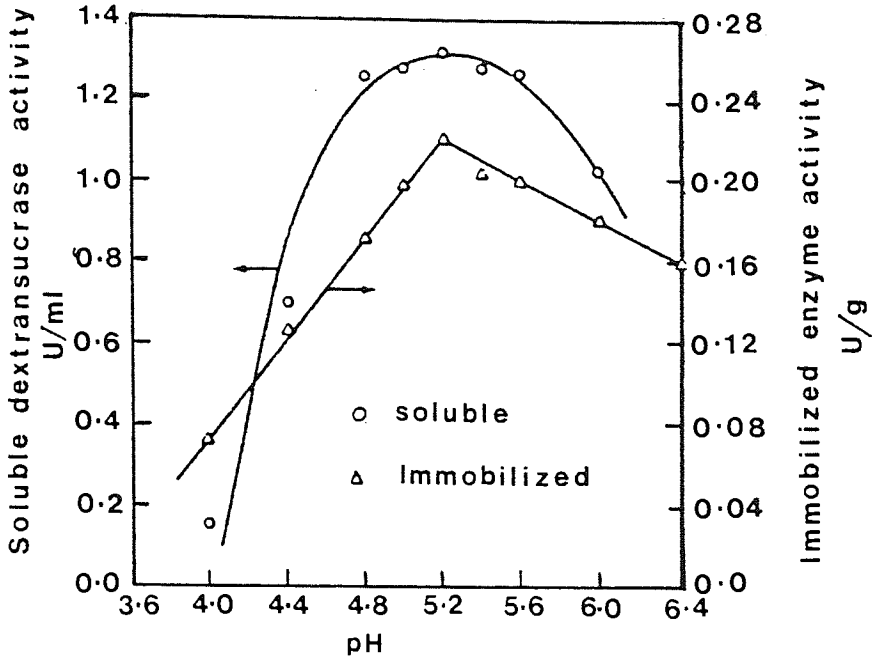

Figure 3.12 Effect of Ph on Dextransucrase Activity (87)

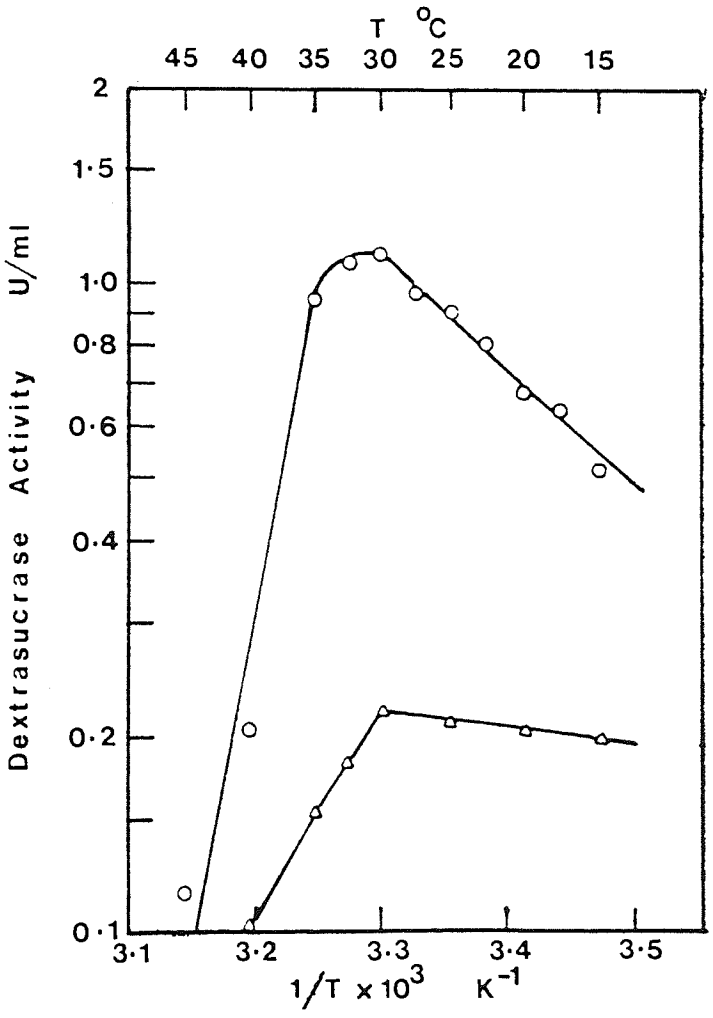

Figure 3.13 Effect of Temperature on Dextransucrase Activity (87)

caused the release of the dextran chains from the enzyme and thus the enzyme was easier to attach to the support. However despite the 100 fold increase in activity over previous workers their yields remained relatively low.

Edwards [79] immobilized dextransucrase onto polyacrylamide gel and more interestingly to cellulose acetate membranes and hollow fibres using glutaraldehyde. In all cases Edwards found that the activity of the immobilized enzyme was far lower than the free form.

While experimenting with the hollow fibre system Edwards found that the molecular weights of the dextrans produced were flow rate dependent. At low flow rates higher molecular weight dextran was formed while at high flow rates more low molecular weight material was formed.

4.0 ANALYTICAL EQUIPMENT

4.0 ANALYTICAL EQUIPMENT

4.1 INTRODUCTION

To assess the rejection characteristics of a membrane system it is necessary to calculate weight changes in selected molecular weight bands. To obtain this information the molecular weight distribution and concentration of the dextran product must be found.

The overall dextran concentrations were calculated using a polarimeter, since this was found to be the most accurate method.

The molecular weight distribution was determined using analytical gel permeation chromatography (GPC).

Using the molecular weight distribution the weight fractions for each molecular weight band can be found. Using the bulk concentration the weight in each band can be calculated. The rejection of each band can then be assessed by comparing the weight in each band to that in the feed.

4.2 CALCULATION OF SAMPLE CONCENTRATION

4.2.1 EQUIPMENT DESCRIPTION

Two types of polarimeter were used. The first manufactured by Bellingham and Stanley (model D) was a simple design. A sodium light provided the illumination. The optical rotation was measured by rotating duel polarizers until both halves of the view finder were of equal darkness. The optical rotation was then read from a scale on the adjusting mechanism.

This polarimeter was replaced by another more accurate model manufactured by Bellingham and Stanley Ltd, England. This polarimeter used a photoelectric cell to match the screen densities. This design of polarimeter was accurate to within 0.05 degrees of optical rotation.

A cell 100 mm long and with an approximate volume of 10 cm^3 was used in both polarimeters.

4.2.2 EXPERIMENTAL TECHNIQUE

From simple theory the optical rotation (θ)can be calculated using the relationship;

$$\theta = R.L.C \qquad \ldots. 4.1$$

where R is constant for the particular substance being used

L is the cell length

C is the concentration

Since the cell length remained constant the relationship can be simplified to;

$$\theta = \text{constant}. C \qquad \ldots. 4.2$$

The value of the constant was determined using a range of dextran samples with known concentration. The relationship can be found in Figure 4.1.

Polarimetry was found to be a very robust method of calculating the concentration of the dextran samples. Since the polarimeter only responds to optically active substances such as dextran, bacteriocides such as sodium azide could be used without affecting the accuracy of the results. Furthermore the concentration could be calculated faster using

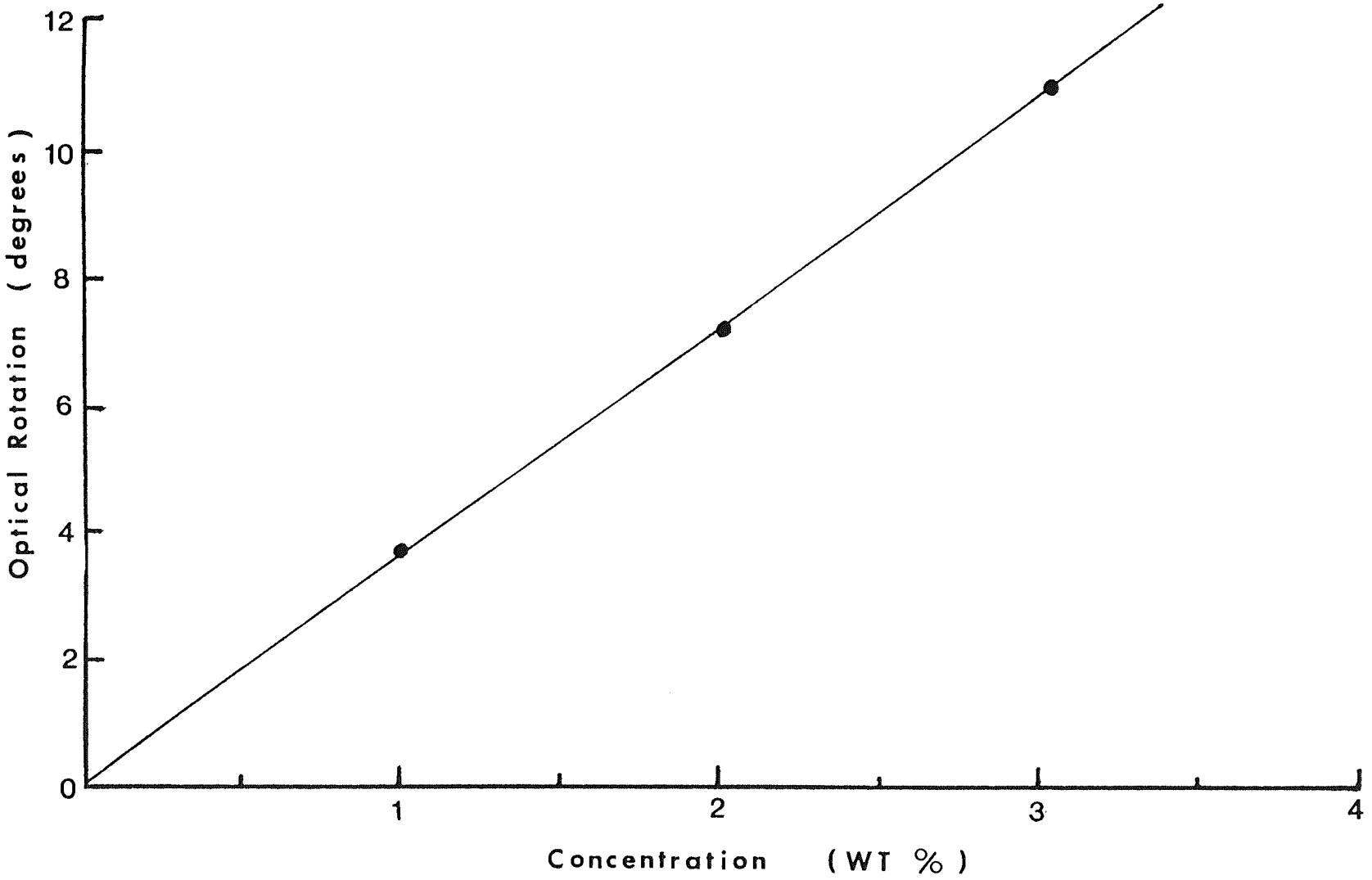

Figure 4.1 Calibration of the Polarimeter

polarimetry than with other comparable methods such as HPLC. Typically the concentration of a sample could be measured in under three minutes using the polarimeter, compared to twenty minutes for HPLC. The accuracy of the HPLC method was also affected by the background concentration of sodium azide.

For convenience the concentration was measured at ambient temperature. Since the samples were often stored in a refrigerator it was necessary to allow time for the samples to warm up before analysis could take place.

4.3 CALCULATION OF THE MOLECULAR WEIGHT DISTRIBUTION (MWD) USING ANALYTICAL GEL PERMEATION CHROMATOGRAPHY (GPC)

4.3.1 EQUIPMENT DESCRIPTION

A schematic diagram of the GPC analysis system can be found in Figure 4.2.

The eluent used was distilled water with 0.02% W/V sodium azide to prevent bacterial growth in the columns. The eluent reservoir held approximately ten litres and was maintained at 50°C to degas the eluent. The eluent was prefiltered using a 0.45 µm sintered metal filter before passing through a debubbler to the pump. The pump was a duel piston, low pulsation pump (model 1330 Biorad Laboratories, Watford, UK) with a flow rate range of 0.1 to 9.9 cm^3/min.

The samples were injected through a 6 port injection valve (model 30100 Spectroscopic Accessory Co, London) with a 100 µl sample loop. The samples were prefiltered using a 0.45 µm disposable syringe filters. (Millipore, London).

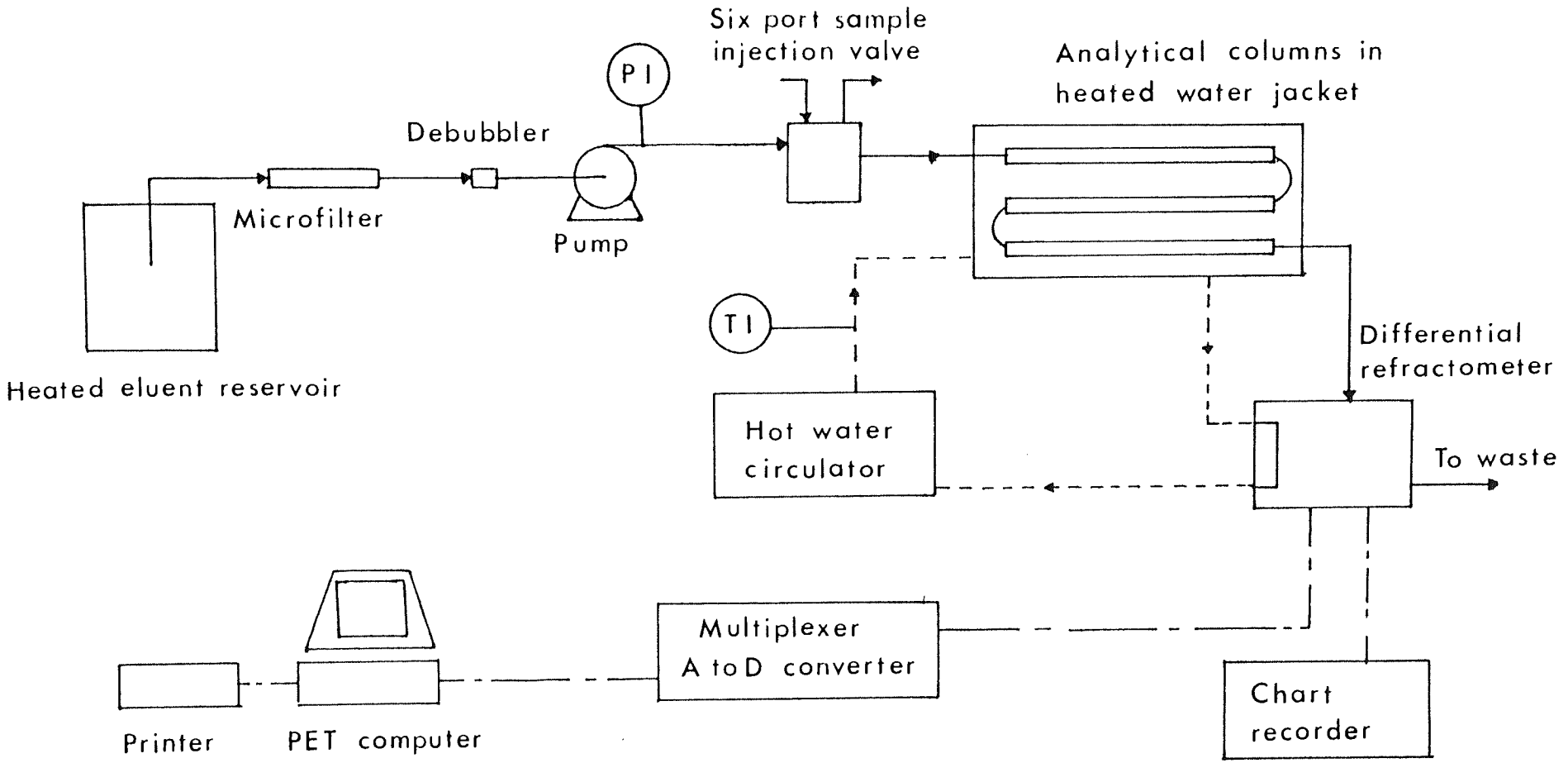

Figure 4.2 Schematic Diagram of GPC Analytical System

The three GPC columns were held within a heated stainless steel waterbath at 40°C. The temperature was maintained by a hot water circulator (C400 Techne, Cambridge, UK).

The concentrations of the product leaving the columns were measured using a differential refractometer (model R401, Waters Asssociates Ltd, London). A 0.02% sodium azide solution was used in the refractometer reference cell since the eluent stream contained a similar concentration of sodium azide. Furthermore the refractometer cell was maintained at 40°C to avoid temperature differences between product and reference streams.

The analogue signal from the refractometer was transmitted to a multiplexer (model PCI 1001, CIL Electronics Ltd, Sussex) which converted it to a digital signal. The digital signal was then used by a PET computer (model CBM 4032, 32K bytes, Commodore UK) to calculate the molecular weight distribution of the sample. As a back-up to the PET computer a flat bed potentiometric chart recorder (Venture Servoscribe RE541.2 Smiths Ltd) was used.

4.3.2 DESCRIPTION OF GPC COLUMNS

Three types of GPC columns were used. Two were manufactured by the Toya Soda Manufacturing Co, Tokyo, Japan, and the other by E Merck (supplied by BDH Atherstone).

Initially the TSK PW columns were used, however these were later replaced by TSK PW-XL columns. Both these columns used a vinyl polymer packing specifically designed for aqueous systems. These columns have a wide fractionation range and low adsorption characteristics, combined with stability in the pH range 2-12. In both cases the system consisted of three columns. The first two were TSK G5000 columns designed to fractionate within the molecular weight range 10,000 to 2×10^6. The

third column was a TSK G3000 column to fractionate up to 10,000 MW.

The TSK PW columns were 60 cm in length by 0.75 cm ID, the TSK PW-XL columns were 30 cm in length and 0.78 cm ID.

The TSK PW-XL columns have a smaller particle size packing which gives a higher number of theoretical plates per meter and allows a shorter elution time, see table 4.1.

The PW system was used at a flow rate of 1.0 cm^3/min. At this flow rate the PW system gave an analysis time of approximately 1 hour. The PW-XL system was used at 0.9 cm^3/min giving a cycle time of 35 minutes. To improve the stability of the PW-XL columns the flow rate was later reduced to 0.7 cm^3/min.

Although the TSK PW series of columns exhibited low adsorption characteristics they were not satisfactory for solutions with a high protein content, for example the dextran/dextransucrase solutions from the enzyme bioreactor (see section 7.0). To analyse these solutions Lichrospher Diol columns were used. The Diol columns were 25 cm in length and 0.4 cm ID. The packing was a 10 µm spherical hydrophilic support material coated with 1,2 - dihydropropoxypropl chains. Three columns were used in series. The first column was a 1000 Diol/2 with a fractionation range 10,000 to $2x10^6$. The second was a 500 Diol/2 column fractionating the molecular weight range 4000 to 700,000. The final column was a 100 Diol/2 cartridge fractionating the molecular weight range 200 to 40000.

These columns were used at 25°C with a flow rate of 0.3 cm^3/min. This gave an analysis time of approximately 30 minutes.

To protect the columns a guard column was used.

Table 4.1 Manufacturers Specification for TSK PW and PW XL columns

Description	Number of Theoretical Plates (NTP)	
	PW	PW-XL
	(60 cm x 0.75 ID)	(30 cm x 0.78 ID)
TSK 3000	10,000	14,000
TSK 5000	6,000	10,000

4.3.3 ASSESSMENT OF COLUMN PERFORMANCE

To assess the performance of the GPC columns two parameters were used. These were the number of theoretical plates (NTP) and the asymmetry factor (As).

Although there are several methods available to calculate the NTP values the most convenient method is;

$$NTP = 5.54 \left(\frac{Vp}{W_{o.5}} \right)^2 \qquad \ldots 4.3$$

where $W_{o.5}$ is the peak width at one-half peak height. Vp is the elution volume for the peak. See figure 4.3.

The asymmetry factor (As) is calculated at one tenth the peak height and is given by the equation;

$$As = \frac{b}{a} \qquad \ldots 4.4$$

See figure 4.4.

To test the columns a 2.5 mg/cm^3 Ethylene Glycol solution was used, this was the same as Toya Soda used for their quality control tests.

In total three sets of PW-XL columns were used. The efficiency of these columns and the factors affecting their useful life was studied in detail. This work was performed for Toya Soda in Japan.

The columns were supplied with information on their performance. This information gave a useful check on the results obtained at Aston. Normally reasonable agreement was found, see table 4.2.

Initially the system was operated at 0.9 cm^3/min and a pressure of 4000 KPa, however after two months of intensive use a significant deterioration of the systems performance was found. The system was dismantled and the individual columns tested, see table 4.3. The problem was identified as a loss of efficiency within the two G5000 PW-XL columns. The efficiency could be recovered in part by backflushing the columns at 0.1 cm^3/min, however this improvement normally lasted only three or four days. This suggested that the reduced efficiency was caused by compaction of the packing. After consultation with Toya Soda, the flow rate was lowered to 0.7 cm^3/min, this reduced the system pressure to 2900 KPa. At this point the two G5000 PW-XL columns were replaced. The reduction in flow rate significantly improved the stability of the system, since the damage to the G5000 columns was greatly reduced. See table 4.4.

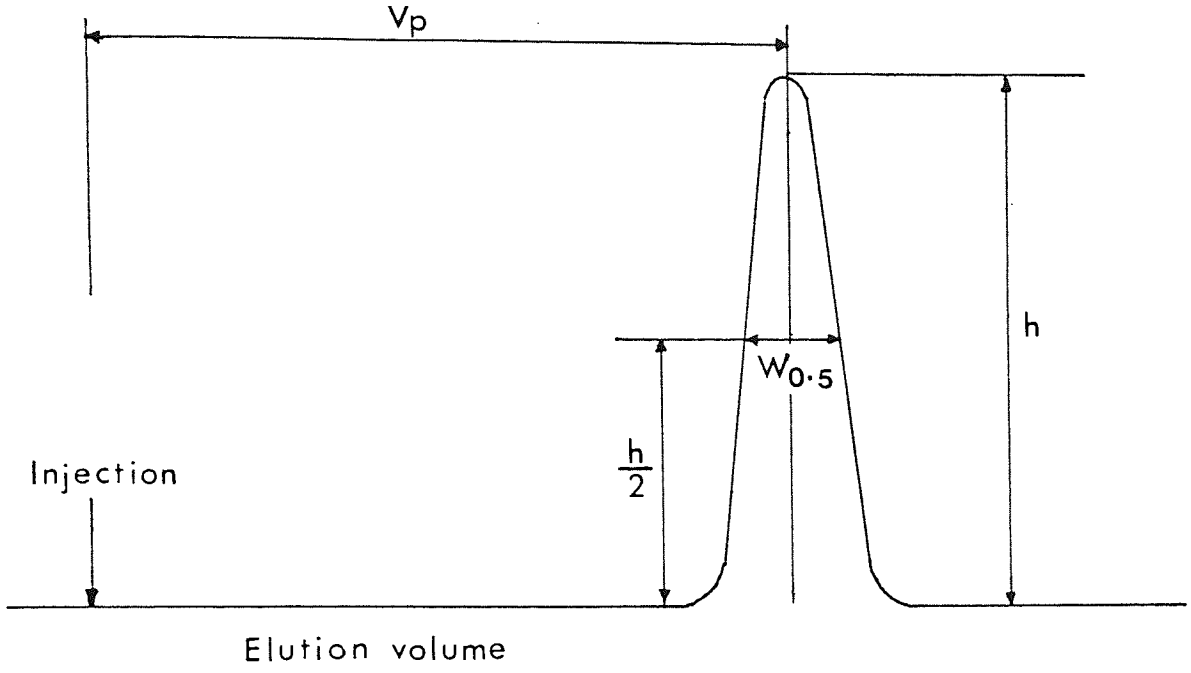

Figure 4.3 Calculation of the Number of Theoretical Plates

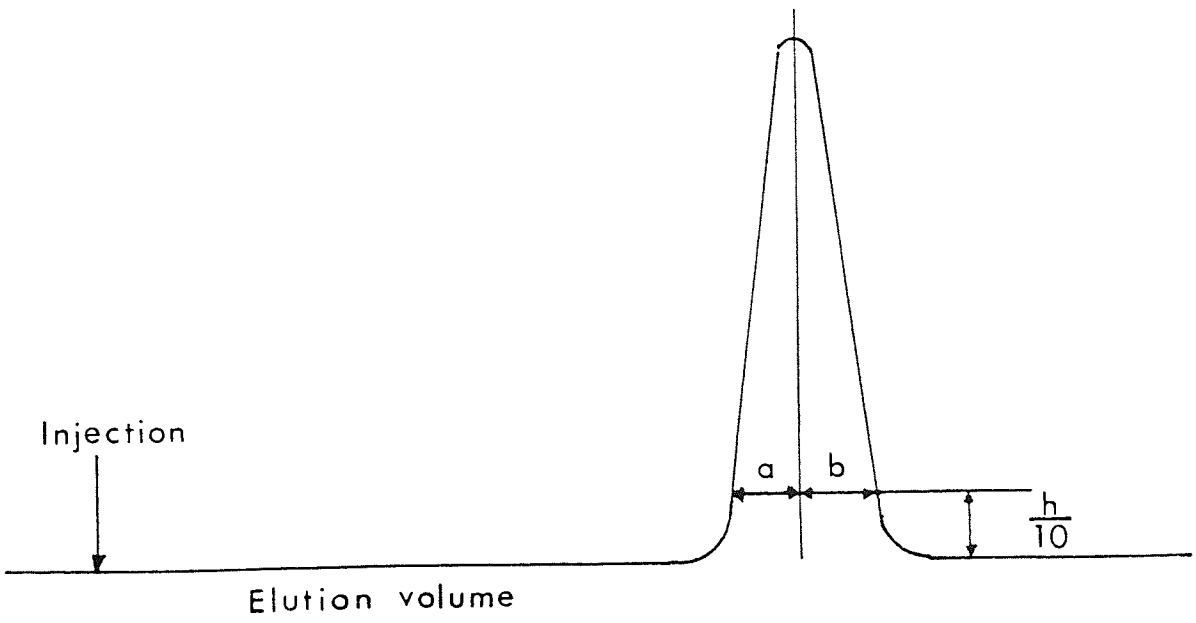

Figure 4.4 Calculation of the Asymmetry Factor

The life expectancy of these columns depended significantly on how carefully they were used. The packing appeared to be damaged by excessive pressure, so it was necessary to avoid pressure peaks when injecting samples. Furthermore the columns were easily damaged by accidental injection of air since this caused channelling in the packing [94]. Typically the useful life of a G5000 PW-XL column was 6-7 months. The life time of the G3000 PW-XL column was approximately 12 months because it was protected by the other two columns.

The useful life of the PW-XL system unfortunately appears to be far shorter than the TSK PW system. The TSK PW originally used by Poland [6] lasted for almost 3 years, however it is difficult to assess how many samples were run during this period. The TSK PW-XL columns however were typically used on average for 100 samples per month.

Although the useful life of the TSK PW-XL columns was noticably shorter than TSK PW columns their performance far exceeded their predecessor. Since the resolution of the individual molecular weights was of great importance when analysing the dextran molecular weight distribution, the TSK PW-XL columns must be considered the better option. Furthermore the elution time for these columns was approximately one third less that the older system, which gave a significant reduction in analysis time.

Table 4.2 Commissioning Results for Toya Soda PW XL Columns

COLUMN	TOYA SODA TEST		ASTON TEST		POSITION IN SYSTEM
	NTP	A_s	NTP	A_s	
G3000 PW-XL (Code PW3XF0228)	25105.7	1.11	21053.7	1.10	3
G5000 PW-XL (Code PW5XF0153)	15885	0.95	13108.3	1.11	1
G5000 PW-XL (Code PW5XF0152)	16104.9	0.86	14055.9	0.885	2

Table 4.3 Test Results on Toya Soda PW-XL Columns After Two Months Use

Column	ASTON TEST				% LOSS OF EFFICIENCY		POSITION IN SYSTEM
	Commissioning		Retest				
	NTP	A_s	NTP	A_s	NTP	A_s	
G3000 PW-XL (PW3XF0228)	21053.7	1.10	19191	1.16	8.84	5.54	3
G5000 PW-XL (PW5XF0153)	13108.3	1.11	7448 10339+	1.25 1.25	43.18 21.12	12.61 12.61	1
G5000 PW-XL (PW5XF0152)	14055.9	0.885	7999	1.0	43.09	12.99	2

(+ after backflushing)

In total 200 samples were run.

Table 4.4 History of TSK PW-XL columns

G5000 PW-XL (PW 5XG0068)

Date	NTP	AS	Pressure (bar)
17.07.87	10786	1.0	15
16.09.87	10848	0.968	15
10.01.88	10665	1.0	15
	10391	1.0	
10.02.88	6942	0.9	15

G5000 PW-XL (PW5XG0069)

Date	NTP	AS	Pressure (bar)
17.07.87	13850	1.16	15
16.09.87	14088	1.07	16
10.01.88	10940	1.00	16
10.02.88	8619	1.00	16

G3000 PW-XL (PW3XF0228)

Date	NTP	AS	Pressure (bar)
10.01.87	21053.7	1.10	33
12.03.87	19191	1.16	33
17.07.87	11006	1.28	33
16.09.87	11826	1.17	35
10.01.87	9526	1.14	35

4.3.4 CALIBRATION OF THE GPC COLUMNS

The calibration of a GPC system can be achieved by using a variety of methods [95-104]. However a detailed investigation by Vlachogiannis [5] and Bhrambra [105] showed that the most convenient method was that proposed by Nillson and Nillson [106]. The molecular weight (M) is expressed as a five term polynominal, where;

$$M = b_5 + \exp \{b_4 + b_1 (K_d) + b_2 (K_d)^2 + b_3 (K_d)^3\} \quad \ldots 4.5$$

$b_1 - b_5$ are constants

K_d is the distribution coefficient. The distribution coefficient is determined from the elution volume V_R of dextran samples with known molecular weights using the simple relationship;

$$V_R = V_o + K_d Vi \quad \text{or} \quad K_d = (V_R - V_o)/V_i \quad \ldots. 4.6$$

$$V_i = V_t - V_o \quad \ldots. 4.7$$

V_i is the internal (pore) volume of the column

V_t is the total liquid volume of the column

V_o is the void volume of the column

The values of V_o and V_t can be found experimentally by using glucose and high molecular weight dextran standards. The glucose penetrates the pores freely so it can be used to give V_t. The high molecular weight dextran is totally excluded hence it gives the interstitial volume V_o.

The limits of the calibration are naturally dependent on the molecular weight of the material which penetrates the pores freely and

that which is totally excluded. Normally the calibration profile follows a characteristic S shape. Figure 4.5 shows the relationship between molecular weight and elution volume (V_R) on a semi-logarithmic scale. In the region a-b total exclusion occurs, the value of M_o for the Toya Soda columns was approximately $1x10^7$ MW. In the region e-f total penetration occurs, this corresponds to a molecular weight (M_t) of 180 MW. Within the limits c-d a linear relationship occurs, in this region the fractionation is at its best. In sections b-c and d-e fractionation is still occurring, however the relationship is non-linear. Ideally the GPC column should only be calibrated and used within the region c-d, however this is often not possible. Simply extrapolating the calibration outside this region is also inadvisable since erroneous results are likely.

To calibrate over the whole fractionation range a series of Pharmacia dextran T fractions were used. The molecular weight average (M_W) of each T fraction had been previously measured using light scattering techniques. Once the elution profiles from each T fraction had been obtained, (see Figure 4.6) the calibration constants b_1-b_5 could be found using an optimisation program. The program written by Vlachogiannis used the Hartley modification of the Gaussian-Newton optimisation method [106] to calculate the new constants. The refractometer heights from each profile, the elution volumes which were converted to the K_d values and light scattering M_W values were entered into the program. Furthermore an inital guess of the constants was required. The program produces a comparison of M_W values obtained from light scattering and the GPC systems, see tables 4.5 and 4.6. To check the accuracy of the calibration the standard deviation between the two sets of values was calculated. Normally if the standard deviation was less than 5% the calibration was acceptable.

Figure 4.5 A Typical Calibration Curve for a GPC System

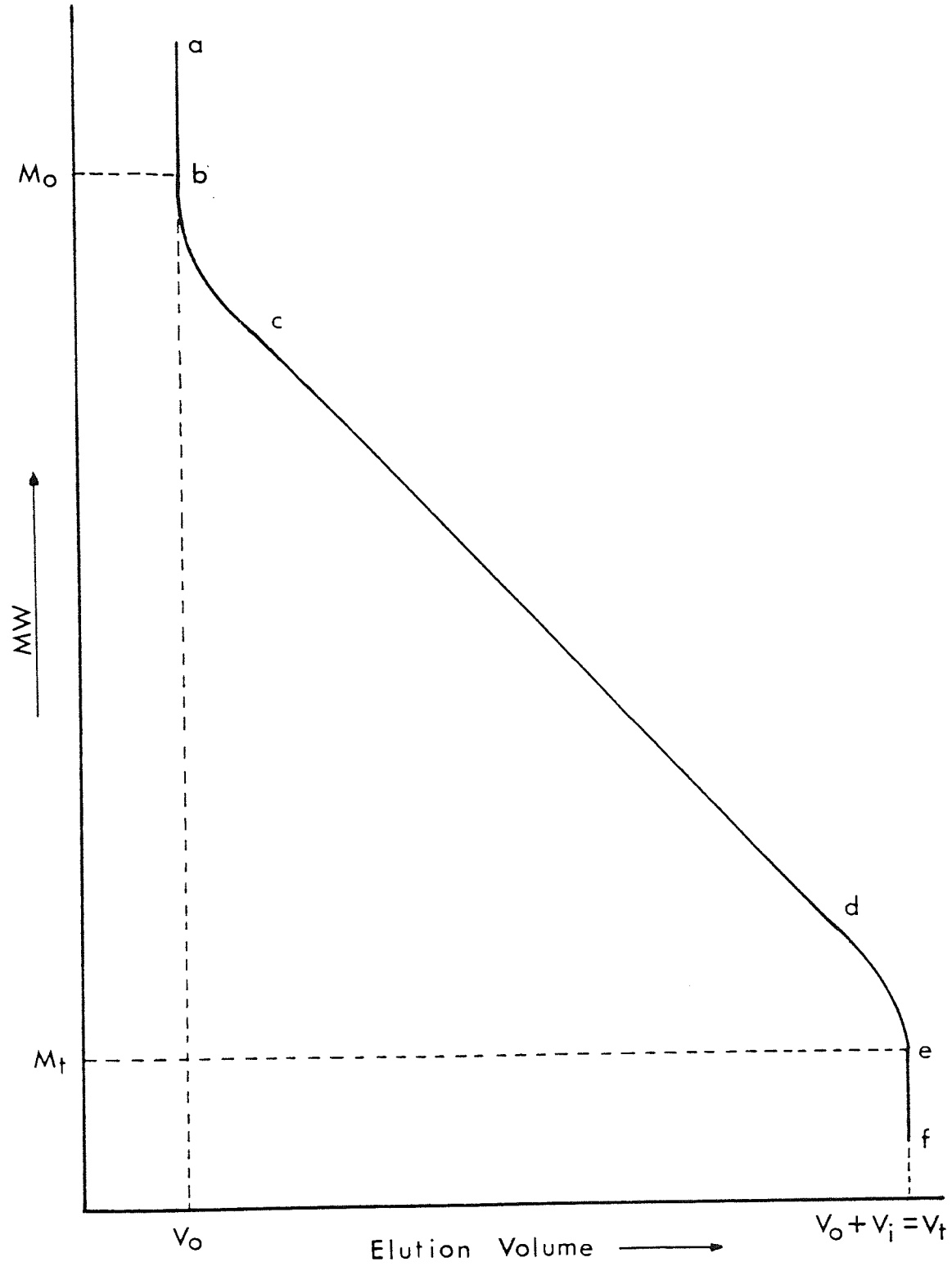

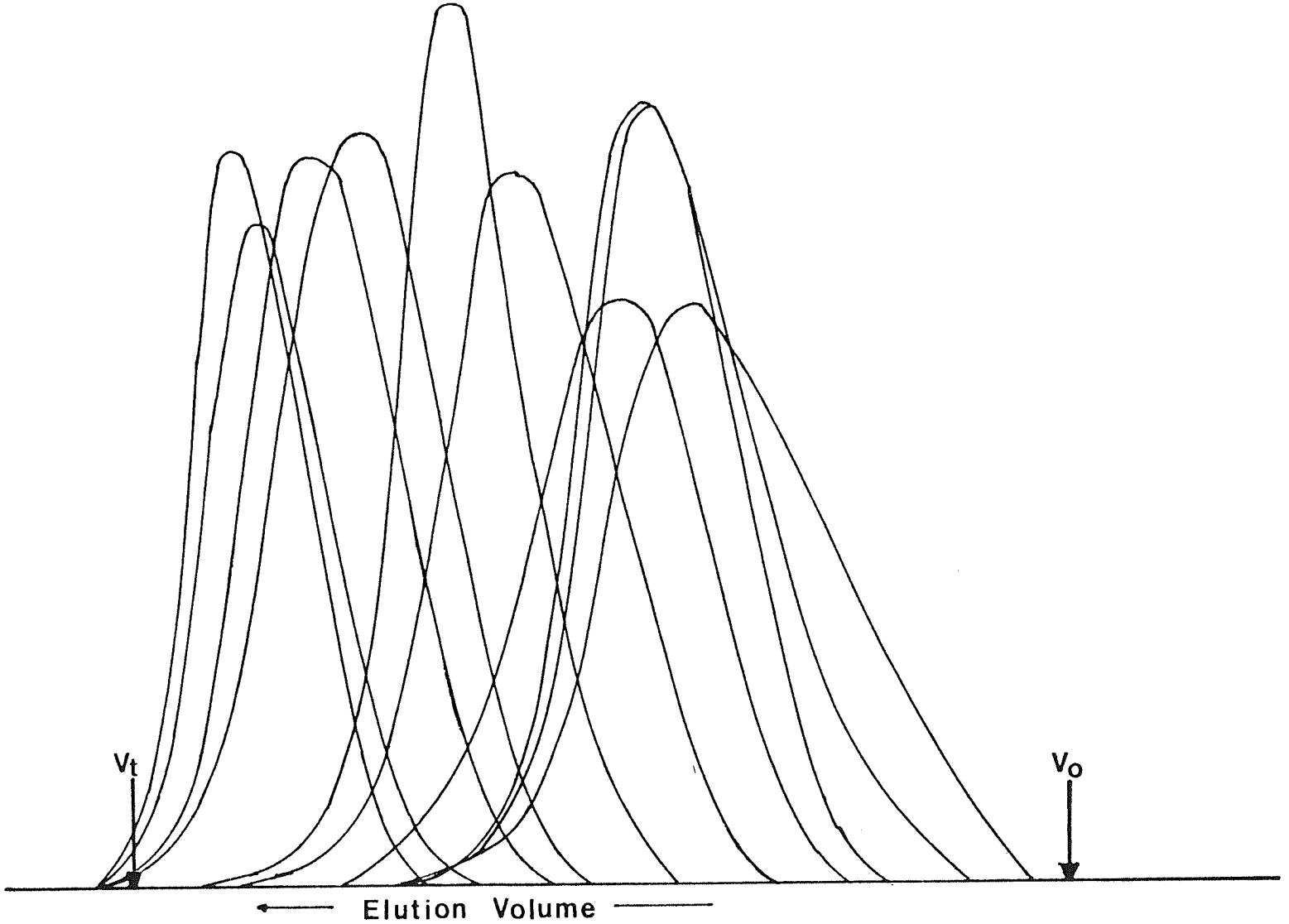

Figure 4.6 Elution Profiles from the Range of T Fractions used to Calibrate the Diol Columns

Table 4.5 Calibration of the TSK PW-XL System

Batch Number	Weight Average Molecular Weights		$\frac{GPC \times 100}{LS}$
	light scattering (LS)	GPC	
PT3636	239825	241866	100.8
PH1076	149600	147539	98.62
PG7427	104450	103919	99.49
PF1601	73625	74280	100.9
PB5227	42150	41528	98.52
PE5382	21975	23063	104.9
PA0094	11500	11092	96.45
JD2985	8825	8536	96.73
DK8868	5250	5387	102.6
PD2335	4100	4112	100.3
Glucose	180	180	100.0

Calibration constants

b_1	b_2	b_3	b_4	b_5
-15.946	17.065	-11.713	16.197	-91.331

Table 4.6 Calibration of the Diol Systems

Batch Number	Weight Average Molecular Weights		$\frac{GPC}{LS} \times 100$
	Light scattering (LS)	GPC	
PT3636	239825	243473	101.5
PH1076	149600	147934	101.12
PG7427	104450	101024	103.39
PF1601	73625	74824	98.39
PB5227	42150	40305	104.57
PE5382	21975	23877	92.03
PA0094	11500	11232	102.38
JD2985	8825	8546	103.26
DK8868	5250	5174	104.7
PD235	4100	4205	97.5
Glucose	180	180	100.0

Calibration constants

b_1	b_2	b_3	b_4	b_5
-13.797	14.649	-5.346	15.498	-59961.678

To test the calibration constants a T40 sample (batch BT IJ) was analysed, the GPC value of the weight average molecular weight (M_w) being compared to the light scattering value of 41500. Furthermore a calibration curve was drawn to check the limits of the calibration. See figure 4.7.

4.3.5 EXPERIMENTAL TECHNIQUE

The experimental procedure for the GPC system was as follows:-

(1) Before analysis commenced the columns were run at 0.2 cm^3/min for a minimum of ten minutes, this avoided any sudden pressure increase which may have damage the columns. After this period the flow rate was increased to the normal operating flow rate of 0.7 cm^3/min. The system was left for a further 45 minutes to reach equlibrium and to remove any residue from the system.

(2) A reference sample containing glucose and high molecular weight dextran was run to check the V_o and V_t values. The elution times were always checked before analysis was started. Furthermore the eluent flow rate was checked on a weekly basis. The eluent flow rate was measured by weighing the eluent collected over a known time period.

(3) The differential refractometer was zeroed according to the Waters Associates Operating Manual [107].

(4) Before the samples were injected their concentrations were checked. The columns could accurately analyse samples in the concentration range 0.5 to 2.5% W/V. However 2% W/V was found to be the optimum. If the samples were too dilute they were concentrated using a Buchi rotary evaporator. Solutions which were too concentrated were diluted using distilled water.

(5) Finally the samples were prefiltered using a 0.45 μm disposable filter before injected via the six part injection valve.

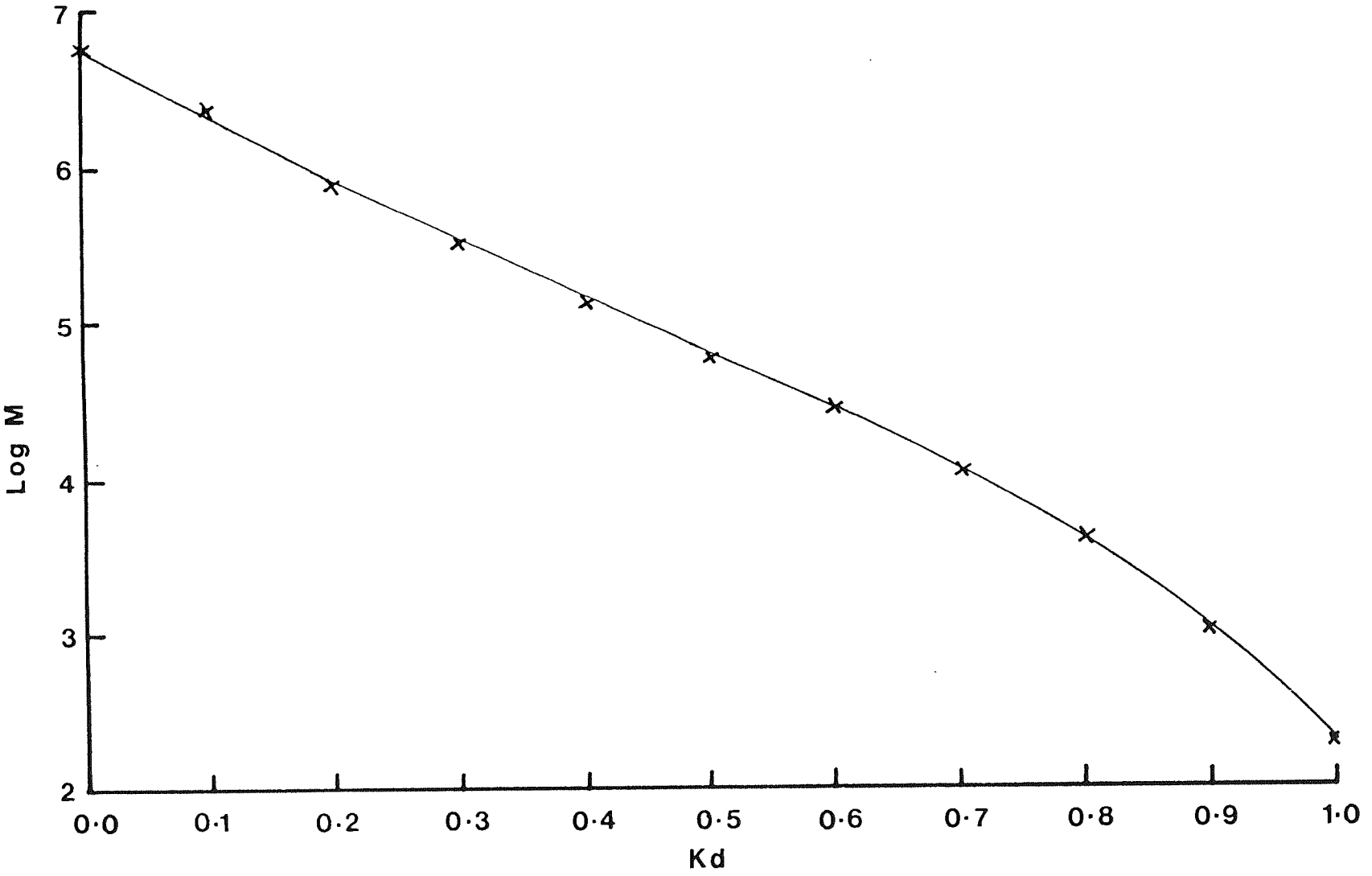

Figure 4.7 GPC Calibration for the TSK PW-XL Columns used at Aston

(6) After the sample had been eluted, the refractometer zero was rechecked. The system was then ready for the next sample.

4.3.6 CALCULATION OF THE MOLECULAR WEIGHT DISTRIBUTION AND MOLECULAR WEIGHT AVERAGES USING PET COMPUTER

Initially the calculation of the molecular weight distribution (MWD) was accomplished in two stages. The first stage was the data aquisition stage which involved the conversion of the electrical signal from the refractometer to a height using a multiplexer and PET computer. These heights were directly proportional to the sample concentration. The heights and their corresponding elution times were then printed out using a Commodore printer. This data was then processed by hand. The beginning and end of the profile was determined and the heights corrected for any minor base line movement. The second stage involved the computerized calculation of the MWD from these refractometer heights. Typically each profile consisted of approximately fifty heights, each height had to be typed into the computer manually. Naturally this method had the disadvantage that it was slow and tedious especially when large amounts of data was involved. Furthermore the process was prone to error since the data transfer relied on the accuracy of the operator.

To overcome these problems a program was written which combined data aquisition and storage with automatic calculation of the MWD, weight average M_W and number average M_N. The program also contained an override which allowed the operator to calculate the MWD manually if required.

The program was written in a modular form so that the data aquisition and storage could be kept separate from the calculations required to obtain the MWD. This had the advantage that it was easier to salvage data if a program error occurred. A listing of the program can be found in appendix 1.

The data acqusition stage of the program simply involved the conversion of the electrical signal produced by the refractometer into a normalised height which could be used by the computer.

At the moment of sample injection the program was started. The computers internal clock was set to zero and after a two second delay the first reading from the refractometer was taken. After five readings had been obtained an average was made. This value was then stored within an array within the computers memory, the computer then reset itself and the cycle started again over the next ten second interval. The refractometer heights and elution times were displayed on the VDU to aid the operator. An interval timer was used to terminate the data acquisition when the appropriate time period had been completed. Normally the timer was set to operate at one minute after the glucose reference peak had eluted. The computer program had been developed so that it could be used to either determine the elution volumes of the glucose and high molecular weight dextran standards or to determine the elution profile from a sample.

If the elution volumes for the two reference peaks were required the computer would scan the data array until a threshold height was found, after which the computer would compare the heights until the peak height had been obtained. The corresponding elution time and hence the elution volume were then calculated. These values would then be stored and the program would repeat this process for the second peak.

The method used to determine the elution profile from a sample was very similar to the method mentioned above. Once the data had been stored the computer would calculate a mean base line from a three minute interval just before the start of the peak. The data was then tested until a set deviation above this mean base line was found. This identified the start of the peak. Although this method may appear simple it proved to be very effective since the refractometer base line was very stable.

After the start of the profile had been determined the computer calculated the peak height and the end of the profile. Finding a suitable method to calculate the end point was more difficult, two methods were tried. Initially the same approach was used, as was used to determine the beginning of the profile, but this method was shown to be inconsistent under normal working conditions. The main problem was that the base line would often shift slightly during analysis. Furthermore the base line noise was normally greater since remnants of the sample would be present for several minutes after the actual profile had been completed. These problems were overcome by considering the rate of change within the data rather than magnitude of the data. This method worked well since the profiles normally had a steep rise and fall.

Once the heights had been obtained from the raw data they could be used to calculate the MWD.

The calibration method discussed in section 3.3.3 was used where;

$$Mi = b_5 + \exp[b_4 + b_1 (K_{di}) + b_2 (K_{di})^2 + b_3 (K_{di})^3] \qquad \ldots 4.6$$

$$\text{and } K_{di} = \frac{V_i - V_o}{V_t - V_o} \qquad \ldots 4.7$$

where V_o is found using high molecular weight dextran and V_t by using glucose.

The weight fraction of each component was found using the chromatogram height for each component (hi).

$$\text{Weight fraction} = \frac{\text{chromatographic height, hi}}{\text{Sum of chromatographic heights. } \Sigma hi} \quad \ldots 4.8$$

Due to the polydisperse nature of dextran it is not normally possible to characterize it by a single molecular weight. To overcome this problem various averages can be used. The most common are:-

$$\text{Weight average, } M_W = \frac{\Sigma hiMi}{\Sigma hi} \quad \ldots 4.9$$

$$\text{Number average, } M_N = \frac{\Sigma hi}{\Sigma hi/Mi} \quad \ldots 4.10$$

For a polydisperse polymer M_W is always greater than M_N. The values are the same for a monodisperse polymer.

Polydispersity is often used to describe the breath of the molecular weight distribution. The polydispersity (D) is defined as;

$$D = \frac{M_W}{M_N} \quad \ldots 4.11$$

The polydispersity ratio is 1.0 for a monodisperse sample, typically commercial polymers have ratios in the range 2-20.

5.0 THE ULTRAFILTRATION CASCADE

5.0 THE ULTRAFILTRATION CASCADE

5.1 INTRODUCTION

Both Vlachogiannis [5] and Poland [6] used a variety of batch ultrafiltration systems to produce a clinical dextran within the British Pharmocapiea (BP) specification of 7.5% below 12,000 MW. Although the correct specification could be obtained they found that there was a significant loss of 'saleable' material. To overcome this problem Poland considered the use of an ultrafiltration cascade. The ultrafiltration cascade constructed by Poland was based on a system proposed by Cooper [49]. Cooper showed theoretically that a diafiltration cascade would improve the efficiency of separation and also reduce the amount of diafiltrate required, however no practical system was ever produced. A schmatic diagram of Coopers system can be found in figure 2.20.

The principle of operation is simple, a counter-current movement of the retentate and permeate products occurs along the cascade, for example considering stage (K), the permeate from this stage is transferred to stage (K+1) and the retentate to stage (K-1). The permeate from stage (K-1) is transferred to stage (K) and is used as diafiltrate in this stage. This process being repeated along the cascade. In Cooper's system the fresh feed enters into stage K and the fresh solvent into stage one. Naturally the permeate which is to be recycled contains a mixture of the impurity and the lost solute. If the solute has a higher rejection coefficient than the impurity then the solute will be recaptured in preference to the impurity, hence an overall improvement of separation will occur.

Using 'Process' (written by Simulation Sciences Ltd) a computer mass balance package, Poland assessed the optimum number of stages for his ultrafiltration cascade. He showed that there was little to be gained by extending the system above four stages since only a marginal improvement in efficiency occurred with the addition of subsequent stages. Furthermore the number of stages which could be incorporated into the cascade was limited by the memory of the BBC model B microcomputer used for the computer control of the cascade.

Using four Amicon 5000 MW cut-off ultrafiltration membranes (code HIP5-20) Poland investigated the possibility of removing material below 12,000 MW from a dextran polymer (code RB5R) supplied by Fisons Pharmaceuticals.

Poland found that the cascade did indeed operate in a manner predicted by Cooper. When the average batch rejection profiles of the membranes used were compared to the cascades rejection profile a cross-over point was found at, or close to, the nominal cut-off of the membranes used. Above this point the rejection was enhanced, below it the rejection was significantly reduced. Unfortunately Poland was unable to consider how the operating parameters such as feed concentration, feed distribution, number of diavolumes used and membrane characteristics would effect the performance of the cascade.

5.2 EXPERIMENTAL CASCADE EQUIPMENT

A detailed schematic diagram of the ultrafiltration cascade and a process description can be found in figure 5.1

Several significant changes were made to the original cascade to improve the systems flexibility and reliability. Initially the volume of permeate collected within each stage was fixed at two litres. The permeate volume was measured by a single float level switch located on

Figure 5.1 Schematic Diagram of the Four Stage Ultrafiltration Cascade and Equipment Description

Key	Item	Description
D	Diafiltration tank	four units each of litre volume manufactured in stainless steel.
F	Feed/Retentate tanks	four units each of 1 litre volume manufactured in stainless steel.
P	Permeate collection tanks	four units each of 1 litre volume manufactured in stainless steel.
LF	Float level switch on feed tanks	Supplied by RS Components, Birmingham.
LP	Capacitance level controller for permeate collection tanks	four units supplied by RS Components
FP	Back-up float level switches for permeate collection tanks	four units supplied by RS Components.
LP	Capacitance level controller for diafiltration feed tank	1 unit supplied by RS Components.
LD	Back-up float level switch for diafiltration feed tank	1 unit supplied by RS Components.
M	Ultrafiltration membrane	Four units - Amicon H1P5-20 or Amicon H1P10-20
PH 1,2,3,4	Peristaltic pump	Two dual head variable speed masterflex pumps flow rate 16.8 to 1680 cm^3/min supplied by Barrel and Tatlock, England.
PG	Pressure Gauge	four units 207 KPa full scale deflexion.
NV	Needle valve	-
PS	Pressure switch	Type DCM1 Texcel Ltd, St Albans, Herts
V	AC Solenoid valves	23 units

Key	Item	Description
G	Glass filters	Porous glass filter (grade 2)
NF	New feed to stage	-
PF	Permeate flux from membranes	-
RP	Final retentate product	-
W	Permeate waste from cascade	-

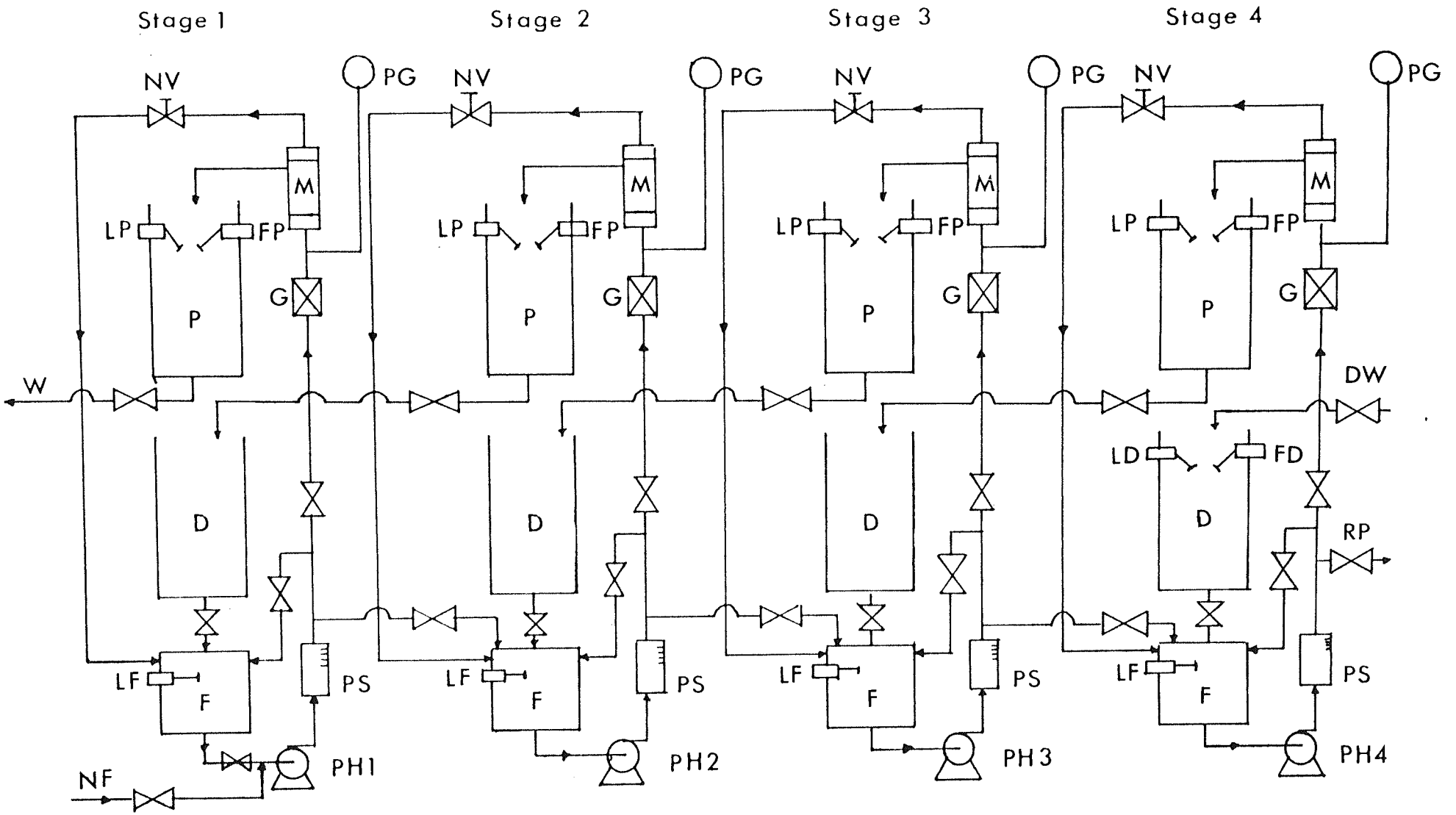

Figure 5.1 A Detailed Schematic Diagram of the UF Cascade

Figure 5.2 Photograph of the Ultrafiltration Cascade

the side of the tank, naturally these could not be adjusted. Furthermore they were difficult to fit and hence obtaining a precise volume was difficult. These units were replaced by capacitance level controllers; each level controllers consisted of two probes which could be used to measure upper and lower limits within the tank. This system worked well with dextran solutions, however when used with deionised water these level controllers occasionally failed to operate correctly. To check that the tanks had filled correctly a back-up level controller was employed, this consisted of a float type level switch attached to the end of an adjustable rod.

On several occasions the computer control program was scrambled by spikes and interruptions in the mains power supply. This was a particularly serious problem as the solenoid valves tended to remain open, rather than fail closed. Since the cascade was connected to a 100 litre deionised water tank this was not a satisfactory state. Once the program had been scrambled it was impossible to continue the run, hence it was felt that a fail safe switch in the mains supply would be the best approach. Since the solenoid valves would automatically shut when the power was switched off the run would not be spoilt and could be restarted once the fault had been corrected.

Also the lifetime of the silicon peristaltic piping used in the peristaltic pump was far from satisfactory at 100 hours of continuous use. This was replaced by Norprene tubing with a lifetime of up to 1000 hours, however a new Marprene variety with a 3000 hour life span later became available.

The opening and closing of the solenoid valves was accomplished by using a BBC model B microcomputer via solid state relays (supplied by RS Components Birmingham). These relays were rated for a continuous 2.5 amps and 250 volts, while the solenoid valves operated at 240 volts and 100 milli amps. Although the relays were rated well above the solenoid valves, high voltage and current spikes generated by the solenoids caused an annoying number of relay failures. Anti-surge suppressors were fitted, and the operating voltage was reduced from 250 to 160 volts, but neither approach was successful. Finally the relays were replaced by a heavy duty variety rated at 25 amps and 250 volts. This required extensive redesign of the control board since these units were far larger than before. After these relays were fitted no further failures occurred.

The software was also up-dated to handle the new level controllers. Several new alarm conditions were also added. There were a variety of alarm modes, each resulted in the suspension of the operating cycle until the fault was corrected by the operator. These alarm modes will be discussed in more detail later in this section. The software was modified further to allow the number of stages in operation to be varied between two and four. Both the electronics and machine code software used for controlling the rig was developed by D Bleby (Electronics Workshop, Aston University).

To prepare the cascade for operation the following steps must be followed:

The mains power for the computer and rig was switched on at the mains isolation switch. The software was then loaded into the BBC microcomputer using a five and a quarter inch floppy disc drive. When the software has been loaded the desired number of stages could be selected. Once this had been completed the feed (F) tanks could be filled with deionised water. Since the LF level controllers would show

empty, the valve VD1 would be open and so each F tank could be filled via the D tank. Once the F tanks were full the next stage was to check or adjust the level controllers on the P tanks, this was accomplished by filling the tanks with the correct volume of deionised water, if necessary the probes could then be adjusted until the level controllers operated. The liquid in the P tanks was then drained into the D tanks by manually opening the VP2 valves. Finally the D4 tank was filled with deionised water by opening valve VP7. The F and D tanks then contained the correct liquid volumes.

The peristaltic pumps (PH1-PH4) were adjusted to give the correct flow rate, this varied between 300 cm^3/min to 1000 cm^3/min depending on the membranes being used. After setting the flow rate the trans-membrane pressure could be set to 70 KPa using the needle valves (NV). The membranes (M) were protected from over pressure by the pressure switches (PS), the pressure switches were set at 104 KPa. If the inlet pressure exceeded this set value the pressure switch would automatically switch off the pump drive until the pressure had decreased. Once the flow rate and pressure had been set the rig could operate completely under computer control.

The computer cycle can be broken down into several steps.

(i) Permeate collection. See figure 5.3. During the permeate collection stage each of the four stages operated independently. To allow flow through the membranes the VF3 valves must be open. As the permeate collects within the permeate tanks (P) the level in the F tank would drop, this would be detected by the LF level controller. The computer would then open valve VD1 until enough diafiltrate had entered to restore the feed volume, the valve would then close. This would continue until the correct permeate volume had been collected.

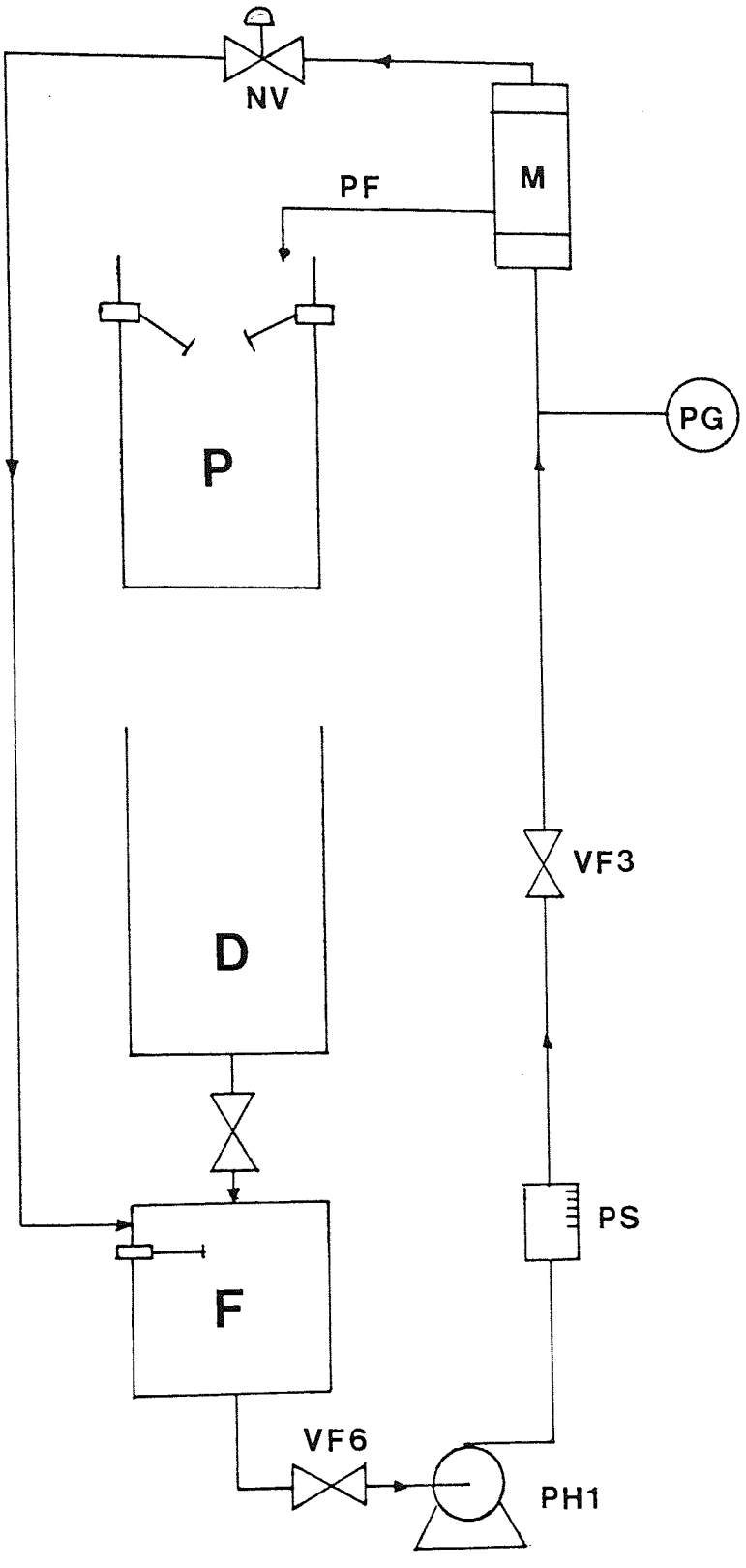

Figure 5.3 Diagram showing the Valves used for Setting Transmembrane Pressure, and for Permeate Collection from Stage One

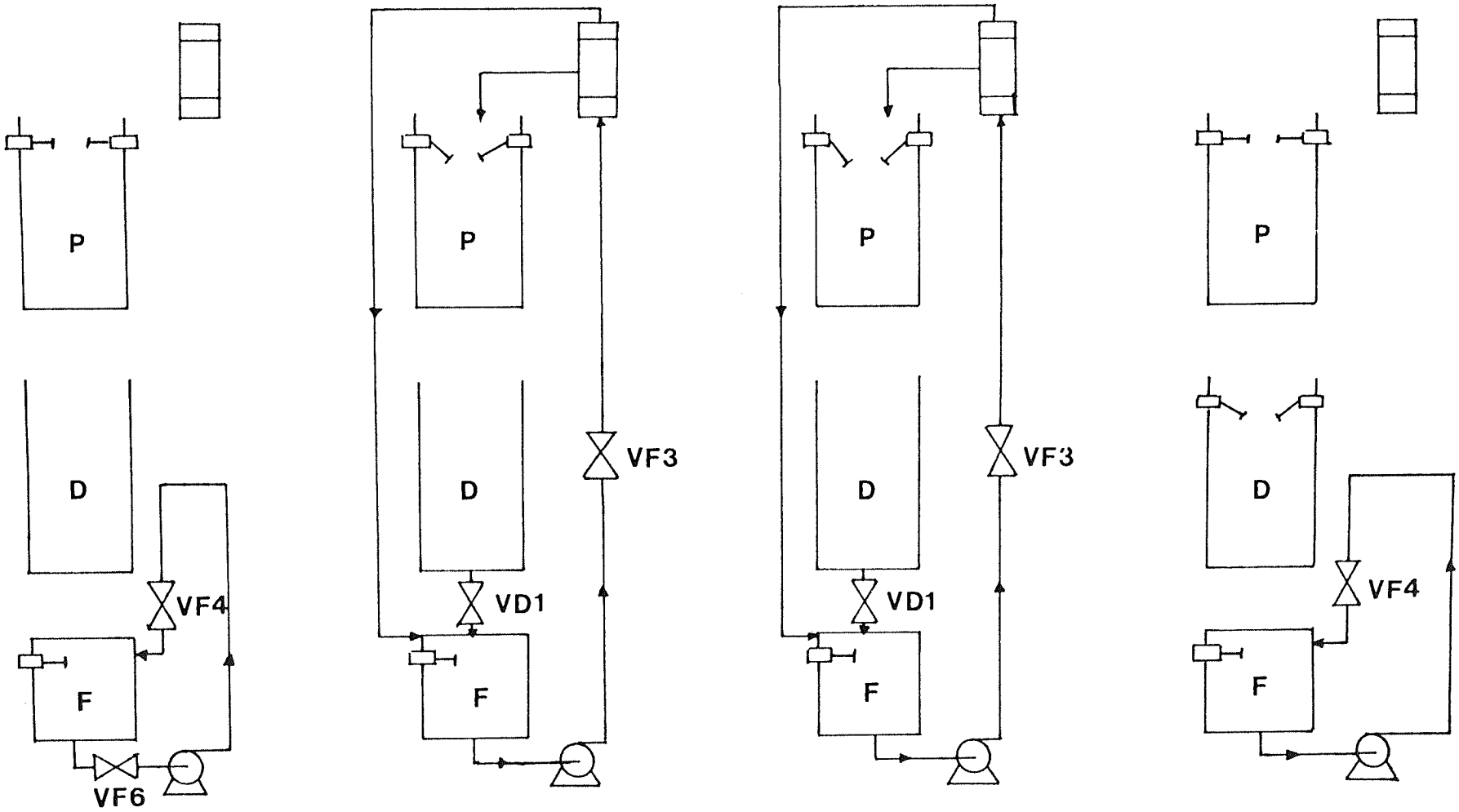

Figure 5.4 Diagram showing the Valves used when Stage 1 and 4 have Completed a Cycle and Stage 2 and 3 are still Collecting Permeate

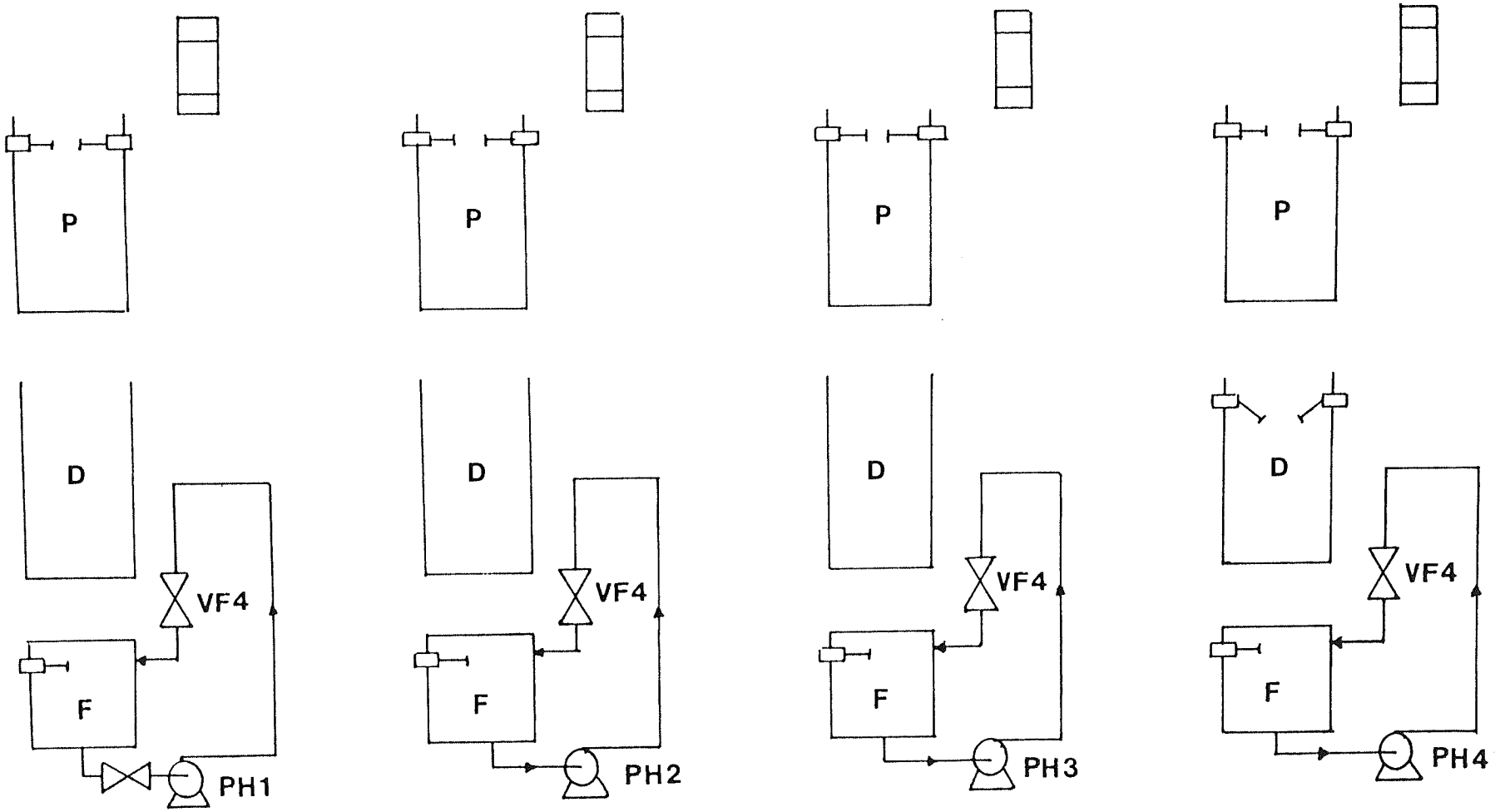

Figure 5.5 Diagram showing Valves used when Setting the Recirculation Rate

Once the LP level controller operates, the stage switches to a recycle mode. However if the back-up FP level controller had not operated then the computer would also go into an alarm mode until the level in the tank had been checked. Also if the LF level switch showed that the F tank was empty at the end of the cycle the computer would also go into an alarm mode.

(ii) As mentioned earlier each stage works independantly. Once a particular stage has finished collecting permeate the stage goes into a recycle mode where valve VD3 closes and VF4 opens. This stops the flow of retentate through the membrane and causes the continual recycle of the retentate back into the F tank. This process was repeated within each of the remaining stages as they finished collecting permeate. See figure 5.4.

(iii) When all of the stages had collected the desired volume of permeate, the recirculation valve VF4 on the final stage was closed and product valve VF6 was simultaneously opened. See figure 5.6. This drains the retentate product from the F tank. The product from tank four was the final retentate product from the cascade. The length of time valve VF6 (on stage 4) remained open was determined by a internal timer within the program.

(iv) The product from tank F within stage 3 can then be transferred to tank F within stage 4. See figure 5.7. This was achieved by closing VF4 on stage 3 and opening VF5 on stage 4. Once the LF switch on stage 4 showed full the transfer was stopped by closing valve VF5 on stage 4 and opening valve VF4 on stage 3.

This process was then repeated for the transfer from stage 2 to 3 and stage 1 to 2.

(v) Next fresh feed could be introduced into stage 1. See figure 5.8. This was accomplished by opening VF5 and closing VF6. Once the level controller showed that the tank was full, VF5 was closed and VF6 opened.

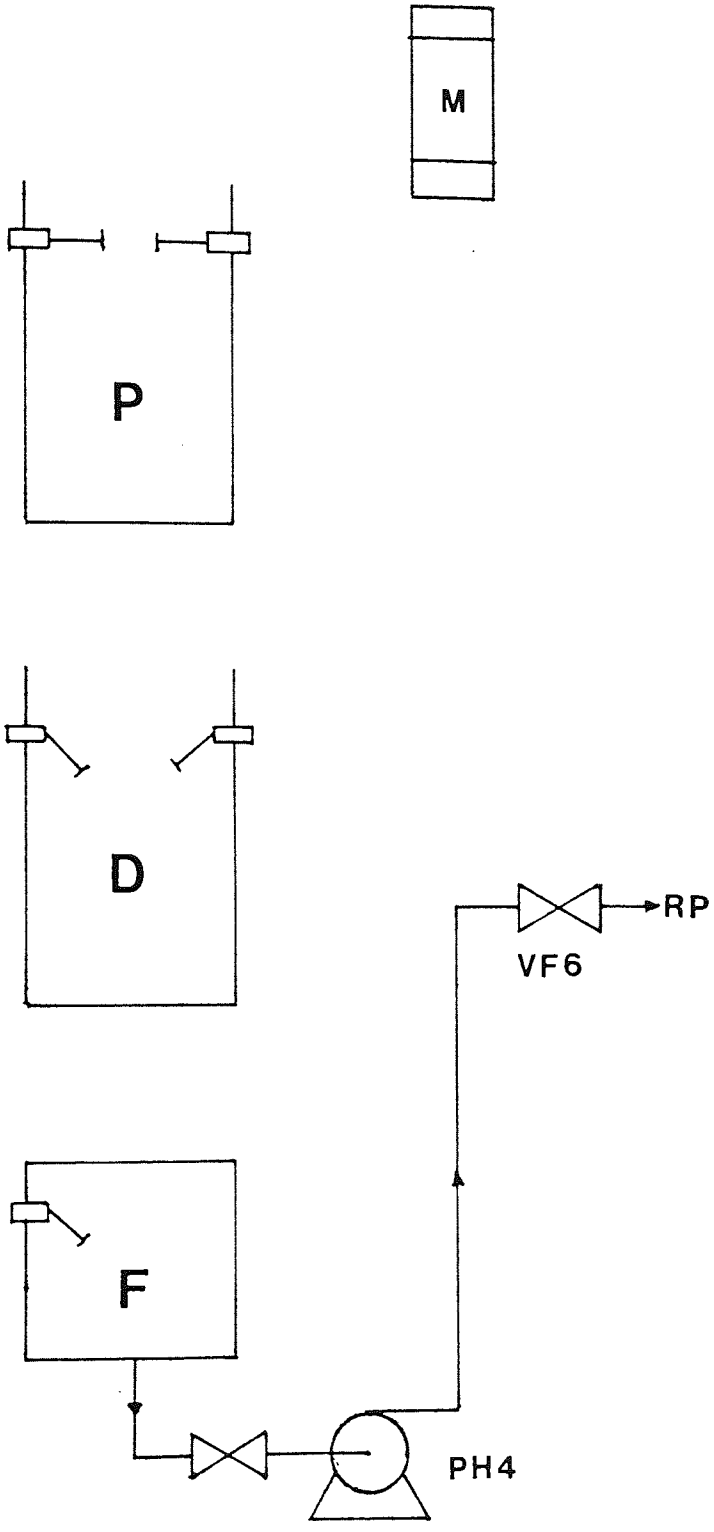

Figure 5.6 Diagram showing the Valves used for Draining the Product from Stage 4

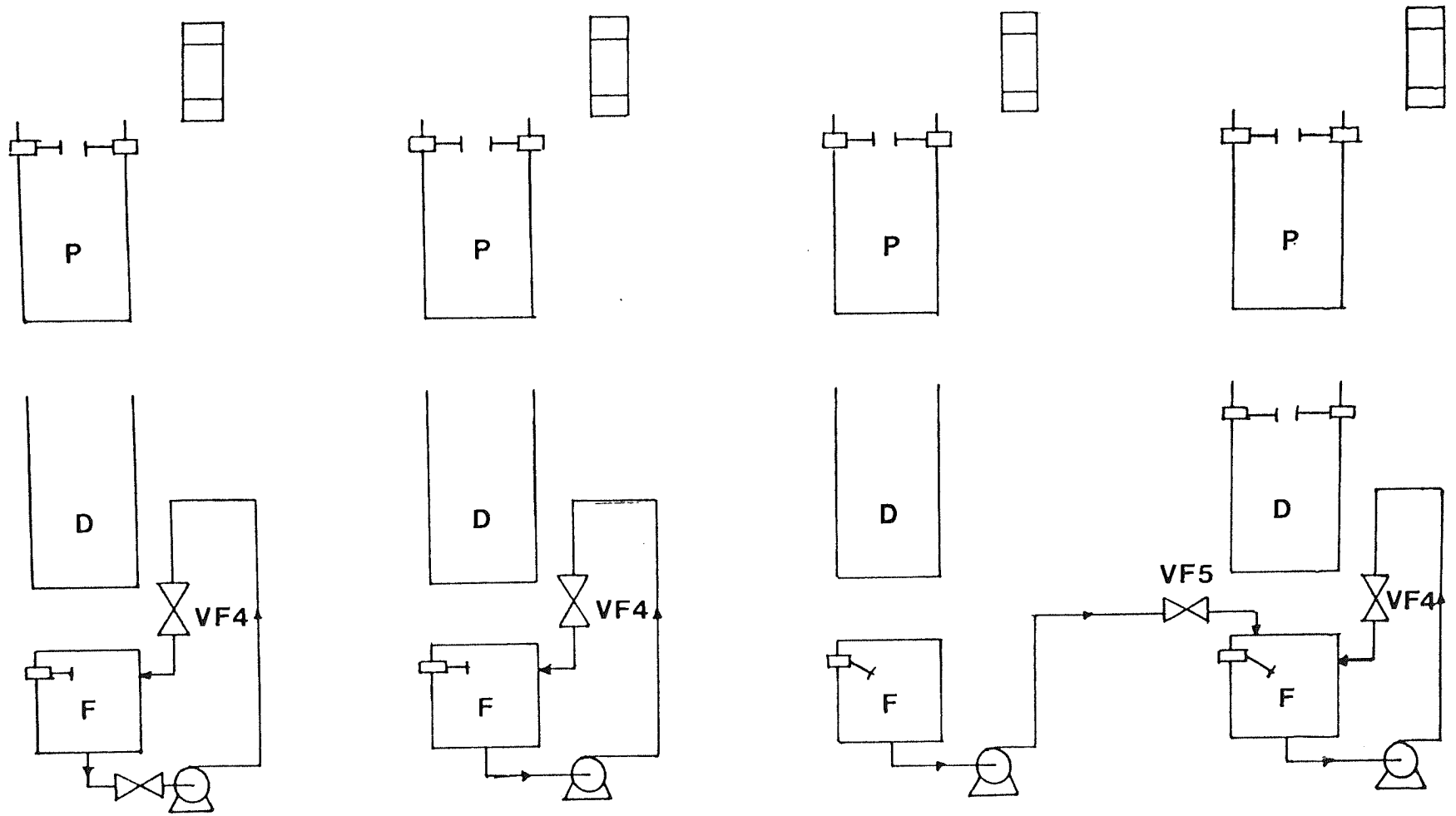

Figure 5.7 Diagram showing the Transfer of Product from Stage 3 to Stage 4

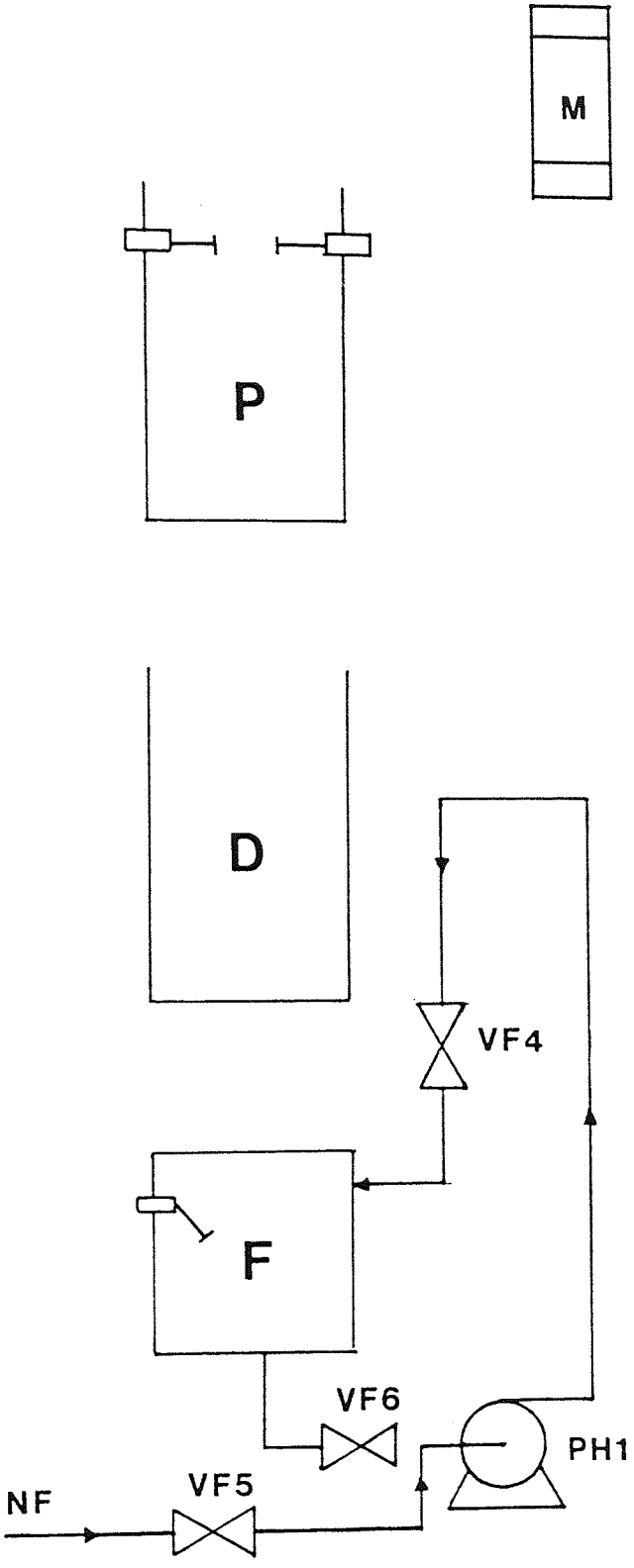

Figure 5.8 Diagram showing the Replenishment of Stage 1 with Fresh Feed

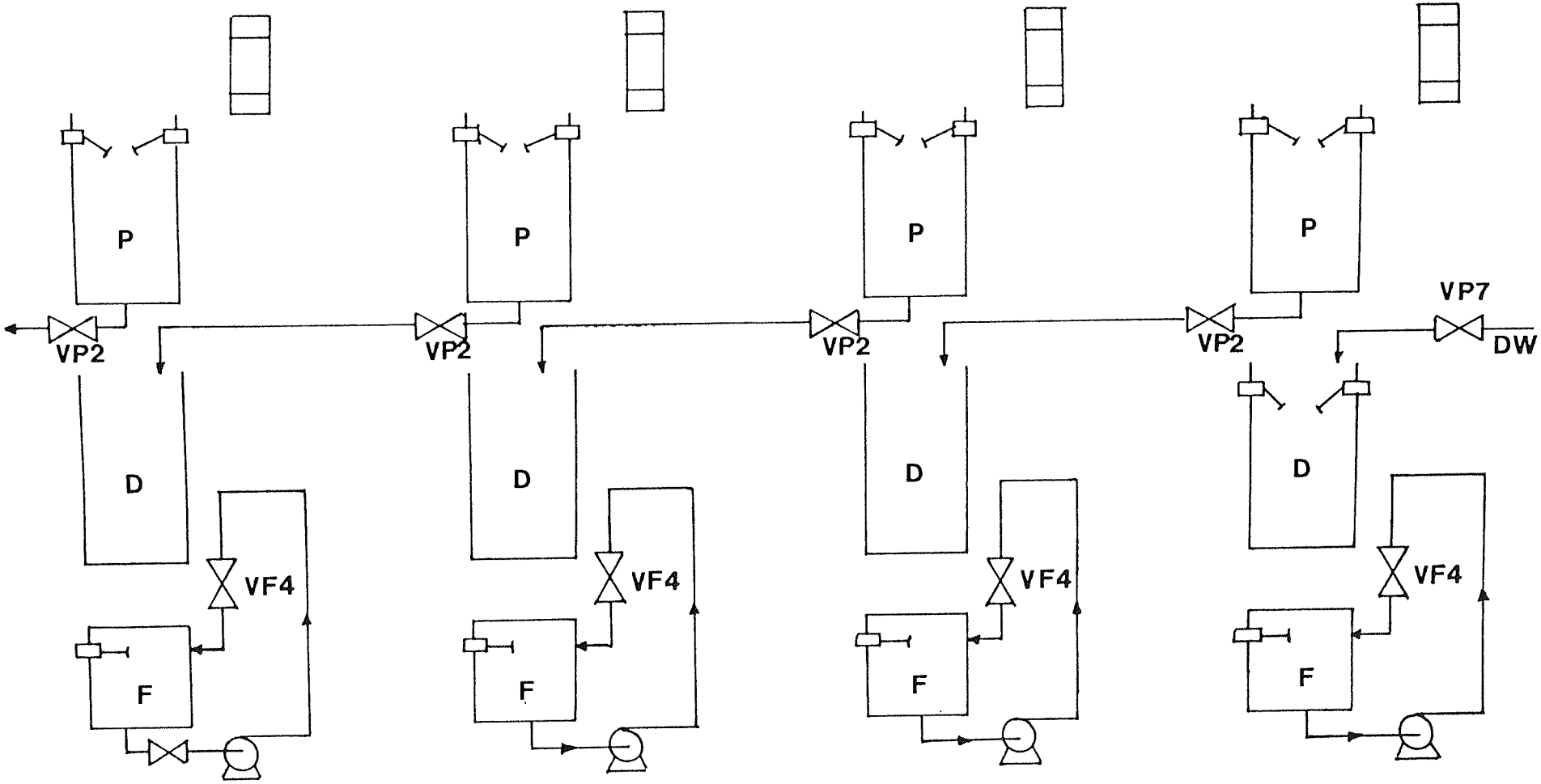

Figure 5.9 Diagram showing the Recycle of Permeate and the Addition of Fresh Solvent to Stage 4

(vi) The retentate transfer was followed by the permeate transfer. See figure 5.9. The VP2 valves were opened allowing the permeate from stage N to drain down into the diafiltration tank (D) of stage (N-1). The product leaving stage 1 was the final permeate product. When a LP level controller showed that a particular P tank was empty the appropriate VP2 valve was closed.

(vii) Finally the diafiltration tank (D) for stage 4 was filled with deionised water from the main storage tank. This was achieved by opening VP7 until the LD level controller operated, the valve was then closed.

(viii) The cycle was then complete and the program returned to step (i).

All the operations performed by the computer were displayed on the computer monitor. At all times the monitor displayed a flow diagram of the cascade. Valves which were closed were shown as green and those which were open were red. Similarly the level controllers which show empty were green and those which show full were red.

5.3 THE DEXTRAN FEED

The dextran used throughout these experiments was obtained from Fisons Pharmaceutical PLC, Cheshire. The dextransucrase enzyme used to produce the dextran was from the bacterium Luconostoc Mensenteroides. This strain of bacterium is well known and is used extensively for the manufacture of clinical dextran. The dextran produced by this enzyme is predominantly straight chained.

Two batches of dextran were used, code numbers RB5R and HZ1S. These were both syrup 1 products since the hydrolysate contained excessive amounts of low molecular weight dextran. The HZ1S feed was used almost exclusively to investigate the removal of material above 98,000 MW, the RB5R feed was used in the experiments involving the

removal of material below 12,000 MW.

There were unfortunately problems with the RB5R feed during the first stage of this research. There was sudden and unexpected change of the dextrans distribution. At first it was felt that the problem must be the analytical GPC equipment. The calibration was checked using the range of T fractions mentioned in section 4.3.4, however no change had occurred within their distributions. The change was finally traced to a barrel to barrel variation of the RB5R feed. Fortunately the distribution at the lower end of the molecular weight range remained unchanged. Since this feed was used for the fractionation of material below 12,000 MW this variation should not effect the comparability of the results. The same problem occurred with the HZ1S feed, however the variation was noticed before it could have any effect on the experimental program. The barrel to barrel variation found within the RB5R feed was far more severe than the BT1J feed, however this made it possible to investigate how the feed distribution would effect the operation of the cascade. Table 5.1 shows the barrel to barrel variation found within the two dextran batches.

5.4 REMOVAL OF DEXTRAN BELOW 12,000 MW

5.4.1 TESTING THE AMICON 10,000 MW CUT-OFF MEMBRANES USING BATCH DIAFILTRATION

Poland was able to show that the ultrafiltration cascade optimised the fractionation process. He also showed that the cross-over point occurred at 5000-6000 MW; this approximately matched the nominal cut-off of the Amicon membranes used. Using this approximate relationship it was reasonable to assume that a membrane with a quoted cut-off of 10,000-12,000 MW should produce the appropriate cross-over point at 12,000 MW.

Table 5.1 Variation found with the Barrels of the RB5R and HZ1S Batches

FISONS

Batch Code Number	%below 12000 MW	%change	%between 12000 & 98000 MW	%change	%above 98000 MW	%change
RB5R	25.0		61		14	
	24.63	-1.5	63.08	3.4	12.29	-12.21
HZ1S	24.31		67.016		8.674	
	31.01	+27.56	60.37	-9.91	8.62	-0.62
	25.04	+ 3.00	65.52	-2.23	9.44	+8.83

Since the performance of the Amicon membranes had been shown by Poland to be superior to those produced by the other major manufacturers such as DDS Ltd and Millipore, it was felt that it would be advisable to continue using these membranes. Therefore four Amicon H1P10-20 membranes were purchased.

These membranes were manufactured from polysulphone and were of a hollow fibre design. The hollow fibre cartridge contained approximately 300 fibres, each fibre had an internal diameter of 0.5 mm, this gave a surface area of 0.06 m^2.

All the membranes were tested on an Amicon DC2A module. A schematic diagram can be found in Figure 5.10. The equipment can be used in either a concentration, dialysis or diafiltration mode. However for the purpose of these experiments the diafiltration mode was used.

The transmembrane pressure was pre-set by a pressure cut-off switch which was incorporated into the DC2A unit. The switch was set to cut-off above 70KP, this therefore ensured that the pressure was the same during all the experiments.

Since the cascade was designed to operate up to a maximum of 2 diavolumes it was felt that an extended analysis of all the membranes would be pointless. Therefore two of the membranes were analysed for up to nine diavolumes, the other two to half this number.

When the fourth Amicon membrane was tested it was found to be significantly different from the other membranes. The membranes rejected dextran far better than the others, in fact it had a rejection higher than some Amicon 5000 MW cut-off membranes.

Figure 5.10 The Amicon DC2A UF System - Diafiltration Mode

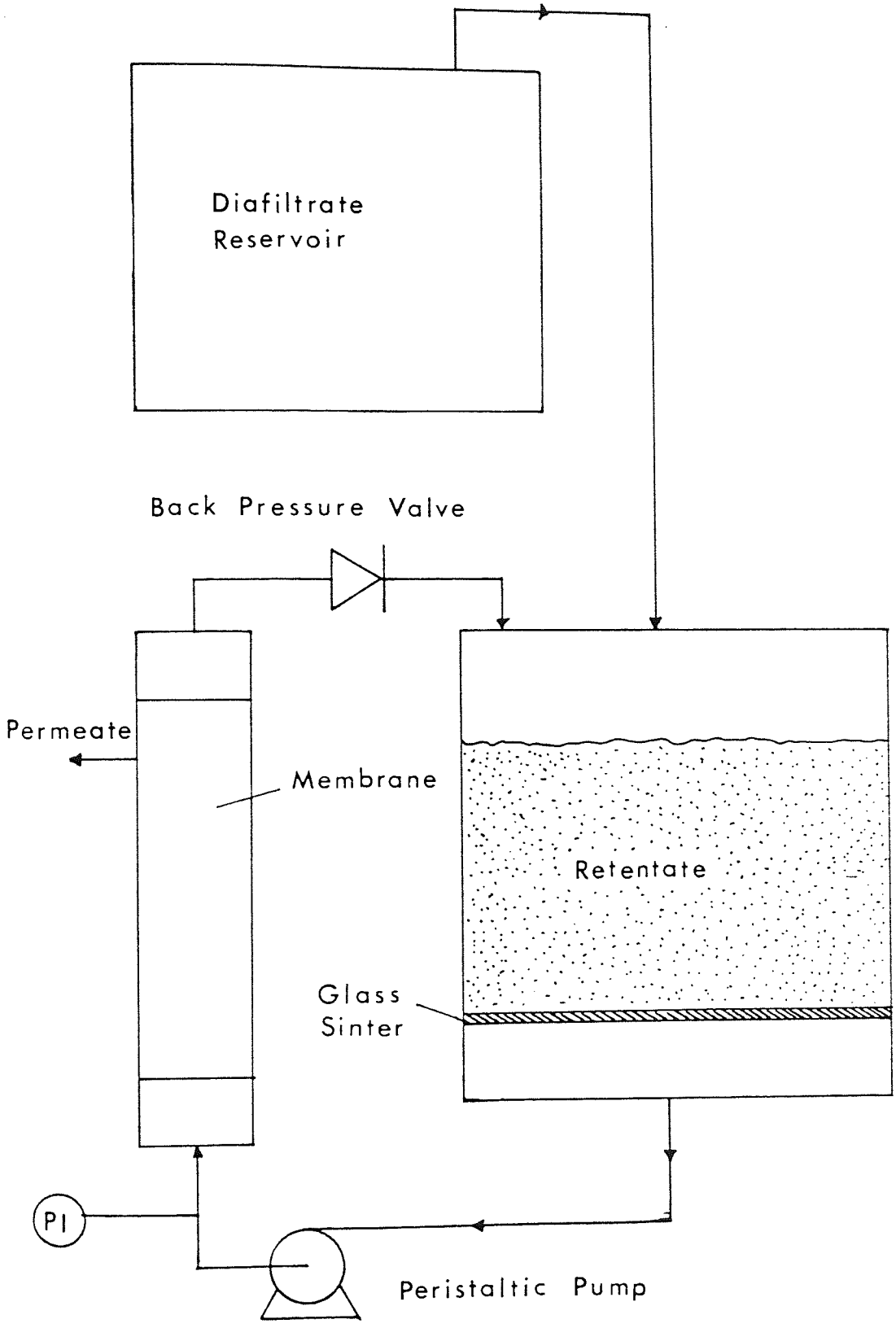

Table 5.2 Operating Conditions Used to Test the Amicon Membranes

Equipment Used	:	Amicon DC2A
Membrane Area	:	600 cm^2
Retentate Recirculation Rate	:	300 cm^3/min
Transmembrane Pressure	:	70KPa
Operating Temperature	:	20°C
Feed	:	2% W/W Fisons batch RB5R
Mode of Operation	:	Diafiltration

Definitions:

$$\text{Number of Diavolumes} = \frac{\text{Volume of permeate collected}}{\text{Volume of feed solution}}$$

$$\text{Efficiency of Retention} = \frac{\text{Weight of saleable material in product}}{\text{Weight of saleable material in feed}}$$

$$\text{Efficiency of Removal} = \frac{\text{Weight of material below 12000 MW in product}}{\text{Weight of material below 12000 MW in feed}}$$

Table 5.3 Diafiltration results for AMICON 10,000 MW cut-off membrane number 1

		RETENTATE PRODUCT				
Number of Diavolumes used	Concentration (g/100g Sol)	% below 12000 MW	Efficiency of Removal (%)	% between 12000 - 98000 MW	Efficiency Retention (%)	% above 98000 MW
Feed	1.856	25.02	0	61.0	100	13.98
1	1.577	21.83	25.9	63.32	88.16	14.83
2	1.322	16.56	52.83	66.7	77.82	16.74
3	1.159	12.83	68.12	66.83	68.37	20.34
4	1.068	10.52	75.88	68.24	64.31	21.24
5	0.941	8.33	83.2	68.32	56.71	23.35
6	0.763	6.67	89.05	67.7	45.58	25.63
7	0.712	5.96	90.95	66.92	42.05	27.12
8	0.661	4.59	93.53	67.11	39.13	28.30
9	0.651	2.46	96.55	69.86	40.16	27.68

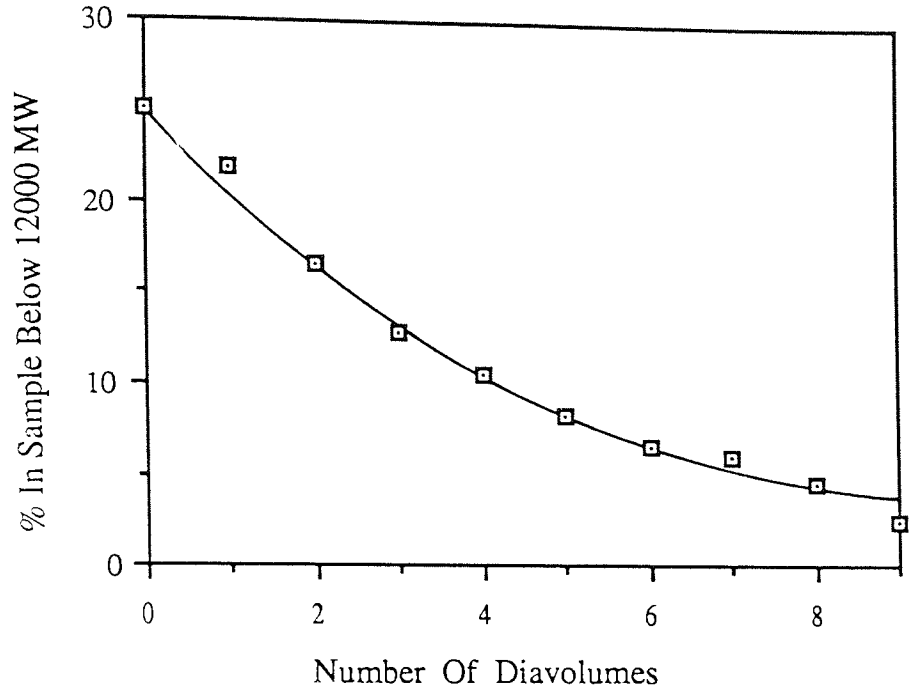

Figure 5.11 How the Number of Diavolumes used Effects the Percentage of the MWD below 12,000 MW in the Retentate

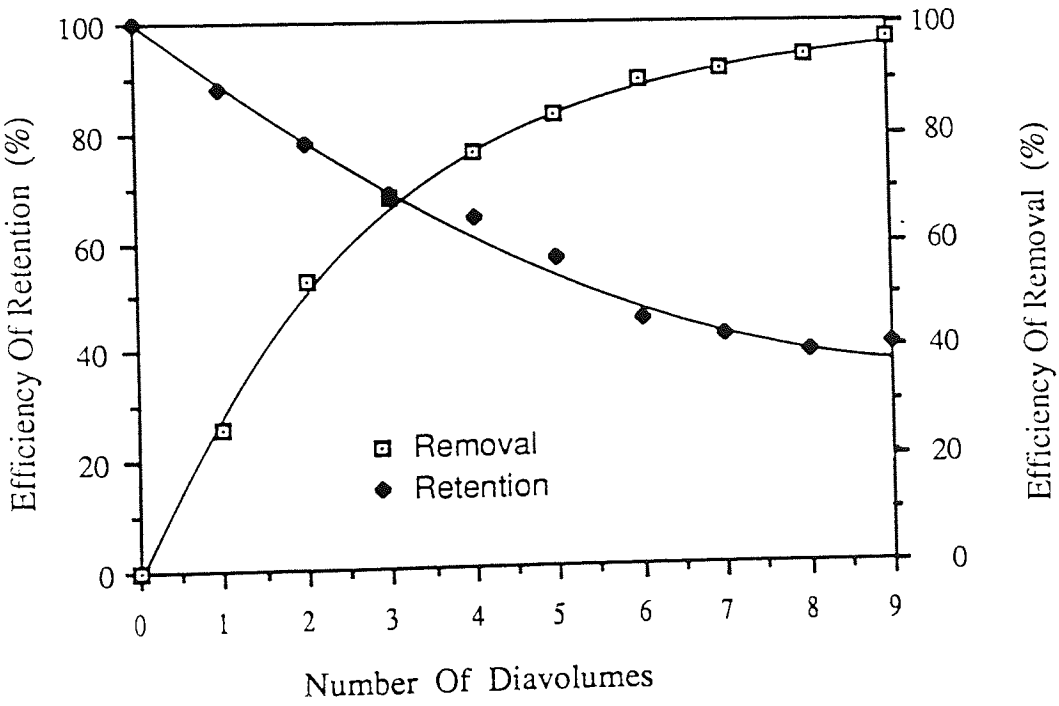

Figure 5.12 The Relationship between Efficiency and Number of Diavolumes used. Membrane Number 1

Table 5.4 Diafiltration Results for Amicon 10,000 MW cut-off Membrane Number 2

		RETENTATE PRODUCT				
Number of Diavolumes used	Concentration (g/100g Sol)	% below 12000 MW	Efficiency of removal (%)	% between 12000 - 98000 MW	Efficiency of Retention (%)	% above 98000 MW
Feed	2.3	25.0	0	62.51	100	12.49
1	1.802	22.91	28.21	65.23	81.84	11.86
2	1.526	20.1	46.66	67.35	71.47	12.55
3	1.42	18.21	55.04	68.73	67.97	13.06
4	1.32	16.32	62.6	70.52	64.78	13.14

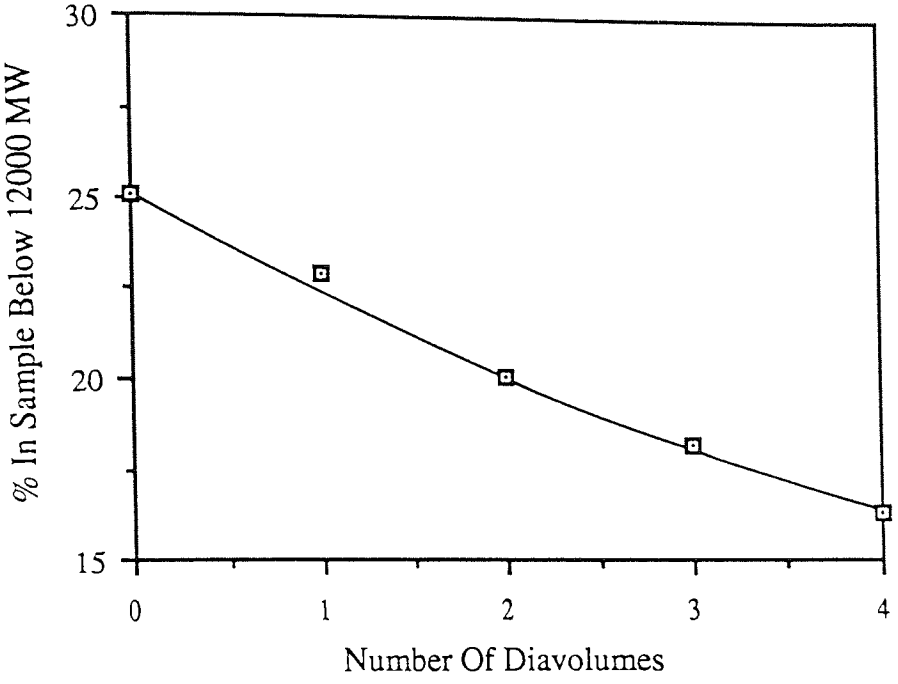

Figure 5.13 How the Number of Diavolumes used Effects the Percentage of the MWD below 12,000 MW in the Retentate

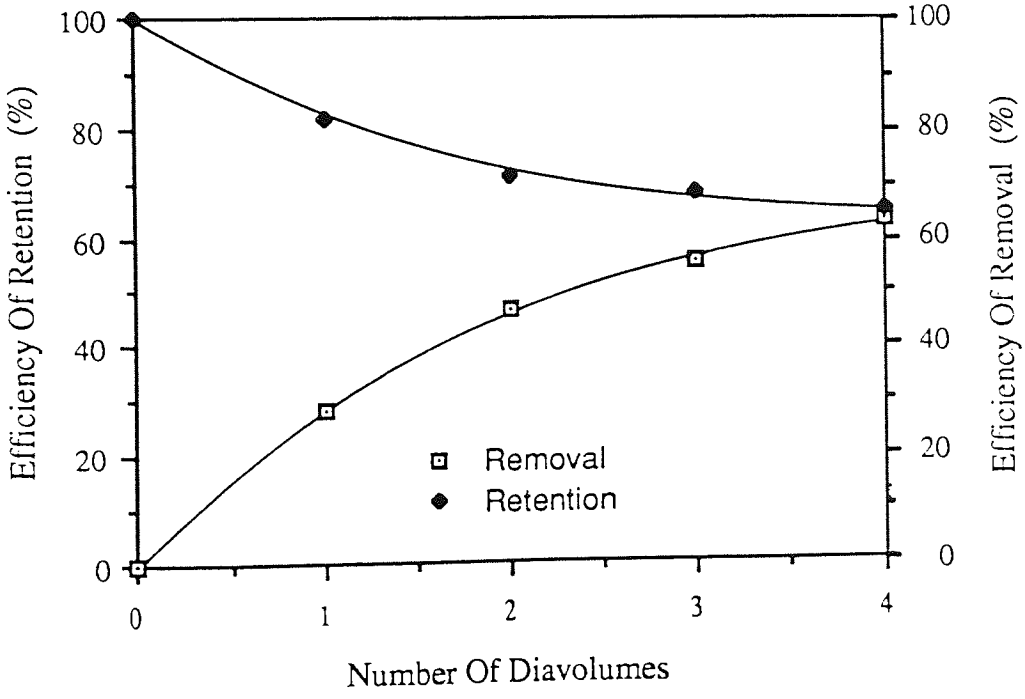

Figure 5.14 The Relationship between Efficiency and Number of Diavolumes used. Membrane Number 2

Table 5.5 Diafiltration Results for the Amicon 10,000 MW cut-off Membrane Number 3

	RETENTATE PRODUCT					
Number of diavolumes used	Concentration (g/100g Sol)	% below 12000 MW	Efficiency of removal	% between 12000 - 98000 MW	Efficiency of retention	% above 98000 MW
Feed	2.15	25.0	0	62.51	100	12.49
1	1.704	17.29	45.25	63.32	80.28	15.14
2	1.42	12.28	67.59	66.7	70.46	18.14
3	1.17	10.14	78.02	66.83	58.17	19.24
4	0.992	8.15	84.91	68.24	50.37	20.43
5	0.99	6.42	88.27	68.32	50.3	22.20

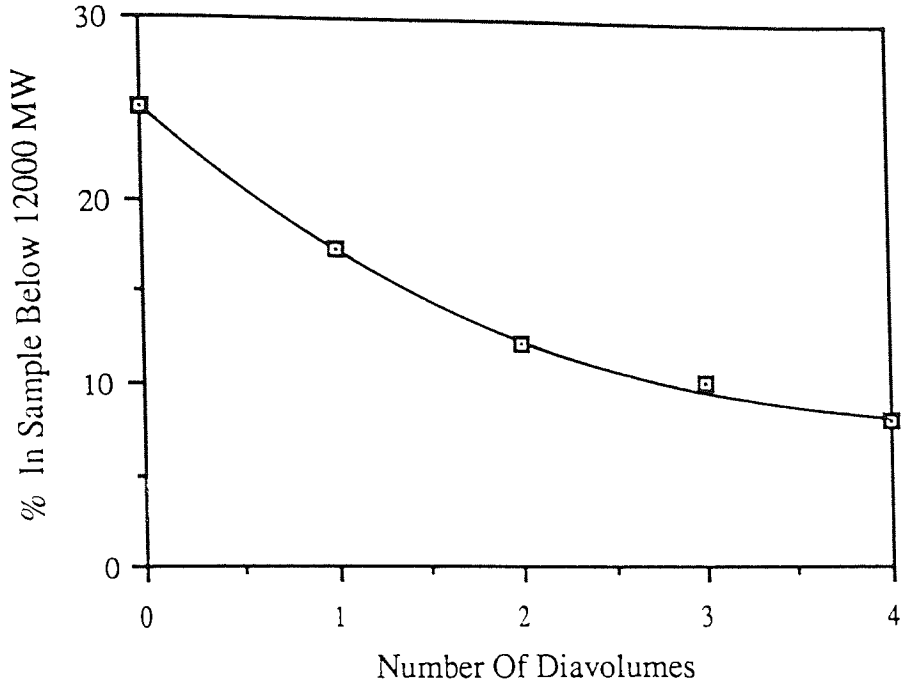

Figure 5.15 How the Number of Diavolumes used Effects the Percentage of the MWD below 12,000 MW in the Retentate

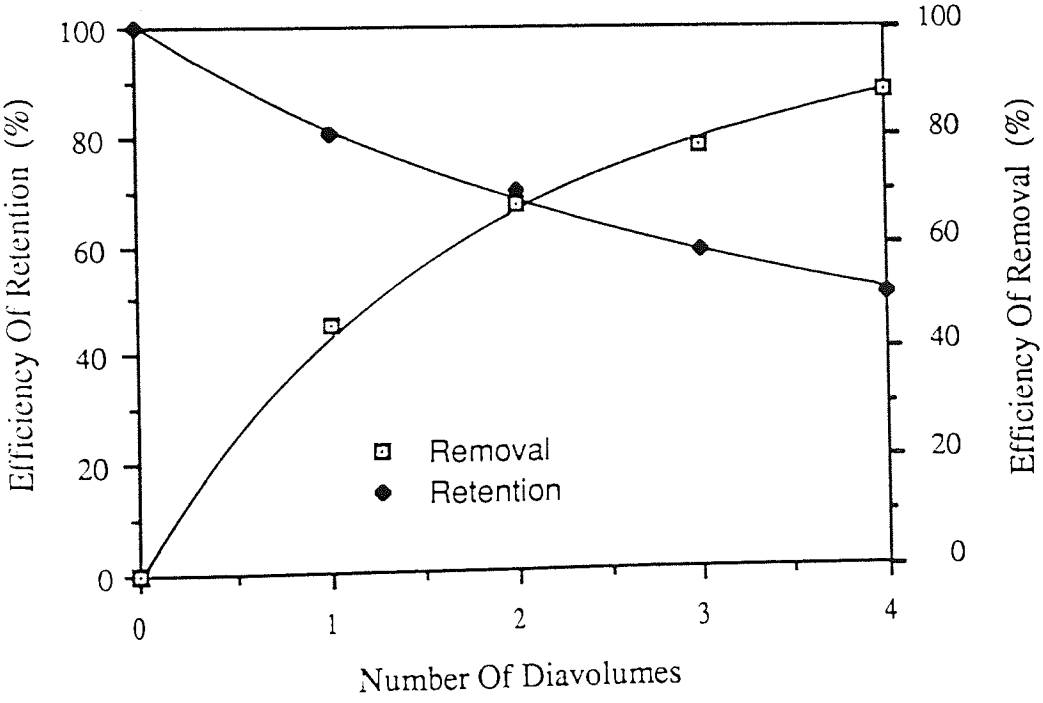

Figure 5.16 The Relationship between efficiency and Number of Diavolumes used. Membrane Number 3

Table 5.6 Diafiltration Results for the Amicon 10,000 MW cut-off Membrane Number 4

	RETENTATE PRODUCT					
Number of diavolumes used	Concentration (g/100g Sol)	% below 12000 MW	Efficiency of removal	% between 12000 - 98000 MW	Efficiency of retention	% above 98000 MW
Feed	2.03	25.0	0	62.51	100	12.49
1	1.88	22.57	16.45	64.43	95.42	13.0
2	1.678	19.03	37.14	67.96	89.91	13.10
3	1.526	12.79	61.54	71.15	85.64	16.06
4	1.45	11.94	65.91	70.81	80.91	17.25
5	1.37	10.76	71.03	72.61	78.47	16.63
6	1.297	9.68	75.36	73.25	74.92	17.07
7	1.246	8.87	78.32	73.68	72.39	17.45
8	1.144	7.98	82.07	74.37	67.11	17.65

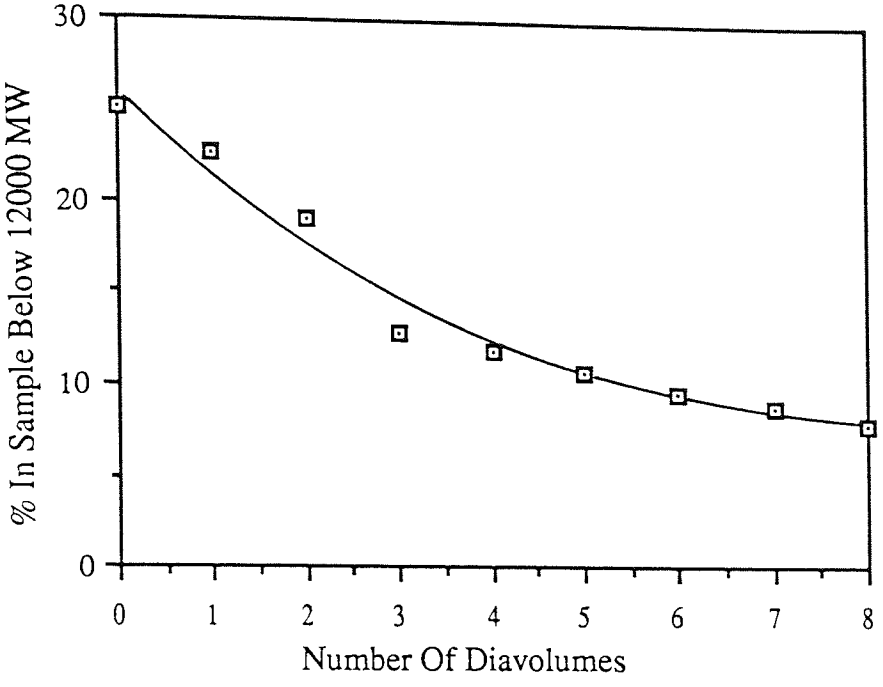

Figure 5.17 How the Number of Diavolumes used Effects the Percentage of the MWD below 12,000 MW in the Retentate

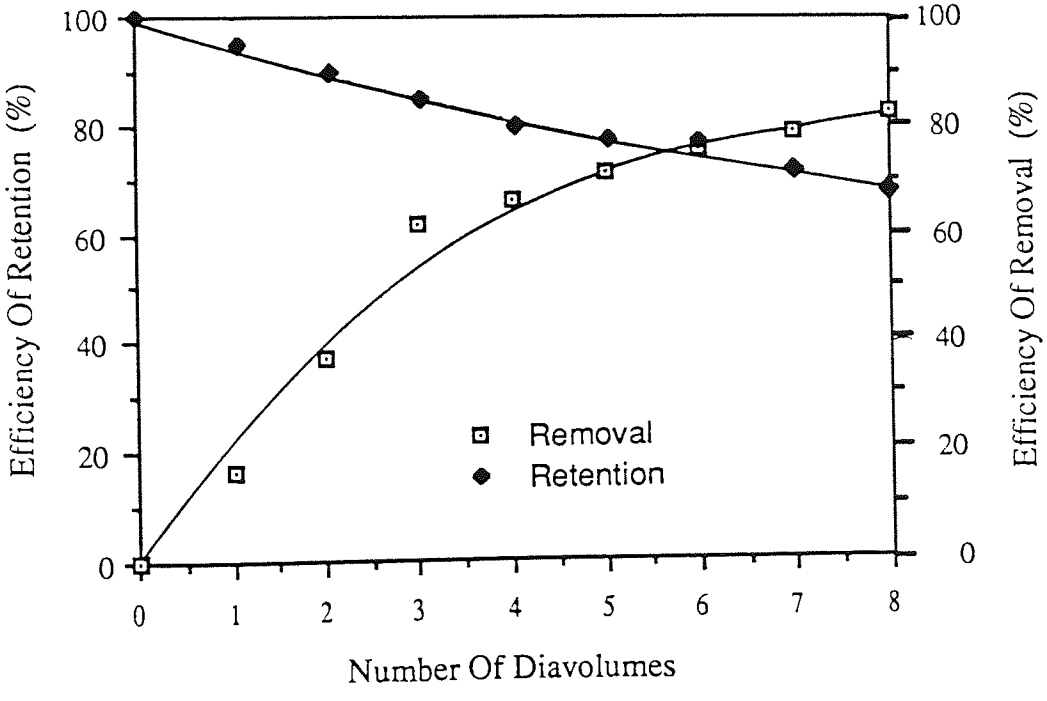

Figure 5.18 The Relationship between Efficiency and Number of Diavolumes used. Membrane Number 4

Table 5.7 Diafiltration Results for the Amicon 10,000 MW cut-off Membrane Number 5

		RETENTATE PRODUCT				
Number of diavolumes used	Concentration (g/100g Sol)	% below 12000 MW	Efficiency of removal	% between 12000 - 98000 MW	Efficiency of retention	% above 98000 MW
Feed	1.88	24.7	0	61.44	100	13.86
1	1.57	19.5	34.05	66.01	89.69	14.49
2	1.42	13.81	57.76	69.28	85.10	16.91
3	1.32	9.51	72.9	71.38	81.55	19.11
4	1.24	7.4	80.17	71.43	76.7	21.17
5	1.09	6.87	83.8	71.23	67.18	21.9
6	1.068	5.29	87.93	70.78	65.45	23.93
7	1.04	4.38	89.87	70.91	63.80	24.71
8	0.99	3.87	91.8	69.56	59.56	26.57
9	0.966	3.15	93.3	68.23	58.78	28.62

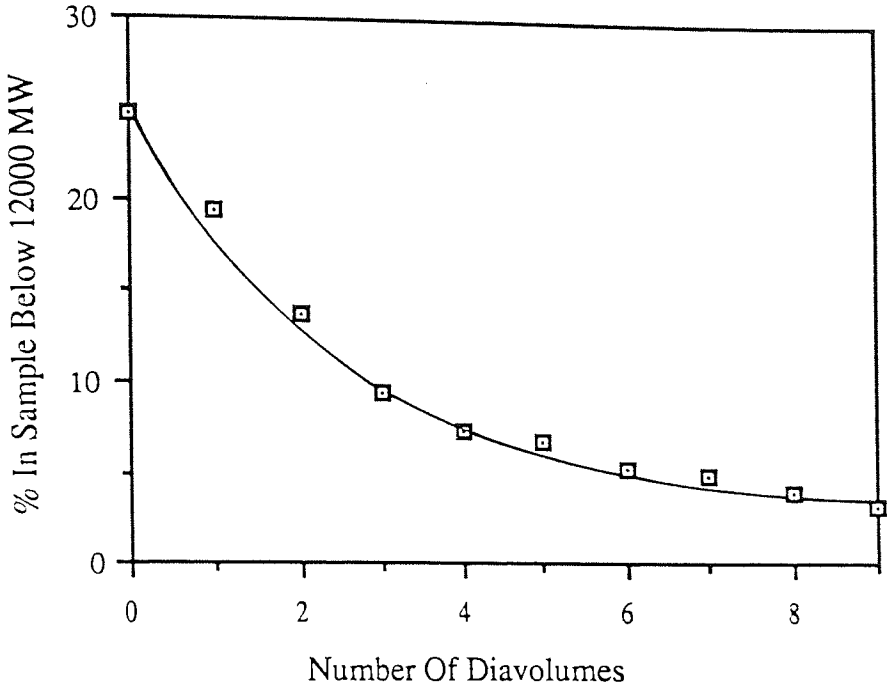

Figure 5.19 How the Number of Diavolumes used Effects the Percentage of the MWD below 12,000 MW in the Retentate

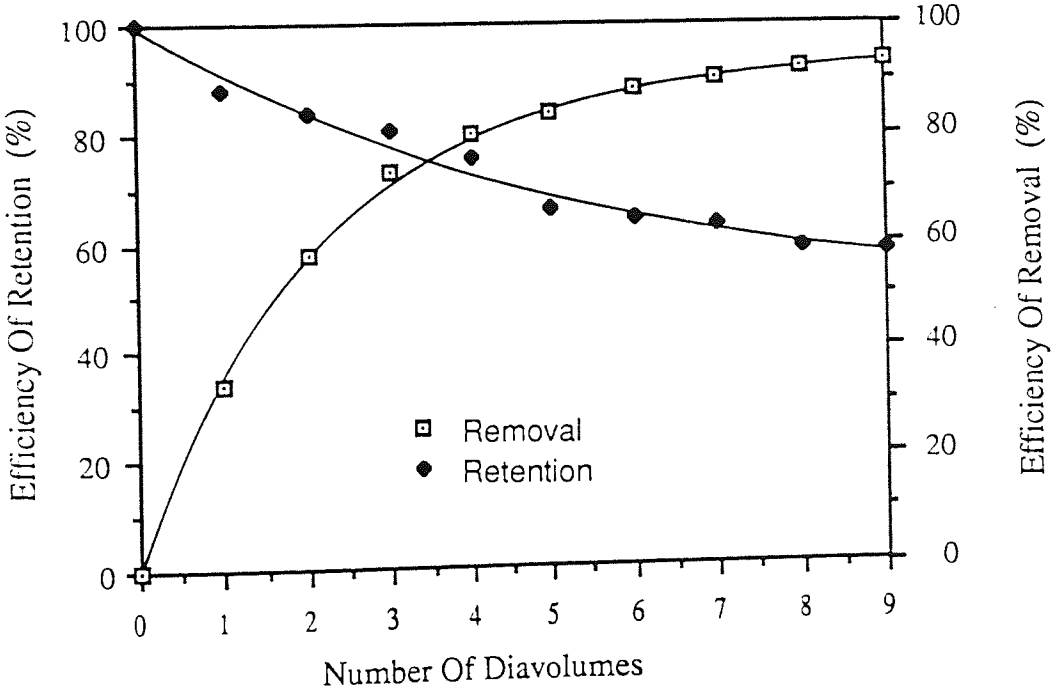

Figure 5.20 The Relationship between Efficiency and Number of Diavolumes used. Membrane Number 5

Since this membrane could not be classed as a typical 10,000 MW cut-off membrane it was returned to Amicon and replaced by another membrane.

The rejection curves for the five membranes after two diavolumes can be found in figure 5.21. Since all the membranes had the same nominal molecular weight cut-off it was surprising that the rejection curves varied so much. This degree of scatter must be a reflection of the inconsistency within the manufacturing process. Furthermore it must also show the limitations and dangers of using the overall rejection as a method of calculating the nominal molecular weight cut-off of a membrane.

The rejection curve for membrane number 2 also suggested that some of the 10,000 MW cut-off membranes could indeed be 5000 MW cut-off membranes which have not reached the correct specification.

Rather than considering the rejection data at a particular diavolume, the rejection of each molecular weight band can be followed as the number of diavolume increases. Figure 5.22 shows the results for a 10,000 MW cut-off membrane (number 5) and figure 5.34 the results for a 5000 MW cut-off membrane (number 5). The rejection of each band can be expressed as a form of isotherm. The gradient of a isotherm will reflect the membranes ability to reject a particular molecular weight. As the number of diavolumes used was increased the rejection obtained from the 10,000 MW cut-off membrane fell faster than the 5000 MW cut-off membrane, this is shown by the steeper isotherms. The differences between the 5000 MW cut-off and 10,000 MW cut-off membranes becomes more apparent as the molecular weight of the band being considered increases. These graphs show clearly the limitations of the batch diafiltration system. Using a 10,000 MW cut-off membrane to improve the removal of material below 12,000 MW also results in a greater loss of 'saleable' material. Typically six to seven diavolumes were required to obtain the

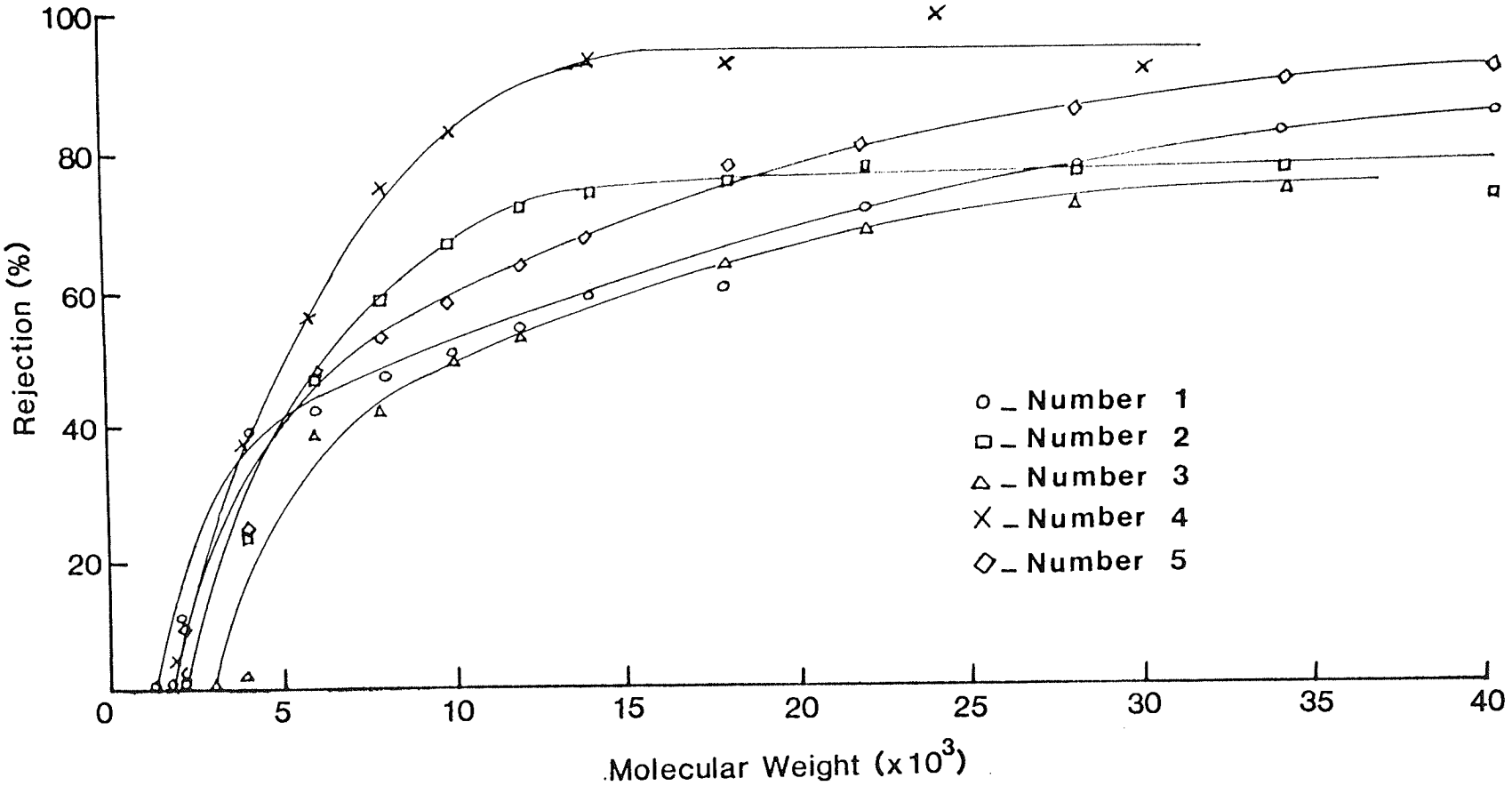

Figure 5.21 The Rejection Curves Obtained from the Five 10,000 MW Cut-off Membranes after Two Diavolumes

Figure 5.22 The Effect of Increasing the Number of Diavolumes used on the Rejection of a Range of Molecular Weight Bands in the Dextran Sample. 10,000 MW cut-off Membrane used.

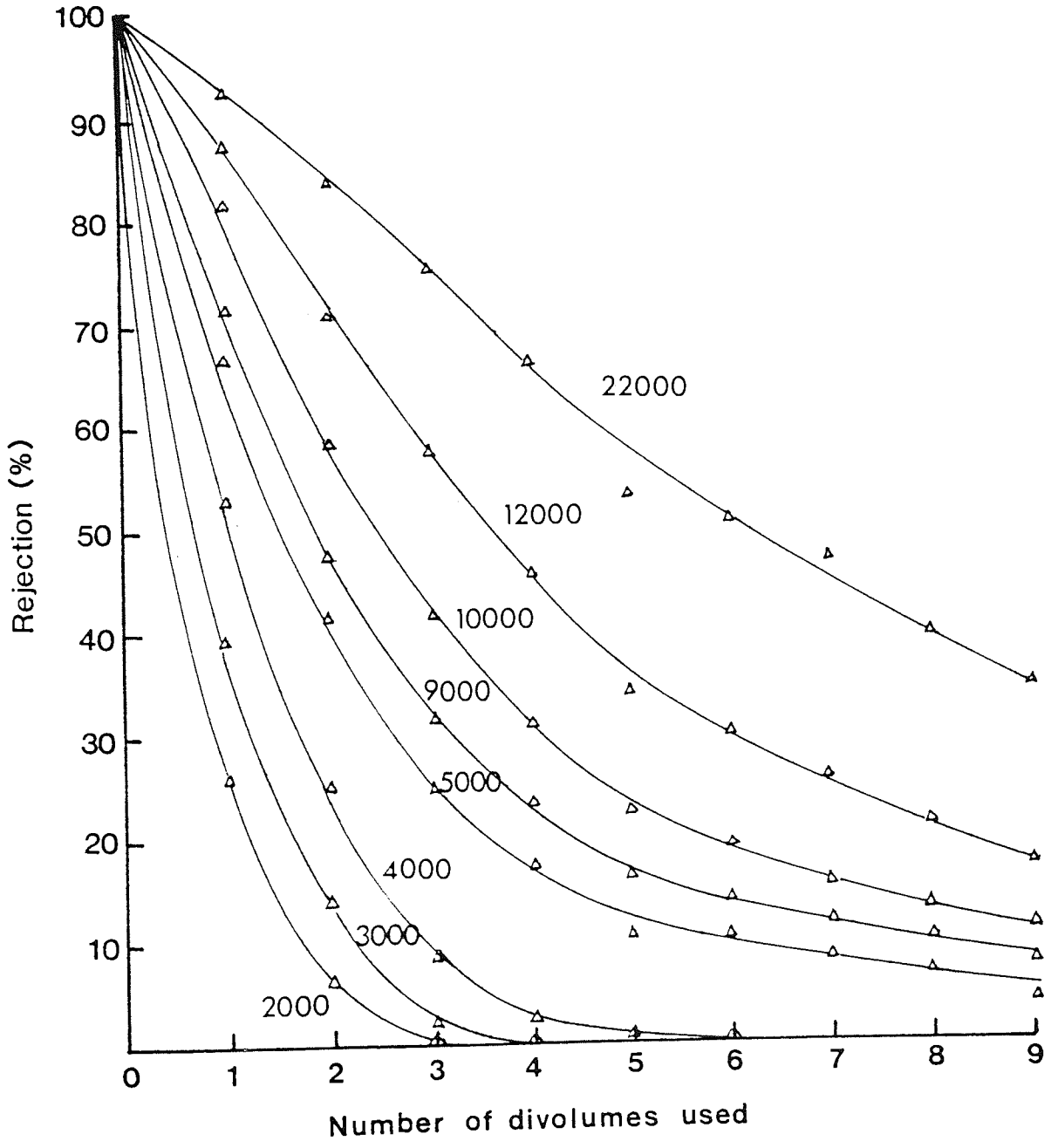

correct BP specification below 12,000 MW, however this gave an efficiency of retention of only 55% for the 'saleable' band. Based on Poland's [6] analysis of the 5000 cut-off membranes, 10 to 12 diavolumes were required to obtain the same specification, however the average efficiency of retention for the 'saleable' material was higher at 64%.

These results confirmed that the 5000 MW cut-off membranes were more suitable for the batch removal of material below 12,000 MW.

In conclusion the general performance of the four 10,000 MW cut-off membranes was a disappointment. Although these membranes had a lower rejection below 12,000 MW, dextran molecules in excess of $1x10^5$ MW were able to pass through them.

5.4.2 TESTING THE AMICON 5000 MW CUT-OFF MEMBRANES USING BATCH DIAFILTRATION

Poland used four Amicon 5000 MW cut-off membranes for his research into the ultrafiltration cascade (code H1P5-20), these membranes had been used intensively for more than 18 months. Since some of these membranes were to be reused within the cascade, it was felt that it would be important to retest them. A new membrane was also purchased as a spare and this was also tested.

As expected the rejection characteristics of some of the membranes had changed. In most cases the membranes ability to reject the dextran had reduced, this was particularly noticable below 12,000 MW. The retention of the 12,000 MW to 98,000 MW band however had been less significantly effected. This suggests that the changes found were caused by changes within the pore distribution rather than damage to the hollow fibres. Interestingly no significant change was found within membrane number four, however this membrane was purchased six months after the others and had been used less intensively.

It is possible that these changes were the result of creep under load, a common problem with thermoplastics. Each cascade experiment typically took over one week to complete and the cascade operated 24 hours a day. These membranes were therefore subjected to positive pressures for long periods. Under these conditions creep would occur, stretching the membrane skin and altering the pore distribution. Changing the pore distribution would naturally alter the rejection characteristics of the membrane.

This deterioration could have a significant effect on the operation of a production membrane system. A membrane life of three years was assumed by Poland in an economic evaluation of a full scale fractionation process. This would now appear to be unrealistic; a more reasonable figure would probably be two years. Since the cost of membranes is a major operating cost this must affect the viability of the membrane process.

The rejection curves for these membranes can be found in figure 5.33. The rejection curves showed the same degree of scatter that was found with the 10,000 MW cut-off membranes. Membrane five has a particularly interesting rejection curve since it was very similar to the off specification 10,000 cut-off membrane (number four) mentioned earlier.

Table 5.8 Diafiltration Results for Amicon 5000 MW cut-off Membrane Number 1

		RETENTATE PRODUCT				
Number of diavolumes used	Concentration (g/100g Sol)	%below 12000 MW	Efficiency of removal	% between 12000 - 98000 MW	Efficiency of retention	% above 98000 MW
Feed	1.78	24.15	0	63.47	100	12.38
1	1.67	19.25	25.30 (20.85)	67.17	99.2 (98.6)	13.58
2	1.531	15.70	44.18 (33.84)	69.91	94.6 (97.4)	14.39
3	1.40	12.70	58.6 (49.72)	70.94	87.89 (96.1)	16.36
4	1.339	11.11	65.4 (59.15)	71.06	84.15 (93.2)	17.83
5	1.314	9.93	69.76 (66.7)	71.54	83.18 (90.3)	18.53
6	1.275	8.91	73.72 (69.6)	72.34	81.59 (86.0)	18.75
7	1.25	8.11	76.51 (-)	72.10	79.73 (-)	19.80
8	1.22	7.37	79.30 (77.32)	72.51	78.23 (81.4)	20.12

( ) brackets denotes Polands results

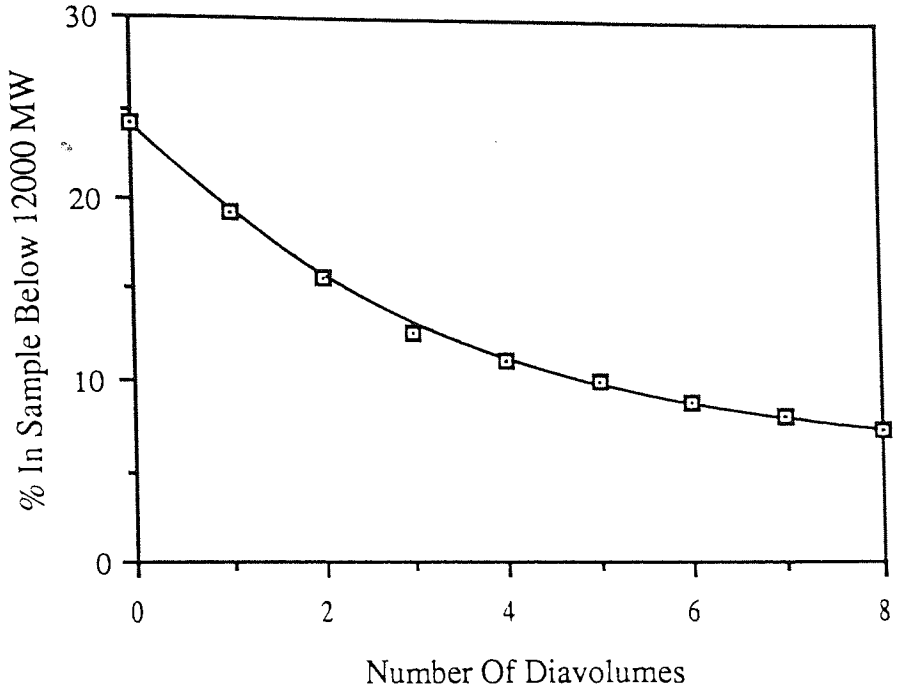

Figure 5.23 How the Number of Diavolumes used Effects the Percentage of the MWD below 12,000 MW in the Retentate

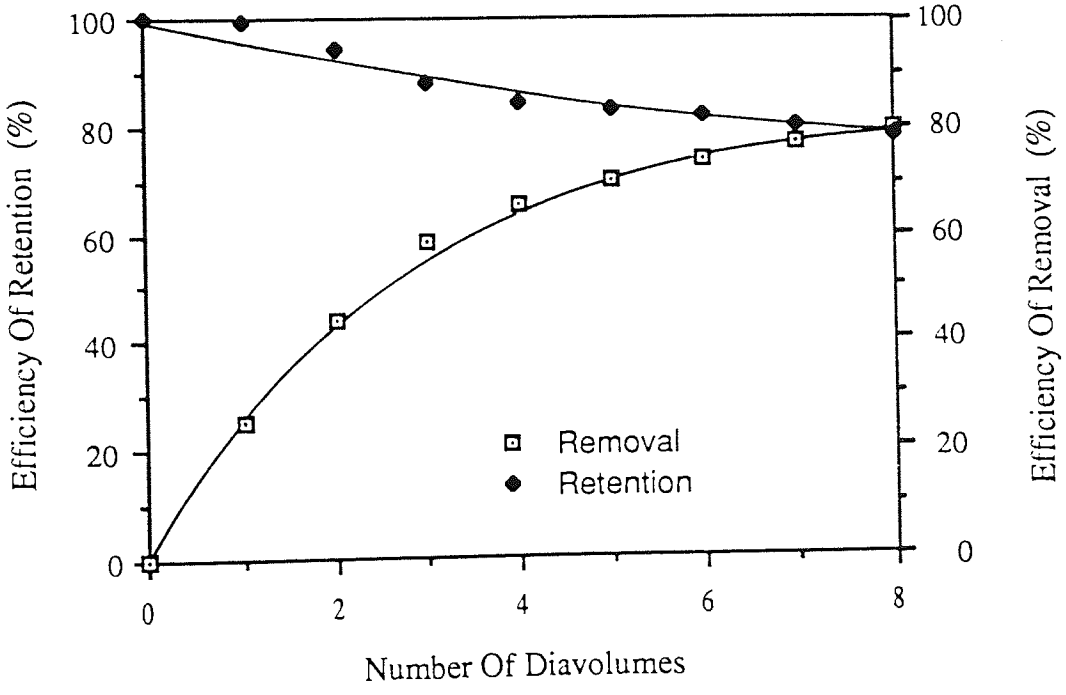

Figure 5.24 The Relationship between Efficiency and Number of Diavolumes used. Membrane Number 1

Table 5.9 Diafiltration Results for Amicon 5000 MW cut-off Membrane Number 2

RETENTATE PRODUCT

Number of diavolumes used	Concentration (g/100g Sol)	%below 12000 MW	Efficiency of removal	%between 12000 - 98000 MW	Efficiency of retention	%above 98000 MW
Feed	1.901	24.63	0	63.08	100	12.29
1	1.810	21.55	16.66 (8.0)	65.15	99.08 (97.0)	12.90
2	1.739	17.41	35.47 (24.9)	68.38	99.16 (97.0)	14.21
3	1.668	13.85	50.64 (32.27)	70.32	97.74 (92.0)	15.83
4	1.526	12.21	60.25 (37.68)	71.42	90.07 (88.0)	16.37
5	1.416	10.77	67.30 (42.7)	71.94	85.07 (84.0)	17.29
6	1.306	9.68	73.07 (47.8)	72.90	79.39 (79.0)	17.42
7	1.293	8.88	75.42 (-)	73.29	78.98 (-)	17.83
8	1.267	7.78	74.05 (63.25)	73.41	77.56 (75.0)	18.81

( ) brackets denotes K Polands results.

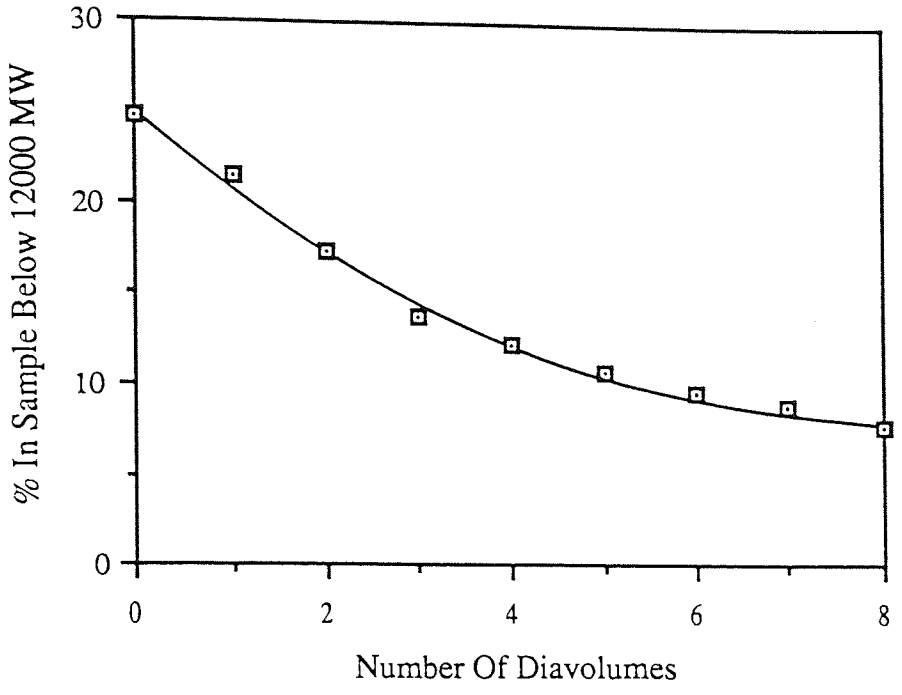

Figure 5.25 How the Number of Diavolumes used Effects the Percentage of the MWD below 12,000 MW in the Retentate

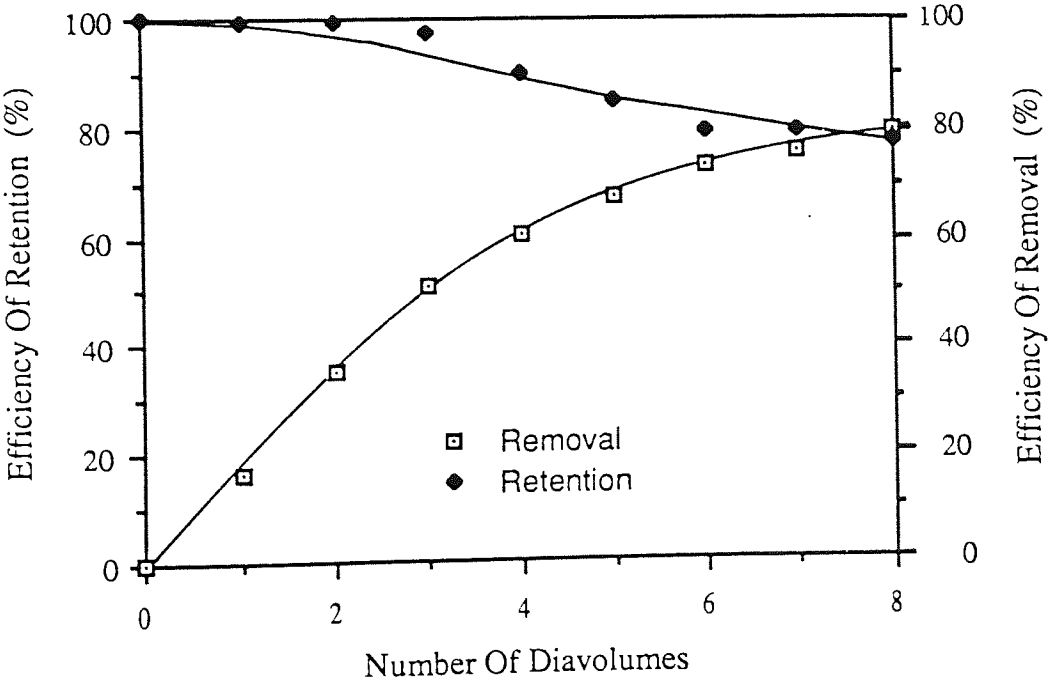

Figure 5.26 The Relationship between Efficiency and Number of Diavolumes used. Membrane Number 2

Table 5.10 Diafiltration results for Amicon 5000 MW cut-off Membrane Number 3

		RETENTATE PRODUCT				
Number of diavolumes used	Concentration (g/100g Sol)	%below 12000 MW	Efficiency of removal	%between 12000 - 98000 MW	Efficiency of retention	%above 98000 MW
Feed	1.78	24.15	0	63.47	100 (100.0)	12.38
1	1.58	17.93	34.18 (19.4)	68.65	95.5 (97.0)	13.42
2	1.44	14.98	49.76 (41.0)	69.63	88.40 (96.0)	15.39
3	1.35	12.68	60.23 (49.8)	71.63	85.57 (90.0)	15.69
4	1.26	9.77	71.39 (62.23)	71.70	79.91 (86.0)	18.53
5	1.21	8.97	74.88 (66.59)	71.59	76.63 (79.0)	19.44
6	1.15	7.62	79.53 (71.90)	71.90	73.18 (75.0)	20.48
7	1.10	7.30	81.39 (-)	72.29	70.35 (-)	20.41
8	1.04	6.60	83.9 (80.7)	72.40	66.63 (68.)	21.00

( ) brackets denotes K Polands results.

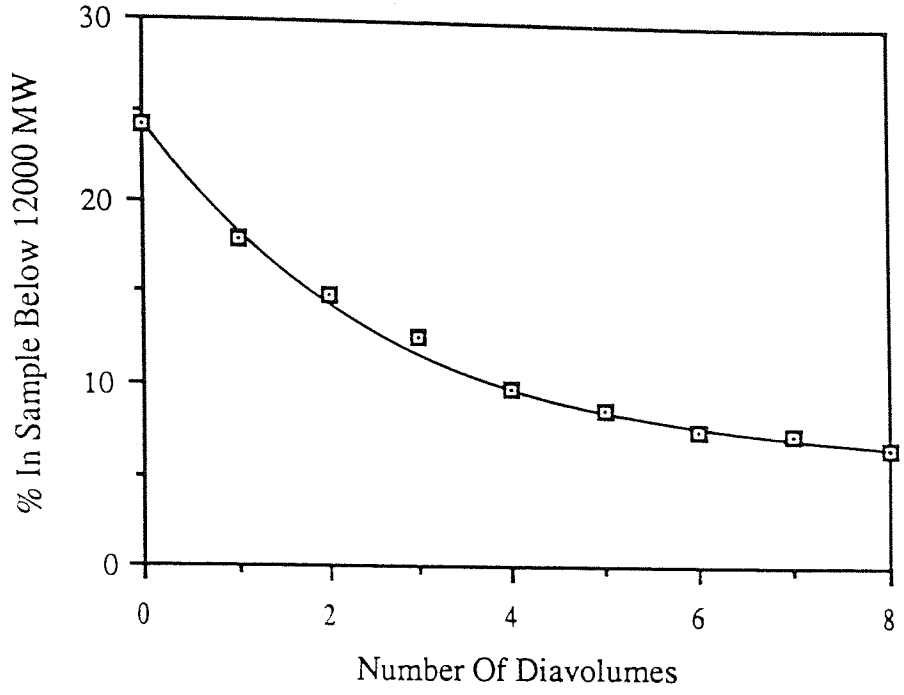

Figure 5 27 How the Number of Diavolumes used Effects the Percentage of the MWD below 12,000 MW in the Retentate

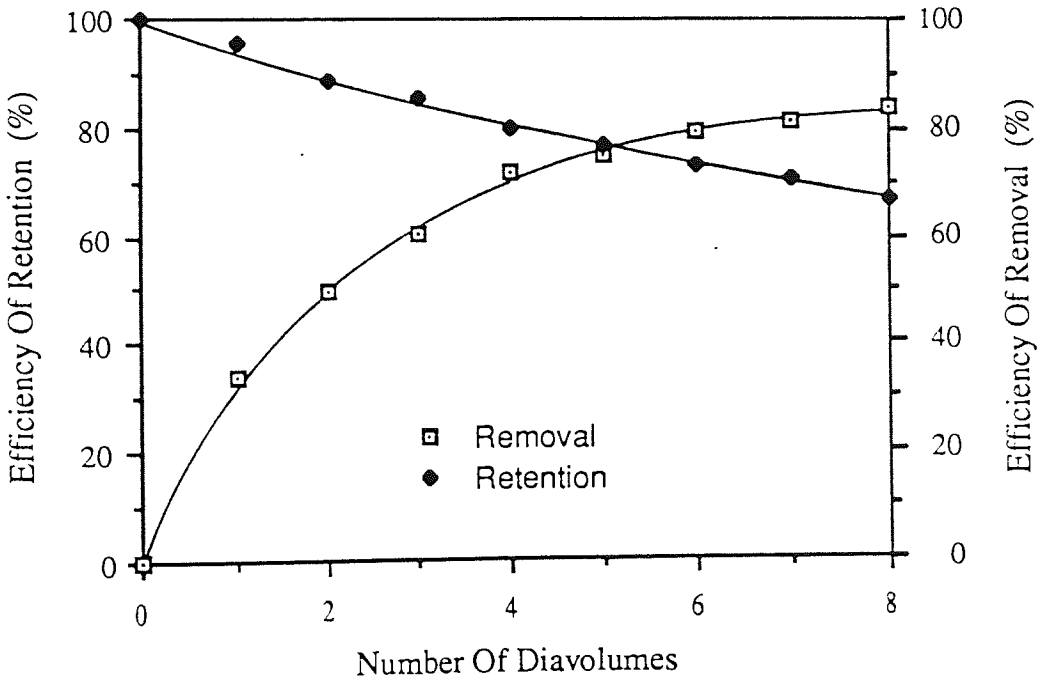

Figure 5.28 The Relationship between Efficiency and Number of Diavolumes used. Membrane Number 3

Table 5.11 Diafiltration Results for Amicon 5000 MW cut-off Membrane Number 4

		RETENTATE PRODUCT				
Number of diavolumes used	Concentration (g/100g Sol)	% below 12000 MW	Efficiency of removal	% between 12000 - 98000 MW	Efficiency of retention	% above 98000 MW
Feed	1.984	24.15	0	63.47	100	12.38
1	1.83	19.69	24.8 (28.1)	66.37	97.42 (95.0)	13.94
2	1.68	17.59	38.41 (36.27)	68.04	90.78 (88.0)	14.37
3	1.526	16.14	48.64 (49.09)	69.21	83.87 (85.0)	14.65
4	1.424	13.09	61.17 (58.36)	71.26	80.54 (77.0)	15.65
5	1.32	11.55	68.26 (66.47)	72.29	75.77 (74.0)	16.16
6	1.27	10.5	72.23 (71.4)	72.92	73.55 (70.0)	16.58
7	1.17	9.98	75.78 (-)	73.31	68.14 (-)	16.71
8	1.09	7.98	82.04 (84.0)	73.49	63.62 (62.0)	18.61

( ) brackets denotes K Polands results

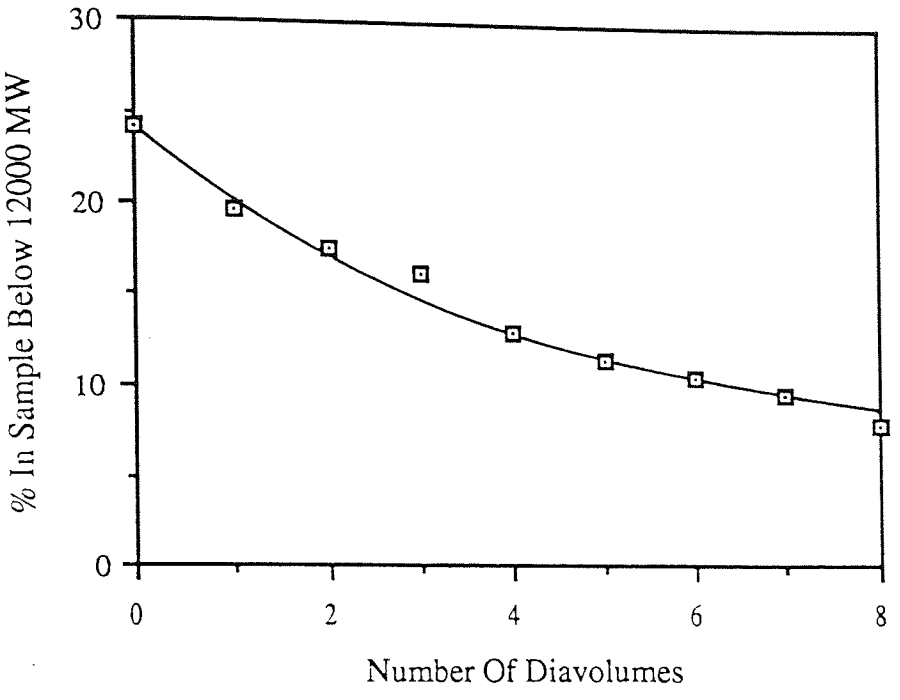

Figure 5.29 How the Number of Diavolumes used Effects the Percentage of the MWD below 12,000 MW in the Retentate

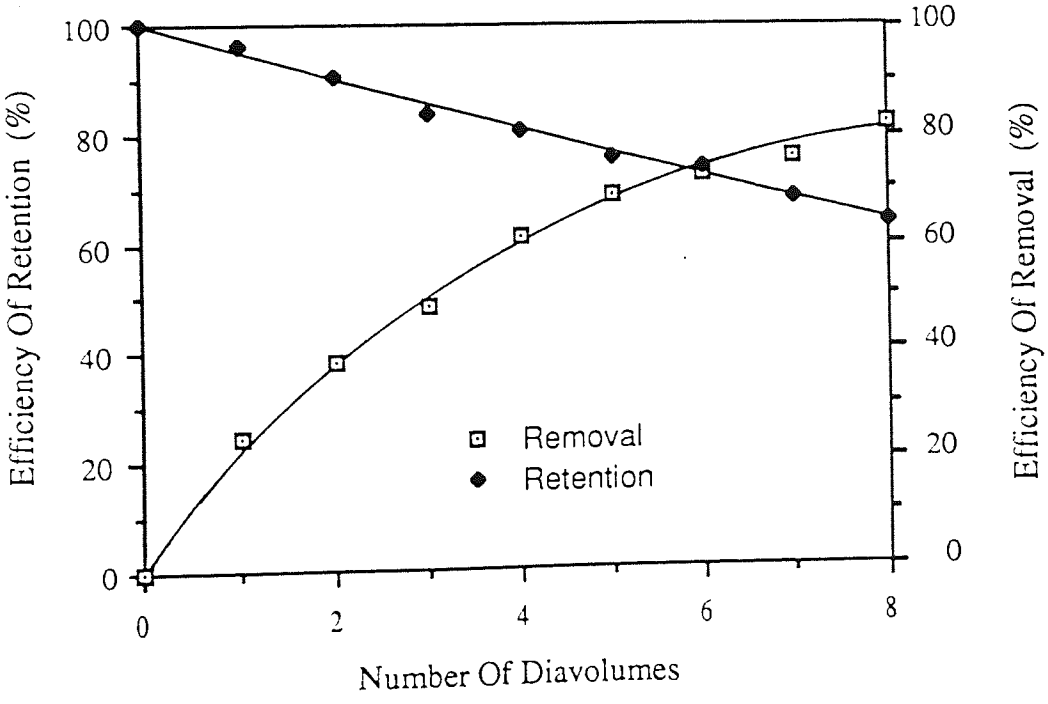

Figure 5.30 The Relationship between Efficiency and Number of Diavolumes used. Membrane Number 4

Table 5.12 Diafiltration Results for the Amicon 5000 MW cut-off Membrane Number 5

	RETENTATE PRODUCT					
Number of diavolumes used	Concentration (g/100g Sol)	%below 12000 MW	Efficiency of removal	% between 12000 - 98000 MW	Efficiency of retention	% above 98000 MW
Feed	1.907	24.63	0	63.08	100	12.29
1	1.698	22.61	18.24	65.22	92.02	12.17
2	1.627	18.89	34.6	67.67	91.44	13.44
3	1.37	14.85	56.78	70.62	80.40	14.53
4	1.32	12.55	64.74	71.62	78.58	15.83
5	1.22	10.48	72.79	72.56	73.57	16.96
6	1.14	9.18	77.64	72.87	69.08	17.95
7	1.068	8.25	81.24	73.53	65.25	18.22
8	1.017	7.15	84.46	73.4	61.76	19.81
9	0.966	6.74	86.16	73.35	58.85	19.91

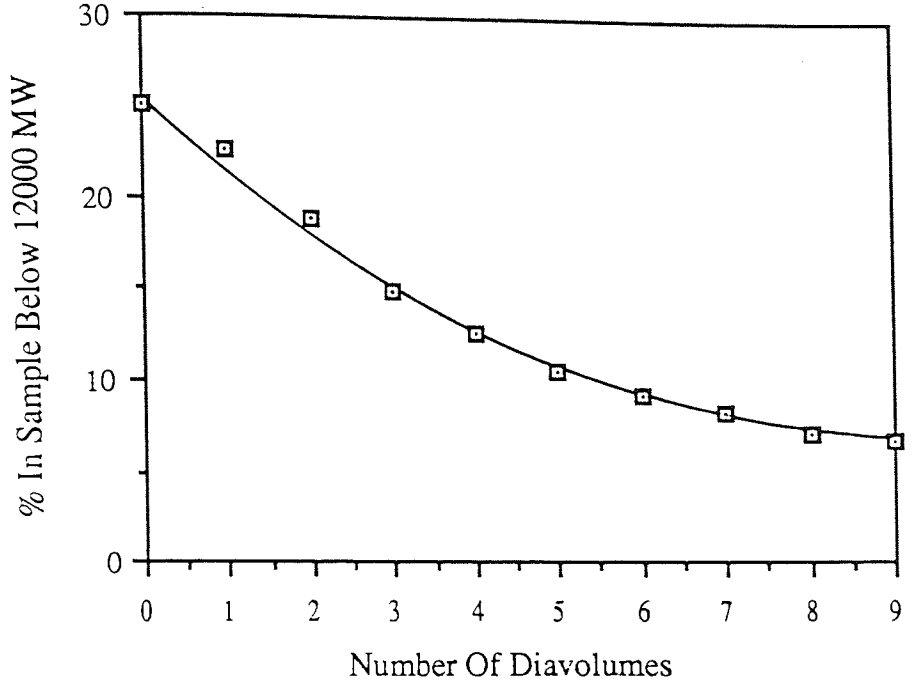

Figure 5.31 How the Number of Diavolumes used Effects the Percentage of the MWD below 12,000 MW in the Retentate

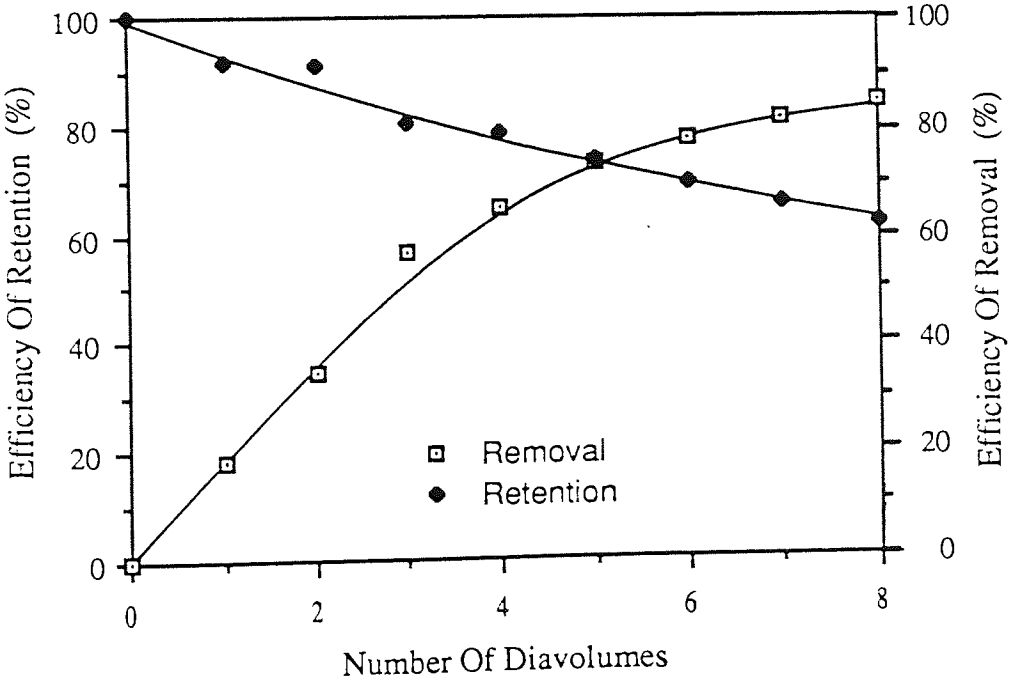

Figure 5.32 The Relationship between Efficiency and Number of Diavolumes used. Membrane Number 5

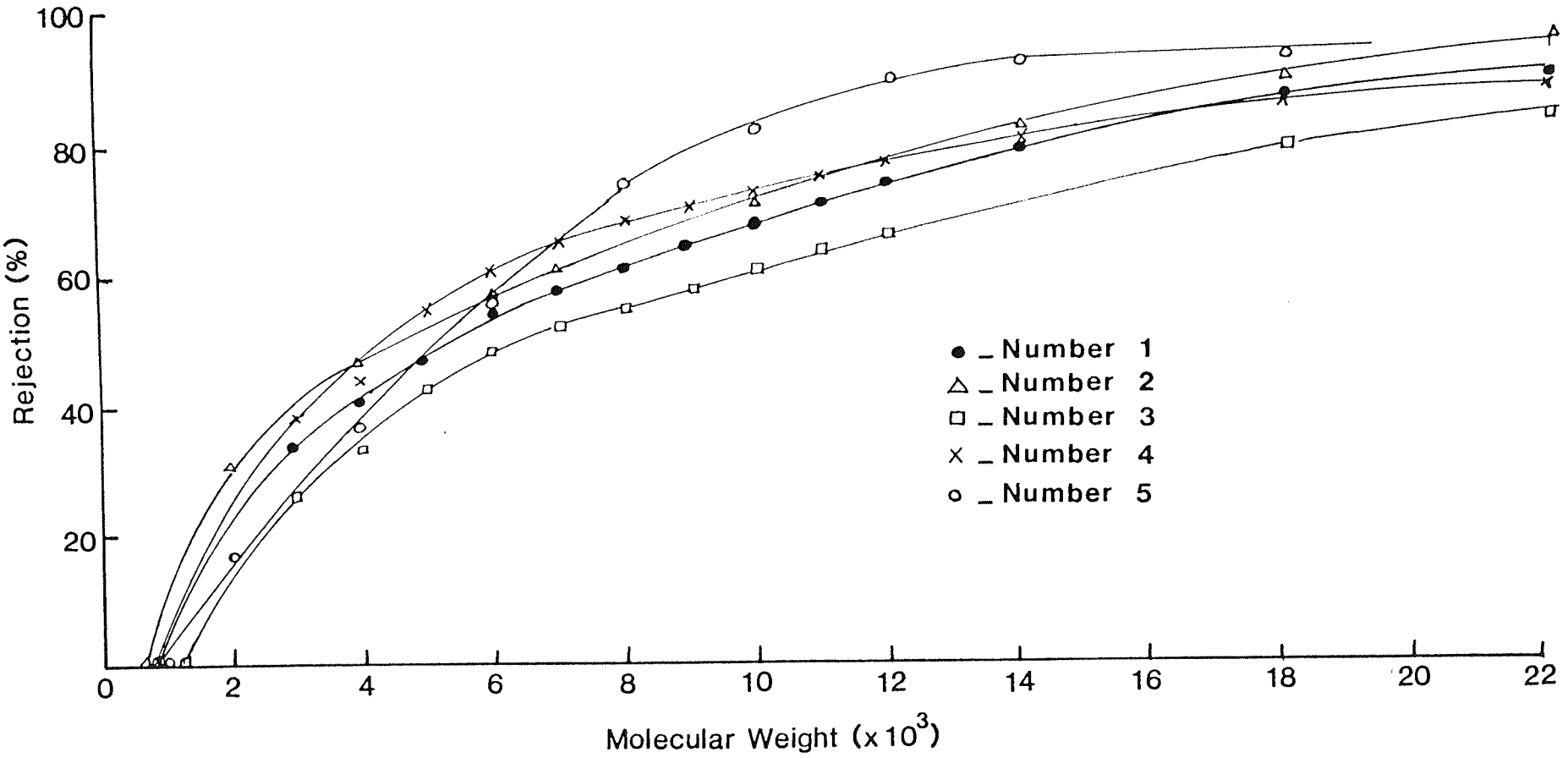

Figure 5.33 The Rejection Curves Obtained from the Five 5,000 MW Cut-off Membranes after Two Diavolumes

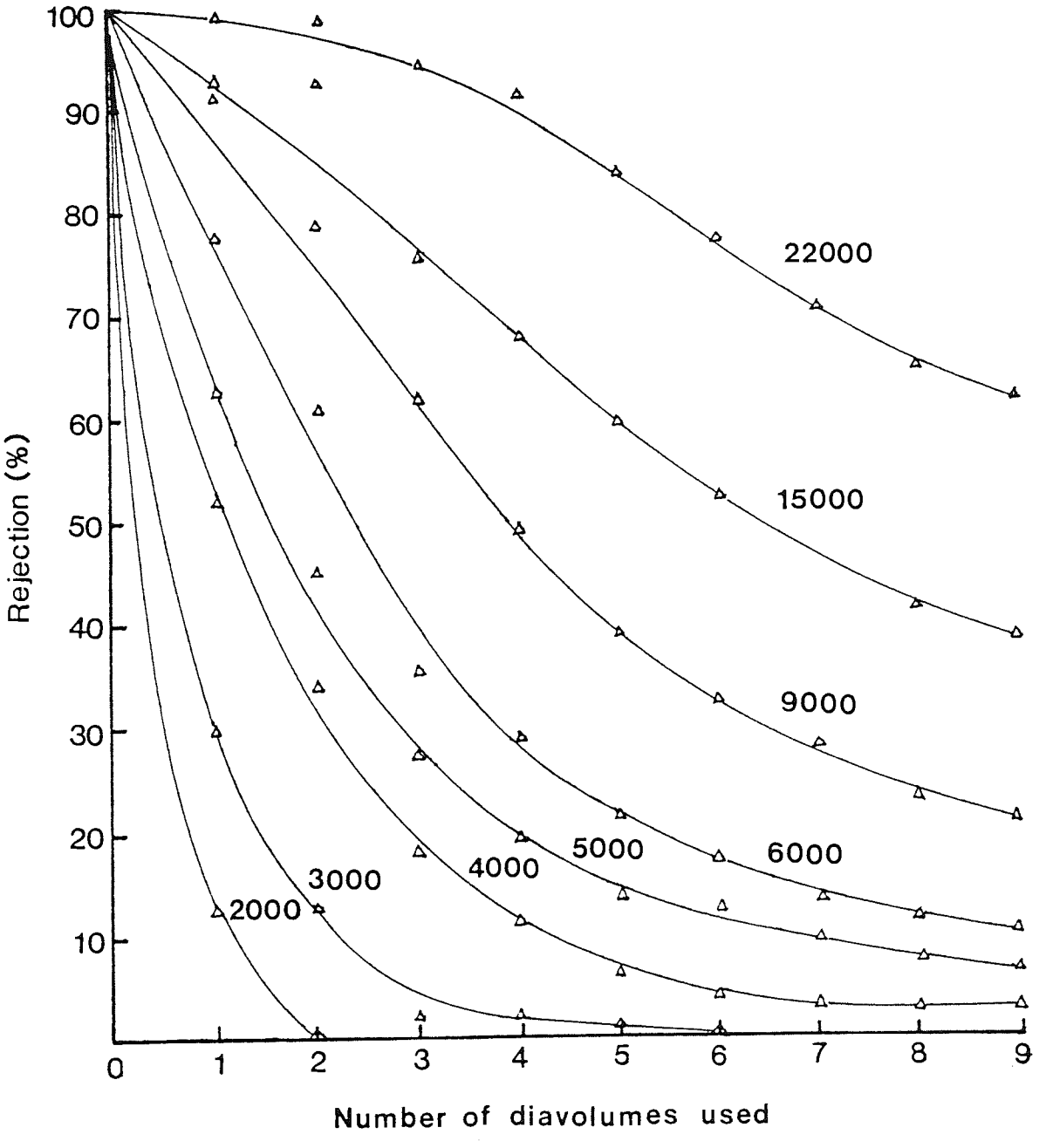

Figure 5.34 The Effect of Increasing the Number of Diavolumes used on the Rejection of a Range of Molecular Weight Bands in the Dextran Sample. 5,000 MW Cut-off Membrane used

5.4.3 USING THE AMICON 10,000 MW CUT-OFF MEMBRANES WITHIN THE ULTRAFILTRATION CASCADE

In section 5.4.1 the performance of membrane number four had been shown to be significantly different from the other membranes. The rejection curve from this membrane showed this most clearly. See figure 5.35. The rejection curve had a very steep initial rise which peaked at about 12,000 MW after which it remained relatively constant. To investigate how the performance of a single membrane could effect the operation of the cascade two experiments were conducted using this membrane. See table 5.14. In the first experiment (1.1) membrane number four was positioned in stage one, the stage into which fresh feed was introduced. In the other experiment (1.2) the membrane was placed in stage four. The fresh diafiltrate was introduced into this stage. To assess the performance of the cascade the rejection curves for these two cascade runs were compared to the average batch rejection curve from the membranes used. See figure 5.36. When membrane number four was positioned in stage one a very steep rejection curve resulted which exceeded the batch rejection after 7500 MW, and continued to rise until it reached a maximum at approximately 12,000 MW. When membrane four was placed in stage four the rejection curve from the cascade was significantly different, a long flat rejection curve resulted which failed to exceed the batch average. The explanation of this effect is simple. Since stage one was the final stage before the permeate left the system, placing a tight membrane in this stage aids recapture of material lost from the other stages. However with the reversed membrane sequence (1.2) quite a different effect would occur. Since the fresh diafiltrate was introduced into stage four most of the fractionation occurred within this stage and hence the permeate would be rich in dextran. Placing a tight membrane in this stage caused a lean permeate.

Table 5.13 Operating Conditions for the Ultrafiltration Cascade

Number of stages	:	4
Number of membranes	:	4
Membrane area per stage (unit area)	:	600 cm^3
Transmembrane pressure	:	70 KPa
Retentate recirculation rate	:	300 cm^3/min
Operting temperature	:	20^oC
Feed	:	2% W/W Fisons batch RB5R
Mode of operation	:	Diafiltration
Number of diavolumes used (unless otherwise stated)	:	2

Definitions:

$$\text{Efficiency of Retention} = \frac{\text{Weight of saleable material in permeate}}{\text{Weight of saleable material in feed}}$$

$$\text{Efficiency of Removal} = \frac{\text{Weight of material below 12000 MW in product}}{\text{Weight of material below 12000 MW in feed}}$$

Figure 5.35 Comparison of the Rejection Curve Obtained from the 10,000 MW Cut-off Membrane Number 4 to the Average of the other Three Membranes

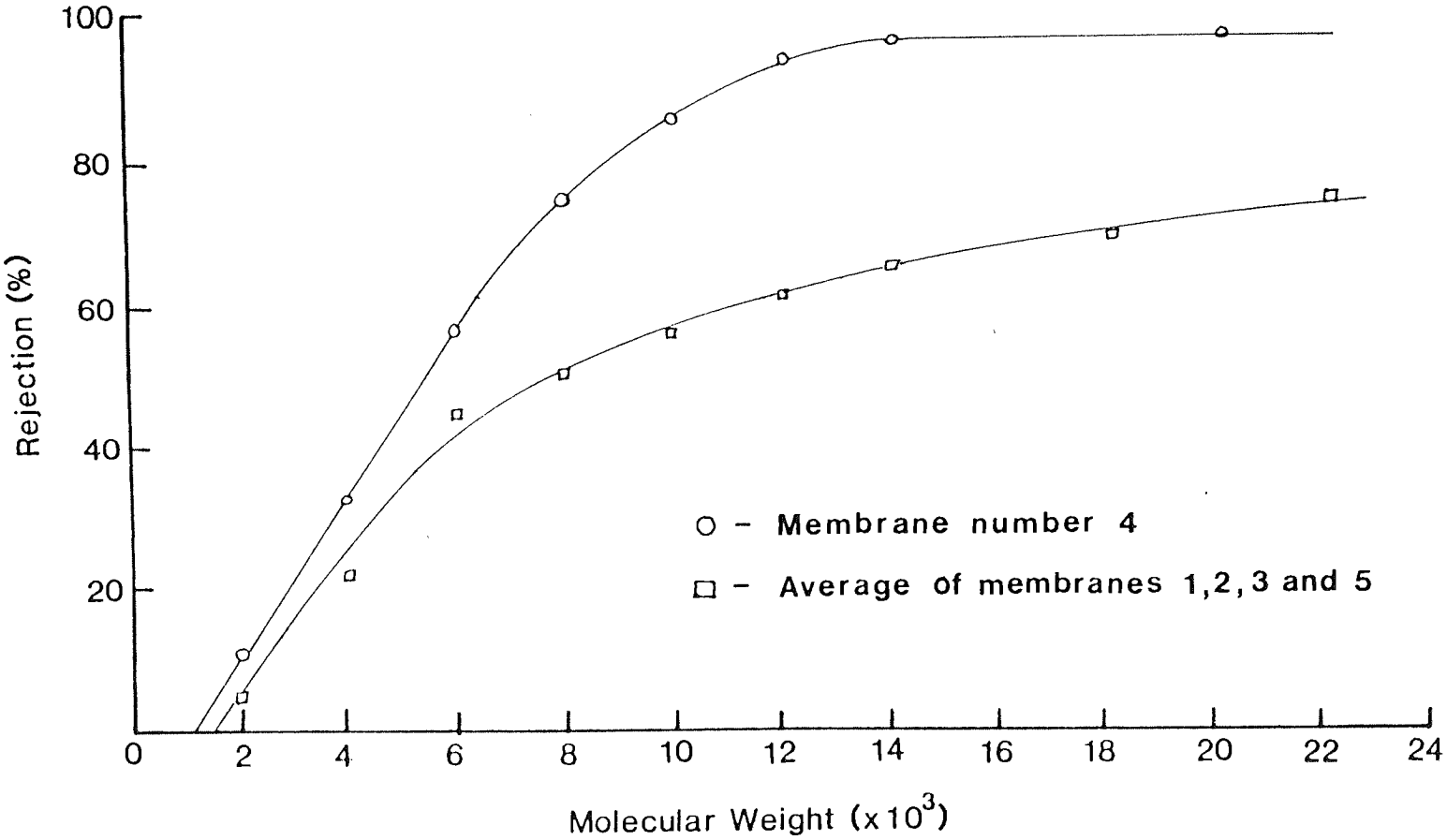

Table 5.14 Using four 10,000 MW cut-off Membranes in the Cascades

		FEED			RETENTATE PRODUCT				
Run	Membrane order	Concentration (g/100g Sol)	%below 12000MW	%between 12000 - 98000MW	Concentration (g/100g Sol)	%below 12000MW	Efficiency of removal	%between 12000 - 98000 MW	Efficiency of retention
1.1	4,3,2,1	2.238	25.00	62.51	1.678	17.38	47.85	69.82	83.77
1.2	1,2,3,4	2.11	25.02	61.00	1.42	15.02	59.12	68.72	75.81

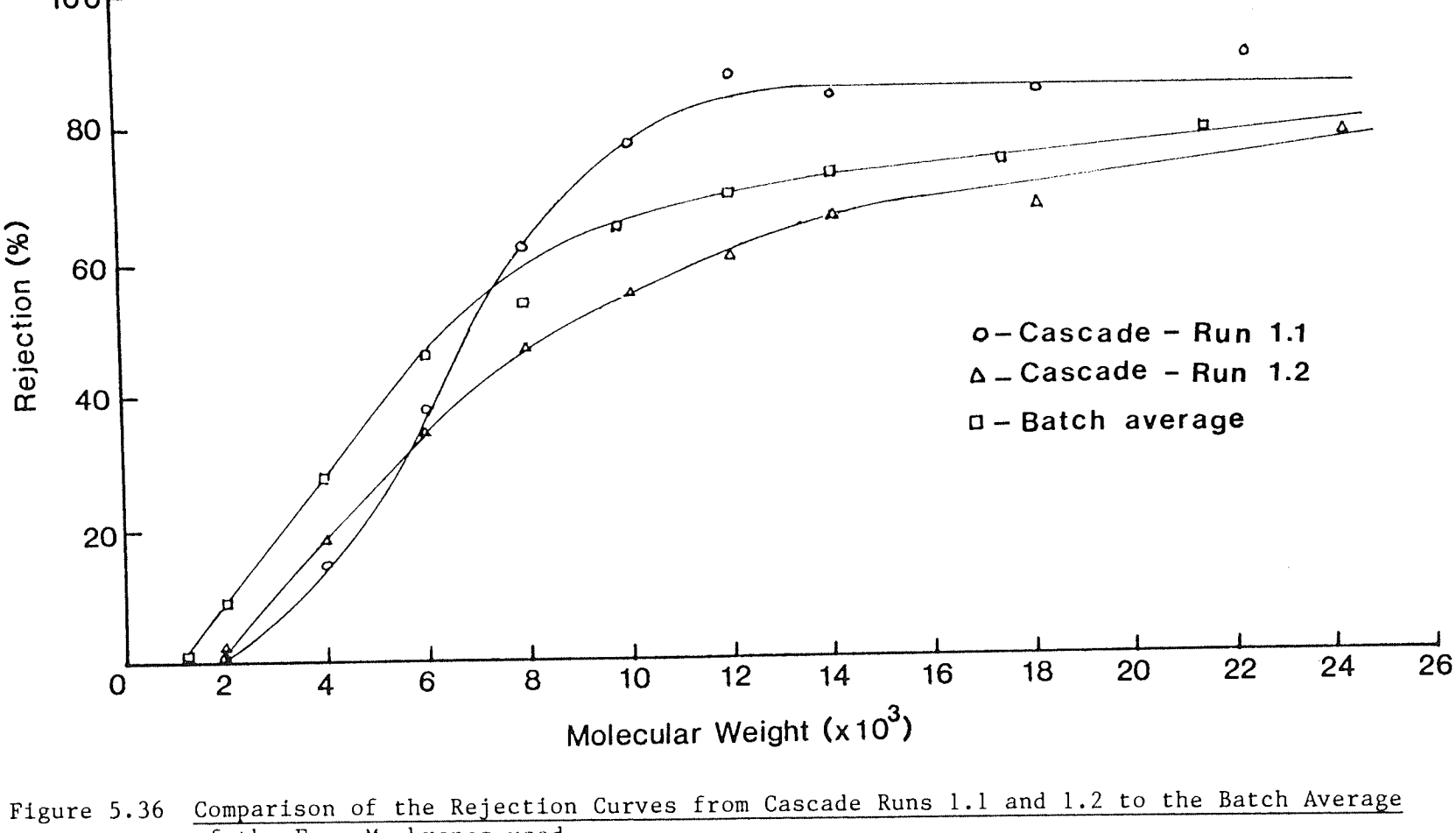

Figure 5.36 Comparison of the Rejection Curves from Cascade Runs 1.1 and 1.2 to the Batch Average of the Four Membranes used

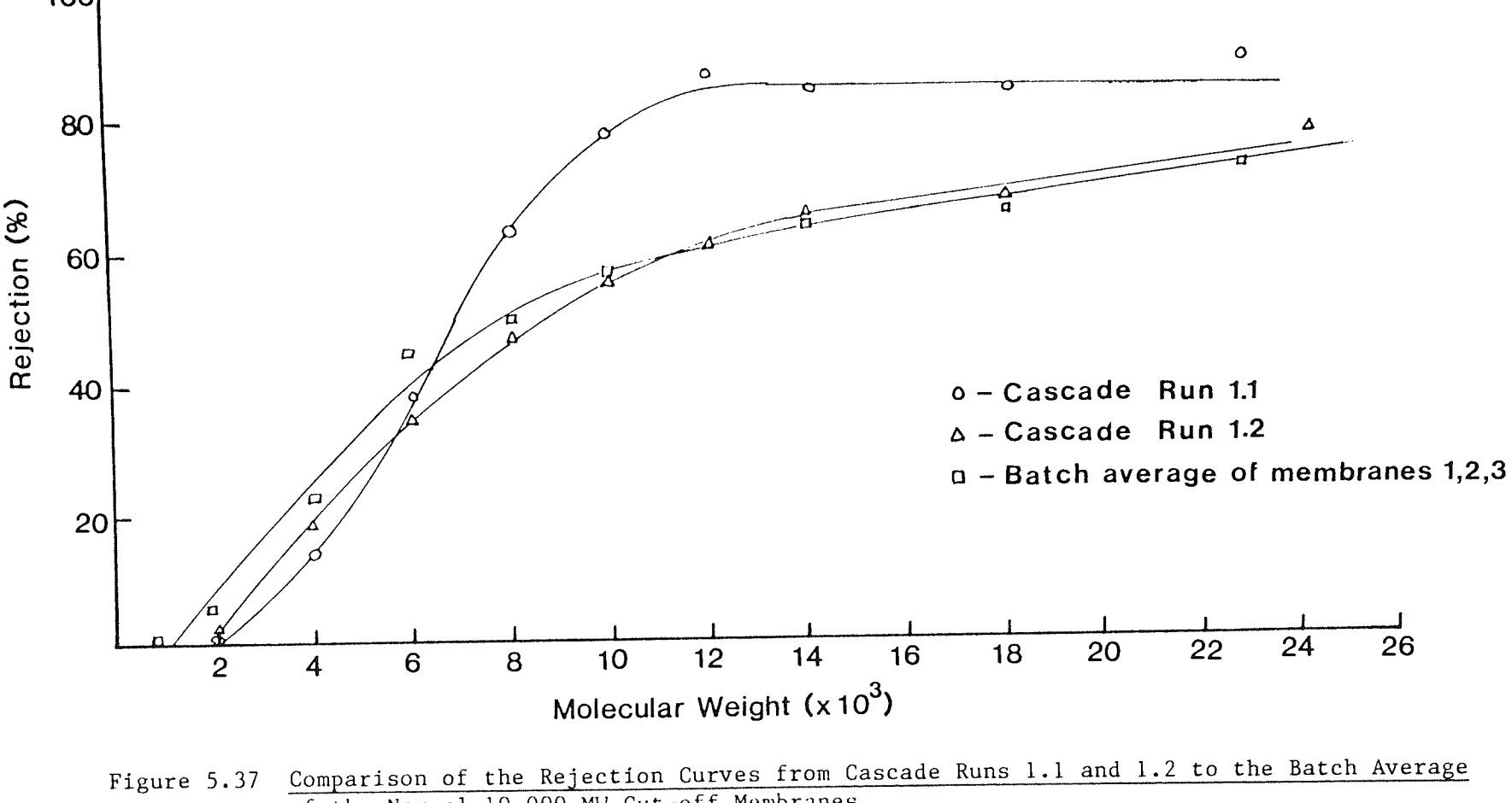

Figure 5.37 Comparison of the Rejection Curves from Cascade Runs 1.1 and 1.2 to the Batch Average of the Normal 10,000 MW Cut-off Membranes

Figure 5.38 Comparison of the Cascade System to the Batch System on an Efficiency Basis

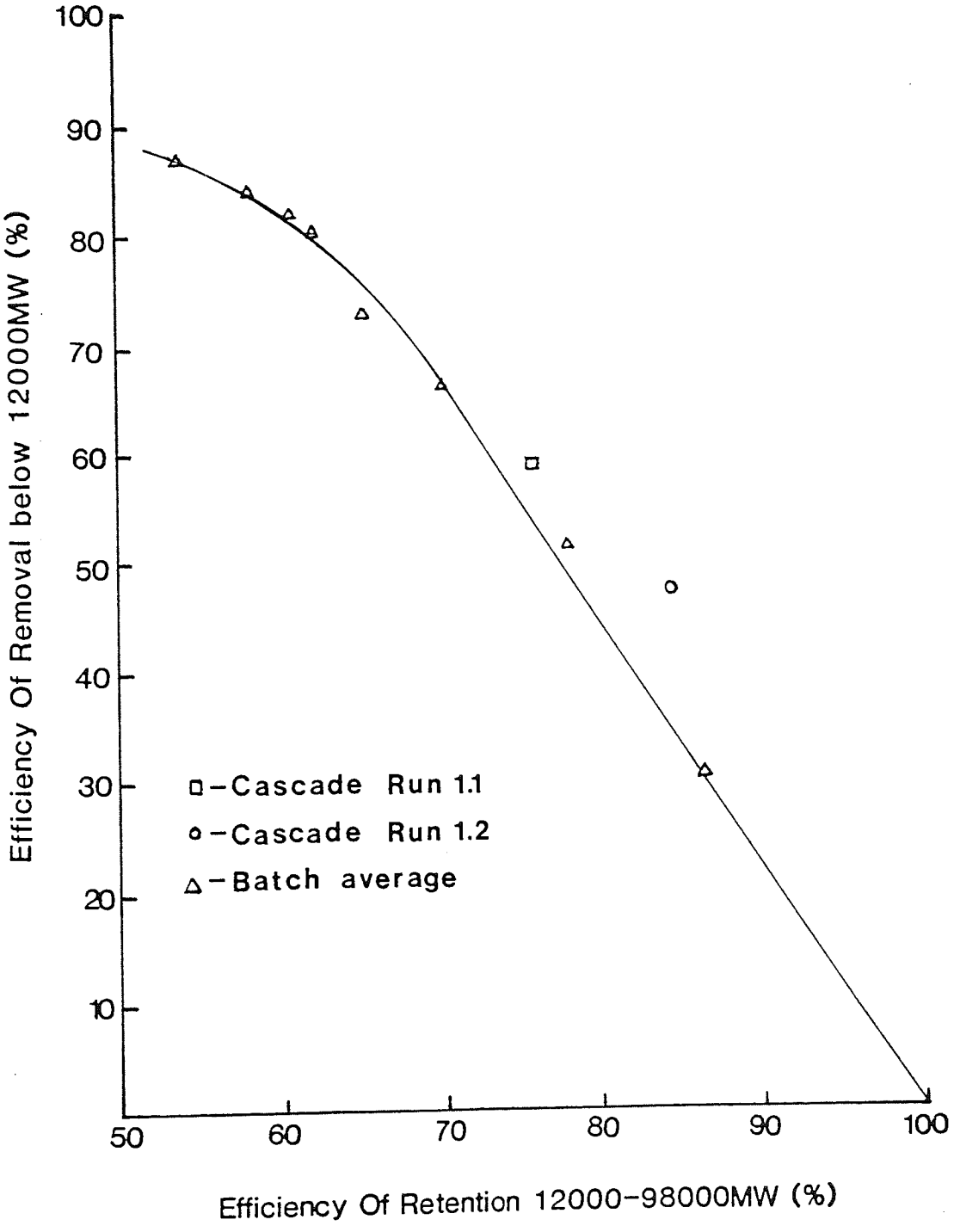

Since the permeate was more dilute the recycle effect of the cascade was reduced and the four stages acted more as if they were independent batch units. Even though the efficiency of the cascade was impaired, the cascade still produced a rejection curve superior to the average of the other three 10,000 MW cut-off membranes, see figure 5.37.

Figure 5.38 shows the two runs compared to the batch results on an efficiency of removal and efficiency of retention basis.

The fact that run 1.2 was very similar to the batch average was not surprising; however run 1.1 also appeared relatively poor. This can be explained by considering the position of the cross-over point which occurred at 7500 MW. Although the cascade removed significantly more material than the batch system below 7500 MW it retained far more above this value, therefore the overall efficiency of removal below 12,000 MW appears to be lower than the batch average. This shows the dangers of using this basis alone to assess the performance of the cascade.

Since the performance of the cascade could be significantly enhanced by using a 'tight' membrane, a series of experiments were later conducted using a mixture of 5000 MW and 10,000 MW cut-off membranes to further investigate the phenomenon.

Once a more typical 10,000 MW cut-off membrane had been obtained from Amicon the main operating variable of the cascade and the number of diavolumes used per stage was studied. To see how the number of diavolumes used effected the operation of the cascade experiments 2.1 to 2.4 were conducted. The number of diavolumes used was varied between 0.5 and 2.0 in 0.5 diavolume increments, see table 5.15. As the number of diavolumes increased the cascades operating line rapidly diverged from that for the batch. See figure 5.39. Comparing the cascade rejection curve to the batch average (at two diavolumes) showed clearly the improvement which could be achieved by using the cascade system. See figure 5.40. As expected the cross over-point occurred at 12,500 MW.

Table 5.15 Diafiltration Results of the Ultrafiltration Cascade using 10,000 MW cut-off Membrane

	FEED				RETENTATE PRODUCT				
Run	Number of Diavolumes used	Concentration (g/100g Sol)	%below 12000 MW	%between 12000 - 98000MW	Concentration (g/100g Sol)	%below 12000MW	Efficiency of removal	%between 12000 - 98000MW	Efficiency of retention
2.1	0.5	1.78	24.7	61.44	1.526	21.64	24.83	64.57	90.06
2.2	1.0	1.80	24.7	61.44	1.373	16.49	49.09	67.61	83.91
2.3	1.5	1.78	24.7	61.44	1.271	11.63	66.28	71.20	82.66
2.4	2.0	1.78	24.7	61.44	1.195	9.64	73.8	71.77	78.36

Below the cross-over point the rejection of the unwanted low molecular weight material was significantly lower than the batch system, although the improvement above the cross-over point was not as high as was hoped. The effect on the distribution within the dextran product was also very significant. See figure 5.41 and 5.42. The percentage of the molecular weight distribution below 12,000 MW was approximately 40% lower than the batch system at two diavolumes and the percentage of the molecular weight distribution between 12,000 and 98,000 MW was 7% higher.

The fact that the cascade operates more efficiently at a higher number of diavolumes is not really surprising. As the number of diavolumes increases more low molecular weight dextran would be 'washed' through the membranes. Since the higher weight material is recaptured the removal of material below 12,000 MW occurs in preference to the 12,000 to 98,000 MW band.

Since the efficiency of retention was not as high as was initially hoped another run was performed using a different membrane order. Since membrane number five was the 'tightest' membrane out of the four used it was placed in stage one to mimic the effect found in run 1.1. This run was also used to follow the unsteady state operation of the cascade. See table 5.16. The run showed that the efficiency of retention could be improved by careful selection of the membrane order. Using this membrane configuration the efficiency was improved by 6.5%. However the cross-over point was also affected and dropped to 9000 MW. See figure 5.43. This confirmed that the cross-over point was not stationary but shifted depending on what membrane order was used. This was unfortunate since it suggested that it would be difficult to improve the efficiency of retention without causing a lower cross-over point and hence impairing the efficiency of removal.

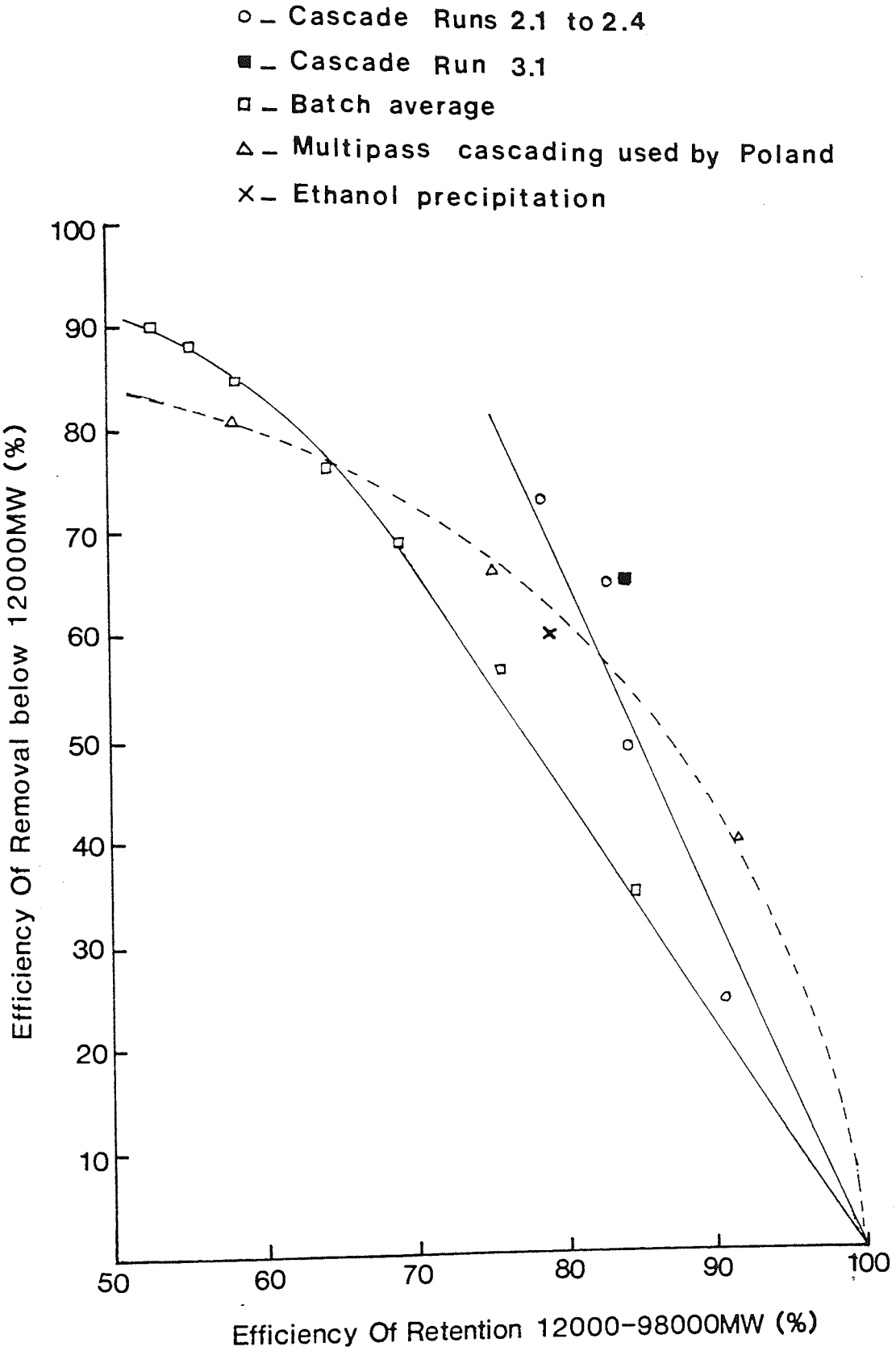

Figure 5.39 Comparison of the Cascade System to the Batch System on an Efficiency Basis. Runs 2.1 to 2.4

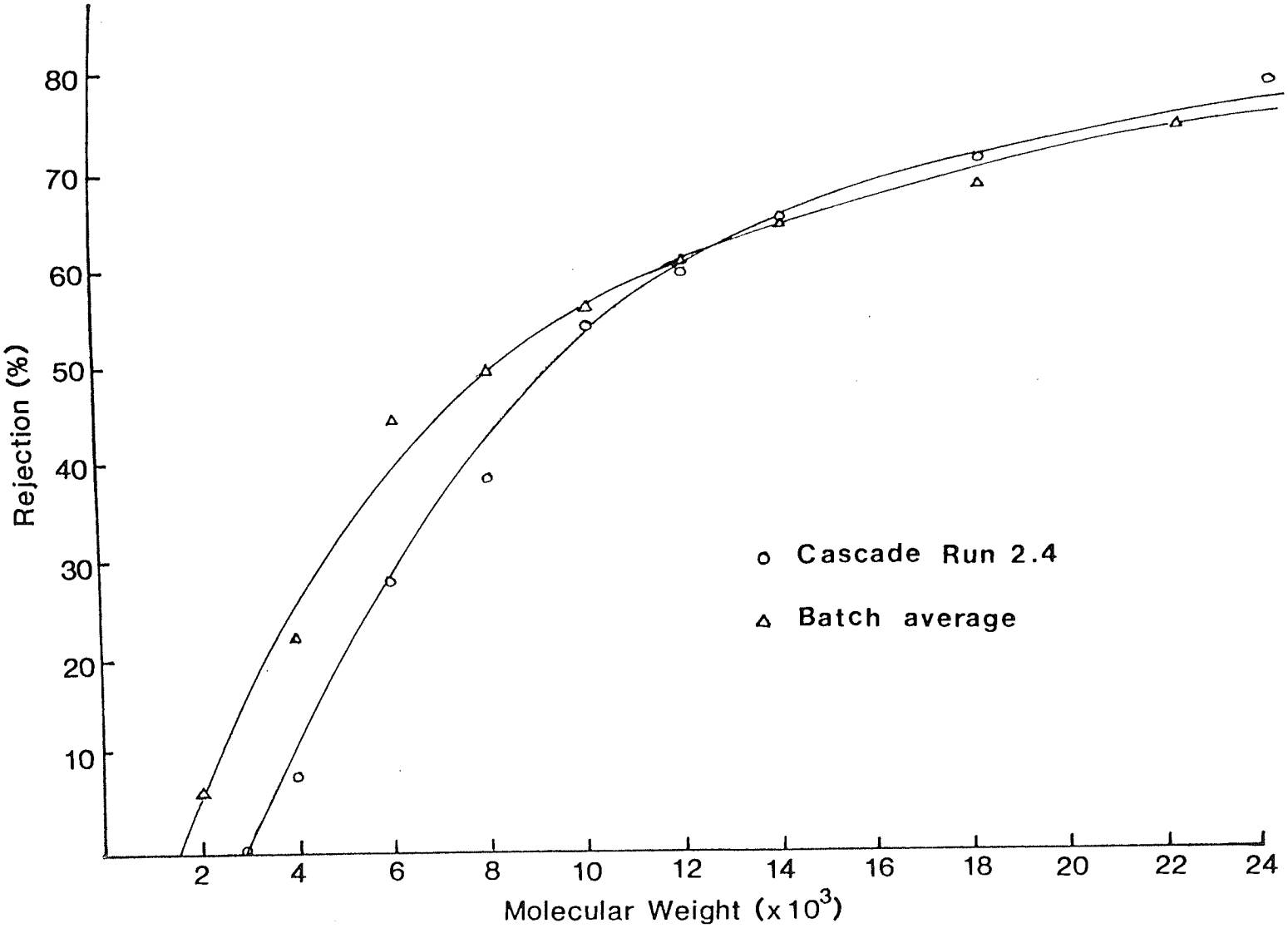

Figure 5.40 Rejection Curve from Cascade Run 2.4

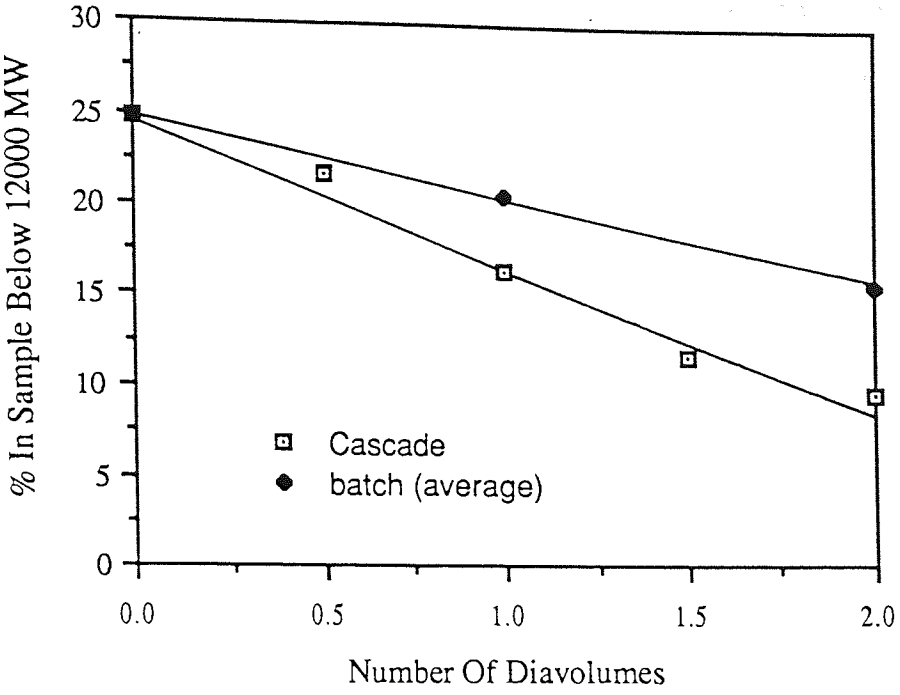

Figure 5.41 The Effect of Changing the Number of Diavolumes used on the Molecular Weight Distribution of both the Batch and Cascade System (0-12,000 MW Band)

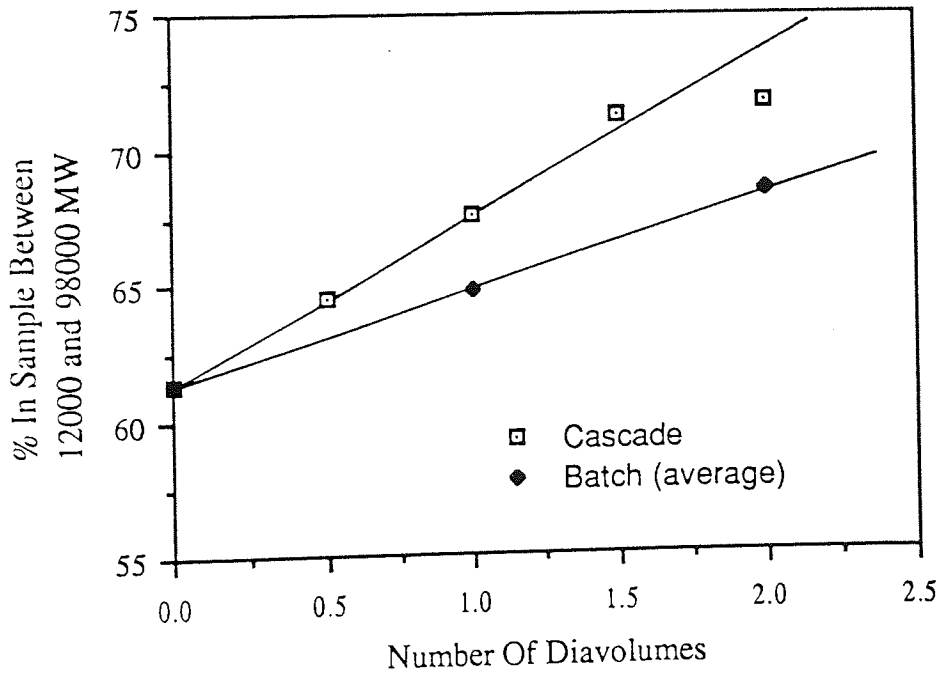

Figure 5.42 The Effect of Changing the Number of Diavolumes used on the Molecular Weight Distribution of both the Batch and Cascade System (12,000 - 98,000 MW Band)

The unsteady state of the study also showed up several interesting points. Firstly the cascade appeared to reach steady state earlier than expected. Poland felt that steady state was not achieved below 20 cycles; however this run showed that steady state was achieved by 17 cycles. Again this was an important consideration since this will effect the cost effectiveness of a production system. Naturally any off specification product must be recycled or disposed of. Also the quicker the cascade reaches equilibrium, the shorter the start up time after maintenance or breakdown.

The results also show how a single membrane can have a significant effect on the cascade. As the cascade reached equilibrium an unexpected peak in efficiency of retention and a reduction in efficiency of removal was found in stage two. Initially it was felt that a fault had occurred with the level controllers. Since the effect developed from the early cycles it could only have been caused if the level controller on stage two had been set incorrectly. This would have manifested itself as an accumulation within or a drainage of the diafiltration tank. This was easy to recognize and did not occur during this experiment. To further check the accuracy of the data a steady state mass balance across the cascade was performed, the results of which can be found in appendix 4.1 and 4.2. The mass balance confirmed that no significant error was present.

Since the cascade was operating correctly the accumulation of material could only have been caused by the membrane (number two) used in that stage. As this membrane had a relatively high rejection, up to 12,000 MW, this would cause the low molecular weight material to accumulate within the stage. Both Cooper [48] and Bottino [44] showed that increasing the amount of low molecular weight material present increased the rejection of the higher molecular weight material. Since the the membrane in the second stage of the cascade was retaining the

Table 5.16 Unsteady State Study of Ultrafiltration Cascade

Membrane order 5,2,1,3 Run 3.1

Cycle & stage number	Concentration (g/100gSol)	%below 12000 MW	Efficiency of removal	%between 12000 & 98000 MW	Efficiency of retention	%above 98000 MW
Feed	2.00	24.15	0	63.47	100	12.38
1-1	1.086	13.90	67.08	70.71	60.05	15.39
2-1	1.513	15.23	52.29	69.67	83.05	15.10
2-2	0.853	12.19	78.46	72.63	48.77	15.18
3-1	1.603	15.57	48.34	69.50	87.78	14.93
3-2	1.298	13.15	64.68	70.93	72.57	15.92
3-3	0.55	8.79	90.00	73.81	31.98	17.40
4-1	1.564	15.05	51.34	69.27	85.10	15.68
4-2	1.571	13.08	57.55	71.17	88.10	15.75
4-3	0.918	8.45	84.05	72.79	52.64	18.76
4-4	-	-	-	-	-	-
5-1	1.55	15.62	49.89	68.96	84.23	15.42
5-2	1.70	13.99	50.7	71.03	95.11	14.98
5-3	1.22	9.98	74.94	72.09	62.27	17.92
5-4	0.756	6.39	90.06	71.63	42.63	21.98
9-1	1.636	15.36	48.03	69.10	89.04	15.54
9-2	1.80	16.50	38.50	69.94	99.13	13.56
9-3	1.52	11.74	63.14	73.0	87.39	15.26
9-4	1.176	8.61	79.08	72.57	67.24	18.82
13-1	1.629	16.01	45.96	68.59	88.02	15.39
13-2	1.95	17.94	27.53	69.25	106.38	12.81
13-3	1.668	13.96	51.76	72.21	94.89	13.83

Cycle & stage number	Concentration (g/100gSol)	%below 12000 MW	Efficiency of removal	%between 12000 & 98000 MW	Efficiency of retention	%above 98000 MW
13-4	1.28	10.20	73.08	72.59	73.20	17.21
17-1	1.70	16.89	40.57	69.22	92.67	14.89
17-2	2.06	21.72	7.45	66.53	107.9	11.75
17-3	1.726	16.79	40.16	69.67	94.70	13.54
17-4	1.448	11.94	64.18	72.24	82.43	15.82
21-1	1.69	17.09	40.37	67.72	90.15	15.19
21-2	2.017	21.66	9.73	66.12	105.0	12.22
21-3	1.797	17.15	36.23	69.42	98.20	13.43
21-4	1.47	10.81	67.08	72.46	83.92	16.73
29-1	1.77	19.89	27.12	65.94	92.19	14.17
29.2	2.03	22.51	5.59	65.34	104.5	12.15
29-3	1.82	18.24	31.14	68.19	97.97	13.57
29-4	1.474	11.21	65.83	72.0	83.60	16.79

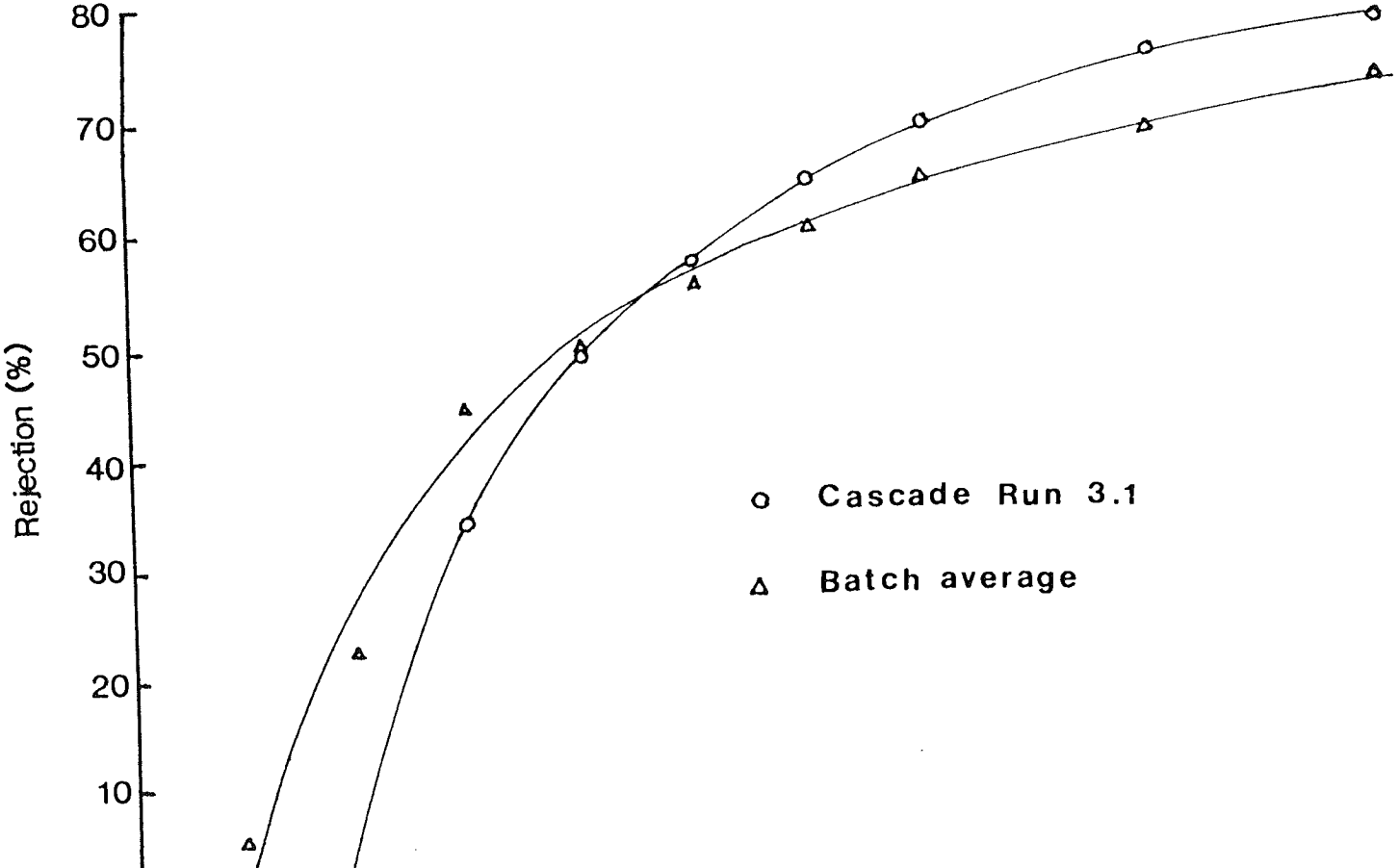

Figure 5.43 The Rejection Curve from Cascade Run 3.1

material below 12,000 MW, the rejection characteristics of the 12,000 MW to 98,000 MW band would be effected in the same manner.

Although the mathematical model correctly predicted the efficiency profile for the material below 12,000 MW the agreement for the 12,000-98,000 MW band was not as good. The model predictions are discussed in more detail in section 6.5.1.

Since the material was accumulating within stage two the efficiency of the cascade must be impaired. Table 5.16 shows only stages three and four were being used to fractionate the low molecular weight dextran and stage one was effectively redundant.

A comparison of these cascade results to those obtained by Poland using the 5000 MW cut-off membranes (Table 5.17) shows that for a single pass through the cascade the 10,000 MW cut-off membranes removed significantly more material below 12,000 MW. Naturally this was accompanied by a greater loss of material between 12,000 MW and 98,000 MW, the efficiency of retention being 15% lower than that found by Poland. At first this would appear to suggest that the 5000 MW cut-off membranes are the better option. However Poland's results show that three cascade passes would be required to obtain the same molecular weight distribution as a single pass through the 10,000 MW cascade. This results in an efficiency of retention 33% below that obtained from the 10,000 MW cascade.

Extrapolating the experimental results suggests that the correct BP specification below 12,000 MW could be achieved using a single cascade unit containing four 10,000 MW cut-off membranes operating at 2.5 diavolumes per stage. While Polands results suggested that four cascade units would be required if the 5000 MW cut-off membranes were used. Using the 10,000 MW cut-off membranes would therefore significantly reduce the operating costs because the pumping costs and the number of membranes used would be reduced.

Table 5.17 Results for Multipass Cascading Extracted from K Polands PhD

			RETENTATE PRODUCT					
Concentration (g/100g Sol)	%below 12000	%between 12000 - 98000MW	Concentration (g/100g Sol)	%below 12000MW	Efficiency of removal	%between 12000 - 98000MW	Efficiency of retention	%above 98000MW
1.765	25.0	61.0	1.45	18.0	40.84	68	91.50	14
Second Pass			1.11	13.0	67.29	73	75.26	14
Third Pass			0.83	10.0	81.18	75	57.82	15

The aim of this project was to develop a production system which used ultrafiltration to remove both ends of the molecular weight distribution. The initial problem was to decide which part of the molecular weight distribution should be removed first.

It was found that the removal of the material above 98,000 MW was more satisfactory at concentrations of 4% W/W or higher. If the material below 12,000 MW was to be removed first it would be necessary to use an initial feed concentration of 4 to 5% W/W. This would give a product concentration of 3.5 to 4.5% W/W which could then be used in subsequent cascade units. A membrane order of 1,2,3,5 was used since this was identical to the earlier experiments conducted at 2% W/W. See table 5.18. The results from these experiments were particularly unexpected since working at the higher concentration signficantly affected the efficiency of removal and the efficiency of retention, as well as the molecular weight distribution of the product. The percentage below 12,000 MW in the sample was approximately 16% compared to 9.5% for the same operating conditions at 2%. This effect can be explained by a combination of factors. At the higher concentration there was double the amount of low molecular weight material present. Since the cascade used the same number of diavolumes at both concentrations it may be simply that the cascade could not compensate for the greater amount of dextran present. The other possible factor involved was gel layer formation. As the concentration increased the gel layer could become thicker and more consolidated and this could interfere with the passage of molecules through the membrane and so affect the rejection characteristics of the cascade.

Table 5.18 Using a 4% Feed Concentration in the Cascade

	FEED				RETENTATE PRODUCT				
Run	Membrane order	Concentration (g/100g Sol)	%below 12000MW	%between 12000 - 98000MW	Concentration (g/100g Sol)	%below 12000	Efficiency of removal	%between 12000 - 98000MW	Efficiency of retention
4,1	1,2,3,5	3.698	24.63	63.18	2.65	15.74	54.22	69.91	79.19
4,2	1,2,3,5	4.69	24.63	63.18	3.427	15.57	53.65	70.21	81.50
4,3	1,2,3,5*	4.69	24.63	63.18	2.922	13.49	65.72	71.23	70.38

* product from run above used as feed for cascade.

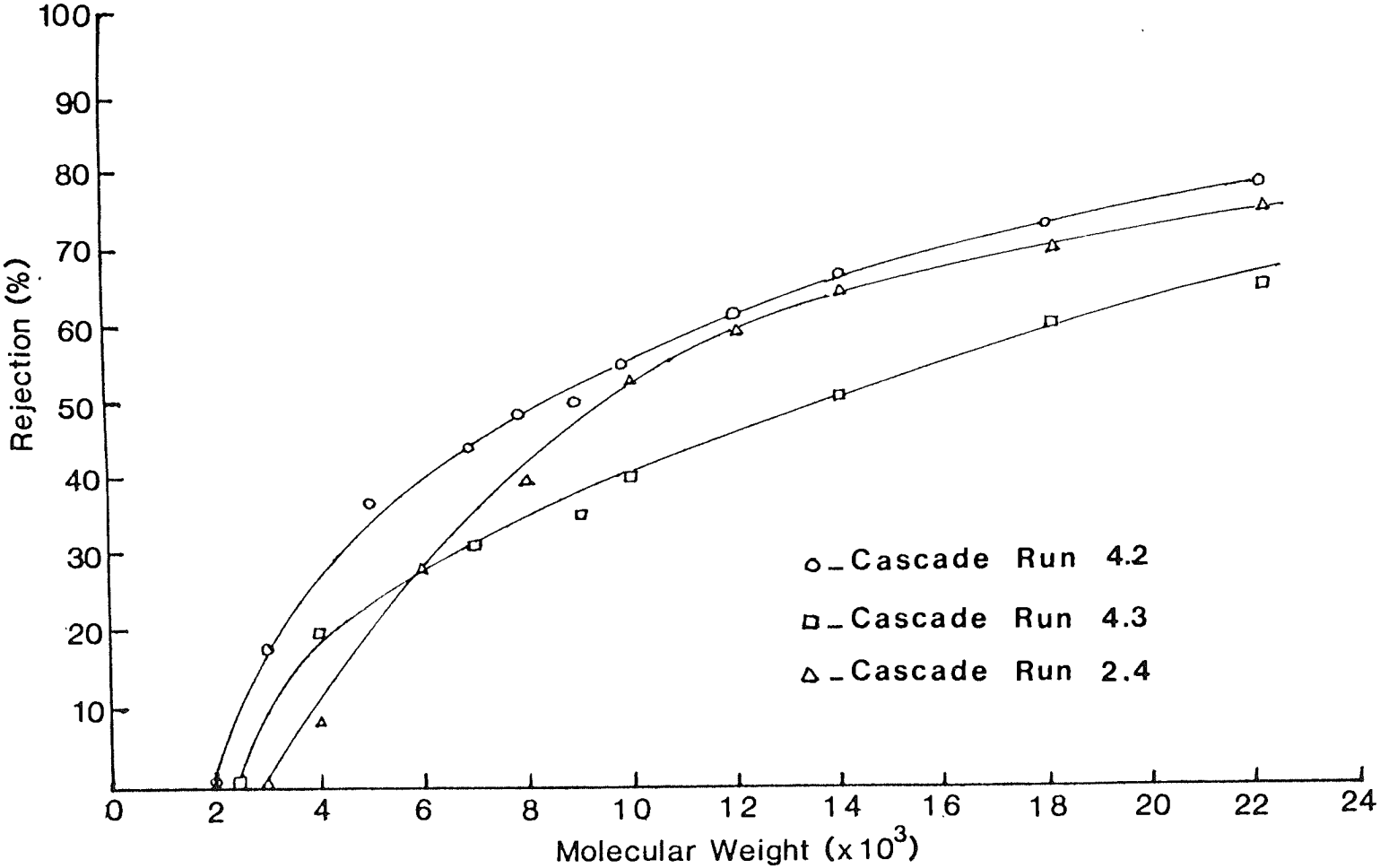

Figure 5.44 Comparing the Rejection Curves from the Cascade when using a 2% and 5% Feed Concentration

Since the correct distribution could not be obtained using a single pass through the cascade, multipass cascading was tried. Unfortunately, at this higher concentration this was also unsuccessful and the results could still not match those obtained using a single cascade pass with a 2% feed. See figure 5.44.

In conclusion these results show that the fractionation process must start with the removal of material above 98,000 MW.

5.4.4 USING MEMBRANES OF VARYING REJECTION PROPERTIES IN THE CASCADE

In the previous section it was shown that the rejection characteristics of the ultrafiltration cascade could be altered significantly by the careful selection of membranes. The earlier experiments had identified stage one and four as the two key stages. To expand on these results several different membrane configurations were investigated by using two 5000 MW cut-off membranes and two 10,000 MW cut-off membranes.

Placing the two 5000 MW cut-off membranes in stage one and four produced results almost identical to those obtained by Poland [6] using four 5000 MW cut-off membranes (see figure 5.45). This suggested that stages two and three had little effect on the fractionation process. This theory was tested by reversing the membrane sequence so stages two and three contained the 5000 MW cut-off membranes. As expected the rejection curve was significantly different from the previous experiment (5.1). See figure 5.46. If the two middle stage had not contributed to the fractionation process, run 5.2 should have matched the earlier experiment 2.4 which used only 10,000 MW cut-off membranes in the order 1,2,3,5. Although the two rejection curves had similar shapes, the rejection was noticeably higher over the whole molecular weight range in experiment 5.2.

Table 5.19 Mixing both 5000 MW and 10,000 MW cut-off Membranes in the Cascade

		FEED			RETENTATE PRODUCT				
Run	Membrane order	Concentration (g/100g Sol)	% below 12000 MW	% between 12000 - 98000 MW	Concentration (g/100g Sol)	% below 12000 MW	efficiency of removal	% between 12000 - 98000 MW	Efficiency of retention
5.1	5,10,10,5	1.84	24.15	63.47	1.513	16.31	44.37	69.88	90.49
5.2	10,5,5,10	1.84	24.15	63.47	1.377	13.34	58.62	72.35	85.27
5.3	5,5,10,10	1.836	24.63	63.08	1.422	16.61	47.74	70.62	86.72
5.4	10,5,10,10	1.849	24.63	63.08	1.474	15.68	49.20	69.28	87.56

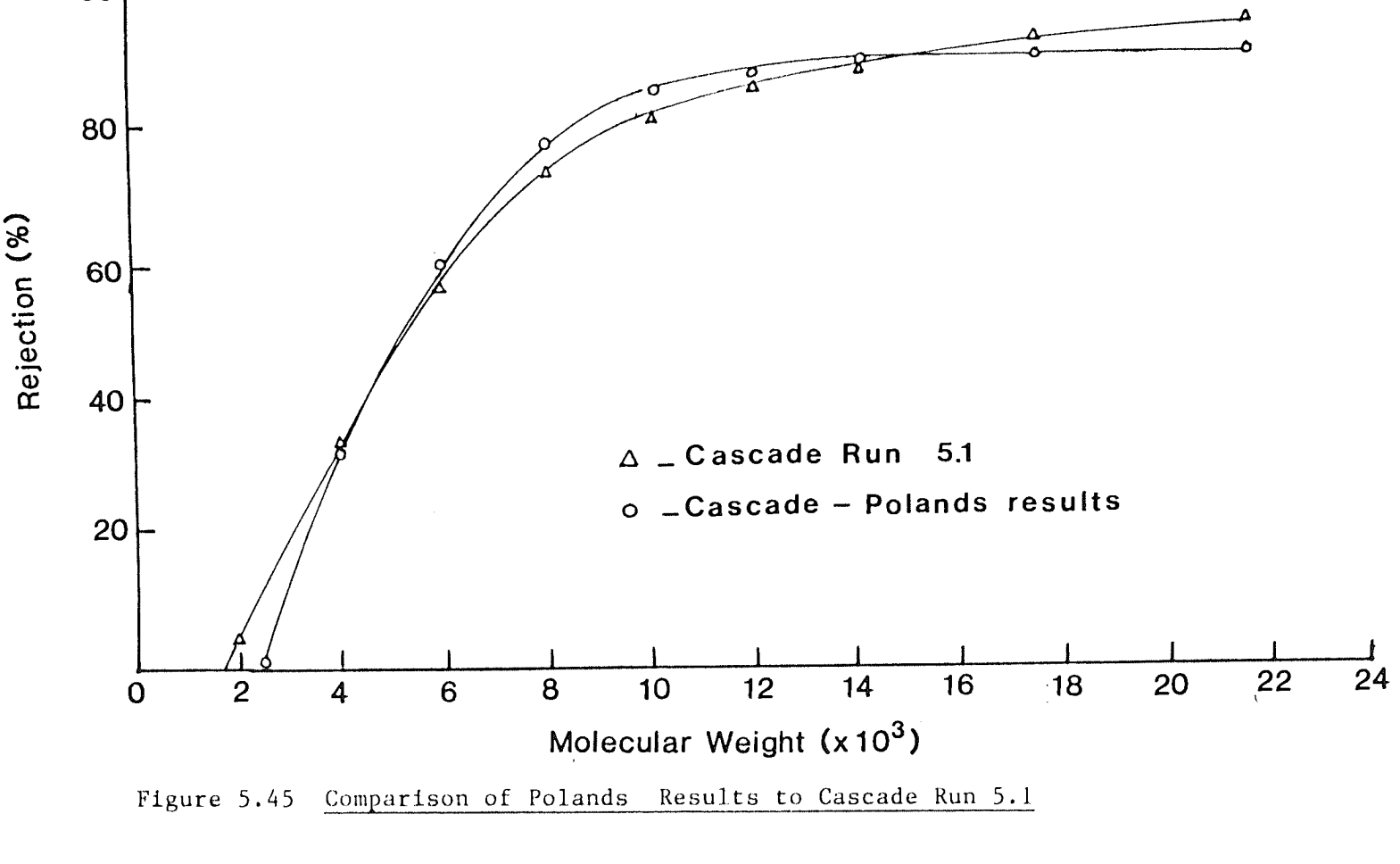

Figure 5.45 Comparison of Polands Results to Cascade Run 5.1

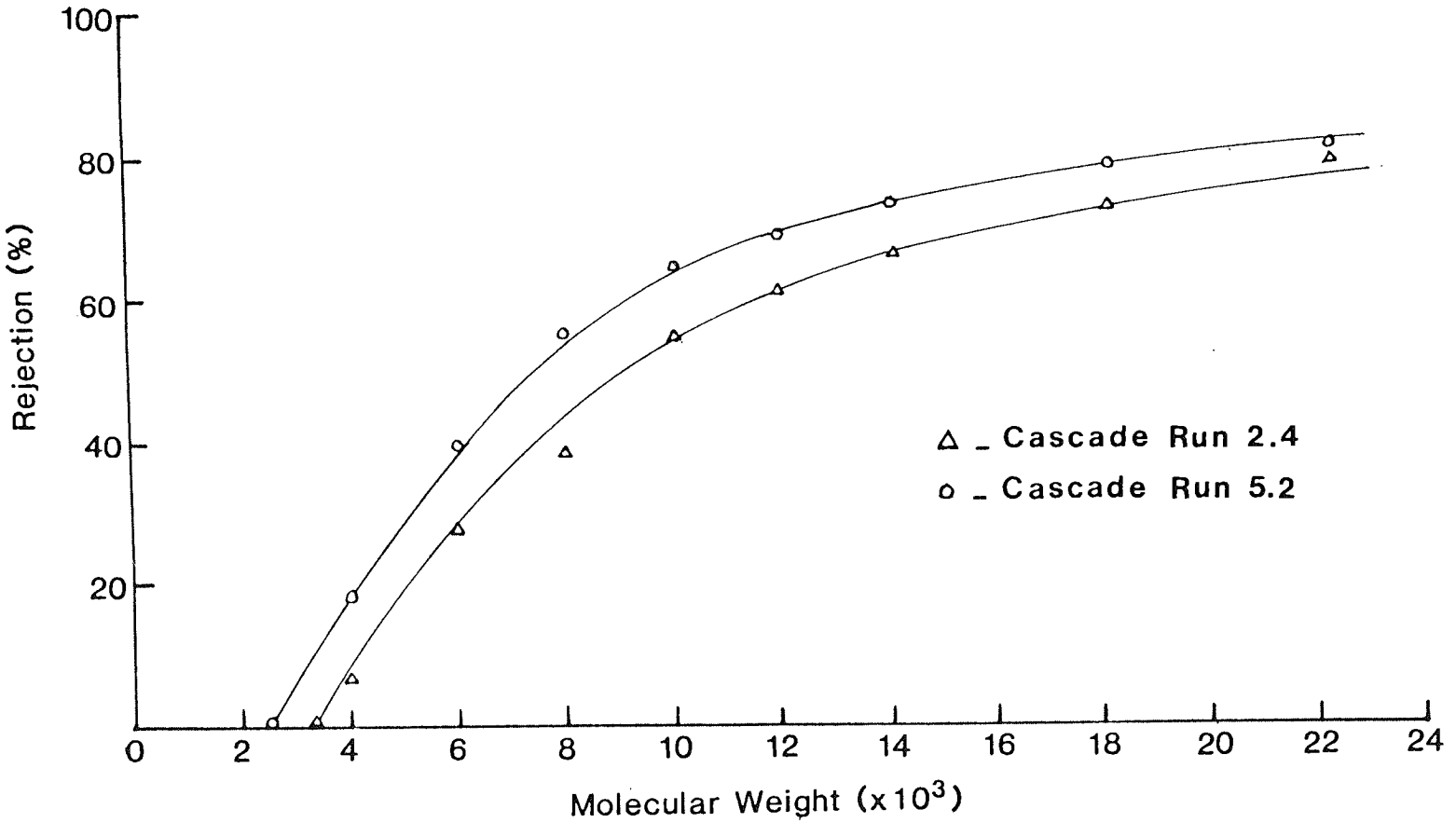

Figure 5.46 Mixing 5000 MW and 10,000 MW Cut-off Membranes within the Cascade (Run 5.2)

The main contribution of the two middle stages would appear to be to aid separation above and below the cross-over point. Their individual effect on the final product being less significant than either stage one or four. When the 5000 MW cut-off membranes were used in these stages their contribution was obviously more significant. The mathematical model was used to find out why this should be the case. The model predicted that these membranes would cause the retention of material within these stages simply because their rejection was significantly higher than the 10,000 MW cut-off membranes. Naturally this would effect the fractionation process and alter the final product specification.

To obtain a better assessment of the cascades performance in run 5.1 and 5.2 the rejection curves from these experiments were compared to the average batch rejection curve from the four membranes used. See figure 5.47. The two runs both exhibited a higher rejection above 12,000 MW than the other comparable experiments using the four 10,000 MW cut off membranes. However the cross-over points fell to 4500 MW and 9000 MW respectively; this was lower than required and was reflected in the lower efficiency of removal obtained from these two runs. When these runs were compared to the batch average rejection curve from the four 10,000 MW cut-off membranes, the higher rejections obtained were shown even more graphically, see figure 5.48. When compared on this basis the cross-over points fell to 3500 MW and 6800 MW. Again this appears to show that it will be impossible to increase the efficiency of retention without lowering the cross-over point.

Two further experiments were conducted to see if the results obtained from run 1.1 could be repeated by using the 5000 MW cut-off membranes. These results can be found in table 5.19. Interestingly the efficiency of removal and retention were very similar, however the shape of the rejection curves were completely different. See figure 5.49.

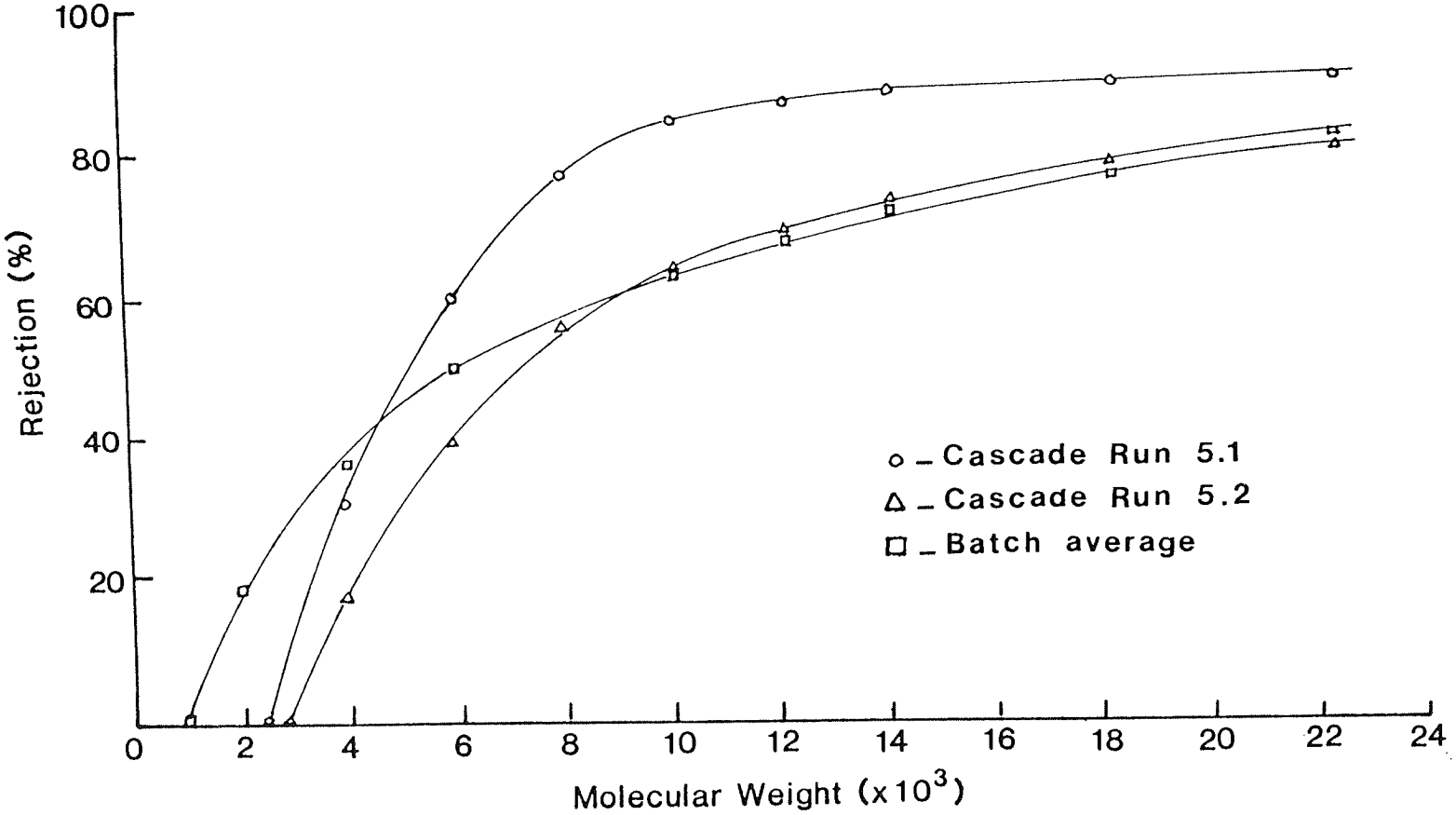

Figure 5.47 Rejection Curves from Cascade Runs 5.1 and 5.2

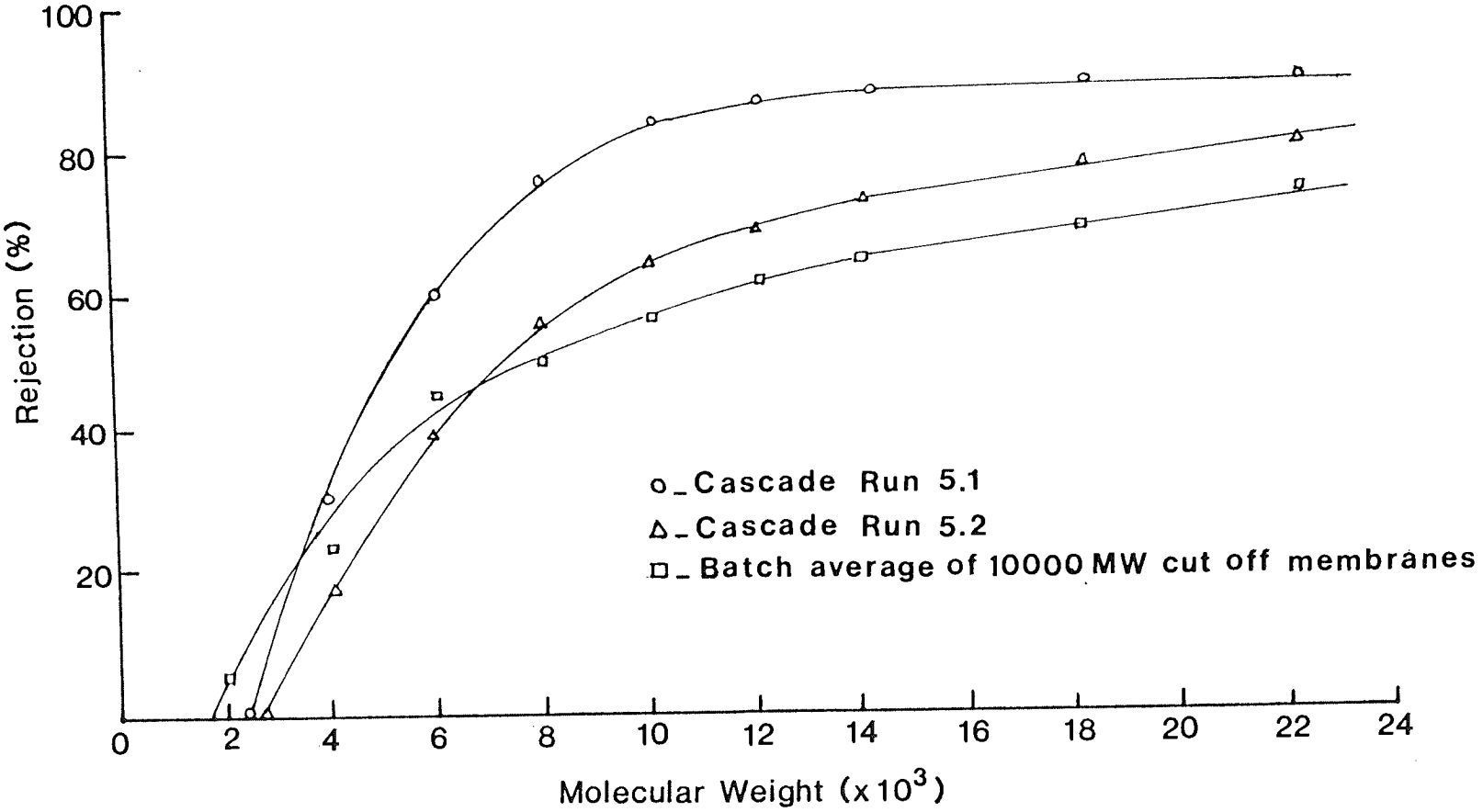

Figure 5.48 Comparing Cascade Runs 5.1 and 5.2 to the Batch Average of the 10,000 MW Cut-off Membranes

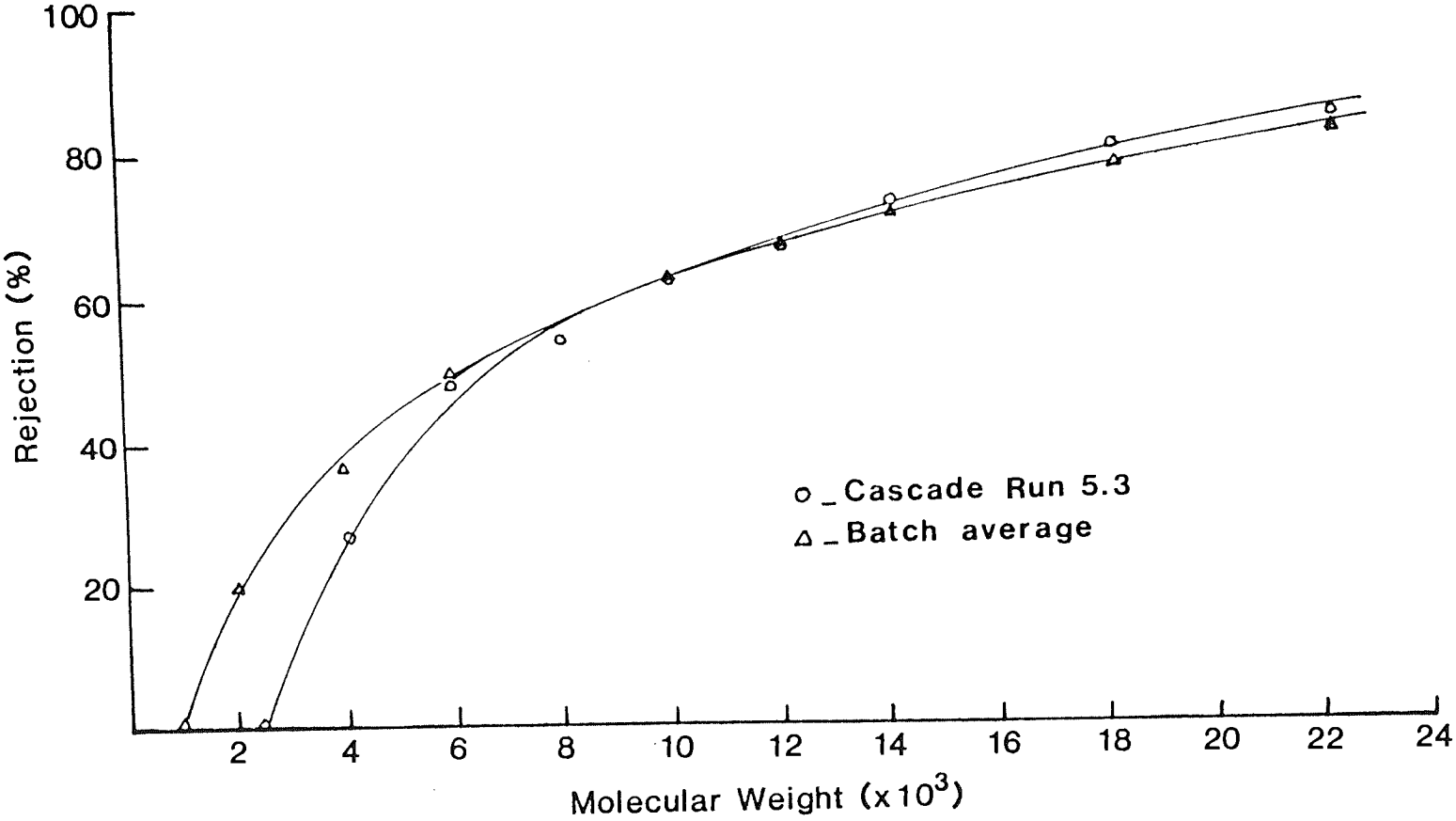

Figure 5.49 Rejection Curve from Cascade Run 5.3

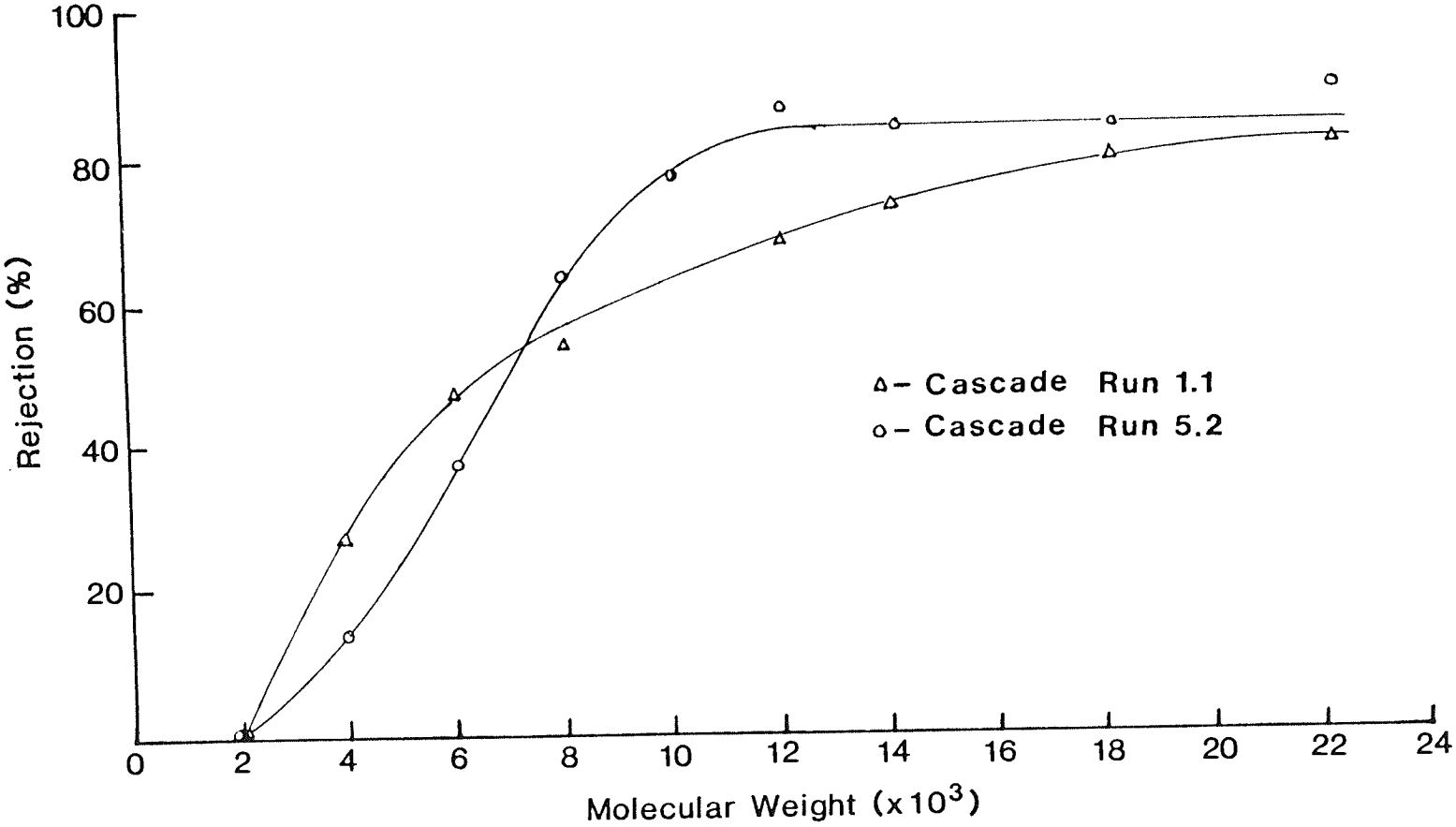

Figure 5.50 Comparing the Rejection Curve from Cascade Run 1.1 to Run 5.2

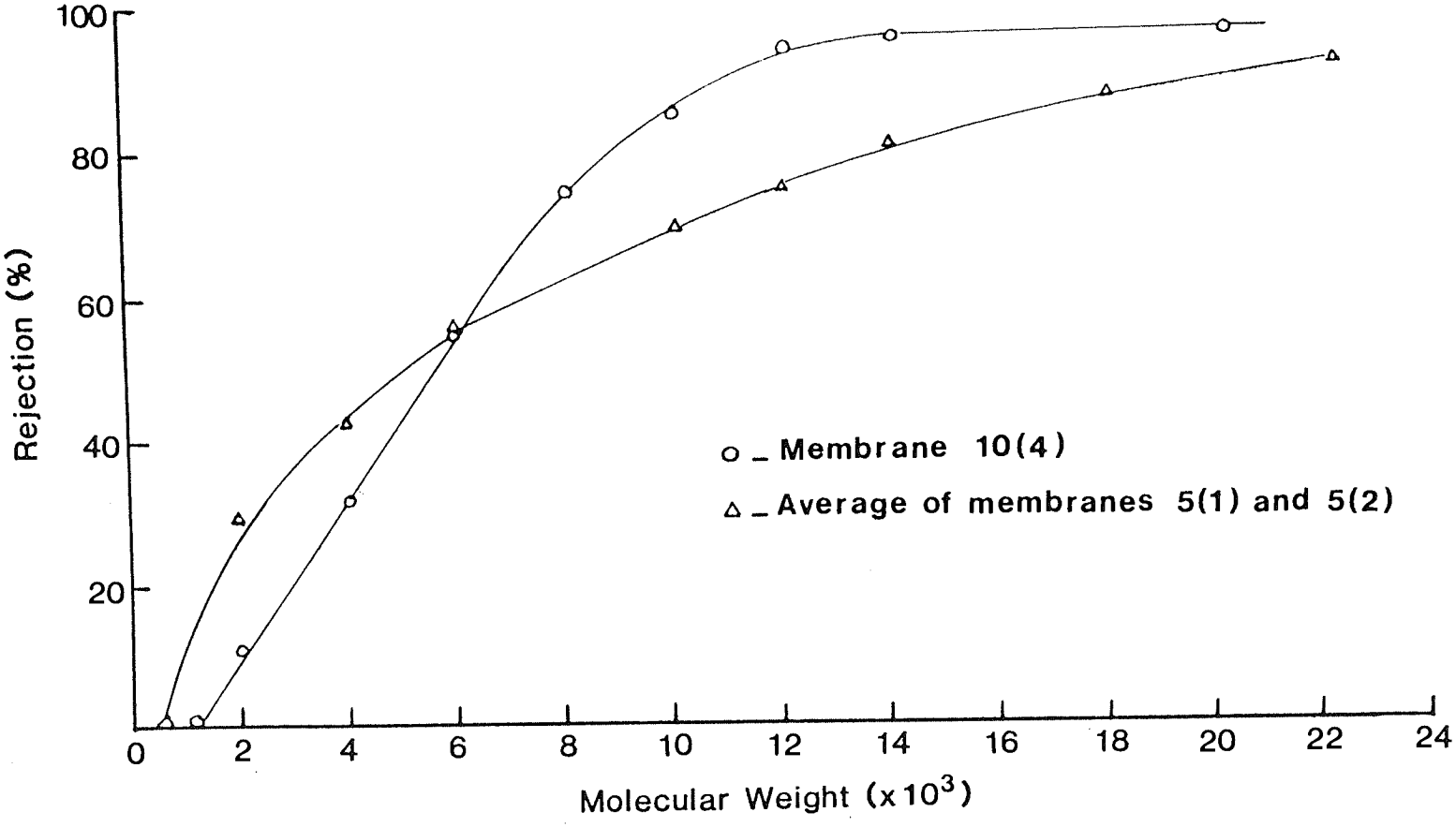

Figure 5.51 Comparing the Batch Rejection Curve from the 10,000 MW Cut-off Membrane Number 4 to the Average of the 5000 MW Cut-off Membranes 1 and 2

The rejection curve from cascade run 1.1 had a distinctly sharper profile than that obtained from cascade run 5.3. In run 5.3 the two 5000 MW cut-off membranes were positioned in stages one and two. This difference can be was explained by comparing the batch rejection curve from the 10,000 MW cut-off membrane number four to that for the two 5000 MW cut-off membranes. See figure 5.50. The 5000 MW cut-off membranes reject more dextran below 6000 MW, but after this value the rejection increases far slower than the 10,000 MW cut-off membrane. This shape was mirrored almost perfectly in the cascade results. See figure 5.51. These results must confirm that stage one is the controlling stage in the cascade.

These experiments have shown how the specification of the product from the cascade can be affected by the rejection characteristics of an individual membrane. In a production system the ability to maintain a consistent product will be of considerable importance. To maintain a consistent product it is clear that it will be necessary to set a very strict specification for the rejection characteristics of the membranes. Unfortunately this could result in the high failure rate and could have a significant affect on the economics of process unless an agreement could be obtained with the manufacturer for the return of any off specification membranes.

5.4.5 COMPARING THE EFFICIENCY OF ULTRAFILTRATION CASCADING TO ETHANOL FRACTIONATION PROCESS

A comparison of the two processes was made more difficult since the two processes were very different. The inital problem with the data obtained from the ethanol fractionation process was it included the removal of both the high and low molecular weight material, see figure 5.52 and table 5.20. Another problem was that the mass balances between

the syrup I and the final syrup were only approximate, since the data was obtained from the actual process which was not equipped for precise measurement.

The two methods of fractionation can be compared by considering two factors:-

1) The overall efficiency of removal and retention.

2) The molecular weight distribution of the product.

The overall efficiencies are compared graphically in figure 5.53. At first sight the results for the ultrafiltration cascade appear to be better than the ethanol process, but it must be remembered that the ethanol fractionation efficiency also incorporates the removal of the high molecular weight material.

To give the same efficiency of removal below 12,000 MW as the ethanol process the ultrafiltration cascade at best gave an efficiency of retention of 86%, this was only 9% better than the ethanol process.

When the molecular weight distribution of the final products were compared the results from the ultrafiltration cascade appeared more encouraging. The final product from the ethanol fractionation process still contained 16% below 12,000 MW and therefore had not reached the correct BP specification. Since further precipitation stages would be required to achieve this specification the final efficiency of retention was likely to be far lower.

To achieve a final syrup product within the BP specification below 12,000 MW it was clear that at least one or two further ethanol precipitations would be required, giving a total of four to five. While the ultrafiltration cascade could give the correct BP specification using an estimated 2.5 diavolumes in a single cascade unit. These results suggest that it would be easier to achieve the BP specification using the ultrafiltration cascade.

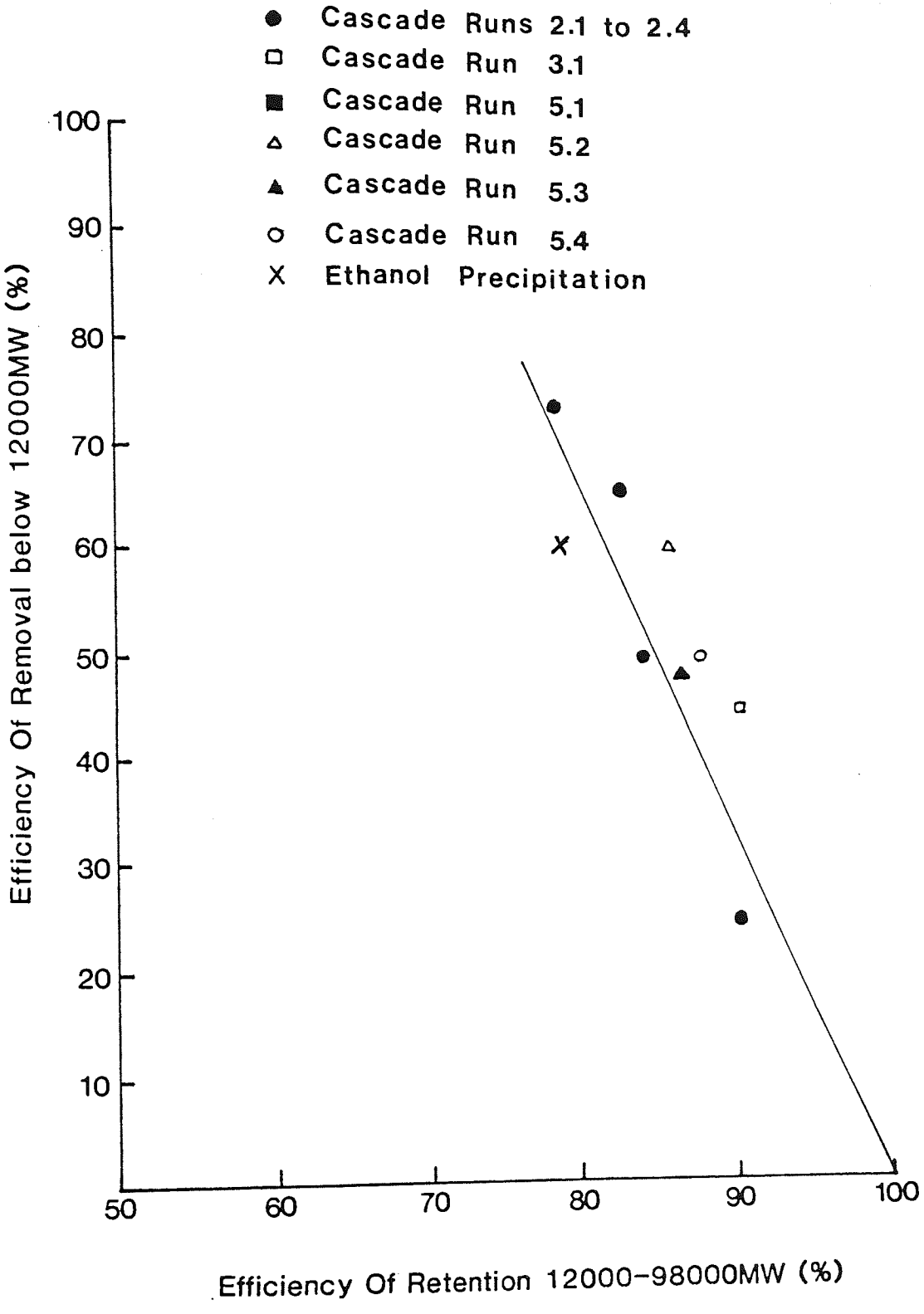

Figure 5.52 Comparing the Efficiency of the Cascade System to the Industrial Ethanol Precipitation Process

Although the ultrafiltration cascade showed great promise these results suggested that once the high molecular weight material had been removed the efficiency of retention of the 'saleable' band would drop to below that obtained using ethanol fractionation. Therefore on a purely economic basis the ultrafiltration cascade would not be able to match the current state of art ethanol fractionation process. It must be noted however that the efficiency of the ultrafiltration cascade was only limited by the quality of the membranes presently available. Once the quality of the 10,000 MW cut-off membranes are improved it is probable that this process could replace the current industrial process.

Figure 5.53 Fractionation Process for Dextran (batch RB 5R)

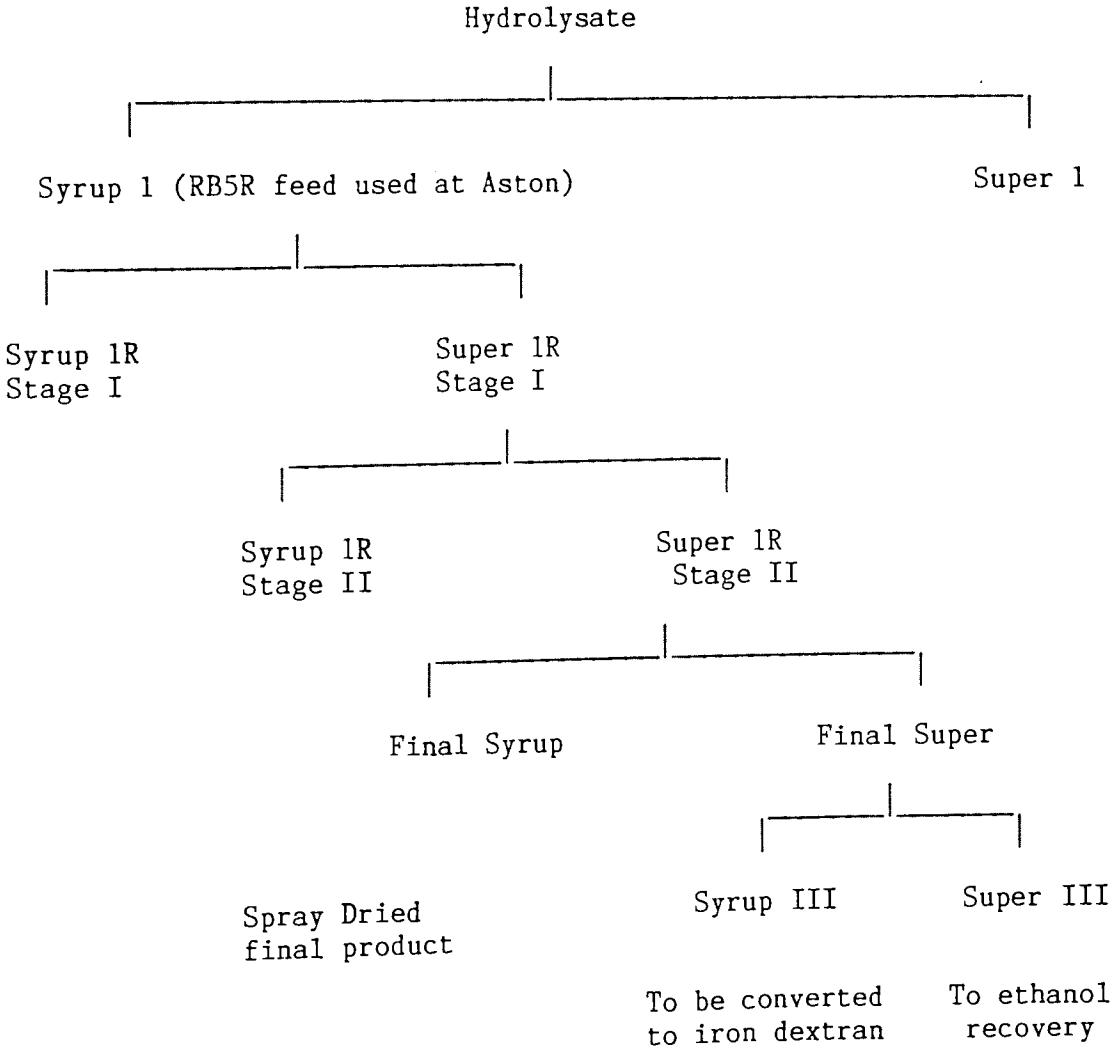

Table 5.20 The Ethanol Precipitation Process

Fractionation step	Mass in stage (Kg)	% below 12000 MW	Ethanol efficiency of removal	% between 12000 and 98000 MW	Ethanol efficiency of retention	% above 98000 MW
Hydro	2815	38.75	-	51.8	-	9.45
Syrup I	2530	25.0	0	61.0	100	14.0
Super I	239	90.94	-	9.0	-	0.06
Syrup 1RS1	259	15.98	-	39.33	-	44.69
Super 1RS1	2271	27.52	1.19	63.25	93.04	9.23
Syrup 1RS2	349	8.21	-	57.34	-	34.45
Super 1RS2	1922	31.27	4.98	65.79	81.93	2.94
Final Syrup	1548	16.14	60.49	79.31	79.22	4.55
Final Super	374	77.69	-	22.18	-	0.13
Syrup III	281	72.76	-	27.17	-	0.07
Super III	93	96.40	maximum molecular weight 88790			

5.5 REMOVAL OF DEXTRAN ABOVE 98,000 MW

5.5.1 INTRODUCTION

Since the ethanol fractionation process could be used to remove both ends of the dextran distribution, it was important that the ultrafiltration process could compete on the same basis. Usually an ultrafiltration system would be used to remove small amounts of low molecular weight impurity from a high molecular weight product. Normally the high molecular weight product would be present in far greater amounts than the impurity. To obtain the correct specification for the removal of dextran above 98,000 MW it was necessary for the membrane to remove up to 90% if the dextran in the permeate and retain the remaining 10%. Since little useful experimental data was found within the literature it was considered to be desirable to investigate both the batch ultrafiltration processes and the ultrafiltration cascading system for the removal of this material.

5.5.2 TESTING ALTERNATIVE BATCH TECHNIQUES FOR THE REMOVAL OF DEXTRAN ABOVE 98,000 MW

The range of membranes available for the removal of material above 98,000 MW was found to be limited. The Amicon range of membranes only contained two possible alternatives, a 30,000 MW and a 100,000 MW cut-off membrane. The 30,000 MW cut-off membrane would certainly inhibit the removal of the 'saleable' 12,000 MW to 98,000 MW band so the 100,000 MW cut-off membrane (code HIP100-20) was purchased. The membrane was used in the Amicon DC2A unit mentioned in section 5.4.1. The test conditions used were identical to those mentioned in section 5.4.1 except that the recirculation rate was increased to 500 cm^3/min.

Table 5.21 Amicon 100,000 MW cut-off Membrane using a 2% feed

		RETENTATE PRODUCT				
Number of Diavolumes used	Concentration g/100gSol	% below 12000 MW	% between 12000 MW - 98000 MW	Efficiency of removal below 98000 MW	% above 98000 MW	Efficiency of retention above 98000 MW
Feed	2.05	24.63	63.08	0	12.29	100
1	1.01	18.45	62.98	54.28	18.57	74.50
2	0.653	14.17	62.81	72.08	23.02	59.76
3	0.368	8.337	59.943	86.04	31.72	46.21
4	0.213	6.79	50.89	93.01	42.32	35.86

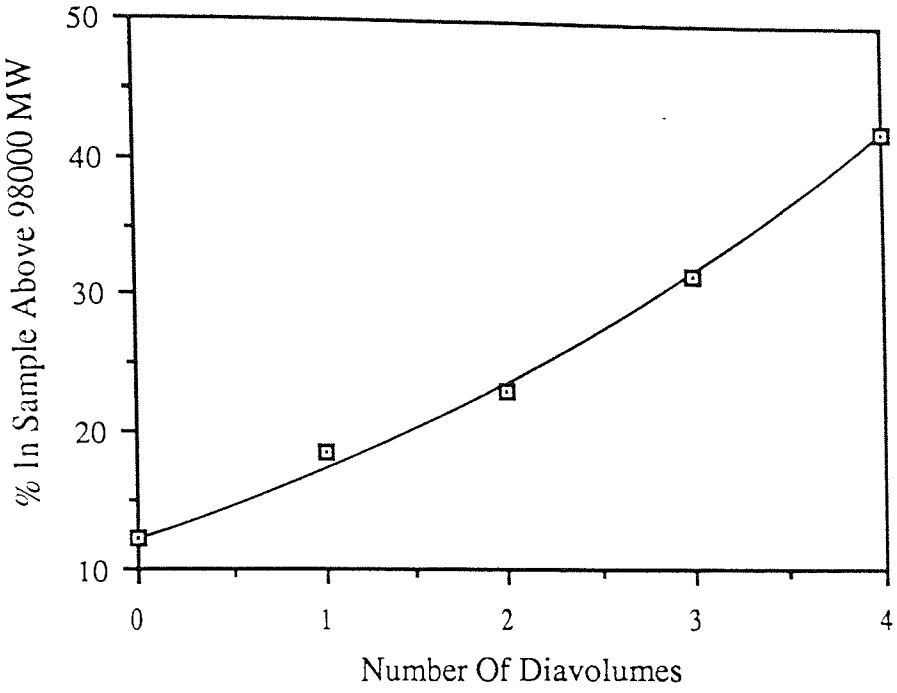

Figure 5.54 How the Number of Diavolumes used Effects the Percentage of Material above 98,000 MW in the Retentate

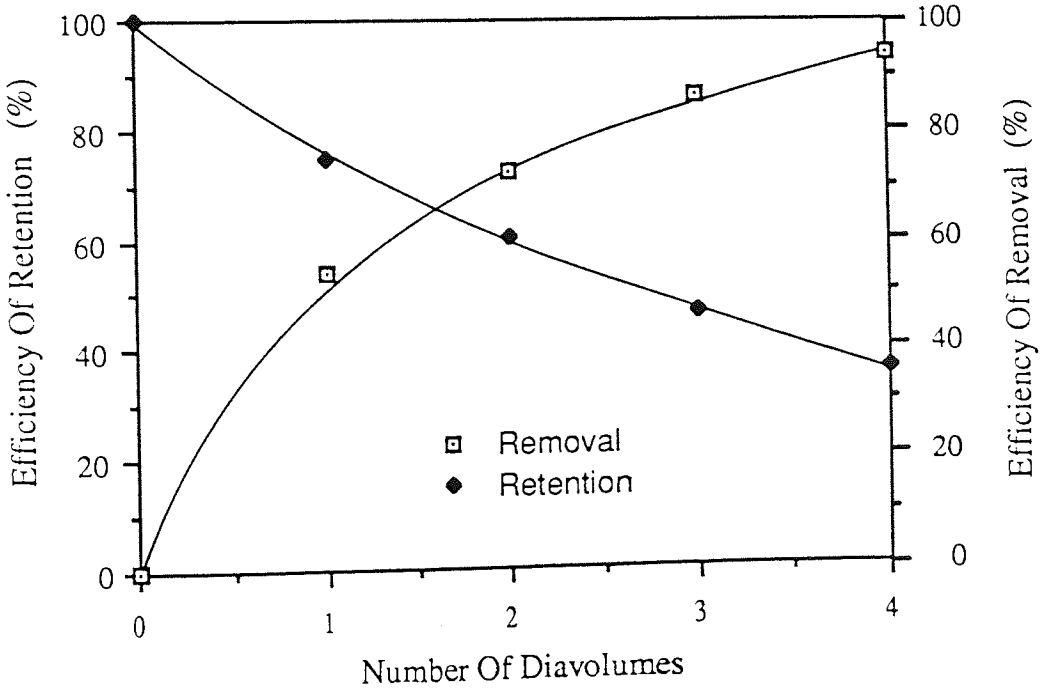

Figure 5.55 The Relationship between Efficiency and Number of Diavolumes used. 2% Feed Concentration

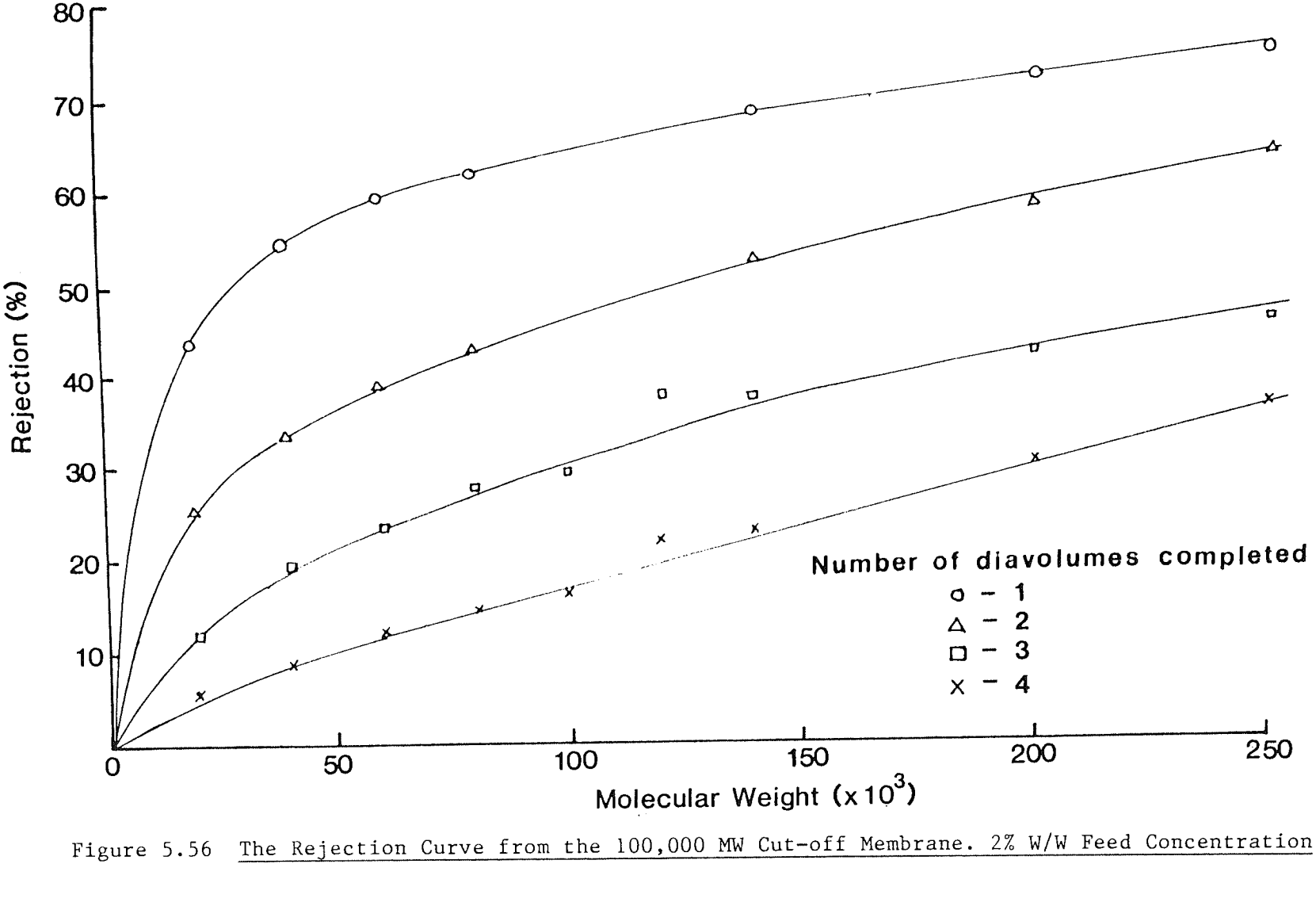

Figure 5.56 The Rejection Curve from the 100,000 MW Cut-off Membrane. 2% W/W Feed Concentration

Table 5.22 Amicon 100,000 MW cut-off Membrane in Concentration Mode

Volume of Retentate remaining (cm^3)	Concentation of permeate (g/l)	PERMEATE PRODUCT % below 98000 MW	Efficiency of removal below 98000 MW	% above 98000 MW	Efficiency of retention above 98000 MW
2000 (Feed)	19.50	87.71	0	12.29	100
1800	9.267	93.50	5.06	6.50	97.49
1600	11.01	93.36	11.07	6.64	94.45
1400	10.95	94.08	17.09	5.92	91.76
1200	11.54	93.68	23.41	6.32	88.71
1000	12.06	94.24	30.06	5.76	85.82
800	13.365	96.24	37.34	6.76	82.05
600	13.627	93.12	44.76	6.88	78.13
400	15.253	93.72	53.11	6.28	74.14
200	18.458	93.73	63.23	6.27	69.31

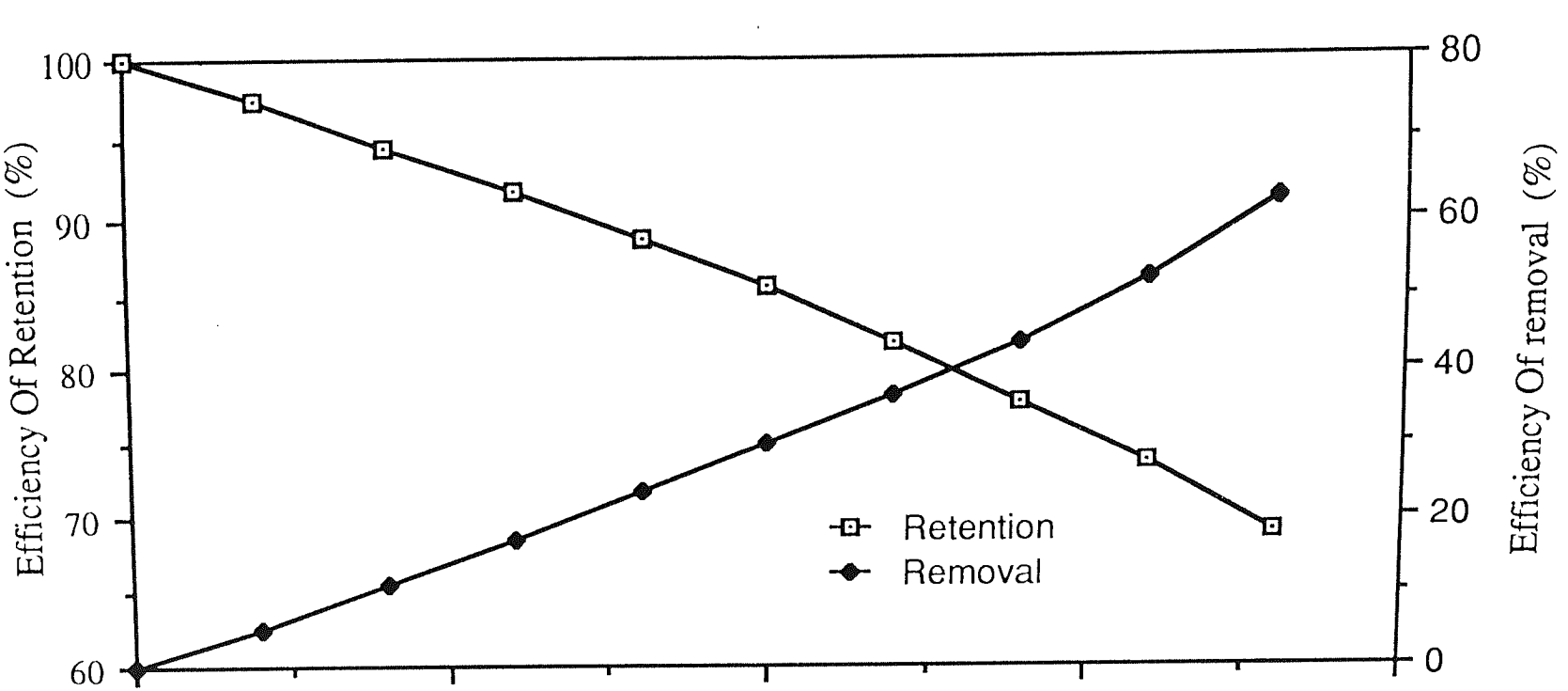

Figure 5.57 Using the 100,000 MW Cut-off Membrane in the Concentration Mode of Operation

Table 5.23 Amicon 100,000 MW cut-off Membrane using a 5% feed

RETENTATE PRODUCT

Number of Diavolumes used	Concentration g/100g Sol	% below 12000 MW	% between 12000 MW - 98000 MW	Efficiency of removal below 98000 MW	% above 98000 MW	Efficiency of retention above 98000 MW
Feed	4.462	24.63	63.08	0	12.29	100
1	2.741	21.72	61.78	41.46	16.50	82.48
2	1.759	12.62	63.5	65.74	23.88	76.64
3	1.151	8.06	59.94	80.01	32.0	67.15
4	0.782	4.96	53.39	88.34	41.65	59.31

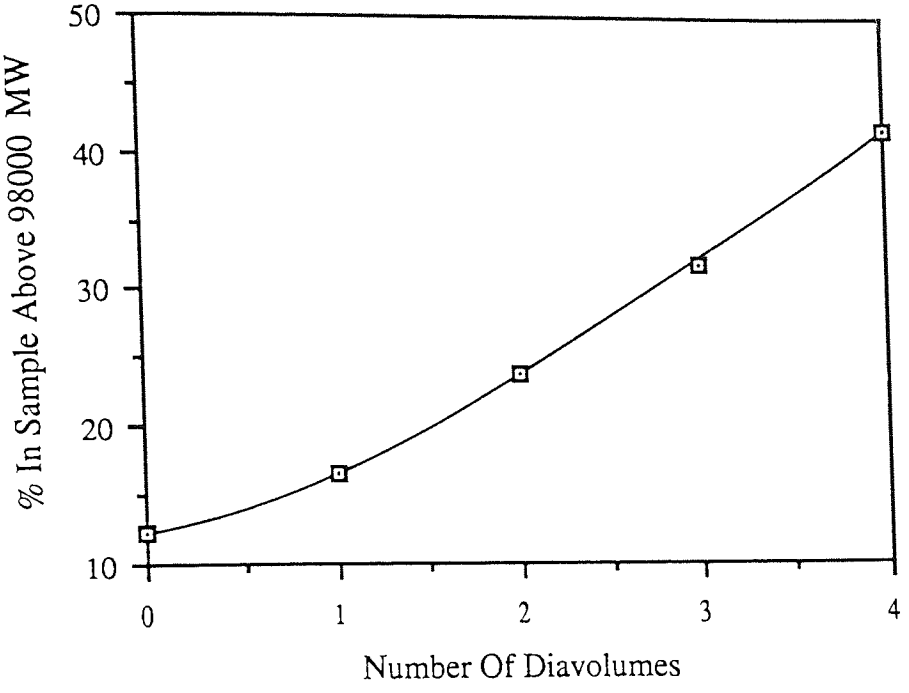

Figure 5.58 How the Number of Diavolumes used Effects the Percentage of Material above 98,000 MW in the Retentate

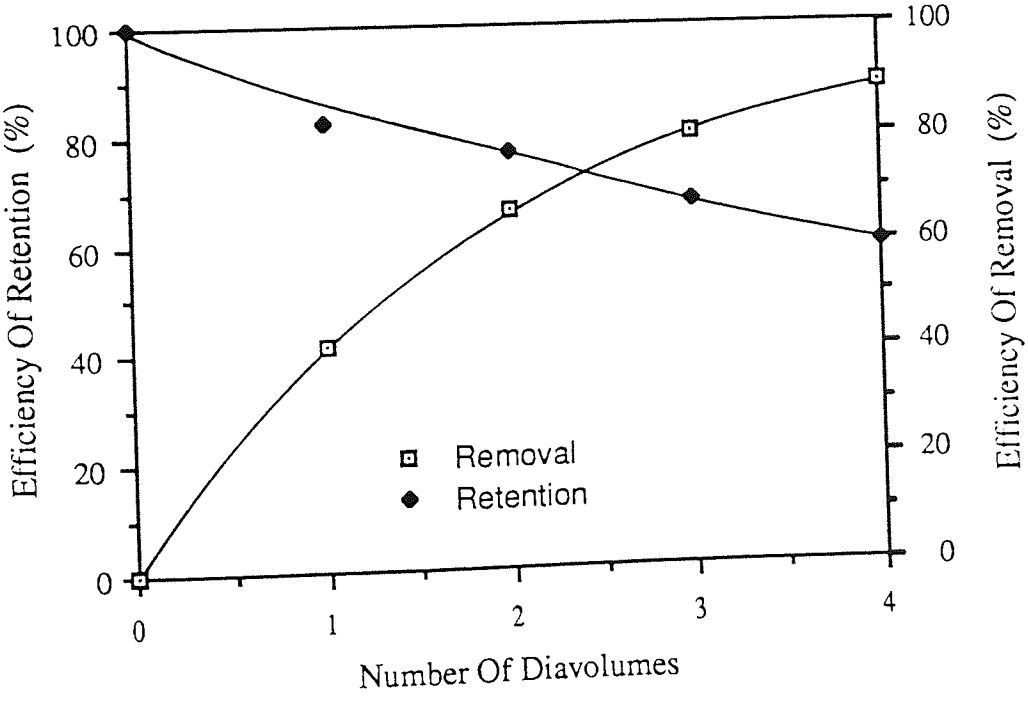

Figure 5.59 The Relationship between Efficiency and Number of Diavolumes used. 5% Feed Concentration

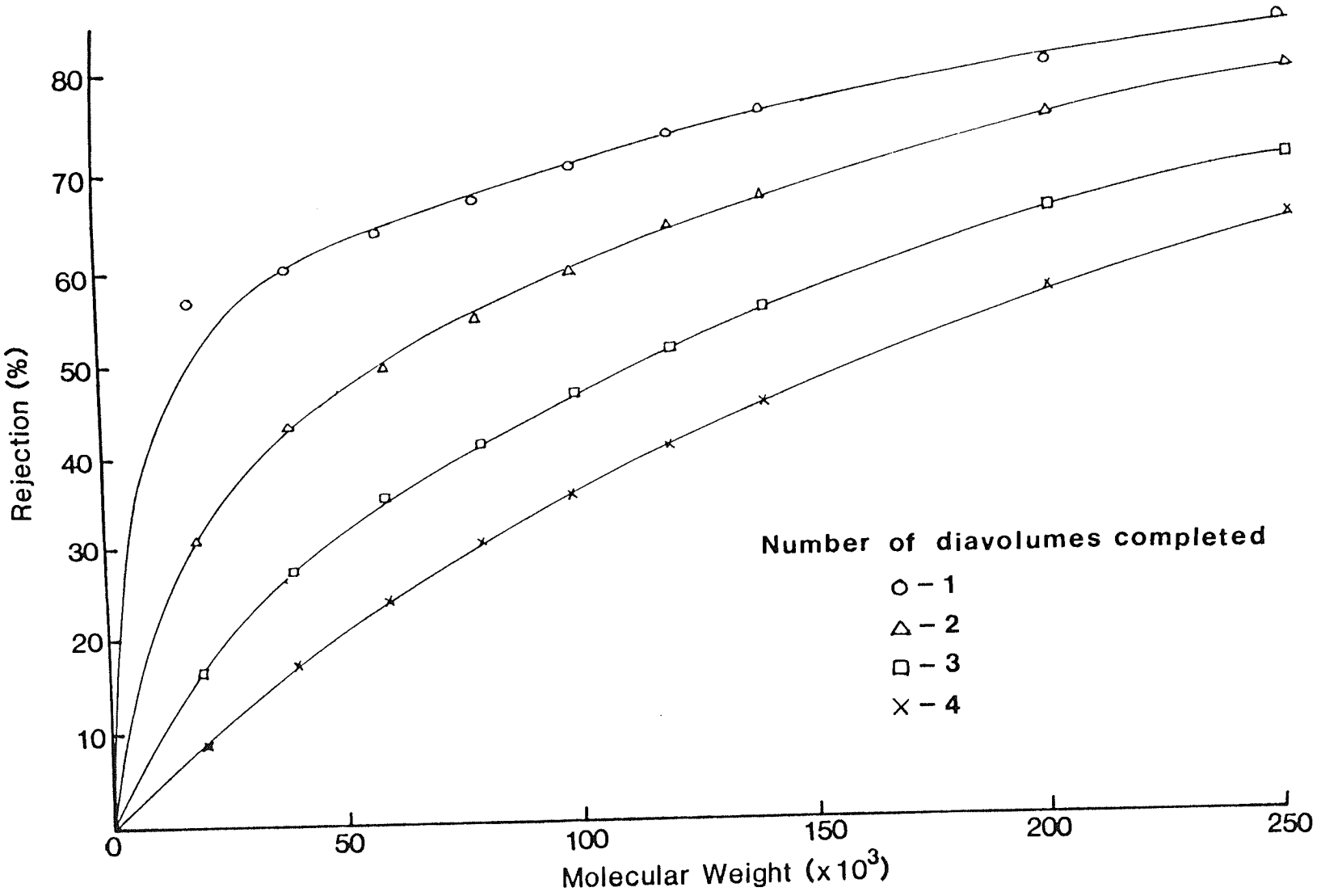

Figure 5.60 The Rejection Curves from the 100,000 MW Cut-off Membrane. 5% Feed Concentration

The membrane was tested in both the diafiltration and concentration modes of operation. Initially a 2% W/W feed concentration was used. The diafiltration mode of operation was highly satisfactory at removing the material below 98,000 MW since the molecules were 'washed' through by the diafiltrate. See table 5.21 and figures 5.54 to 5.55. Using four diavolumes, 93% of the material below 98000 MW was removed in the permeate but a large proportion of the larger molecules were also lost. After four diavolumes only 35% of the dextran above 98,000 MW had been retained. The rejection curves obtained at each of the four diavolumes can be found in figure 5.56. The rejection of each molecular weight band rapidly decreases as the number of diavolumes used was increased. The rejection of dextran with a molecular weight of 98,000 MW drops from 64% at one diavolume to only 17% at four diavolumes.

Using the same membrane in the concentration mode improved the retention of the dextran above 98,000 MW and the process had the added advantage that the waste dextran was in a concentrated form, making storage and treatment easier. Unfortunately the efficiency of removal was significantly lower than that obtained when using diafiltration. See table 5.22 and figure 5.57. Although the retentate could be rediluted and the concentration procedure repeated, there was little to be gained by doing this since the retention of the high molecular weight dextran would be impaired.

The membrane was again tested using the diafiltration mode, however the feed concentration was increased to 5% W/W. See table 5.23 and figures 5.58 to 5.59. The higher concentration was found to give a higher retention of material particularly above 98,000 MW. At four diavolumes the efficiency of retention was 59% and the efficiency of removal below 98,000 MW was 88%. In comparison, a 2% W/W feed gave an efficiency of retention of 59% after only 2 diavolumes and by four diavolumes had dropped to only 35%. The efficiency of removal below

98,000 MW after 4 diavolumes was 93%. The rejection curves obtained from the membrane at the higher feed concentration can be found in figure 5.60. The greater retention of the high molecular weight material is shown by the steeper gradient of each rejection curve. The effect becomes more noticable as the number of diavolumes increases. An analysis of the data from the two experiments showed that when the 5% W/W feed concentration was used the total mass of dextran passing through the membrane significantly increased. This indicates that the diafiltrate was being used more efficiently at the higher concentration.

Although it is clear that the dialysates ability to 'wash' material through the membrane was the critical factor affecting both the efficiency of removal and retention, there was some indication that the presence of the gel layer alters the rejection of the dextran molecules. When the 2% W/W feed was used the majority of the experiment was conducted at a concentration below which the gel layer could be present, at the higher concentration the reverse was the case. Since the efficiency of retention above 98,000 MW was significantly higher when the higher feed concentration was used, the gel layer may be partly responsible for the higher retention of the very large dextran molecules. These molecules have a molecular weight from 98,000 MW to in excess of 1×10^7 MW.

To obtain a higher efficiency of retention without reducing the efficiency of removal a hybrid process was considered. Initially the system was operated in the diafiltration mode after which the retentate was concentrated. The results can be found in table 5.24 to 5.28. The process was found to be satisfactory between 0.5 and 1.5 diavolumes. If the number of diavolumes used was increased above this value, the retentate became too dilute. This process was also affected by the feed concentration in a similar manner to the diafiltration experiments

Table 5.24 Diafiltration followed by Concentration (2% Feed)

PERMEATE PRODUCT

Volume of retentate remaining (cm^3)	Concentration of permeate (g/l)	% below 98000 MW	Efficiency of removal below 12000 MW	% above 98000 MW	Efficiency of retention above 98000 MW
2000 (Feed)	18.09	87.71	0	12.29	100
(1 Diavolume completed)					
2000	8.14	91.25	46.83	8.75	68.04
1450	6.104	91.08	56.47	8.92	61.32
1000	6.605	90.57	64.95	9.43	55.03
500	7.609	90.05	75.75	9.95	46.54
100	8.65	92.27	85.81	7.73	40.54

Table 5.25 Diafiltration followed by Concentration (4% Feed)

		PERMEATE PRODUCT			
Volume of retentate remaining (cm^3)	Concentration of permeate (g/l)	% below 98000 MW	Efficiency of removal below 98000 MW	% above 98000 MW	Efficiency of retention above 98000 MW
2000 (Feed)	35.0	87.71	0	12.29	100
(1 Diavolume completed)					
2000	13.24	94.54	40.77	5.46	83.19
1500	11.43	91.09	49.25	8.91	77.27
950	12.53	90.95	59.46	9.05	70.02
500	14.25	90.52	68.92	9.48	62.96
100	22.04	89.78	81.81	10.22	52.48

Table 5.26 Diafiltration followed by Concentration (5% Feed)

Volume of retentate remaining (cm^3)	Concentration of permeate (g/l)	% below 98000 MW	Efficiency of removal below 12000 MW	% above 98000 MW	Efficiency of retention above 98000 MW
		PERMEATE PRODUCT			
2000 (Feed)	47.26	87.75	0	12.25	100
0.5 Diavolumes completed					
2000	22.0	95.03	25.21	4.95	90.55
1500	19.20	95.09	36.21	4.91	86.48
1000	21.54	95.15	48.59	4.85	81.97
500	25.4	94.81	63.08	5.19	76.26
100	41.27	93.10	81.61	6.9	66.41

Table 5.27 Diafiltration followed by Concentration (5% Feed)

PERMEATE PRODUCT

Volume of retentate remaining (cm^3)	Concentration of permeate (g/l)	% below 98000 MW	Efficiency of removal below 98000 MW	% above 98000 MW	Efficiency of retention above 98000 MW
2000 (Feed)	46.74	87.75	0	12.25	100
1.0 Diavolume completed					
2000	18.195	95.13	42.21	4.87	84.19
1450	14.29	93.78	51.19	6.22	79.91
1000	14.81	93.66	58.8	6.34	76.22
500	18.66	92.87	69.36	7.13	70.41
100	29.787	92.41	82.78	7.59	62.52

Table 5.28 Diafiltration followed by Concentration (5% Feed)

Volume of retentate remaining (cm^3)	Concentration of permeate (g/l)	% below 98000 MW	Efficiency of removal below 98000 MW	% above 98000 MW	Efficiency of retention above 98000 MW
		PERMEATE PRODUCT			
2000 (Feed)	47.26	87.75	0	12.25	100
1.5 Diavolumes completed					
2000	15.36	95.16	52.87	4.84	83.72
1500	10.72	92.63	58.85	7.37	77.31
1000	10.93	92.32	64.94	7.68	73.68
500	14.05	92.05	72.73	7.95	68.84
100	24.59	91.03	83.54	8.97	61.21

mentioned earlier. The efficiency of retention increased from 40% to 62% as the feed concentration increased from 2% to 5%. The efficiency of removal only decreased from 85.81% to 82.78%. Unfortunately the hybrid system could only produce a final product with a similar specification to the diafiltration system although the system had the advantage that the volume of retentate and permeate was reduced. The efficiency of retention had not improved as significantly as was first expected.

Although the results show that an ultrafiltration system could fractionate the dextran in the desired manner the efficiency of retention was lower than required. Since Amicon did not manufacture another membrane suitable for this fractionation the Romicon range of hollow fibre membranes were considered. A 50,000 MW cut-off membrane was purchased (code number HF1-43-PM50). The membrane was manufactured in polysulphone and had a surface area of approximately 0.09 m^2. Each fibre was 1 mm in diameter compared to 0.5 mm in the Amicon units. A test rig was also borrowed from Romicon. This unit was of a similar design to Amicon DC2A unit but used a centrifugal pump to recirculate the feed. After consultation with Romicon a recirculation rate of 7 l/min was used.

When tested using the diafiltration mode the membrane was found to be of an exceedingly high quality. See table 5.29 and figures 5.61 to 5.62. After four diavolumes the membrane had still retained 83% of the dextran above 98,000 MW and had removed 87% below 98,000 MW. The Amicon membrane gave efficiencies of 59% and 88% when tested under similar conditions. The rejection curve for this membrane shows very clearly the membranes ability to reject the material above 98,000 MW, see figure 5.63. The rejection of the dextran with a molecular weight of 98000 MW was 55% after four diavolumes compared to only 35% for the Amicon membrane.

Table 5.29 Romicon 50,000 MW cut-off Membrane Number 1

Number of Diavolumes	Concentration g/100g Sol	% below 12000 MW	% between 12000 and 98000 MW	Efficiency of removal below 98000 MW	% above 98000 MW	Efficiency of retention above 98000 MW
Feed	3.965	23.56	67.68	0	8.76	100
0.5	2.847	21.45	66.8	30.55	11.75	96.25
1.0	2.234	17.09	68.06	47.47	14.85	95.38
2.0	1.42	12.06	66.47	69.03	21.47	87.61
3.0	1.02	8.18	62.42	80.09	29.04	86.4
4.0	0.77	5.27	57.39	86.67	37.34	82.71

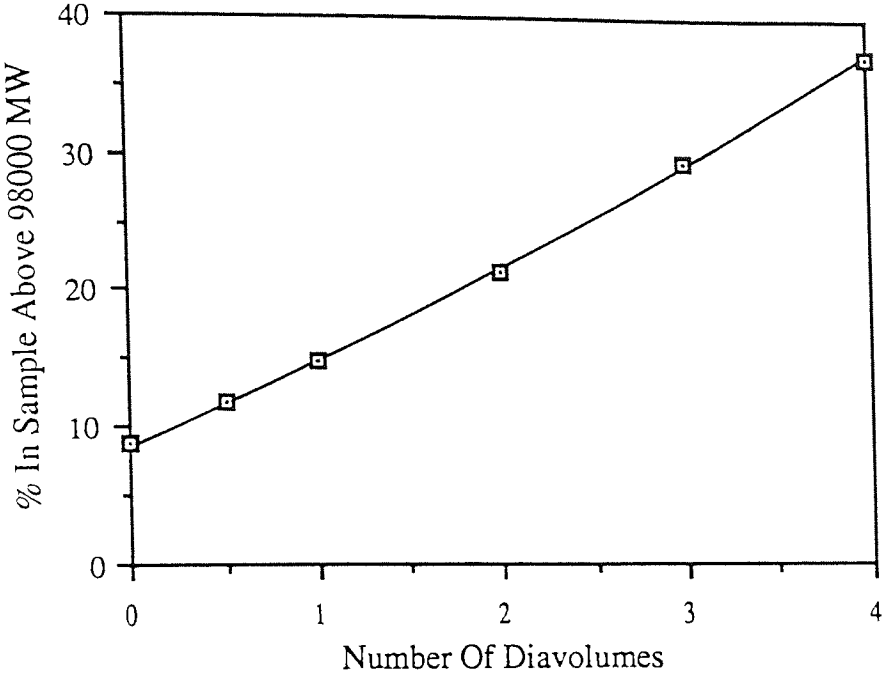

Figure 5.61 How the Number of Diavolumes used Effects the Percentage of Material above 98,000 MW in the Retentate

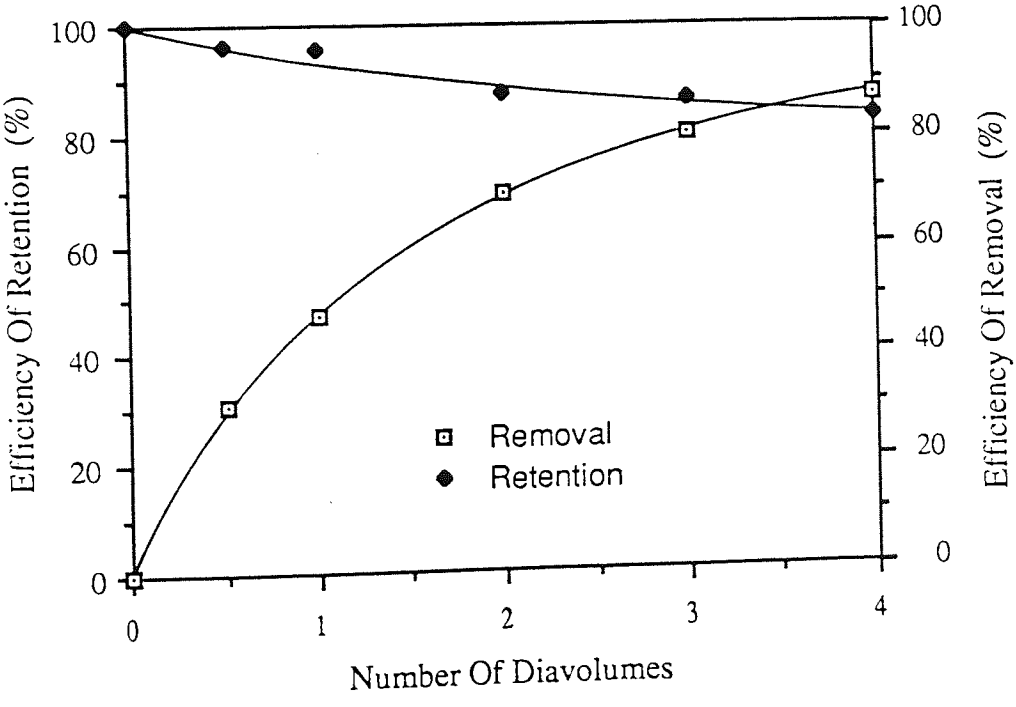

Figure 5.62 The Relationship between Efficiency and Number of Diavolumes used. Recirculation Rate of 7 l/min used

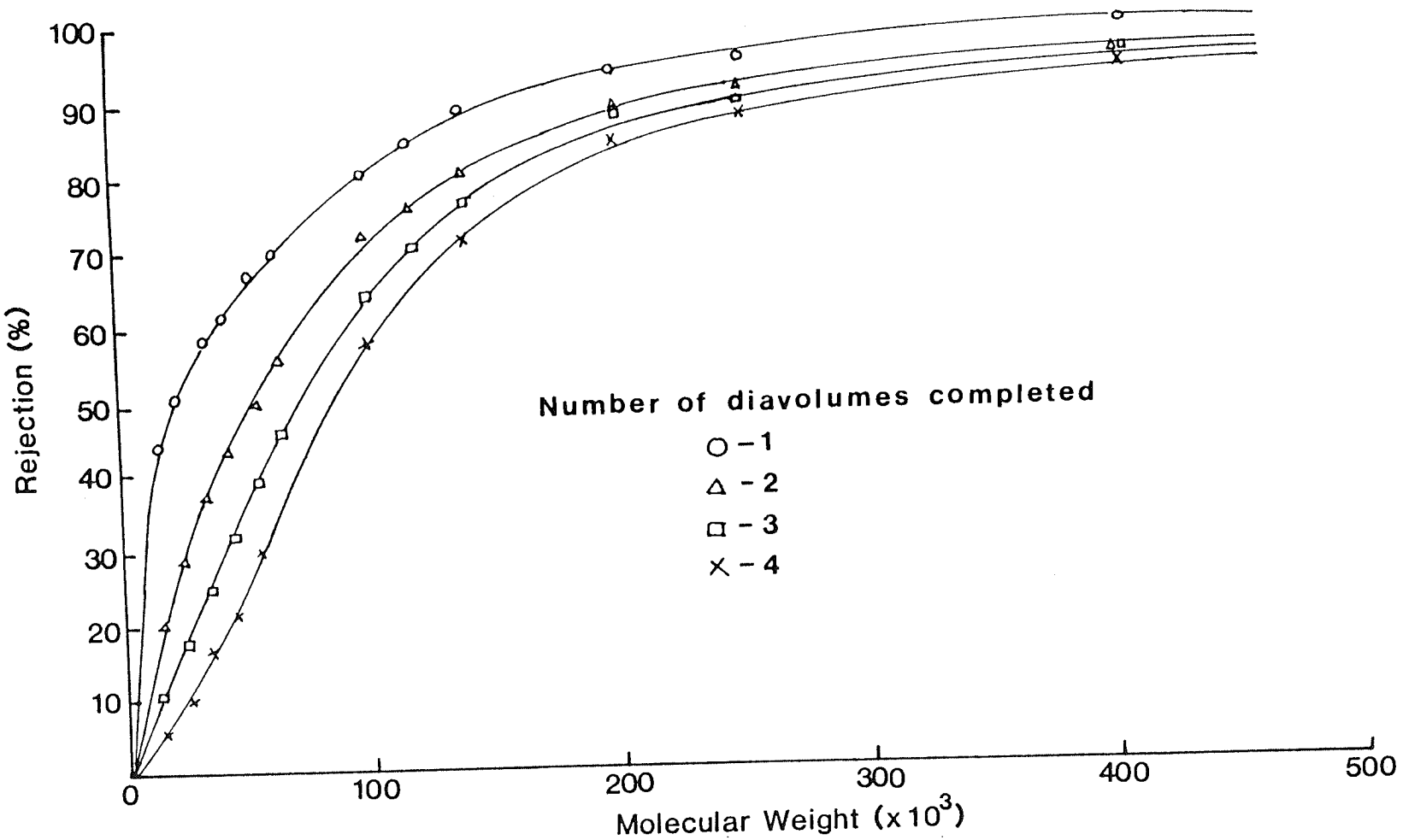

Figure 5.63 Rejection Curves Obtained from the 50,000 MW Cut-off Membrane Number 1. Recirculation Rate of 7 l/min

Table 5.30 Romicon 50,000 MW cut-off Membrane in Concentration Mode

PERMEATE PRODUCT

Volume remaining (cm^3)	Concentration of permeate (g/l)	% below 98000 MW	Efficiency of removal below 98000 MW	% above 98000 MW	Efficiency of retention above 98000 MW
2000 (Feed)	40.61	91.24	0	8.76	100
1500	23.74	98.96	15.86	1.04	98.10
1000	25.55	98.92	32.91	1.08	96.16
500	29.30	98.65	52.41	1.35	93.39
220	35.57	98.16	65.6	1.84	90.79

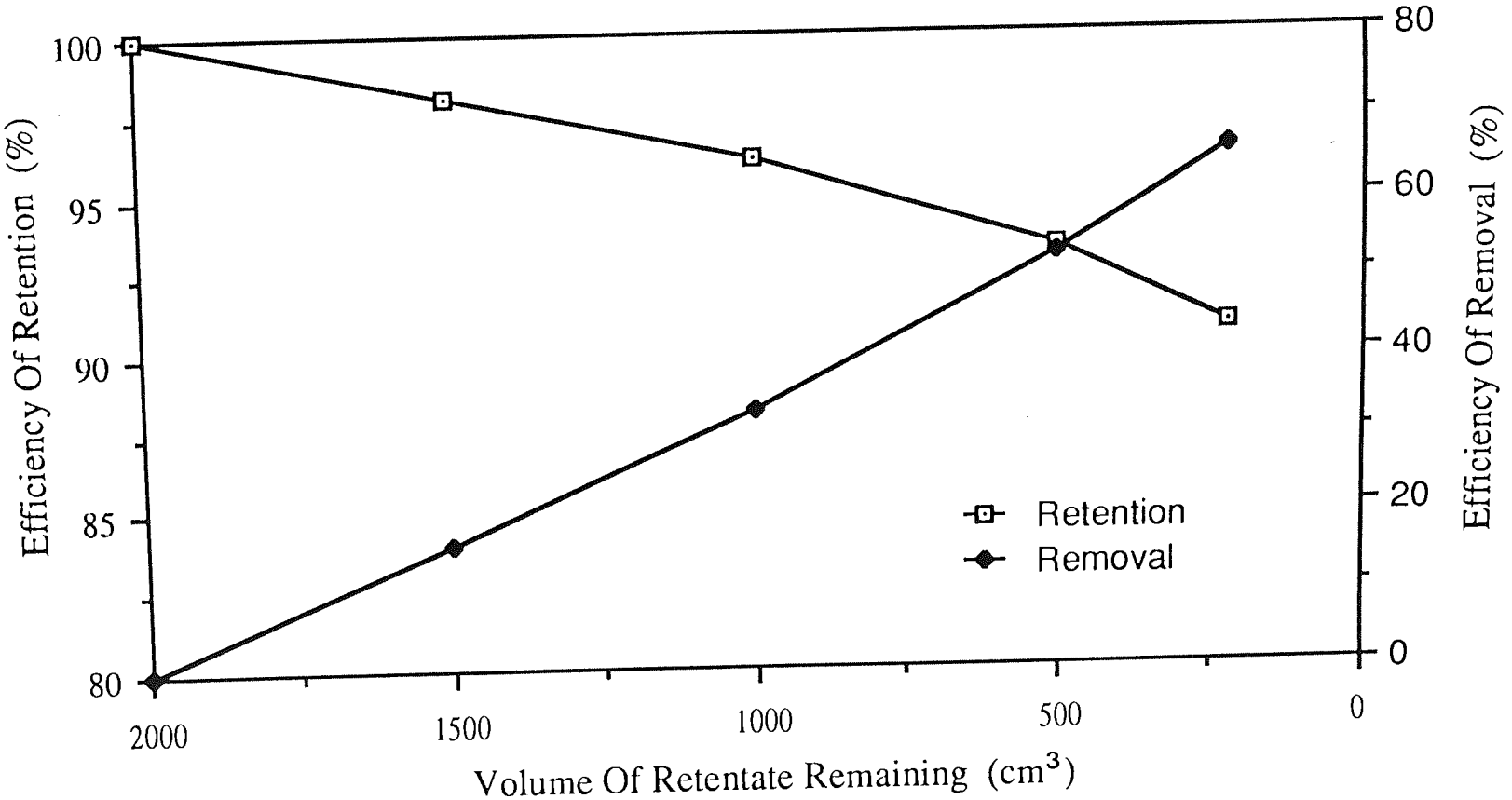

Figure 5.64 Using the Romicon 50,000 MW Cut-off Membrane in the Concentration Mode of Operation

When tested in the concentration mode the membrane showed the same trends as the Amicon membrane. A higher efficiency of retention was obtained, however the efficiency of removal was 26% lower than in the diafiltration mode. See table 5.30 and figure 5.64.

These results confirmed that the diafiltration mode was the most suitable approach for separating the high molecular weight dextran from the 'saleable' material.

It is clear that the Romicon membrane would be the better option for a batch diafiltration system because the Romicon membrane exhibited a far better retention above 98,000 MW than the Amicon membrane and also gave an acceptable efficiency of removal below 98,000 MW.

5.5.3 TESTING THE ROMICON 50,000 MW CUT-OFF MEMBRANES USING BATCH DIAFILTRATION

The Romicon membrane tested in the previous section was shown to be manufactured to a high standard and gave a better separation of the high molecular weight dextran than the Amicon membrane. These membranes were therefore chosen for use in the ultrafiltration cascade.

The membranes were tested using the same conditions as mentioned earlier except that recirculation rate was reduced to 1 litre/minute. This was the maximum continuous flow rate obtainable from the peristaltic pumps used on the ultrafiltration cascade.

The Romicon membranes were found to be effected by feed concentration in the same manner as the Amicon membranes mentioned in section 5.5.2. See table 5.32 and 5.33. Using a 2% W/W feed an efficiency of retention of 56% was obtained at four diavolumes, and when the 4% W/W feed was used the efficiency increased to 72%.

The efficiency of removal of the 12,000 MW to 98,000 MW band was only reduced from 89% to 86%. Since the batch system was found to perform better at the higher concentrations it was realistic to believe that the cascade would be effected in a similar way, therefore a 4% W/W feed was used in the cascade.

The Romicon membranes ability to reject material was found to be improved by increasing the recirculation rate, this effect was also found by Bottinio [44] and Baker [50]. See figure 5.67 and 5.68. The rejection of dextran below 50,000 MW was found to be similar at both recirculation rates, however as the molecular weight increased the rejection at the higher recirculation rate became significantly higher. Since the recirculation rate had a far greater effect on the retention of the high molecular weight material it was unfortunate that the cascade could not be operated at the higher recirculation rate as this would further enhance the fractionation process.

The three remaining membranes were tested using only a 4% W/W feed concentration. See table 5.34 to 5.36. The 50,000 MW cut-off Romicon membranes show the same variation of performance that was found throughout the Amicon range of membranes. The degree of variation was reflected within the rejection curves for the four membranes. See figure 5.75. At 98,000 MW the rejection varied from 47% for membrane number two to 75% for membrane number three (At two diavolumes). The performance of membrane number 2 was only marginally better than the 100,000 MW cut-off membrane (number one) mentioned in section 5.5.5.

Table 5.31 Operating Conditions used to test the Romicon 50,000 MW cut-off Membrane

Membrane area	:	900 cm^2
Membrane recirculation rate	:	1 litre/minute
Transmembrane pressure	:	70 KPa
Operating temperature	:	20°C
Feed	:	4% W/W of Fisons Batch HZIS
Mode of operation used	:	Diafiltration
Number of diavolumes used	:	4

Definitions:

$$\text{Efficiency of removal below 12000 MW} = \frac{\text{Weight of dextran below 12000 MW in retentate}}{\text{Weight of dextran below 12000 MW in feed}}$$

$$\text{Efficiency of removal between 12000–98000MW} = \frac{\text{Wt of dextran between 12000–98000MW in retentate}}{\text{Wt of dextran between 12000–98000MW in feed}}$$

$$\text{Efficiency of retention above 98000MW} = \frac{\text{Weight of dextran above 98000 MW in retentate}}{\text{Weight of dextran above 98000 MW in feed}}$$

Table 5.32 Romicon 50,000 MW cut-off Membrane Number 1 using a 2% feed

		RETENTATE PRODUCT					
Number of diavolumes	Concentration (g/100g Sol)	% below 12000 MW	Efficiency of removal below 12000 MW	% between 12000 and 98000 MW	Efficiency of removal 12000 MW - 98000 MW	% above 98000 MW	Efficiency of retention above 98000 MW
Feed	2.153	23.56	0	67.68	0	8.76	100
0.5	1.634	22.63	27.08	66.75	25.19	10.62	91.73
1.0	1.239	19.44	52.66	67.09	42.96	13.47	88.55
1.5	0.913	18.29	67.26	65.66	58.88	16.05	77.41
2.0	0.708	15.20	78.89	65.12	68.43	19.68	73.7
2.5	0.545	12.98	86.19	62.81	76.52	24.21	69.46
3.0	0.449	11.44	89.94	61.26	81.12	27.30	64.86
3.5	0.354	8.88	93.8	57.26	86.13	33.86	63.09
4.0	0.286	6.79	96.17	56.16	89.02	37.11	56.20

Table 5.33 Romicon 50,000 MW cut-off Membrane Number 1 using a 4% Feed

RETENTATE PRODUCT

Number of diavolumes	Concentration (g/100g Sol)	% below 12000 MW	Efficiency of removal below 12000MW	% between 12000 and 98000 MW	Efficiency of removal 12000 MW - 98000 MW	% above 98000 MW	Efficiency of retention above 98000 MW
Feed	4.005	23.56	0	67.68	0	8.76	100
0.5	3.065	22.84	25.8	66.22	25.09	10.94	95.49
1.0	2.316	20.07	50.71	67.16	42.80	12.77	84.29
1.5	1.825	19.33	62.60	64.65	56.45	16.02	82.66
2.0	1.47	16.39	74.91	64.29	65.74	19.32	81.03
2.5	1.226	13.50	82.51	63.36	71.32	23.14	80.67
3.0	0.994	11.10	88.34	61.14	77.56	27.76	78.39
3.5	0.858	8.99	92.98	58.85	81.36	32.16	78.39
4.0	0.667	6.59	95.33	55.62	86.31	37.79	71.83

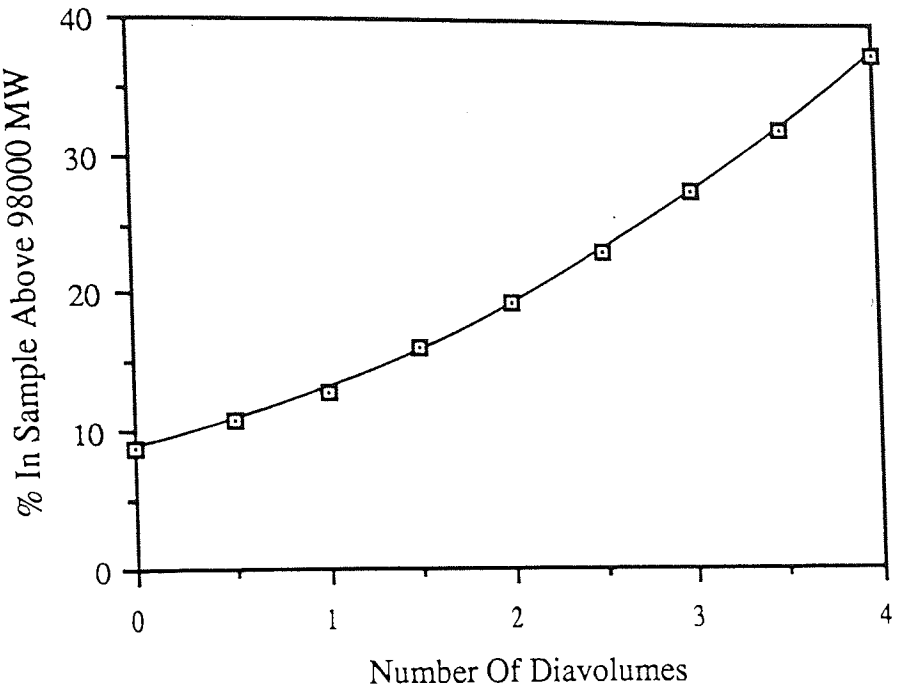

Figure 5.65 How the Number of Diavolumes used Effects the Percentage of Material above 98,000 MW in the Retentate

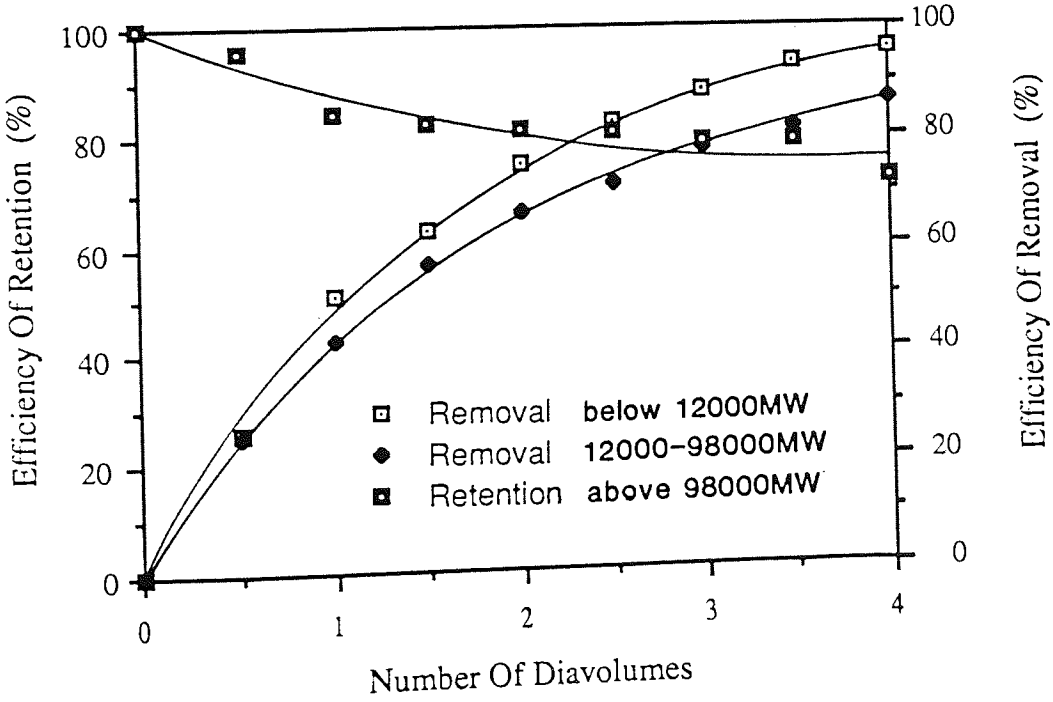

Figure 5.66 The Relationship between Efficiency and the Number of Diavolumes used. Membrane Number 1

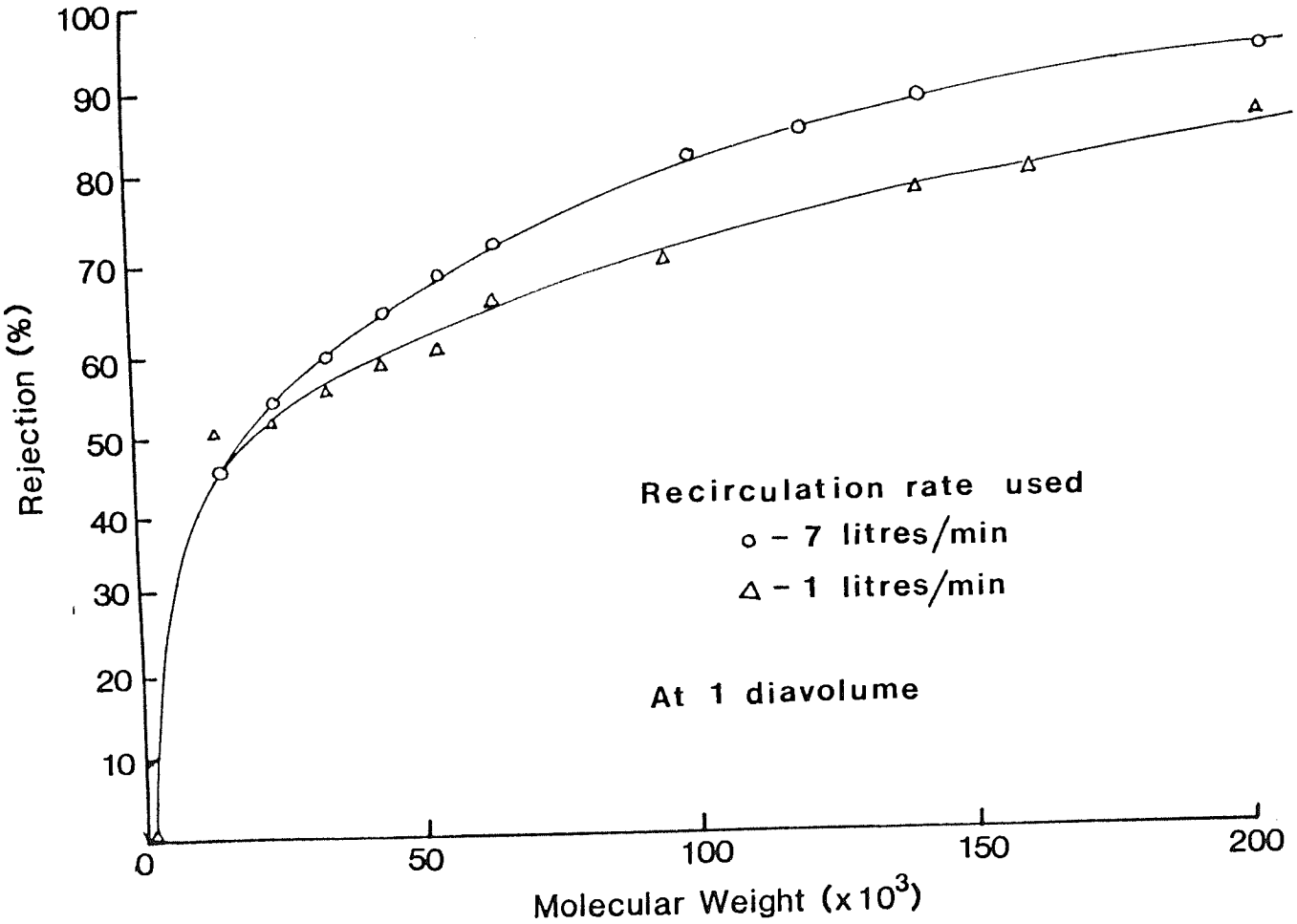

Figure 5.67 The Effect of Recirculation on Rejection. At 1 Diavolume

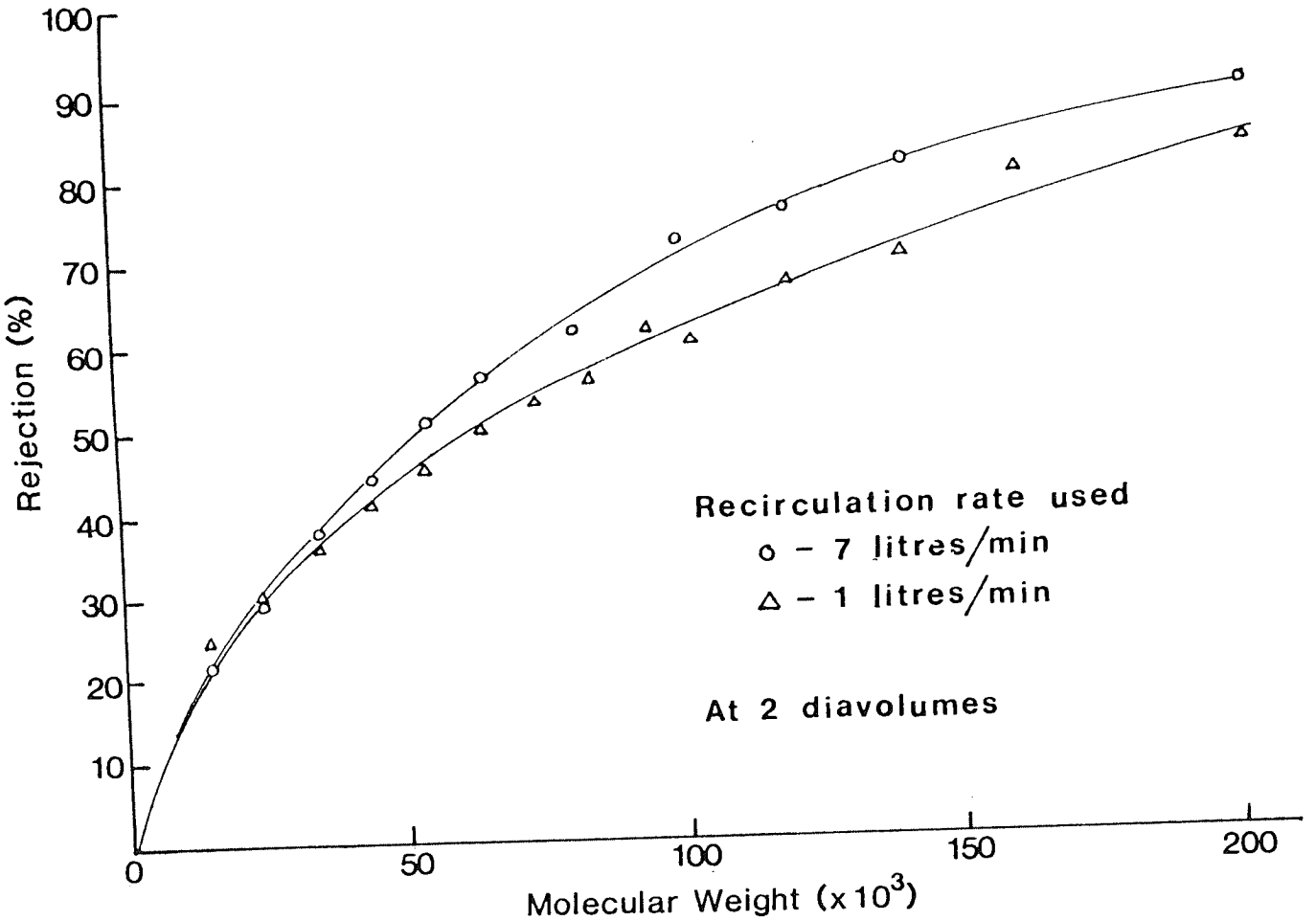

Figure 5.68 The Effect of Recirculation Rate on Rejection. At 2 Diavolumes

Table 5.34 Romicon 50,000 MW cut-off Membrane Number 2

RETENTATE PRODUCT

Number of diavolumes	Concentration (g/100g Sol)	% below 12000 MW	Efficiency of removal below 12000 MW	% between 12000 and 98000 MW	Efficiency of removal 12000 MW - 98000 MW	% above 98000 MW	Efficiency of retention above 98000 MW
Feed	3.855	24.31	0	67.016	0	8.674	100
0.5	2.915	23.30	27.53	66.07	25.43	10.63	92.51
1.0	2.09	18.84	58.05	68.03	44.75	12.86	80.24
1.5	1.58	15.83	73.33	67.3	58.85	16.87	79.64
2.0	1.185	13.58	82.83	65.88	69.76	20.54	72.75
2.5	0.940	10.48	89.54	64.0	76.71	25.52	71.56
3.0	0.746	8.84	92.96	59.10	82.96	32.06	71.56
3.5	0.572	6.98	95.84	55.68	87.69	37.34	63.77
4.0	0.436	5.83	97.33	51.24	91.37	42.93	56.04

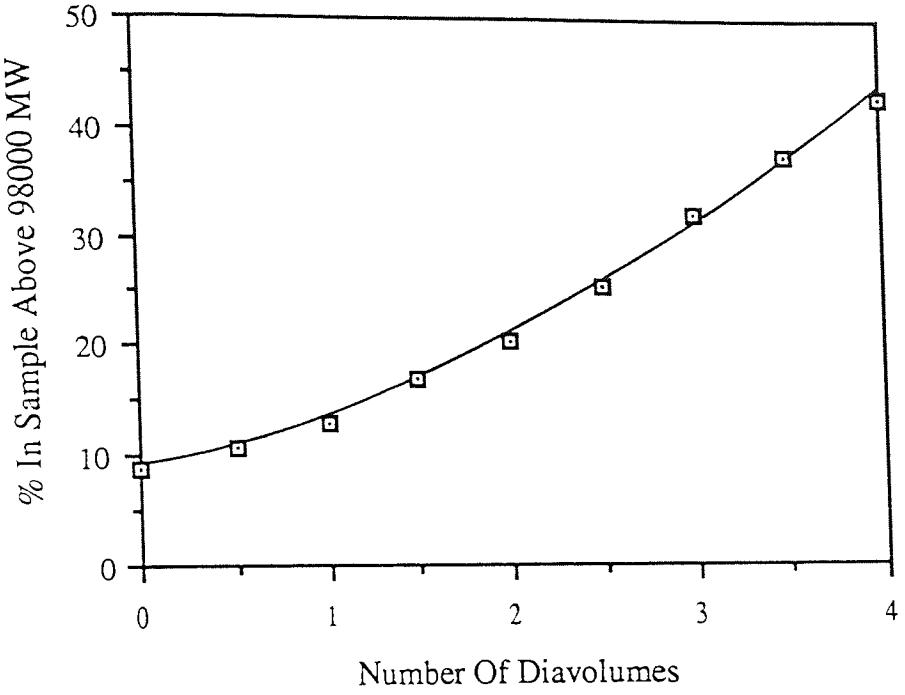

Figure 5.69 How the Number of Diavolumes used Effects the Percentage of Material above 98,000 MW in the Retentate

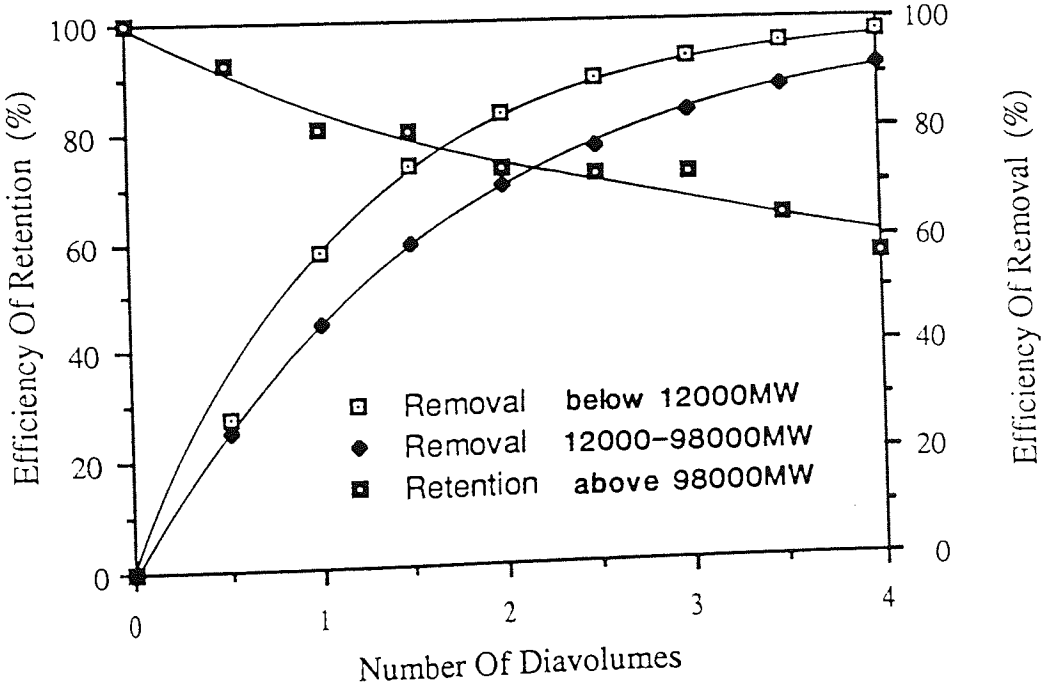

Figure 5.70 The Relationship between Efficiency and Number of Diavolumes used. Membrane Number 2

Table 5.35 Romicon 50,000 MW cut-off Membrane Number 3

RETENTATE PRODUCT

Number of diavolumes	Concentration (g/100g Sol)	% below 12000 MW	Efficiency of removal below 12000 MW	% between 12000 and 98000 MW	Efficiency of removal 12000 - 98000 MW	% above 98000 MW	Efficiency of retention above 98000 MW
Feed	3.95	24.31	0	67.016	0	8.674	100
0.5	3.02	22.71	28.64	66.17	24.51	11.12	98.01
1.0	2.44	18.12	53.96	68.44	36.95	13.44	95.70
1.5	1.92	13.89	72.22	69.22	49.79	16.89	94.60
2.0	1.58	11.23	81.56	68.45	59.16	20.32	93.69
2.5	1.328	10.59	85.35	66.41	66.68	23.00	89.14
3.0	1.08	8.19	90.83	64.54	73.67	27.27	85.81
3.5	0.906	6.09	94.27	61.92	78.77	31.99	84.59
4.0	0.79	4.83	96.03	58.59	82.54	36.58	84.32

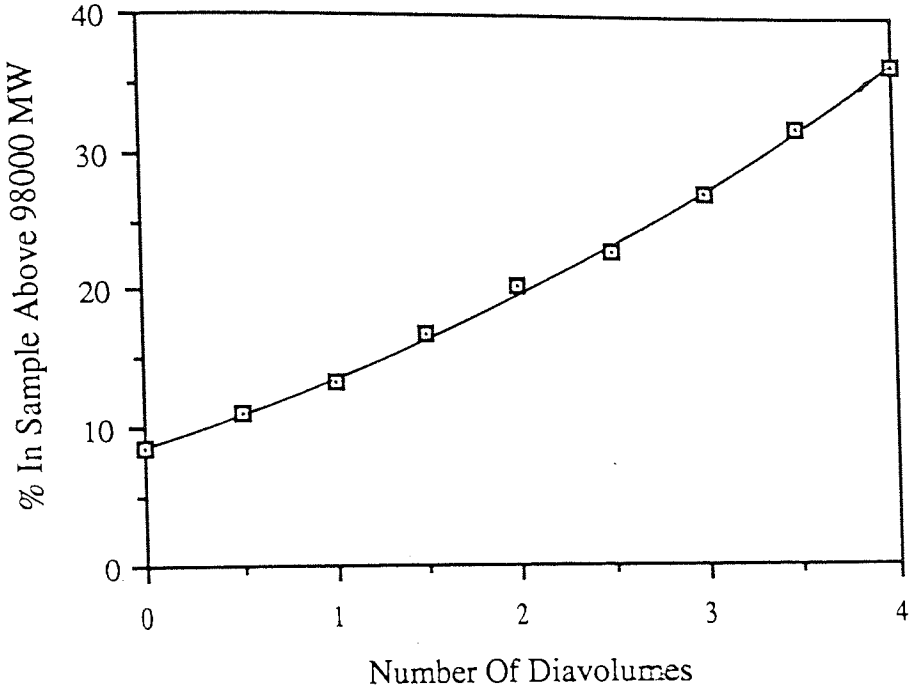

Figure 5.71 How the Number of Diavolumes used Effects the Percentage of Material above 98,000 MW in the Retentate

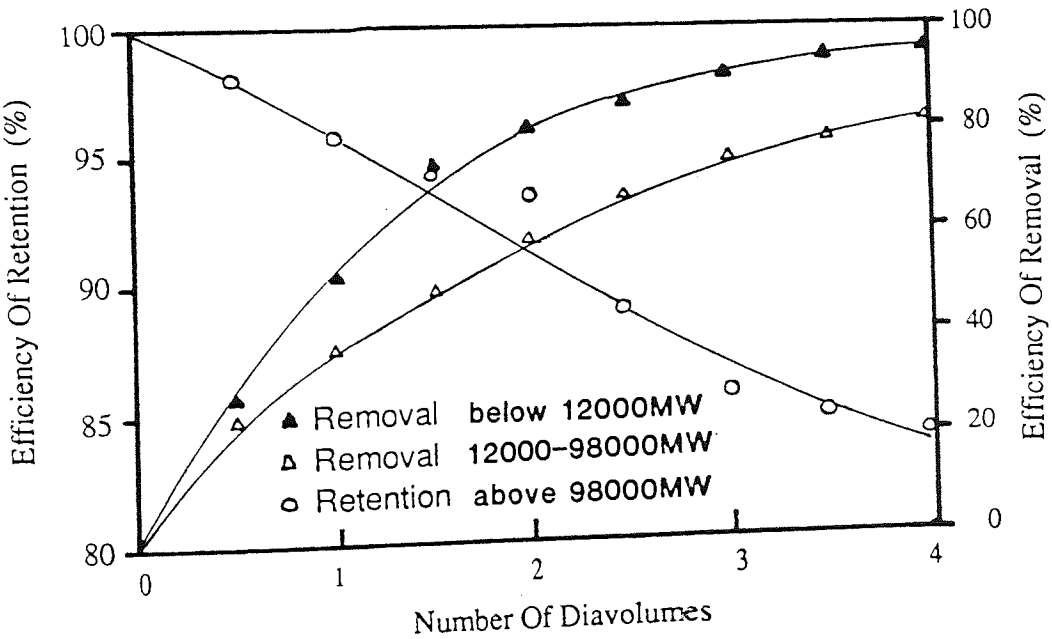

Figure 5.72 The Relationship between Efficiency and Number of Diavolumes used. Membrane Number 3

Table 5.36 Romicon 50,000 MW cut-off Membrane Number 4

RETENTATE PRODUCT

Number of diavolumes	Concentration (g/100g Sol)	% below 12000MW	Efficiency of removal below 12000 MW	% between 12000 and 98000 MW	Efficiency of removal 12000 - 98000 MW	% above 98000 MW	Efficiency of retention above 98000 MW
Feed	3.692	24.1	0	66.99	0	8.91	100
0.5	2.724	22.26	31.83	66.57	26.69	11.17	92.40
1.0	2.09	18.51	56.69	67.24	43.18	14.25	90.27
1.5	1.64	14.51	73.23	67.65	55.15	17.84	88.75
2.0	1.29	11.91	82.67	66.09	65.55	22.00	86.01
2.5	1.00	8.9	89.98	63.27	74.41	27.83	84.58
3.0	0.844	7.36	93.02	60.21	79.45	32.43	82.97
3.5	0.69	5.44	95.83	56.44	84.25	38.12	79.94
4.0	0.585	3.47	97.75	51.74	87.79	44.79	79.63

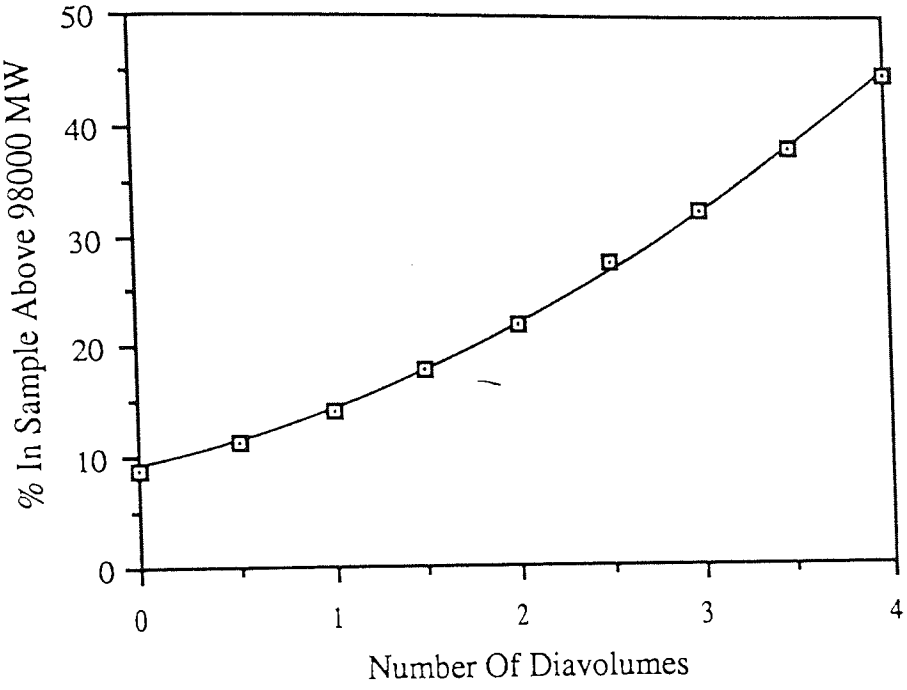

Figure 5.73 How the Number of Diavolumes used Effects the Percentage of Material above 98,000 MW in the Retentate

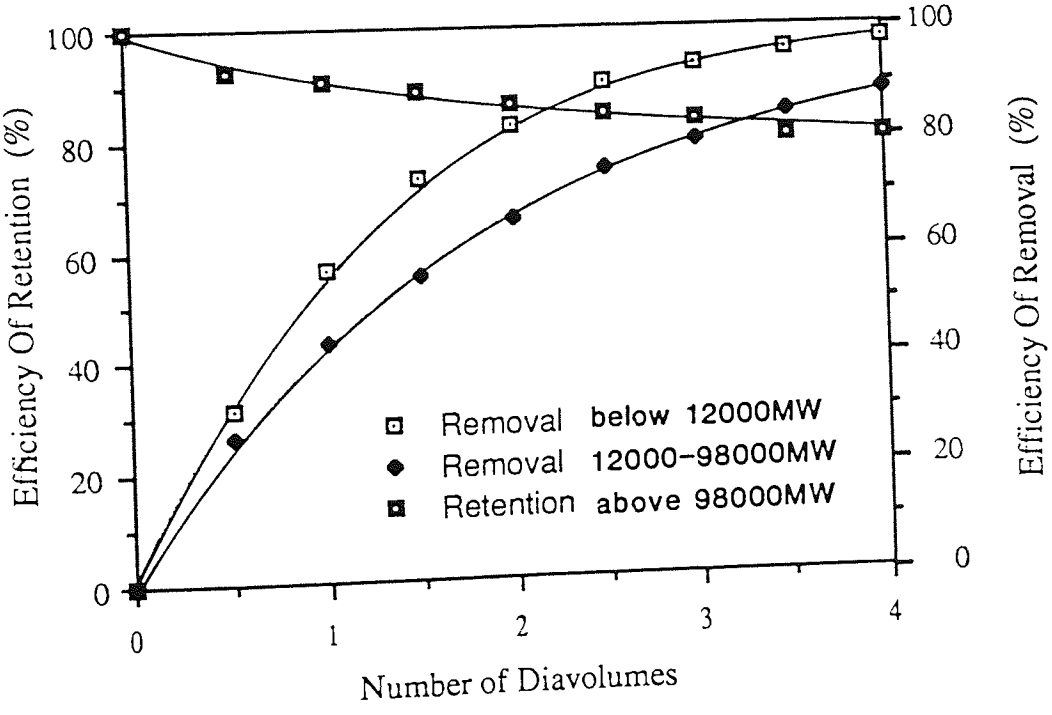

Figure 5.74 The Relationship between Efficiency and Number of Diavolumes used. Membrane Number 4

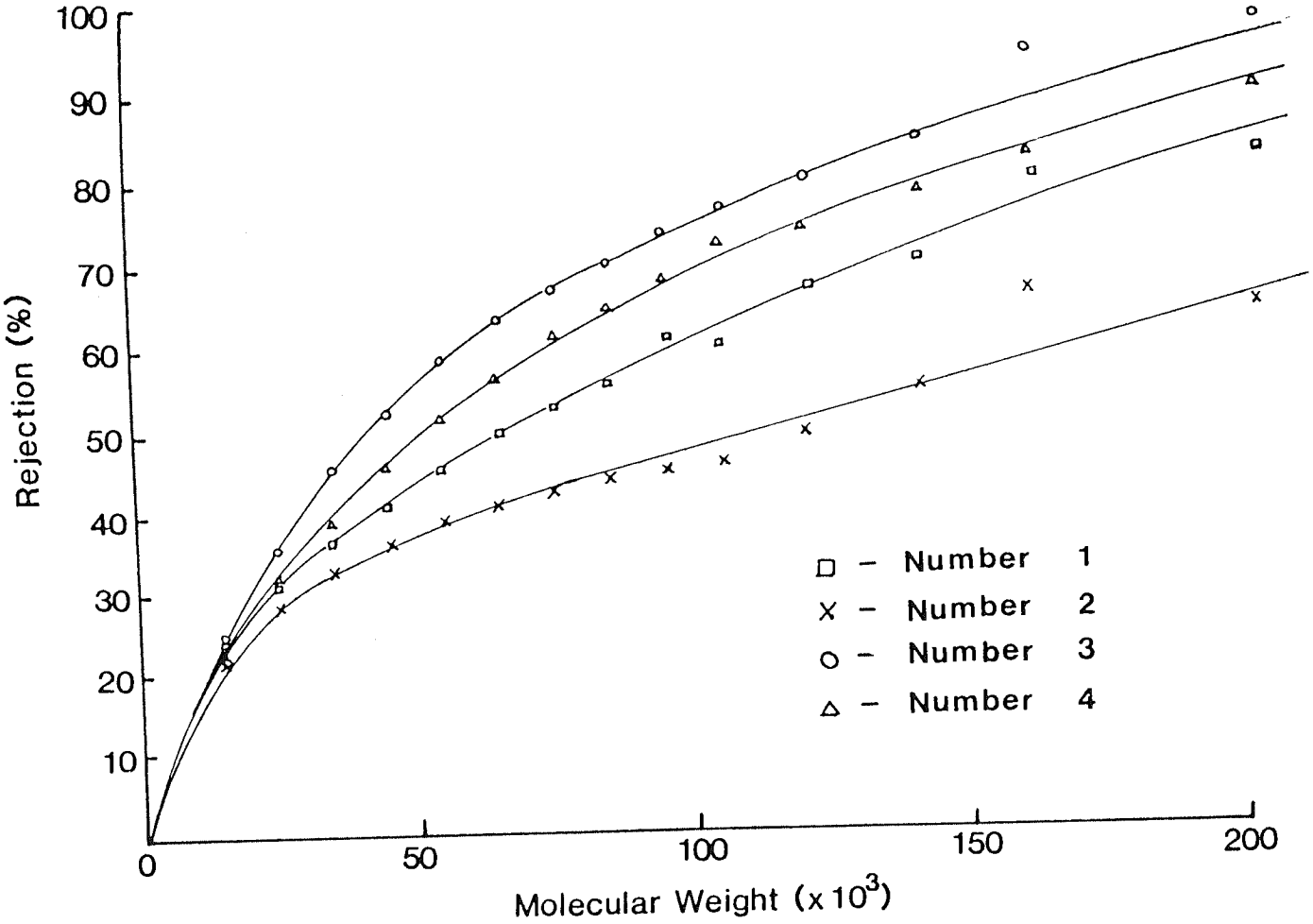

Figure 5.75 The Rejection Curves Obtained from the Four 50,000 MW Cut-off Membranes. At 2 Diavolumes

5.5.4 USING THE ROMICON MEMBRANES WITHIN THE CASCADE

Although the batch diafiltration system gave a satisfactory retention of the high molecular weight dextran an excessive volume of diafiltrate was required to separate the 12,000 to 98,000 MW band. The concentration of the final permeate product containing the "saleable" material was therefore very low. This would make it necessary to use an intermediate concentration stage before any further fractionation could take place. Since the ultrafiltration cascade had already been shown to reduce the amount of diafiltrate required and also improved the separation process this system appeared to be ideal for this particularly fractionation.

In section 5.4.3 a four stage cascade was used, however it was felt that for this particular fractionation a four stage cascade might not be necessary. To test this theory the software used for the computer control of the cascade was altered to allow one or more stages to be made redundant. A series of experiments were then conducted using a two, three and four stage cascade. The number of diavolumes used was also varied to obtain a precise operating line for each cascade, see table 5.37. Using a two stage cascade (experiments 6.1 to 6.3) with two 50,000 MW cut-off membranes (number one and two) the efficiency of retention was increased from 77% to 91% at two diavolumes. However the efficiency of removal of the 12,000 MW to 98,000 MW band had only been marginally improved from 68% to 74%. See figure 5.76. The explanation for the apparent poor removal of the 12,000 MW to 98,000 MW band can be found by comparing the cascades rejection curve with the average batch rejection curve. See figure 5.77 to 5.79. The cross-over point occurred at 55,000 MW rather than the required value of 98,000 MW, therefore between 55,000 MW and 98,000 MW the cascade was enhancing the

Table 5.37 Using the Romicon Membranes in the Cascade

Run	FEED Conc (g/100g Sol)	%below 12000 MW	%between 12000 - 98000MW	%above 98000 MW	RETENTATE PRODUCT Conc (g/100g Sol)	%below 12000 MW	%between 12000 - 98000MW	%above 98000 MW	Efficiency of removal below 12000 MW	Efficiency of removal 12000 to 98000 MW	Efficiency of Retention
6.1	3.95	24.31	67.016	8.674	1.92	13.94	69.33	16.73	72.12	49.75	93.75
6.2	3.95	24.31	67.016	8.674	1.457	9.79	69.14	21.07	85.20	61.95	89.57
6.3	3.95	24.31	67.016	8.674	1.06	6.70	63.85	29.45	92.61	74.43	91.07
7.1	3.85	24.31	67.016	8.674	1.92	12.25	71.58	15.84	74.25	46.74	91.29
7.2	3.85	24.31	67.016	8.674	0.994	3.85	66.24	29.91	95.94	74.45	89.19
8.1	4.121	23.97	67.00	9.03	2.009	8.62	73.53	17.85	87.27	46.50	96.50
8.2	4.114	23.97	67.00	9.03	1.20	1.36	68.93	29.71	98.34	69.74	96.76
8.3	3.58	24.10	66.99	8.91	0.94	2.07	67.32	30.61	97.75	73.64	90.47
9.1*	3.91	25.04	65.52	9.44	0.6539	0.108	62.07	37.82	99.9	84.19	66.94

* Feed changed - new barrel of HZIS used.

Figure 5.76 Comparing the Efficiency of the Two Stage Cascade to the Batch System

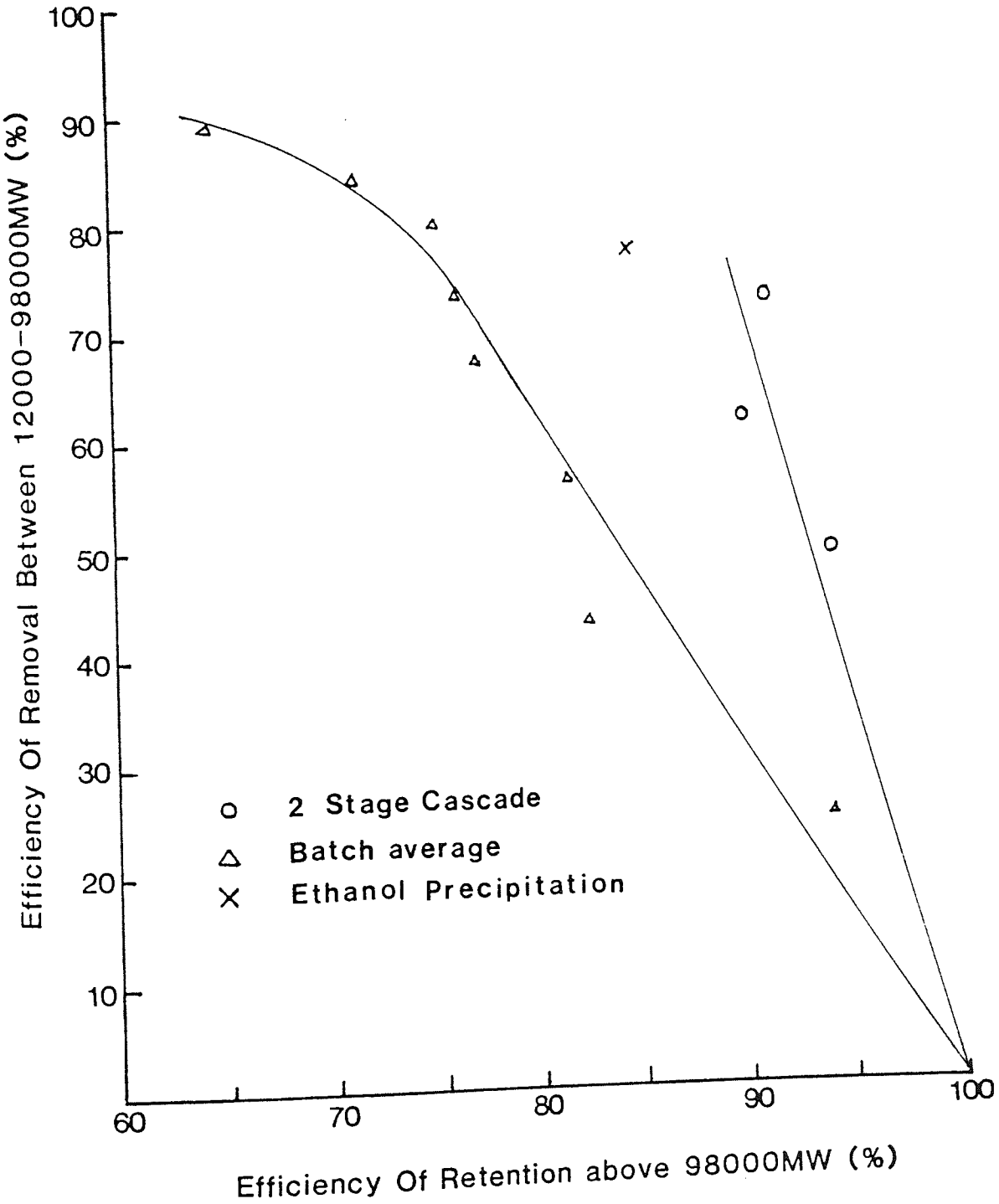

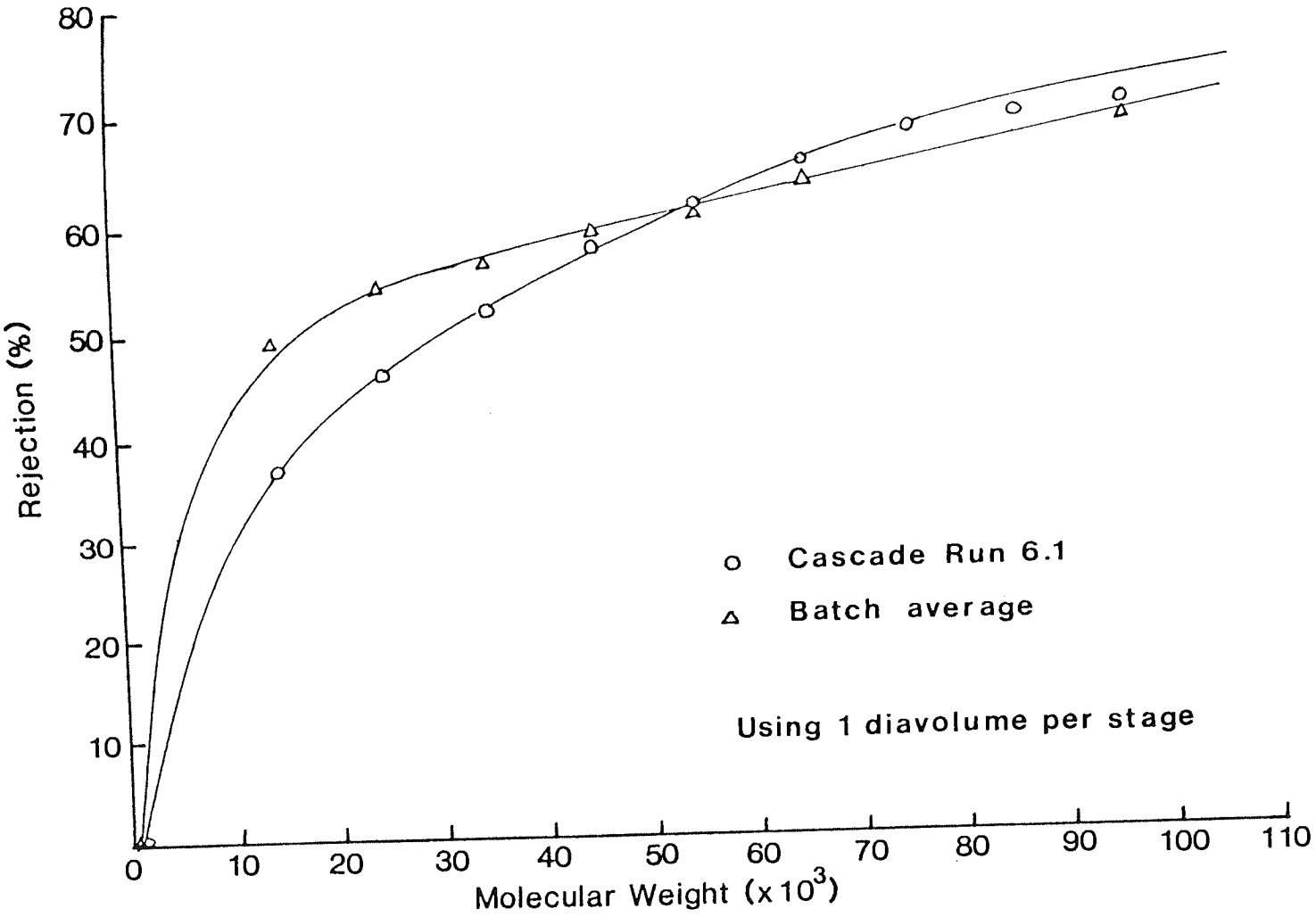

Figure 5.77 Rejection Curve from Cascade Run 6.1

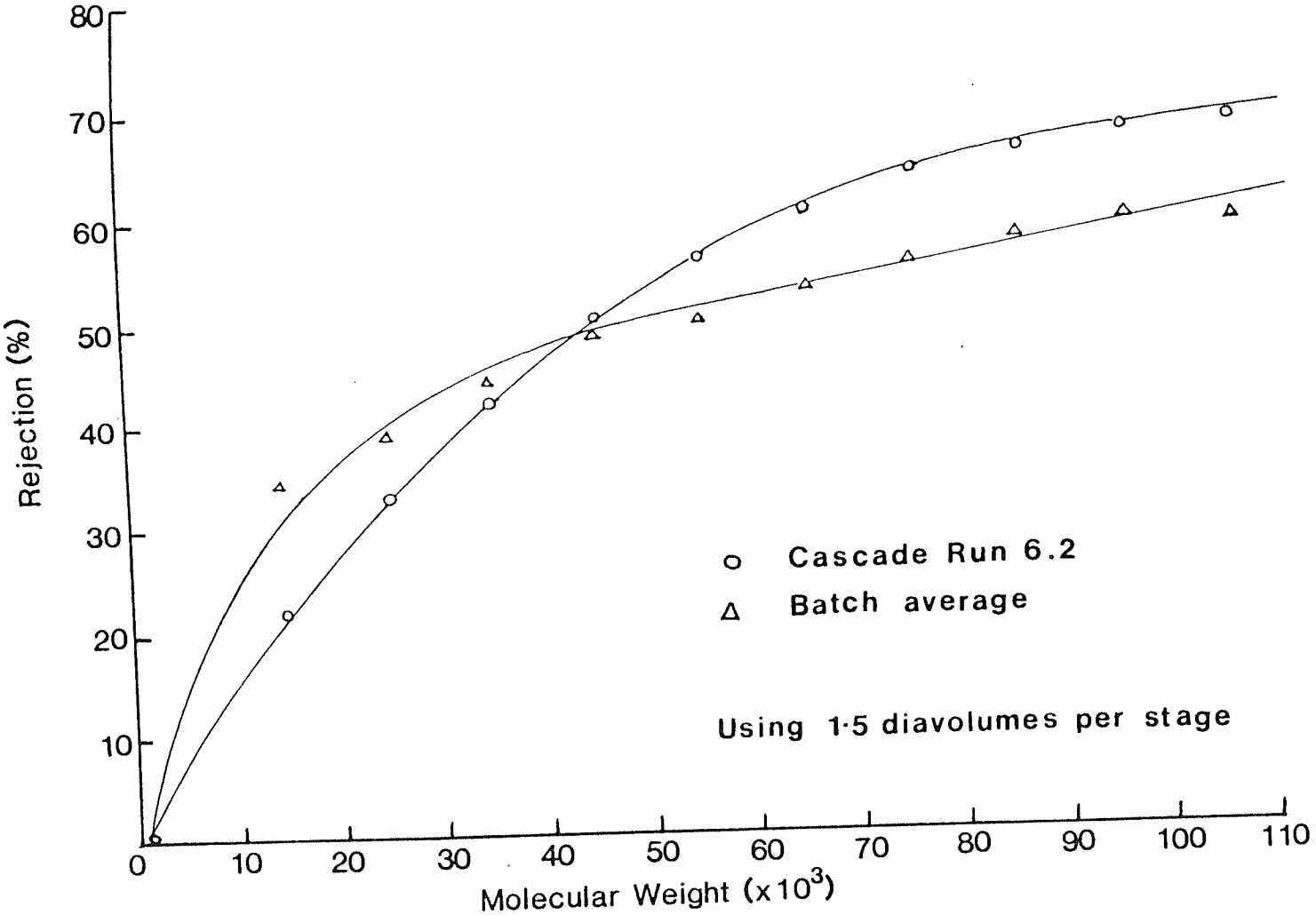

Figure 5.78 Rejection Curve from Cascade Run 6.2

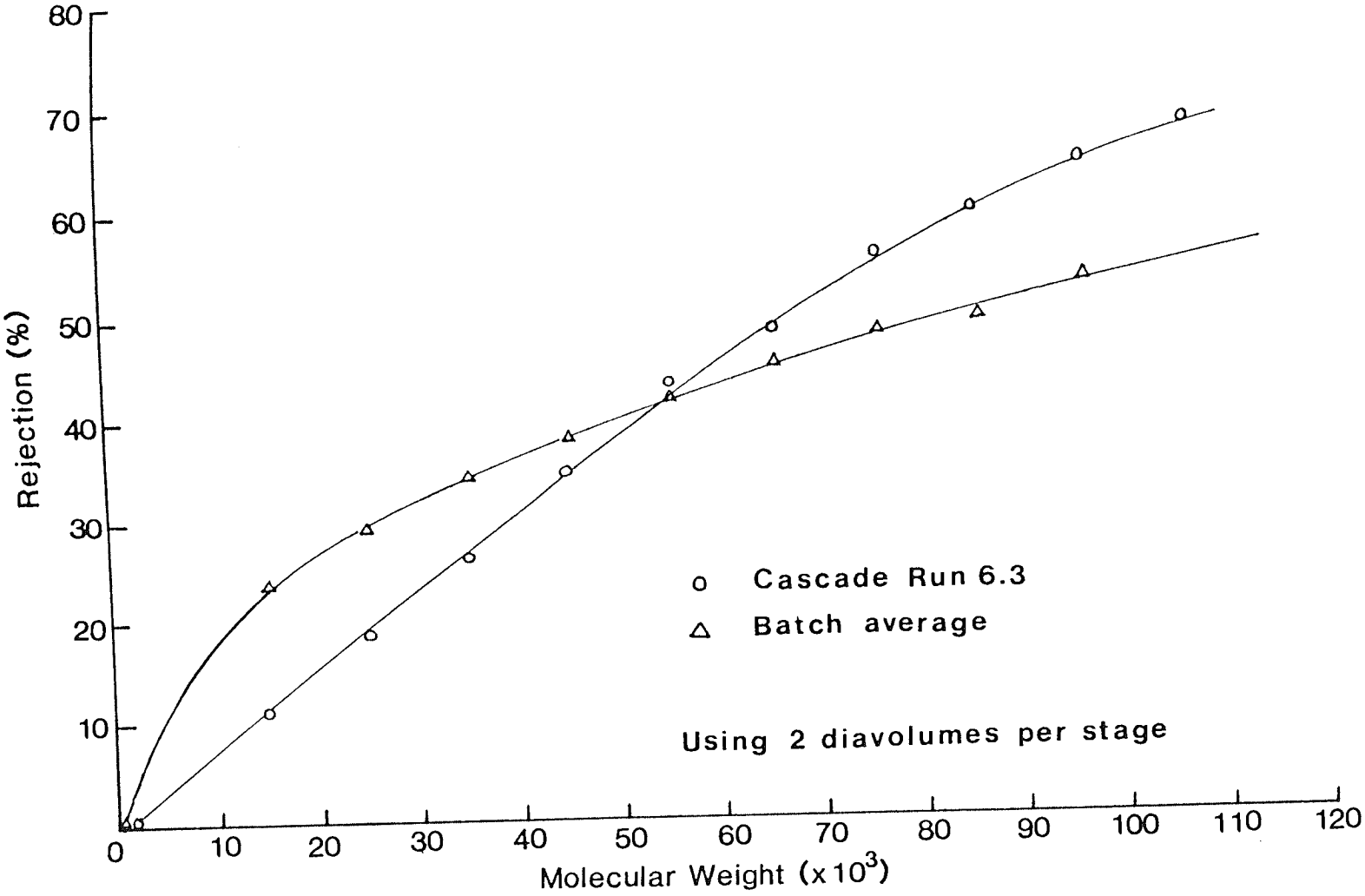

Figure 5.79 Rejection Curve from Cascade Run 6.3

retention of the dextran which should have been removed. Interestingly the number of diavolumes used had little effect on the cross-over point. If the efficiency of the cascade is redefined as the efficiency of retention and removal above and below the cross-over point, a better appreciation of the cascades performance can be obtained. See figure 5.80. On this basis the efficiency of removal can be seen to be far better than that obtained with the batch system. Furthermore the enhancement of the efficiency of retention was far more significant than that obtained with the earlier work involving the removal of material below 12,000 MW.

The close agreement between the cross-over point obtained from the cascade and the quoted nominal molecular weight cut-off appears to suggest that these quoted values can be used with some confidence as a method of estimating the position of the cross-over point.

The effect on the molecular weight distribution was also particularly interesting, the percentage within the retentate sample above 98,000 MW increased far more rapidly than was found with the batch system. See figure 5.82. This trend was identical to that found with the earlier work involving the removal of material below 12,000 MW. If the distribution in the retentate was considered above and below the cross-over point the results were most impressive. See figure 5.81. The percentage within the sample below 55,000 MW was reduced from 67% to 52% at two diavolumes using the cascade. These results show clearly the advantage of using an ultrafiltration cascade although it was unfortunate that the cross-over point occurred at only 55,000 MW. It was initially hoped that a cross-over point would fall at approximately 80,000 MW when using these membranes

An unsteady state study of cascade run 6.2 shows the same trends as those found in the previous unsteady state study mentioned in section 5.4.3. See table 5.38. Since fewer stages were used the cascade

Figure 5.80 Comparing the Efficiency of the Two Stage Cascade to the Batch Average. Based on the Cross-over Point

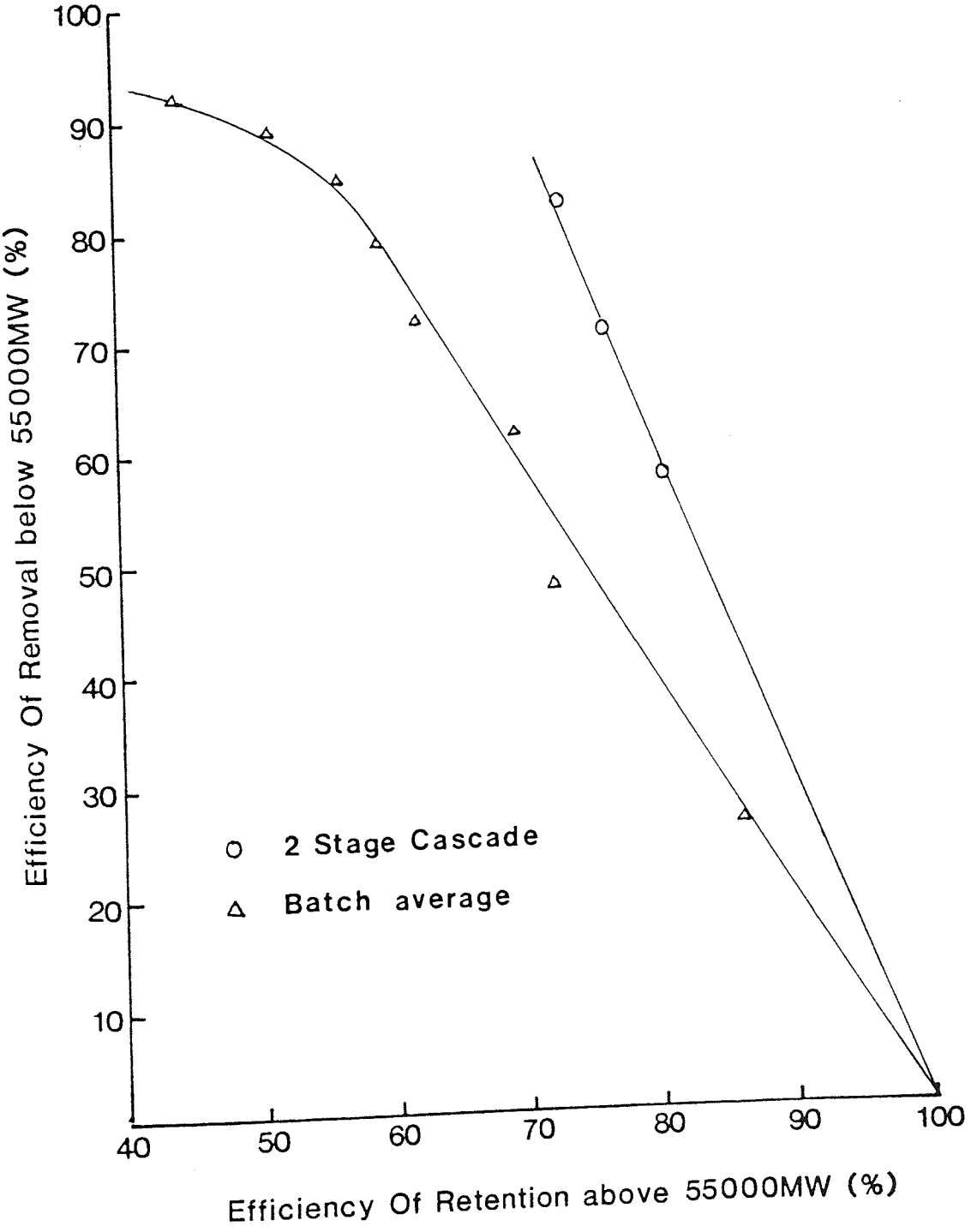

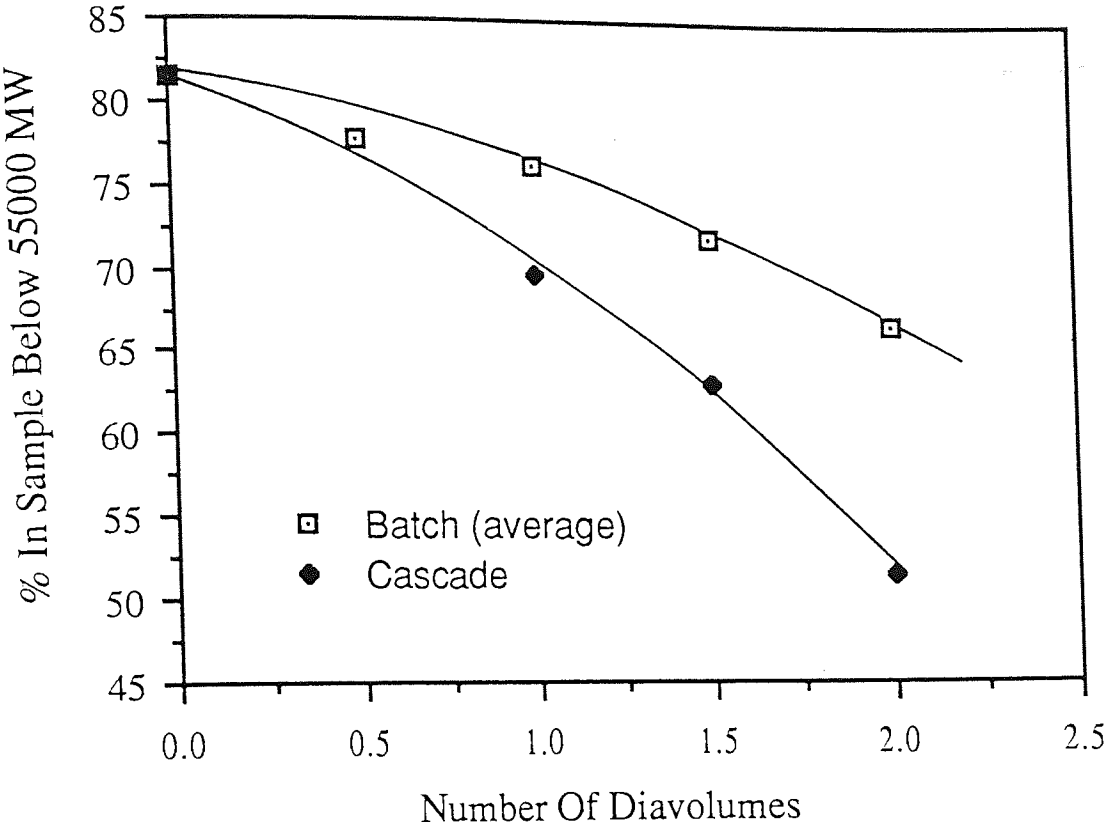

Figure 5.81 Comparison of the Molecular Weight Distribution Obtained from the Batch and Cascade Systems below the Cross-over Point

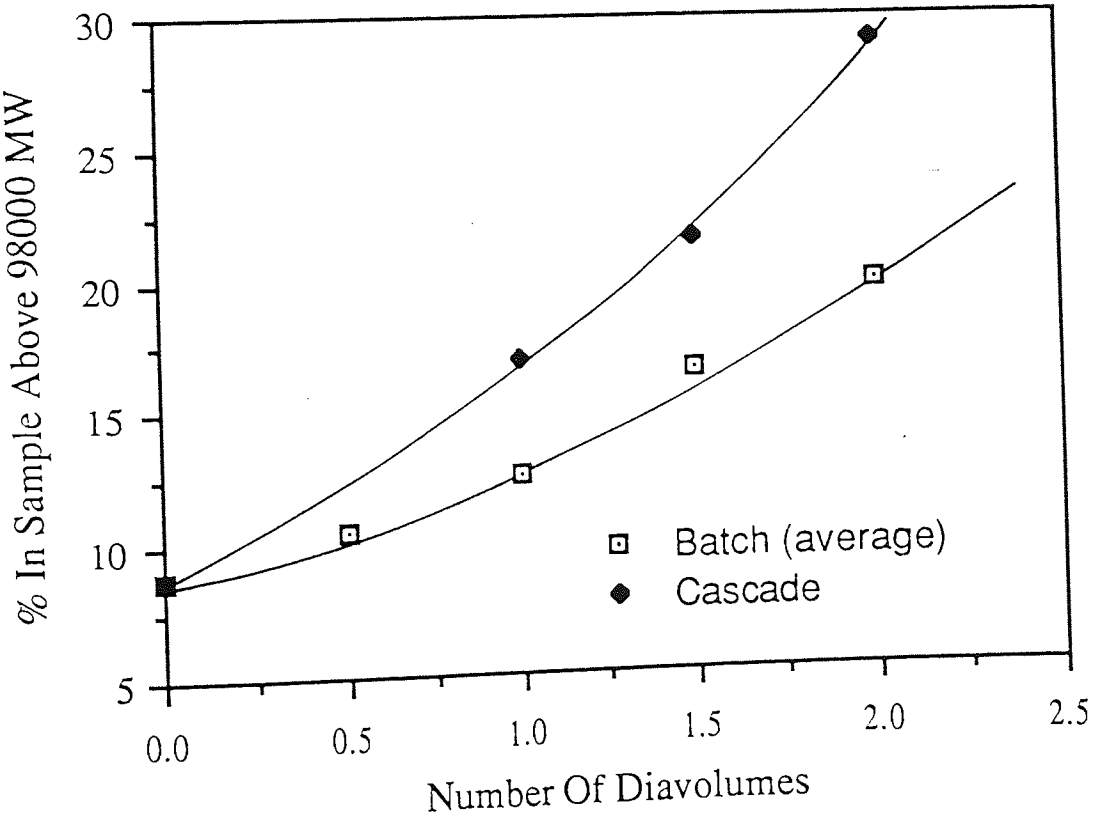

Figure 5.82 Comparison of the Molecular Weight Distribution Obtained from the Batch and Cascade above 98,000 MW

requires fewer cycles to reach equibrium, in total 10 cycles were required compared to 17 cycles for the four stage cascade.

In section 6.5.2 the mathematical model was used to predict the product specification from these experiments. The main assumption of the model was that the membranes rejection characteristics were fixed. The rejection data was obtained from the batch diafiltration experiments. In all cases the model over predicted the losses through the membrane. This difference suggests that the rejection of these membranes were in some way enhanced when used in the cascade.

The unsteady state study of the two stage cascade gives some insight into operation of the cascade.

It can be seen that the efficiency of retention within the first stage rapidly exceeded 100% after only four cycles. Since the first stage was being saturated with material from stage two it was probable that the rejection of the higher molecular weight material was enhanced in a similar manner to that found by Cooper [48] and Bottinio [44] mentioned in section 2.6.

Since the permeate from the 50,000 MW cut-off membrane had a higher concentration and would contain a larger proportion of the dextran distribution this effect should be far more pronounced than would be found with either the 5000 MW or 10,000 MW cut-off membranes.

Further experimentation using a cascade containing three and then four stages gave a clearer picture of the operation of the cascade. To stop the performance of an individual membrane masking the underlying trends caused by changing the number of stages, membranes number one and two were retained in the first and last stages of the cascade. However several further experiments were conducted to optimise the retention of material above 98,000 MW these naturally required an alternative membrane configuration. (Run 8.1 and 8.2).

Table 5.38 Unsteady State Study of the Two Stage Ultrafiltration Cascade using 50000 MW cut-off Membranes

Sample	Concentration (g/100gSol)	% below 12000 MW	Efficiency of removal below 12000 MW	% between 12000 - 98000 MW	Efficiency of removal 12000-98000 MW	% above 98000 MW	Efficiency of retention above 98000 MW
Feed	3.95	24.31	0	67.016	0	8.674	100
C1 S1	0.735	17.64	86.5	67.68	81.22	14.68	31.52
C2 S+1	1.893	17.19	66.14	67.84	51.48	14.97	82.69
S+2	0.313	8.79	97.13	59.05	93.01	32.16	29.36
C3 S+1	2.22	19.45	55.03	66.70	44.08	12.85	89.6
S+2	0.708	11.7	91.46	64.19	82.84	24.11	49.79
C4 S+1	2.45	16.8	57.12	69.04	36.1	14.16	101.28
S+2	0.899	9.84	90.83	64.42	78.12	25.74	67.54
C5 S+1	2.602	16.16	56.2	69.59	31.58	14.25	108.2
S+2	1.062	10.02	88.92	64.7	74.04	25.28	78.22
C6 S+1	2.725	19.44	44.82	67.62	30.41	12.94	102.74
S+2	1.131	9.57	88.75	66.0	71.81	24.43	80.56

Table 5.38 continued

Sample	Concentration g/100gSol	% below 12000 MW	Efficiency of removal below 12000 MW	% between 12000 - 98000 MW	Efficiency of removal 12000-98000 MW	% above 98000 MW	Efficiency of retention above 98000 MW
C8 S+1	2.88	19.87	40.21	67.56	26.26	12.57	105.95
S+2	1.28	9.31	87.60	68.3	66.98	22.39	83.47
C10 S+1	3.01	20.61	35.38	67.04	23.8	12.35	108.49
S+2	1.335	11.59	83.88	65.15	67.17	23.26	90.48
C13 S+1	3.08	19.46	37.6	68.44	20.36	12.10	108.58
S+2	-	-	-	-	-	-	-
C14 S+1	3.08	20.17	35.29	68.09	20.78	11.76	105.72
S+2	1.335	10.02	86.07	68.33	65.53	21.65	84.35
C16 S+1	3.099	19.77	36.18	86.50	19.83	11.73	105.95
S+2	1.43	9.92	85.31	68.49	63.01	21.59	89.9
C19 S+1	3.133	20.37	33.53	68.07	19.43	11.56	105.6
S+2	1.457	10.26	84.43	69.07	61.99	20.67	87.86
C20 S+2	1.457	9.79	85.2	69.14	61.95	21.07	89.57

Increasing the number of stages clearly enhances the removal of the material below the cross-over point. For example the percentage in the retentate below 12,000 MW drops from 6.7% to 2.7% as the number of stages increases from two to four. The percentage within the sample above 98,000 MW did not increase by the same proportion, increasing the number of stages from two to four caused an increase from 29.45% to 30.61%. See figure 5.83. These changes are reflected in the efficiency of removal and retention for these two bands; the efficiency of removal increased by 5.5% but the efficiency of retention remained effectively unchanged. The efficiency of removal of the 12,000 MW to 98,000 MW band remained constant throughout these experiments, this was caused by the increased removal below the cross-over point being matched by an equal improvement above it, hence no change within the overall efficiency of removal.

The cross-over point did however vary as the number of stages increased, these changes were more likely due to the varying performance of the additional membranes used rather than the operation of the cascade. The limit of the variation was between 40,000 MW and 60,000 MW. Although each membrane order produced different cross-over points this value was found to be relatively stable as the number of diavolumes used was increased; this confirmed the results obtained from the two stage cascade. See figure 5.84 to 5.88.

To improve the efficiency of retention the membrane order was changed (run 8.1 and 8.2). Membrane number three and four were placed in stages one and two, because these membranes both exibited a very high retention above 98,000 MW. Using this membrane configuration an efficiency of retention of 96% was obtained; unfortunately the efficiency of removal of the 12,000 MW to 98,000 MW band was reduced because the cross-over point dropped to only 37,000 MW. See figure 5.89 and 5.90. This confirmed the trends found in section 5.4.3, the

efficiency of retention could be improved by careful selection of the membranes order used, however this resulted in a lower cross-over point and a lower efficiency of removal.

The failure of a membrane within the cascade was found to have a significant affect on the final product. During run 9.1 a hollow fibre burst in membrane number two, this membrane was positioned in the second stage of the cascade. Although the other stages were unaffected the cascade was unable to compensate for the loss of the membrane and the efficiency of retention was signficantly reduced, the rejection curve for this run can be found in figure 5.91. The Romicon 50,000 MW cut-off membranes appear to be more prone to fibre damage than the Amicon membranes, in total two membranes were damage even though the operating pressure never exceeded 70KPa. This problem was probably caused by the larger fibre diameter used in the Romicon cartridges. Since the fibres were far larger the radial stresses will be far more severe and so any imperfections would be more likely to cause the fibre to burst. Although fibre damage was a significant problem, the broken fibre could be easily blocked by using a piece of copper wire and glue. This allowed the cartridges to be reused, however the flux was lower since the surface area of the membrane was marginally reduced.

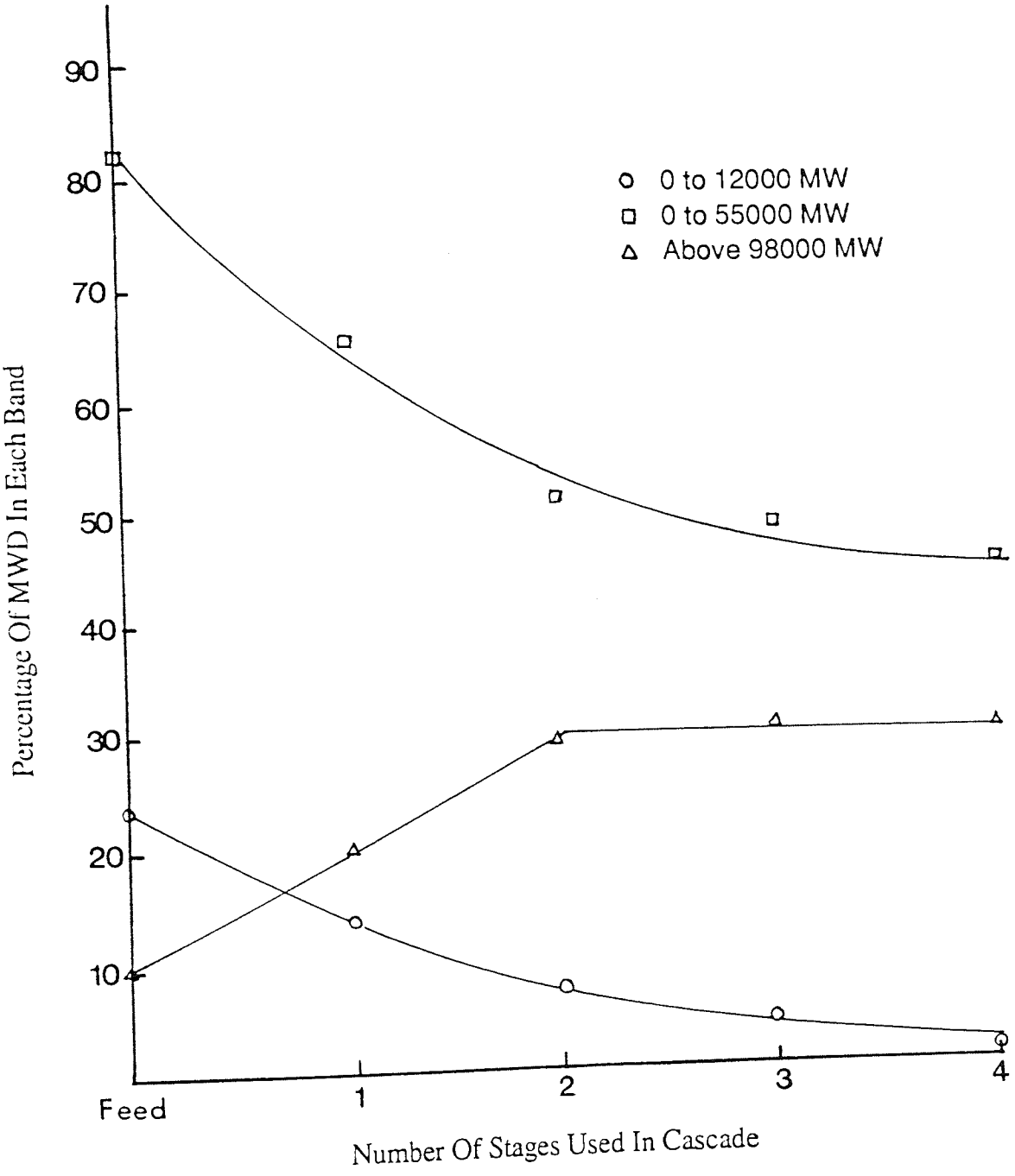

Figure 5.83 The Relationship between the Molecular Weight Distribution of the Final Product and the Number of Stages used in the Cascade

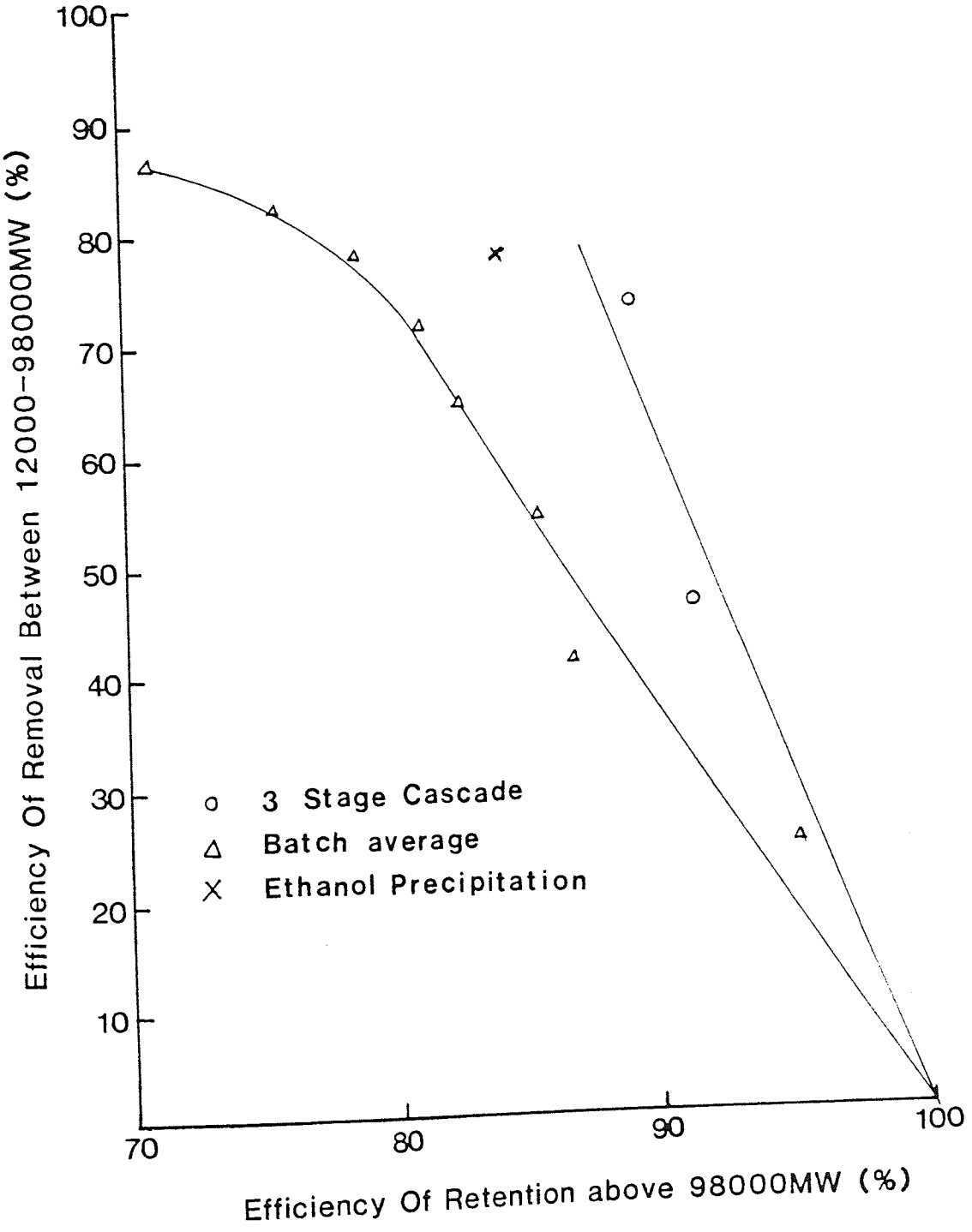

Figure 5.84 Comparing the Efficiency of the 3 Stage Cascade to the Batch System

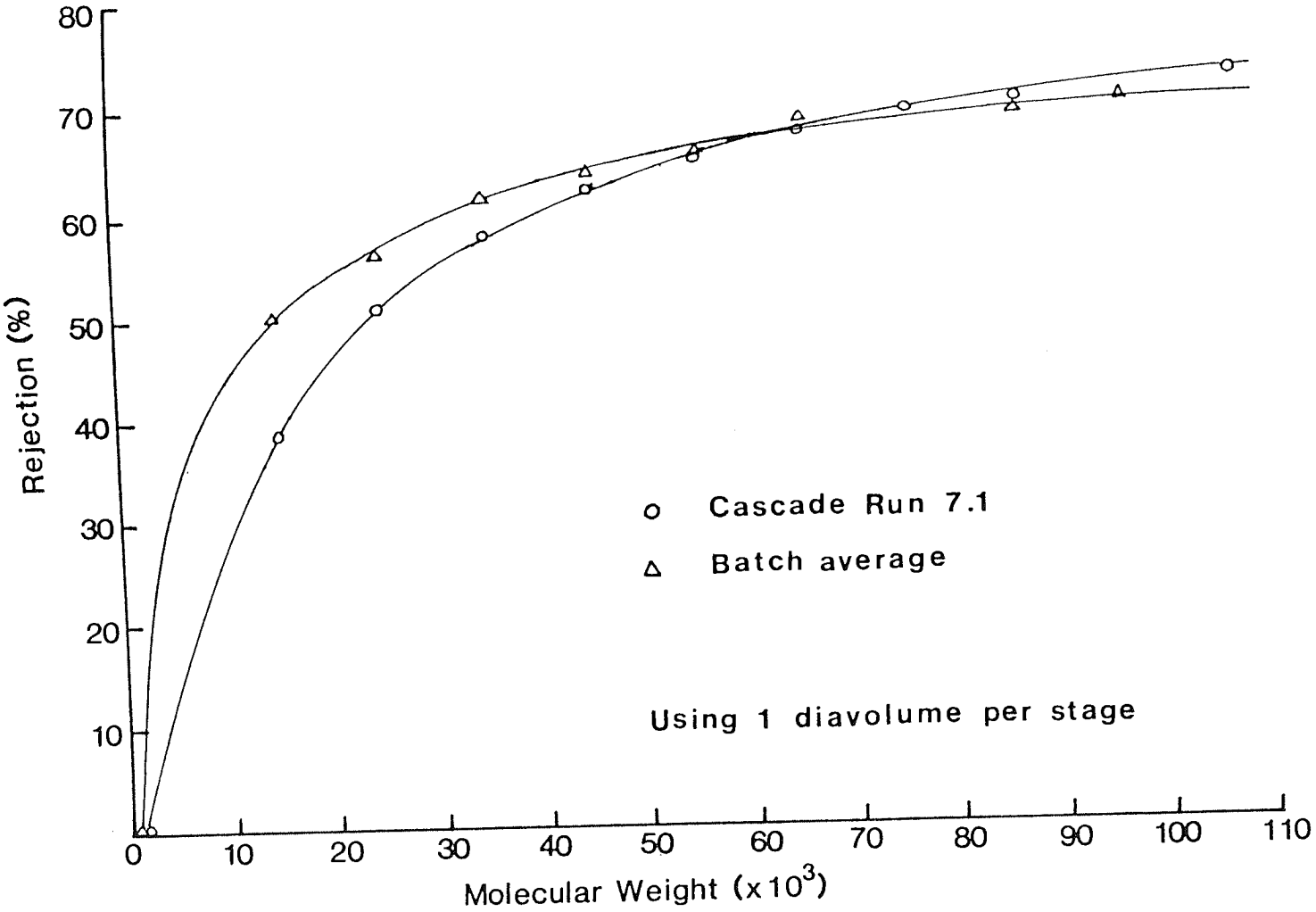

Figure 5.85 Rejection Curve from Cascade Run 7.1

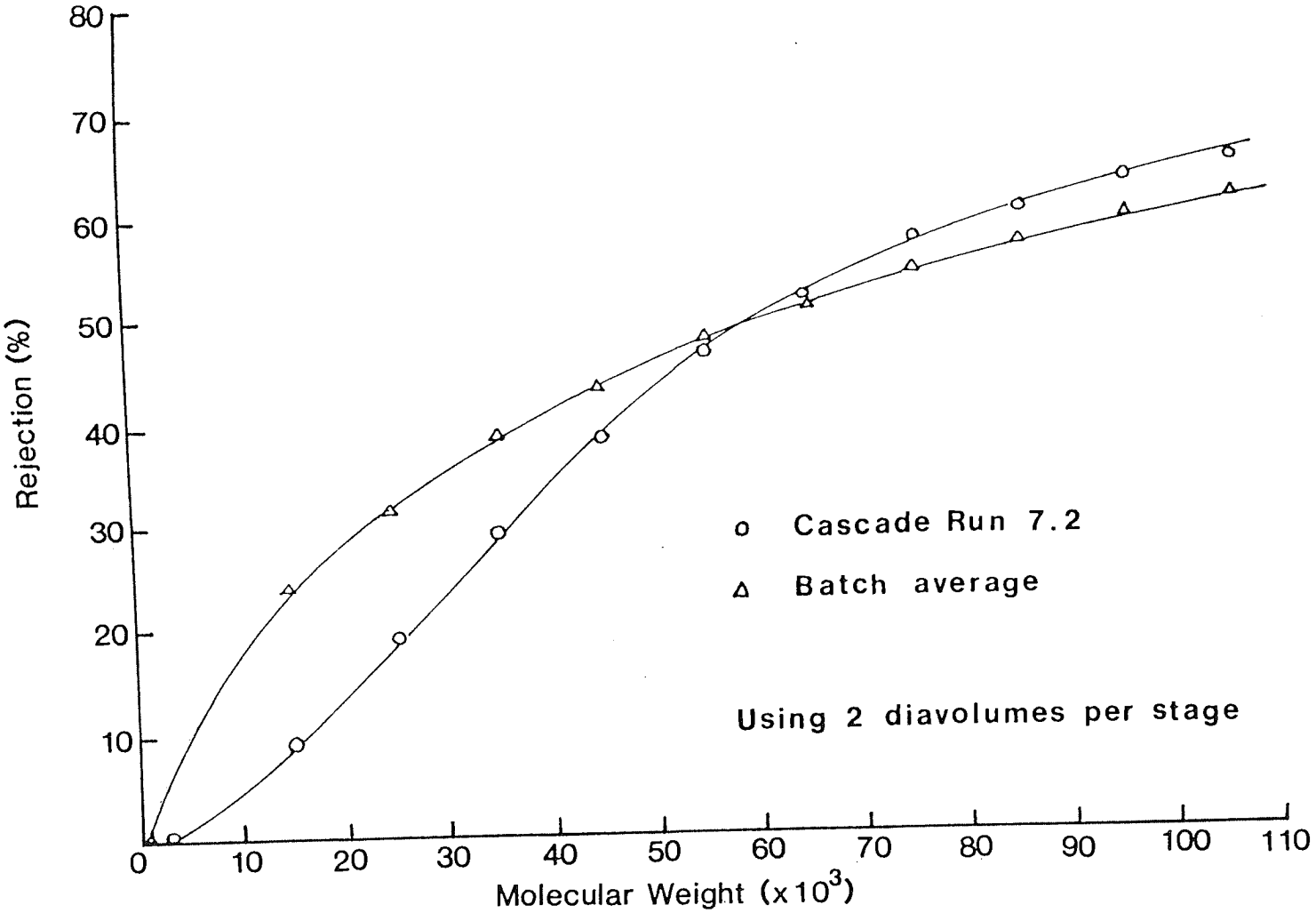

Figure 5.86 Rejection Curve from Cascade Run 7.2

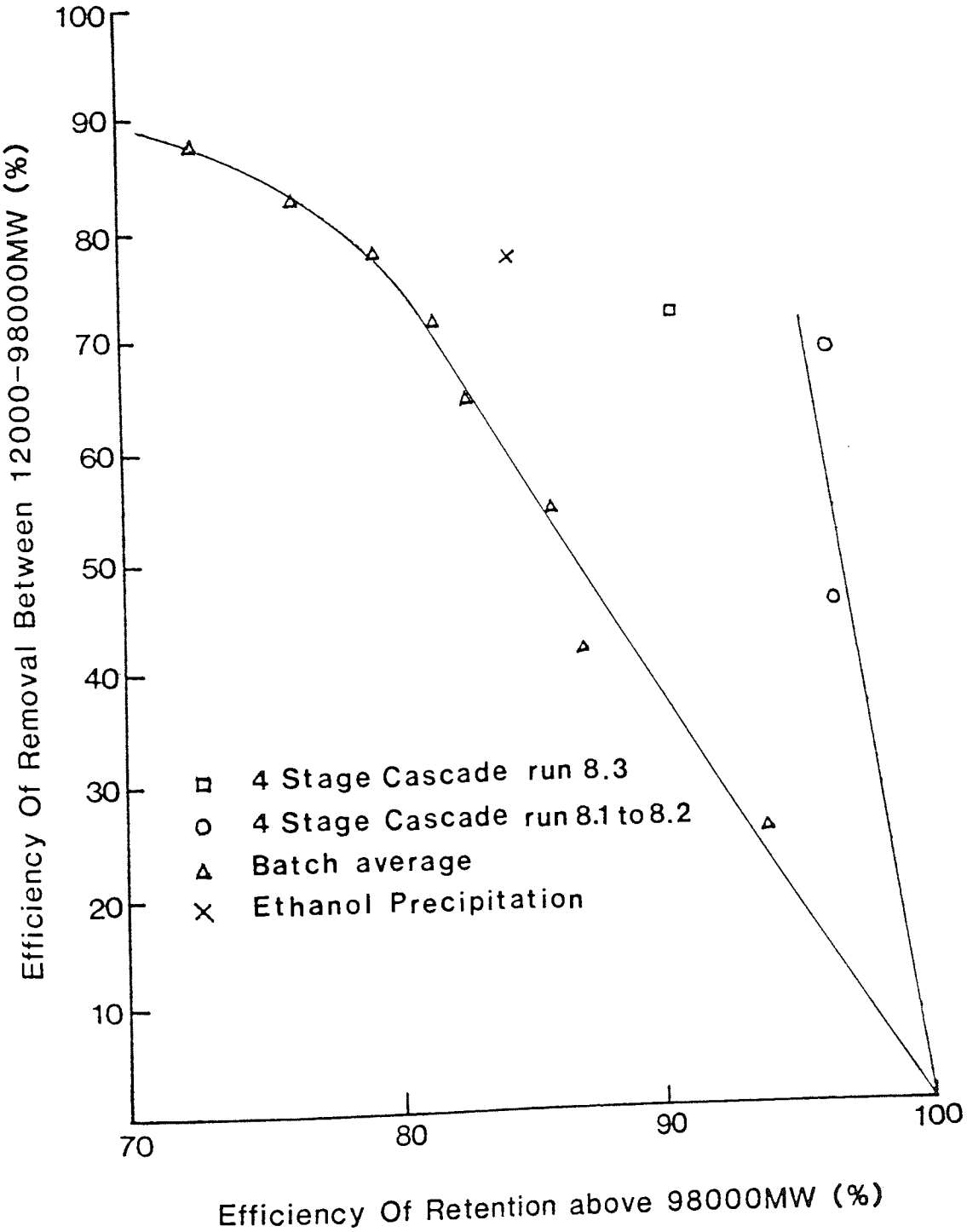

Figure 5.87 Comparing the Efficiency of the 4 Stage Cascade to the Batch System

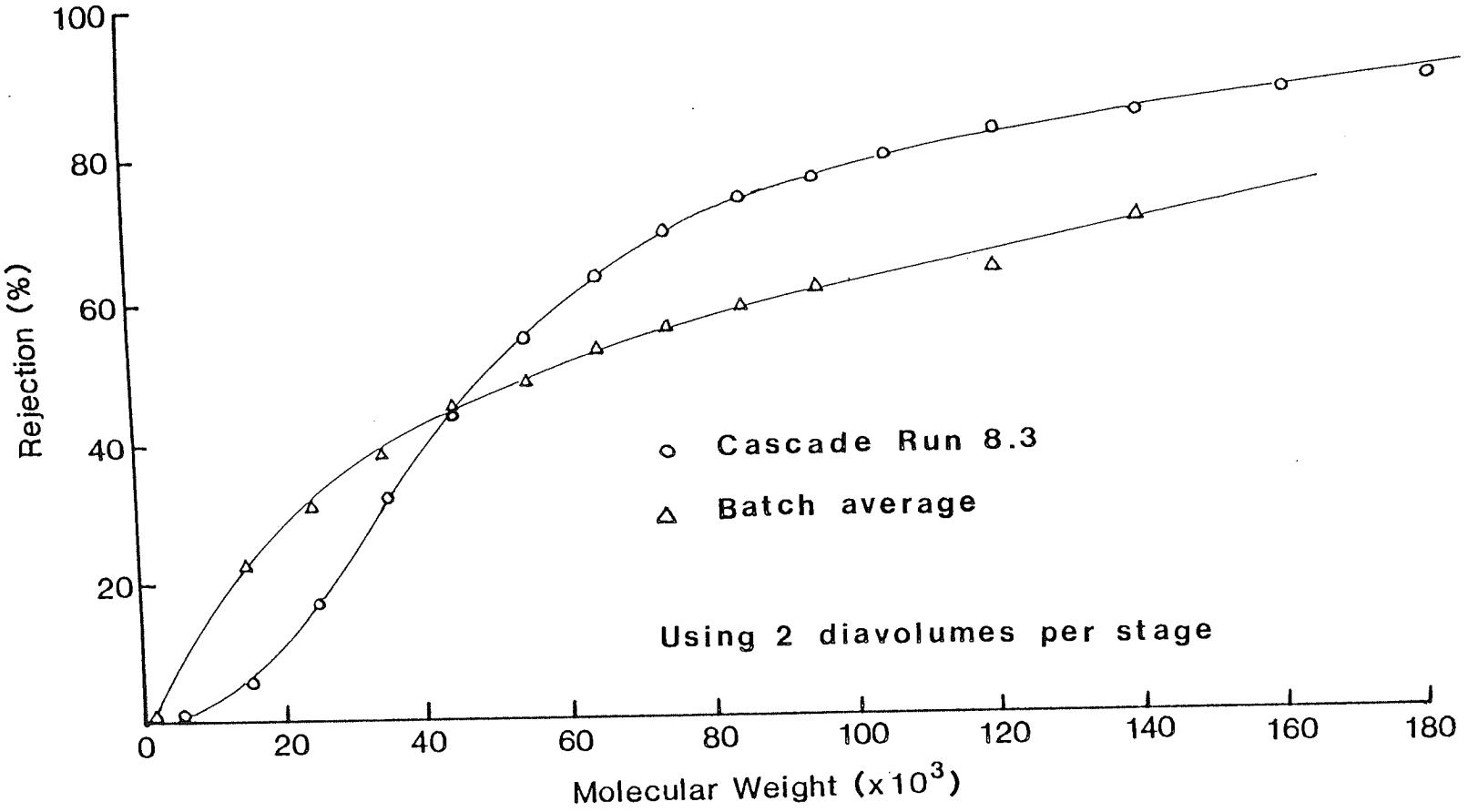

Figure 5.88 Rejection Curve from Cascade Run 8.3

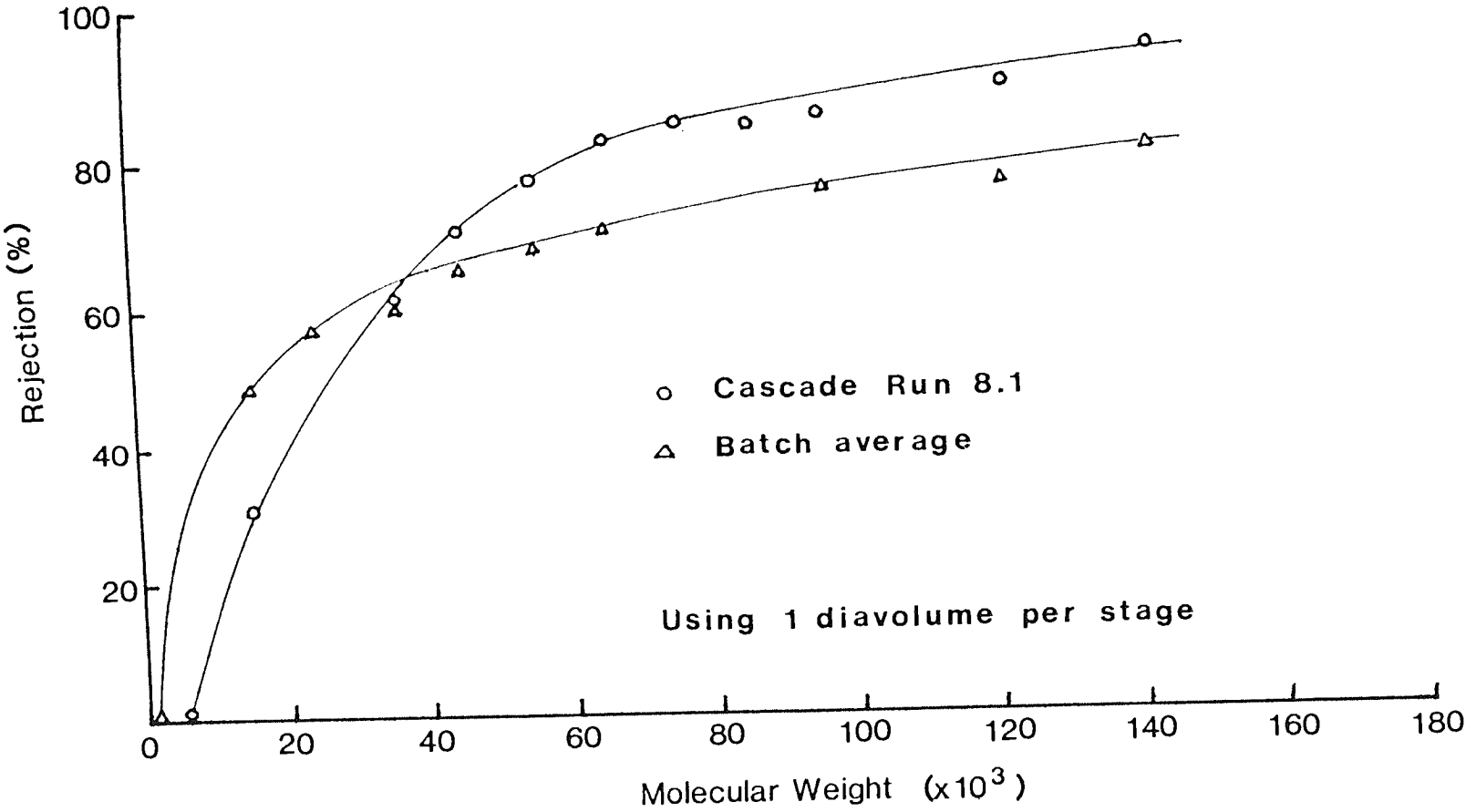

Figure 8.89 Rejection Curve from Cascade Run 8.1

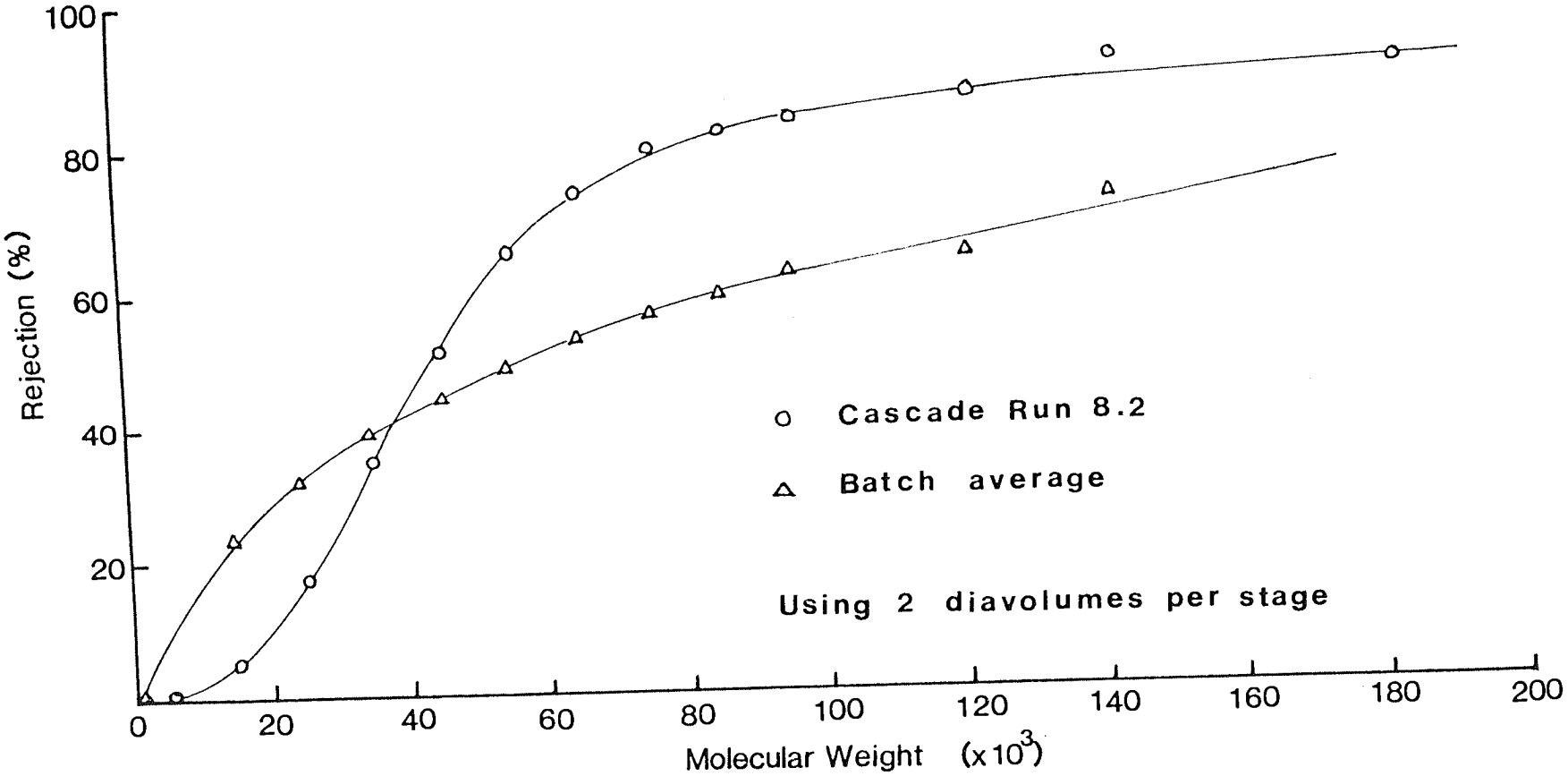

Figure 5.90 Rejection Curve from Cascade Run 8.2

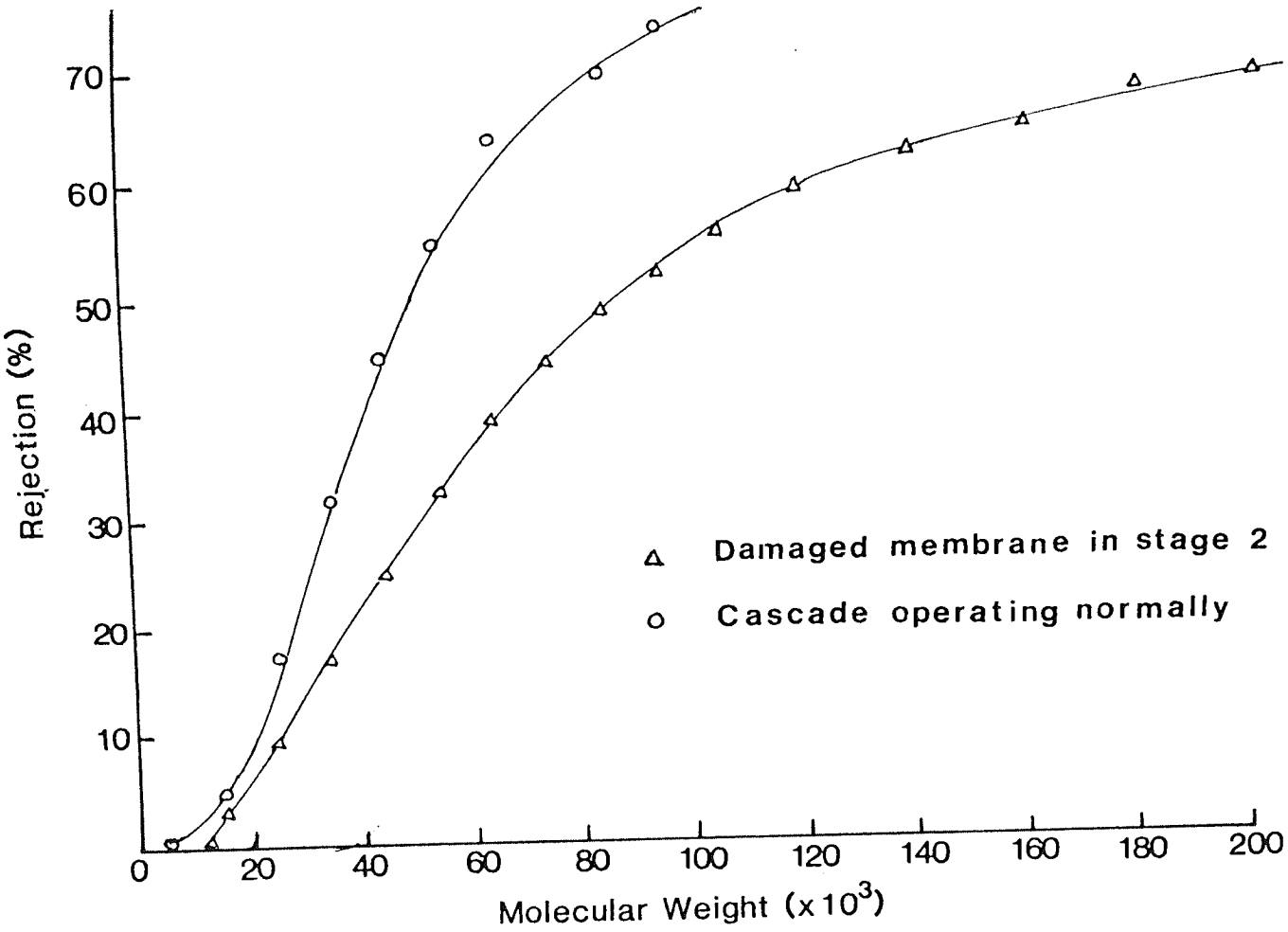

Figure 5.91 The Effect of a Damaged Membrane Within the Cascade

5.5.5 TESTING THE AMICON 100,000 MW CUT-OFF MEMBRANE USING BATCH DIAFILTRATION

The Romicon membranes used in the previous section were found to be highly satisfactory at retaining the dextran above 98,000 MW but the removal of the 12,000 MW to 98,000 MW band was impaired since the cross-over point fell well below the desired value of 98,000 MW. To raise the cross-over point to 98,000 MW the 100,000 MW cut-off Amicon membranes were used.

The Amicon HIP100-20 membrane used in section 5.5.2 was retested using a 4% W/W HZIS feed as was a new membrane obtained specifically for used in the cascade. See table 5.39 and 5.40. The performance of the new membrane was noticeably poorer than the first membrane obtained from Amicon. The rejection curve in figure 5.96 shows this very clearly. Below 30000 MW the rejection curves were very similar, however after this value the two rejection curves rapidly diverge. At 98000 MW the rejection of the new membrane was only 43% compared to 50% for the original membrane.

Table 5.39 Amicon 100,000 MW cut-off Membrane Number 1

		RETENTATE PRODUCT					
Number of diavolumes	Concentration (g/100g Sol)	% below 12000 MW MW	Efficiency of removal below 12000 MW	% between 12000 - 98000 MW	Efficiency of removal 12000 to 98000 MW	% above 98000 MW	Efficiency of retention above 98000 MW
Feed	3.95	24.31	0	67.016	0	8.674	100
0.5	2.929	23.41	28.58	65.98	27.01	10.61	90.68
1.0	2.13	18.55	58.84	68.11	45.22	13.34	82.89
1.5	1.621	15.99	73.01	68.36	58.14	15.65	73.84
2.0	1.21	13.22	83.34	66.8	69.47	19.98	70.34
2.5	0.88	11.06	89.89	65.06	78.39	23.88	61.29
3.0	0.667	9.46	93.44	60.81	84.69	29.73	57.79
3.5	0.49	7.42	96.25	58.32	89.19	34.26	49.03
4.0	0.3679	5.73	97.81	54.23	92.48	40.04	42.91

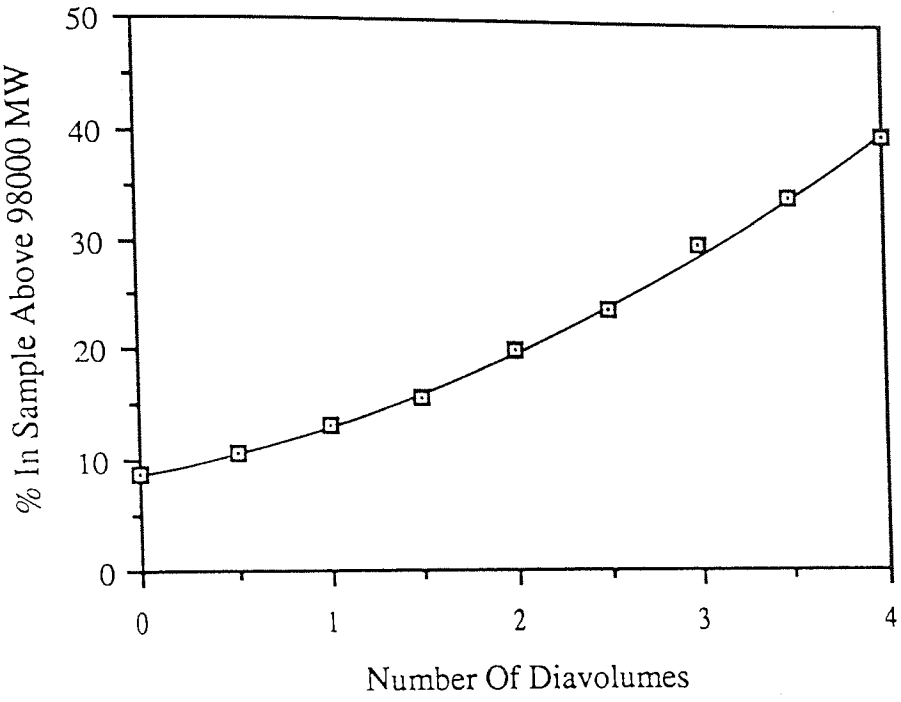

Figure 5.92 How the Number of Diavolumes used Effects the Percentage of Material above 98,000 MW in the Retentate

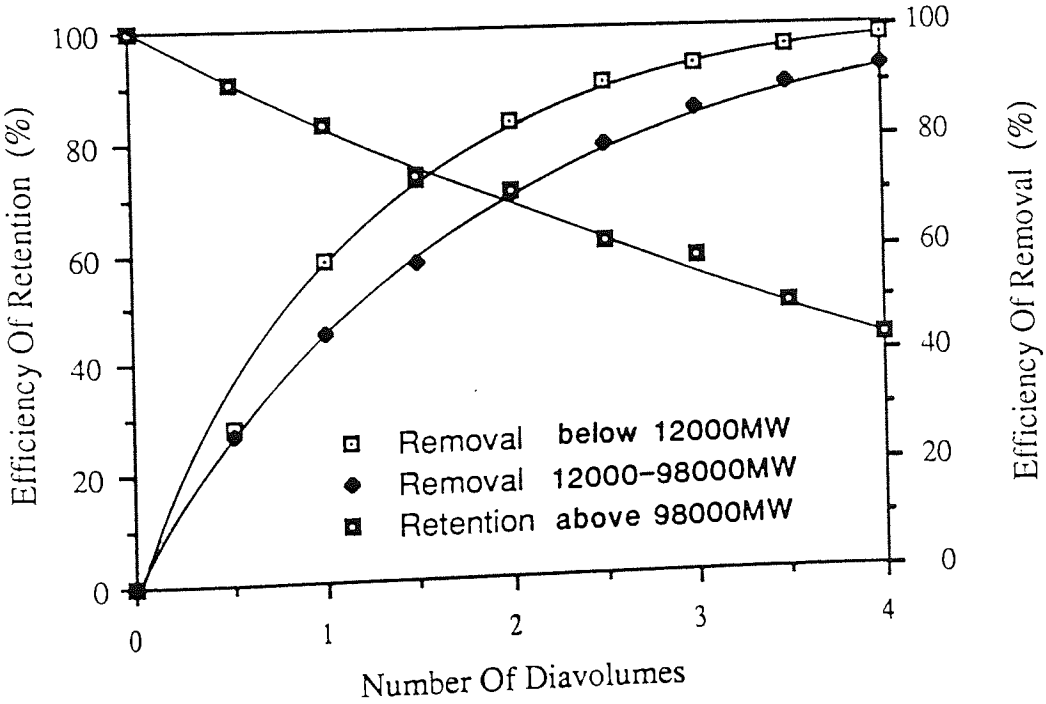

Figure 5.93 The Relationship between Efficiency and Number of Diavolumes used. Membrane Number 1

Table 5.40 Amicon 100,000 MW cut-off Membrane Number 2

Number of diavolumes	Concentration (g/100g Sol)	% below 12000 MW	Efficiency of removal below 12000 MW	% between 12000 - 98000 MW	Efficiency of removal 12000 - 98000 MW	% above 98000 MW	Efficiency of retention above 98000 MW
Feed	3.828	23.97	0	67.00	0	9.03	100
0.5	2.75	22.69	31.99	66.58	28.59	10.73	85.50
1.0	1.97	19.16	58.91	68.23	47.58	12.61	71.88
1.5	1.43	15.95	75.15	69.05	61.50	15.00	62.02
2.0	1.06	13.75	84.19	68.09	71.87	18.16	55.65
2.5	0.708	9.07	93.02	67.02	81.51	23.73	48.69
3.0	0.558	7.82	95.31	63.79	86.11	28.39	45.79
3.5	0.381	5.56	97.71	62.36	90.75	32.08	35.36
4.0	0.299	5.59	98.25	53.65	93.70	40.76	35.07

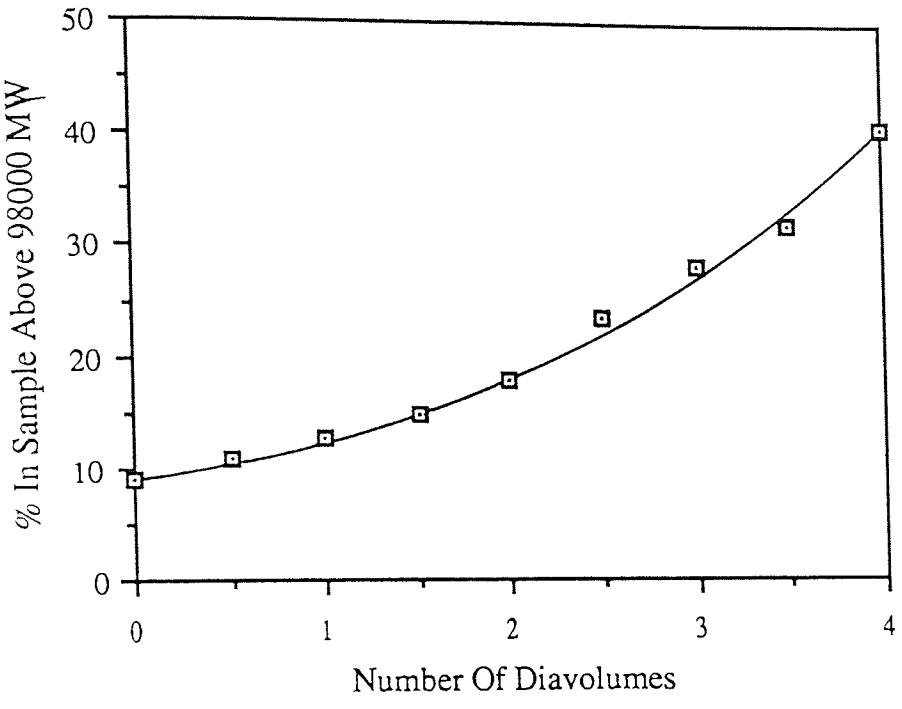

Figure 5.94 How the Number of Diavolumes used Effects the Percentage of Material above 98,000 MW in the Retentate

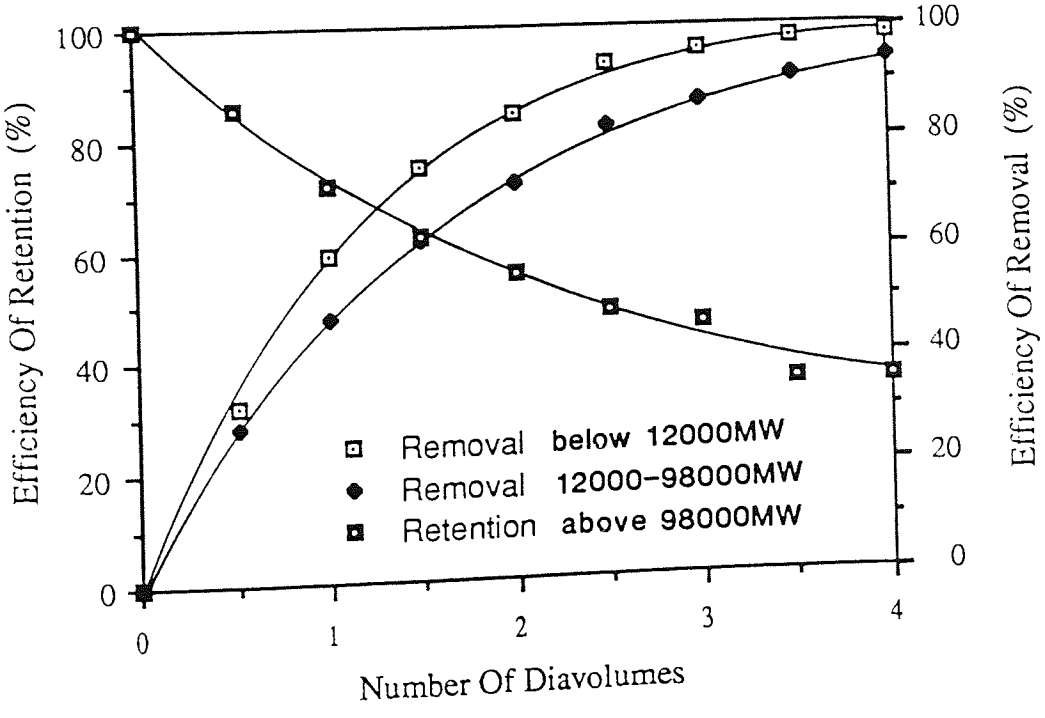

Figure 5.95 The Relationship between Efficiency and Number of Diavolumes used. Membrane Number 2

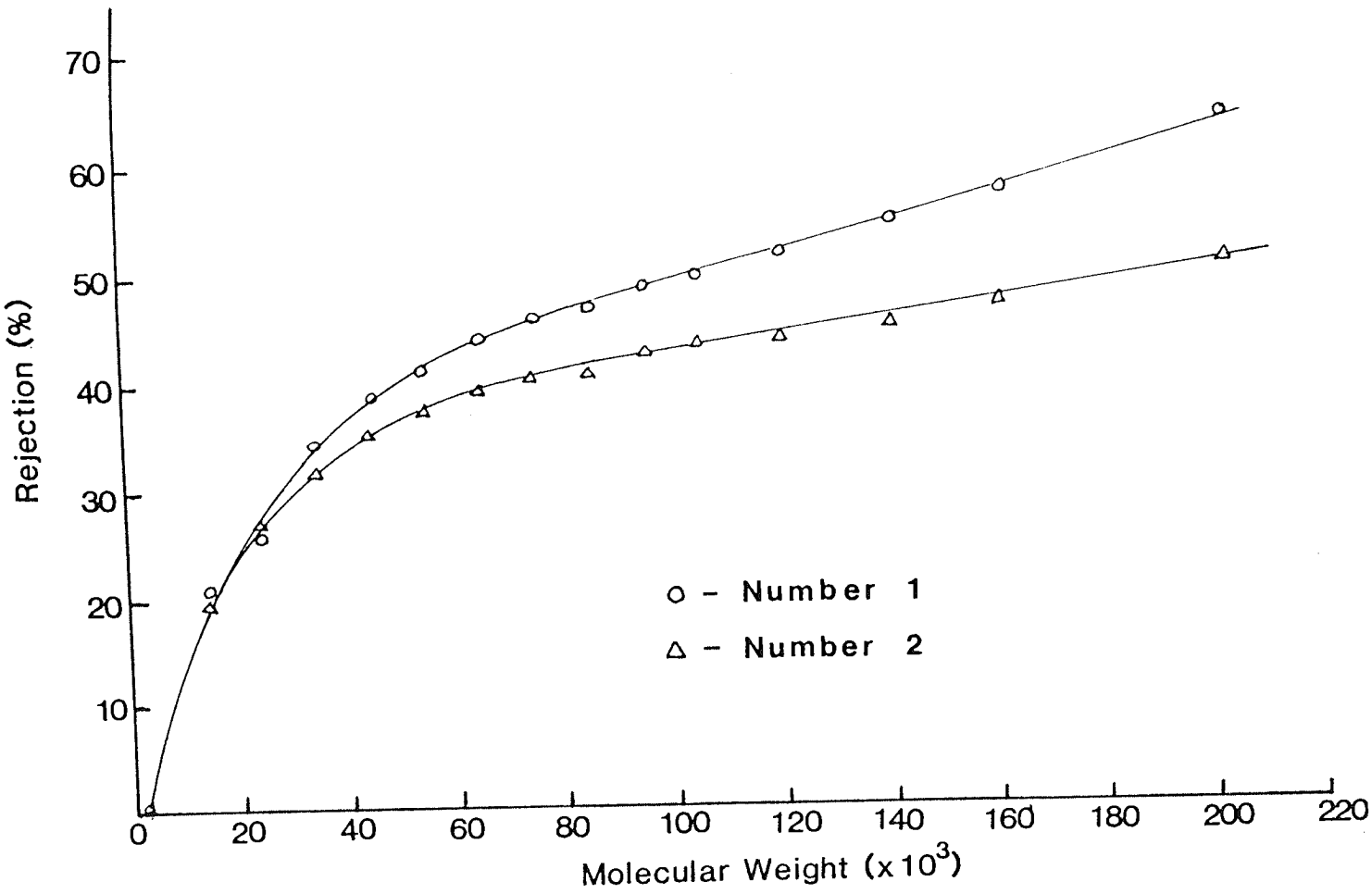

Figure 5.96 The Rejection Curves Obtained from the Two 100,000 MW Cut-off Membranes. At 2 Diavolumes

5.5.6 USING THE AMICON 100,000 MW CUT-OFF MEMBRANES WITHIN THE CASCADE

A two stage cascade was used to study the fractionation obtained when using the 100,000 MW cut-off Amicon membranes. Since the two membranes had significantly different rejection curves, their position within the cascade was varied to see how the cross-over point could be altered (see runs 10.1 to 10.3 and 11.1 to 11.2). When the membrane with the higher rejection (number one) was placed in stage one an efficiency of retention of 83% was obtained, this dropped to only 70% when the membrane sequence was reversed, however the efficiency of removal increased from 76% to 78%. See figure 5.97. At best this was only a 6% improvement on the comparable 50,000 MW cut-off cascade, but the efficiency of retention had dropped by 23% in the worst case. The rejection curves for these experiments can be found in figures 5.98 to 5.101. Using the first membrane sequence the cross-over point occurred at 60,000 MW this was only marginally higher than the mean value obtained for the earlier experiment using the Romicon membranes. Again the cross-over point was found to remain relatively constant as the number of diavolumes increased. The reversed membrane sequence raised the cross-over point to 145,000 MW, this was far more satisfactory but the removal of the dextran below this molecular weight was not as high as was expected.

Mixing the Romicon and Amicon membranes was also considered, see figure 5.102 positioning a 50,000 MW cut-off membrane (number one) in stage one and an 100,000 MW cut-off membrane (number two) in stage two improved the efficiency of retention by 5% however again the efficiency of removal was similar to results obtained in section 5.5.4. This was again caused by the position of the cross-over point which occurred at 55,800 MW rather than the desired value of 98,000 MW. See figure 5.103. In all cases the relatively poor improvements achieved for the

efficiency of removal can be explained by comparing the rejection curves for the 50,000 MW and 100,000 MW cut-off membrane used in these experiments. See figure 5.104 and 5.105. Below 60,000 MW the rejection curves were almost identical, it was only when the molecular weight exceeded 100,000 MW that the two rejection curves rapidly diverged. Naturally since the batch rejection curves were very similar it was not surprising that cascade runs 6.3 and 10.3 were also similar in this region. Furthermore the rejection curve of the poor 50,000 MW cut-off membrane (number two) was almost identical to that found for the original 100,000 MW cut-off membrane (number one) hence the similarity between runs 13.1 and 6.3.

Since the main objective was to improve the efficiency of removal these results show that there would be little gained by using the Amicon membranes within the cascade. As the Amicon membranes were unsatisfactory the only other alternative would be to use the Romicon membrane but at a higher number of diavolumes. This should enhance the efficiency of removal since more material would be 'washed' through the membrane by the diafiltrate, while the rejection of the dextran above 98,000 MW should still be acceptable since the Romicon membranes give such a high rejection of this band. Unfortunately it was impossible to investigate this approach experimentally because the cascade was only designed to operate up to a maximum of two diavolumes.

The enhanced rejection of the large dextran molecules by the presence of the low molecular weight material has been discussed in previous sections. A feed rich in dextran below 12,000 MW was obtained to quantify this effect and to test the theory discussed in section 5.5.4 regarding the higher than expected retention of dextran by the cascade. The feed contained 31% below 12,000 MW compared to 24% for the normal HZIS feed, while the proportion of dextan above 98,000 MW was very

similar. Experiments 12.1 and 12.2 were conducted using identical operating conditions as experiments 11.1 and 11.2 so that the results would be directly comparable. See figure 5.106. The experiments proved conclusively that the percentage of the low molecular weight material present directly effects the rejection of the higher molecular weight dextran. The efficiency of retention above 98,000 MW increased from 70% to 80% while the efficiency of removal below 12,000 MW remained almost unchanged. The rejection curves for these experiments shows the effect more clearly (see figure 5.107); the rejection above 12,000 MW had noticably increased but the rejection of the dextan below this value had not changed at all. The significance of this is unclear, however since these molecules have such a low rejection it may simply by that these molecules could permeate freely through the membrane. The modification of the rejection curve can be put into context when these results are compared to the batch average of the two membranes used; using the normal feed the cross-over point occurred at 145,000 MW, however this fell to only 40,000 MW when the other feed was used. This shows clearly how the rejection was enhanced. See figure 5.108 and 5.109.

Both Cooper [48] and Bottino [44] showed that this effect was present in the batch system, however the effect should be more pronounced in the cascade system since the the permeate product containing the majority of the low molecular weight material is recycled along the cascade. For example the amount of this material present in the the diafiltrate in stage (n-1) would be greater than stage n, hence the effect would be amplified as the low molecular material moved along the cascade.

These results appear to give more weight to the enhanced retention theory discussed in section 5.5.4.

Table 5.41 Cascade Experiments using Amicon 100,000 MW cut-off Membranes

Run	Conc (g/100g Sol)	%below 12000 MW	%between 12000 - 98000 MW	%above 98000 MW	Conc (g/100g Sol)	%below 12000 MW	%between 12000 - 98000 MW	%above 98000 MW	Efficiency of removal below 12000 MW	Efficiency of removal 12000 to 98000 MW	Efficiency of retention above 98000 MW
10.1	4.107	23.61	67.591	8.799	2.064	14.59	70.36	15.05	68.93	47.69	85.94
10.2	4.155	23.61	67.591	8.799	1.58	9.52	71.15	19.33	84.67	59.97	83.90
10.3	4.155	23.61	67.591	8.799	1.049	6.44	64.64	28.92	93.11	75.85	83.35
11.1	3.85	25.04	65.52	9.44	1.744	16.61	68.06	15.33	70.02	52.93	73.64
11.2	4.11	23.61	67.591	8.799	0.912	6.55	65.73	27.72	93.84	78.42	70.08
12.1	3.855*	31.01	60.37	8.62	1.81	18.64	65.83	15.53	71.79	48.82	84.60
12.2	3.855*	31.01	60.37	8.62	0.98	6.67	66.30	27.03	94.53	72.11	79.81
13.1	3.95**	24.31	67.016	8.674	1.022	6.69	64.04	29.27	92.91	75.29	87.30

* new feed used with higher percentage of low molecular weight material
** mixed membrane run 50(1),100(1)

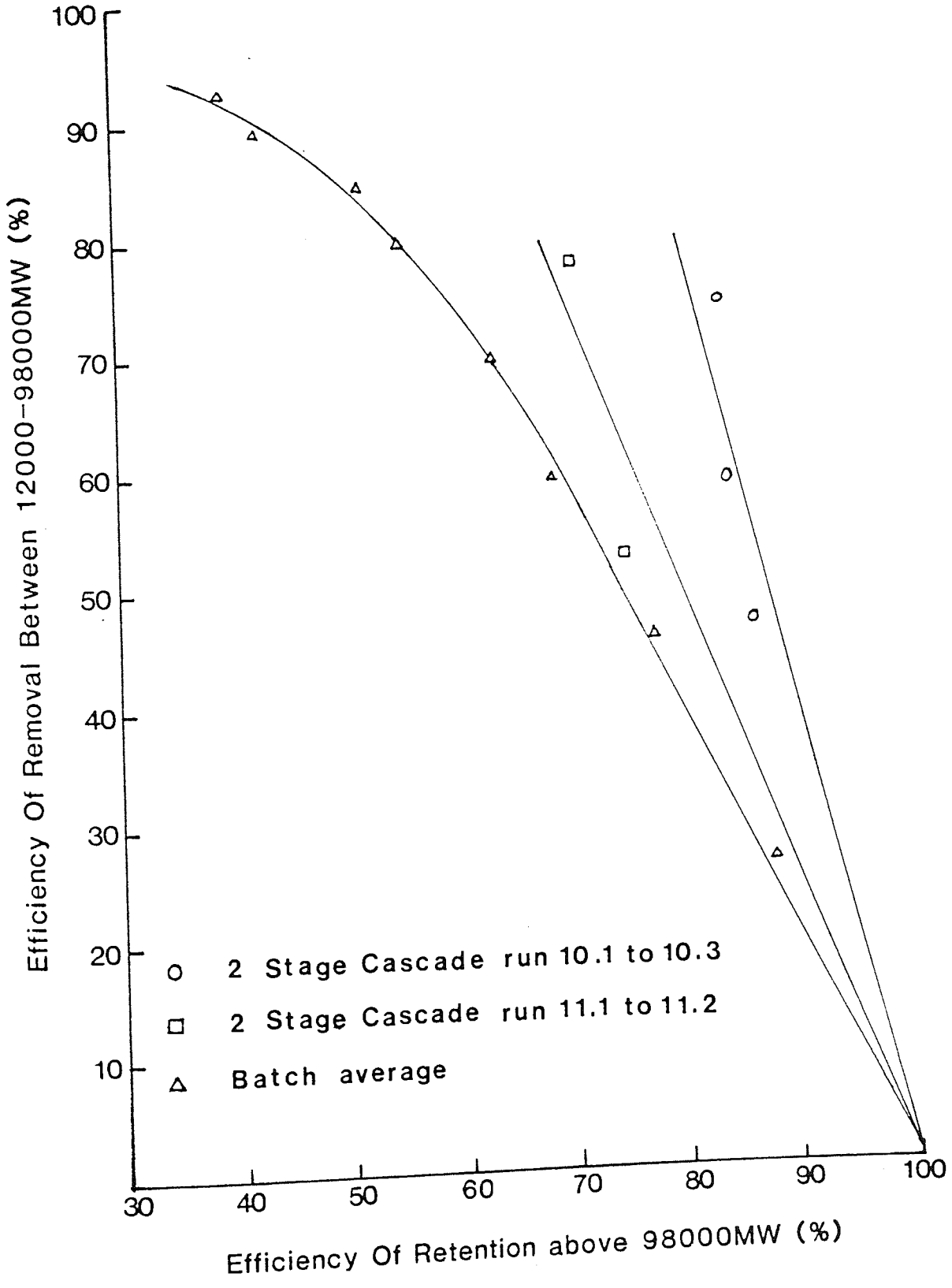

Figure 5.97 The Effect of Membrane Order on the Performance of the Cacade

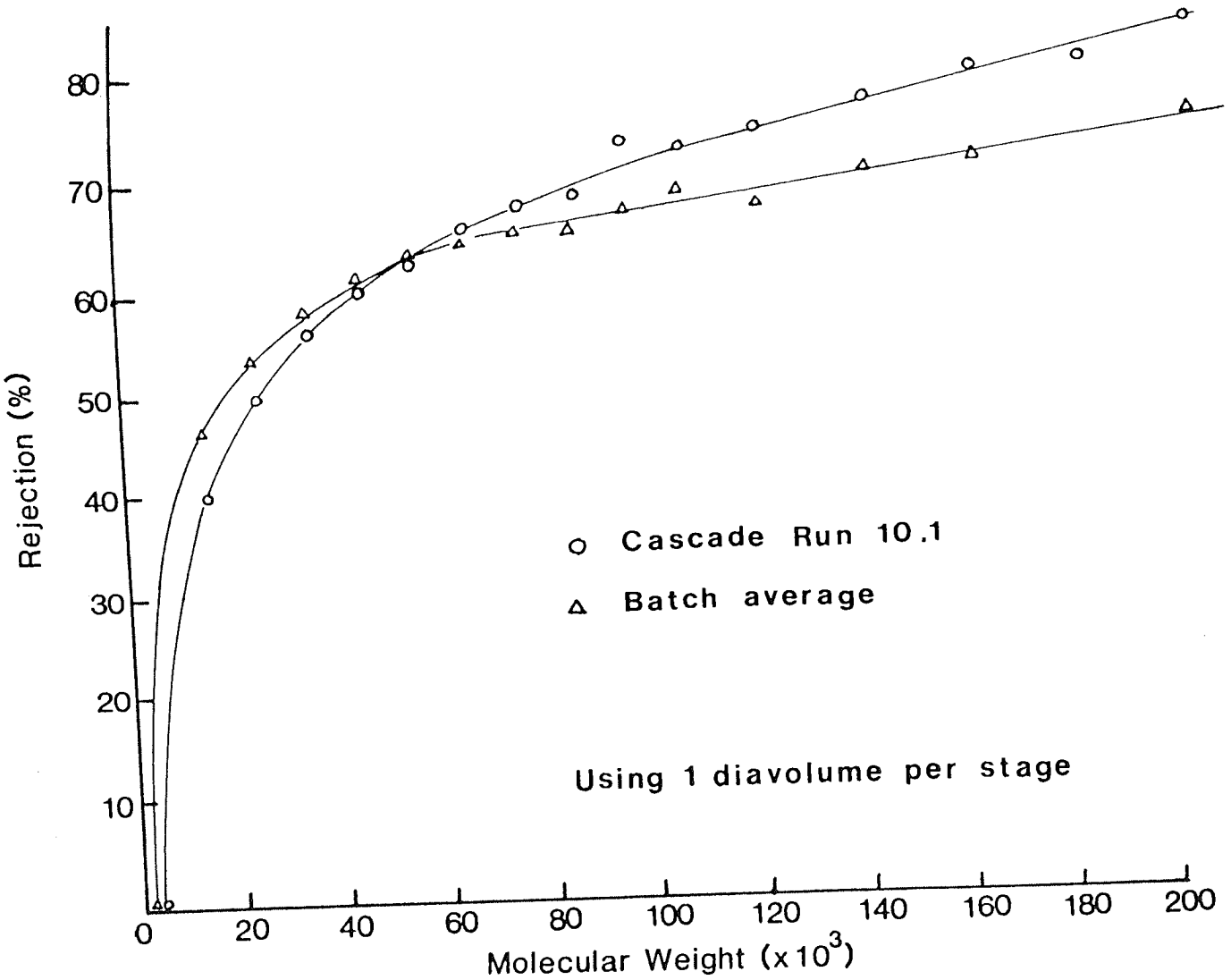

Figure 5.98 Rejection Curve from Cascade Run 10.1

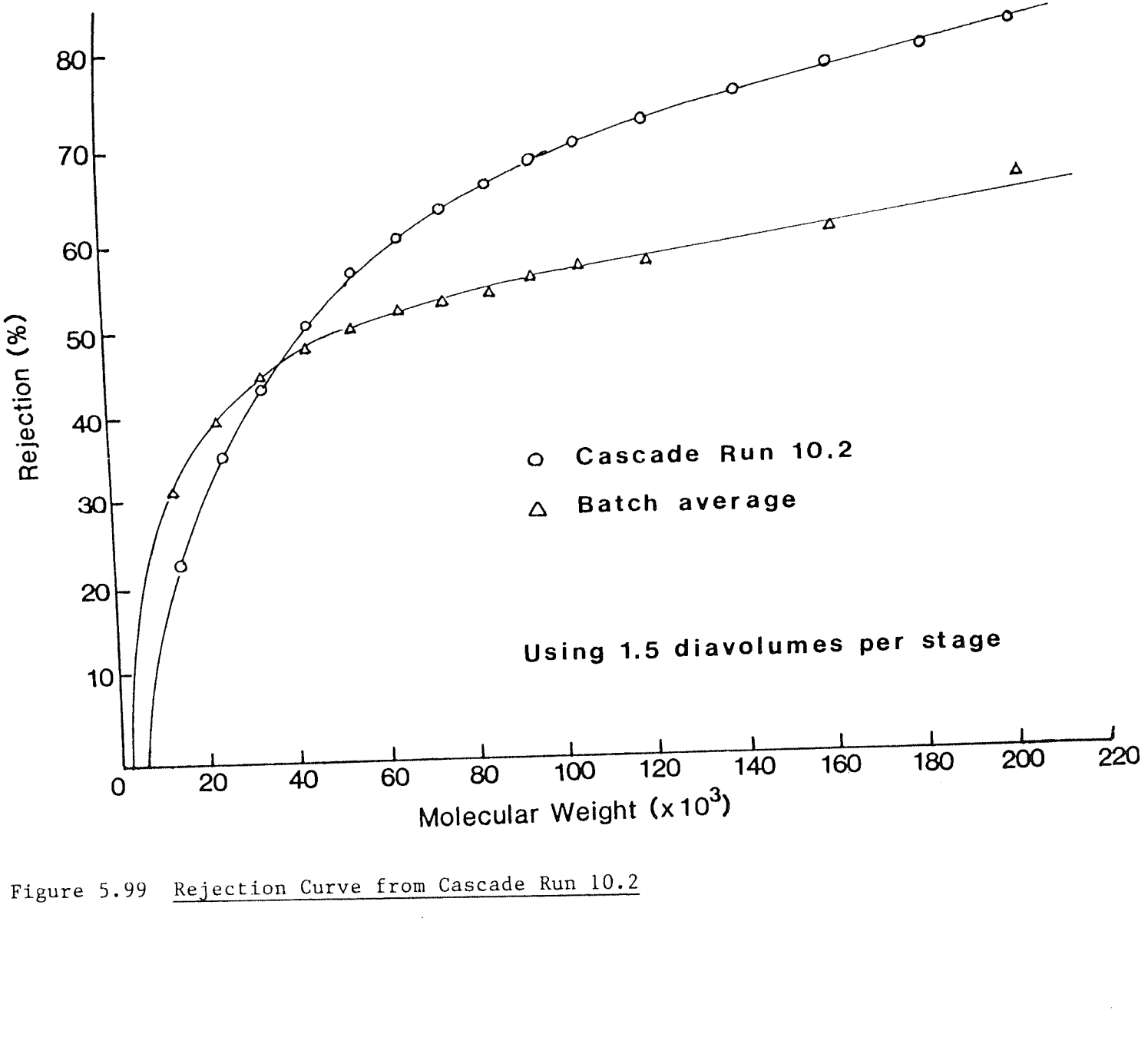

Figure 5.99 Rejection Curve from Cascade Run 10.2

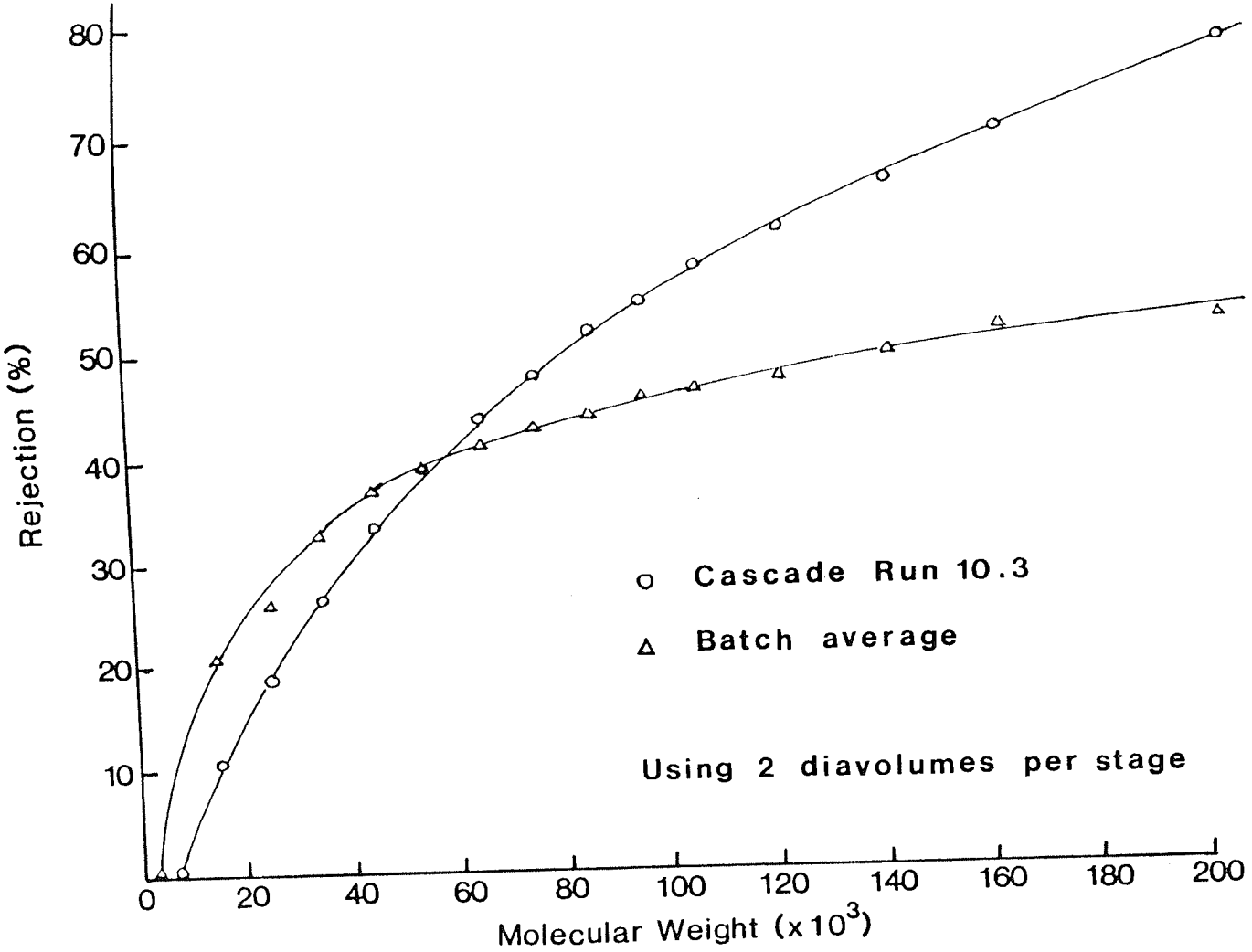

Figure 5.100 Rejection Curve from Cascade Run 10.3

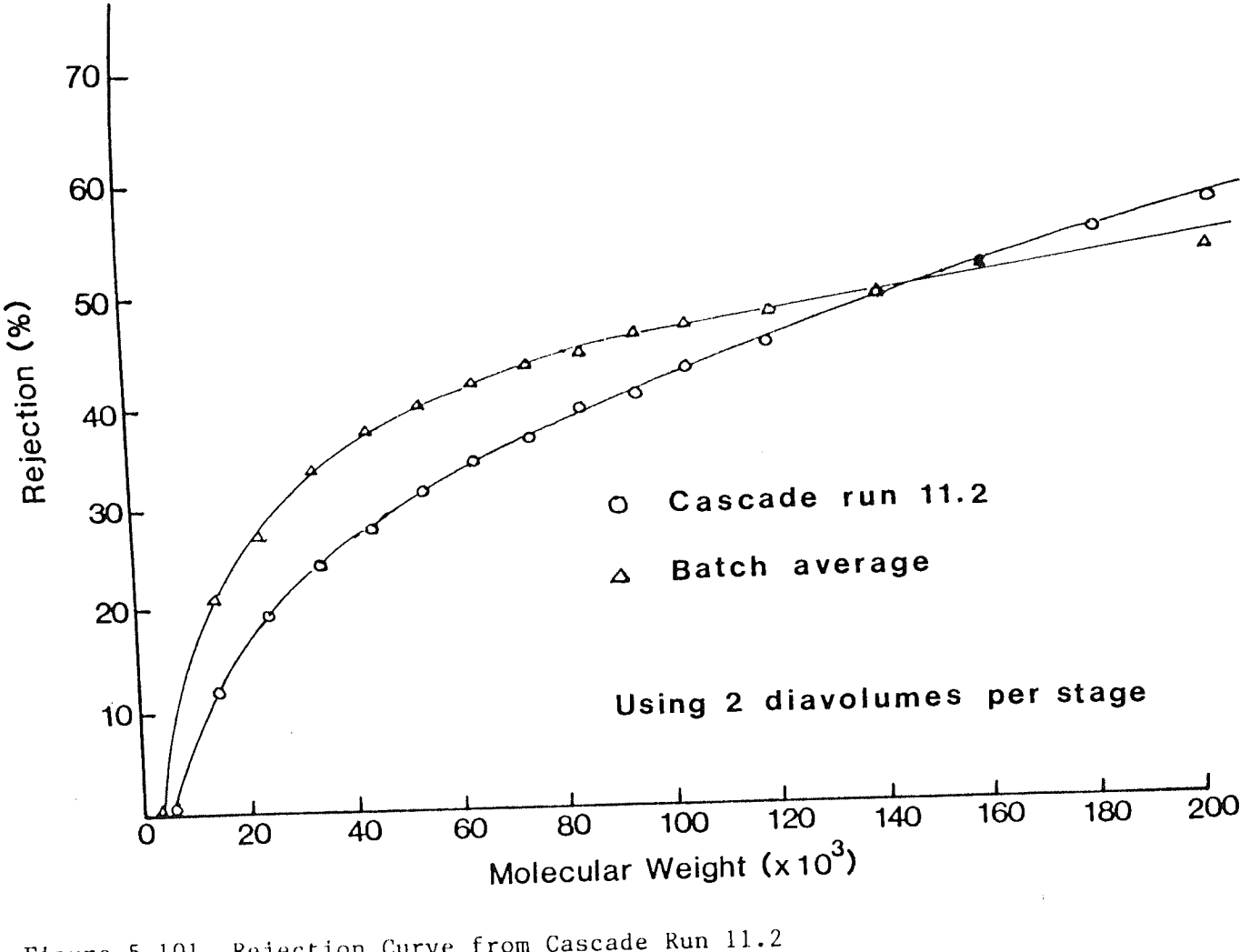

Figure 5.101 Rejection Curve from Cascade Run 11.2

Figure 5.102 Mixing 50,000 MW and 100,000 MW Cut-off Membranes in the Cascade

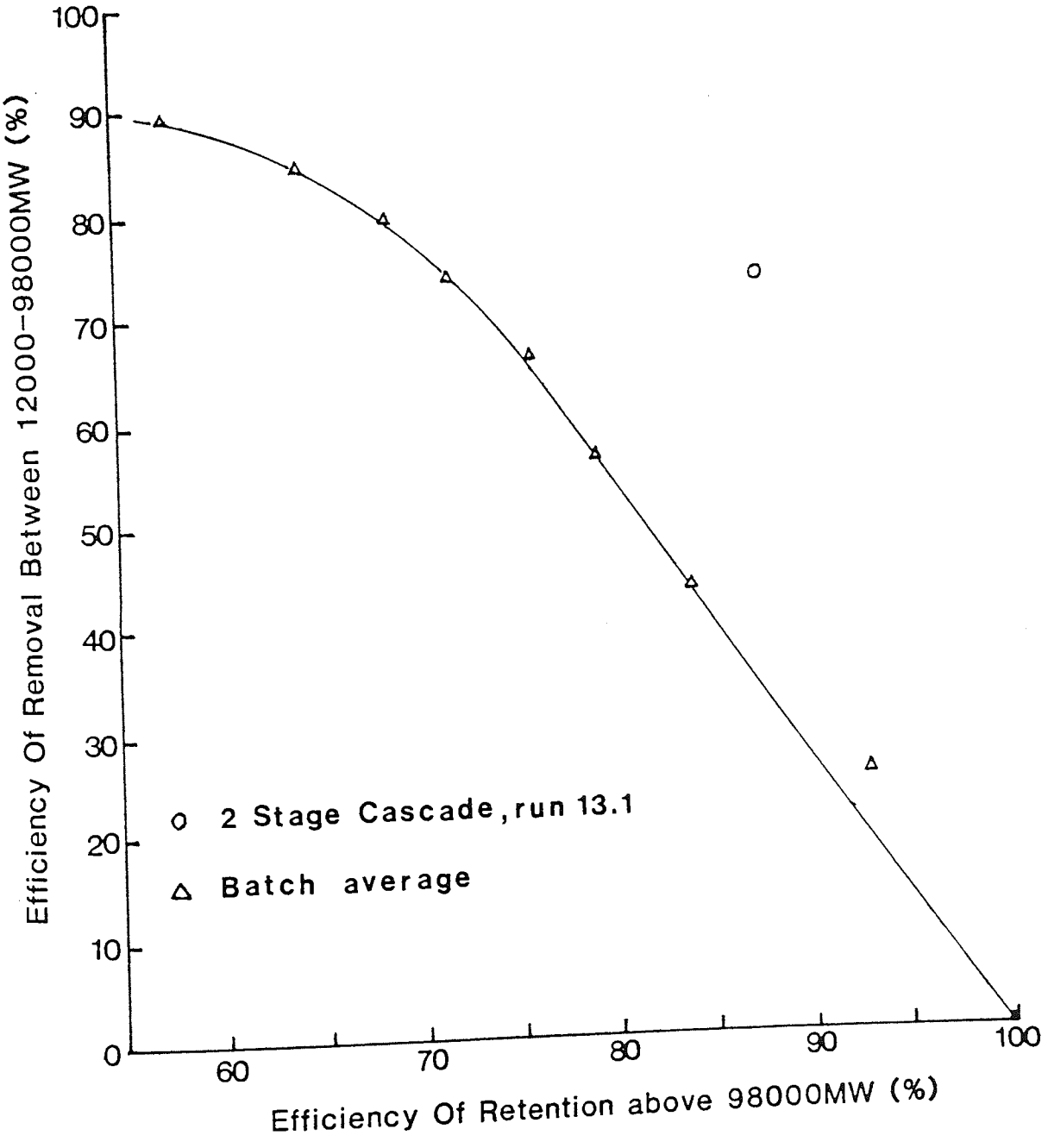

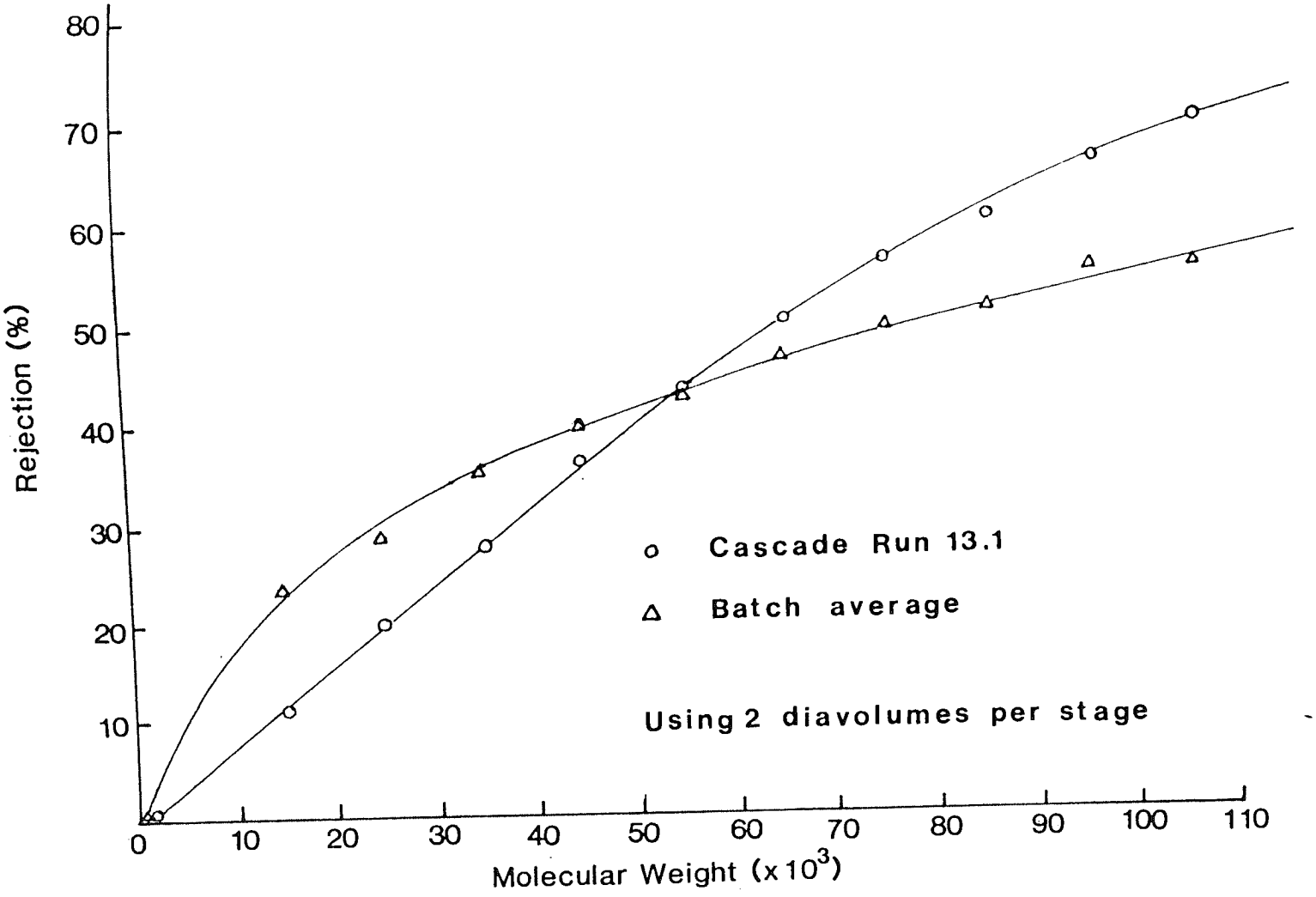

Figure 5.103 Rejection Curve from Cascade Run 13.1

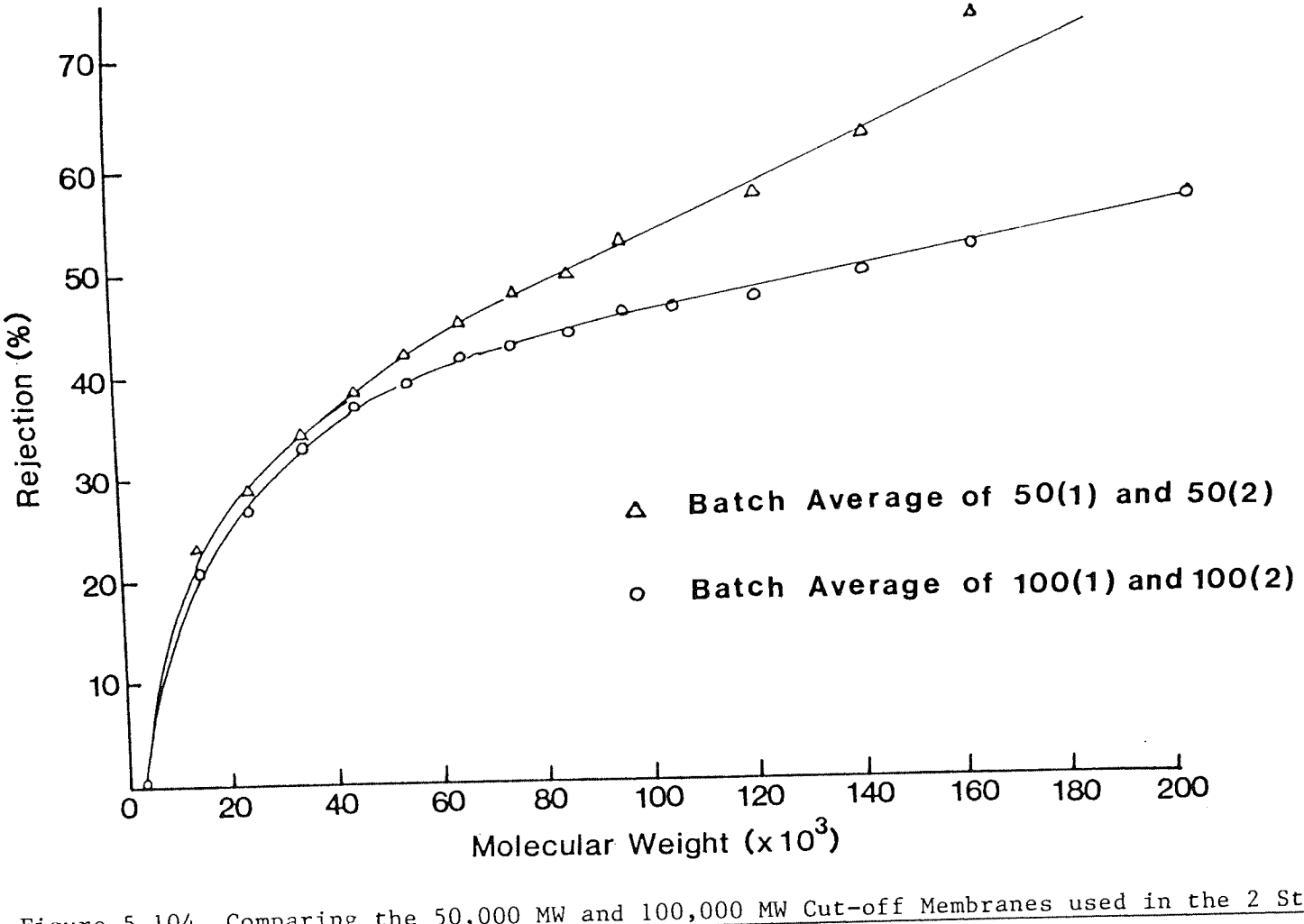

Figure 5.104 Comparing the 50,000 MW and 100,000 MW Cut-off Membranes used in the 2 Stage Cascade

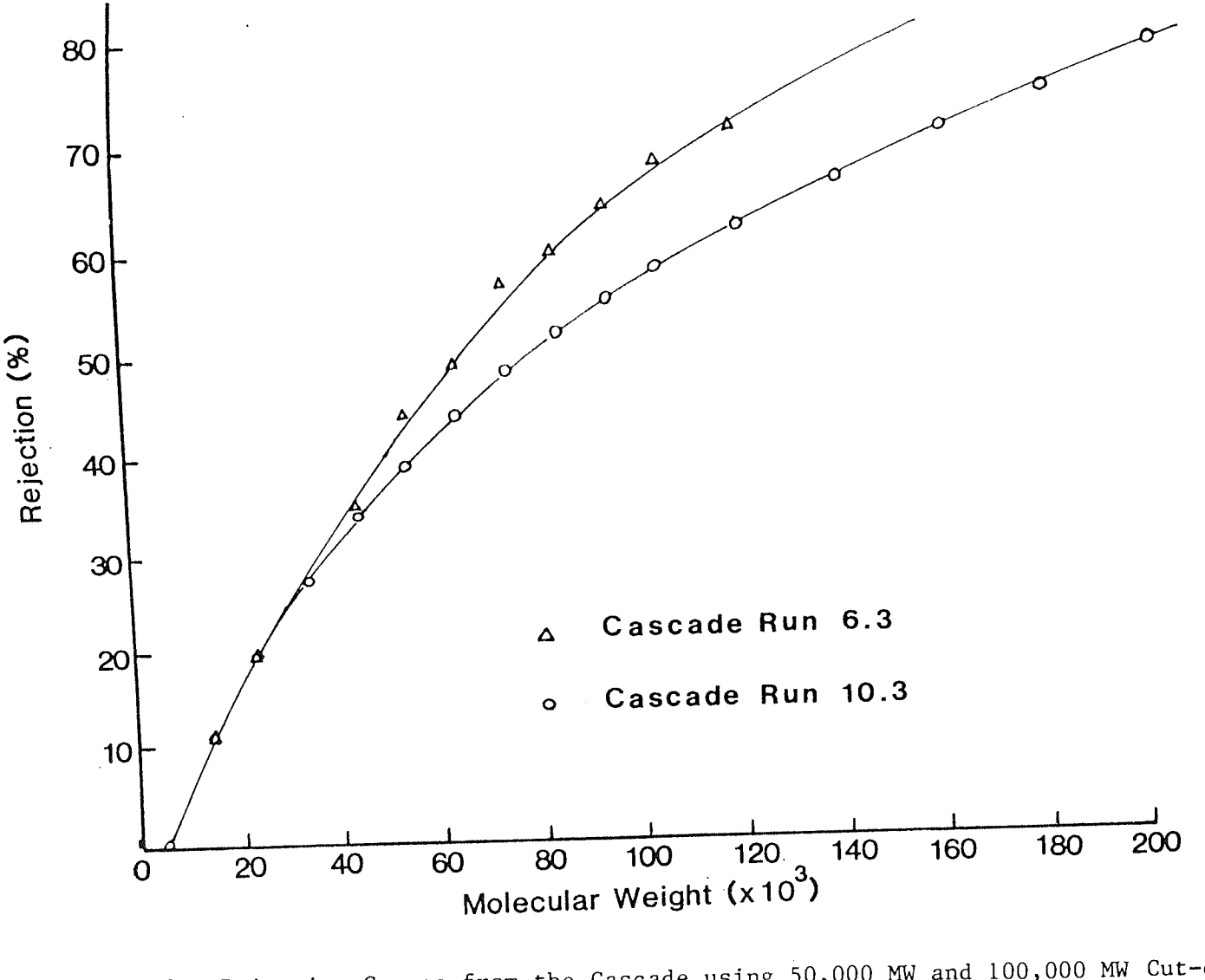

Figure 5.105 Rejection Curves from the Cascade using 50,000 MW and 100,000 MW Cut-off Membranes

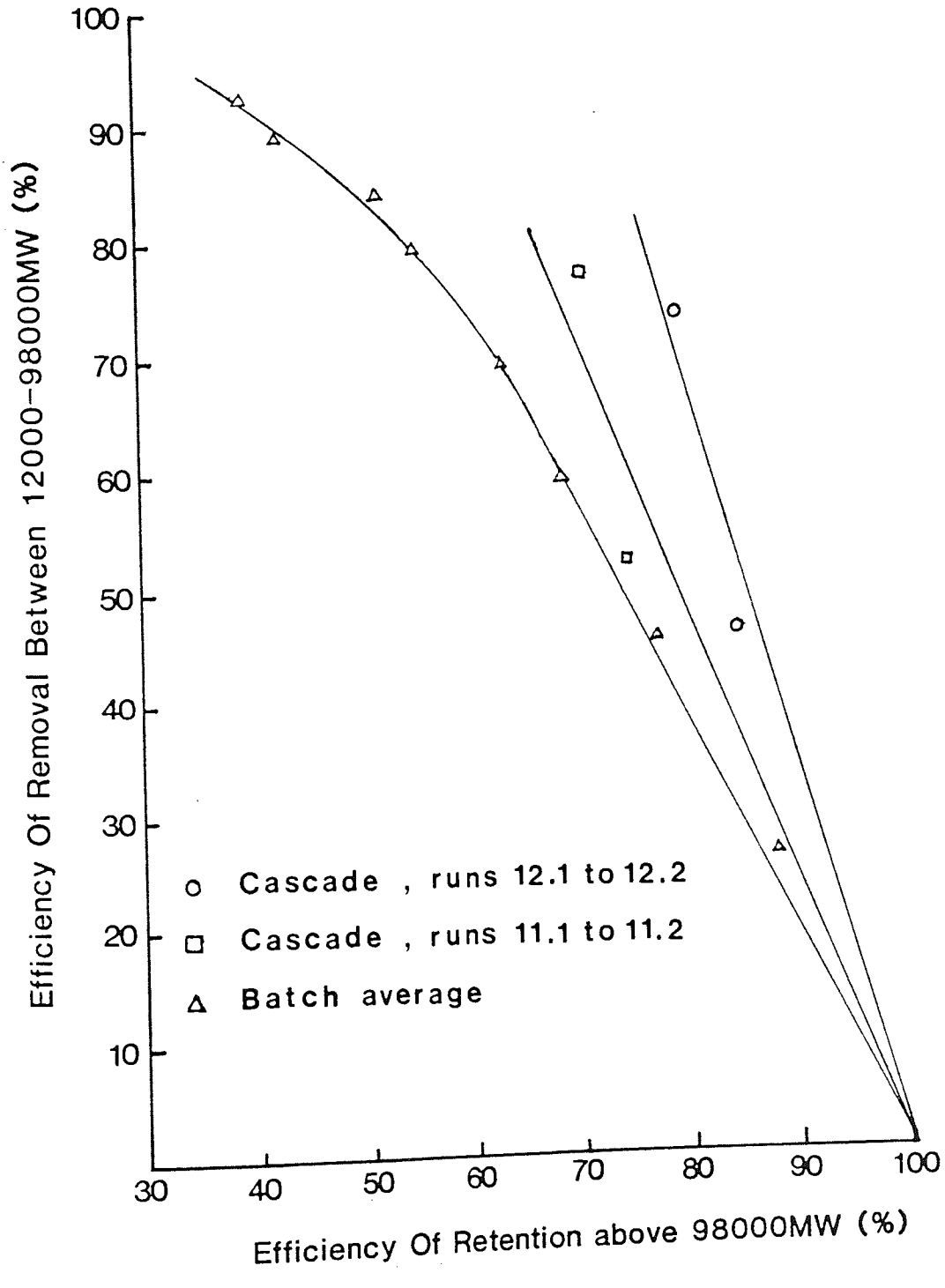

Figure 5.106 The Effect the Molecular Weight Distribution of the Feed has on the Performance of the Cascade

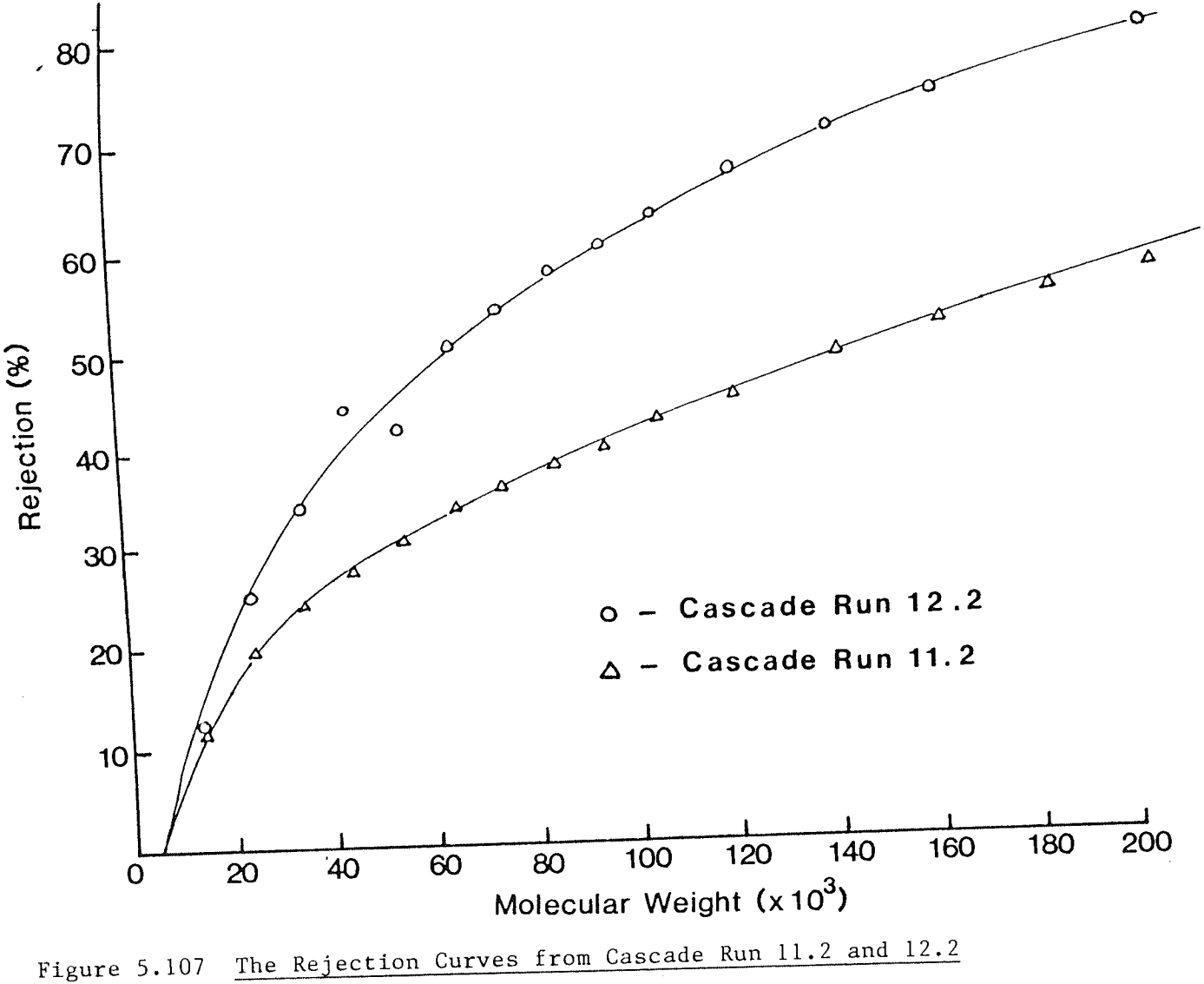

Figure 5.107 The Rejection Curves from Cascade Run 11.2 and 12.2

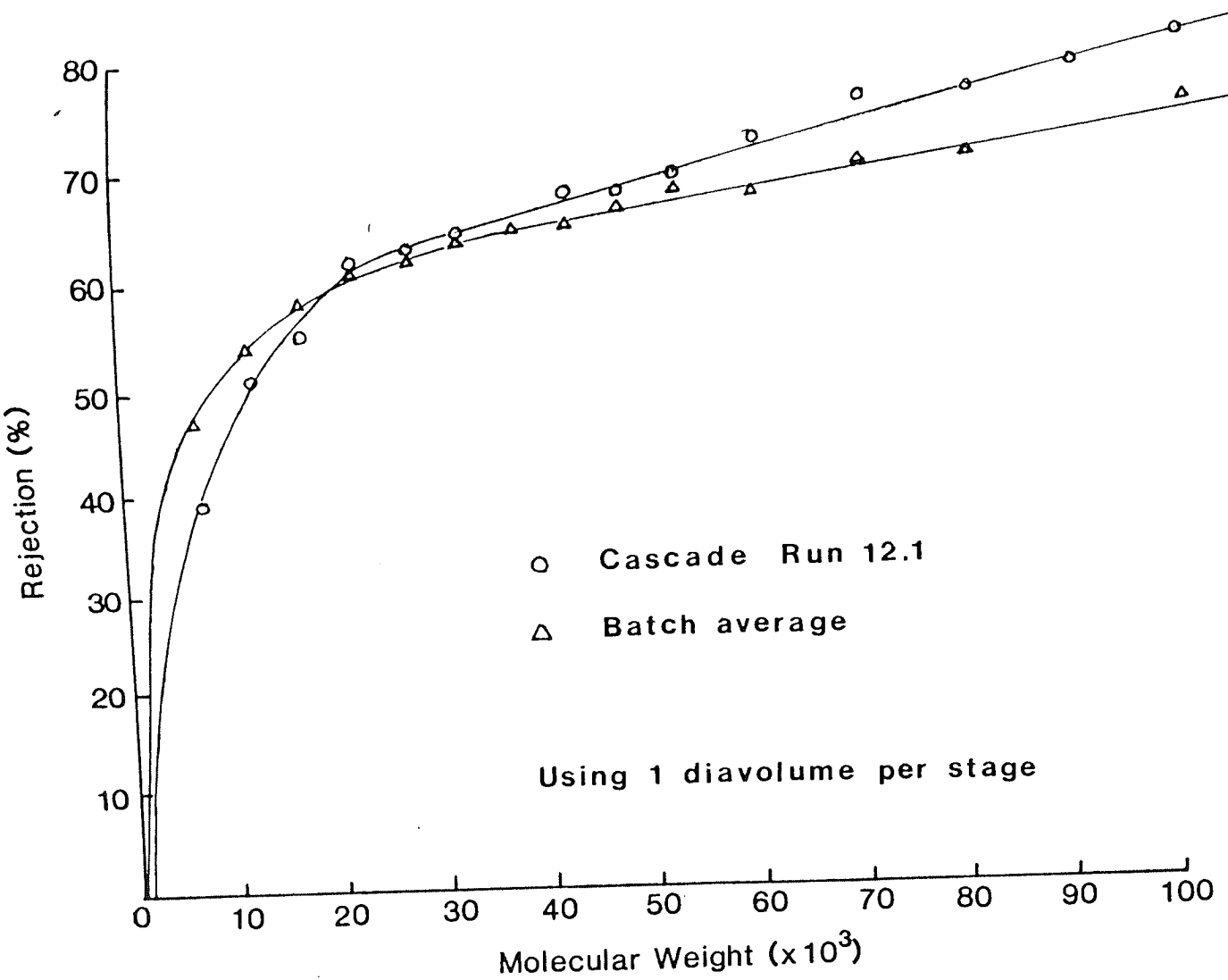

Figure 5.108 Rejection Curve from Cascade Run 12.1

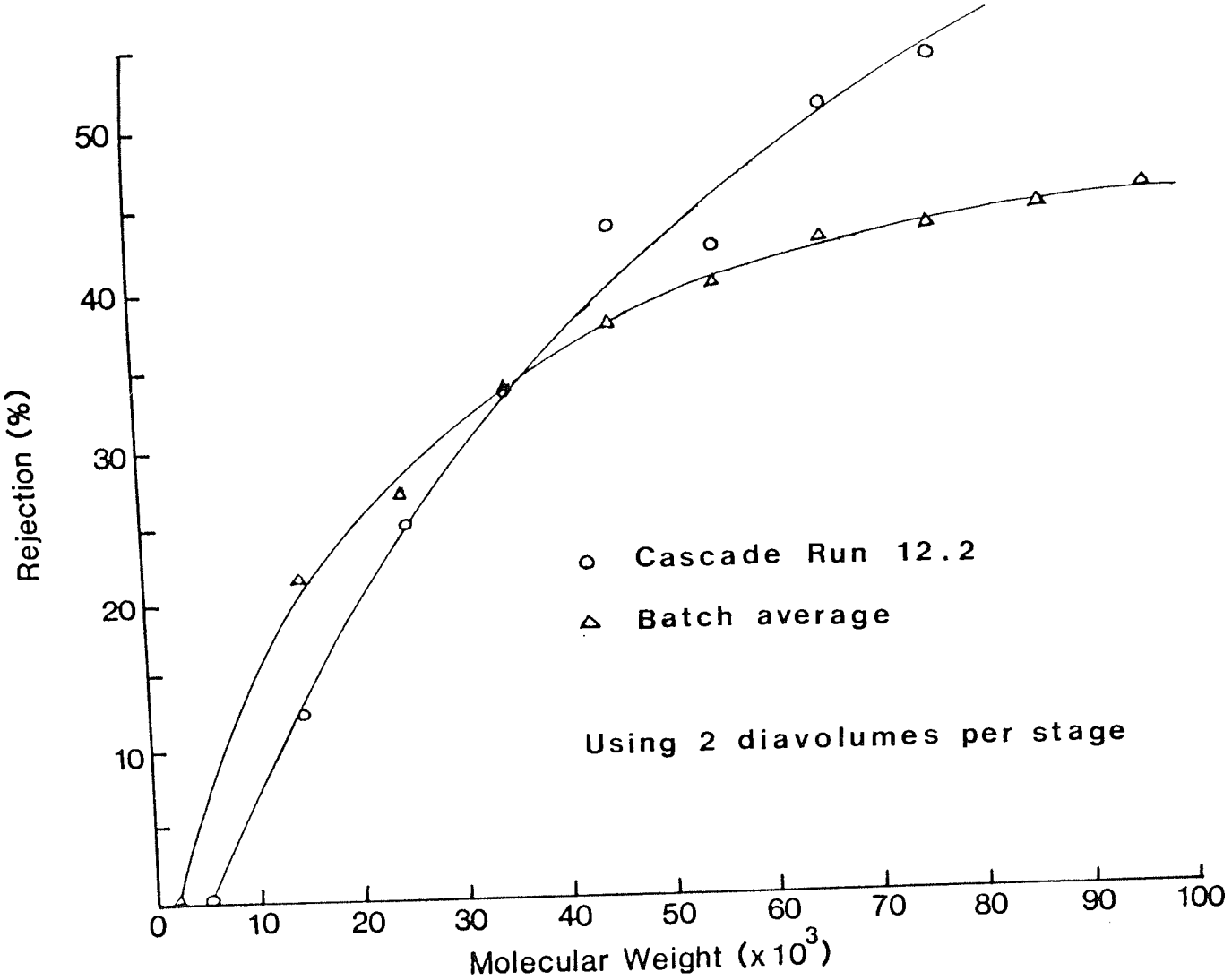

Figure 5.109 Rejection Curve from Cascade Run 12.2

5.5.7 COMPARING THE ULTRAFILTRATION CASCADE TO THE ETHANOL FRACTIONATION PROCESS

The comparison of the two processes was again made more difficult since the data obtained from the ethanol fractionation process included the removal of both the low and the high molecular weight dextran. Although the ultrafiltration process removed up to 96% of the high molecular weight material compared to only 84% for the ethanol fractionation process, the retention of the 12,000 MW to 98,000 MW band was only 74% compared to 78% for the ethanol process, see table 5.42. As mentioned earlier the separation of this material was inhibited by the low cross-over point which resulted in the material between 50,000 MW and 98,000 MW being retained by the action of the cascade rather than being removed in the permeate. Since a more suitable membrane could not be found to enhance the removal of the 12,000 MW to 98,000 MW band the ultrafiltration cascade was again unable to compete with the ethanol fractionation process on a purely economic basis.

A closer inspection of the ethanol precipitation results does however show some interesting points. This particular fractionation required four ethanol precipitation steps to obtain the final syrup products, this was one more than the previous example and the specification of the final product was significantly different. This suggests that the process was relatively unpredictable and a consistent product was difficult to achieve. The product from the ultrafiltration cascade in comparison was easier to control. For example the specification of the final product could be altered by a predictable amount by simply altering the number of diavolumes used.

The ethanol precipitation process appears to be very effective at removing the high molecular weight material, but both the results from this fractionation and the previous example suggests that this process was far less effective at removing material below 12,000 MW.

The conclusions for this particular fractionation must be the same as the earlier case. The main problem was again the difficulty obtaining membranes suitable for this fractionation. Both the Amicon and Romicon membranes were unsatisfactory simply because they retained too much of the 'saleable' band. If a range of membranes could be obtained with their rejection characteristics tailored to this process then these problems could be overcome.

Figure 5.110 Ethanol Fractionation Process used to Produce HZ1S Feed

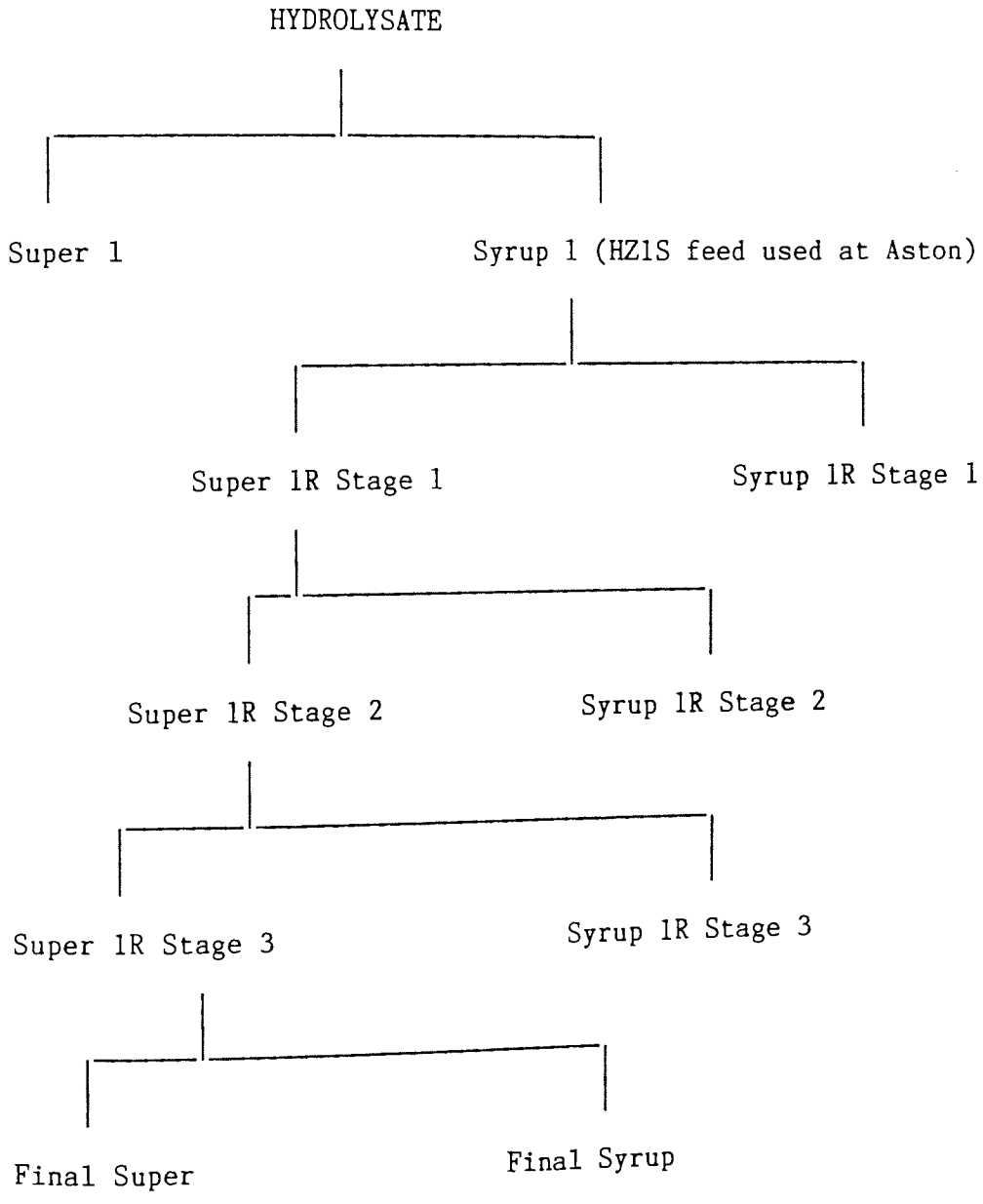

Table 5.42 Ethanol Precipitation Steps for HZ1Z Feed

Fractionation step	Mass in stage (Kg)	% below 12000 MW	Ethanol efficiency of removal	% between 12000 - 98000 MW	Ethanol efficiency of retention	% above 98000 MW	Ethanol efficiency of removal
Hydrolysate	2621	Distribution not available					
Super 1	386	Distribution not available					
Syrup 1	2067*	23.56	0	67.68	100	8.76	0
Super 1R ST1	1925	24.5	3.15	68.45	94.19	7.05	25.05
Super 1R ST1	142	10.81	-	57.24	-	31.94	-
Super 1R ST2	1683	24.91	13.91	71.37	85.86	3.72	65.42
Syrup 1R ST2	242	21.65	-	48.12	-	30.23	-
Super 1R ST3	1608	25.83	14.71	72.08	82.85	2.09	81.44
Syrup 1R ST3	75	5.19	-	56.14	-	38.67	-
Final Super	195	61.11	-	33.29	-	2.60	-
Final Syrup	1413	20.55	40.37	77.43	78.20	2.02	84.23

* 168 Kg sent to Aston leaving 2067 Kg

6.0 COMPUTER SIMULATION OF THE ULTRAFILTRATION CASCADE

6.0 COMPUTER SIMULATION OF THE ULTRAFILTRATION CASCADE

6.1 INTRODUCTION

Several worker [49, 6] have attempted to model the diafiltration cascade system. Cooper [49] for example developed a satisfactory model by solving a series of material balances over the cascade, although he made several important assumptions to simplify the solution of the problem. Cooper assumed that the product to be purified was completely rejected, the rejection characteristics of the membranes used were identical and that only two components were used. These assumptions were not acceptable when modelling the cascade development by Poland [6]. Poland purchased five 5000 MW cut-off membranes from Amicon and although they had identical quoted nominal molecular weight cut-off their individual performance varied significantly from each other. These membranes exhibited a mean rejection of 68% at 12,000 MW and only exceeded 90% rejection after 26,000 MW. Clearly the rejection of the 12,000 MW to 98,000 MW band which was equivalent to the product to be purified in Coopers model was not completely rejected. Finally the feed used in the cascade was a polymer with a wide molecular weight distribution which could not be expressed as a simple component.

The model developed by Poland was more satisfactory for this particular application, however he also made several assumptions which limited the effectiveness of his model. Poland split the dextran distribution into three bands, (a) material below 12,000 MW (b) material between 12,000 MW and 98,000 MW (c) material above 98,000 MW. He then obtained an average rejection for each of the three bands. For simplicity Poland then assumed that all the cascade stages contained identical membranes. Using this information Poland then used the 'Process' computer package (written by Simulation Sciences Inc) to solve

the mass balances involved. Although this model was able to predict broad trends such as number of stages required it was not satisfactory for the detailed examination required for this project. For this reason a new model was developed from first principles which overcame the limitations of the earlier models.

6.2 DETERMINATION OF MASS TRANSFER COEFFICIENTS AND GEL LAYER CONCENTRATIONS

The preliminary requirement was to determine the most satisfactory method of calculating the mass transfer coefficients for the membranes, for incorporation into the mathematical model. Probably the most well known method for determining the mass transfer coefficient of a membrane was that proposed by Porter [14] using mass transfer, heat transfer analogies for laminar and turbulent flow.

For laminar flow the Leveque [16] equation can be used:

$$Sh = 1.62\ (Re.Sc.\ d/L)^{0.333} \qquad \ldots 6.1$$

$$\text{for } 100 < Re\ Sc\ \frac{d}{L} < 5000$$

where Re is the Reynolds number, Sh is the Sherwood number, Sc the Schmitt number, L is the fibre length and d the fibre diameter while for the turbulent region:-

$$Sh = 0.023\ Sc^{0.33}\ Re^{0.8} \qquad \ldots 6.2$$

$$Re = \frac{\rho V d}{\mu} \qquad \ldots 6.3$$

$$Sc = \frac{\mu}{\rho D} \qquad \ldots 6.4$$

$$Sh = \frac{K\ d}{D} \qquad \ldots 6.5$$

where ρ is the density, μ the viscosity, D the diffusity, v the velocity, d the fibre diameter and K the mass transfer coefficient.

Since the dextran feed was fractionated in each of the four cascade stages its molecular weight distribution altered as it moved through the cascade, this in turn caused the physical properties of the solution to change and therefore the flux also changed. Although some empirical equations were found which related the molecular weight distribution to the physical properties of the dextran solution [108, 109] these required a precise knowledge of the M_W value for the sample and were also only available for the more commonly used properties such as osmotic pressure and viscosity. Therefore it became necessary to obtain the physical properties at a mean molecular weight distribution; this corresponded to a dextran T70 solution [19, 20, 110, 111].

To determine the flux the simple expression:

$$J = K\ In\ \frac{C_g}{C_B} \qquad \ldots 6.6$$

for a retentive membrane may be used.

The gel layer concentration (C_g) for dextran is dependent on a number of factors. Goldsmith [112] for example found that the gel layer concentration was dependent on the molecular weight distribution of the dextran sample. The higher the M_W value the higher the gel layer concentration. See figure 6.1. Furthermore other workers [110] have commented that the gel layer concentration was dependent on the conditions under which the membrane system was used. For these reasons it was necessary to determine the gel layer concentrations experimentally. Using simple theory a plot of J versus InC_g will give an intercept on the concentration axis of C_g and a gradient of K. The results for the 5000 MW, 10,000 MW and 100,000 MW cut-off Amicon membranes and the Romicon 50,000 MW membranes can be found in figures 6.2 to 6.5. The results strongly suggest that the gel layer concentration increases as the nominal molecular weight cut-off of the membrane used increases. See figure 6.6. This fits in well with the results obtained by Goldsmith. Increasing the nominal molecular weight cut-off will result in the gel layer being almost exclusively made up from dextran molecules with a molecular weight above the nominal cut-off since a high proportion of the lower molecular weight material will pass through the membrane. Goldsmith found that increasing the M_W value of the sample used resulted in a higher gel layer concentration hence in both cases the high molecular weight material present at the membrane wall resulted in a higher gel layer concentration. The gel layer concentrations determined for the mathematical model were comparable to those obtained by Vlachogiannis [45] using similar Amicon membranes and process conditions.

The effect of operating pressure on the flux of each of these membranes was also determined at the normal recirculation rate used with these membranes. For the Amicon 5000 MW and 10,000 MW cut-off membranes this was 300 cm^3/min while for the 100,000 MW cut-off membrane this was

500 cm^3/min, and for the Romicon 50,000 MW cut-off membrane this was 1 litre/min. The results can be found in figures 6.7 to 6.10. All three Amicon membranes exhibit the same trends. Below 70 KPa they all exhibit some pressure dependance, however at higher pressures all but the most dilute solution of 0.5% W/W were pressure independant. This therefore suggested that at these particular recirculation rates the gel layer started to form at concentrations as low as 1%. The Romicon membrane showed a different profile, the pressure independant region occurred at higher pressures than the Amicon membranes in all cases except the 4% W/W solution. This difference between the two types of membrane can be directly attributed to the higher recirculation rate which would remove material from the membrane wall and hence reduce the degree of concentration polarization present.

Normally reasonable agreement could be obtained between the experimentally determined flux and that determined expirically. However when using the empirical calculations the value of the mass transfer coefficient was found to increase slightly as the concentration increased, this resulted in a slight curve rather than the normal linear relationship. This error was however small and could be ignored. Although the physical property data was obtained from well known publications [19, 20, 110, 111] this error was most likely caused by inaccuracies in this data. Porter commented that only small errors in the physical property data would cause relatively large errors in the calculated mass transfer coefficient.

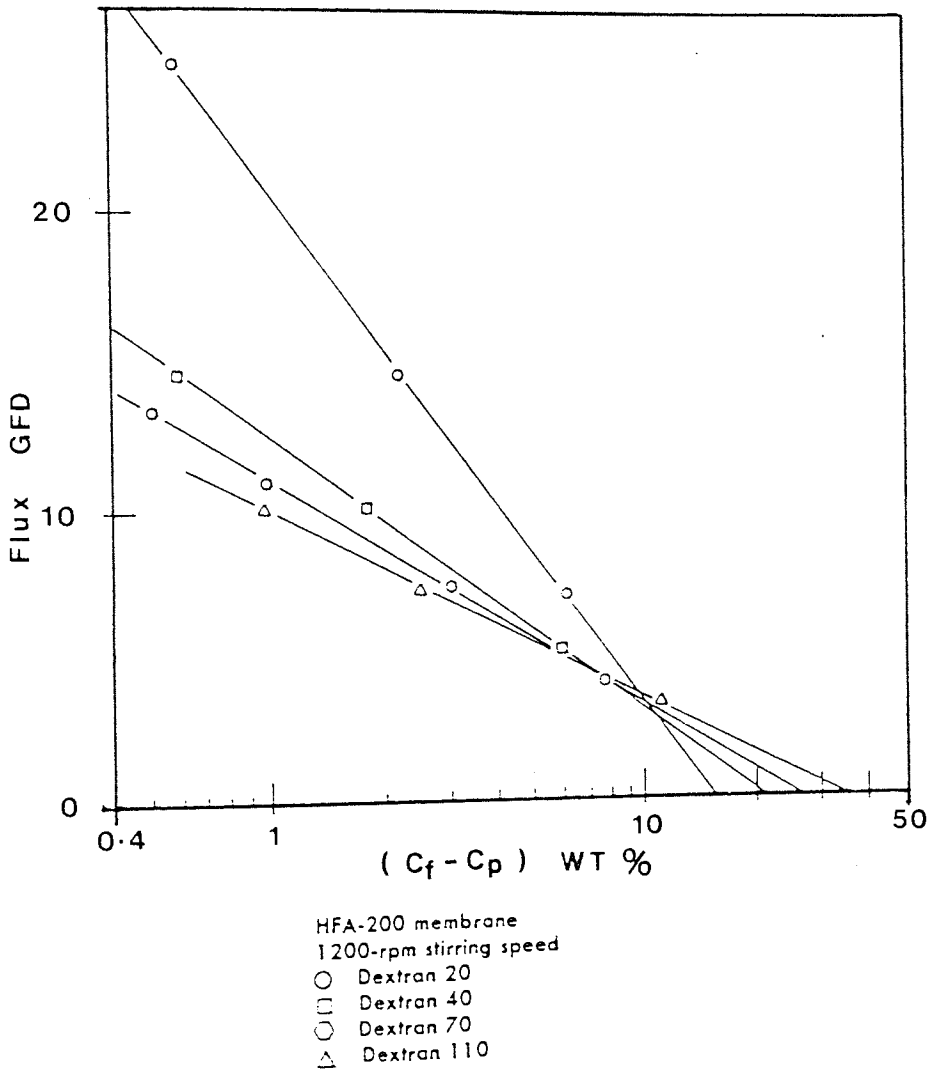

Figure 6.1 Effect of Dextran Molecular Weight Distribution on the Gel Layer Concentration (112)

Figure 6.2 Determining the Gel Layer Concentration for the 5000 MW Cut-off Membrane

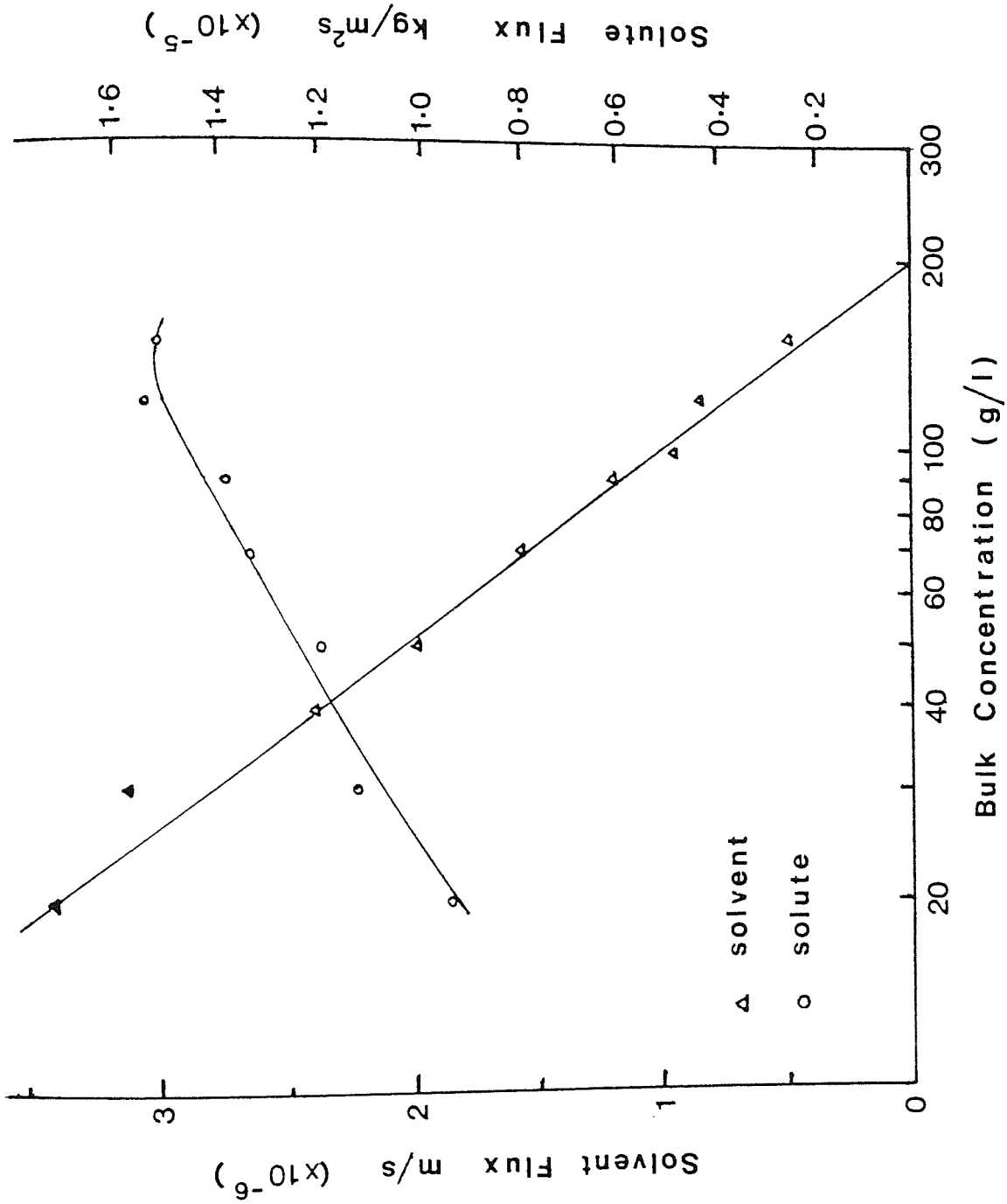

Figure 6.3 Determining the Gel Layer Concentration for the 10,000 MW Cut-off Membrane

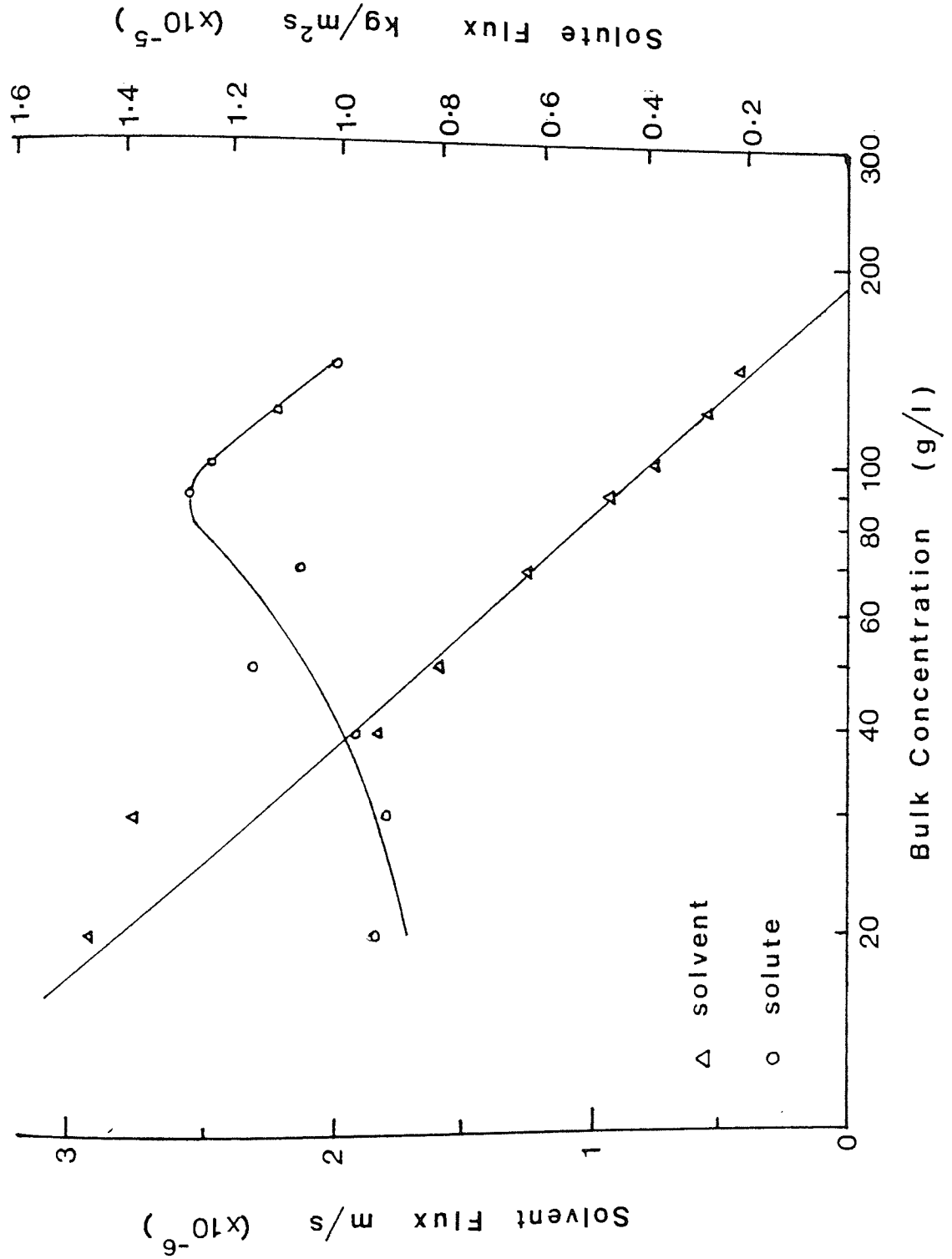

Figure 6.4 Determining the Gel Layer Concentration for the 50,000 MW Cut-off Membrane

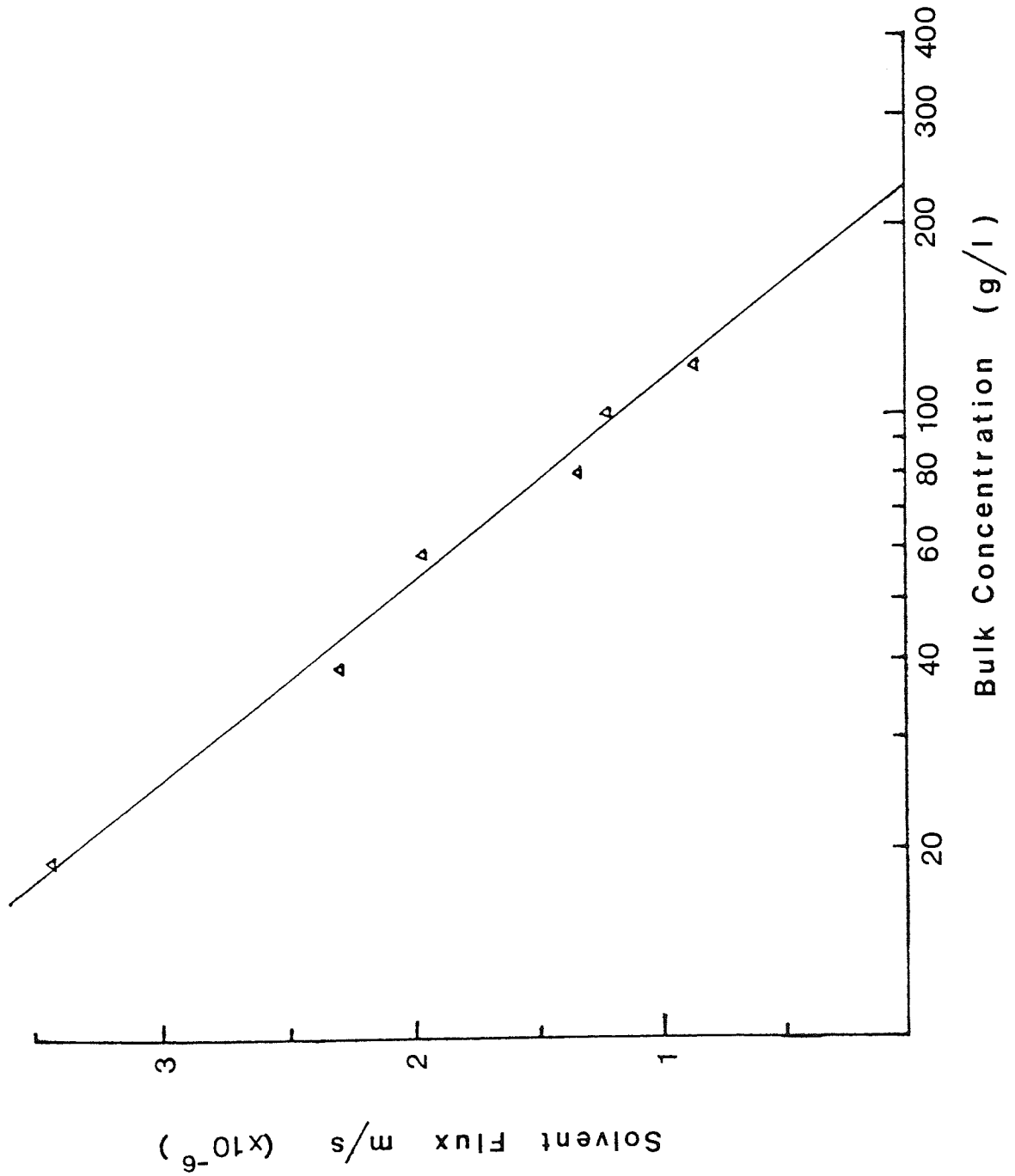

Figure 6.5 Determining the Gel Layer Concentration for the 100,000 MW Cut-off Membrane

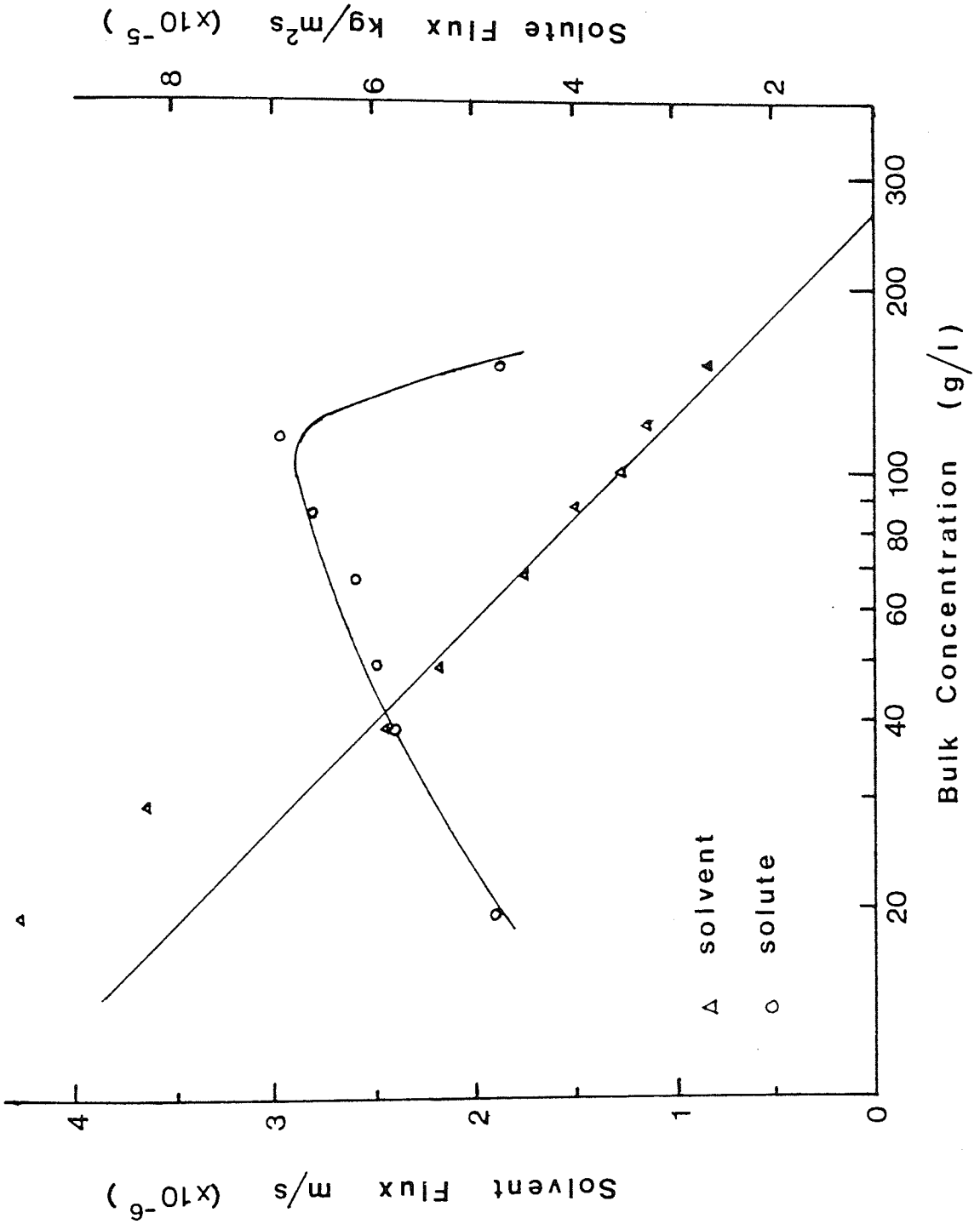

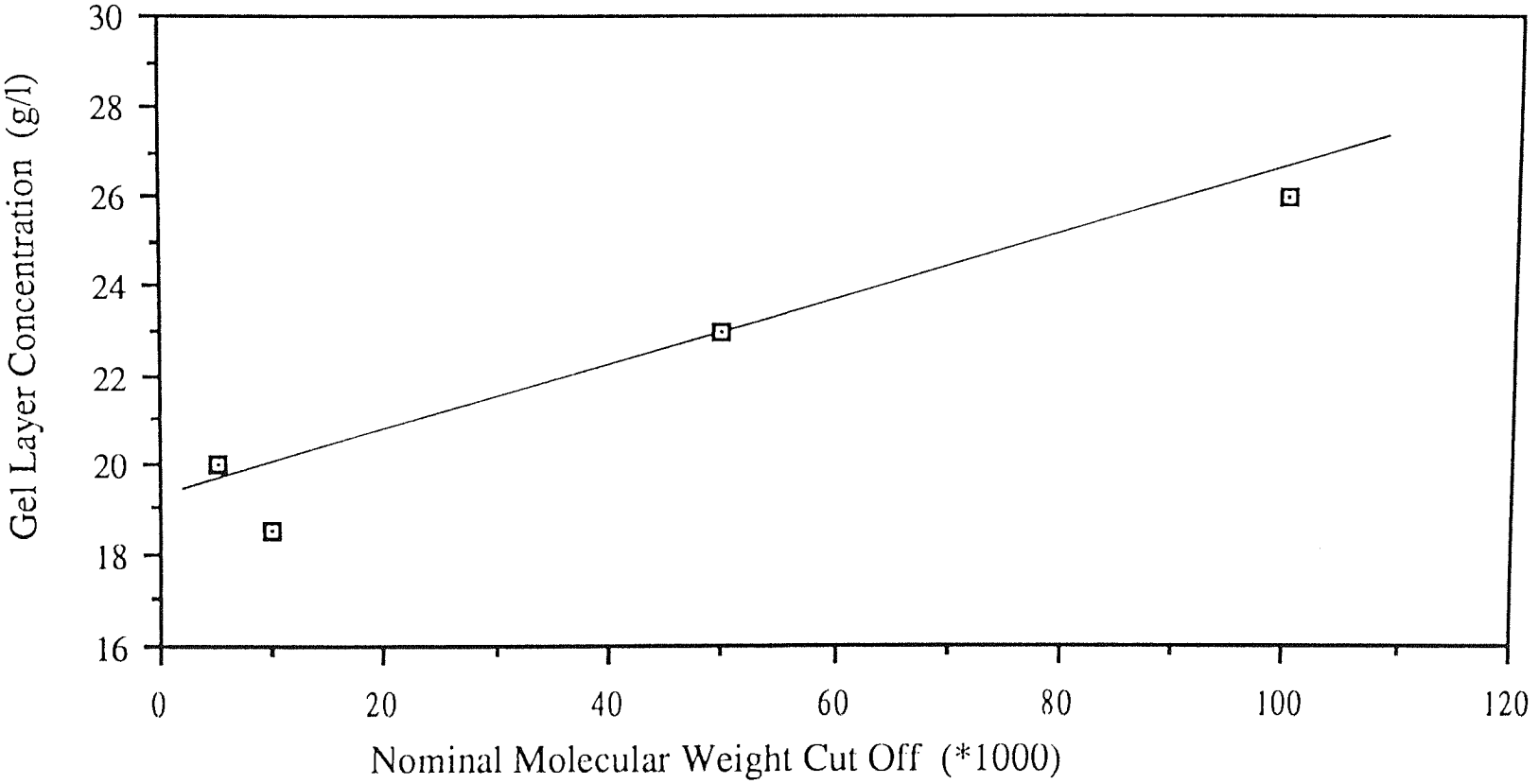

Figure 6.6 The Effect of Molecular Weight Cut-off of the Membrane on the Gel Layer Concentration

Figure 6.7 The Relationship between Flux and Pressure for the 5000 MW Cut-off Membrane Number 5

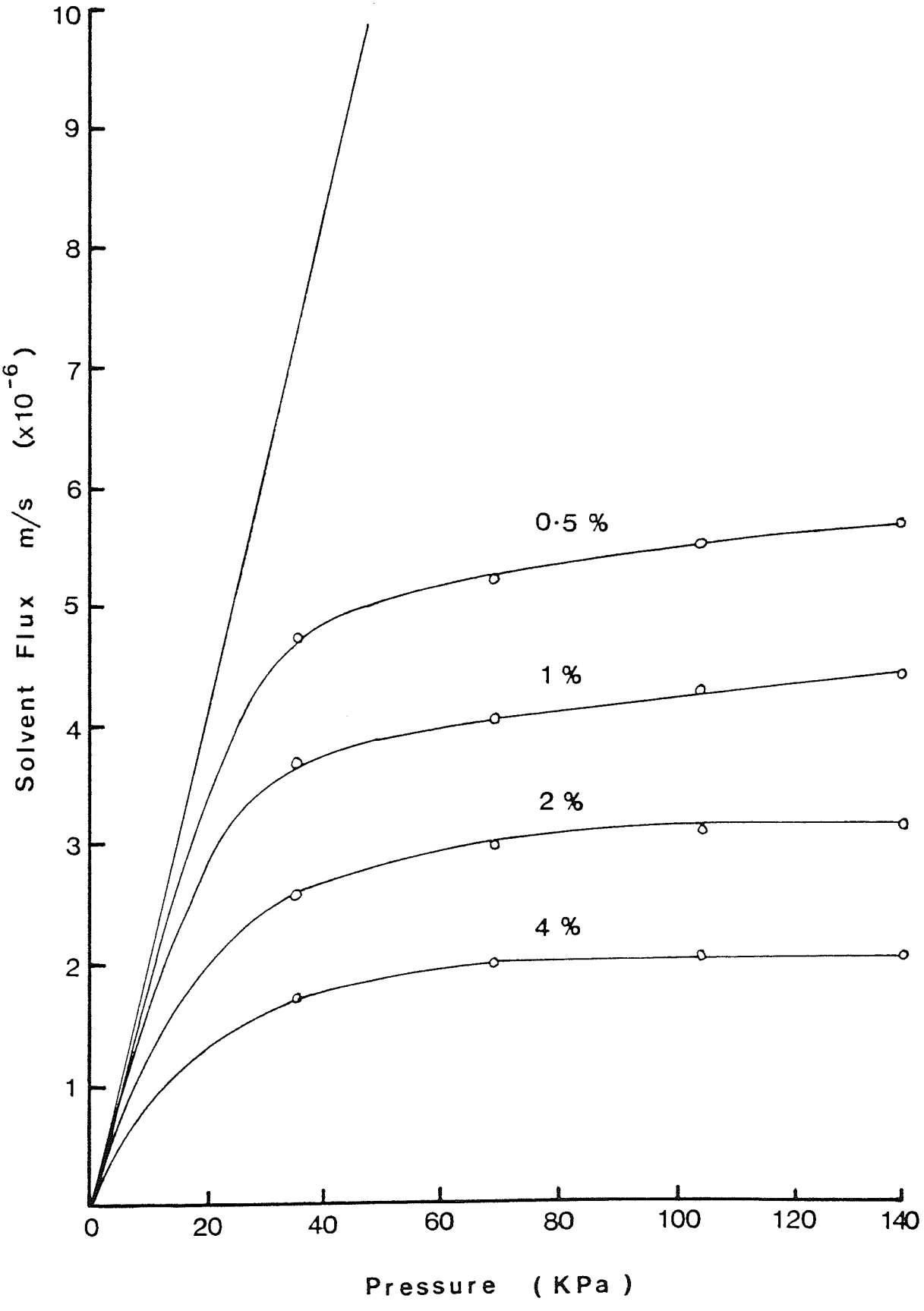

Figure 6.8 The Relationship between Flux and Pressure for the 10,000 MW Cut-off Membrane Number 5

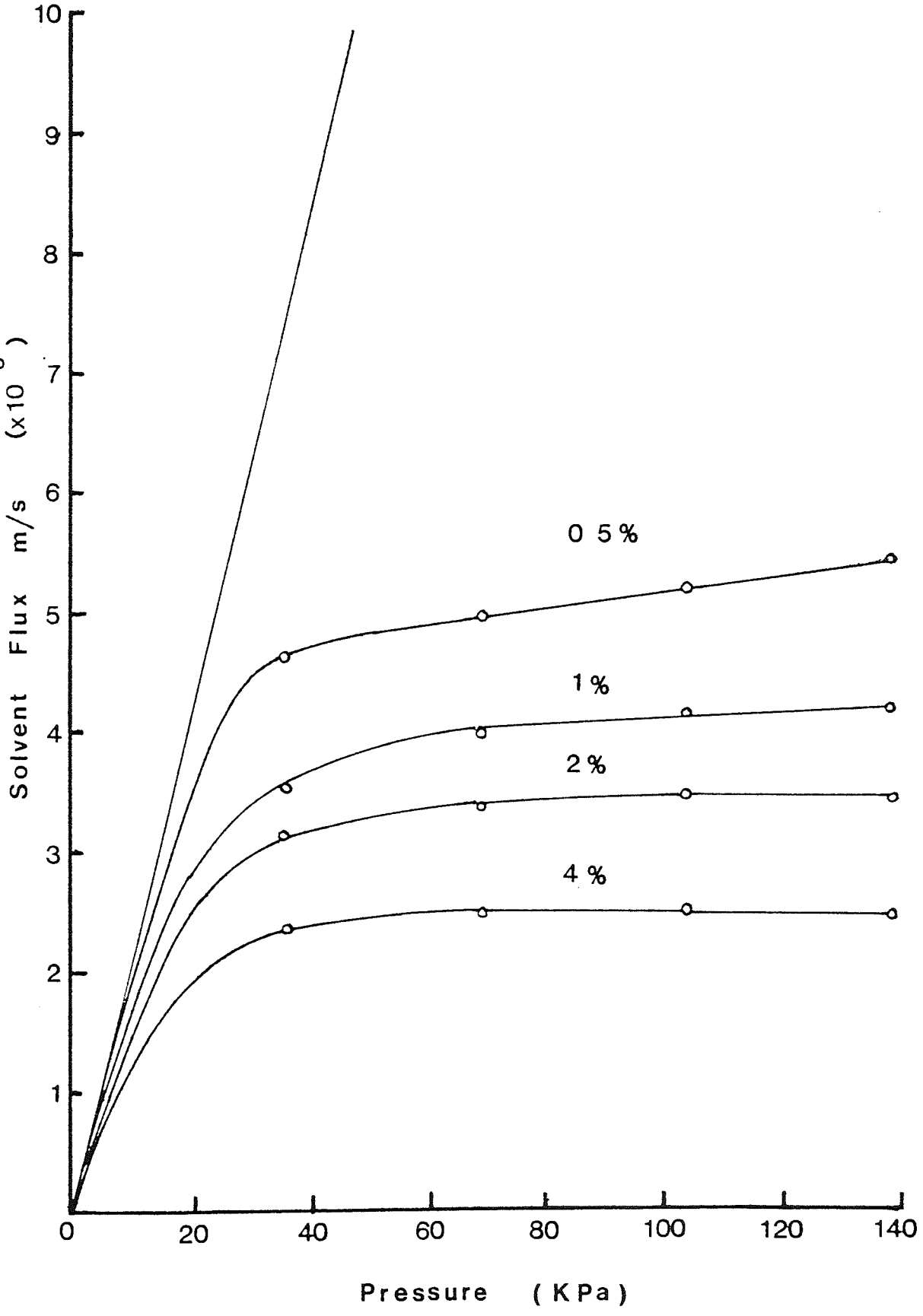

Figure 6.9 The Relationship between Flux and Pressure for the 100,000 MW Cut-off Membrane Number 1

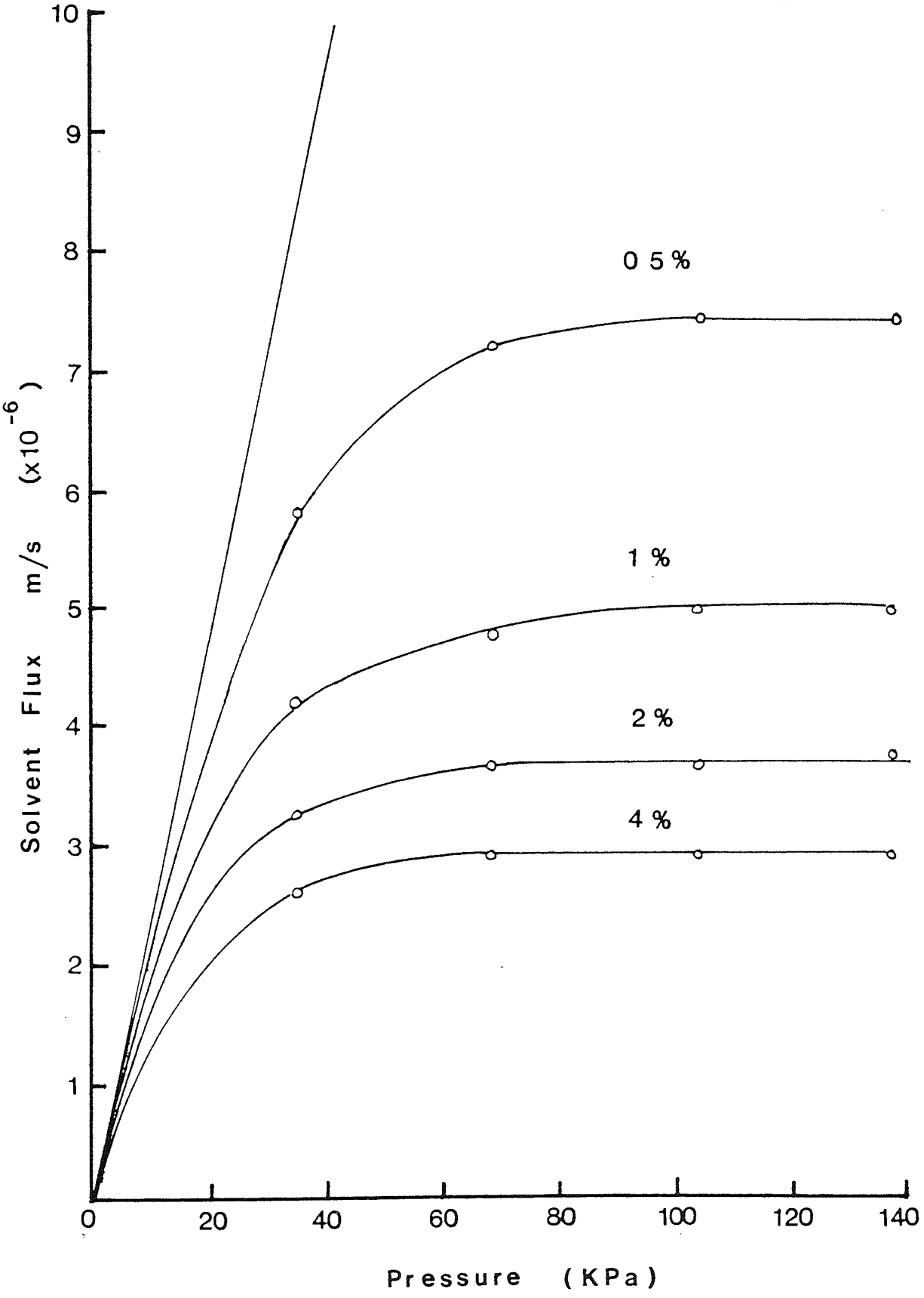

Figure 6.10 The Relationship between Flux and Pressure for the 50,000 MW Cut-off Membrane Number 1

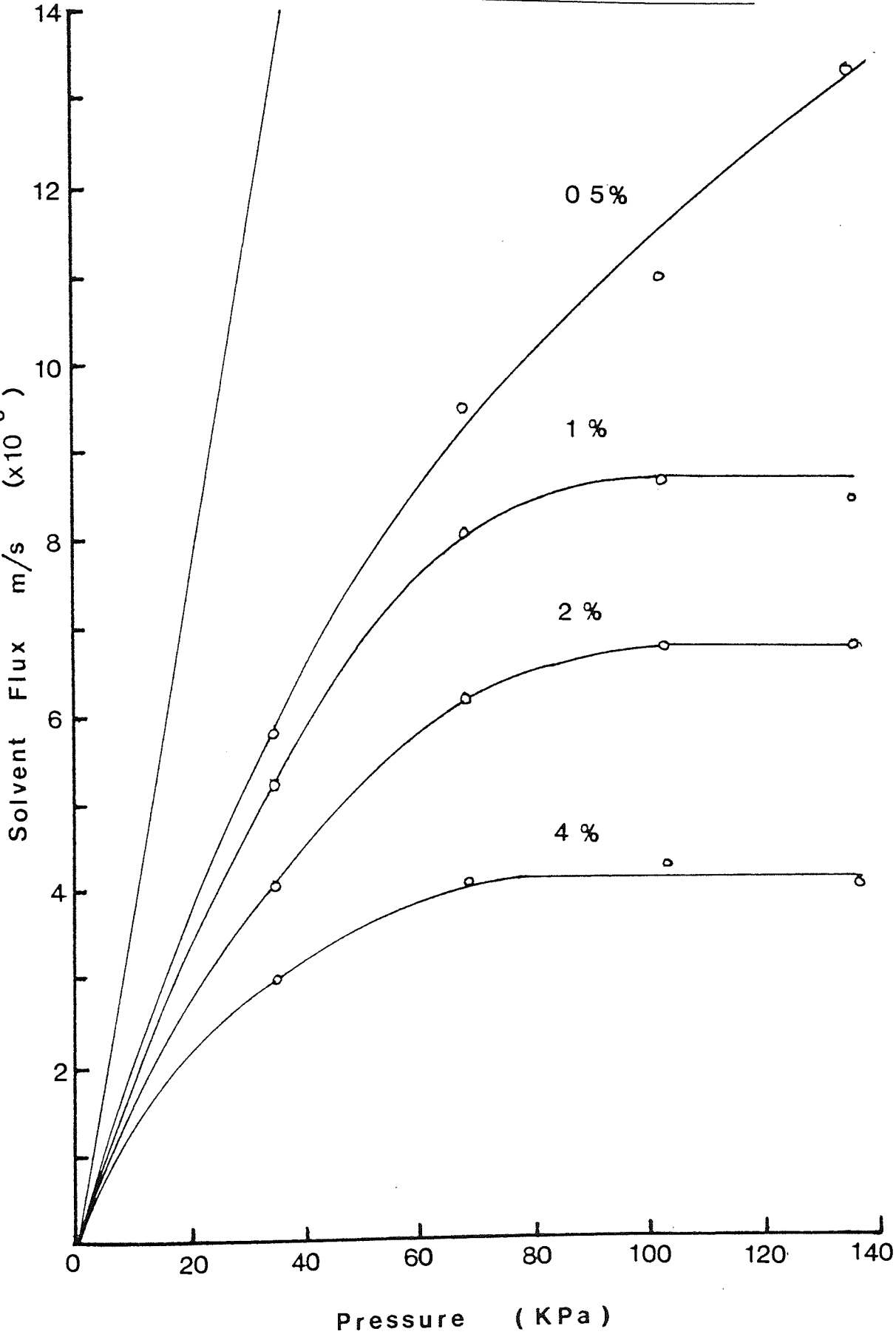

6.3 SOLVING THE MASS BALANCE OVER A CASCADE STAGE

The development of the model was simplified because each of the four cascade stages could be considered to be independent for the purpose of developing the mass balance. This was possible since transfer of material between each stage occurred only at the end of each cycle and the composition of the products, the retentate and permeate could be calculated from a mass balance over the stage from which they originated.

An unsteady state mass balance over stage N was developed. See figure 6.11. The mass balance was particularly simple since there was only one stream into the system and one leaving. The input stream was the flow of diafiltrate. This stream contained dextan lost in the permeate from stage N+1. The composition of this stream was assumed to be fixed, ie. did not change as the level in the diafiltration tank dropped. This would be true in the real system since the solution would be well mixed. The only output stream was the permeate flow through the membrane. Finally the flow rate of the diafiltrate must equal the flow rate of permeate if the volume in the tank is to remain constant.

The mass balance gives:

$$C_{Di}F_D - C_{Pi}F_P = V \frac{dC_{ti}}{dt} \qquad \ldots 6.7$$

where C_{Di} is the concentration of component i in the diafiltrate, C_{Pi} the concentration of component, i in the permeate; C_{ti} the concentration of component i leaving the tank, V is the volume of the tank, F_D and F_P are the flow rates into and out of the system.

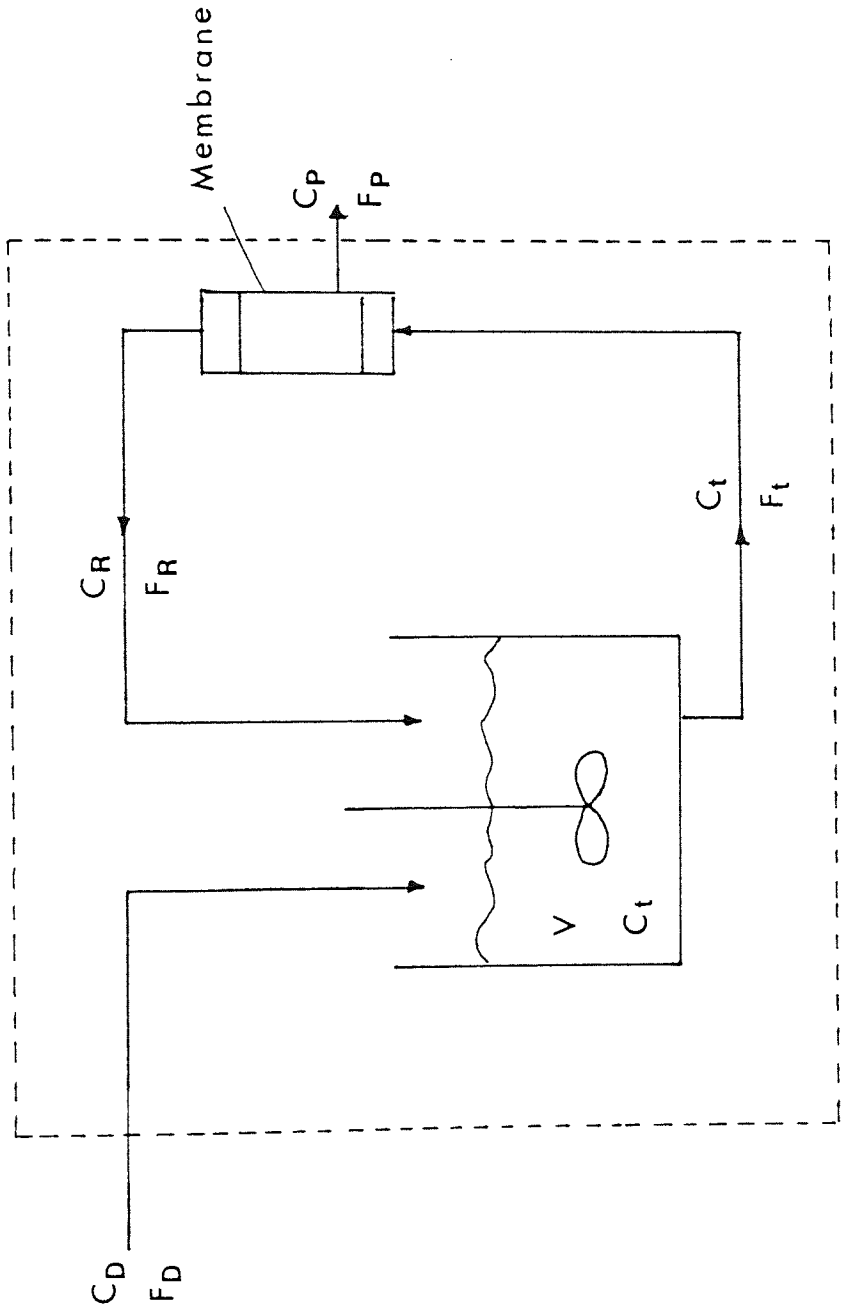

Figure 6.11 Boundary Conditions used for the Mathematical Model

For simplicity the rejection of the membrane was assumed to be constant, ie. would not change with composition:-

$$R = \frac{F_R\ C_{Ri}}{F_t\ C_{ti}} \qquad \ldots 6.8$$

$$\text{or} \quad R = \left| - \frac{C_{Pi}\ F_P}{C_{ti}\ F_t} \right. \qquad \ldots 6.9$$

The rejection was defined in this form since the experimental batch rejection data could be simply incorporated into the model. The validity of this will be discussed in more detail later.

Equations 6.7 and 6.9 can be combined to give:-

$$C_{Di}F_D + (R-1)\ F_t\ C_{ti} = V\ \frac{dC_{ti}}{d_t} \qquad \ldots 6.10$$

This equation can be solved using Laplace transforms to give:

$$C_{ti} = \frac{C_{Di}(F_t - F_R)}{(F_t - F_t\ R)} \left(1 - EXP\left(\frac{-\ (F_t - F_t R)\ t}{V} \right) \right)$$

$$+ C_{oi}\ \ EXP\ \left(- \frac{(F_t - F_t\ R)\ \ t}{V} \right) \qquad \ldots 6.11$$

but $F_t - F_R = F_p = F_D$

therefore

$$C_{ti} = \frac{C_{Di}\ F_D}{F_t\ (1-R)} \left(1 - \text{EXP} \left(\frac{-\ F_t\ (1 - R)\ t}{V} \right) \right)$$

$$+ C_{oi} \quad \text{EXP} \left(\frac{-\ F_t\ (1-R)\ t}{V} \right) \qquad \ldots 6.12$$

where C_{oi} is the initial concentration in the tank.

This expression was satisfactory until the values of R reached a value of one (100% rejection) or very close to one. To overcome this minor problem the incorporation of a power series expansion of e^{-t} was considered, this would allow the expression to be rearranged.

where $$e^{-t} = 1 - t + \frac{t^2}{2!} - \frac{t^3}{3!} \quad \ldots\ \frac{t^n}{n!} \qquad \ldots 6.13$$

Although the expression was easily incorporated into the model, when the model was tested the model still failed to work correctly. This error was caused because the power series did not converge correctly when t became greater than one. This problem occurred when the value of R became close to 1.0, so there was little to gain by using the power series expansion.

To overcome this problem the mass balance was redefined for the case where R = 1.0 since C_{pi} will be zero:-

$$F_D C_{Di} = V \frac{dC_{ti}}{dt} \qquad \ldots 6.14$$

This can again be solved using Laplace transforms to give:

$$C_{ti} = \frac{C_{Di} F_D}{V} t + C_{oi} \qquad \ldots 6.15$$

Equations 6.12 and 6.15 can be used to determine the concentration changes in the retentate tank.

6.4 OBTAINING REJECTION DATA FOR THE MODEL

Using a steric rejection model Zeman [31] was able to successfully predict the rejection of dextran molecules by a membrane. Although this model could correctly predict the rejection, it was most accurate under ideal conditions, ie. no concentration polarization and with a membrane with a uniform pore distribution. Because the cascade operated under conditions which were far from ideal this particular model and the others discussed in section 2 were of little use. It was mentioned in section 5.0 that each membrane used had its own unique rejection characteristics. Since the aim of the work was to predict the specification of the product from the experimental cascade it was important to include this variation within the model.

To obtain sufficiently accurate rejection data for the model it was necessary to use the batch rejection data obtained when each of the membranes were originally tested.

Since the model was to be used to predict how the number of diavolumes would effect the specification of the product the rejection data was obtained over a wide range of diavolumes. Normally the rejection would be calculated by comparing the mass of dextran in the feed solution to that in the retentate product at a particular diavolume, however for use in this model the rejection was considered incrementally. For example the incremental rejection of the membrane at two diavolumes was calculated using the retentate product after one diavolume as if it were the feed and this was compared to the retentate product after two diavolumes. Interestingly when this approach was used the rejection curves obtained remained relatively stable over the range of diavolumes considered. The incremental rejection curves from the 10,000 MW cut-off membrane number five can be found in figure 6.12 This suggested that it was probable that a constant sieving factor was involved when these membranes were used in this simple batch diafiltration mode.

The rejection curves for all the 5000 MW, 10,000 MW and 50,000 MW cut-off membranes used in the cascade were calculated in the manner mentioned above and the data incorporated into the computer program. Since both the rejection data and the molecular weight distribution of the dextran feed were continuous functions, not fixed values as in Coopers model [49] the data was fitted to a series of three term polynominal equations which covered the whole molecular weight range being considered.

Figure 6.12 Calculating the Mean Rejection for the 10,000 MW Cut-off Membrane Number 5

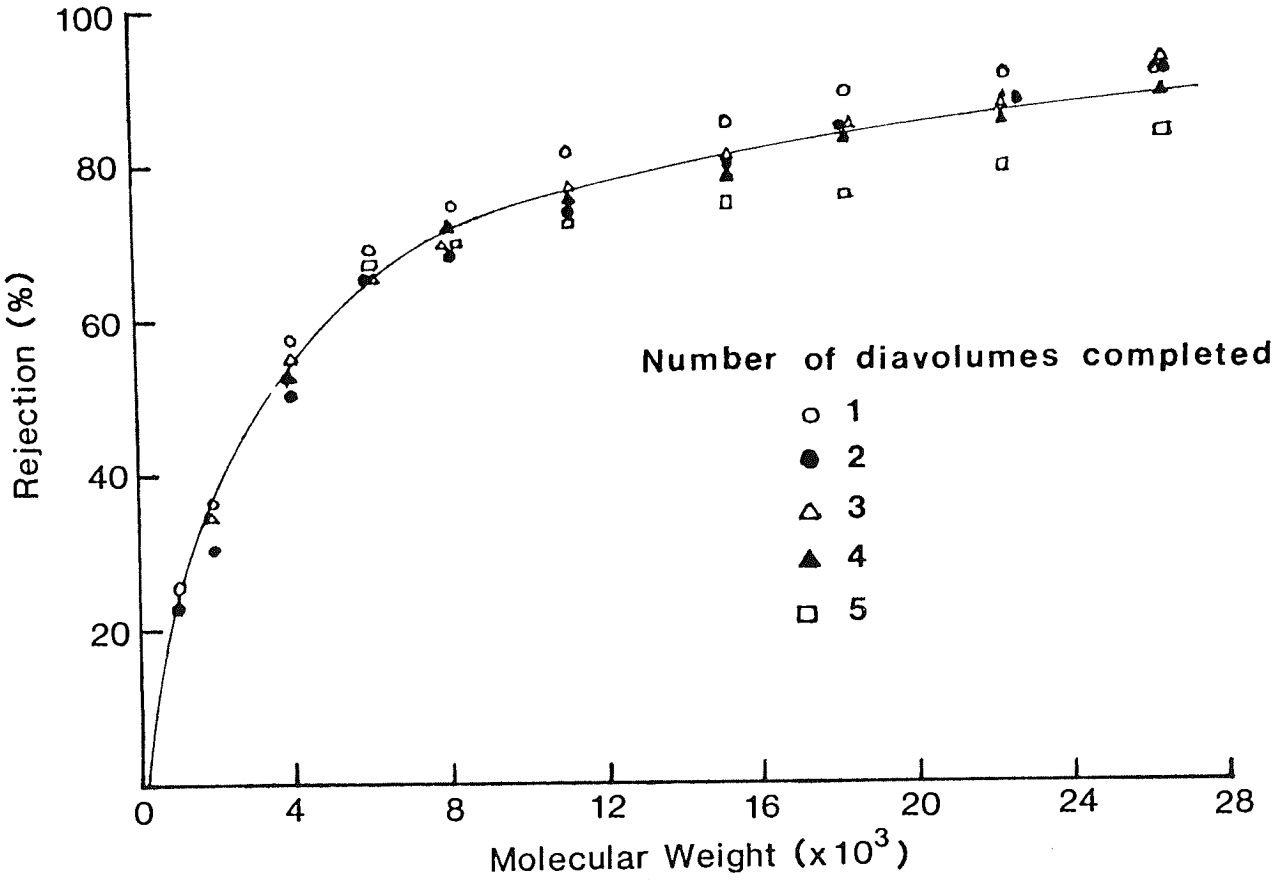

Figure 6.13 Model Prediction for 5000 MW Cut-off membrane Number 5

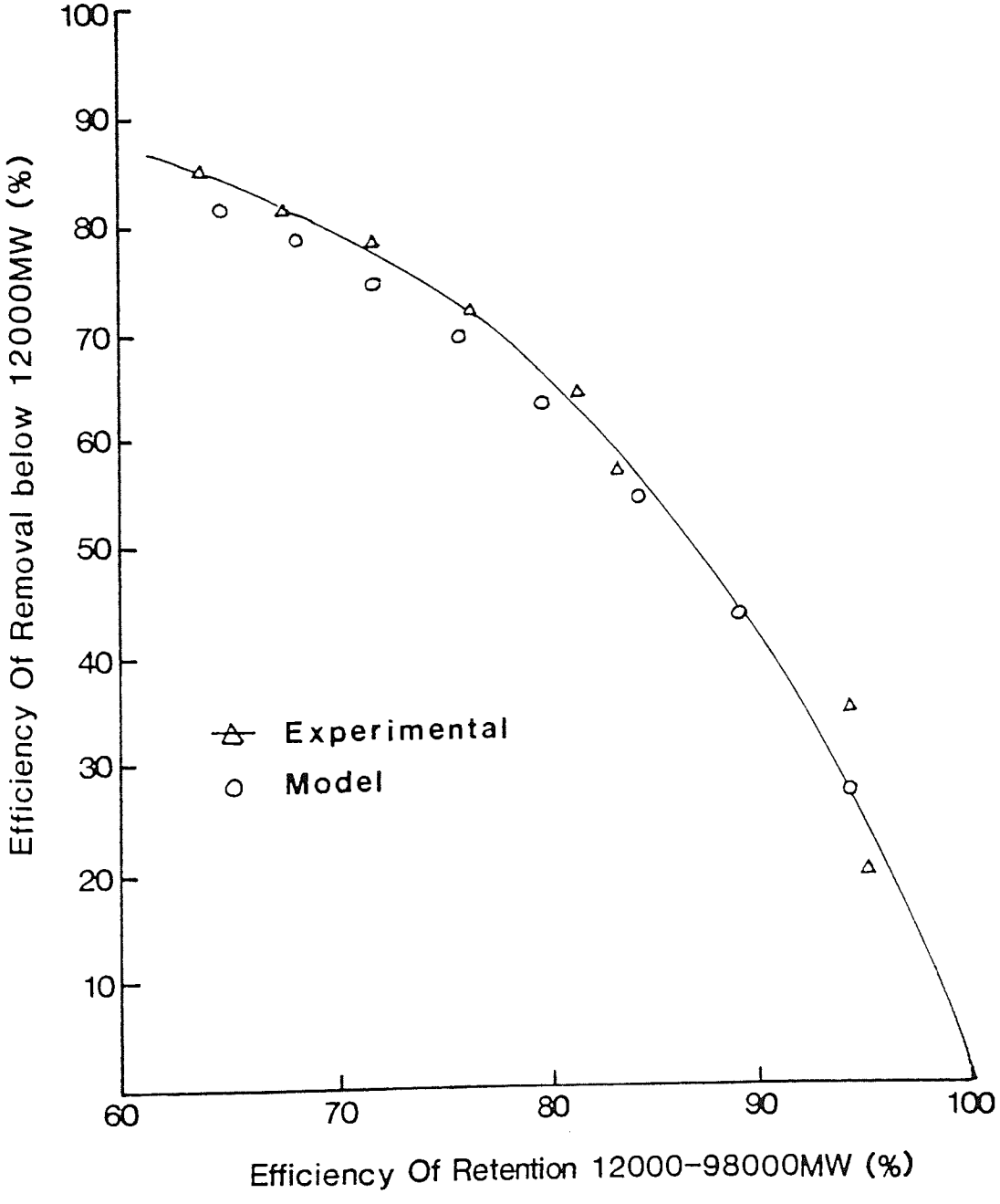

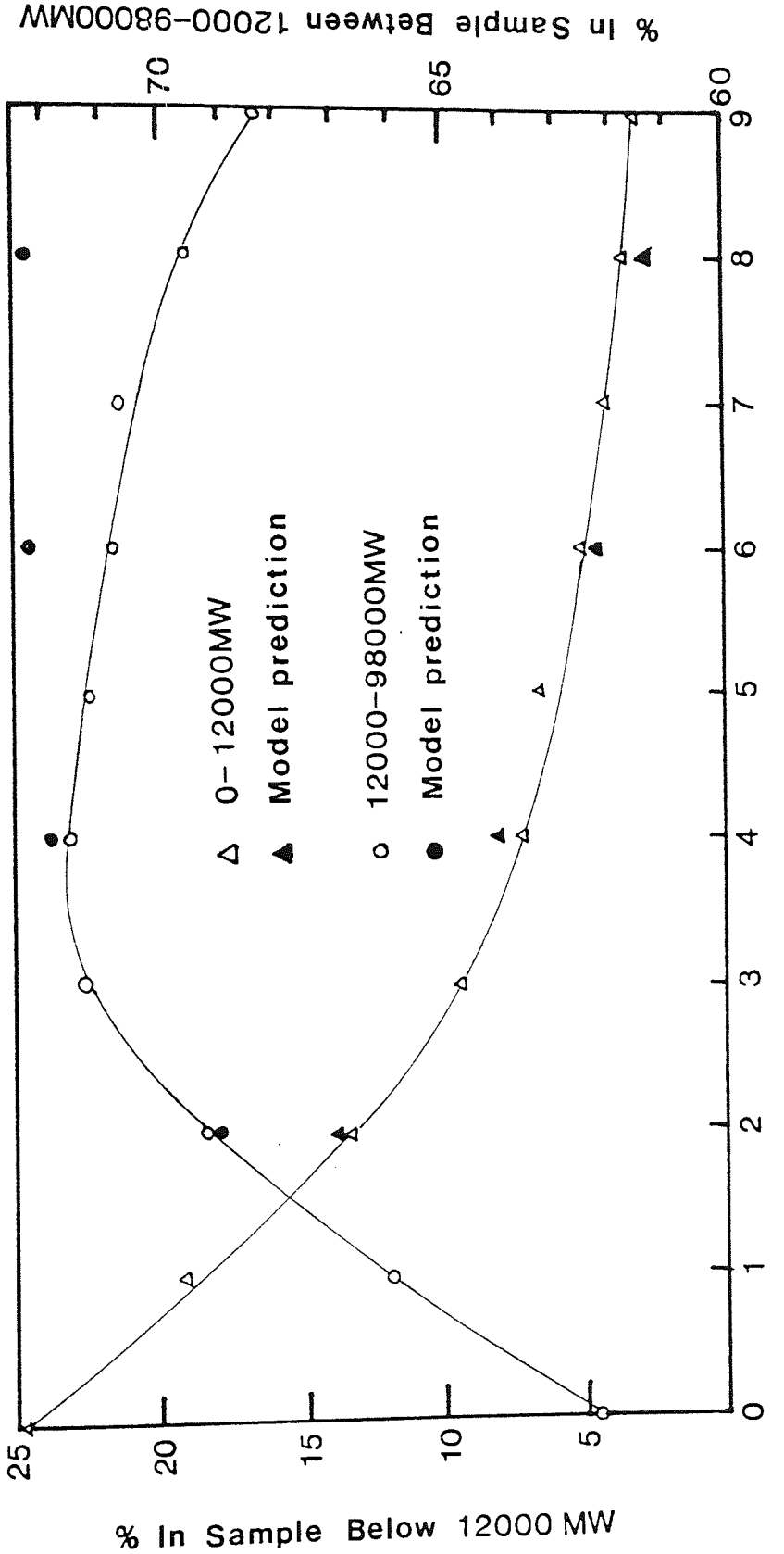

Figure 6.14 Model Prediction showing Changes in the Molecular Weight Distribution. 10,000 MW Cut-off Membrane Number 5

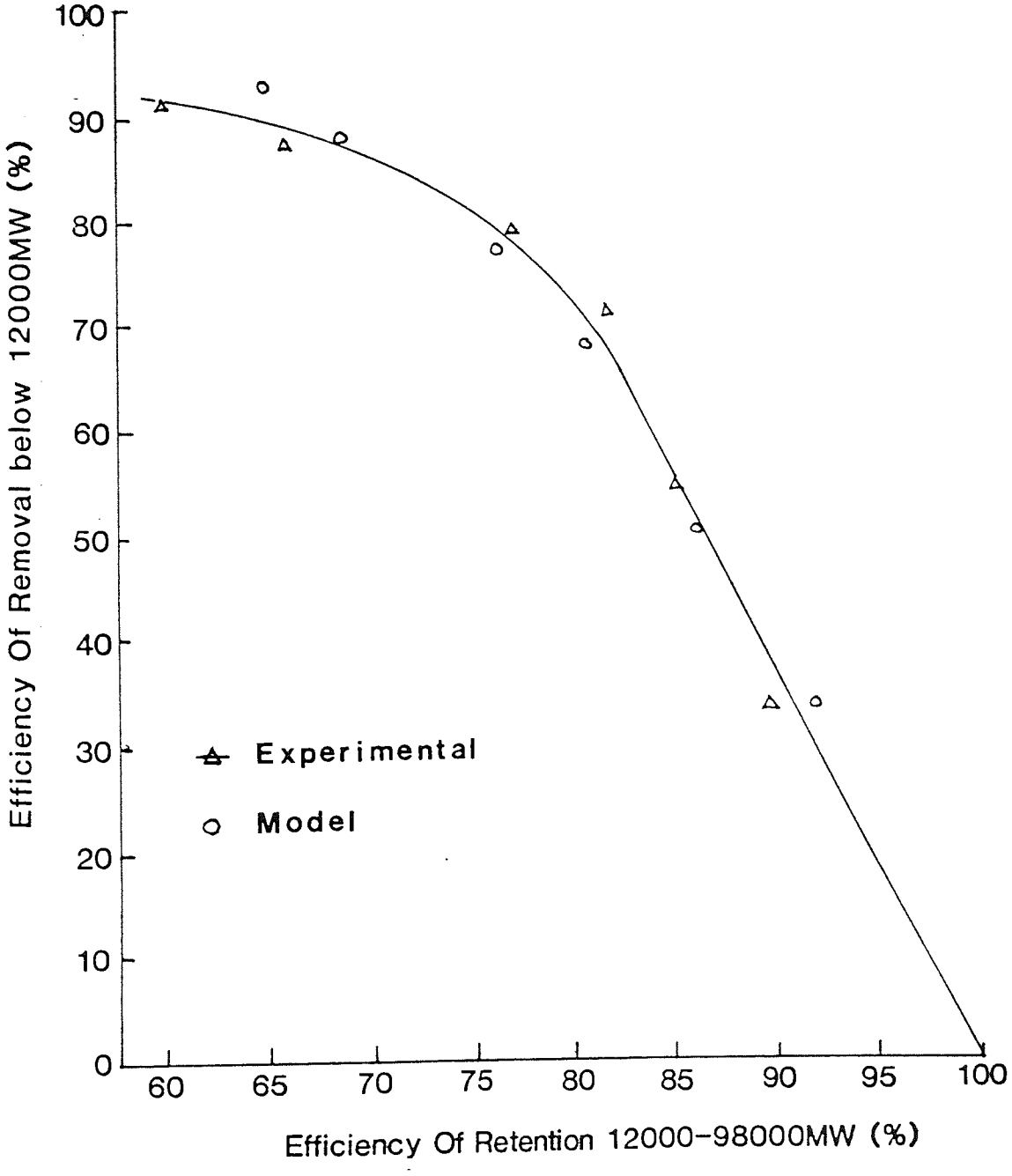

Figure 6.15 Model Prediction for 10,000 MW Cut-off Membrane Number 5

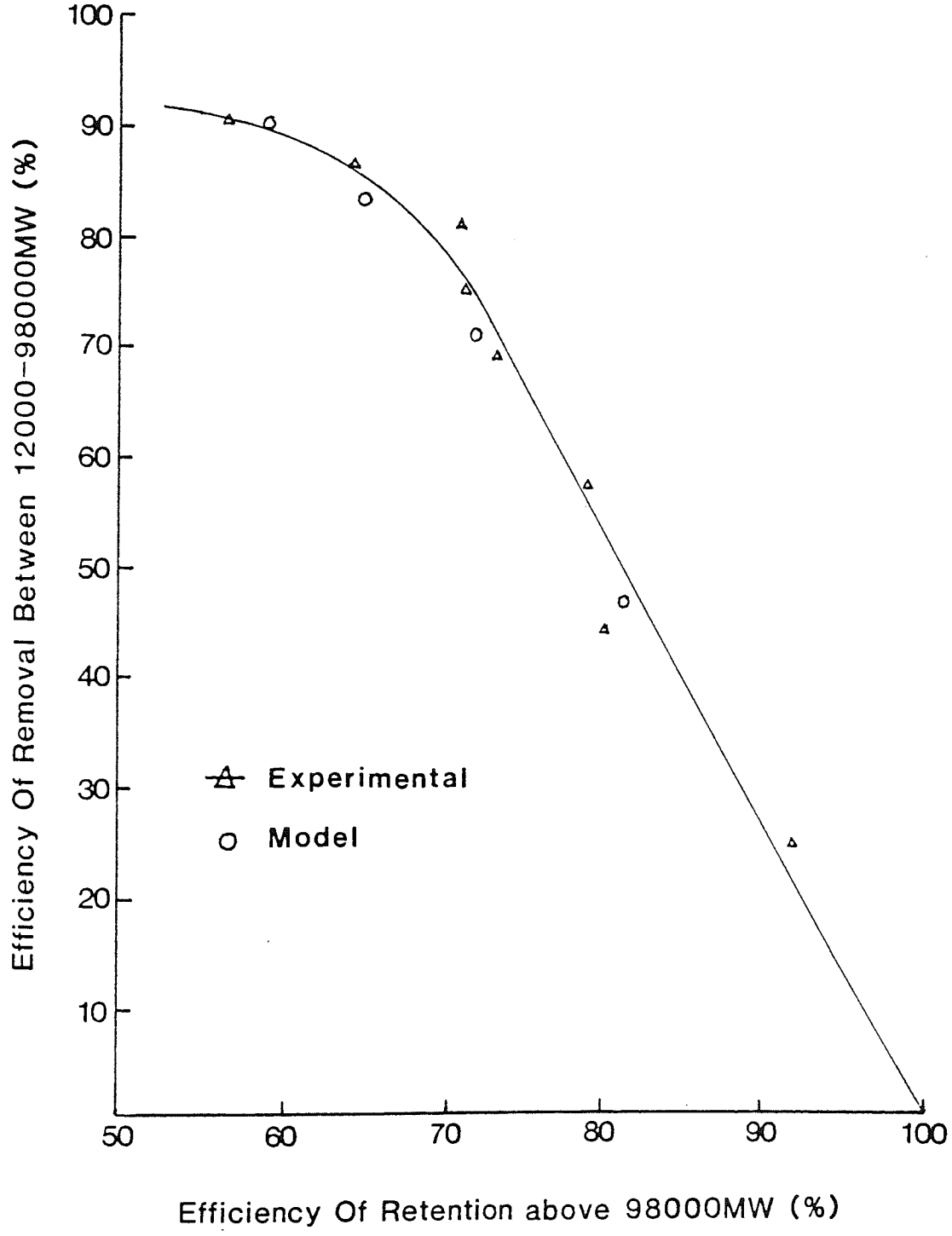

Figure 6.16 Model Prediction for 50,000 MW Cut-off Membrane Number 2

The accuracy of this approach was tested by comparing the model predictions to the batch experimental data. An example of the fit obtained for each of the membranes used can be found in figures 6.13 to 6.16. As the results show this approach was satisfactory and the model correctly followed the changes in overall efficiency and also the changes in the molecular weight distribution.

6.5 RESULTS

Before the model was used it was extensively tested. The model predictions for the cascade were checked by producing an overall steady state mass balance for the cascade and mass balances over each individual stage. The two sets of mass balances were then compared to check the accuracy of the computer simulation. Two examples can be found in appendix 5 and 6.

The results obtained from this model have been split into two sections for simplicity. The first section considers the removal of dextran with a molecular weight below 12,000 MW and the other the removal of dextran above 98,000 MW

6.5.1 MODELLING THE REMOVAL OF DEXTRAN BELOW 12,000 MW

The model was initially used to investigate the operation of an ideal cascade, ie. where all four membranes have identical rejection characteristics. The rejection data from the 10,000 MW cut-off membrane number five was used as the basis for this study. The results can be found in figure 6.17 and 6.18. It can be seen that the cascade removed the low molecular weight material far more successfully than the batch system, furthermore the retention of the 'saleable' band was maintained by recycling the permeate containing the lost material. The cascade

became more effective as the number of diavolumes increased. Also the number of stages within the cascade can be seen to be an important factor. When less than one diavolume was used increasing the number of stages had only a marginal effect, but as the number of diavolumes increased the number of stages within the cascade became more important for the recapture of lost material. These results also show that as the number of stages increased the effect of adding further stages became more limited. This suggests that there must be an optimum number of stages for any separation. This would depend on the required product specification, ie. the degree of removal required which in turn would dictate the number of diavolumes used and hence the number of stages required to obtain the satisfactory recapture of lost material. Furthermore the economic aspects would also have to be considered, in particular the capital cost and operating costs of the equipment.

To test the accuracy of the model the model predictions were compared to the experimental results. See table 6.1. The main aspects considered were how successfully the model could predict the product specification as the number of diavolumes changed and when the membrane order was changed (the effect of varying the rejection characteristics of the membranes in the cascade).

The models ability to predict how the number of diavolumes used effected the product specification was tested by comparing it to experiments 2.1 to 2.4. The model correctly predicted the overall efficiency of removal and retention and also changes in the molecular weight distribution within the product. See figure 6.19 to 6.21. Although the agreement between the model and the experiment data was good it was noticed that the model was beginning to under predict the efficiency of retention after 1.5 diavolumes.

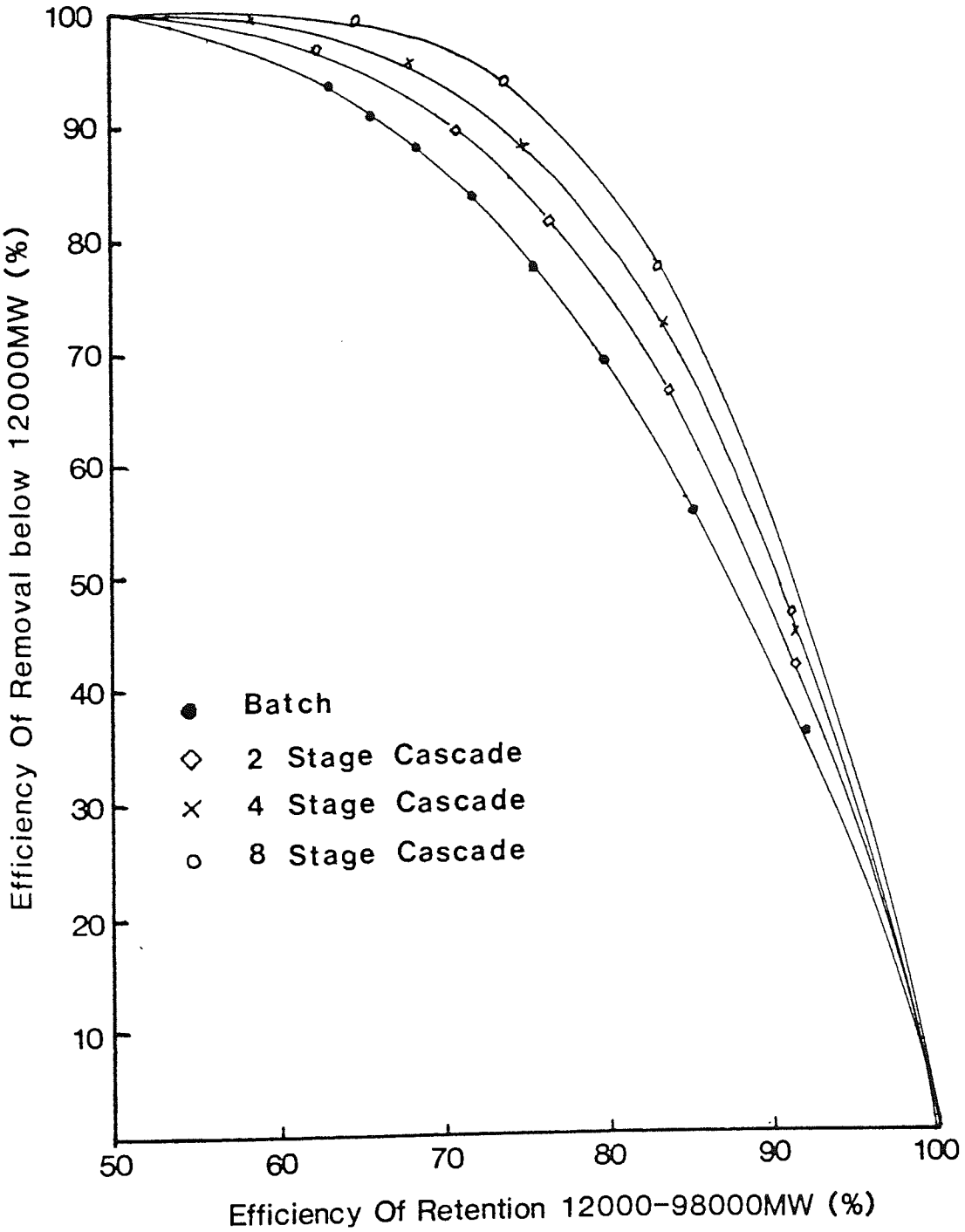

Figure 6.17 Model Predictions Showing the Effect of Increasing the Number of Stages within the Cascade

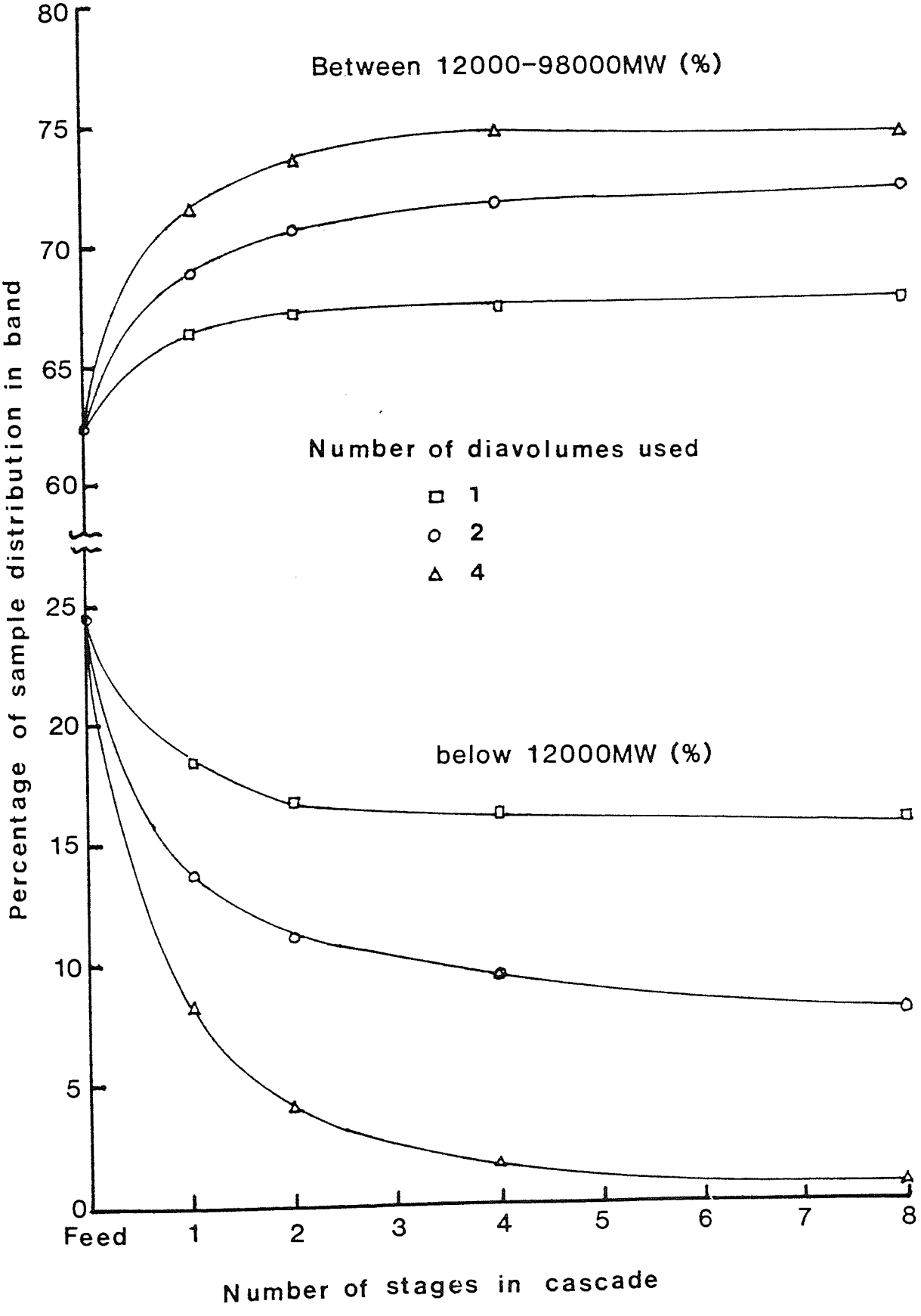

Figure 6.18 Model Prediction Showing how the Number of Stages in the Cascade Effects the Molecular Weight Distribution of the Final Product

Table 6.1 Model Predictions for the Experimental Cascade Using 10,000 MW cut-off Membranes

Number	Membrane order	Number of Diavolumes	%below 12000 MW		Efficiency of removal below 12000MW (%)		% between 12000 MW and 98000 MW		Efficiency of retention (%)	
			EXP	MODEL	EXP	MODEL	EXP	MODEL	EXP	MODEL
1	1,2,3,5	0.5DIA	21.64	20.35	24.83	26.25	64.57	64.92	90.06	93.5
2	1,2,3,5	1.0DIA	16.49	16.71	49.09	45.26	67.58	66.99	83.91	87.19
3	1,2,3,5	1.5DIA	11.63	13.44	66.28	60.09	71.2	68.60	82.66	80.97
4	1,2,3,5	2.0DIA	9.64	10.45	73.8	71.8	71.77	69.78	78.36	74.84
5	5,2,1,3	2 DIA	11.21	10.3	64.83	69.81	72.0	71.50	83.60	83.31

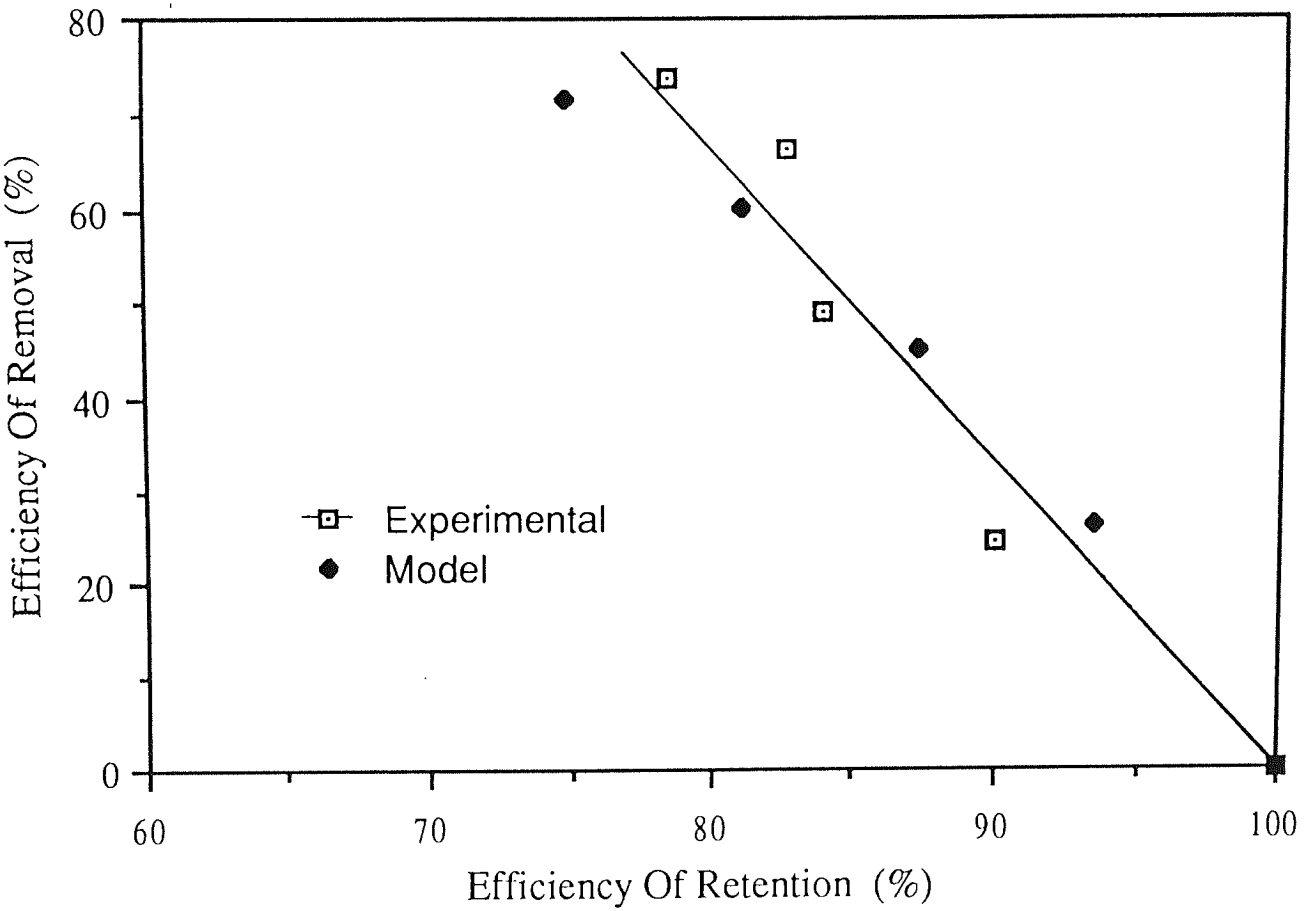

Figure 6.19 Comparison of Cascade Runs 2.1 to 2.4 to the Model Predictions

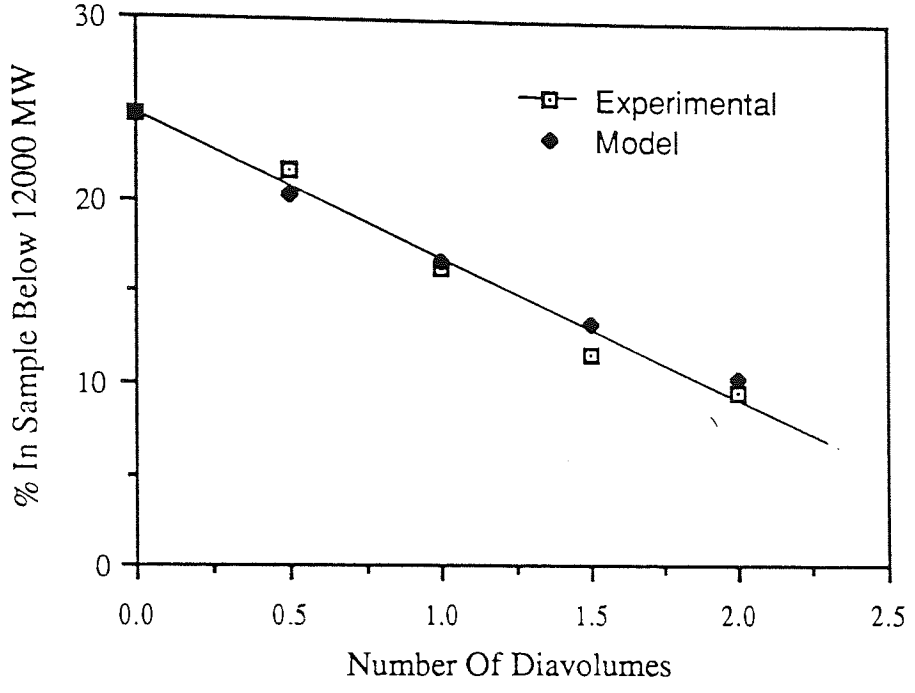

Figure 6.20 Model Prediction showing the Changes in the Molecular Weight Distribution (0-12,000 MW)

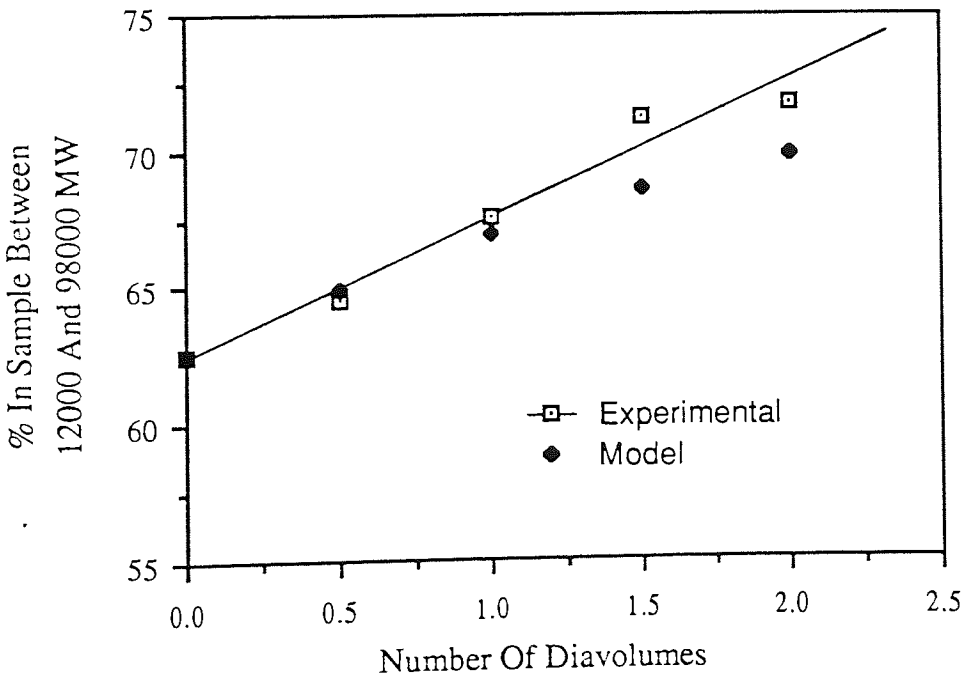

Figure 6.21 Model Predictions showing the Changes in the Molecular Weight Distribution (12,000 - 98,000)

Table 6.2 Model Predictions for the Mixed Membrane Cascade Runs

Number	Number Order	% below 12000 MW		Efficiency of removal below 12000MW (%)		% between 12000 MW and 98000 MW		Efficiency of retention 12000-98000MW (%)	
		EXP	MODEL	EXP	MODEL	EXP	MODEL	EXP	MODEL
	Mixed membrane runs (at 2 DIA)								
6	5(2),10(1),10(5),5(1)	16.31	14.07	44.37	52.45	69.88	70.16	90.49	94.28
7	10(1),5(2),5(1),10(5)	13.34	12.46	58.62	64.52	72.35	68.79	85.27	77.81
8	5(2),5(1),10(1),10(5)	16.61	15.42	47.74	46.57	70.62	69.18	86.72	95.27
9	10(4),10(3),10(2),10(1)	17.38	14.33	49.46	53.09	69.8	69.37	83.77	90.27
10	10(1),10(2),10(3),10(4)	15.77	10.75	56.09	70.83	68.24	69.57	77.92	74.98

* Number of outside bracket denotes nominal molecular weight cut-off of membrane used while number inside denotes the membrane reference number

Although the under prediction was only 4.5% at 2 diavolumes it was unclear if the model predictions would continue to diverge. Ideally further experimental data would have been obtained, but the cascade could only operate up to two diavolumes.

The models ability to predict the changes caused by varying membrane performance was also acceptable, however the results showed a higher degree of scatter especially when 'tight' membranes such as the 10,000 MW cut-off membrane number four had been used. In most cases the model over predicted the efficiency of removal. This suggested that within the experimental cascade a further factor was involved which was not accounted for by the model.

The model predicted the same agreed trends as found in the experimental cascade, see tables 6.1 and 6.2. The model correctly showed that stage one was the controlling stage in the cascade because the membrane placed in that stage had the greatest effect on the cascade product. This is shown in predictions number 5, 6 and 9, ie. where a 'tight' membrane had been placed in stage one. The model also correctly predicted that the middle stages had some effect on the overall fractionation of the cascade but their main purpose was to aid the recapture of lost material. The fourth stage was shown by the model to cause the greatest degree of fractionation, see table 6.3. This was also found in the experimental cascade and occurred since fresh diafiltrate was used in this stage.

Tables 6.4 and 6.5 clearly show the effect of placing one or more 'tight' membranes within the cascade.

The predictions clearly show that these membranes cause accumulation of material within the stage they occupy.

In the extreme case so much accumulation can result in the stage efficiency of removal actually becoming negative. These results are consistent with the results found in the experimental cascade.

The model predictions for the unsteady state experiment number 3.1 are shown graphically in figure 6.22. Close agreement between the model and the experimental results was achieved for the individual stage efficiency of removal across the cascade. The model correctly showed that low molecular weight material accumulated within stage two. The model prediction of the efficiency of retention across the cascade was noticably different from experimental cascade. The reason for this difference was unclear, but was probably due to the simplicity of the model and because the rejection was assumed to be constant.

The model was also used to determine how many cycles were required before the cascade would reach equilibrium, see table 6.6. The results were surprising, the cascade had been shown experimentally to reach equilibrium between 17 and 20 cycles by Poland [6] and myself, while the model predicted that the cascade product specification would require 30 cycles before equilibrium was achieved. However between cycle 22 and 30 the changes were very small. This difference between the model prediction and the experimental can be attributed to the unavoidable experimental scatter found in the real cascade, masking the very small changes predicted by the model. However it must be noted that the experimental cascade was operated for more than 30 cycles before samples were taken and so would be at equilibrium.

Table 6.3 Model Prediction for a ideal Cascade with Membrane order 10(5), 10(5), 10(5), 10(5)

Stage	% below 12000MW (%)	Efficiency of removal below 12000 MW	% between 12000 - 98000MW	Efficiency of retention 12000 - 98000 MW
1	20.73	20.45	65.37	99.72
2	18.23	32.59	67.35	98.99
3	15.10	47.50	69.55	96.12
4	9.43	72.64	72.19	83.25

Table 6.4 Model Prediction for Membrane Order 5(2), 10(1), 10(5), 5(1) @ 2 Diavolumes

Stage	% below 12000MW (%)	Efficiency of removal below 12000 MW	% between 12000 - 98000MW	Efficiency of retention 12000 - 98000 MW
1	28.20	-48.07	61.64	128.65
2	24.49	-9.42	63.56	112.86
3	17.89	33.55	67.74	99.98
4	14.06	52.45	70.16	94.28

Table 6.5 Model Prediction for Membrane Order 10(1), 5(2), 5(1), 10(5) @ 2 Diavolumes

Stage No	% below 12000MW (%)	Efficiency of removal below 12000 MW	% between 12000 - 98000 MW	Efficiency of retention 12000 - 98000 MW
1	17.99	43.61	64.99	80.89
2	18.89	39.08	64.58	82.82
3	20.54	27.55	64.34	90.22
4	12.46	64.54	68.79	77.81

Table 6.6 Predicting the Number of Cycles to reach Equilibrium based on Run 2.4

Cycle	% in sample below 12000 MW	Efficiency of removal below 12000 MW	% in sample between 12000-98000 MW	Efficiency of retention 12000 - 98000 MW
4	3.80	94.01	62.36	39.08
6	5.64	88.11	69.05	57.83
8	6.94	83.56	70.54	66.41
10	7.88	80.25	70.81	70.48
12	8.58	77.88	70.74	72.56
14	9.08	76.18	70.57	73.55
16	9.45	74.96	70.4	74.12
18	9.72	74.08	70.26	74.42
20	9.92	73.45	70.14	74.60
22	10.06	72.99	70.05	74.70
24	10.17	72.65	69.98	74.76
26	10.25	72.4	69.92	74.79
28	10.31	72.23	69.88	74.81
30	10.35	72.09	69.85	74.82
40	10.45	71.8	69.78	74.84
50	10.45	71.8	69.78	74.84

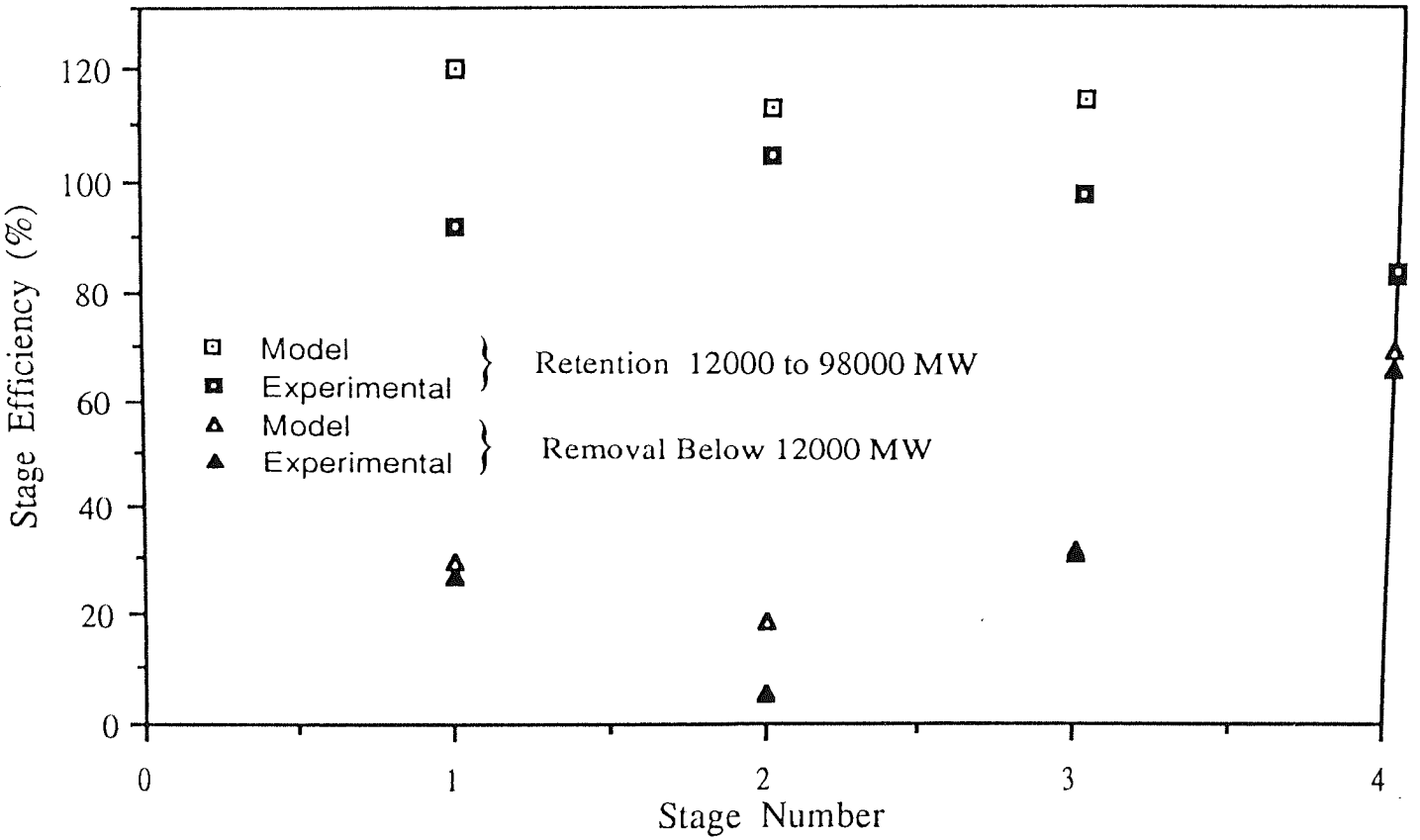

Figure 6.22 Experimental Stage Efficiencies Obtained from Run 3.1 Compared to Model Predictions

6.5.2 MODELLING THE REMOVAL OF DEXTRAN ABOVE 98,000MW

Modelling of the removal of the dextran above 98,000 MW was found to be far more difficult to model than the removal of material below 12,000 MW. The problems were not specifically with the model itself but with the computer program in which the model was incorporated. The main problem was that the Romicon 50,000 MW cut-off membranes could not be assumed to completely reject dextran below 500,000 MW compared to 98,000 MW for the other membranes. This made it necessary to make two important changes to the program:-

1) The arrays containing the rejection data and molecular weight distribution were changed to cover the wider molecular weight range being considered.

2) The incremental step size used for each calculation was increased from 200 MW in the previous case to 1,000 MW to make the volume of data manageable.

These changes could not be incorporated into the original program so a second version of the program was written so that both fractionations could be considered.

The model predictions for the removal of the high molecular weight material can be found in table 6.7. The model gave good agreement for the removal of material below 12,000 MW for all experiments. However for the 12,000 MW to 98,000 MW band and above 98,000 MW the model consistently over predicted the removal of material. On average this over prediction was about 12%.

If the trends are considered it can be seen that the model correctly predicts the effect of changing membrane order, for example for the four stage cascade predictions 7 and 8. Furthermore the model shows clearly how increasing the number of stages within the cascade improves the removal of the low molecular weight material, for example

Table 6.7 Model Predictions for the Removal of Material above 98,000 MW

No	Description	% below 12000		Efficiency of removal below 12000 MW		% between 12000-98000 MW		Efficiency of removal 12000 - 98000 MW		% above 98000		Efficiency of retention above 98000 MW	
		MODEL	EXP	MODEL	EXP	MODEL	EXP	MODEL	EXP	MODEL	EXP	MODEL	EXP
1	(1,2) 1.0DIA	14.94	13.94	70.38	72.12	68.82	69.33	52.53	49.75	16.22	16.73	86.44	93.75
2	(1,2) 1.5DIA	9.87	9.79	87.26	85.2	66.39	69.14	70.17	61.95	23.73	21.07	82.37	89.57
3	(1,2) 2.0DIA	5.99	6.70	94.79	92.61	60.52	63.85	81.704	74.43	33.49	29.45	78.23	91.07
4	(1,3,2) 1.0DIA	12.58	12.25	75.94	74.25	70.437	71.58	53.14	46.74	16.97	15.84	87.26	91.29
5	(1,3,2) 2.0DIA	2.27	3.86	98.20	95.94	59.46	66.24	83.69	74.45	38.27	29.91	81.06	89.19
6	(4,3,2,1) 1.0DIA	9.79	8.62	82.39	87.27	71.62	73.53	55.18	46.5	18.58	17.85	89.83	96.5
7	(4,3,2,1) 2.0DIA	0.687	1.36	99.51	98.34	54.72	68.93	86.37	69.74	44.59	29.71	85.79	96.76
8	(1,4,3,2) 2.0DIA	0.77	2.07	99.47	97.75	55.19	67.32	86.93	73.64	44.04	30.61	80.59	90.47

* Numbers in bracket denotes the reference number of Romicon membrane used.

the model predicts an increased efficiency of removal below 12,000 MW from 94% to 99.5% by increasing the number of stages from two to four while the experimental results show an increase from 92.5% to 98%.

6.6 DISCUSSION

The modelling of the removal of the material below 12,000 MW can be considered satisfactory. The model correctly predicted the effect of changing the number of diavolumes used and also changing the membrane order within the cascade. The agreement was more satisfactory when membranes with similar rejection characteristics were used. Where tight membranes were introduced into the cascade they tended to cause accumulation of material. In the experimental cascade this effect would probably cause the rejection of the membrane to be modified by the presence of the low molecular material, and hence the model predictions for these runs were less accurate since a constant rejection was assumed. Generally however the assumption of a constant rejection was reasonable.

This model can be considered to be more flexible and is certainly more applicable to the real system than that produced by Poland. Poland was unable to consider in detail the complex relationship between product specification, number of diavolumes used and the number of stages required. Poland for example only considered a cascade system operating at two diavolumes with a varying number of stages. He found that after six stages no further change in product specification occurred. This would appear to be unreasonable and this new model is probably more realistic in that it predicts that increasing the number of cascade stages does effect the product specification, but the effect of adding each additional stage becomes less and less significant. This effect continues well past six stages and is more noticable if more

noticable if more than two diavolumes are used.

Modelling of the removal of the high molecular weight material was expected to be more difficult since the majority of the dextran was being transported along the cascade in the permeate streams and not the retentate stream. Although the model predicted the correct trend, ie. the effect of changing the membrane order and the number of stages used, in all cases it over predicted losses of the material above 12,000 MW. Interestingly there was good agreement between the model and the experimental data for the removal of material below 12,000 MW this suggested that the inaccuracy was not due to the model itself but the assumption of a constant rejection.

As mentioned in section 5.5.4 the first stage of the cascade would be saturated by material lost from the other stages, this material would include the majority of the material below 12,000 MW which was shown experimentally to effect the rejection of the other material and so the rejection characteristics of the membranes within the cascade would probably not be constant. Therefore it is clear that this more complex system cannot be accurately predicted by this model in its present form. To predict this particular fractionation more accurately it is clear that it will be necessary to experimentally determine how the rejection of these membranes was altered by the widely varying concentrations and molecular weight distributions found along the cascade. This data could then be expressed as a correction factor in the model. Clearly this is a very intensive project beyond the scope of this particular study.

7.0 A DEXTRANSUCRASE BIOREACTOR - A FEASIBILITY STUDY

7.0 A DEXTRANSUCRASE BIOREACTOR - A FEASIBILITY STUDY

7.1 INTRODUCTION

Presently dextran production consists of three stages. Firstly the crude dextran is produced in a batch reactor using the enzyme dextransucrase. It is then hydrolysed to reduce the molecular weight of the dextran and finally fractionated to give a clinical product.

The aim of this work was to develop an ultrafiltration bioreactor system which combined biosynthesis (the production of native dextran from sucrose using the enzyme dextansucrase) and dextran separation in a single unit. Ideally the product from the reactor would be close to the clinical specification and so little further fractionation would be required. Industrially this approach would represent a substantial cost saving because the number of process stages would be reduced.

The immobilized dextransucrase bioreactor system varies from the most other commonly found immobilized enzyme systems in that the product of the reaction is of a larger molecular weight than the substrate (sucrose). In all other examples found the products of the reaction were either of a lower molecular weight than the substrate or involved only a molecular rearrangement.

Edwards [79] showed that the dextransucrase enzyme could be immobilized on an ultrafiltration membrane using glutaldahyde, however as with all other workers looking at the chemical immobilization of dextransucrase enzyme he found that the retained activity was very low. This problem was caused by the instability of the dextransucrase enzyme, even when kept under ideal conditions.

Since the stability of the dextransucrase enzyme cannot be significantly inproved, the use of chemical immobilization techniques cannot be considered satisfactory. This is because the membranes could

not be reused once the enzyme had denatured. After reviewing the literature for alternative techniques and testing those which were considered to be practical, the final choice was a design proposed by Michaels [68]. The reactor system proposed by Michaels consists of a membrane sandwich, the enzyme being retained between the two membranes. The reactor could be operated in a diffusion mode or a convective transport mode by applying a positive pressure across the cell. This design of cell was chosen for two reasons:

1) The factors effecting enzyme immobilization and dextran production could be easily observed

2) Scale up to a hollow fibre system would be simple because the principles of operation would be identical.

7.2 ANALYTICAL EQUIPMENT AND TECHNIQUE

7.2.1 INTRODUCTION

A high pressure liquid chromatography (HPLC) system was used to calculate the concentrations of fructose, sucrose and dextran in the bioreactor feed and product streams. HPLC was chosen in preference to the polarimeter since complex mixtures of the three components were involved. Unfortunately the polarimeter was unable to differenciate between each component and so could only be used to give a bulk concentration.

The molecular weight distribution of the dextran was determined using gel permeation chromatography.

Figure 7.1 Schematic Diagram of the HPLC Analytical System

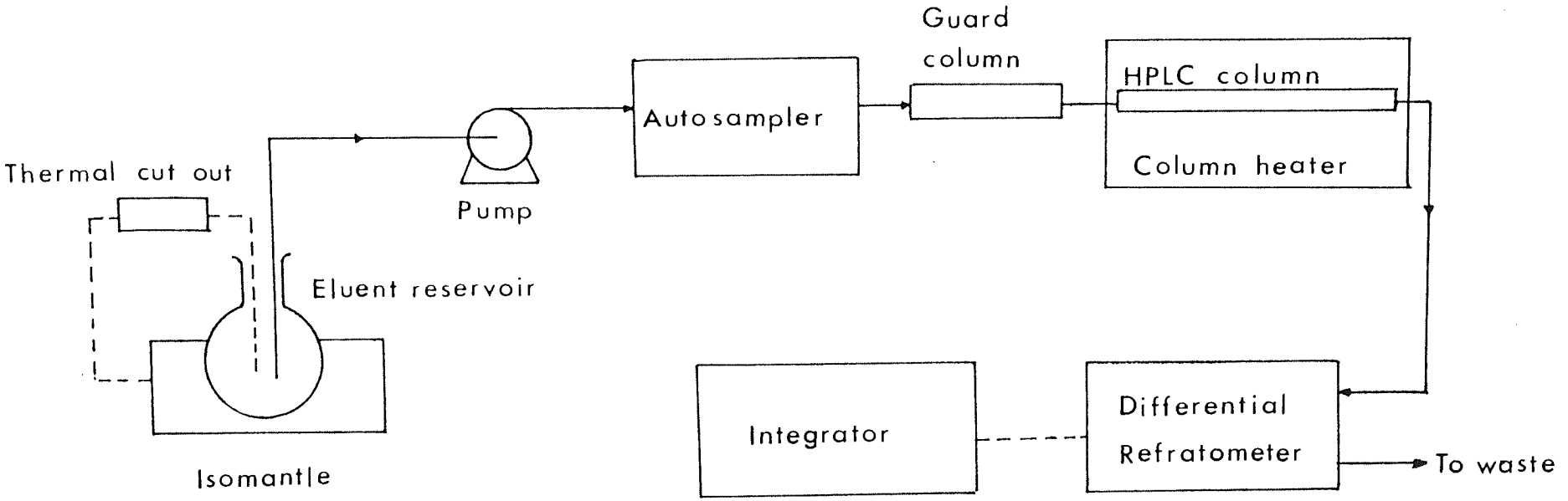

7.2.2 DETERMINING CONCENTRATIONS USING ANALYTICAL HPLC

7.2.2.1 EQUIPMENT DESCRIPTION

A resin based high performance liquid chromatography (HPLC) system was employed to analyse the feed and products from the enzyme bioreactor. See figure 7.1. The system consisted of the following:-

An eluent reservoir was heated to 80°C using an isomantal to degas the eluent. To prevent the system boiling dry a thermal cut-out was used, (supplied by Laboratory Thermal Equipment, Greenfield, London). The eluent used was distilled water (pH 6.5) with 0.02 gl^{-1} of calcium acetate to maintain the calcium form of the packing.

The eluent was pumped using a low pulsation positive displacement pump (model 1330 Biorad Laboratories, Watford, UK), at a flow rate of 0.5 cm^3/min. An Anachem (Luton, Bedfordshire) debubbler was used to remove any bubbles which had found their way inside the eluent delivery pipe.

The samples were injected using a Talbot autosampler (Talbot model ASI-3, Cheshire, UK). All the samples were prefiltered using a 0.45 µm disposable filter (supplied by Millipore Ltd, UK).

The column used was an Aminex HPX-87C column supplied by Biorad. The column was 30 cm long by 0.78 cm ID. The column operated at approximately 8300 KN/m^2. The column was protected by a guard column. The guard column used Hibar Lichrocart 4-4 cartridges (supplied by BDA Chemical Ltd Atherstone, Warwickshire). The guard column was found to be essential when analysing enzyme samples since it was impossible to remove all the cell debris during the purification stage.

The column was heated to 85°C using a column heater (HPLC Technology Ltd, Model TC831).

The concentrations of the products leaving the column were measured using a differential refractometer. (Biorad, Model 1750).

The electrical signal from the refractometer was passed to an intergrator (Model SP207 Spectra Physics Ltd, UK) which used it to calculate the area of the peak.

7.2.2.2 EXPERIMENTAL TECHNIQUE

Since the HPLC system was used to analyse samples containing enzyme a very strict operating procedure was required.

The column was placed in the column heater and allowed to reach the operating temperature of 85°C before the full flow rate of 0.5 cm^3/min was used. The column was then allowed to reach equilibrium.

The refractometer and intergrator parameters were then checked according to their operating manuals (116,117).

The eluent used was a 0.02 g/l calcium acetate solution. This was used to replace any calcium ions lost from the packing.

The samples containing the enzyme were first heated above 80°C for 15 minutes to denature the enzyme. The samples were then pre-filtered using a 5um filter followed by a 0.45 um disposable filter.

Whenever samples were analysed, fructose, glucose and dexran standards were also included. The standards were accurately weighed to give a concentration of 1% W/V.

After all the analysis has been completed the system was allowed to run for an extra half an hour before shut down to remove any residue from the system.

After 50 samples the columns were reversed and backflushed at 0.2 cm^3/min for six hours.

If the column performance decreases or the pressure increases by more than 10% the columns were cleaned with a 30% acetonitrile solution at 0.1 cm^3/min and then regenerated using 0.1 M calcium acetate.

7.2.3 DETERMINING THE ENZYME ACTIVITY

The enzyme activity was determined using Hostettlers method [91]. This method works by measuring the fructose released from the reaction. 1.0 cm^3 of enzyme solution was added to 4.0cm^3 of 6.25% W/V sucrose solution in 0.1 M sodium acetate buffer at pH 5.2 and incubated for up to 20 minutes at 25°C. Samples of 0.5cm^3 were taken at 0, 5, 10 and 20 minutes, each sample was added to 1.0 cm^3 of sumner reagent (10g of 3,5 dinitrosalicylic acid and 300g of potassium-sodium tartrate dissolved in 1 litre of 0.4 M NaOH) and then heated in boiling water for 3 minutes and cooled. To this 11 cm^3 of distilled water was added. The absorbency of these samples was measured against a blank at a wavelength of 530 nm. The blank contained 0.5 cm^3 of 6.25% W/V sucrose in a 0.1 M sodium acetate solution, 1.0 cm^3 sumner reagent and 11 cm^3 of distilled water. The spectrophotometer used to measure the absorbency was a Pye Unicam SP1800 ultraviolet spectrophotometer.

Defining one dextransucrase unit as the amount of enzyme which will convert 1 mg of sucrose to dextran in 1 hour at 25°C and pH5.2; the enzyme activity of a solution can be obtained using the following formula:

$$\text{Enzyme activity } (DSU/cm^3) = \frac{(OD_t - OD_o) \times 2 \times d \times 60}{OD_s \times 0.52 \times 0.2 \times t} \quad \ldots 7.1$$

where OD_t, OD_o and OD_s are the optical densities of the samples incubated at time t, ie. 5, 10, 15 and 20 minutes, at zero time and a standard 2% W/V fructose solution. d is the dilution factor and t the incubation time in minutes.

7.3 ENZYME PURIFICATION

The crude dextransucrase present in the fermentation broth must be purified to remove impurities such as dead cells, dextran, fructose, leucrose, mannitol, proteins and small quantities of levansucrase and invertase before it can be used. These impurities much be removed since the cell debris will foul the membranes and the mannitol and fructose present would prevent accurate quantification of the fructose formed.

The purification of the dextransucrase enzyme has been investigated extensively at the University of Aston by Zafar [113] and Ganetsos [114].

The purification procedure was split into two stages, the first stage involved the removal of the cells and the second stage the removal of the other impurities. The cell removal was achieved by using an ultracentifuge, model 1A LAB T1 (supplied by Pennwalt Sharples, Surrey, England). When using a centifuge force of 20000G a single pass through the centifuge would remove between 80-90% of the cells with only a 10% loss of enzyme activity. Higher centifugal forces were also used but these resulted in an appreciable loss of enzyme activity. This loss of enzyme activity was probably the result of the higher shear forces denaturing the enzyme.

The low molecular weight impurities were removed using diafiltration. The system used consisted of a peristaltic pump (supplied by Watson Marlow, Falmouth, England, model 701S/R) operating at four litres per minute. The ultrafiltration unit was a thin channel

Pellicon cassette module (supplied by Millipore, Hartford, Cheshire, England). A 30,000 MW cut-off membrane with an area of 0.05 m^2 was used at a transmembrane pressure of 172 KPa. The enzyme solution was kept in a fridge at 6°C during the whole procedure to maintain the enzyme activity.

Generally it was found that between four and six diavolumes were required to give a satisfactory removal of the low molecular weight impurities. Typically the ultrafiltration system gave an efficiency of 50%. The losses could be attributed to two factors, the shear forces present in the ultrafiltration system and adsorption onto the membrane surface.

The final activity of the enzyme varied depending on the original activity of the feed, however typically the purified enzyme had an activity of 60 to 150 DSU/cm^3. The purified enzyme was then stored frozen to maintain the activity of the enzyme.

7.4 SELECTION OF MEMBRANES FOR THE BIOREACTOR SYSTEM

The selection of membranes for the bioreactor was particularly critical for two reasons.

(1) The membranes must retain the enzyme within the bioreactor.

(2) The membranes must control the molecular weight distribution of the dextran product leaving in the permeate.

A range of membranes were obtained from Amicon, Millipore, New Brunswick and DDS and examined to determine the optimum molecular weight cut-off for use in the bioreactor. The Amicon membranes (Stonehouse, Gloucestershire, England) and DDS membrane (Nakstiou, Denmark, code GB90PP) were tested in a Amicon 402 stirred cell ultrafiltration system. The Millipore membrane (Harrow, Middlesex, England) was tested in a

thin channel Pellicon unit and the New Brunswick Scientific membranes (Watford, England) in the Megaflow thin channel unit, model TM-100. Both the New Brunswick and Millipore thin channel systems were operated at a recirculation rate of 1 litre/minute. The test solution was a 2% W/W dextran solution (code HZ1S) protected using a 0.02% sodium azide. A transmembrane pressure of 70 KPa was used when testing all membranes.

The performance of each membrane was quantified by examining the dextran molecular weight distribution found in the permeate.

Since the main objective of the project was to produce a dextran product as close to the clinical specification as possible, a specification of 85% between 12,000 MW and 98,000 MW was set, this was identical to that used in the earlier fractionation work. The factors used to determine the membranes ability to achieve this specification were:

1) The maximum molecular weight detected in permeate.

2) The percentage of the molecular weight distribution within the 12000 MW to 98000 MW band.

3) The percentage of the molecular weight distribution above 98,000 MW.

The amount of dextran above 98,000 MW present in the permeate (the final product) was an important factor since this material is known to interfere with the blood clotting process. It was reasonable to assume that whatever design of bioreactor was chosen some high molecular weight material would be produced, this would not be a problem if this material could be retained in the bioreactor by the membrane. Infact this would be advantageous since the presence of this material has been shown to improve the stability of the dextransucrase enzyme [115]. Once the amount of high molecular weight material within the reactor became excessive or when the enzyme was replaced this material could be separated and hydrolysed to give the correct specification, so reducing losses from the system.

The results obtained for all the membranes can be found in table 7.1. The results show that the performance of the Amicon membranes were generally superior to the other makes. The DDS and New Brunswick membranes were the most disappointing, both makes allowed the passage of molecules far larger than the comparable Amicon YM membranes did.

In all cases the membrane allowed the passage of molecules far larger than their quoted molecular weight cut-off would suggest. The relationship between the maximum molecular weight found in the permeate and the quoted nominal molecular weight cut-off of the Amicon membranes tested can be found in figure 7.2.

A significant difference in performance was found between the Amicon YM and PM membranes. The PM series of membranes were designed to give high fluxes, however this was found to be at the expense of rejection. The elution profiles obtained for the YM and PM membranes show clearly the differences between the two types of membranes. See figure 7.3 to 7.5. The PM membranes can be seen to produce a higher and broader peak than the YM membranes. The greater height reflects the higher concentrations and the wider peak the wider molecular weight range present.

In terms of rejection of dextran only, it was clear that either the YM30 or XM50 membranes were suitable for use in the bioreactor. Both give elution profiles which peaked within the 12,000 to 98,000 MW band and both exhibit satisfactory retention of material above 98,000MW.

To examine how well the membranes retained the dextransucrase enzyme the following test procedure was used. The membranes were sealed in the Amicon 402 stirred cell and the cell filled with an enzyme solution with an activity of approximately 200 DSU/cm^3. The cell was then pressurized to 70 KPa and permeate samples collected. These samples were then tested for any enzyme activity. In both cases no enzyme activity was found.

Table 7.1 The Molecular Weight Distribution found in the Permeate Products from the Range of Membranes Tested for use in the Bioreactor

Membrane	PERMEATE PRODUCT: % in sample below 12000 MW	% in sample between 12000 - 98000 MW	% in sample above 98000 MW	% in sample below membrane nominal MW cut-off	Maximum detectable molecular weight in permeate
Feed distribution	23.56	67.68	8.76	-	-
Amicon YC05	Too dilute to determine molecular weight distribution				
YM2	Too dilute to determine molecular weight distribution				
YM5	100	-	-	95.47	10525
YM10	72.94	27.06	-	63.77	65003
YM30	48.82	51.027	0.153	87.95	167847
YM50	46.37	52.51	1.12	93.56	265750
PM10	41.16	57.886	0.974	33.78	287623
PM30	35.89	61.64	2.47	74.35	433073

Table 7.1 (Continued)

PERMEATE PRODUCT

Membrane	% in sample below 12000 MW	% in sample between 12000 - 98000 MW	% in sample above 98000 MW	% in sample below membrane nominal MW cut-off	Maximum detectable molecular weight in permeate
DDS 2000 MW cut-off	63.21	36.79	-	25.27	93356
Millipore Durapore 30,000 MW cut-off	43.46	56.138	0.402	85.61	140331
New Brunswick					
10,000 MW cut-off	40.18	59.492	0.328	31.11	162869
50,000 MW cut-off	28.47	68.51	3.02	87.00	360441
100,000 MW cut-off	28.32	76.67	4.99	95.18	973010

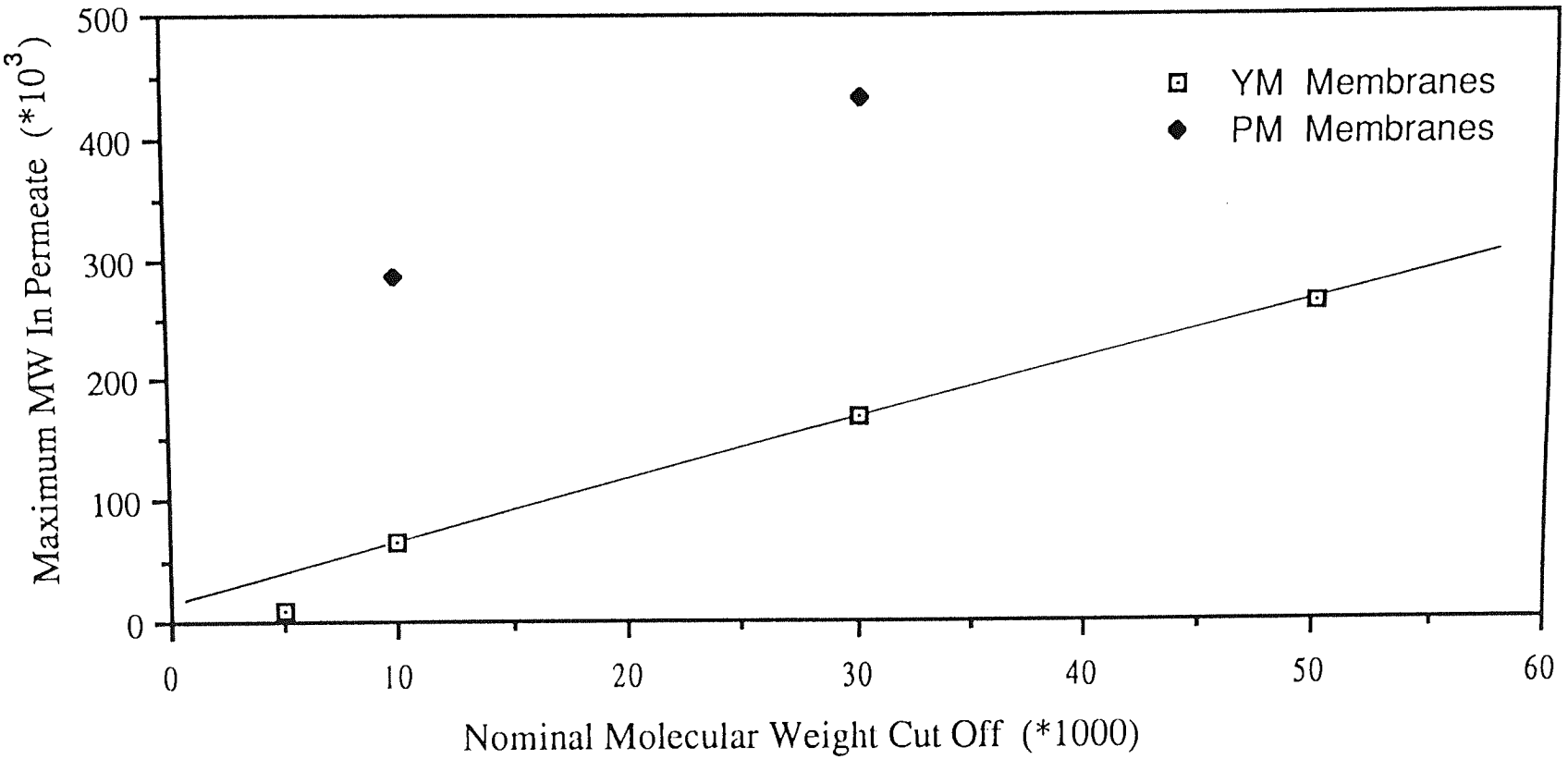

Figure 7.2 Maximum Molecular Weight of Dextran Found in Permeate

Figure 7.3 The Elution Profiles from a Range of Amicon Membranes

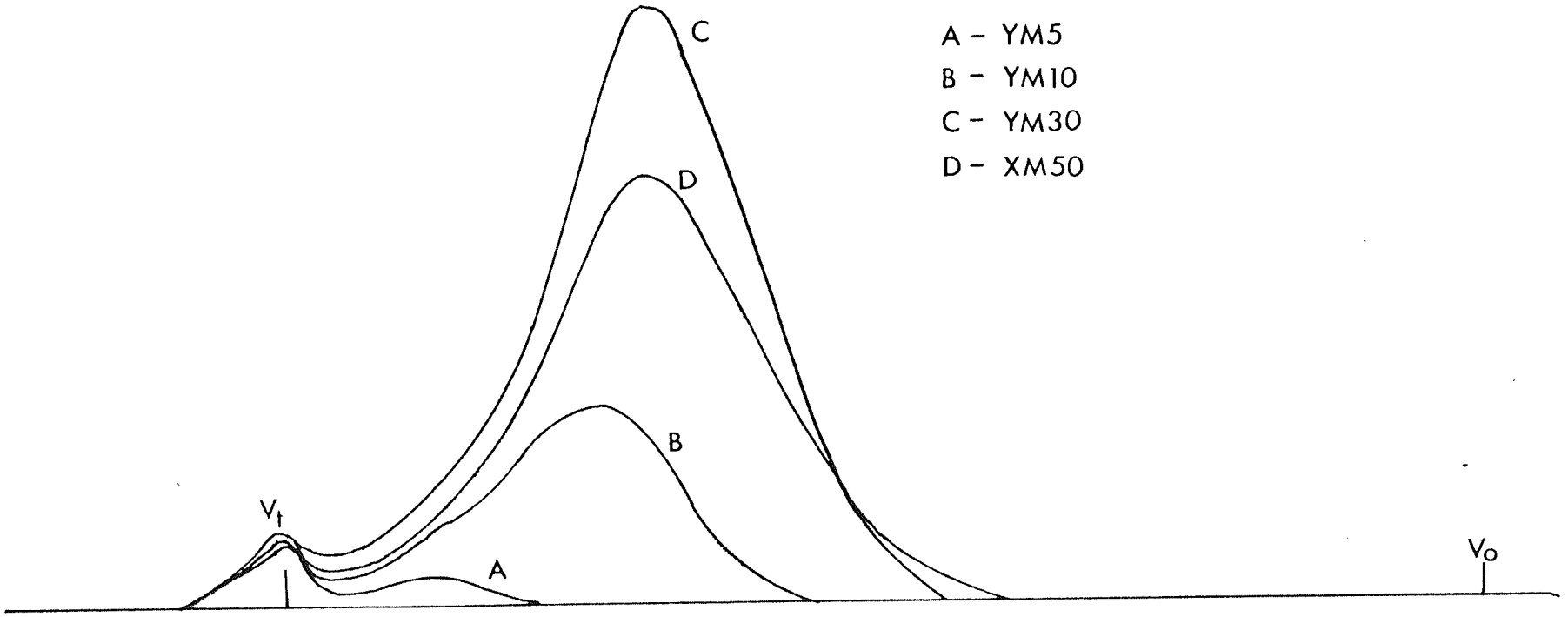

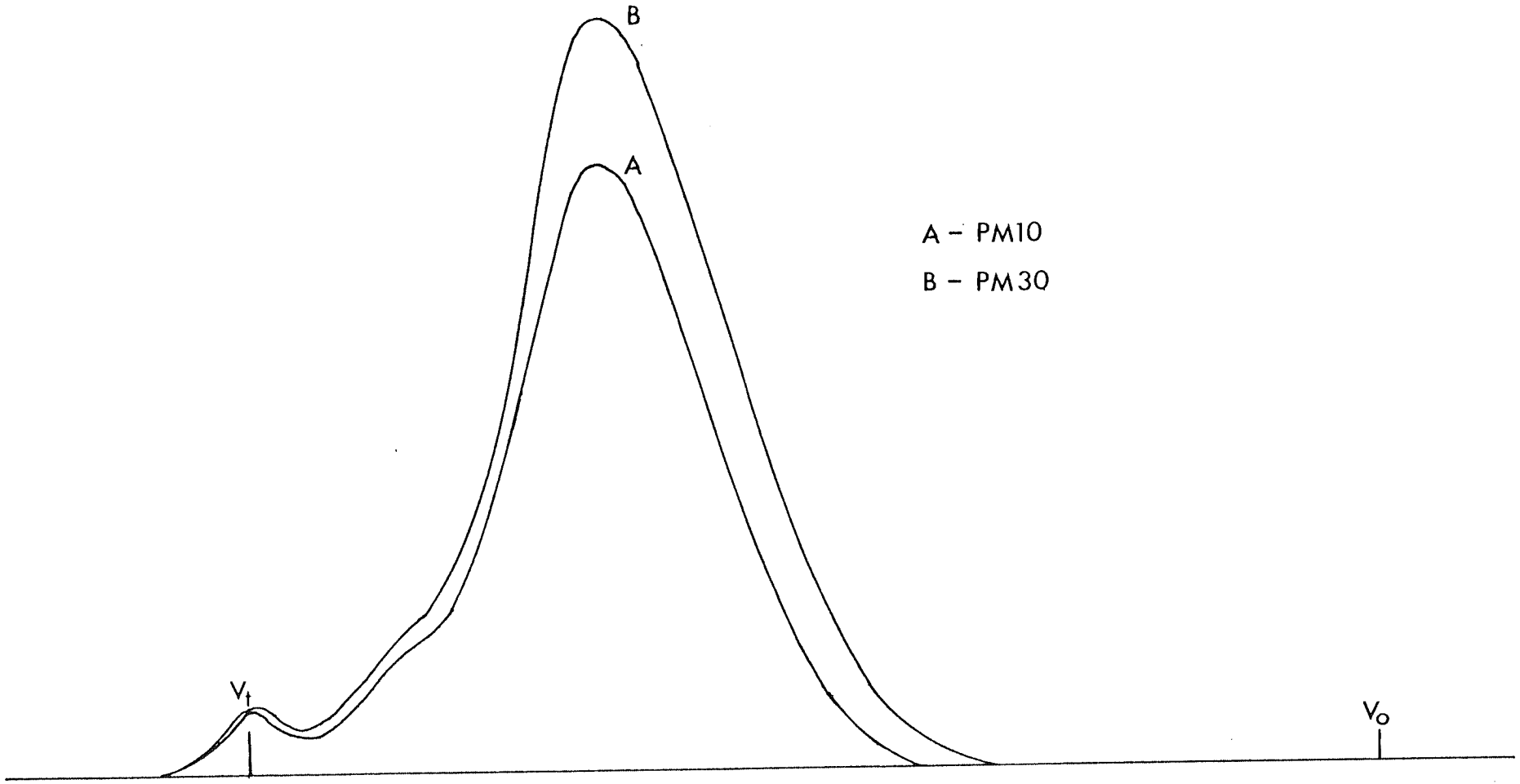

Figure 7.4 The Elution Profiles from the Two Amicon PM Membranes

Figure 7.5 The Elution Profiles from the DDS and Millipore Membranes

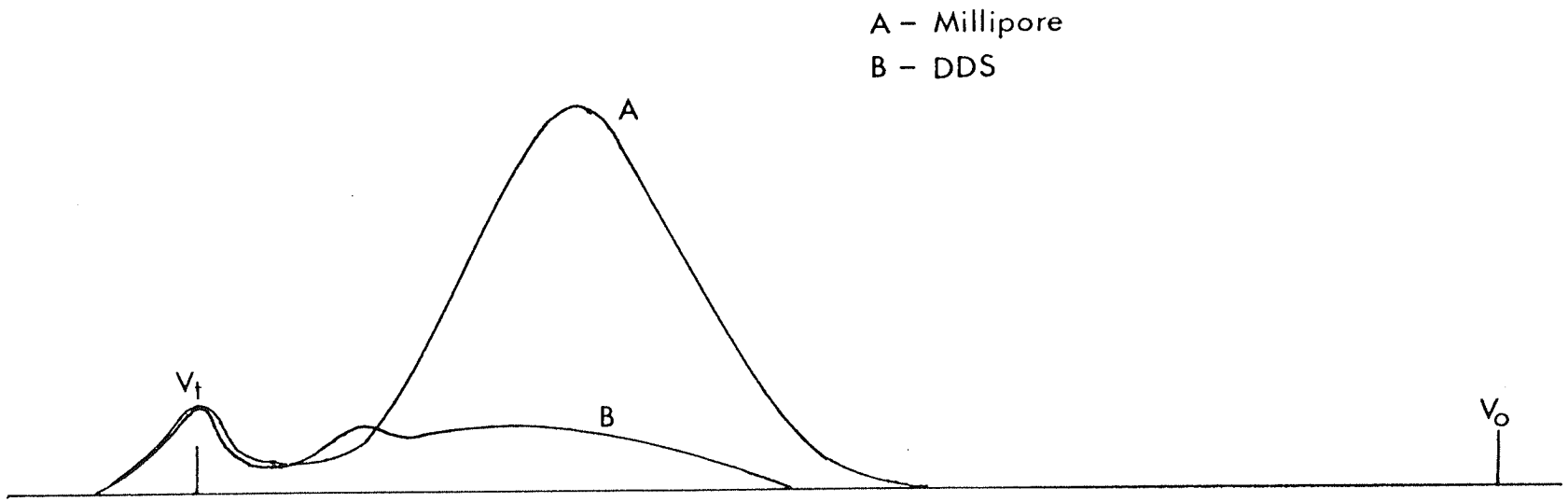

7.5 PRELIMINARY EVALUATION OF ALTERNATIVE BIOREACTOR SYSTEMS

The literature survey identified three methods of non-chemical immobilization which could be applied to the dextransucrase bioreactor system. These were:-

(1) Physical immobilization into the porous substructure of the membrane.

(2) Gel layer immobilization.

(3) Entrapment within the shell side of a hollow fibre cartridge or membrane sandwich as proposed by Michaels [68].

The physical immobilization into the porous substructure of a membrane was investigated using the New Brunswick thin channel system (Megaflow System Model TM-100). The enzyme loading was achieved by reversing the membrane and continually recirculating the enzyme solution through the unit. Two transmembrane pressures of 70 KPa and 140 KPa were used. The degree of enzyme adsorption was measured by weighing the membrane before and after loading. Using 70 KPa no significant enzyme loading could be detected. This was confirmed by bringing the membrane into contact with a sucrose solution, no reaction could be detected. At 140 KPa an enzyme loading of 0.0147 g/cm^2 was obtained, however the immobilization process damaged the membrane. The membrane exhibited blistering where the membrane skin had separated from the porous substructure. The experiments were repeated several times with the same results. In conclusion using a low transmembrane pressure results in little or no detectable enzyme loading while higher pressures damage the membrane.

The second method investigated was gel layer immobilization. The procedure used was as follows. An Amicon XM50 membrane was sealed into the Amicon 402 stirred cell. 50 cm^3 of enzyme solution with an activity of 50 DSU/cm^3 was placed in the cell and a transmembrane pressure of 140

KPa applied. The solution was then ultrafiltered until less than 5 ml of solution remained.

Using this technique an average enzyme loading of 0.01447 g/cm^2 was achieved, this was very similar to the other method mentioned above. This method of immobilization had a significant effect on the flux, for example before immobilization the membrane had a fresh water flow rate of 2.7 cm^3/min, after immobilization the average flow rate was 0.4 cm^3/min.

Another problem found with this technique was the instability of the gel layer. When the sucrose feed solution was added to the ultrafiltration cell the gel layer rapidly disintegrated and much of the gel layer was lost before the experiment could start. Typically the activity of this type of system were very low, this could have been because the enzyme was lost from the gel layer or that the enzyme was being denatured by the immobilization procedure.

These experiments confirmed that a higher enzyme loading was required than could be achieved by using either gel layer immobilization or immobilization into the porous substructure of the membrane. The only other practical methods of obtaining a higher activity were by immobilizing the enzyme within the shell side of a hollow fibre cartridge or by containing it within a membrane sandwich. The design chosen was the membrane sandwich. This design was chosen for its simplicity since it would make it easier to identify the factors affecting the immobilization of the enzyme and the molecular weight distribution of the product. A detailed analysis of this design can be found in the following sections.

Figure 7.6 Exploded View of the Bioreactor

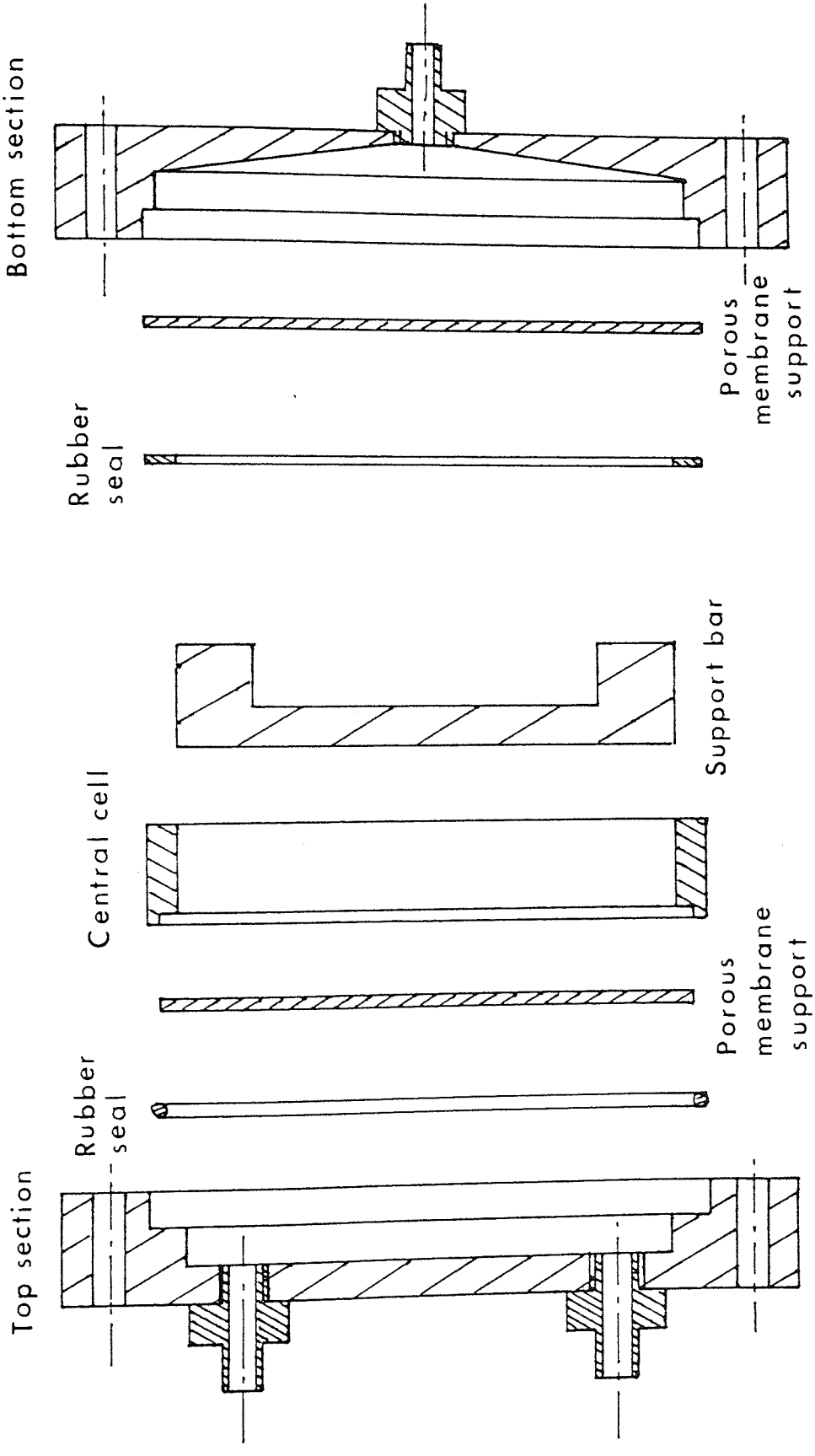

7.6 IMMOBILIZING ENZYME BETWEEN TWO MEMBRANES

7.6.1 EQUIPMENT DESCRIPTION

The reactor cell consists of 8 components as described below. A schematic diagram can be found in figure 7.6.

(1) Top Section : manufactured in perspex the component was 180 mm in diameter and was 15 mm thick. Cut into this section was a channel 150 mm diameter. Screwed into the back of the component were three fittings, two outlet and one inlet connections so that the sucrose feed could enter into the feed channel and then be recirculated back to the feed tank. A rubber seal was glued onto the inside face of the component to give a good seal between it and the central cell.

(2) Central cell : manufactured in perspex, the central cell was 150 mm in diameter and had a wall thickness of 4 mm. The cell height was 8 mm. On one side a groove was cut into which a sintered metal support for the membrane was placed.

(3) Sintered metal membrane support : manufactured in sintered stainless steel. Two membrane supports were required. The first fitted into a groove cut into the top of the central cell, this was 146 mm in diameter. The other fitted flush to the other side of central cell and was 150 mm in diameter. The sintered metal supports were both 1.5 mm thick and contained 75 micron pores.

(4) Support bar : made in mild steel with two rubber feet to prevent damage to the membrane underneath it. The support bar was 142 mm long. The support fitted inside the central cell and was required to prevent the cell collapsing when a transmembrane pressure was applied.

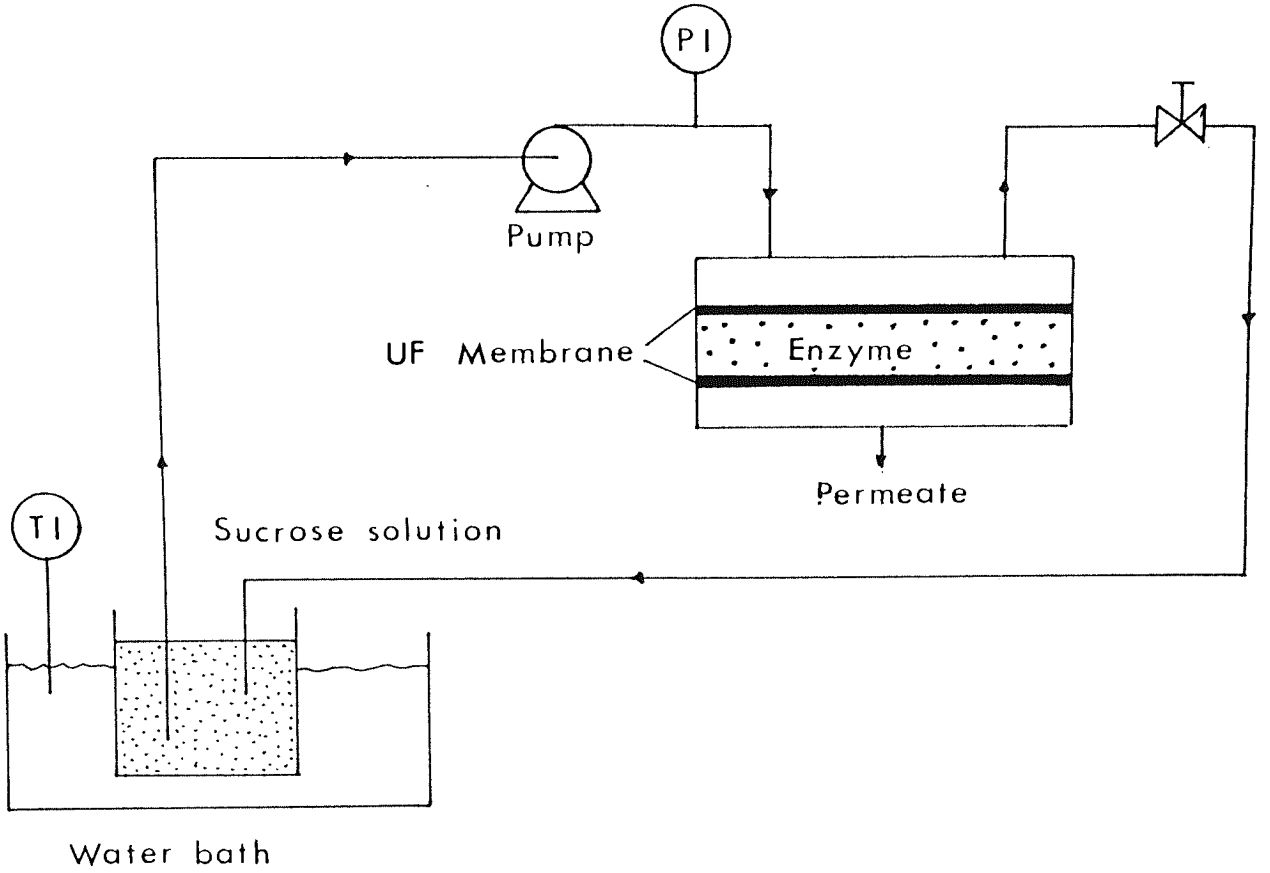

Figure 7.7 Schematic Diagram of the Bioreactor System

(5) Rubber seal : the rubber seal was required to prevent leaks from between the bottom of the central cell and the membrane which fitted on top of the second sintered metal support. This seal was manufactured in 1 mm thick neoprene rubber.

(6) Bottom section : manufactured in perspex the bottom section was 180 mm diameter and 20 mm thick. Cut into this section was the permeate drain channel. The channel was tappered so that the liquid would run out of a single drain hole in the middle of the channel.

The top and bottom sections were clamped together with the central cell placed between them. In total the reactor was held together by 8 mild steel bolts.

A schematic diagram of the complete system can be found in figure 7.7.

The sucrose feed solution was contained in a reservoir (two litre volume). The reservoir was maintained at 25^{o}C using a water bath and a heater (Tecam model TE7 Cambridge, England). A masterflex peristaltic pump (Baird and Tatlock, England) was used to recirculate the sucrose solution through the first compartment of the bioreactor cell. A transmembrane pressure of 70 KPa was applied, the pressure was adjusted using a needle valve fitted into the outlet pipe. A pressure gauge was connected onto the inlet pipe to the reactor cell.

The permeate leaving the bioreactor cell was collected in a 10 ml measuring cylinder.

7.6.2 EXPERIMENTAL TECHNIQUES

Before any experiment could be started the bioreactor cell must be filled with enzyme. The procedure used was as follows:

(1) The bottom sintered metal support was placed into the groove present in the bottom section of the biorector unit. On top of this a

Amicon XM50 membrane was placed. A small amount of silicon sealant was then placed around the edge of the membrane.

The rubber seal was then glued onto the bottom of the central cell. This was required to stop the seal slipping out of place.

The central cell was placed on top of the bottom section and pressure applied so that the silicon sealant would give a good seal between the two parts. The sealant was then given ten minutes to harden.

The support bar was then placed into the central cell.

(2) The central cell was completely filled with enzyme solution. The top sintered metal support was then placed into the groove in the top of the central cell. The other membrane an Amicon YM30 was placed on top of this support and the top section put into place. The whole unit was then bolted together.

(3) The central cell was then examined to check if the central cell had been correctly filled. Finally the sucrose feed channel and permeate channel were flushed with deionised water to remove any traces of enzyme. The bioreactor unit was then ready to be connected into the rest of the reactor system.

Typically one litre of sucrose feed was used for each experiment, the sucrose concentration used varied between 2 to 10% W/V. The pH of the solution was maintained at 5.2 by using a 0.1 M sodium acetate buffer, the pH being adjusted to the desired value using acetic acid. The sucrose solution was left in the heated water bath for at least 15 minutes before the experiment was started to allow the solution time to reach the normal operating temperature of 25^{o}C.

Once the bioreactor unit had been connected into the rest of the system and the sucrose solution was up to temperature the experiment could be started. The peristaltic pump was adjusted to give a sucrose

flow rate of 1 litre/minute and the transmembrane pressure set at 70 KPa. The cell could be operated up to 172 KPa, but due to the presence of concentration polarization inside the central cell there was no significant advantage operating at this pressure.

The permeate product from the bioreactor was collected for analysis in a 10 ml measuring cylinder.

After the experiment had been completed the bioreactor was split and the product in the central cell collected for analysis. The enzyme solution was denatured by heating to 80^{o}C for 15 minutes before storage.

Finally the membranes were cleaned in deionised water and put into storage for future use.

7.7 EXPERIMENTAL RESULTS AND DISCUSSION

During this work the key areas of interest were the flux from the cell, the loss of sucrose in the permeate and the molecular weight distribution of the dextran product.

The molecular weight of the dextran had been shown by Edwards [79] and Monsan and Lopez [84] to be highly dependant on the residence time within the reaction system, therefore the flow through the reactor would be a critical factor. The residence time in the central cell was completely dependant on the membrane flux. The central cell containing the enzyme was stagnant and so it was anticipated that the flux would decline at the beginning of the experiment but would reach a constant value once steady state had been reached. The final flux was difficult to assess before using the reactor since so many unknown factors were involved.

The preliminary investigation of the reactor system was performed using a sucrose feed concentration of 2% W/V. At this concentration the dextran produced by the batch system would be predominantly above $1x10^{6}$

MW. If the results of Monsan and Lopez [84] and Edwards [79] were correct the molecular weight of the dextran leaving the bioreactor would have been far lower than this because the dextran molecules would have been removed from the reactor system before chain growth could continue. The molecular weight distribution obtained from the bioreactor can be found in table 7.2.

The initial flux decline was as anticipated, during the first hour of the experiment the flux dropped by two thirds of its original value (measured at the beginning of the experiment). After one hour the rate of decline had dropped significantly but the flux still continued to fall. See figure 7.8.

The analysis of the permeate product identified the reason for the flux decline. The sucrose concentration typically increased for the first hour but then began to fall until it reached a low steady state value, while the fructose concentration would rapidly increase as the experiment proceeded. See figures 7.9 and 7.10. However no dextran was found in any permeate sample taken, the dextran was therefore accumulating within the central cell. Clearly as the amount of dextran in the cell increased it caused the flux to decline still further.

When the central cell containing the enzyme was split it was clear what had happended. The enzyme and the dextran produced during the experiment were present as a gel on the surface of the second membrane. The gel was relatively solid and could only be removed by scraping it off the membrane surface.

These experiments were repeated at sucrose concentrations of 4% and 10% W/V. At the higher concentrations the flux decreased faster than at the lower concentrations. In all cases the dextran was retained within the central cell, at the higher concentrations the mass of dextran produced increased which explained the faster flux decline.

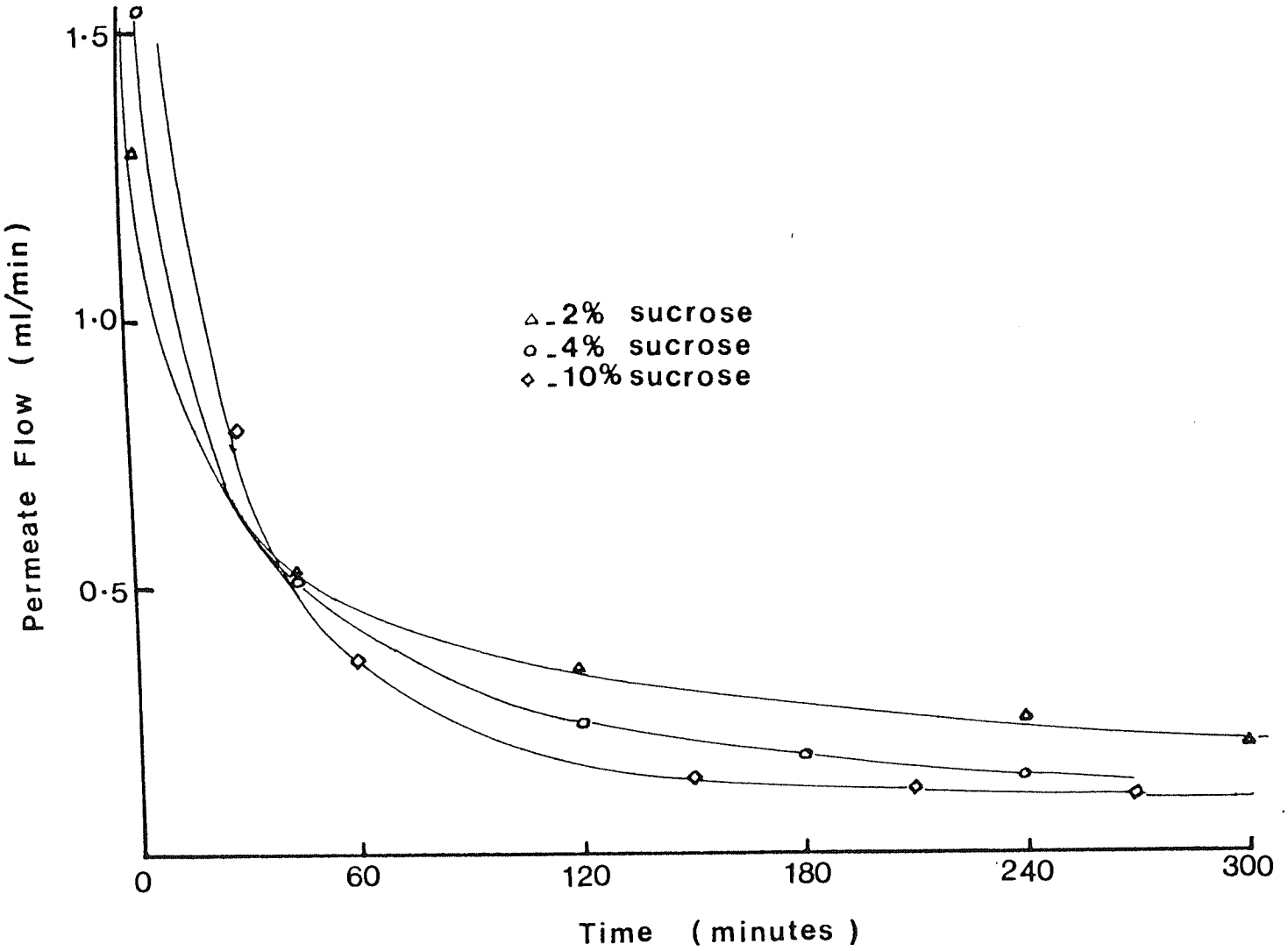

Figure 7.8 Permeate Flow Rates from the Bioreactor

In every experiment the membranes used were completely retentive to the dextransucrase enzyme.

Initially it was felt that the retention of the dextran within the central cell was caused by the high residence times in the reactor allowing the dextran chains to grow to a molecular weight too large to pass through the XM50 membrane. Although this would be true to some degree it did not explain why dextran molecules as small as 20,000 MW found in the central cell did not pass through the membrane. This was even more surprising when it was realised that the majority of the enzyme was found within the gel layer on the face of the second membrane, so the majority of the reaction must have occurred at the membranes surface.

It it probable that these small dextran molecules were attached to the dextransucrase enzyme and so were unable to leave through the membrane. Robyt [82] commented that the chain growth was normally only terminated when an acceptor molecule attached itself to the active site of the enzyme. This would suggest that at low fructose concentrations the growing dextran molecules would not be released from the enzyme until they were very large. Monsan and Lopez [84] would not have observed this effect in their work simply because they were looking exclusively at the batch system and the dextran would have been released once they denatured the enzyme prior to analysis. Edwards [79] found that at different recirculation rates through his reactor different molecular weight dextrans were produced. This would have been caused by the shear forces exerted on the enzyme resulting in the premature release of the dextran molecule. Since the flux through the central cell of our bioreactor was low then the shear forces present would have been insufficient to cause the release of the dextran.

Unfortunately insufficient time was available to continue an experimental investigation into this problem. A further survey of the literature has shown an approach which could solve this problem. It was mentioned earlier that the presence of acceptor molecules could significantly effect the molecular weight of the dextran produced, since these molecules caused the release of the growing dextran chains from the enzymes active site. Alsop [83] investigated the effect of maltose and low molecular weight dextran (T5) on the growth of the dextran chains. Alsop found that the molecular weight of the final product was far lower when these materials were added. Alsop showed that the effect of these molecules was very predictable and that repeatable results could be obtained. Alsop was also able to show that the greater the amount of acceptor used the smaller the amount of high molecular weight dextran present.

Using these molecules in the bioreactor system could help to separate the dextran from the enzyme molecules and therefore allow the dextran molecules to pass through the membrane.

Although the bioreactor was not operating as anticipated the bioreactor was successfully removing the fructose from the reaction system. Zafer [113] had showed that if the fructose was removed from the reaction system the molecular weight of dextran produced increased. At the low sucrose concentrations of 2% and 4% W/V the bioreactor gave some marginal improvements in the molecular weight distribution. At these concentrations the fructose concentration is normally very low and its effect on the chain growth would be limited, therefore at best only small improvements could be expected. When a 10% sucrose feed was used the amount of dextran above 10^6 MW was less than the batch system, even though the fructose concentration in the bioreactor cell was typically less than half that of the batch system. This apparent anomaly can be simply explained. As mentioned earlier the majority of the enzyme was

located in the gel layer on the face of the second membrane. Since the reaction occurred in this region it was probable that the localized concentration of the fructose was far higher than in the bulk solution. This problem would be more apparent at the higher sucrose concentration because the rate of fructose production would have been far higher and would have probably exceeded the rate of removal through the membrane.

To improve the operation of the bioreactor cell some redesign will be required. The main problem with the design was the stagnant middle reactor cell which resulted in excessive concentration polarization. Ideally a magnetic stirrer could be incorporated into the cell or the enzyme solution could be continually recirculated by pumping enzyme feed into and out of the central cell. Although these ideas would solve the problem they would be very difficult to apply in practice since the central cell was only 6 mm deep. The only practical alternative would be to significantly reduce the amount of enzyme solution present in the cell, probably to below 0.5 DSU/cm^3. To reduce the pressure drop across the cell and to reduce the residence time in the cell, the cell depth should also be reduced to 3 mm or less.

Table 7.2 Molecular Weight Distributions of Dextran Produced in the Batch and Bioreactor Systems

Run Number	% below 10^5 MW	% between 10^5 to 10^6 MW	% above 10^6 MW
2% Sucrose Batch	2.06	11.56	86.38
1	3.59	10.18	86.23
2	3.72	11.29	84.99
3	2.91	8.2	88.89
4% Sucrose Batch	5.09	8.16	86.75
4	2.03	6.24	91.73
10% Sucrose Batch	7.38	7.95	84.67
5	13.27	12.08	74.65
6	4.52	15.75	79.73
7	11.95	7.81	80.24

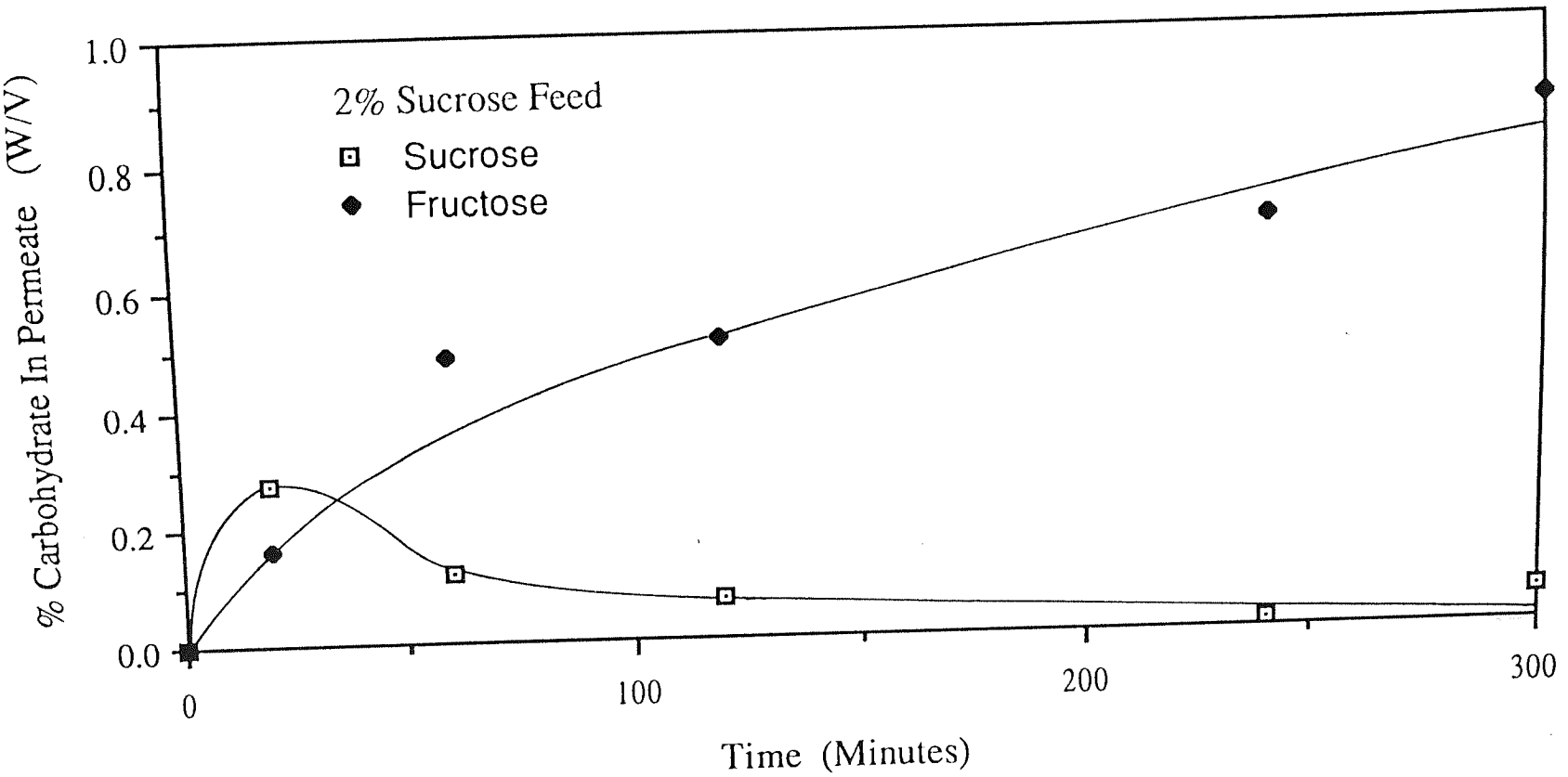

Figure 7.9 Concentrations of Sucrose and Fructose in the Permeate from the Bioreactor

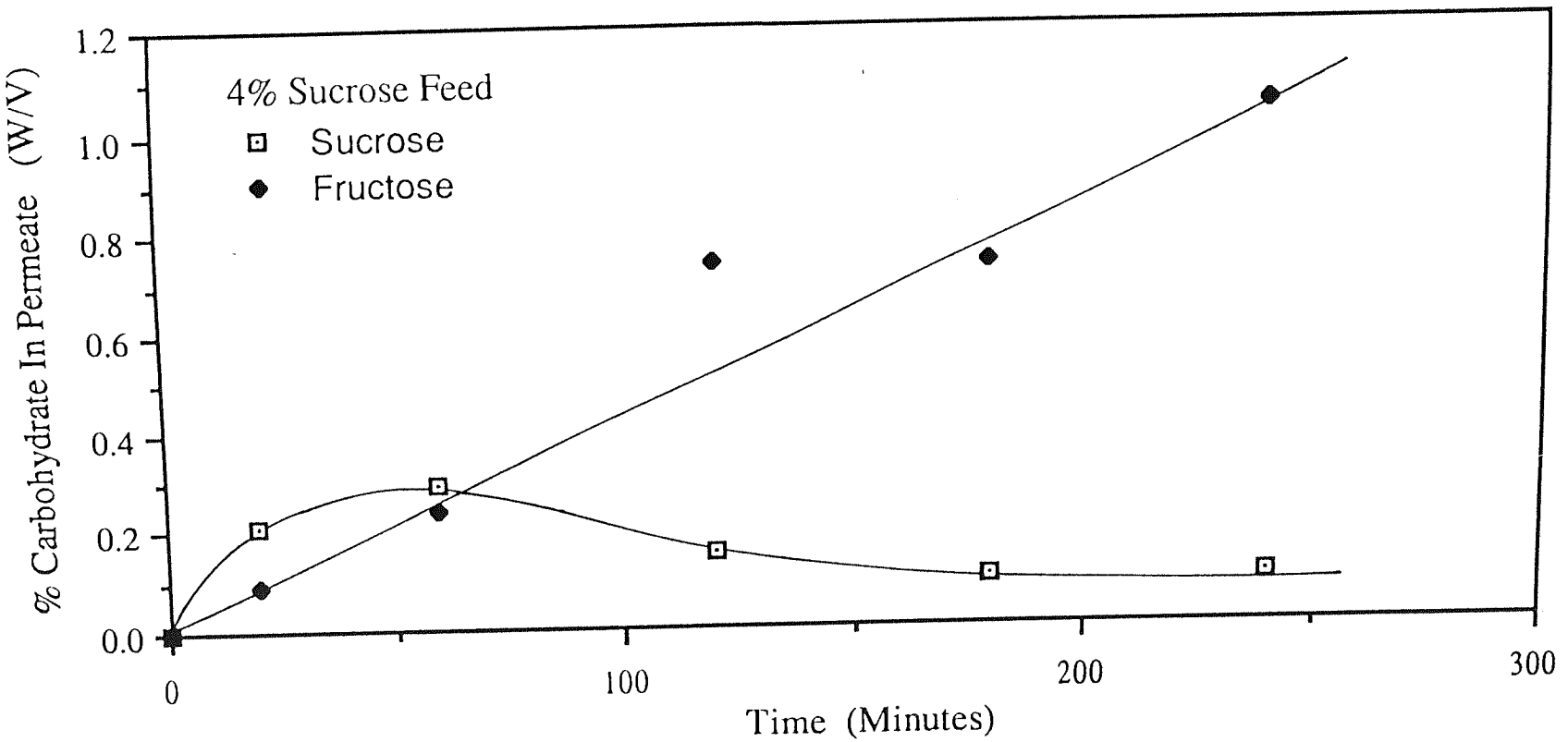

Figure 7.10 Concentrations of Sucrose and Fructose in the Permeate from the Bioreactor

7.8 CONCLUSIONS

This work has shown the problems involved with the development of an ultrafiltration bioreactor system for the dextransucrase enzyme.

Of the three designs of bioreactor considered only the membrane sandwich design showed any potential. Both gel layer immobilization and immobilization onto the porous substruction of the membrane gave very low enzyme activities and gave low fluxes.

The membrane sandwich bioreactor showed that the enzyme could be successfully immobilized, although several unexpected problems limited its operation. The most important of these being the retention of the dextran molecules. This problem was probably the result of the dextran chains being associated with the very much larger enzyme molecules, and to some degree the high residence time in the central cell. Although extensive research is required to solve this problem the most promising approach is to use maltose or low molecular weight dextran to encourage termination of chain growth and the release of the dextran molecules from the enzyme.

The use of these acceptor molecules must also be complemented by the redesign of the bioreactor to reduce the residence time in the cell. Finally the enzyme concentration must also be lowered to reduce the effect of concentration polarization in the central cell.

8.0 CONCLUSIONS AND RECOMMENDATIONS

8.0 CONCLUSIONS

THE REMOVAL OF DEXTRAN WITH A MOLECULAR WEIGHT BELOW 12,000 MW

Batch Diafiltration Studies

1) The batch studies performed on the Amicon membranes showed the limitations of the present manufacturing and quality control procedures. Although the H1P10-20 hollow fibre membranes obtained from Amicon had the same nominal molecular cut-off, the rejection curves obtained from these membranes varied dramatically. The same variation was found when the Amicon H1P5-20 membranes (with a nominal molecular weight cut-off of 5000 MW) were tested.

2) The performance of the Amicon 10,000 MW cut-off membranes were disappointing. When using diafiltration these membranes gave a greater removal of dextran below 12,000 MW for a given number of diavolumes than the Amicon 5000 MW cut-off membranes. However the retention of the 'saleable' 12,000 MW to 98,000 MW band was lower. For example after two diavolumes all the 5000 MW cut-off membranes had a rejection of 90% at 18,000 MW, while only one 10,000 MW cut-off membrane had reached a 90% rejection by 40,000 MW (excluding membrane number 4).

3) Both the 5000 MW and 10,000 MW cut-off membranes could be used to obtain the correct BP specification below 12,000 MW, but the 5000 MW cut-off membranes gave an efficiency of retention 15% higher than the 10,000 MW cut-off membranes.

4) The Amicon 5000 MW cut-off membranes gave a higher efficiency of retention but required between 10 to 12 diavolumes to achieve the correct BP specification. This would not be practical on an industrial scale since large volumes of sterile water would be required and an equivalent volume of waste product would be produced. The waste product would require effluent treatment before it could be disposed of.

5) The operation of the cascade was found to be effected by a number of factors.

Membrane order. Changing the position of membranes within the ultrafiltration cascade had a significant effect on the final dextran product. This could be attributed to the relative importance of each stage within the cascade. Stage one was the most critical stage within the cascade since material lost from this stage was lost from the cascade. Typically the shape of the rejection curve from the cascade mirrored the rejection curve of the membrane placed in stage one. Placing a 'tight' membrane in stage one gave a higher retention of the 'saleable' 12,000 MW to 98,000 MW band since this aided recapture of this material and reduced losses from the cascade.

Stage four was critical since the majority of the fractionation occurred in this stage, this was simply because fresh diafiltrate was introduced into this stage.

Individually the two middle stages had far less effect on the final product from the cascade. Their main function within the cascade was to enhance retention above the cross-over point and removal below the cross-over point. If a 'tight' membrane was placed in either of the central stages it caused accumulation within that stage, this was generally a disadvantage since it reduced the cascades ability to fractionate the dextran feed.

Several general rules were found. The cross-over point varied according to the membrane order used. The efficiency of removal and retention were also dependant on the membrane order used. Placing a 'tight' membrane in stage one increased the efficiency of retention but also lowered the value of the cross-over point and hence lowered the efficiency of removal. Placing a 'tight' membrane in stage four

generally caused a poorer fractionation and impaired the recycle effect of the cascade.

Number of diavolumes used. As the number of diavolumes used increased the cascade operating line rapidly diverged from that of the batch. This confirmed that the recycle effect predicted for the cascade was indeed occurring.

Concentration. The concentration of the dextran feed had a significant effect on the fractionation achieved by the cascade. The efficiency of removal below 12,000 MW was significantly lower when a 4% W/W feed solution was used rather than the normal 2% W/W concentration. This effect was probably caused by two factors.

i) The inability of the diafiltrate to remove the greater mass of low molecular weight material present. (The same number of diavolumes were used at both concentrations).

ii) The presence of a gel layer which could have effected the rejection characteristics of the membranes.

6) The ultrafiltration cascade was shown to make far better use of solvent than the batch system, for example using 2 diavolumes per stage (using four 10,000 MW cut-off membranes - run 2.4) gave an efficiency of removal only slightly less than the batch system using four diavolumes. The cascade also gave a higher efficiency of retention.

7) The 10,000 MW cut-off Amicon membranes gave better results when used in the cascade than the 5000 MW cut-off membranes. Although the 5000 MW cut-off membranes gave a higher efficiency of retention, the cross-over point produced by these membranes fell between 5000 MW to 6000 MW. This naturally impaired the efficiency of removal. The 10,000 MW cut-off membranes gave a cross-over point of between 9000 MW and 12,000 MW depending on the membrane order used.

Mixing the 5000 MW and 10,000 MW membranes within the cascade gave a higher efficiency of retention but in all cases lowered the value of the cross-over point and hence lowered the efficiency of removal.

8) The main advantage of the diafiltration cascade was to give a significantly enhanced removal below the cross-over point. Generally the enhancement below the cross-over point was more significant than that above it. This was expected since the objective of diafiltration is to aid removal of material by 'washing' low molecular weight material through the membrane.

9) The ethanol fractionation process currently used industrially is a complex process requiring 5 or more steps to achieve the correct BP specification. In comparison a single four stage cascade could achieve the same specification below 12,000 MW by using 2.5 diavolumes per stage. The product specification achieved using ethanol fractionation also appears to be relatively unpredictable, while the product specification from the cascade could be easily altered by varying the number of diavolumes used.

Although the efficiency of the ultrafiltration cascade came close to that obtained from the ethanol fractionation process, it is unable to improve on this system.

When it is understood that the ethanol fractionation process has been used for many years and a great deal of research had been performed to optimise its efficiency then the results obtained from the ultrafiltration cascade must still be considered relatively impressive. The only factor limiting the performance of the ultrafiltration cascade was the poor quality of the 10,000 MW cut-off membranes currently available. Once these membranes are improved then it is likely that the ultrafiltration cascade could replace the ethanol fractionation process.

THE REMOVAL OF DEXTRAN WITH A MOLECULAR WEIGHT ABOVE 98,000 MW

Batch Studies

10) The batch studies using the Amicon H1P100-20 (100,000 MW nominal molecular weight cut-off) membranes and the Romicon HF1-43-PM50 membranes (50,000 MW nominal molecular weight cut-off) showed conclusively that both membranes could be used to remove material above 98,000 MW. However it was clear that the Romicon membranes were better than the Amicon membranes for this batch fractionation. For example after four diavolumes the Amicon membrane (number 1) had retained only 42% of the high molecular weight material compared to over 80% for the Romicon membrane (number 3).

The diafiltration mode of operation was found to give a better separation below 98,000 MW while the concentration mode typically gave a higher efficiency of retention above 98,000 MW.

11) An hybrid process was considered which combined a diafiltration stage with a concentration step. The efficiency of removal and retention for this process was little different from the diafiltration system but the concentration of the waste product was far higher, making storage and disposal easier. The concentration of the purified material was also marginally higher.

12) The concentration of the feed solution was found to have a very significant effect on the efficiency of the batch diafiltration process. Although the efficiency would be expected to change because the diafiltrate would be unable to compensate for the greater mass of material present, there was some indication that the presence of a gel layer was effecting the rejection of the larger molecules.

13) The recirculation rate was found to have an effect on the rejection of the dextran molecules. Increasing the recirculation rate from 1 litre/minute to 7 litre/minute noticably increased the rejection of the dextran molecules. The degree of enhancement was strongly dependant on the molecular weight of the dextran molecule, the greater the molecular weight the greater the effect.

14) In total four Romicon and two Amicon membranes were purchased and tested. The four Romicon membranes all had the same nominal molecular weight cut-off as did the two Amicon membranes. The rejection curves obtained for these membranes exhibited the same degree of variation that was found with the Amicon 5000 MW and 10,000 MW cut-off membranes. This would appear to confirm that this was a common problem with all current commercial membranes.

Ultrafiltration Cascade Studies

15) During this work further factors were identified which effected the operation of the cascade.

Number of stages used. The number of stages used in the cascade had a pronounced effect on the composition of final retentate product. Increasing the number of stages increased the removal of dextran below the cross-over point, for example the percentage below 12,000 MW in the final retentate product dropped from 6.7% when two stages were used to 1.3% when four stages were used. The efficiency above the cross-over point was also improved but this was not as significant.

The composition of the dextran feed. Increasing the amount of low molecular weight material present (with a molecular weight below 12,000 MW) significantly altered the rejection characteristics of the cascade. Although the amount of dextran with a molecular weight above 98,000 MW was almost identical its retention markedly increased from 70% to 80%.

This confirmed the results of Cooper [48] and Bottino [44] who found similar trends in the batch system.

16) The batch ultrafiltration system was shown to require at least 4 diavolumes to satisfactorily separate the material with a molecular weight below 98,000 MW. Since the permeate contained the final purified product it would require concentrating before further processing could continue. The ultrafiltration cascade reduced the volume of diafiltrate required, so the final permeate product from the cascade could probably be used without any concentration.

17) The Romicon membranes were very efficient at removing the dextran above 98,000 MW, up to 96% could be removed in a single pass through the cascade. The separation of the 12,000 MW to 98,000 MW band was impaired since the cross-over point fell between 40,000 MW and 60,000 MW depending upon membrane order used. Using the Amicon membranes raised the value to the cross-over point but far more dextran above 98,000 MW was lost in the permeate (23% lower efficiency of retention). The Amicon membranes could therefore not be considered a satisfactory alternative to the Romicon membranes.

18) This work confirmed that varying the membrane order varied the position of the cross-over point, but increasing the number of diavolumes used did not. The cross-over point was found to vary as the number of stages was increased, however this was more likely caused by the the varying performance of the additional membranes rather than the operation of the cascade.

19) The enhancement achieved above the cross-over point was far more significant than anticipated. An unsteady state study of the cascade showed that the first stages of the cascade were being saturated by material removed from the retentate stream further along the cascade. This effect was more pronounced when the 50,000 MW and 100,000 MW cut-

off membranes were used since a larger proportion of the molecular weight distribution was found in the permeate stream and hence the concentrations found in this stream were far higher. The greater presence of this material would cause the rejection of the larger dextran molecules to be enhanced in a similar manner as was found by Cooper [48] and Bottino [44].

20) When compared to the ethanol fractionation process the cascade results were again encouraging, but because a suitable membrane could not be obtained to optimise the removal of the 12,000 MW to 98,000 MW band the cascade was at a disadvantage. Again the successful operation of the ultrafiltration cascade was hampered by the quality and limited range of membranes available from the major manufacturers.

MATHEMATICAL MODELLING

The models ability to predict the removal of the dextran below 12,000 MW was found to be satisfactory. The main assumption that the membranes rejection was uneffected by the action of the cascade would appear to be reasonable in this case. The model was most successful at predicting the results obtained when the 10,000 MW cut-off membranes were used. The model correctly predicted the effect of changing the membrane order and also how the number of diavolumes effected the efficiency of removal and retention.

The relative importance of each stage was also predicted correctly by the model.

The results for the mixed membranes experiments were more difficult to predict correctly. It was probably that the 5000 MW cut-off membranes caused material to accumulate within the stage in which they were placed, simply because they had a higher rejection than the other membranes. This effect was predicted by the model and if present would

alter the rejection characteristics of the membranes involved. With one or two exceptions the predictions were normally within 10% of the experimental results.

When the model was adapted to predict the removal of dextran above 98,000 MW the model was found to consistently over-predict the amount of material lost through the membrane. Typically the model under predicted the efficiency of retention above 98,000 MW by 12%. This consistent under prediction suggested that the constant rejection assumptions cannot be as valid in this case. The removal of the high molecular weight dextran involved a far more complex system, where widely varying concentrations and molecular weight distributions were involved. This was naturally a far more difficult situation to model correctly.

THE DEXTRANSUCRASE ENZYME BIOREACTOR

The experiments conducted showed that the dextransucrase enzyme could be easily contained by using an ultrafiltration membrane.

Three types of enzyme bioreactor were examined:

(i) gel layer immobilization

(ii) immobilization into the porous substructure of the membrane

(iii) immobilization inbetween two membranes

Both method (i) and (ii) suffered from low enzyme activity and low flux which made them ineffective and research was discontinued.

The immobilization between two membranes overcame the problem of low activity but suffered from several unexpected problems. The dextran product which was expected to leave the reaction cell in the permeate stream was completely retained within the cell, even though some of the molecules had a molecular weight below the nominal molecular weight cut-off of the XM50 membrane. Although the problem was partly caused by the

residence time in the reactor cell, the main problem was that the dextran molecules were attached to the enzyme making it impossible for them to leave though the membrane.

At low sucrose concentrations there were indications that the removal of the fructose from the bioreactor increased the molecular weight of the dextran product. However at high concentrations the rate of fructose production was higher than the rate of removal through the membrane. This resulted in high localized fructose concentrations at the membrane surface which reduced the amount of high molecular weight dextran present (compared to the batch system).

RECOMMENDATIONS

The future of this product should include:

(a) Linking the removal of material below 12,000 MW with the removal of material above 98,000 MW in a dual cascade system. The cascade should also be scaled up to a small pilot plant scale with a 5 litre retentate volume compared to the present 1 litre volume. This would allow the potential problems of scale up to be investigated. The cascade should also be able to operate up to four diavolumes per stage, making it possible to obtain the BP specification using a single pass through the cascade.

(b) Further investigation is required to find membranes more suitable for this particular fractionation. Ideally membranes should be manufactured specifically for this application, although it is unlikely that any company will do this.

(c) The diafiltration cascade system should be used with a wider range of feed stocks. Other potential separations include:

(i) Separation of salts and other low molecular weight impurities from dextrins.

(ii) Purification of enzyme solutions - removal of low molecular weight impurities and aiding the retention of the enzyme. For example the dextransucrase enzyme.

(iii) Purification of high cost pharmaceuticals such as Monoclonal antibodies and hormones.

(d) Work is also required to see if the ultrafiltration system can be maintained as a sterile environment. This is a critical factor since medical products are involved.

(e) To improve the accuracy of the mathematical model the assumption of a constant rejection should be abandoned and should be replaced with empirical equations, expressing how the rejection changes with concentration and molecular weight distribution.

(f) The bioreactor requires extensive work if it is to operate successfully. The main problem to overcome is the retention of the dextran product within the reactor cell. The most promising route appears to be the use of either low molecular weight dextran or maltose as an acceptor. These molecules terminate chain growth by releasing the chain from the enzyme molecule. The bioreactor cell should also be redesigned, the central reactor cell should be made thinner to reduce the pressure drop across the cell and to reduce the residence time in the central cell. Furthermore using a more dilute enzyme solution should reduce concentration polarization in the reactor cell and so further reduce the residence time.

REFERENCES

1 SCHEIBER C, Rudenzuker Ver Ind, 24 (1874) p309

2 NILSSON K, SODERLUND G Clinical Dextrans. Specification and Quality of Preparation on the Market. Acta Pharmaceuticals Suec, 15 (1978) p439-454

3 FOSTER FH Dextran - Manufacture and Use. Part 1. Process Biochem, February (1968) p15-19

4 FOSTER FH Dextran - Manufacture and Use. Part 2. Process Biochem, March (1968) p55-62

5 VLACHOGIANNIS GJ Dextran Polymer Fractionation by Production Scale Chromatography and Ultrafiltration. PhD Thesis, University of Aston in Birmingham, 1982

6 POLAND KR The Fractionation of Dextran Polymer by Ultrafiltration to Yield Clinical Products. PhD Thesis, University of Aston in Birmingham, 1986

7 MEARES P Membrane Separation Processes. Elsevier Scientific Publishing Company, Amsterdam (1976)

8 KEDEM O, KATCHALSKY A A Physical Interpretation of the Phenomenological Coefficients of Membrane Permeability. J Gen Physiol, 45, (1961) p143

9 LACEY RE Industrial Processing with Membranes. Robert K Krieger Publishing Company, New York, (1979)

10 RAUTENBACH R, ALBRECHT R Separation by Membranes, Ger Chem Eng, 5, (1979) p329

11 KIMURA S, SOURIRAJAN K Analysis of Data in Reverse Osmosis with Porous Cellulose Acetate Membranes used. AIChE J, 13 (3), (1967) p497-503

12 MICHAELS AS New Separation Techniques for CPI. Chem Eng Prog, 64, p12-31

13 BLATT WF, DRAVID A, MICHAELS AS, NELSON L Solute Polarization and Cake Formation in Membrane Ultrafiltration,Causes, Consequences and Control Techniques. Membrane Science and Technology, Ed Flinn JE, Plenum Press, p47

14 PORTER MC Concentration Polarization with Membrane Ultrafiltration. Ind Eng Chem Prod Res Develop, 11 (3),(1972) p234-248

15 GRAETZ L Ann Phys Chem, 18, (1883)

16 LEVEQUE MA Ann Mines, 13, (1928)

17 DITTUS FW, BOELTER LMK Univ Calif. Publ Engng, 2, (1930) p443

18 VILKER VL, COLTON CK, SMITH KA The Osmotic Pressure of Concentrated Protein Solutions. Effect of Concentration and pH in Saline Solutions of Bovine Serum Albumin. J Colloid Interface Sci. 79, (1981) p548

19 CLIFTON MJ, ABIDINE N Growth of the Concentration Polarization Layer in Ultrafiltration with Hollow Fibre Membranes. Submitted for Publication in J Mbr Sci.

20 WIJAMS JG, NAKAO S, VAN DEN BERG JWA Hydrodynamic Resistance of Concentration Polarization Boundary Layer in Ultrafiltration. J Mbr Sci. 22 (1985) p117-135

21 COLTON CK, FRIEDMAN S, WILSON DE, LEE SM Ultrafiltration of Lipoproteins through a Synthetic Membrane. J Clin Inv, 51, (1972)

22 STRATHMANN H Membrane Separation Processes. J Membrane Science 9, (1981), p121-189

23 JOHNSON JD Reverse Osmosis Membrane. Research Ed HK Lonsdale and HE Podall. Plenum Press, NY, (1973)

24 NAKAO S, YUMOYO D, KIMURA S Analysis of Rejection Characteristics of Macromolecular Gel Layer for Low Molecular Weight Solutes in Ultrafiltration. J Chem Eng Jpn, 15 (6), (1982) p463-468

25 JAGUR-GRODZINSKI J, KEDEN O Transport Coefficient and Salt Rejection in Uncharged Hyperfiltration Membranes. Desalination, 1, (1966) p327

26 FANE AG Factors Effecting Flux and Rejection in Ultrafiltration. J Separ Proc Technol, 4(1), (1983) p15-23

27 CHANNABASPPA KC Need for New and Better Membranes. 18, p15 (1976)

28 WANG SS, DAVIDSON B, GILLESPIE C Nippon Shokukin Kogyo Gakkaish, 26 (6), p260

29 MATHIASSON E The role of Macromolecular Adsorption in Fouling of UF Membranes. J Membr Sci, 16, (1983) p23

30 ZEMAN JL Adsorption Effects in Rejection of Macromolecules by Ultrafiltration Membranes. J Membr Sci, 15, (1983) p213-230

31 ZEMAN L, WALES M Steric Rejection of Polymeric Solutes by Membranes with Uniform Pore Size Distribution. Separation Science and Technology, 16 (3),(1981), p275-290

32 ZEMAN L, WALES M Polymer Solute Rejection by Ultrafiltration Membranes. Synthetic Membranes Vol 2 (Hyper and Ultrafiltration Uses) Ed AF Turbak (1980) p411-434

33 FERRY JD Ultrafiltration Membranes and Ultrafiltration. Chem Rev, 18, (1936) p373-448

34 LONG TD, JACOBS DL, ANDERSON JL Configuration Effect on Membrane Rejection, J Membr Sci, 9 (1981) p13-27

35 MUNCH DW, ZESTER LP, ANDERSON JL Rejection of Polyelectrolytes from Microporous Membranes, J Membr Sci, 5 (1979) p77

36 DE GENNES PG Coil Stretch Transition of Dilute Flexable Polymers Under Ultrafiltration Velocity Gradients. Journal of Chemical Physics, 60 (12), (1976), p5030-5042

37 DE GENNES PG Dynamics of Entangled Polymer Solutions. The Rouse Model. Macromolecules, 9, (1976) p587

38 DAOUDI S, BROCHARD F Flow of Flexable Polymer Solutions in Pores. Macromolecules. 11 (1978) p751-758

39 EDWARDS SF The Statistical Mechanics of Polymerized Material. Proc Phys Soc, 92, (1967), p9-16

40 QUANG TRONG NGUYEN Characterization of UF Membranes. Part IV. Influence of the Deformation of Macromolecular Solutions on the Transport Through Ultrafiltration Membranes. J Membr Sci, 14, (1983), p111-128

41 ARTURSON G, GRANATH K Dextran as Test Molecules of the Functional Ultrastructure of Biological Membranes. Clin Chim Acta, 37, (1972), p309-322

42 BRODZEK M Physico-Chemico Characterization of Ultrafiltration Membrane. Polish Journal of Chemistry, 56, (1983), p919-930

43 BAKER RW, STRATHMANN H Ultrafiltration of Macromolecular Solution with High Flux Membranes. Journal of Applied Polymer Science, 14, (1979), p1197-1214

44 BOTTINO A, CAPANNELLI G, IMPERATO A, MUNARI S Ultrafiltration of Hydrosoluble Polymers. Effect of Operating Conditions on the Performance of the Membrane. J Membr Sci, 21, (1984), p247-267

45 BARKER PE, ALSOP RM, VLACHOGIANNIS GJ Fractionation, Purification and Concentration of Dextran Solutions by UF. J Membr Sci, 20, (1284), p79-91

46 EDBERG SC, BRONSON PM The Fractionation of Hydrolysed Dextran by UF through a Series of Anisotropic Cellulose Acetate Membranes. Preparative Biochemistry, 1 (3) (1971), p249-257

47 PORTER MC, MICHAELS AS Membrane Ultrafiltration. Chem Technol, 1, (1971), p56-63

48 COOPER AR, VAN DER VEER DS Ultrafiltration Membrane Characterization. 2nd World Filtration Congress, (1979), p455-461

49 COOPER AR, PETTINGILL DB Improved UF Processes by Partial Recycle of Ultrafiltrate. J Membr Sci, 15, (1983), p3-13

50 BAKER MW Methods of Fractionating Polymers by Ultrafiltration. Jounal of Applied Polymer Science, 13, (1969), p369-376

51 TUTANJIAN RS, RETI AR Molecular Fractionation by Staged Ultrafiltration. AIChE Symp Ser, 74 (1978), No 178, p210-216

52 WARD R, KLEIN E, FELDHOLF PW Ultrafiltration Separation Enhancement by Counter Current Cascading. J Membr Sci, 33 (1987) p97-111

53 MITROVIC M, RADOVANOVIC FR, KNEZIC L Dual Membrane Separation. I. Stage Wise Dual Separation. The Chemical Engineering Journal, 28 (1984) p53-57

54 KINOSHITA M, NARUSE Y Improvement of the Mathematical Simulation Model for a Multicomponent Separation Cascade. Nucl Science and Eng, 82 (4) (1982), p469-75

55 GRUZDEV EB, LAGUNTSOV NI A Method of Calculating Membrane Element Cascades for Separation Multi Component Mixtures. Atomnaya Energiya, 54 (1984) p205-232

56 ASH R, FOLEY T Transcient State Transport in Some Finite Systems. Part 1. A Simple (Two Stage) Cascade. J Membr Sci, 13 (1983) p205-232

57 NODA I, GRYTE C Multicomponent Membrane Separation Processes for the Continuous Fractionation of Solutes Having Similar Permeabilities. AIChE, 27, (1981) p904-12

58 BLATT WF, HUDSON BG A Modified Ultrafiltration Cell for Separating the Products of Proteolysis. Analytical Biochemistry, 22 (1968) p161-165

59 MICHAELS AS, STRATHMAN H Membrane Science and Technology News. Journal of Membrane Science, 15 (1983) p118-119

60 JANDEL AS, HUSTEDT H, WANDREY C European J Appl Microbiol Biotechnol, 15 (1982)

61 RONY RR Multiphase Catalysis II. Hollow Fibre Catalysts. Biotech Bioeng, Vol XIII p431-447 (1971)

62 RONY PR Hollow Fibre Enzyme Reactors. J Am Chem Soc, 94 (1972) p8247

63 KITANO H, YOSHIJIMA S, ISE N Kinetic Study of a Hollow Fibre Enzyme Reactor. Biotech Bioeng, Vol XXII pp2643-2653 (1980)

64 KATOAKA H, SAIGUSA T, MAKATUKA S The Effect of Axial Dispersion and Mass Transfer Resistance on Conversion in a Hollow Fibre Enzyme Reactor. J Ferment Technol, 58 (1980) p438

65 KLEI HE, SUNDSTROM W, COUGHLIN RW Hollow Fibre Enzyme Reactors in Cellulose Hydrolysis. Biotech Bioeng Sym, No 11 p593-601 (1981)

66 DAVIS J Kinetic Studies in a Continuous Steady State Hollow Fibre Membrane Enzyme Reactor. Biotech Bioeng, Vol XVI p1113-1122 (1974)

67 KAN JK, SHULER ML Urocanic Acid Production Using Whole Cells Immobilized in a Hollow Fibre Reactor. Biotech Bioeng, Vol XX p217-230 (1978)

68 MICHAELS AS Membrane Technology and Biotechnology. Desalination. 35 (1980) p329-351

69 REED I, DUDLEY L Adsorption of Proteins by Membranes. Biosep Report, 1985

70 KORUS RA, OLSON AC The Use of -Glactosidase in Hollow Fibre Reactors. Biotech Bioeng, Vol XIX p1-8 (1977)

71 BRESLAU BR, KILCULLEN BM Hollow Fibre Enzymic Reactors, An Engineering Approach. Third International Conference on Enzyme Engineering, Portland Oregon, 1975

72 CAPOBIANCO G, DRIOLI E A Study of Gelled Enzyme Ultrafiltration Reactors. Journal of Solid Phase Biochemistry, 2 (4), (1977) p315-328

73 DRIOLI E, SCARDI V Ultrafiltration Processing With Enzyme-Gel Composite Membranes. Journal of Membrane Science, 1 (1976) p237-248

74 CAPOBIANCO G, DRIOLI E, ROSSI M, Malic Enzyme Immobilization in Continuous Capillary Membrane Reactors. Journal of Membrane Science, 22 (1985) p317-324

75 DRIOLI E, GIANFREDA L, PALESCANDOLO R The Kinetic Behaviour of Enzymes Gelified on Ultrafiltration Membranes. Anal Control. Immobilized Enzyme Systems Proc Int Symp Meeting, (1975) p179-186 pub 1986

76 GRECO G, SCARDI V Experimental Techniques for Multilayer Enzyme Immobilization. Biotech Bioeng, Vol XXII p215-219 (1980)

77 STAUDE E, JORISCH W, ANSORGE W Reactions with Enzyme Covalently Bonded to Hetrogeneous Ultrafiltration Membranes. Journal of Membrane Science, 11 (1982) p289-296

78 GREGOR HP, RAUF RW Enzyme Coupled Ultrafiltration Membranes. Biotech Bioeng, Vol XVII (1975) p445-449

79 EDWARDS CR, DREW SW Immobilized Dextransucrase Isolated From Leuconostoc Mesenteroides. Abstr Annual Meeting Am Soc Microbiol, 77 (1977)

80 MELDRUM A Hollow Fibre Membrane Bioreactors. The Chemical Engineer, Oct 1988 p28-31

81 DRIOLI E, IORIO G, DE ROSA M High Temperature Immobilized-Cell Ultrafiltration Reactors. Journal of Membrane Science, 11 (1982) p365-370

82 ROBYT JF, EKLUND S Stereochemistry Involved in the Mechanism of the Action of Dextransucrase in the Synthesis of Dextran and the Formation of Acceptor Products. Bioorganics Chemistry, 11 (1982) p115-132

83 ALSOP RM Industrial Production of Dextrans Process in Industrial Microbiology. Ed Bushell ME, Elsevier Press (1983) p1-45

84 MONSAN P, LOPEZ A Dextran Production by Free and Immobilized Dextransucrase. Adv Biotech, 1 (1981) p679-684 Pergamon Press

85 BRASWELL E, GOODMAN A, STERN KG Studies on the Enzyme Synthesis of Dextrans. Part II, I Polym Sci, 61 (1962) p143-154

86 BOVEY FA Enzyme Polymerization I. Molecular Weight and Branching During the Formation of Dextran. J Polym Sci, 35 p138-204

87 KABOLI H, REILLY PJ Immobilization and Properties of Leuconostoc Mesenteroides Dextransucrase. Biotech Bioeng 22 (1980) p1055-1069

88 KABOLI H, CHAN YE Properties of Soluble and Immobilized Dextransucrase. Biotech Bioeng, 23 (1981) p1-10

89 MONSAN P On the Production of Dextran by Free and Immobilized Dextransucrase. Biotech Bioeng, 23 (1981) p2027-2037

90 LOPEZ, MONSAN P Dextran Synthesis by Immobilized Dextransucrase. Biochemie, 62 (1980) p323-329

91 HOSTETTLER F, BOREL E Uber Die Reduktion Der 3,5 - Dinitrosalicylsaure Durch Zucker. Helv Chem Acta, 34 (1951) p2132-2139

92 JACKSON C, STEWARD G Fisons UK, Loughborough. Personal Communication

93 EBERT KH, SCHENK G, Mechanisms of Biopolymer Growth. The Formation of Dextran and Levan. Adv Enzymol, 30 (1968) p179-221

94 TOYA SODA Instruction Manual for TSK PW-XL Gel Permeation Chromatography Columns (1987)

95 YAU WW, KIRKLAND JJ, BLY DD Modern Size Exclusion Liquid Chromatography. Johy Wiley and Sons (1979)

96 HATT BW Polymer Molecular Weight Distribution by Gel Permeation Chromatography. Developments in Science Publ. Essex (1979) p157-199

97 GRABISTIC Z, REMPP R, BENOIT H, A Universal Calibration for Gel Permeation Chromatography. Jon Polym Sci, Part B, 5 (1967) p753-759

98 FRANK FC, WARD IM, WILLIAMS T Calibration Procedure for Gel Permeation Chromatography. Jon Polm Sci, 6 A2 (1968) p1357-1369

99 BALKE ST, HAMIELEC AE Gel Permeation Chromatography Calibration Curve from Polydisperse Standards. Ing Eng Prod Res Dev, 8 (1969) p54-57

100 CERVENKA A, BATES TW Characterization of Polydispersed Branched Polymer by Means of Gel Permeation Chromatography. Jou of Chromatography, 53 (1970) p85-93

101 LANSING W, KRAEMER E A New Method of GPC Calibration Using Dextran Fractions of Low Polydispersity. Jou Am Chem Soc, 57 (1935) p1369-1385

102 McCRACKIN FL Calibration of GPC Columns Using Polydisperse Polymer Standards. Jou Appl Polymer Sci, 21 (1977) p191-198

103 CHAPLIN RP, CHANG W Accurate Calibration of GPC by Use of Broad Molecular Weight Distribution Standards. J Macro Mol Sci Chem, A14 (1980) p257-263

104 MOLOWER EG, MONTANA AJ Algorithm for the Determination of Linear GPC Calibration Curves of a Polydisperse Standard. Jou Polym Sci, Polym Phys Ed, 118 (1980) p2303-2305

105 BHRAMBRA KS The Fractionation of Dextran Using Ethanol. PhD Thesis. University of Aston in Birmingham. 1985

106 HARTLEY HO The Modified Gauss-Newton Method for Fitting of Non-Linear Regression Function by Least Squares. Technometrices 3 (1961) p269-280

107 INSTRUCTIONS MANUAL Differential Refractometer R401, Waters Associates Ltd, Hartford, Cheshire

108 SENTI FR, HELLMAN NN, LUDWIG H Viscosity Sedimentation and Light Scattering Properties of Fractions of an Acid-Hydrolyzed Dextran. Journal of Polymer Science, Vol XVII (1955) p527-546

109 CERNY LC, TIERNAN MC, STASINO DM Dextran: A Branched Polymer and Plasm Expander. J Polymer Sci Symposium, No 42 (1973) p1455-1465

110 JONSSON G Boundary Layer Phenomenon During Ultrafiltration of Dextran and Whey Protein Solutions. Desalination, 51 (1984) p61-77

111 THE HANDBOOK OF PHYSICAL AND CHEMICAL PROPERTIES Weast RC, Astle MS 62nd Edition, CRC Press, p1981-1982

112 GOLDSMITH RL Macromolecular Ultrafiltraton with Microporous Membranes. Ind Eng Chem Fundam, 10 (1), (1971) p113-120

113 ZAFER I Biosynthesis and Separation of Dextran Fructose Mixtures in a Chromatographic Reactor. PhD Thesis. Aston University in Birmingham 1986

114 GANETSOS G The Chromatographic Separation of Carbohydrate Mixtures. PhD Thesis. Aston University in Birmingham (1986)

115 MILLER AW, ROBYT JF Stabilization of Dextransucrase From Leuconostoc Mesenteriodies NRRL B-512F By Non-Ionic Detergents, Polyethylene Glycol and High Molecular weight Dextran. Biochemica at Biophysica Act, 785 (1984) p89-96

116 OPERATING MANUAL Bio Rad Differential Refractometer.

117 SPECTRA PHYSICS AUTOLAB AUTOSAMPLER Basic Operators Manual

NOMENCLATURE

A_s	Asymmetry factor of a GPC column
B	Back diffusion
B_{1-5}	GPC calibration constants
C_B	Concentration of bulk solution
C_{Di}	Concentration of component i in diafiltrate
C_g	Concentration of the gel layer
C_o	Initial concentration of solute
C_{oi}	Initial concentration of component i
C_p	Concentration of solute in the permeate
C_{pi}	Concentration of component i in the permeate
C_t	Concentration of solute at time t
C_{ti}	Concentration of component i in tank
C_{Ri}	Concentration of component i in retentate
C_r	Concentration of solute in retentate
D	Diffusivity of solute (Chapter 2)
D	Polydispersity of a dextran sample (Chapter 3)
dp	Diameter of a membrane pore
F_D	Flow rate of diafiltrate
F_P	Flow rate of permeate
F_R	Flow rate of retentate
F_t	Flow rate from tank
F(V)	Surface area per unit volume
h_i	GPC chromatogram height of component i
J_1	Membrane solvent flux
J_2	Membrane solvent flux
J_v	Total volume of membrane flux
J*	Critical flux
K	Overall mass transfer coefficients

K_c	Carman factor
K_d	GPC distribution coefficients
K_m	Mass transfer coefficient of solute
K_1, K_2	Solute drag coefficients
k_B	Boltzmann constant
L	Length of pore
L_p	Membrane permeability constant
M_N	Number average molecular weight
M_W	Weight average molecular weight
N	Number of monomer units in a polymer chain
NTP	Theoretical number of plates
N_A	Avergadro's number
P	Permeability of solute
P_p	Permeate pressure
R	Rejection coefficient
R_e	Einstein radius
R_F	Flory radius of gyration
R_o	True rejection
R_{perm}	Rejection based on permeate
R_{ret}	Rejection based on retentate
r	radius of membrane pore
r_R	Reptation time
r_Z	Zimm relaxation fequency of a polymer chain
r_2	Solute radius
r_3	Membrane capillary radius
S_c	Kelvin temperature
U	Average velocity
V	Volume of tank
V_o	Initial retentate volume
V	Volume of permeate

V_t	Retentate volume at time t (Chapter 2)
V_o	Void volume
V_R	Elution volume
V_t	Total liquid volume (Chapter 3)
v	Kinematic viscosity
W	Hindrance to convection
$W_{o.5}$	Peak width at one half peak height
X	Thickness of membrane
Y_B	Boundary layer thickness

GREEK LETTERS

ξ	Correlation length
ρ	Density
Γ_2, Γ_3	Virial coefficients
ϵ	Fraction of membrane skin containing pores
η_o	Intrinsic viscosity
μ	Viscosity of solvent
λ	Ratio of solute radius to pore radius
π	Osmotic pressure
θ	Optical rotation
σ	Rejection coefficient
σ	Reflection coefficient (section 2.4.2)
ω	Rotational velocity
ϕ	Sieving coefficient

APPENDIX

APPENDIX 1

Computer program used to calculate the molulecular weight distribution

```
5 REM PROGRAM USED TO CALCULATE THE MOL
10 REM WEIGHT DISTRIBUTION OF A DEXTRAN
12 REM SAMPLE
15 REM      BY A.TILL  1986
17 REM
20 DIM A(400),Z(5),B(170),VIN(170),S(170),S5(170),
MAX(2),AMIN(170)
40 X=0.0
60 PRINT 'RUN A VO-VT ... YES OR NO'
80 INPUT ANS$
100 IF ANS$='YES' THEN X=1 : GOTO 320
120 PRINT 'THEN INPUT TO AND TT'
140 INPUT MAX(1),MAX(2)
150 X=2.0
160 PRINT 'INPUT THE FLOW RATE'
180 INPUT RATE
200 PRINT 'TYPE IN BATCH NUMBER;
220 INPUT KR$
240 PRINT 'TYPE IN DATE'
260 INPUT KP$
280 PRINT 'READY TO START ... TYPE GO'
300 INPUT NUM$
320 I=1:T1=TI:Y=1
340 GOSUB 1570
360 E=TI-T1
380 IF E<120 THEN 360
400 IF Y=5 THEN 460
420 Y=Y+1:T1=TI
440 GOTO 340
460 T1=TI
480 A(I)=(Z(1)+Z(2)+Z(3)+Z(4)+Z(5))/5
500 PRINT 'READING AT';I/6;'MINS =';A(I)/4
520 IF I>=282 THEN 580
540 Y=1.0:I=I+1
560 GOTO 340
580 IF X=1.0 THEN GOSUB 1380
600 IF X=0.0  THEN 150
610 GOSUB 1860
620 GOSUB 2140:GOSUB 2520
640 OPEN1,4
660 OPEN2,4,1
680 OPEN3,4,2
700 F$='999  99999999.99  99999999999999.  9999.99
  99999999.9999  999999.99'
720 PRINT#3,F$
740 PRINT#1,CHR$(1)'BATCH NUMBER :';KR$
760 PRINT#1 : PRINT#1
780 PRINT#1,CHR$(1)'DATE OF ANALYSIS:';KP$
800 PRINT#1:PRINT#1
```

```
820 PRINT#1,'FLOWRATE=';RATE;'ML/MIN'
840 PRINT#1,'     VO=';MAX(1)
860 PRINT#1,'     VT=';MAX(2)
880 PRINT#1,'     VS=';BEGIN
900 PRINT#1,'     VF=';FINISH
920 PRINT#1
940 PRINT#1,'WEIGHT AVERAGE MOL WT ='AARW
960 PRINT#1,'NUMBER AVERAGE MOL WT ='AVMN
1000 PRINT#1.'           MW/MN RATIO ='SPR
1020 PRINT#1:PRINT#1:PRINT#1
1040 HD$='POINT'+'       '+'KD VALUE'+'      '
1060 GH$='MOL WEIGHT'+'      '
1080 FH$='HEIGHT'+'      '+'WT FRAC'+'   CUMM%'
1100 EH$=HD$+GH$+FH$
1120 PRINT#1,,EH$
1140 FOR I=NMAX TO 1 STEP -1
1160 PRINT#2,I,VIN(I),AMIN(I),B(I),S(I),S5(I)
1180 NEXT I
1200 PRINT#1:PRINT#1:PRINT#1
1220 PRINT#1,'ASTON GPC CONSTANTS'
1240 PRINT#1,'       B1=';B1
1260 PRINT#1,'       B2=';B2
1280 PRINT#1,'       B3=';B3
1300 PRINT#1,'       B4=';B4
1320 PRINT#1,'       B5=';B5
1340 CLOSE 1:CLOSE 2:CLOSE 3
1345 GOSUB 3060
1355 GOTO 200
1360 END
1380 REM TO FIND TO AND TT
1400 Z=1.0
1420 FOR I=126 TO 282
1440 IF A(I)<200 THEN 1500
1460 IF A(I)>=A(I-1) THEN MAX(Z)=I/6:GO TO 1500
1480 Z=2.0
1500 NEXT I
1510 PRINT '   '
1520 PRINT 'TO ='';MAX(1);'TT=';MAX(2)
1530 PRINT ' '
1540 X=0.0
1560 RETURN
1570 REM HEIGHTS FROM REWFRACTOMETER
1580 OPEN1,9,15
1600 GET#1,J$,K$
1620 IF K$=' ' THEN K=-224:GOTO 1660
1640 K=ASC(K$)-224
1660 IF K<0 THEN D=(K+32)*-1
1680 IF K>=0 THEN D=K
1700 D=D*256
1720 IF J$=' ' THEN J=0:GOTO 1760
1740 J=ASC(J$)
1760 IF K<0 THEN J=J*-1
1780 Z(Y)=J+D
1800 PRINT Z(Y),Z(Y)/4
```

```
1820  CLOSE 1
1840 RETURN
1850 REM CALC START AND FINISH TIMES
1860 SUM=0.0:NMAX=1.0:SAP=0.0
1870 FOR I=100 TO 270
1880 IF A(I)>SAP THEN SAP=A(I):PEAK=1
1890 IF (I>102) AND (I=<120) THEN SUM=SUM+A(I)/4
1900 NEXT I
1910 MEAN=SUM/18
1920 FOR 1=120 TO PEAK
1930 IF A(I)/4-MEAN>2 THEN S=I:GOTO 1950
1940 NEXT I
1950 FOR I=PEAK+1 TO  282
1955 IF A(I)<0.0 THEN A(I)=0.0:T=I:R=0.0:GOTO 1985
1960 IF (A(I)-A(I+1))/4<0.6 THEN R=A(I+1)/4:T=I+1:
GOTO 1985
1980 NEXT I
1985 B(1)=0.0
1990 FOR I=S TO T
2000 NMAX=NMAX+1
2020 IF PEAK>=I THEN B(NMAX)=A(I)/4-MEAN:GOTO 2050
2040 B(NMAX)=A(I)/4-R
2050 NEXT I
2060 BEGIN=(S-1)/6:FINISH=(T)/6
2120 RETURN
2130 REM CALC OF ELUTION VOLUMES
2140 VIE=RATE*BEGIN
2160 VFE=RATE*FINISH
2180 VI=(VIE-(RATE*MAX(1)))/(RATE*(MAX(2)-MAX(1)))
2200 VF=(VFE-(RATE*MAX(1)))/(RATE*(MAX(2)-MAX(1)))
2220 VH=(VF-VI)/(NMAX-1)
2240 RETURN
2520 REM CALC OF MWD
2540 B1=-14.539:B2=14.233:B3=-10.008:
B4=16.068:B5=-135.503
2560 S1=0.0:S2=0.0:S3=0.0
2580 FOR I=1 TO NMAX
2600 VIN(I)=VI+VH*(I-1)
2620 IF VIN(I)>1.0 THEN 2680
2640 IF VIN(I)<0.0 THEN 2720
2660 AMIN(I)=B5+EXP(B4+B1*VIN(I)+B2*(VIN(I)^2)+
B3*(VIN(I)^3)):GOTO 2740
2680  AMIN(I)=B5+EXP(B4+B1+B2+B3)
2700 GOTO 2740
2720 AMIN(I)=B5+EXP(B4)
2740 S1=S1+B(I):S2=S2+(AMIN(I)*B(I))
2760 S3=S3+(B(I)/AMIN(I)):NEXT I
2780 AAAW=S2/S1
2800 AVMN=S1/S3
2820 SPR=AAAW/AVMN
2840 PRINT 'WEIGHT AVERAGE MOL WT=';AAAM
2860 PRINT 'NUMBER AVERAGE MOL WT=';AVMN
2880 PRINT '                MW/MN RATIO';SPR
```

```
2900 S4=0.0
2920 FOR I=1 TO NMAX:S4=S4+B(I):NEXT I
2940 FOR I=1 TO NMAX:S(I)=B(I)*100/S4:NEXT I
2960 S5(NMAX+1)=0.0
2980 FOR I=NMAX TO 1 STEP -1
3000 S5(I)=S5(I+1)+S(I)
3020 NEXT I
3040 RETURN
3060 PRINT 'IS THE DATA OK ....IF SO TYPE YES'
3080 PRINT 'ELSE PRESS ANY LETTER'
3100 INPUT ROP$
3120 IF ROP$='YES' THEN 3640
3140 FOR I=126 TO 282
3160 OPEN1,4,1
8180 OPEN2,4,2
3200 F$='9999.99     S99999.99     S9999.99'
3220 PRINT#2,F$
3240 PRINT#1,I/4,A(I),A(I)/4
3260 CLOSE1:CLOSE2
3280 NEXT I
3300 PRINT 'DO YOU WISH TO RUN THE '
3320 PRINT 'DISTRIBUTION YOURSELF IF SO '
3340 PRINT 'INPUT ANY LETTER , ELSE TYPE'
3360 PRINT 'NO'
3380 INPUT POP$
3400 IF POP$='NO' THEN GOTO 3640
3420 PRINT 'TYPE IN THE START AND FINISH TIMES'
3440 INPUT AB,BC
3460 NMAX=0.0:SAP=0.0
3500 FOR I=100 TO 270
3520 IF S(I)>SAP THEN SAP=A(I):PEAK=I
3530 NEXT I
3535 IF A(BC)<0.0 THEN A(BC)=0.0
3540 FOR I=AB TO BC
3550 NMAX=NMAX+1
3560 IF PEAK>=I THEN B(NMAX)=(A(I)-A(AB)))/4:GOTO 3600
3580 B(NMAX)=(A(I)-A(BC))/4
3600 NEXT I
3620 BEGIN=AB/6:FINISH=BC/6
3630 GOTO 620
3640 RETURN
```

APPENDIX 2

Computer program used to model the removal of material below 12000MW

```
*PROGRAM TO MODEL A ULTRAFILTRATION CASCADE BASED ON A USS
*MASS BALANCE SOLVED BY LAPLACE TRANSFORMS
*
*  PROPERTY              SYMBOL          UNITS
*
* FIBRE DIAMETER         DI              M
* FIBRE NUMBER           F               -
* LENGTH OF FIBRE        L               M
* DENSITY                DE              Kg/M3
* VISCOSITY              VE              Kg/M S
* DIFFUSSIVITY           DIF             M2/S
* VELOCITY               U               M/S
* CONCENTRATION          C               Kg/M3
* REYNOLDS NO            RE              -
* SCHMIDT NO             SC              -
* SHERWOOD NO            SH              -
* FLUX                   J               M/S
*
      REAL C,F,U,DI,DE,VE,RE,L,K,CG.DIF,FP,FR,FT,PC
      REAL CI,REJ,PEC,PARA,PARB,FRAC,A,CR,SH,LAM,SC
      REAL TF,MASFRAC,X,DIA,LOW,H,ERM,ER,HIGH,DA,G,B
      REAL CONC1,CONC2,RI,EX,MASS
      CHARACTER ANS*3,DSA*3
      INTERGER ZU,Q,P,N,M,R,I,MAX,STAGE
      DIMENSION CT(11,500),ARR(8,18),CI(11,500),CD(11,500)
      DIMENSION CP(11,500),MBR(10)
      DATA ARR/ -0.627332,0.30,0.3,-0.81061,
     +  0.24891,0.30,0.81884,0.83298,
     +  3.36187E-3,0.0,0.0,3.92937E-3,
     +  1.1785E-3,0.0,2.87365E-4,1.96272E-4,
     +  -1.89336E-6,0.0,0.0,-2.23759E-6,
     +  -5.6064E-7,0.0,-1.58973E-7,-9.08554E-8,
     +  0.7647,-0.7042,0.52489,0.87207,
     +  0.71990,-0.36691,0.91656,0.89253,
     +  1.05283E-4,1.79383E-3,3.61802E-4,3.88055E-5,
     +  1.8880E-4,1.38698E-3,4.02428E-5,5.89518E-5,
     +  -1.35607E-8,-5.06487E-7,-8.00714E-8,-3.845E-9,
     +  -4.10264E-8,-3.72196E-7,-72459E-1,-1.22866E-8,
     +  0.7647,0.73396,0.84058,0.87207,
     +  0.85502,0.81439,0.93868,0.92181,
     +  1.05283E-4,1.006E-4,5.43264E-5,3.8805E-5,
     +  5.00173E-5,7.02697E-5,1.83673E-5,2.51749E-5,
     +  -1.35607E-8,-1.1073E-8,-6.205E-9,-3.845E-9,
     +  -5.16434E-9,-7.54771E-9,-1.80514E-9,-2.64873E-9,
     +  0.93247,0.88268,0.9223,0.91785,
     +  0.92587,0.91862,0.95745,0.95267,
     +  1.33579E-5,2.81809E-5,1.19087E-5,1.63493E-5
     +  1.58037E-5,1.91301E-5,9.03254E-6,8.805E-6
     +  -9.895E-10,-1.9305E-9,-6.88025E-10,-1.09675E-9,
     +  -1.01385E-9,-1.2555E-9,-6.17975E-10,-4.84E-10,
     +  0.98028,0.9656,0.95749,0.96594,
     +  0.97039,0.96886,0.98026,0.98026,
     +  -1.17289E-9,3.77757E-6,2.08995E-6,2.12346E-6,
```

```
     +   2.95351E-6,4.49063E-6,1.866E-6,1.866E-6,
     +   1.14554E-10,-1.30714E-10,-9.67854E-12,-4.8338E-11,
     +   -8.29658E-11,-1.81446E-10,-6.60536E-11,-6.60536E-11,
     +   0.9773678,0.9897878,0.976545,0.976383,
     +   0.992902,0.9974348,0.987302,0.990307,
     +   4.48E-7,0.0,3.77E-7,6.66E-7,
     +   9.70E-8,0.0,5.06E-7,2.9E-7,
     +   0.0,0.0,0.0,0.0,0.0,0.0,0.0,0.0/
*
        V=0.001
        DI=0.0005
        F=300.0
        L=0.22
        CG=18.0

*
 2      PRINT*,'INPUT THE NUMBER OF CYCLES OF OPERATION'
        READ*,R
        PRINT*,'INPUT THE NUMBER OF CASCADE STAGES REQUIRED'
        READ*,MAX
 5      PRINT*,'INPUT THE FEED CONCENTRATION AS A WT%'
        READ*,C
        PRINT*,'INPUT THE FLOW RATE ....FT (M3/S)'
        READ*,FT
        PRINT*,' INPUT THE NUMBER OF DIAVOLUMES'
        READ*,DA
         DIA=DA*0.001
        PRINT*,'DO YOU WISH TO USE EMPERICAL CALCULATIONS TO'
        PRINT*,'FIND K ....TYPE   YES OR NO'
        READ*,ANS
*
        IF (ANS.NE.'YES') THEN
        PRINT*,'INPUT K IN M/S'
        READ*,K
        GOTO 9
        END IF
*
        PRINT*,' '
        PRINT*,' '
        PRINT*,'NOW INPUT THE MEMBRANE REQUIRED AT EACH STAGE'
        PRINT*,'INPUT MEMBRANE NUMBER FROM LIST BELOW'
        PRINT*,'AMICON 10K NO1      ....1'
        PRINT*,'AMICON 10K NO2      ....2'
        PRINT*,'AMICON 10K NO3      ....3'
        PRIMT*,'AMICON 10K NO4      ....4'
        PRINT*,'AMICON 5K NO6       ....5'
        PRINT*,'AMICON OFF SPEC 10K ...6'
        PRINT*,'AMICON 5K NO2       .....7'
        PRINT*,'AMICON 5K NO1       .....8'
        PRINT*,' '
        DO 7 I=1,MAX
 6         READ*,MBR(I)
           IF (MBR(I).GT.8) THEN
           PRINT*,'TRY AGAIN'
           GOTO 6
           END IF
 7      CONTINUE
*
```

```
* CALCULATE THE MASS TRANSFER COEFFICIENT AND FLUX
*
      A=3.14*DI**2/4.0
      CR=C*0.0103
      U=FT/(F*A)
 8    VE=0.000908*(1+CR*EXP(8.678*CR+3.313))
      DIF=(5.96E-11+2.12E-11*TANH(28.4*CR-1.491))
      DE=(0.003884*C+0.9974)*1000
      RE=U*DI*DE/VE
      SC=VE/(DE*DIF)
      LAM=RE*SC*DI/L
     IF (RE.GE.2000) THEN
        SH=0.023*(RE**0.8)*(SC**0.33)
     ELSE IF (LAM.GE.100.AND.LAM.LE.5000) THEN
        SH=1.62*(RE*SC*DI/L)**0.33
     ELSE
        PRINT*,'OUT OF RANGE OF EQUATION TRY AGAIN'
        GOTO 5
     END IF
*
      K=SH*DIF/DI
 9    J=K*LOG(CG/C)
      FP=0.06*J
      TF=DIA/FP
      FR=FT-FP
      PRINT*,'-----------------------------------------------'
      PRINT*,'THE MASS TRANSFER COEFFICIENT IS ',K,'M/S'
      PRINT*,'THE FLUX IS ',J,'M/S'
      PRINT*,'-----------------------------------------------'
      PRINT*,'PRESS 1 TO RESTART, ELSE ANY NUMBER'
        READ*,ZU
        IF (ZU.EQ.1) THEN
        GOTO 5
        END IF
*
      PRINT*,'PRESS ...1 FOR DISPLAY OF RESULTS FROM EACH'
      PRINT*,'CYCLE  ELSE ANY NUMBER FOR FINAL CYCLE ONLY'
      READ*,STAGE
* CALCULATE THE CONCENTRATION IN THE TANKS
*
      Q=1
 10   PC=0.0
      X=200.0
      M=1.0
      DO 20 N=1,490
         IF (X.LE.1000) THEN
         PEC=(-2.59999E-2-3.73411E-4*X+7.11387E-7*X**2)/100
         ELSE IF (X.GT.1000.AND.X.LE.4000) THEN
         PEC=(-0.66126+9.511321E-4*X+1.96391E-7*X**2)/100
         ELSE IF (X.GT.4000.AND.X.LE.20000) THEN
         PEC=(-4.4587+2.62146E-3*X-1.67835E-8*X**2)/100
         ELSE IF (X.GT.20000.AND.X.LE.68000) THEN
         PEC=(9.667+1.8839E-3*X-1.24335E-8*X**2)/100
         ELSE
         PEC=(2.223424E-4*X+64.872)/100
         END IF
         FRAC=PEC-PC
         PC=PEC
         CI(M,N)=FRAC*C*10.0
         X=X+200.0
```

```
 20      CONTINUE
*
 25     H=MBR(M)
        X=200.0
        DO 30 N=1,490
             IF (X.LE.1000) THEN
             REJ=ARR(H,1)+ARR(H,2)*X+ARR(H,3)*X**2
             ELSE IF (X.GT.1000.AND.X.LE.2000) THEN
             REJ=ARR(H,4)+ARR(H,5)*X+ARR(H,6)*X**2
             ELSE IF (X.GT.2000.AND.X.LE.4000) THEN
             REJ=ARR(H,7)+ARR(H,8)*X+ARR(H,9)*X**2
             ELSE IF (X.GT.4000.AND.X.LE.7000) THEN
             REJ=ARR(H,10)+ARR(H,11)*X+ARR(H,12)*X**2
             ELSE IF (X.GT.7000.AND.X.LE.12000) THEN
             REJ=ARR(H,13)+ARR(H,14)*X+ARR(H,15)*X**2
             ELSE IF (X.GT.12000) THEN
             REJ=ARR(H,16)+ARR(H,17)*X+ARR(H,18)*X**2
             IF (REJ.GT.1.0) THEN
             REJ=1.0
             END IF
             END IF
             G=(1-REJ)*FT
             B=FP*CD(M,N)
             RI=TF/V
             EX=G*RI
             CONC1=CI(M,N)
             IF (REJ.LE.0.9999) THEN
             CALL MODEL1(CONC2,EX,B,G,CONC1)
             ELSE
             CALL MODEL2(CONC2,B,RI,CONC1)
             END IF
             CT(M,N)=CONC2
             MASS=CD(M,N)*DIA+(CI(M,N)-CT(M,N))*V
             IF (MASS.GT.1.0E-9) THEN
             CP(M,N)=MASS/DIA
             ELSE
             CP(M,N)=0.0
             END IF
             CD(M,N)=0.0
             X=X+200.0
 30     CONTINUE
        IF (M.LT.MAX) THEN
             M=M+1
             GOTO 25
        END IF
*
        IF (STAGE.NE.1.AND.Q.NE.R) THEN
        GOTO 80
        END IF
        PRINT*,'TO DISPLAY RESULTS TABLE ...PRESS YES'
         READ*,ANS
         IF (ANS.NE.'YES') THEN
         GOTO 80
         END IF
 35     PRINT*,'WHICH STAGE DO YOU WISH TO CONSIDER'
 40      READ*,P
         IF (P.GT.1.AND.P.LE.MAX) THEN
*
         LOW=0.0
         HIGH=0.0
```

```
      MASFRAC=0.0
       DO 62 I=1,490
61     MASFRAC=MASFRAC+CT(P,I)
      IF  (I.LE.60 ) THEN
      LOW=LOW+CT(P,I)
      ELSE
      HIGH=HIGH+CT(P,I)
      END IF
62    CONTINUE
      ERM=1-LOW/(C*10.0*0.247)
      ER=HIGH/(C*10.0*0.6213)
      PRINT*,'CYCLE ',Q
      PRINT*,LOW,HIGH,MASFRAC
*
      PRINT*,'************************************'
      PRINT*,' '
      PRINT*,'    EFFICIENCY OF REMOVAL ='
      PRINT*,'        ',ERM*100,'%'
      PRINT*,' '
      PRINT*,'    EFFICIENCY OF RETENTION ='
      PRINT*,'        ',ER*100,'%'
      PRINT*,' '
      PRINT*,' FRACTION IN SAMPLE BELOW 12000'
      PRINT*,'        ',LOW/(MASFRAC+C*10.0*0.1317)
      PRINT*,' '
      PRINT*,' FRACTION BETWEEN 12000-98000'
      PRINT*,'        =',HIGH/(MASFRAC+C*10.0*0.1317)
      PRINT*,' '
      PRINT*,'************************************'
*
      ELSE
            PRINT*,'OUT OF RANGE ... TRY AGAIN'
            GOTO 35
      END IF
      PRINT*,'TO TRY ANOTHER STAGE TYPE ...YES'
      READ*, ANS
      IF (ANS.EQ.'YES') THEN
      GOTO 35
      END IF
*
80    M=1
90    DO 95 N=1,500
       CI(M+1,N)=CT(M,N)
       CD(M,N)=CP(M+1,N)
95    CONTINUE
      IF (M.LT.MAX) THEN
      M=M+1
      GOTO 90
      END IF
         IF (Q.LT.R) THEN
         Q=Q+1
         GOTO 10
         END IF
      PRINT*,'END OF SIMULATION'
      PRINT*,'PRESS S TO RESTART'
      READ*,DSA
      IF (DSA.EQ.'S') THEN
         GOTO 2
      END IF
      END
```

```
      SUBROUTINE MODEL1(CT,EX,B,G,CI)
      REAL PARA,PARB,EX,B,G,CT,CI
*
      PARA=B*(1-EXP(-EX))/G
      PARB=CI*EXP(-EX)
      CT=PARA+PARB
      RETURN
      END
*
      SUBROUTINE MODEL2(CT,B,RI,CO)
      REAL B,RI,CT,CO
      CT=B*RI+CO
      RETURN
      END
```

APPENDIX 3

Computer program used to model the removal of material above 98000MW

```
*PROGRAM TO MODEL A ULTRAFILTRATION CASCADE BASED ON A USS
*MASS BALANCE SOLVED BY LAPLACE TRANSFORMS
*       BY A . TILL     1987
      REAL MASS,C,V,J,K,CG,FP,FR,PC,CONC1,CONC2
      REAL CI,REJ,PEC,PARA,PARB,FRAC,A,RI,EX,MID
      REAL TF,MASFRAC,X,DIA,LOW,H,ERM,ER,HIGH,DA,G,B
      CHARACTER ANS*3,DSA*3
      INTERGER ZU,Q,P,N,M,R,I,MAX,STAGE
      DIMENSION CT(11,500),ARR(8,18),CI(11,500),CD(11,500)
      DIMENSION CP(11,500),MBR(10),POC(7,3)
      DATA ARR/ 0.98422,0.97689,0.97896,0.97557,
     +   6.3525E-7,2.17315E-6,1.47225E-6,3.05355E-6,
     +   -1.085E-11,-1.365E-10,-1.3875E-11,-2.237E-10,
     +   0.98440,0.97949,0.98508,0.98191,
     +   6.70879E-7,1.36895E-6,3.91575E-7,8.2502E-7,
     +   -2.22249E-11,-5.09875E-11,-3.8125E-12,-2.705E-11,
     +   0.98448,0.98661,0.98187,0.98356,
     +   5.34964E-7,1.77298E-7,8.29837E-7,4.07146E-7,
     +   -1.13625E-11,-8.32136E-13,-1.76965E-11,-3.28582E-12,
     +   0.98626,0.98635,0.98538,0.98562,
     +   2.59989E-7,1.97181E-7,3.71372E-7,2.81277E-7,
     +   -2.04086E-12,-1.25857E-12,-3.46143E-12,-2.20372E-12,
     +   0.98747,0.9893,0.98894,0.98642,
     +   1.85478E-7,8.19493E-8,1.76169E-7,2.15842E-7,
     +   -9.323358E-13,-2.50144E-13,-7.81571E-13,-1.07829E-12,
     +   0.98891,0.99052,0.99293,0.98688,
     +   1.27264E-7,5.09925E-8,8.51416E-8,1.75993E-7,
     +   -4.24998E-13,-5.67125E-14,-2.59073E-13,-6.585E-13,
     +   0.99646,0.992221,0.996784,0.995367,
     +   1.3412E-8,3.00312E-8,2.133E-8,2.643E-8,
     +   0.0,0.0,0.0,0.0/
      DATA POC/-1.03202E-2,-24.254,-7.6469,27.891,58.11,
     +   80.455,93.471,-1.04356E-4,4.83524E-3,3.39947E-3,
     +   1.54222E-3,5.7317E-4,1.49276E-4,1.49694E-5,
     +   1.85783E-7,-6.5298E-8,-3.45341E-8,-1.01801E-8,
     +   -2.38367E-9,-3.60031E-10,-1.30902E-11/
*
      V=0.001
      CG=23.0
      C=4.0
      FT=0.000016666
*
 2    PRINT*,'INPUT THE NUMBER OF CYCLES OF OPERATION'
      READ*,R
 5    PRINT*,'INPUT THE NUMBER OF CASCADE STAGES REQUIRED'
      READ*,MAX
      PRINT*,' INPUT THE NUMBER OF DIAVOLUMES'
      READ*,DA
       DIA=DA*0.001
*
      PRINT*,' '
      PRINT*,'NOW INPUT THE MEMBRANE REQUIRED AT EACH STAGE'
      PRINT*,'INPUT MEMBRANE NUMBER FROM LIST BELOW'
```

```
      PRINT*,'ROMICON 50K NO1        ....1'
      PRINT*,'ROMICON 50K NO2        ....2'
      PRIMT*,'ROMICON 50K NO3        ....3'
      PRINT*,'ROMICON 50K NO4        ....4'
      PRINT*,' '
      DO 7 I=1,MAX
         READ*,MBR(I)
 6       IF (MBR(I).GT.8) THEN
         PRINT*,'TRY AGAIN'
         GOTO 6
         END IF
 7    CONTINUE
*
* CALCULATE THE MASS TRANSFER COEFFICIENT AND FLUX
*
      K=1.422E-6
 9    J=K*LOG(CG/C)
      FP=0.0929*J
      TF=DIA/FP
      FR=FT-FP
      PRINT*,'-------------------------------------------'
      PRINT*,'THE MASS TRANSFER COEFFICIENT IS ',K,'M/S'
      PRINT*,'THE FLUX IS ',J,'M/S'
      PRINT*,'-------------------------------------------'
      PRINT*,'PRESS 1 TO RESTART, ELSE ANY NUMBER'
        READ*,ZU
        IF (ZU.EQ.1) THEN
        GOTO 5
        END IF
*
      PRINT*,'PRESS ...1 FOR DISPLAY OF RESULTS FROM EACH'
      PRINT*,'CYCLE  ELSE ANY NUMBER FOR FINAL CYCLE ONLY'
      READ*,STAGE
* CALCULATE THE CONCENTRATION IN THE TANKS
*
      Q=1
 10   PC=0.0
      X=1000.0
      M=1.0
      DO 20 N=1,500
         IF (X.LE.10000) THEN
         PEC=POC(1,1)+POC(1,2)*X+POC(1,3)*X**2
         ELSE IF (X.GT.10000.AND.X.LE.20000) THEN
         PEC=POC(2,1)+POC(2,2)*X+POC(2 3)*X**2
         ELSE IF (X.GT.20000.AND.X.LE.40000) THEN
         PEC=POC(3,1)+POC(3,2)*X+POC(3,3)*X**2
         ELSE IF (X.GT.40000.AND.X.LE.60000) THEN
         PEC=POC(4,1)+POC(4,2)*X+POC(4,3)*X**2
         ELSE IF (X.GT.60000.AND.X.LE.1.0E5) THEN
         PEC=POC(5,1)+POC(5,2)*X+POC(5,3)*X**2
         ELSE IF (X.GT.1.0E5.AND.X.LE.2.0E5) THEN
         PEC=POC(6,1)+POC(6,2)*X+POC(6,3)*X**2
         ELSE
         PEC=POC(7,1)+POC(7,2)*X+POC(7,3)*X**2
         END IF
         FRAC=(PEC-PC)/100
         PC=PEC
         CI(M,N)=FRAC*C*10.0
         X=X+1000.0
 20      CONTINUE
```

```
*
 25     H=MBR(M)
        X=1000.0
        DO 30 N=1,490
             IF (X.LE.6000) THEN
             REJ=ARR(H,1)+ARR(H,2)*X+ARR(H,3)*X**2
             ELSE IF (X.GT.6000.AND.X.LE.12000) THEN
             REJ=ARR(H,4)+ARR(H,5)*X+ARR(H,6)*X**2
             ELSE IF (X.GT.12000.AND.X.LE.20000) THEN
             REJ=ARR(H,7)+ARR(H,8)*X+ARR(H,9)*X**2
             ELSE IF (X.GT.20000.AND.X.LE.40000) THEN
             REJ=ARR(H,10)+ARR(H,11)*X+ARR(H,12)*X**2
             ELSE IF (X.GT.40000.AND.X.LE.80000) THEN
             REJ=ARR(H,13)+ARR(H,14)*X+ARR(H,15)*X**2
             ELSE IF (X.GT.80000.AND.X.LE.120000) THEN
             REJ=ARR(H,16)+ARR(H,17)*X+ARR(H,18)*X**2
             ELSE IF (X.GT.120000) THEN
             REJ=ARR(H,19)+ARR(H,20)*X+ARR(H,21)*X**2
             IF (REJ.GT.1.0) THEN
             REJ=1.0
             END IF
             END IF
             G=(1-REJ)*FT
             B=FP*CD(M,N)
             RI=TF/V
             EX=G*RI
             CONC1=CI(M,N)
             IF (REJ.LE.0.9999) THEN
             CALL MODEL1(CONC2,EX,B,G,CONC1)
             ELSE
             CALL MODEL2(CONC2,B,RI,CONC1)
             END IF
             CT(M,N)=CONC2
             MASS=CD(M,N)*DIA+(CI(M,N)-CT(M,N))*V
             IF (MASS.GT.1.0E-11) THEN
             CP(M,N)=MASS/DIA
             ELSE
             CP(M,N)=0.0
             END IF
             CD(M,N)=0.0
             X=X+1000.0
 30     CONTINUE
        IF (M.LT.MAX) THEN
             M=M+1
             GOTO 25
        END IF
*
        IF (STAGE.NE.1.AND.Q.NE.R) THEN
        GOTO 80
        END IF
        PRINT*,'TO DISPLAY RESULTS TABLE ...PRESS YES'
         READ*,ANS
         IF (ANS.NE.'YES') THEN
         GOTO 80
         END IF
 35     PRINT*,'WHICH STAGE DO YOU WISH TO CONSIDER'
 40      READ*,P
         IF (P.GT.1.AND.P.LE.MAX) THEN
*
```

```
      LOW=0.0
      NID=0.0
      HIGH=0.0
      MASFRAC=0.0
      DO 62 I=1,500
61    MASFRAC=MASFRAC+CT(P,I)
      IF  (I.LE.12 ) THEN
      LOW=LOW+CT(P,I)
      ELSE IF ( I.GT.12.AND.I.LE.98) THEN
      MID=MID+CT(P,I)
      ELSE
      HIGH=HIGH+CT(P,I)
      END IF
62    CONTINUE
      ERM=1-LOW/(C*2.356)
      ERI=1-MID/(C*6.768)
      ER=(HIGH+C*0.1942)/(C*0.876)
      PRINT*,'CYCLE ',Q
      PRINT*,LOW,HIGH,MID,MASFRAC
*
      PRINT*,'************************************************'
      PRINT*,' '
      PRINT*,'    EFFICIENCY OF REMOVAL  12000MW'
      PRINT*,'        ',ERM*100,'%'
      PRINT*,' '
      PRINT*,'    EFFICIENCY OF REMOVAL 12000-98000MW'
      PRINT*,'        ',ERI*100,'%'
      PRINT*,' '
      PRINT*,'    EFFICIENCY OF RETENTION  98000MW'
      PRINT*,'        ',ER*100,'%'
      PRINT*,' '
      PRINT*,'    FRACTION IN SAMPLE BELOW 12000'
      PRINT*,'      =',LOW/(MASFRAC+C*0.1942)
      PRINT*,' '
      PRINT*,'    FRACTION BETWEEN 12000-98000 '
      PRINT*,'      =',MID/(MASFRAC+C*0.1942)
      PRINT*,' '
      PRINT*,'    FRACTION ABOVE 98000 MW '
      PRINT*,'      =',(HIGH+C*0.1942)/(MASFRAC+C*0.1942)
      PRINT*,' '
      PRINT*,'************************************************'
*
        ELSE
             PRINT*,'OUT OF RANGE ... TRY AGAIN'
             GOTO 35
        END IF
        PRINT*,'TO TRY ANOTHER STAGE TYPE ...YES'
        READ*, ANS
        IF (ANS.EQ.'YES') THEN
        GOTO 35
        END IF
*
80      M=1
90      DO 95 N=1,500
         CI(M+1,N)=CT(M,N)
         CD(M,N)=CP(M+1,N)
95      CONTINUE
        IF (M.LT.MAX) THEN
        M=M+1
```

```
      GOTO 90
      END IF
         IF (Q.LT.R) THEN
         Q=Q+1
         GOTO 10
         END IF
      PRINT*,'END OF SIMULATION'
      PRINT*,'PRESS S TO RESTART'
      READ*,DSA
      IF (DSA.EQ.'S') THEN
         GOTO 2
      END IF
      END
      SUBROUTINE MODEL1(CT,EX,B,G,CI)
      REAL PARA,PARB,EX,B,G,CT,CI
*
      PARA=B*(1-EXP(-EX))/G
      PARB=CI*EXP(-EX)
      CT=PARA+PARB
      RETURN
      END
*
      SUBROUTINE MODEL2(CT,B,RI,CO)
      REAL B,RI,CT,CO
      CT=B*RI+CO
      RETURN
      END
```

APPENDIX 4.1

Mass balance across the cascade, run 3.1 (0-12,000 MW band)

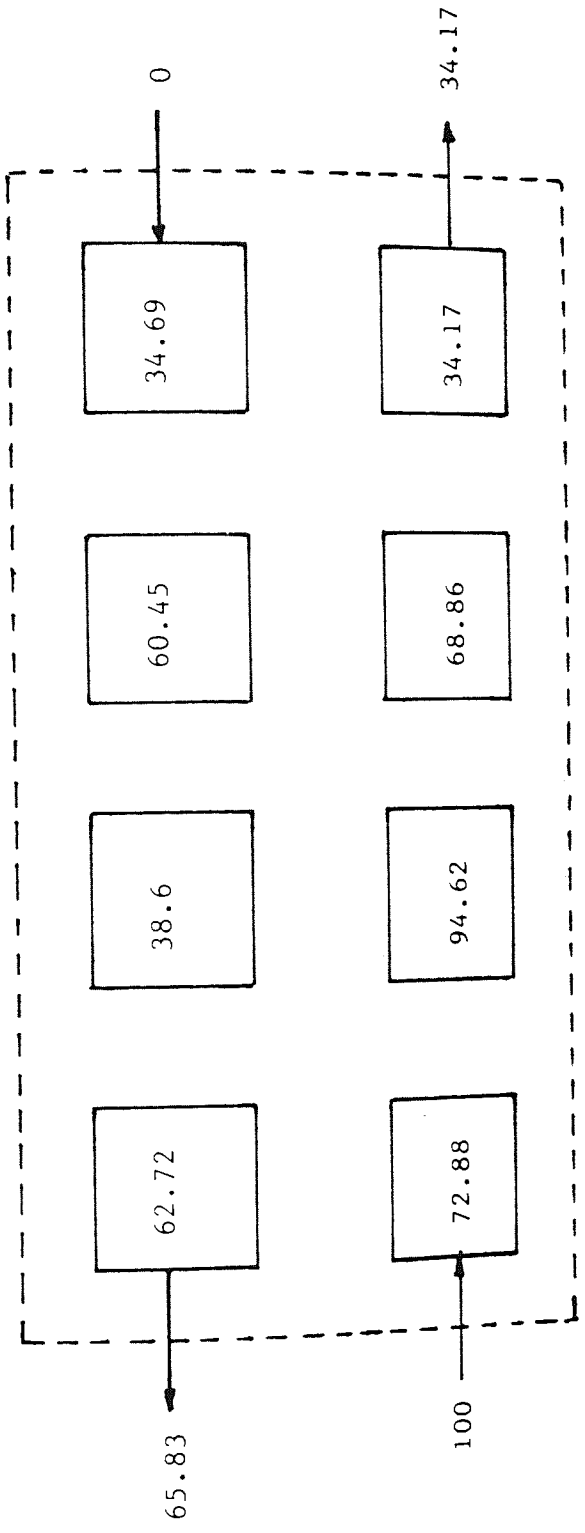

Mass input (beginning of cycle)	100	72.88	94.62	68.86
	+38.6	+60.45	+34.69	
Mass output (end of cycle)	70.88	94.62	68.86	34.17
Mass in permeate	62.72	38.6	60.45	34.69

APPENDIX 4.2

Mass balance across the cascade, run 3.1 (12,000-98000 band)

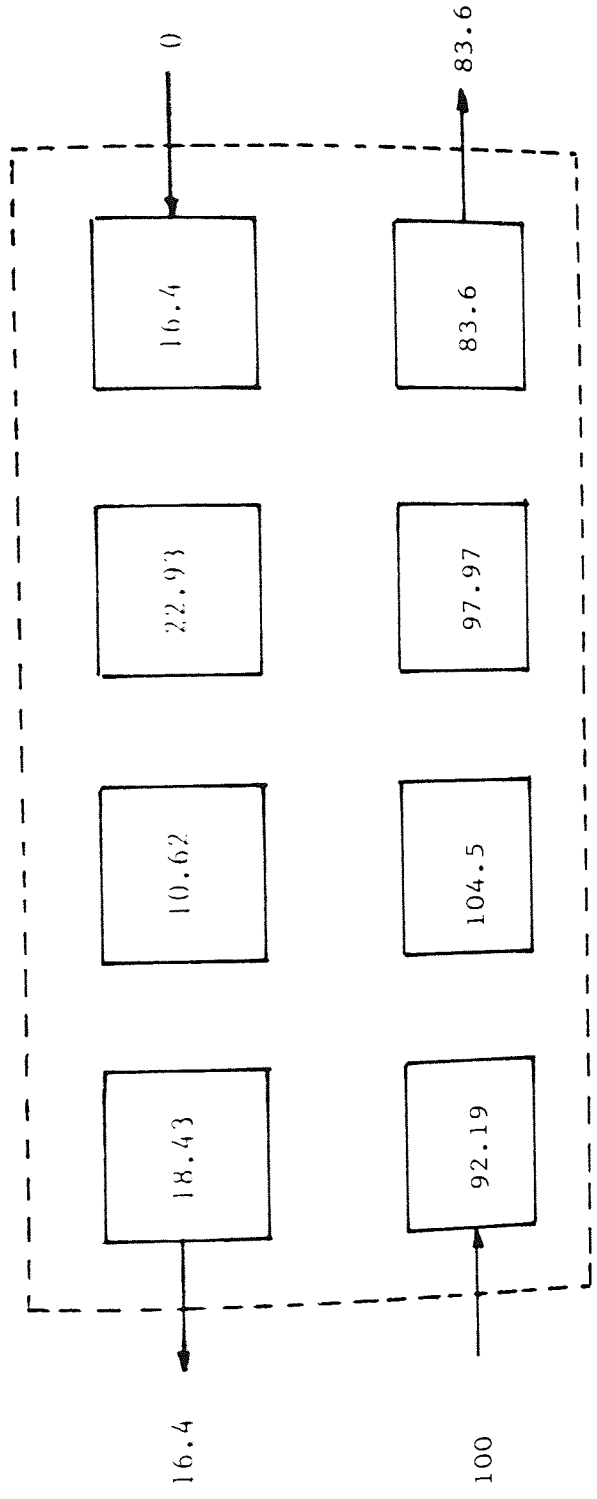

Mass input (beginning of cycle)	100	+10.62	92.19 +22.93	104.8 +16.4	97.97
Mass output (end of cycle)	92.19		104.5	97.97	83.6
Mass in permeate	18.43		10.62	22.93	16.4

APPENDIX 5.1

Model prediction for ideal cascade. (0-12,000 MW band)

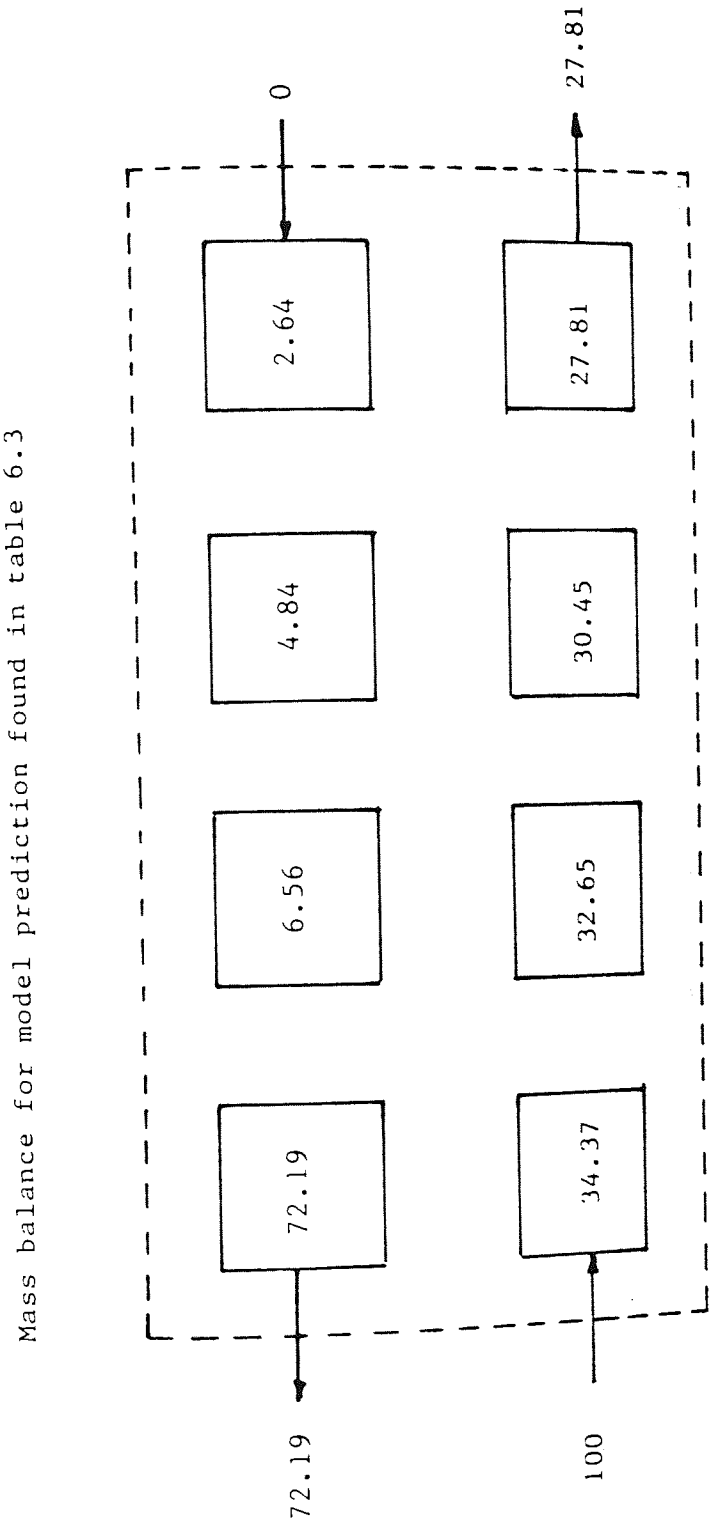

APPENDIX 5.2

Model prediction for ideal cascade (12,000-98,000 MW band)

Model prediction for mixed membrane run 5.1 (0-12,000 MW band)

Mass balance for model prediction found in table 6.4

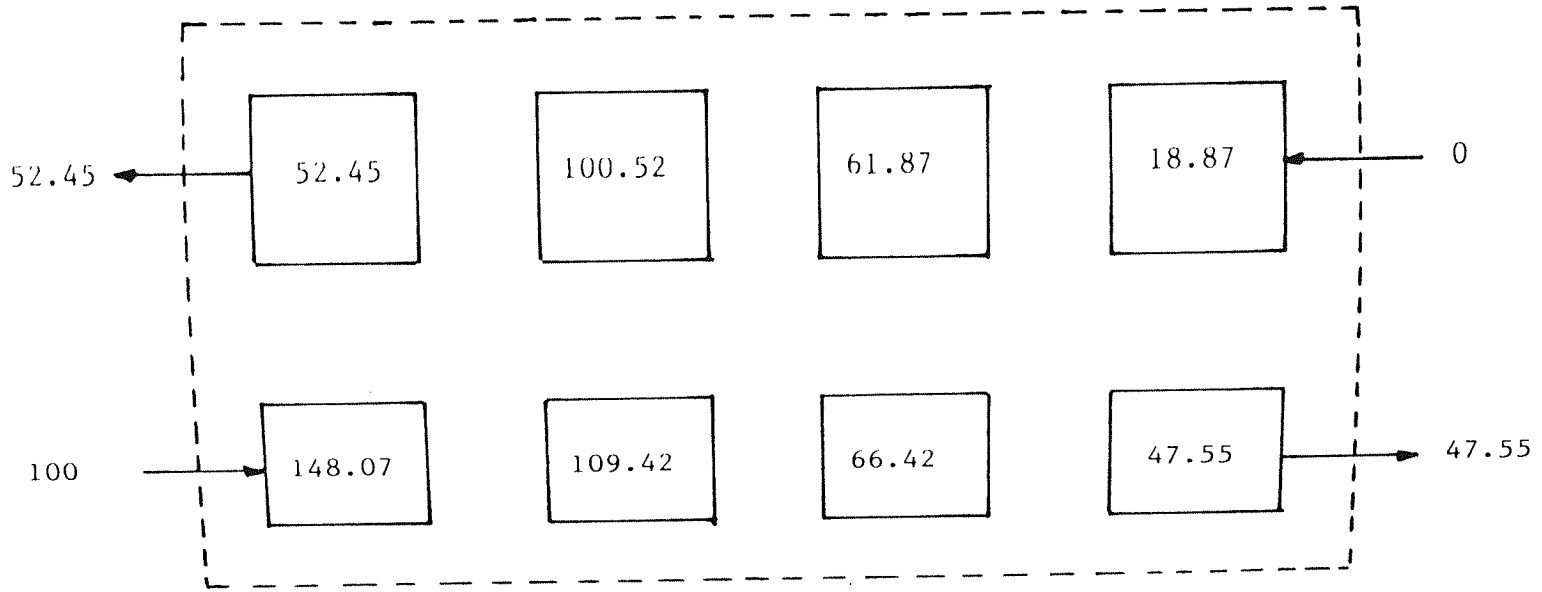

Mass input (beginning of cycle)	100 +100.52	148.07 +61.87	109.42 +18.87	66.42
Mass output (end of cycle)	148.07	109.42	66.42	47.55
Mass in permeate	52.45	100.52	61.87	18.87

APPENDIX 6.2

Model prediction for mixed membrane run 5.1 (12,000-98,000 MW band)

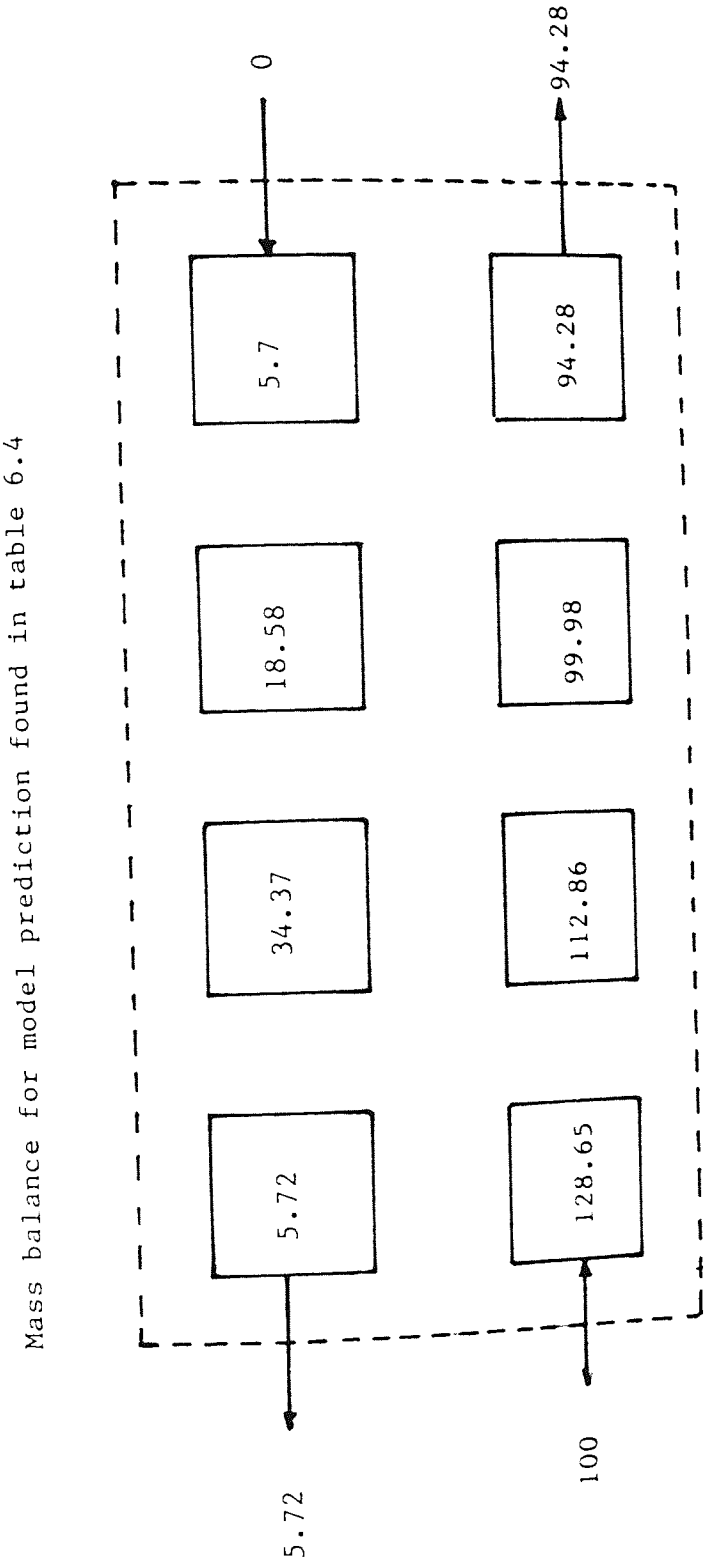

Mass balance for model prediction found in table 6.4

Mass input (beginning of cycle)	100	+35.37	128.65 +18.58	112.86 +5.7
Mass output (end of cycle)	128.65		112.86	99.98
Mass in permeate	5.72		34.37	18.58

Mass input (beginning of cycle)	99.98
Mass output (end of cycle)	94.28
Mass in permeate	5.7

Appendix 7

Results obtained from the bioreactor.

RUN 2

Sucrose feed concentration - 2% W/V

Enzyme activity - 10.16 DSU/cm^3

Total activity - 965 DSU

Membranes used - XM50 : YM100

Time (Minutes)	Permeate flow cm^3/min	Permeate Concentrations % W/V		
		Sucrose	Fructose	Dextran
50	-	-	0.147	-
120	-	0.086	0.41	-
240	-	0.086	0.674	-
Cell concentration		-	0.846	0.856
2% batch concentration		-	0.981	0.808

RUN 3

Sucrose feed concentration - 2% W/V

Enzyme activity - 19.89 DSU/cm^3

Total activity - 1890 DSU

Membranes used - YM30 : XM50

Time (minutes)	Permeate flow cm^3/min	Permeate Concentrations % W/V		
		Sucrose	Fructose	Dextran
20	1.30	0.278	0.164	-
60	0.533	0.121	0.49	-
120	0.341	0.071	0.515	-
240	0.26	0.013	0.697	-
300	0.202	0.058	0.874	-
Cell concentration		-	0.78	1.383
2% batch concentration		-	0.981	0.808

RUN 4

Sucrose feed concentration - 4% W/V

Enzyme activity - 19.68 DSU/cm^3

Total activity - 1870 DSU

Membrane used - YM30 : XM50

Time (minutes)	Permeate flow (cm^3/min)	Permeate Concentration % W/V		
		Sucrose	Fructose	Dextran
20	1.55	0.212	0.0864	-
60	0.525	0.290	0.241	-
120	0.25	0.1493	0.7405	-
180	0.195	0.094	0.746	-
240	0.149	0.0971	1.0473	-
Cell concentration		-	1.22	2.631
4% batch concentration		-	2.24	1.738

RUN 5

Sucrose feed concentration - 10% W/V

Enzyme activity - 9.47 DSU/cm^3

Total activity - 900 DSU

Membrane used - YM30 : XM50

Time (minutes)	Permeate flow (cm^3/min)	Permeate Concentrations % W/V		
		Sucrose	Fructose	Dextran
10	1.833	-	0.0	-
30	0.818	0.051	0.0396	-
60	0.375	0.181	0.2812	-
150	0.146	0.122	0.644	-
210	0.142	0.12	0.783	-
270	0.133	0.123	1.047	-
Cell Concentration		-	1.722	4.41
10% batch concentration		-	4.183	6.278

RUN 6

Sucrose feed concentration - 10% W/V

Enzyme activity - 19.7 DSU/cm^3

Total cell activity - 1872 DSU

Membranes used - YM30 : XM50

Time (minutes)	Permeate flow (cm^3/min)	Permeate Concentration W/V%		
		Sucrose	Fructose	Dextran
10	1.15	0.803	0.073	-
25	0.7	1.216	0.158	-
60	0.412	1.373	0.347	-
90	0.2727	1.322	0.545	-
150	0.129	1.04	0.898	-
210	0.115	0.777	1.157	-
Cell concentration		-	1.959	4.013
10% batch concentration		-	4.1833	6.278

RUN 7

Sucrose feed concentration - 10% W/V

Enzyme activity - 19.7 DSU/cm^3

Total activity - 1872 DSU

Membranes used - YM30 : XM50

Time (minutes)	Permeate flow (cm^3/min)	Permeate Concentration % W/V		
		Sucrose	Fructose	Dextran
10	0.7	0.134	0.85	-
30	0.58	0.291	0.1618	-
60	0.335	0.55	0.1816	-
120	0.2	0.608	0.409	-
180	0.133	0.509	0.709	-
Cell concentration		-	1.511	3.01
10% batch concentration		-	4.1833	6.278